

WOODHEAD PUBLISHING IN MATERIALS



Polymer modified bitumen

Properties and characterisation

Edited by Tony McNally

WP
WOODHEAD
PUBLISHING

Polymer modified bitumen

Related titles:

Polymer–carbon nanotube composites

(ISBN 978-1-84569-761-7)

Polymer–carbon nanotube composites reviews the use of carbon nanotubes as reinforcements in a polymer matrix, creating a new class of nanocomposites with useful properties and wide potential applications. Part I discusses preparation and processing techniques. Part II analyses key properties and ways of characterising polymer–carbon nanotube composites. The final part of the book covers some of the important applications of this new group of materials.

Interface engineering of natural fibre composites for maximum performance

(ISBN 978-1-84569-742-6)

There is a growing trend towards the use of natural (sustainable) fibres as reinforcements in composites. One of the major mechanisms of failure in such composites is the breakdown of the bond or interface between the reinforcement fibres and the matrix. When this happens, the composite loses strength and fails. By engineering the interface between fibres and the matrix, the properties of the composite can be manipulated to give maximum performance. This book reviews both processing and surface treatments to improve interfacial adhesion in natural fibre composites as well as ways of testing their resulting properties.

Non-crimp fabric composites

(ISBN 978-1-84569-762-4)

Non-crimp fabric (NCF) composites are composites that are reinforced with woven mats of straight (non-crimped) fibres. Straight fibres deform much less under tension. NCF composites are being used in applications in the aerospace, automotive, civil engineering and wind turbine sector where strength is important. *Non-crimp fabric composites* reviews production, properties and applications of this important class of composites.

Details of these and other Woodhead Publishing materials books can be obtained by:

- visiting our web site at www.woodheadpublishing.com
- contacting Customer Services (e-mail: sales@woodheadpublishing.com; fax: +44 (0) 1223 832819; tel.: +44 (0) 1223 499140 ext. 130; address: Woodhead Publishing Limited, 80 High Street, Sawston, Cambridge CB22 3HJ, UK)
- contacting our US office (e-mail: usmarketing@woodheadpublishing.com; tel.: (215) 928 9112; address: Woodhead Publishing, 1518 Walnut Street, Suite 1100, Philadelphia, PA 19102-3406, USA)

If you would like to receive information on forthcoming titles, please send your address details to: Francis Dodds (address, tel. and fax as above; e-mail: francis.dodds@woodheadpublishing.com). Please confirm which subject areas you are interested in.

Polymer modified bitumen

Properties and characterisation

Edited by
Tony McNally



Oxford Cambridge Philadelphia New Delhi

Published by Woodhead Publishing Limited,
80 High Street, Sawston, Cambridge CB22 3HJ, UK
www.woodheadpublishing.com

Woodhead Publishing, 1518 Walnut Street, Suite 1100, Philadelphia,
PA 19102-3406, USA

Woodhead Publishing India Private Limited, G-2, Vardaan House,
7/28 Ansari Road, Daryaganj, New Delhi – 110002, India
www.woodheadpublishingindia.com

First published 2011, Woodhead Publishing Limited
© Woodhead Publishing Limited, 2011; Chapter 10 © Government of Canada
The authors have asserted their moral rights.

This book contains information obtained from authentic and highly regarded sources.
Reprinted material is quoted with permission, and sources are indicated. Reasonable efforts
have been made to publish reliable data and information, but the authors and the publisher
cannot assume responsibility for the validity of all materials. Neither the authors nor the
publisher, nor anyone else associated with this publication, shall be liable for any loss,
damage or liability directly or indirectly caused or alleged to be caused by this book.

Neither this book nor any part may be reproduced or transmitted in any form or by any
means, electronic or mechanical, including photocopying, microfilming and recording, or by
any information storage or retrieval system, without permission in writing from Woodhead
Publishing Limited.

The consent of Woodhead Publishing Limited does not extend to copying for general
distribution, for promotion, for creating new works, or for resale. Specific permission must
be obtained in writing from Woodhead Publishing Limited for such copying.

Trademark notice: Product or corporate names may be trademarks or registered trademarks,
and are used only for identification and explanation, without intent to infringe.

British Library Cataloguing in Publication Data
A catalogue record for this book is available from the British Library.

Library of Congress Control Number: 2011934933

ISBN 978-0-85709-048-5 (print)
ISBN 978-0-85709-372-1 (online)

The publisher's policy is to use permanent paper from mills that operate a sustainable
forestry policy, and which has been manufactured from pulp which is processed using
acid-free and elemental chlorine-free practices. Furthermore, the publisher ensures that the
text paper and cover board used have met acceptable environmental accreditation standards.

Typeset by Replika Press Pvt Ltd, India
Printed by TJI Digital, Padstow, Cornwall, UK

Contents

	<i>Contributor contact details</i>	ix
1	Introduction to polymer modified bitumen (PmB) T. McNALLY, Queen's University Belfast, UK	1
1.1	Bitumen	1
1.2	Polymer modified bitumen	8
1.3	Introduction to <i>Polymer modified bitumen: properties and characterisation</i>	14
1.4	References	15
	Part I Types of polymer modified bitumen	23
2	Polymer modified bitumen emulsions (PMBEs) D. LESUEUR, Lhoist R&D, Belgium	25
2.1	Introduction	25
2.2	Manufacturing polymer modified bitumen emulsions (PMBEs)	26
2.3	Uses of PMBE	35
2.4	Conclusions	38
2.5	References	40
3	Modification of bitumen using polyurethanes P. PARTAL and F. J. MARTÍNEZ-BOZA, Universidad de Huelva, Spain	43
3.1	Introduction	43
3.2	Bitumen modification by polymers	44
3.3	Modification by isocyanate-based reactive polymers	46
3.4	The role of the bitumen colloidal nature	49
3.5	Polyurethane/urea-based modified bitumen	55
3.6	Bitumen foaming and future trends	59
3.7	Sources of further information and advice	67
3.8	References	68

4	Rubber modified bitumen	72
	I. GAWEL, Wrocław University of Technology, Poland, J. PIŁAT, P. RADZISZEWSKI, K. J. KOWALSKI and J. B. KRÓL, Warsaw University of Technology, Poland	
4.1	Introduction	72
4.2	Waste rubber recycling	73
4.3	Shredding of scrap rubber from tyres	75
4.4	Methods of bitumen modification with crumb rubber	76
4.5	Rubber-bitumen interactions	78
4.6	Properties of rubber modified bitumen	84
4.7	Properties of asphalt-rubber mixture	87
4.8	Performance of pavement with asphalt-rubber mixture	90
4.9	Economic benefits	92
4.10	Conclusions	93
4.11	References	93
5	The use of waste polymers to modify bitumen	98
	F. J. NAVARRO DOMÍNGUEZ and M. GARCÍA-MORALES, Universidad de Huelva, Spain	
5.1	Introduction	98
5.2	Processing of waste polymer modified bitumens	100
5.3	Thermomechanical properties of waste polymer modified bitumens	111
5.4	Future trends	132
5.5	Sources of further information and advice	133
5.6	References	133
6	Polypropylene fiber-reinforced bitumen	136
	S. TAPKIN, Ü. UŞAR and Ş. ÖZCAN, Anadolu University, Turkey and A. ÇEVİK, University of Gaziantep, Turkey	
6.1	Introduction to polypropylene modification of asphalt concrete	136
6.2	Using polypropylene fibers to improve the fatigue life of asphalt concrete	138
6.3	Experiments used to enhance the physical and mechanical properties of polypropylene fiber-reinforced asphalt mixtures	139
6.4	Analysing the fatigue life of bituminous concrete	145
6.5	Analysing the repeated creep behaviour of bituminous concrete by utilising wet basis modification	152
6.6	Using artificial neural networks to predict physical and mechanical properties of polypropylene-modified dense bituminous mixtures	161

6.7	Determining the optimal polypropylene fiber modification of asphalt concrete utilising static creep tests, Marshall tests and fluorescence microscopy analyses	181
6.8	Conclusions	189
6.9	References	190
Part II Characterisation and properties		195
7	Rheology of polymer-modified bitumens C. GALLEGOS and M. GARCÍA-MORALES, Universidad de Huelva, Spain	197
7.1	Introduction	197
7.2	Rheological characterisation of polymer-modified bitumen at in-service temperatures	200
7.3	Case studies	218
7.4	Conclusions and future trends	231
7.5	Sources of further information and advice	232
7.6	References	232
8	Factors affecting the rheology of polymer modified bitumen (PMB) G. D. AIREY, University of Nottingham, UK	238
8.1	Introduction	238
8.2	Polymer modification	239
8.3	Conventional physical property tests	243
8.4	Advanced rheological characterisation	248
8.5	Ageing	251
8.6	Asphalt mixture performance	256
8.7	Conclusions	260
8.8	Sources of further information and advice	261
8.9	References	262
9	Ageing of polymer modified bitumen (PMB) J.-Y. YU, Z.-G. FENG and H.-L. ZHANG, Wuhan University of Technology, P. R. China	264
9.1	Introduction	264
9.2	Main causes of ageing for polymer modified bitumens (PMBs)	265
9.3	Simulative ageing methods of polymer modified bitumens (PMBs)	269
9.4	Ageing performance and characterization of polymer modified bitumens (PMBs)	272

9.5	Methods for improving the ageing resistance of polymer modified bitumens (PMBs)	292
9.6	Future trends in research on polymer modified bitumen (PMB) ageing	293
9.7	Sources of further information and advice	294
9.8	References	295
10	Natural weathering of styrene–butadiene modified bitumen J-F. MASSON, P. COLLINS, J. R. WOODS and S. BUNDALO-PERC, National Research Council of Canada, Canada and I. L. AL-QADI, University of Illinois at Urbana-Champaign, USA	298
10.1	Introduction	298
10.2	Background	299
10.3	Bituminous sealants and methods of analysis	300
10.4	Weathering of bituminous sealants	309
10.5	Future trends	330
10.6	References	332
11	Fuel resistance of bituminous binders G. POLACCO, S. FILIPPI, M. PACI and S. MARKANDAY, University of Pisa, Italy and F. MERUSI and F. GIULIANI, University of Parma, Italy	336
11.1	Introduction	336
11.2	Solubility of bituminous binders	338
11.3	Bitumen modification to enhance fuel resistance	340
11.4	Conclusions	362
11.5	References	363
12	Physico-chemical techniques for analysing the ageing of polymer modified bitumen V. MOUILLET, Centre d'Etudes Techniques de l'Equipement-Méditerranée, France and F. FARCAS and E. CHAILLEUX, Institut Français des Sciences et Technologies des Transports, de l'Aménagement et des Réseaux, France	366
12.1	Introduction	366
12.2	Usual methods for physico-chemical characterization of polymer modified bitumen (PmB) ageing	367
12.3	Investigation at the microscopic scale of polymer modified bitumen (PmB) ageing	382
12.4	Conclusions	389
12.5	Acknowledgements	392
12.6	References	392
	<i>Index</i>	396

Contributor contact details

(* = main contact)

Editor and Chapter 1

Dr Tony McNally
School of Mechanical and
Aerospace Engineering
Queen's University Belfast
University Road
Belfast BT7 7NN
UK

E-mail: t.mcnamara@qub.ac.uk

Chapter 2

Dr Didier Lesueur
Lhoist R&D
Rue de l'Industrie, 31
1400 Nivelles
Belgium

E-mail: didier.lesueur@lhoist.com

Chapter 3

Pedro Partal* and Francisco J.
Martínez-Boza
Departamento de Ingeniería
Química
Universidad de Huelva
Campus del Carmen, 21071 Huelva
Spain

E-mail: partal@uhu.es;
martinez@uhu.es

Chapter 4

Professor Irena Gaweł*
Wrocław University of Technology
Department of Fuels Chemistry and
Technology
ul. Gdańsk 7/9
50-344 Wrocław
Poland

E-mail: irena.gawel@pwr.wroc.pl

Professor Jerzy Piłat, Professor
Piotr Radziszewski, Dr Karol J.
Kowalski and Dr Jan B. Król
Warsaw University of Technology
Faculty of Civil Engineering
Department of Building Materials
Engineering
Al. Armii Ludowej 16
00-637 Warsaw
Poland

E-mail: j.pilat@il.pw.edu.pl;
p.radziszewski@il.pw.edu.pl;
k.kowalski@il.pw.edu.pl;
j.krol@il.pw.edu.pl

Chapter 5

Francisco J. Navarro Domínguez*
and Moisés García-Morales
Departamento de Ingeniería
Química
Facultad de Ciencias
Experimentales
Avenida del 3 de marzo
Campus del Carmen
Universidad de Huelva
21071 Huelva
Spain

E-mail: frando@uhu.es

Chapter 6

Professor Serkan Tapkıń*, Ün Uşar
and Şenol Özcan
Anadolu University
İki Eylül Campus
Civil Engineering Department
Transportation Division
26555 Eskişehir
Turkey

E-mail: serkan.tapkin@gmail.com;
estapkin@anadolu.edu.tr

Professor Abdulkadir Çevik
Civil Engineering Department
University of Gaziantep
Turkey

Chapter 7

Críspulo Gallegos* and Moisés
García-Morales
Departamento de Ingeniería
Química
Facultad de Ciencias
Experimentales
Universidad de Huelva
21071 Huelva
Spain

E-mail: cgallego@uhu.es

Chapter 8

Professor Gordon D. Airey
Nottingham Transportation
Engineering Centre
University of Nottingham
University Park
Nottingham NG7 2RD
UK

E-mail: Gordon.Airey@nottingham.
ac.uk

Chapter 9

Jianying Yu*, Zhengang Feng and
Henglong Zhang
School of Materials Science and
Engineering
Wuhan University of Technology
Luoshi Road 122#
Wuhan, 430070
Hubei
P. R. China

E-mail: jyyu@whut.edu.cn

Chapter 10

J.-F. Masson*, Peter Collins, John R. Woods and Slađana Bundalo-Perc
 National Research Council of Canada
 Ottawa
 Ontario K1A 0R6
 Canada

E-mail: Jean-Francois.Masson@nrc.gc.ca

Imad L. Al-Qadi
 Illinois Center for Transportation
 Department of Civil and Environmental Engineering
 University of Illinois at Urbana-Champaign
 Urbana, IL 61801
 USA

E-mail: alqadi@illinois.edu

Chapter 11

Giovanni Polacco*, Sara Filippi, Massimo Paci and Sureshkumar Markanday
 Department of Chemical Engineering
 University of Pisa
 via Diotisalvi, 2
 Pisa 56122
 Italy

E-mail: g.polacco@ing.unipi.it

Filippo Merusi and Felice Giuliani
 Department of Civil and Environmental Engineering
 University of Parma
 Viale G.P. Usberti 181/A
 Parma 43124
 Italy

Chapter 12

Virginie Mouillet*
 Laboratoire Régional des Ponts et Chaussées d'Aix-en-Provence
 CETE Méditerranée, Pôle d'activité – CS 70499
 13593 Aix-en-Provence Cedex 3
 France

E-mail: virginie.mouillet@developpement-durable.gouv.fr

Fabienne Farcas
 Département Matériaux, Groupe CPDM
 Institut Français des Sciences et Technologies des Transports, de l'Aménagement et des Réseaux
 58 Boulevard Lefebvre
 75732 Paris Cedex 15
 France

E-mail: fabienne.farcas@ifsttar.fr

Emmanuel Chailleux
 Département Matériaux, Groupe MIT
 Institut Français des Sciences et Technologies des Transports, de l'Aménagement et des Réseaux
 Route de Bouaye
 BP 4129
 44341 Bouguenais Cedex
 France

E-mail: emmanuel.chailleux@ifsttar.fr

Introduction to polymer modified bitumen (PmB)

T. McNALLY, Queen's University Belfast, UK

Abstract: Bitumen is a by-product of the fractional distillation of crude oil, but is also found in natural deposits. It has a unique combination of excellent water-proofing and adhesive properties which have been used effectively for more than 5000 years. Bitumen is a low-cost thermoplastic material which is widely used in roofing, road and pavement applications. However, it is brittle in cold environments and softens readily in warm environments. One of the many methods employed to toughen bitumen is to blend it with polymers, either virgin or scrap, to produce polymer modified bitumen (PmB). In this chapter, an introduction to bitumen structure and properties, and a short review of the published literature on PmB is provided. Finally, an outline of the focus and content of each chapter in the book is described.

Key words: bitumen, asphaltenes, aromatics, resins, paraffins, colloid, Iatroscan, polymer modified bitumen, binder, microstructure, rheology, viscoelastic properties, bitumen ageing.

1.1 Bitumen

British Standard 3690, Part 1: 1989 defines bitumen as 'A viscous liquid, or solid, consisting essentially of hydrocarbons and their derivatives, which is soluble in trichloroethylene and is substantially non-volatile and softens gradually when heated. It is black or brown in colour and possesses waterproofing and adhesive properties. It is obtained by refinery processes from petroleum, and is also found as a natural deposit or as a component of naturally occurring asphalt, in which it is associated with mineral matter'.

Man has made use of bitumen and bituminous binders for thousands of years. There are many references to bitumen in the Bible. In Genesis it refers to Noah's waterproofing of the ark which was 'pitched within and without with pitch'. Pitch is the Latin equivalent of 'gwitu-men' which was subsequently shortened to 'bitumen', then passing via French into English. Also, in the description of the building of the Tower of Babel, 'they used bricks for stone and bitumen for mortar' (Whiteoak, 1990). For over 5000 years bitumen has been used as a waterproofing and/or bonding agent (Abraham, 1945). The earliest recorded use was by the Sumerians around 3800 BC and the Egyptians used it in their mummification processes (Volke, 1993; Chirife *et al.*, 1991).

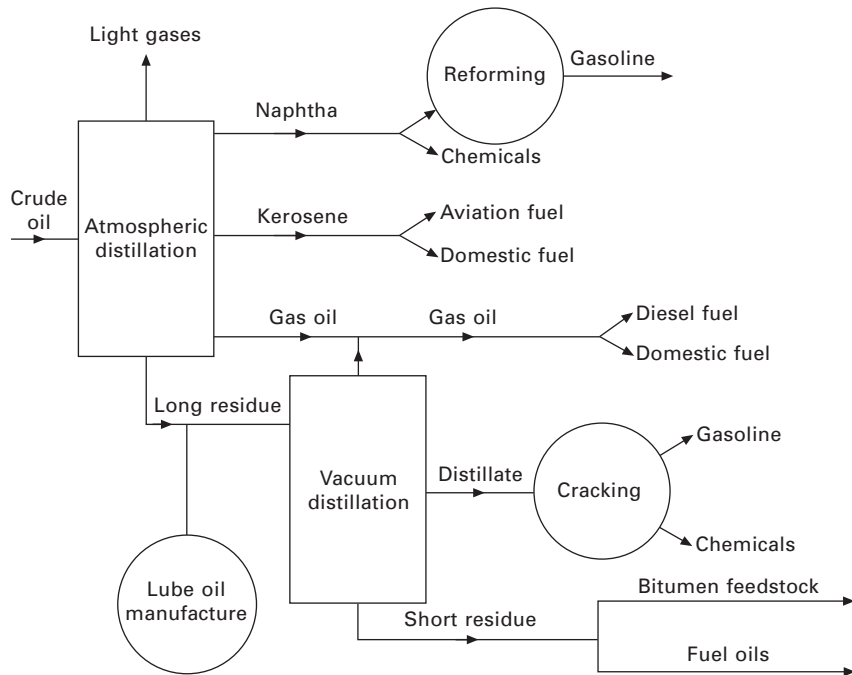
Bitumen occurs naturally, as mentioned above, and also remains after crude oil has been refined. Since the turn of the twentieth century demand for bitumen has far outweighed that available from naturally occurring sources. 'Natural' bitumen is found in the vicinity of subterranean crude oil deposits where surface seepages may occur at geological faults. The amount and nature of this naturally occurring material depend on a number of natural processes which modify the properties of this material. This product is often accompanied by mineral matter, the amount and nature of which depend on the circumstances which caused such an admixture to occur (Whiteoak, 1990).

Crude oil originates from the remains of marine organisms and vegetable matter deposited with mud and fragments of rock on the ocean bed. Over millions of years organic matter and mud accumulate into layers hundreds of metres thick, the immense weight of the upper layers compressing the lower layers into sedimentary rock. Conversion of organisms and vegetable matter into hydrocarbons of crude oil is thought to be the result of the effect of heat from the earth's crust and of pressure applied by the upper sedimentary layers, possibly aided by the effects of bacterial action and radioactive bombardment. As further layers of sediment were deposited on the sedimentary rock where the oil had formed, the additional pressure squeezed the oil sideways and upwards through porous rock. Porous rock extends to the earth's surface, allowing oil to seep through, resulting in surface seepages (Whiteoak, 1990).

In general, there are four main oil producing regions in the world: the USA, Russia, the Middle East and the countries around the Caribbean. Bitumen is obtained by the fractional distillation of the crude oil at 300–350°C. Figure 1.1 shows a schematic diagram of the distillation process.

The lighter fractions (e.g. propane and butane) come off first, followed by naphtha, kerosene and gas oil, distillates and short residue. It is this short residue which is the feedstock used in the manufacture of many different grades of bitumen. Oxygen is blown through the short residue and, depending on the temperatures and pressures used, and how much oxygen is added, different grades of bitumen are obtained. In the UK bitumen is generally classified into four grades:

1. Penetration grades: specified by penetration (British Standard 2000, Part 49: 1983) and softening point (British Standard 2000, Part 58: 1983), tests.
2. Cutback grades (to which kerosene has been added): specified by viscosity.
3. Hard grades: specified by penetration test and softening point range.
4. Oxidised grades: specified by penetration and softening point tests and also by solubility criteria.



1.1 Schematic diagram of the fractional distillation of crude oil to yield bitumen feedstock (Whiteoak, 1990).

Bitumen is considered to be a complex mixture of high molecular weight hydrocarbons and non-hydrocarbons which can be separated into fractions consisting of asphaltenes, resins, aromatics and paraffins (Traxler, 1936). Three types of hydrocarbons are present in bitumen; paraffinic, naphthenic and aromatic. Non-hydrocarbons in bitumen have heterocyclic atoms consisting of sulphur, nitrogen and oxygen. Elemental analysis of bitumen manufactured from a variety of crude oils shows that most bitumens contain:

- Carbon 82–85%
- Hydrogen 8–11%
- Sulphur 0–6%
- Oxygen 0–1.5%
- Nitrogen 0–1%.

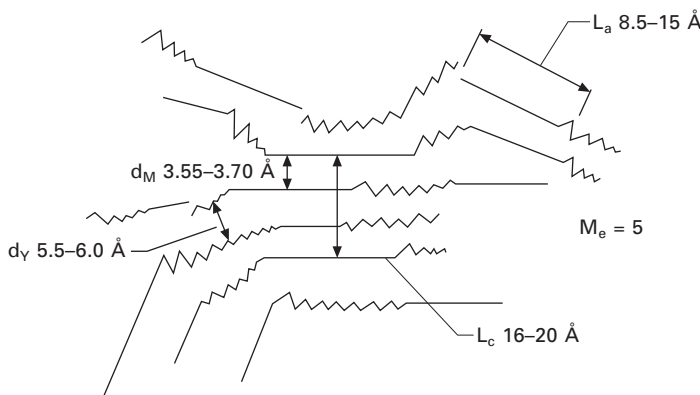
Trace quantities of metals such as nickel, iron, vanadium, calcium, magnesium and chromium are also found in bitumen (Atherton *et al.*, 1987).

Chemically, asphaltenes are multilayer systems containing a great variety of building blocks. Initially, Nellensteyn in 1933 proposed that asphaltenes contained a microcrystalline graphitic-type nucleus (Nellensteyn, 1933), but in 1940 Pfeiffer and Saal suggested that asphaltenes were high molecular

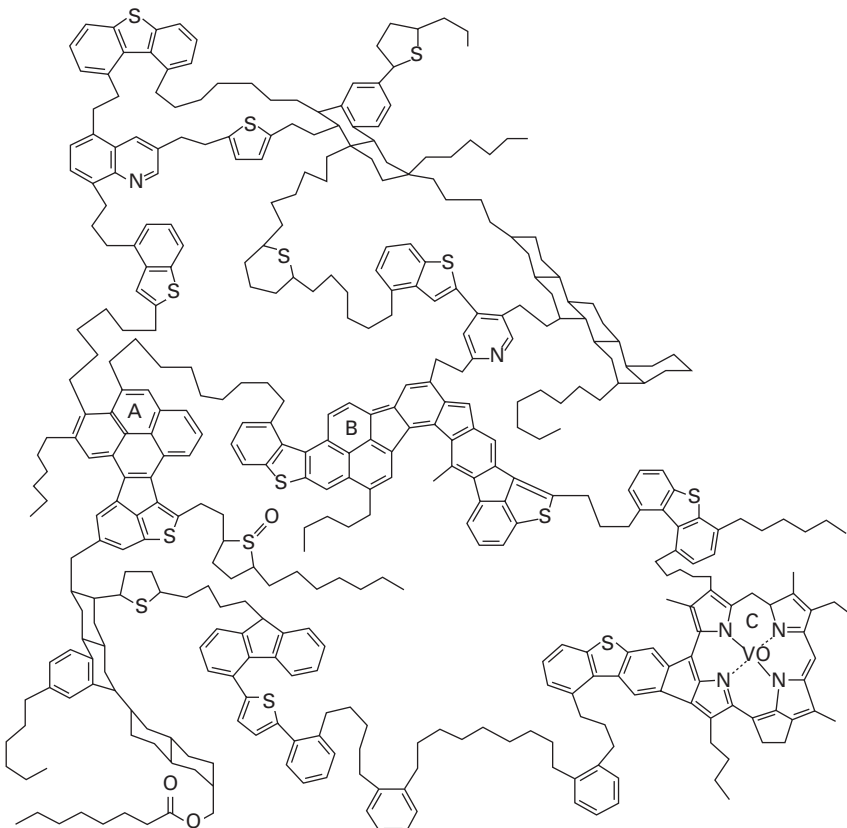
weight hydrocarbons of an aromatic character (Pfeiffer and Saal, 1940). Exhaustive studies by Yen and co-workers (Yen *et al.*, 1961, 1962; Yen and Erdman, 1962, 1963; Yen and Dickie, 1968), Strausz and co-workers (Ignasiak *et al.*, 1977; Rubenstein and Strausz, 1979; Payzant *et al.*, 1979, 1992; Rubenstein *et al.*, 1979) and others have identified many different chemical structures in asphaltenes. The average asphaltene molecule contains a flat sheet of condensed aromatic systems which may be interconnected by sulphur, ether, aliphatic chains or naphthenic ring linkages. Gaps and holes in the aromatic system with heterocyclic atoms coordinated by transition metals such as vanadium (V), nickel (Ni) and iron (Fe) are most likely caused by free radical attack. The flat sheets are associated by π - π interactions and are stacked one above the other with an average distance between sheets ranging from 3–4 Å, giving an overall height for a stack of 16–20 Å (see Figs 1.2 and 1.3).

Asphaltenes are organised as either randomly oriented particle aggregates or ordered micelles (Anderson and Speight, 1993). The polar groups are oriented towards the centre, which can be composed of water, silica or metals. The driving force of the polar groups assembled towards the centre originates from hydrogen bonding, charge transfer or salt formation. Asphaltenes are present as discrete or colloidally dispersed particles in the oily phase or resins. Resins are considered to be smaller analogues of asphaltenes with a much lower molecular weight. The resins contain aromatic compounds substituted with longer alkyls and a higher number of side chains attached to the rings than asphaltenes. The combination of the saturated and aromatic characteristics of the resins stabilises the colloidal structure of asphaltenes in the oily medium. Resins act as peptisers for asphaltenes.

Aromatics comprise the lowest molecular weight fraction and serve as the

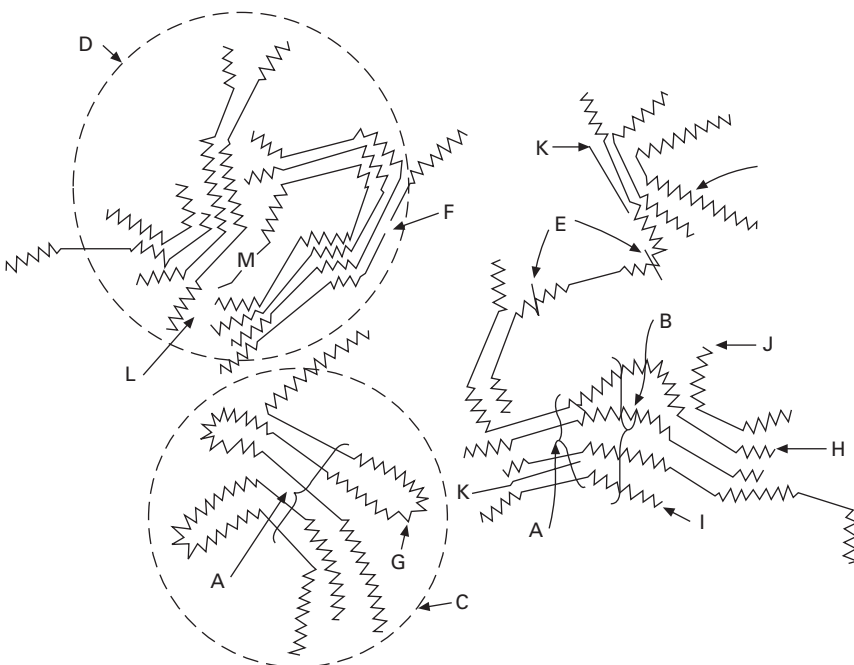


1.2 Cross-sectional view of asphaltene molecule; straight lines represent the edges of flat sheets of condensed aromatic rings (Yen *et al.*, 1961).



1.3 A hypothetical asphaltene molecule (Strausz *et al.*, 1992).

dispersion medium for the peptised asphaltenes. Structurally these aromatics consist mostly of naphthenic–aromatic nuclei with a greater proportion of the side chains than resins. Alkyl naphthenes predominate and straight-chain alkanes are rarely present. Paraffins (or saturates) comprise straight and branched aliphatic hydrocarbons. The average molecular weights of paraffins are similar to those of aromatics. Wax-like and non-waxy components are also found in saturates. As stated above, bitumen is a colloidal system containing four main fractions. The physical properties of bitumen are directly related to the quantity of asphaltenes, the size of the micelle structures, which in turn are dependent on the degree of adsorption of resins and the composition of the dispersion medium (i.e. aromatics and resins). Figure 1.4 shows a schematic diagram of a representative macrostructure of bitumen, illustrating the different possible physical and chemical entities that may be present in bitumen.



1.4 Macrostructure of asphalts. Straight lines denote aromatic constituents; zig-zag lines denote saturated constituents. A, crystallite; B, chain bundle; C, particle; D, micelle; E, weak link; F, gap and hole; G, intra-cluster; H, inter-cluster; I, resin; J, single layer; K, petroporphyrin; L, metal (Dickie and Yen, 1967).

The nature of the aromatic and aliphatic carbon and hydrogen in bitumen, pitch and asphaltenes has been investigated by nuclear magnetic resonance (NMR) spectroscopic methods. Various workers have used high resolution, solution-state ^{13}C and ^1H and solid state ^{13}C NMR to elucidate bitumen structure (Yen, 1991; Hamaguchi and Nishizawa, 1992; Cyr *et al.*, 1987; Giavarini and Vecchi, 1987; Axelson, 1987; Sobol *et al.*, 1985). Characterisation of asphaltene content in bitumen by gel permeation chromatography (GPC) (Acevedo *et al.*, 1985) and ultraviolet (UV) spectroscopy (Zerlia and Pinelli, 1992) and of all bitumen fractions using techniques such as vapour pressure osmometry (VPO) (Champagne *et al.*, 1985), freezing point depression (FPD) (Champagne *et al.*, 1985) and gas chromatography–mass spectrometry (GC–MS) yields useful information in determining the average structure of bitumen. Masson and co-workers have used modulated differential scanning calorimetry to analyse bitumen microstructure (Masson and Polomark, 2001; Masson *et al.*, 2002). The relative amounts of the four general fractions in bitumen can be determined from an Iatroscan (TLC/FID): see Chapter 3 for further detail on this method. The wax content (i.e. the short chain aliphatic

component) in bitumen can be determined from ISO 10512 (1983), but Jain has proposed a more accurate analytical test procedure, accurate to $\pm 2\%$ (Jain, 1989). The metals present in trace amounts in bitumen/asphaltenes, typically vanadium, nickel and iron, have been studied by electron nuclear double resonance (ENDOR) spectroscopy (Yen *et al.*, 1970). Other substances such as naturally occurring interfacial agents including inorganic salts of long chain carboxylic acids, alcohols, mercaptans, acid-bearing molecules, and other metallochelates or complexes such as porphyrins, are concentrated in trace amounts in asphaltene and resin fractions (Yen, 1981). These substances have an important influence on the properties of bitumen. It has been demonstrated that the rheology of bitumen is strongly dependent on the relative amounts of the four main components present in the bitumen and in particular the asphaltene content (Simpson *et al.*, 1961). Neumann *et al.* studied the rheology of the colloidal structure of bitumen and have shown that rheological properties are concentration dependent (Neumann and Rahimian, 1992).

As mentioned above, the two main advantageous properties of bitumen are its adhesiveness and waterproofing character. The loss of adhesion between a bitumen binder and minerals results in, for example, road failure. Khudyakova *et al.* investigated the chemical nature of the adhesiveness of bitumen and concluded that bitumen–mineral adhesiveness is primarily determined by the chemical composition of the dispersion medium (i.e. resins, aromatics and saturates), and by the concentration of the polar compounds capable of forming bonds with acid-based minerals which are not destroyed by water (Khudyakova *et al.*, 1989). Nowell and Powell (1991) and Evans *et al.* (1993) used heat-of-immersion calorimetry to study the chemical factors influencing bitumen–mineral adhesion and the determination of the strength of the chemical bond formed between bitumen and minerals, respectively. Nowell *et al.* concluded that the presence of acidic and basic groups in bitumen promotes bonding between bitumen and filler. Evans *et al.* concluded that the mechanism believed to be most significant in bitumen–mineral adhesion is catalytic oxidation. The cations present in minerals are believed to be able to catalyse bitumen oxidation and the ease with which bitumen can be oxidised is directly proportional to bitumen–mineral interactions. It is also thought that trace metals present in the bitumen (e.g. V, Ni, Fe) can promote oxidation. Adhesion agents such as alkyl propylene diamines have been added to bitumen–mineral mixes to prevent bond separation, particularly in wet conditions. Donbavand has used thermogravimetry (TGA) to detect and identify adhesion agents in bitumen mixes (Donbavand, 1984).

Further and more extensive detail on the colloidal structure of bitumen and the properties of bitumen can be obtained from the review by Lesueur (Lesueur, 2009).

1.2 Polymer modified bitumen

The concept of blending, mixing or alloying two or more materials to form a single product with different physical properties to those of the constituent materials is not new. The mechanical, electrical, chemical and many other properties are determined by the resultant phase behaviour. For example, copper and zinc form a single phase called brass which is mechanically superior to either constituent alone. Polymer blends or polyblends are physical mixtures of structurally different homo- or copolymers. Bates (1991) and Paul and Barlow (1980) have reviewed polymer–polymer phase behaviour and polymer–polymer miscibility, respectively. Homogeneity in mixtures depends on the heat and entropy of mixing. The state of miscibility of any mixture is governed by the free energy of mixing, ΔG_{mix} , given by:

$$\Delta G_{\text{mix}} = \Delta H_{\text{mix}} - T\Delta S_{\text{mix}} \quad 1.1$$

where, ΔH_{mix} is the enthalpy on mixing, ΔS_{mix} is the entropy change on mixing and T is absolute temperature. The necessary conditions for miscibility are that $G_{\text{mix}} < 0$ and

$$\frac{\delta^2 G}{\delta^2 \emptyset} > 0$$

where \emptyset is the mole fraction of one component. In equation 1.1 the combinatorial entropy on mixing depends on the number of molecules per unit volume according to:

$$\Delta S_{\text{mix}}/RT = n_1 \ln \emptyset_1 + n_2 \ln \emptyset_2 \quad 1.2$$

which decreases with increasing molecular size. This means that when the components in the mixture are polymers (i.e. large molecules), entropy change per unit volume will be extremely small and the heat of mixing (ΔH_{mix}) alone will determine the homogeneity of the mixture. Heat of mixing arises to a large extent from the energies of association (e.g. hydrogen bonding) between neighbouring polymer chains. In general, polymers prove to be immiscible with each other, one exception being blends of polystyrene and polyphenylene oxide. Addition of compatibilising agents/polymers or control of phase morphology during processing can aid miscibility.

Bitumen is an important low-cost thermoplastic which finds many applications as a building and engineering material; however, bitumen has poor mechanical properties as it is hard and brittle in cold environments and soft and fluid in hot environments (Whiteoak, 1990). One of the many ways of toughening bitumen is by blending it with synthetic polymers, which can be either virgin or waste polymer. A large number of polymers have been studied for bitumen modification, including polyethylenes (Jew *et al.*, 1986; Bahl *et al.*, 1993; Fawcett *et al.*, 1999a), polyolefins (Morrison *et al.*, 1994; Fawcett and McNally, 2000a; Fawcett *et al.*, 1999b; Yousefi, 2003), most

extensively styrene homopolymers and copolymers (Airey, 2004; Bahl *et al.*, 1993; Blanco *et al.*, 1995; van Beem and Brasser, 1973; Bull and Vonk, 1988, 1992; Lu and Isacsson, 2001; Varma *et al.*, 2002; Vonk and Bull, 1989; Heimerikx, 1993; van Gooswilligen and Vonk, 1986; Fawcett and McNally, 2001a, 2003; Wang *et al.*, 2007; González-Águirre *et al.*, 2009), ionomers (Engel *et al.*, 1991), ethylene vinyl acetate and acrylic copolymers (Denning and Carswell, 1981; Fawcett and McNally, 2001b), rubbers (Fawcett and McNally, 2000b), polymer blends (Fawcett *et al.*, 2002; García-Morales *et al.*, 2007) and many other polymeric materials (Boutevin *et al.*, 1989; Fawcett *et al.*, 2000). More recently, there has been intense interest in the use of recycled or scrap plastic, including tyre rubber crumb to modify bitumen (Singh *et al.*, 2003; Ho *et al.*, 2006; Fang *et al.*, 2008; Fuentes-Audén *et al.*, 2008; Cao *et al.*, 2008; Navarro *et al.*, 2010; Naskar *et al.*, 2010).

Polyethylene (PE) has proven to be an attractive modifier for bitumen finding applications in both the road and roofing trades. This is for several reasons but primarily because of its cost relative to other virgin materials. However, the increasing price of virgin polymers has initiated work to investigate the blending of scrap and recycled polymers with bitumen. Tappeiner and Male as long ago as 1993 found that the addition of recycled low density polyethylene (LDPE) to bitumen was more advantageous than adding virgin LDPE alone (Tappeiner and Male, 1993). Other benefits included greater tensile strength, increased impact properties, greater fatigue resistance and a lowering of the brittle temperature. Moreover, addition of up to 20 wt% of other polymers with recycled LDPE in bitumen has no adverse effects on the properties of the modified bitumen.

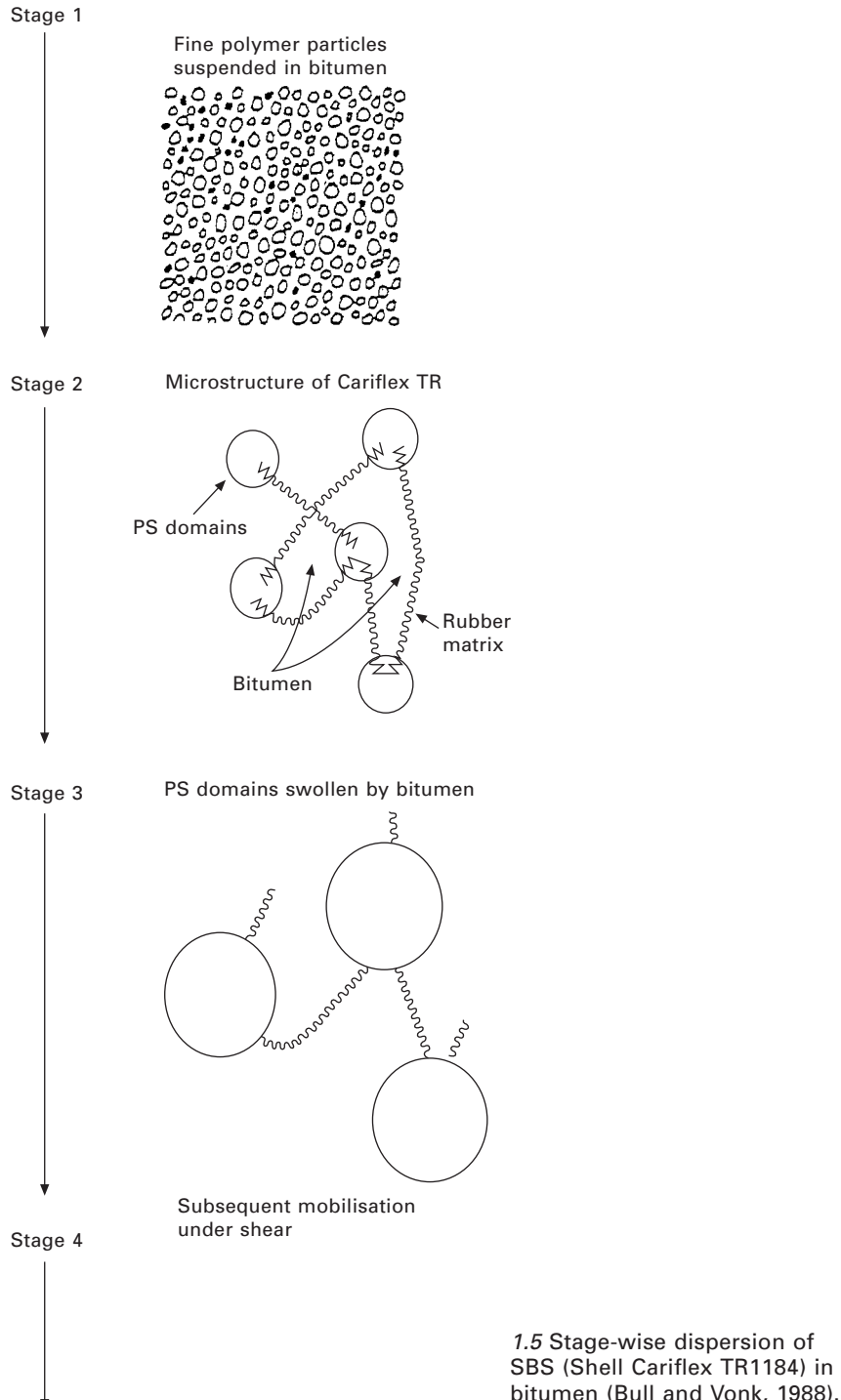
The dispersion of polyethylene in bitumen is readily accomplished at temperatures between 140°C and 180°C under high shear conditions. The molten polyethylene particles gradually absorb the aliphatic components of the bitumen and partially dissolve to form a highly viscous and elastic dispersion. The softening point also increases, particularly at higher loadings of polyethylene. Jew *et al.* have shown that polyethylene modified bitumen dispersions (for paving applications) can be stabilised and their performance influenced by the conditions of mixing and the presence of dispersing agents such as block copolymers (e.g. styrene–butadiene–styrene, SBS) (Jew *et al.*, 1986). The presence of a block copolymer was shown to further contribute to the strength, elongation and toughness but slightly reduce the modulus. One disadvantage of PE modified bitumen is that polyethylene particles tend to float to the surface of liquid bitumen where they coalesce into a highly viscous non-dispersive layer (i.e. no blend is formed, just a physical dispersion). More recently, Polacco and co-workers reported the mechanical and rheological properties of a range of functionalised and non-functionalised polyethylenes and highlighted the marked differences in polymer–bitumen interactions observed (Polacco *et al.*, 2005).

Use of thermoplastic elastomers for bitumen modification continues to grow rapidly. These materials behave as linear polymers during hot processing and as vulcanised rubbers at ambient temperatures. The general types of rubbers used to modify bitumen properties include styrene–butadiene rubber (SBR), crosslinked polymers, thermoplastic rubbers, e.g. styrene–butadiene–styrene (SBS) (Navarro *et al.*, 2010; Wen *et al.*, 2002; Jin *et al.*, 2002; Varma *et al.*, 2002; Airey, 2004) and styrene–isoprene–styrene (SIS) and olefinic rubbers. Bahl *et al.* proposed that when a thermoplastic elastomer of styrenic block-type copolymer is added to hot bitumen, the latter immediately starts to penetrate into the polymer particles whereon the styrene domain of the rubber becomes solvated and swollen (Bahl *et al.*, 1993). Under the influence of shear, the swollen polymer becomes mobile and disperses in the bitumen (see Fig. 1.5). Bull *et al.* have postulated that the polystyrene blocks of SBS agglomerate into micro-domains which form the physical crosslinks for the polybutadiene mid-blocks to give an elastomeric network (Bull and Vonk, 1988). Vonk and Bull investigated the phase morphology of SBS/bitumen blends and showed how the bitumen composition in two-phase blends with SBS elastomers affects blend properties and the composition and properties of each phase (Vonk and Bull, 1989). They concluded among many things that:

1. Bitumen composition has a major effect on blend properties.
2. Blend properties are largely governed by those of the continuous phase.
3. Blends of two elastomers with a bitumen may form a single network if their molecular weights are similar.
4. Bitumen of high aromaticity and low molecular weight gives blends with low softening points.

Rozeveld and co-workers have also studied the network morphology of a number of styrene-based rubber and elastomer–bitumen blends (Rozeveld *et al.*, 1997). The authors proposed a network of fibrils consisting of high molecular weight asphaltene/resin micelles. Atomic force microscopy and confocal laser scanning microscopy have also proved useful in elucidating the microstructure of bitumen and polymer modified bitumen (Jäger *et al.*, 2004; Loeber *et al.*, 1996; Forbes *et al.*, 2001).

Heimerikx demonstrated that bitumen composition and SBS morphology have a significant effect on the properties of SBS modified bitumen (Heimerikx, 1993). SBS-modified bitumen has found many applications, mainly in the road and roofing industries, with a typical blend consisting of between 3% and 15% by weight of SBS. Bull and Vonk (1992) and van Gooswilligen and Vonk (1986) studied such materials for road and roofing applications. Valkering and Vonk have shown that modification of bitumen with a linear SBS copolymer leads to significant changes in rheological properties of



the bitumen even at concentrations as low as 3 wt% (Valkering and Vonk, 1992). These advantageous changes are attributed to the development of a polymer-rich phase that may be regarded as a heavily extended polymer.

The rheological and viscoelastic properties of a range of polymer modified bitumens have been studied extensively, including but not limited to SBS, EVA, PP, PE and PE blends – see González *et al.*, 2002; Wen *et al.*, 2002; Becker *et al.*, 2003; Rojo *et al.*, 2004; García-Morales *et al.*, 2004a, 2004b; Polacco *et al.*, 2004a, 2004b; Yeh *et al.*, 2005; Pérez-Lepe *et al.*, 2005 and references therein.

The performance of SBS modified bitumen when applied to roads and roofing has also been a topic of intense investigation. Vonk *et al.*, for example, studied the ageing resistance of SBS modified bitumen road binders (Vonk *et al.*, 1993). The improved properties (e.g. better low temperature flexibility, resistance to permanent deformation and fretting resistance) obtained with SBS modification were well maintained under the ageing tests carried out in comparison with styrene–ethylene+butylene–styrene, S(EB)S, and EVA modified bitumen. However, excess heating of SBS modified bitumen may lead to gelation and as such S(EB)S modified bitumen may be more advantageous for applications where extreme heat conditions prevail. Ageing of polymer modified bitumen is of immense technical and industrial importance and continues to be a topic of intense research, not just for SBS modified bitumen (Airey, 2004) but for a range of polymer modified bitumens (Lu and Isacsson, 2000).

Blends of polymers, including SBS, with bitumen are thermodynamically unstable and phase separation occurs at high temperatures, resulting in poorer properties of the blend. Much work has concentrated on trying to improve the thermal stability of these blends. One proposal is based on the formation of reversible ionic interactions between the bitumen and SBS (Engel *et al.*, 1991). The bitumen and SBS were chemically modified by grafting on carboxylic acid groups, and mixed, and finally the acid groups were neutralised with zinc acetate dihydrate. No macroscopic phase separation was observed in the resultant blends when examined under an optical microscope ($\times 200$). More recently, researchers have focused on the use of reactive polymers to modify the morphology, rheological properties and storage stability of bitumen. In particular, low molecular weight isocyanates have been shown to react with the asphaltene fraction and alter the mechanical and other properties of bitumen, although the composition and source of the bitumen will play a major role in the extent of these reactions (Martín-Alfonso *et al.*, 2008; Navarro *et al.*, 2007; Izquierdo *et al.*, 2011). Jun and co-workers have also shown that the epoxy terminal group on glycidyl methacrylate functionalised LDPE can react with carboxylic acid and anhydride moieties in asphaltenes to form crosslinks. The resultant

modified bitumen has improved rutting resistance and storage stability (Jun *et al.*, 2008).

Morrison *et al.* blended different chlorinated polyethylenes with bitumen and tried to improve the compatibility between the two components by adding small quantities of Friedel–Crafts catalysts, typically anhydrous aluminium trichloride (Morrison *et al.*, 1994). The catalyst is added to induce a reaction between the polymer and the bitumen phase, as aromatic alkyl substituents and allylic hydrogens are susceptible to both radical induced and electrophilic substitution reactions. Improved compatibility between the chlorinated polyethylenes and the bitumen was observed, resulting in a significant enhancement of both low and high temperature properties. Boutevin *et al.* reviewed the patent literature on bitumen–polymer blends applied to roads and public constructions (Boutevin *et al.*, 1989). Both thermoplastic and thermosetting polymers have been used and significant improvements in properties are observed, particularly increase in softening point and toughness, improved low temperature flexibility and wettability. The properties of polymer–bitumen blends may be improved further by chemical modification of either the polymer (chlorination, sulphonation) or the bitumen, by grafting the polymer onto the bitumen. The main result of such modification is improved compatibility between polymer and bitumen. Enhanced mechanical properties and elongation at break are obtained when thermosets are blended with bitumen. Epoxides and polyurethane resins when blended with bitumen have found widespread use, particularly in anti-corrosion paints. More recently, modification of bitumen itself (Jahromi and Khodaii, 2009; You *et al.*, 2011) and polymer–bitumen blends has been attempted using layered silicates (nanoclays). Ternary blends of polymer, bitumen and nanoclay can be prepared using conventional polymer processing techniques. Sureshkumar and co-workers showed that nanoclay can act as a compatibiliser for EVA–bitumen blends and influence the rheological behaviour of these systems (Sureshkumar *et al.*, 2010). Similarly, Galooyak *et al.* reported a further improvement in storage stability when a nanoclay was added to a SBS–bitumen blend (Galooyak *et al.*, 2010).

The rheological behaviour and viscoelastic properties of bitumen and polymer-modified bitumen are very important both from a practical application perspective but also in understanding fundamentally the effect of polymer addition on mechanical properties, bitumen morphology and polymer–bitumen interactions. The rheology of several polymer modified bitumen systems has now been studied in detail. In particular, Polacco *et al.* (2006) described the relationship between polymer architecture and non-linear viscoelastic behaviour of modified asphalts. Further work by Polacco *et al.* (2006) showed eloquently the usefulness of rheology in the determination of the formation of a crosslinked network.

1.3 Introduction to *Polymer modified bitumen: properties and characterisation*

Bitumen has been used for thousands of years and its importance as a valued engineering material continues to increase. The interest in modification of bitumen using polymers, whether virgin, scrap or polymer blends, is intense. The last two decades in particular have seen an increase in the number of academic groups studying polymer-modified bitumen and correspondingly the peer-reviewed literature in the field has increased. Initially, studies on polymer modified bitumen focused more on engineering and empirical measurements, e.g. ageing and softening point. However, in recent years a plethora of techniques have been employed in the study of the effect of addition of polymers on a range of bitumen properties, polymer-bitumen morphology and polymer-bitumen interactions. Most textbooks in the field tend to be focused solely on bitumen itself with typically a single chapter given over to polymer modified bitumen. Therefore, the stimulus for this book was to bring together the main researchers over the last two to three decades to contribute to a book, the first of its type, which would provide a comprehensive and in-depth coverage of the science and technology of polymer modified bitumen.

To this end, the book is divided into two parts. Part I (Chapters 2–6) focuses on the preparation and properties of a range of polymer modified bitumens. In Chapter 2, Lesueur describes the formulation, manufacture and properties of polymer modified bitumen emulsions (PMBEs). Most notably, the author demonstrates how PMBEs show improved rheological properties of the residue after breaking when compared to unmodified bitumen emulsions. This in turn results in higher softening points and modulus at high operating temperatures (in the 40–50°C range), which in turn imparts higher binder cohesion that generates a better resistance to loading. In Chapter 3, Partal and Martínez-Boza describe the modification of bitumen using isocyanate-based reactive polymers. The authors report a series of chemical reactions describing the *in situ* formation of polyurethane/urea-based polymers in the bituminous matrix to explain the change in bitumen properties obtained. In Chapter 4, Gawel and co-workers describe the methods used to recycle waste rubber from tyres and the methods employed in the modification of bitumen with crumb rubber. The authors describe rubber-bitumen interactions in terms of a diffusion phenomenon, in which rubber particles absorb bitumen components of similar solubility parameters and swell. In Chapter 5, Navarro Domínguez and García-Morales describe the use of waste polymers, both thermoplastics and thermosets alone and thermoplastic/thermoset blends, to modify bitumen. In particular, the authors report the importance of processing conditions, including mixer type, shear rate and temperature on the thermomechanical properties of the resultant waste polymer modified bitumen blend. Finally in

Part I, in Chapter 6 Tapkın and co-workers describe the use of polypropylene fibres to improve the fatigue life of bituminous concrete. Interestingly, the authors also report the use of artificial neural networks to predict the result of Marshall tests on polypropylene modified dense bituminous mixtures.

Part II (Chapters 7–12) addresses the characterisation and properties of polymer modified bitumen. In Chapter 7, Gallegos and García-Morales provide an excellent introduction to the fundamentals of rheology and its application to the study of polymer modified bitumen. The authors then eloquently show the relationship between rheological properties and the rutting and fatigue characteristics of polymer modified bitumen. In Chapter 8, Airey reports the rheological behaviour of polymer modified bitumen using both conventional test methods and advanced rheology measurements. The author also describes the effect of ageing on the rheological properties of both plastomer and elastomer modified bitumen. In Chapter 9, Yu and co-workers start by detailing the main reasons and mechanisms by which polymer modified bitumens age. The authors describe five main methods used to simulate ageing of polymer modified bitumen and discuss methods for improving its ageing resistance. Most relevant and interesting, in Chapter 10, Masson and co-workers report the outcome of 10 years of actual weathering of 12 bituminous sealants containing styrene-based thermoplastic elastomers. The authors used extensive physico-chemical analysis to elucidate the mechanisms by which styrene–butadiene block copolymers degrade, and they discuss the suitability of accelerated ageing tests to assess natural weathering of elastomer–bitumen sealants. In Chapter 11, Polacco and co-workers address the problem of the solubility of bituminous binders in fuels and oil-based products. The authors describe how to measure fuel solubility and the effect of polymer modifiers on bitumen solubility in kerosene, and propose a mechanism based on selective swelling to explain the improvements in fuel resistance obtained. Finally, in Chapter 12, Mouillet and co-workers describe the novel use of Fourier transform infrared spectroscopy to investigate the ageing of SBS and EVA modified bitumen. The authors show clearly the role of oxidation of the bitumen phase in the ageing process and the affinity the polymer has for oxidised asphaltene molecules which in turn affect polymer swelling.

1.4 References

Abraham H (1945), 'Asphalts and allied substances, their occurrence, modes of production, uses in the arts of methods of testing', New York, Van Nostrand.

Acevedo S, Escobar G, Gutiérrez L B and D'Aquino J (1985), 'Synthesis and isolation of octylated asphaltene standards for calibration of g.p.c. columns and determination of asphaltene molecular weight', *Fuel*, 64, 1077–1079.

Airey G D (2004), 'Styrene butadiene styrene polymer modification of road bitumens', *J. Mater. Sci.*, 39, 951–959.

Anderson S I and Speight J G (1993), 'Observations on the critical micelle concentration of asphaltenes', *Fuel*, 72, 1343–1344.

Atherton N M, Fairhurst S A and Hewson G J (1987), 'ENDOR spectra of vanadyl complexes in asphaltenes', *Magn. Res. Chem.*, 25, 829–830.

Axelson D E (1987), 'Solid state ^{13}C nuclear magnetic resonance of heavy oil/bitumen-derived solids', *Fuel*, 66, 40–43.

Bahl J S, Atheya N and Singh H (1993), 'Bitumen properties modification using organic polymers', *Erdöl Kohle. Erdgas. Petrochem.*, 46, 22–25.

Bates F S (1991), 'Polymer–polymer phase behavior', *Science*, 251, 898–905.

Becker Y, Müller A J and Rodriguez Y (2003), 'Use of rheological compatibility criteria to study SBS modified asphalts', *J. Appl. Polym. Sci.*, 90, 1772–1782.

Blanco R, Rodriguez R, Garcia-Gardu M and Castano V M (1995), 'Morphology and tensile properties of styrene–butadiene copolymer reinforced asphalt', *J. Appl. Polym. Sci.*, 56, 57–64.

Boutevin B, Pietrasanta Y and Robin J J (1989), 'Bitumen–polymer blends for coatings applied to roads and public constructions', *Prog. Org. Coat.*, 17, 221–249.

Bull A L and Vonk W C (1988), 'Thermoplastic rubber–bitumen blends for roof and road', *Shell Tech. Manual TR8.15*.

Bull A L and Vonk W C (1992), 'Thermoplastic rubber–bitumen blends for roof and road applications', *Shell Tech. Manual TR8.15*.

Cao D, Cao Y, Gao Y, Guo W and Wu C (2008), 'Studies on the structure, morphology and thermal properties of HDPE/petroleum resin blends', *E-Polymers*, 123.

Champagne P J, Manolakin E and Ternan M (1985), 'Molecular weight distribution of Athabasca bitumen', *Fuel*, 64, 423–425.

Chirife J, Favetto G, Ballesteros S and Kitic D (1991), 'Mummification in ancient Egypt: an old example of tissue preservation by hurdle technology', *Lebensmittel–Wissenschaft und Technologie*, 24, 9–11.

Cyr N, McIntyre D D, Toth G and Strausz O P (1987), 'Hydrocarbon structural group analysis of Athabasca asphaltene and its g.p.c. fractions by ^{13}C n.m.r.', *Fuel*, 66, 1709–1714.

Denning J H and Carswell J (1981), 'Improvements in rolled asphalt surfacing by the addition of organic polymers', Department of the Environment, Department of Transport, TRRL Report 989, ISSN 0305–1293, Transport and Road Research Laboratory, Crowthorne, UK.

Dickie J P and Yen T F (1967), 'Macrostructures of the asphaltic fractions by various instrumental methods', *Anal. Chem.*, 39, 1847–1852.

Donbavand J (1984), 'The use of thermogravimetry to detect and identify adhesion agents in bitumen', *Thermochim. Acta*, 79, 161–169.

Engel R, Vidal A, Papirer E and Grosmangin J (1991), 'Synthesis and thermal stability of bitumen–polymer ionomers', *J. Appl. Polym. Sci.*, 43, 227–236.

Evans M B, Nowell D V and Powell M W (1993), 'Determination of adhesion in bitumen–mineral systems by heat-of-immersion calorimetry. II. Correlation of chemical properties with adhesion', *J. Therm. Anal.*, 40, 121–131.

Fang C, Li T, Zhang Z and Jing D (2008), 'Modification of asphalt by packaging waste-polyethylene', *Polym. Compos.*, 29, 500–505.

Fawcett A H and McNally T (2000a), 'A dynamic mechanical and thermal analysis study of various rubber–bitumen blends', *J. Appl. Polym. Sci.*, 76, 586–601.

Fawcett A H and McNally T (2000b), 'Blends of bitumen with various polyolefins', *Polymer*, 41, 5315–5326.

Fawcett A H and McNally T (2001a), 'Blends of bitumen with polymers having a styrene component', *Polym. Eng. Sci.*, 41, 1251–1264.

Fawcett A H and McNally T (2001b), 'Studies on blends of acetate and acrylic functional polymers with bitumen', *Macromol. Mater. Eng.*, 286, 126–137.

Fawcett A H and McNally T (2003), 'Polystyrene and asphaltene micelles within blends with a bitumen of a SBS block copolymer and styrene and butadiene homopolymers', *Colloid Polym. Sci.*, 281, 203–213.

Fawcett A H, McNally T and McNally G M (1999a), 'Modification of a bitumen with various polymers for use in built-up roofing membranes', *J. Elast. Plast.*, 31, 334–352.

Fawcett A H, McNally T, McNally G M, Andrews F and Clarke J (1999b), 'Blends of bitumen with polyethylenes', *Polymer*, 40, 6337–6349.

Fawcett A H, McNally T and McNally G M (2000), 'Blends of bitumen with polar polymers', *Plast. Rubbers Compos.*, 29, 385–390.

Fawcett A H, McNally T and McNally G M (2002), 'An attempt at engineering the bulk properties of blends of a bitumen with polymers', *Adv. Polym. Technol.*, 21, 275–286.

Forbes A, Haverkamp R G, Robertson T, Bryant J and Bearsley S (2001), 'Studies of the microstructure of polymer-modified bitumen emulsions using confocal laser scanning microscopy', *J. Microsc.*, 204, 252–257.

Fuentes-Audén C, Sandoval J A, Jerez A, Navarro F J, Martínez-Boza F J, Partal P and Gallegos C (2008), 'Evaluation of thermal and mechanical properties of recycled polyethylene modified bitumen', *Polym. Testing*, 27, 1005–1012.

Galooyak S S, Dabir B, Nazarbeygi A E and Moeini A (2010), 'Rheological properties and storage stability of bitumen/SBS/montmorillonite composites', *Constr. Build Mater.*, 24, 300–307.

García-Morales M, Partal P, Navarro F J, Martínez-Boza F J and Gallegos C (2004a), 'Linear viscoelasticity of recycled EVA-modified bitumens', *Energy Fuels*, 18, 357–364.

García-Morales M, Partal P, Navarro F J, Martínez-Boza F J, Gallegos C, González N, González O and Muñoz M E (2004b), 'Viscous properties and microstructure of recycled EVA modified bitumen', *Fuel*, 83, 31–38.

García-Morales M, Partal P, Navarro F J, Martínez-Boza F J and Gallegos C (2007), 'Processing, rheology, and storage stability of recycled EVA/LDPE modified bitumen', *Polym. Eng. Sci.*, 47, 181–191.

Giavarini C and Vecchi C (1987), 'Characterization of visbreaker bitumens by n.m.r. spectroscopy', *Fuel*, 66, 868–869.

González O, Peña J J, Muñoz M E, Santamaría A, Pérez-Lepe A, Martínez-Boza F and Gallegos C (2002), 'Rheological techniques as a tool to analyse polymer–bitumen interactions: Bitumen modified with polyethylenes and polyethylene-based blends', *Energy Fuels*, 16, 1256–1263.

González-Águirre P, Medina-Torres L, Schrauwen C, Fonlex C, Pia F and Herrera-Nájera R (2009), 'Morphology and rheological behaviour of maltene–polymer blends. I. Effect of partial hydrogenation of poly(styrene-block-butadiene-block-styrene-block-) type copolymers', *J. Appl. Polym. Sci.*, 112, 1330–1344.

Hamaguchi M and Nishizawa T (1992), 'Quantitative analysis of aromatic carbon types in pitch by fused-state ^{13}C n.m.r. spectroscopy', *Fuel*, 71, 747–750.

Heimerikx G W J (1993), 'Styrene block copolymers for bitumen based roofing felt', *Eighth Brazilian Symposium of Waterproofing*, São Paulo, Brazil, 26–29 September.

Ho S, Church R, Klassen K, Law B, MacLeod D and Zanzotto D (2006), 'Study of recycled polyethylene materials as asphalt modifiers', *Can. J. Civil Eng.*, 33, 968–981.

Ignasiak T M, Kemp-Jones A V and Strausz O P (1977), 'The molecular structure of Athabasca asphaltene. Cleavage of the carbon–sulfur bonds by radical ion electron transfer reactions', *J. Org. Chem.*, 42, 312–320.

Izquierdo M A, Navarro F J, Martínez-Boza F J and Gallegos C (2011), 'Novel stable MDI isocyanate-based bituminous foams', *Fuel*, 90, 681–688.

Jäger A, Lackner R, Eisenmenger-Sittner Ch and Blab R (2004), 'Identification of four material phases in bitumen by atomic force microscopy', *Road Materials and Pavement Design*, 9–24.

Jahromi S G and Khodaii A (2009), 'Effects of nanoclay on rheological properties of bitumen binder', *Constr. Build Mater.*, 23, 2894–2904.

Jain P K (1989), 'A method for determination of wax content in bitumen', *Research & Industry*, 34, 134–136.

Jew P, Shimizu J A, Svazic M and Woodhams R T (1986), 'Polyethylene-modified bitumen for paving applications', *J. Appl. Polym. Sci.*, 31, 2685–2704.

Jin H, Gao G, Zhang Y, Zhang Yi, Sun K and Fan Y (2002), 'Improved properties of polystyrene modified asphalt through dynamic vulcanisation', *Polym. Testing*, 21, 633–640.

Jun L, Yuxia Z and Yuzhen Z (2008), 'The research of GMA-g-LDPE modified Qinhuangdao bitumen', *Constr. Build Mater.*, 22, 1067–1073.

Khudyakova T S, Strizhev E F, Mashkova I A and Sychev M M (1989), 'Adhesiveness of bitumen as a function of its chemical composition and structure', *Zh. Prikl. Khim.*, 62, 1849–1853.

Lesueur D (2009), 'The colloidal structure of bitumen: Consequences on the rheology and on the mechanisms of bitumen modification', *Adv. Colloid Inter. Sci.*, 146, 42–82.

Loeber L, Sutton O, Morel J, Valleton J-M and Muller G (1996), 'New direct observations of asphalt and asphalt binders by scanning electron microscopy and atomic force microscopy', *J. Microsc.*, 182, 32–39.

Lu X and Isacsson U (2000), 'Artificial aging of polymer modified bitumens', *J. Appl. Polym. Sci.*, 76, 1811–1824.

Lu X and Isacsson U (2001), 'Modification of road bitumens with thermoplastic polymers', *Polym. Testing*, 20, 77–86.

Martín-Alfonso M J, Partal P, Navarro F J, García-Morales M and Gallegos C (2008), 'Use of a MDI-functionalized reactive polymer for the manufacture of modified bitumen with enhanced properties for roofing applications', *Eur. Polym. J.*, 44, 1451–1461.

Masson J-F and Polomark G M (2001), 'Bitumen microstructure by modulated differential scanning calorimetry', *Thermochim. Acta*, 374, 105–114.

Masson J-F, Polomark G M and Collins P (2002), 'Time-dependent microstructure of bitumen and its fraction by modulated differential scanning calorimetry', *Energy Fuels*, 16, 470–476.

Morrison G R, Lee J K and Hesp S A M (1994), 'Chlorinated polyolefins for asphalt binder modification', *J. Appl. Polym. Sci.*, 54, 231–240.

Naskar M, Chaki T K and Reddy K S (2010), 'Effect of waste plastic as modifier on thermal stability and degradation of kinetics of bitumen/waste plastics blend', *Thermochim. Acta*, 509, 128–134.

Navarro F J, Partal P, García-Morales M, Martínez-Boza F J and Gallegos C (2007), 'Bitumen modification with a low-molecular-weight reactive isocyanate-terminated polymer', *Fuel*, 86, 2291–2299.

Navarro F J, Partal P, Martínez-Boza F J and Gallegos C (2010), 'Novel recycled

polyethylene/ground tire rubber/bitumen blends for use in roofing applications: Thermo-mechanical properties', *Polym. Testing*, 29, 588–595.

Nellensteyn F J (1933), 'Theoretical aspect of the relation of bitumen to solid matter', in *Proc. World Petroleum Congress*, 2, 616–618.

Neumann H J and Rahimian I (1992), 'Zur Rheologie des kolloidalen Systems Bitumen', *Erdöl Kohle. Erdgas. Petrochem.*, 1, 41–44.

Nowell D V and Powell M W (1991), 'Determination of adhesion in bitumen–mineral systems by heat-of-immersion calorimetry. I. The effect of crude oil sources on adhesive performance', *J. Therm. Anal.*, 37, 2109–2124.

Paul D R and Barlow J W (1980), 'Polymer blends', *J. Macromol. Sci., Rev. Macromol. Chem.*, 18, 109–168.

Payzant J D, Rubenstein I, Hogg A M and Strausz O P (1979), 'Field-ionization mass spectrometry: application to geochemical analysis', *Geochim. Cosmochim. Acta*, 43, 1187–1193.

Pérez-Lepe A, Martínez-Boza F J and Gallegos C (2005), 'Influence of polymer concentration on the microstructure and rheological properties of high-density polyethylene (HDPE)-modified bitumen', *Energy Fuels*, 19, 1148–1152.

Pfeiffer J P and Saal R N J (1940), 'Asphaltic bitumen as colloid systems', *J. Phys. Chem.*, 44, 139–149.

Polacco G, Stastna J, Biondi D, Antonelli F, Vlachovicova Z and Zanzotto L (2004a), 'Rheology of asphalts modified with glycidylmethacrylate functionalized polymers', *J. Colloid Inter. Sci.*, 280, 366–373.

Polacco G, Stastna J, Biondi D, Antonelli F, Vlachovicova Z and Zanzotto L (2004b), 'Temporary networks in polymer-modified asphalts', *Polym. Eng. Sci.*, 44, 2185–2193.

Polacco G, Berlincioni S, Biondi D, Stastna J and Zanzotto L (2005), 'Asphalt modification with different polyethylene-based polymers', *Eur. Polym. J.*, 41, 2831–2844.

Polacco G, Stastna J, Biondi D and Zanzotto L (2006), 'Relation between polymer architecture and nonlinear viscoelastic behaviour of modified asphalts', *Curr. Opin. Colloid Inter. Sci.*, 11, 230–245.

Rojo E, Fernández M, Peña J J, Peña B, Muñoz M E and Santamaría A (2004), 'Rheological aspects of blends of metallocene-catalysed atactic polypropylene with bitumen', *Polym. Eng. Sci.*, 44, 1792–1799.

Rozeveld S J, Shin E E, Bhrake A, France L and Drzal L T (1997), 'Network morphology of straight and polymer modified asphalt cements', *Micros. Res. Technique*, 38, 529–543.

Rubenstein I and Strausz O P (1979), 'Thermal treatment of the Athabasca oil sand bitumen and its component parts', *Geochim. Cosmochim. Acta*, 43, 1887–1893.

Rubenstein I, Spykerelle C and Strausz O P (1979), 'Pyrolysis of asphaltenes: a source of geochemical information', *Geochim. Cosmochim. Acta*, 43, 1–6.

Simpson W C, Griffen R L and Miles T K (1961), 'Relationship of asphalt properties to chemical constitution', *J. Chem. Eng. Data*, 6, 426–429.

Singh B, Gupta M and Tarannum H (2003), 'Mastic of polymer-modified bitumen and poly(vinyl chloride) wastes', *J. Appl. Polym. Sci.*, 90, 1347–1356.

Sobol W T, Schreiner L J, Milijhovic L, Marcondes-Helene M E, Reeves L W and Pinter M W (1985), 'N.m.r. line shape-relaxation correlation analysis of bitumen and oil sands', *Fuel*, 64, 583–590.

Strausz O P, Mojelsky T W and Lown E M (1992), 'The molecular structure of asphaltene: an unfolding story', *Fuel*, 71, 1355–1363.

Sureshkumar M S, Filippi S, Polacco G, Kazatchkov I, Stastna J and Zanzotto L (2010), 'Internal structure and linear viscoelastic properties of EVA/asphalt nanocomposites', *Eur. Polym. J.*, 46, 621–633.

Tappeiner W J and Male A G (1993), 'Enhancement of asphalt concrete mixtures through the addition of recycled polyethylene', *Proceedings of the Annual Technical Meeting of the Society of Plastics Engineers* (ANTEC), 860–865.

Traxler R N (1936), 'The physical chemistry of asphaltic bitumen', *Chem. Rev.*, 19, 119–143.

Valkering C P and Vonk W C (1992), 'Cariflex TR in bitumen for asphalt mixes: improved elastic recovery and higher performance', *Shell Tech. Manual TR 8.23*.

Van Beem E J and Brasser P (1973), 'Bituminous binders of improved quality containing Cariflex thermoplastic rubbers', *J. Inst. Pet.*, 59, 91–97.

Van Gooswilligen G and Vonk W C (1986), 'The role of bitumen in blends with thermoplastic rubbers for roofing applications', *Shell Tech. Manual TR 8.16*.

Varma R, Takeichi H, Hall J E, Ozawa Y F and Kyu T (2002), 'Miscibility studies on blends of Kraton block copolymer and asphalt', *Polymer*, 43, 4667–4671.

Volke K (1993), 'Die Chemie der Mumifizierung im alten Ägypten', *Chemie in Unserer Zeit*, 27, 42–47.

Vonk W C and Bull A L (1989), 'Phase phenomena and concentration effects in blends of bitumen and Cariflex TR', *Shell Tech. Manual TR 8.17*.

Vonk W C, Philips M C and Roele M (1993), 'Ageing resistance of bitumenous road binders: benefits of SBS modification', *Shell Tech. Manual TR 8.29*.

Wang Q, Liao M, Wang Y and Ren Y (2007), 'Characterisation of end-functionalised styrene–butadiene–styrene copolymers and their application in modified asphalt', *J. Appl. Polym. Sci.*, 103, 8–16.

Wen G, Zhang Y, Zhang Y, Sun K and Fan Y (2002), 'Rheological characterization of storage-stable SBS-modified asphalts', *Polym. Testing*, 21, 295–302.

Whiteoak D (1990), *The Shell Bitumen Handbook*, Chertsey, Surrey, Shell Bitumen UK.

Yeh P-H, Nien Y-H, Chen J-H, Chen W-C and Chen J-S (2005), 'Thermal and rheological properties of maleated polypropylene modified asphalt', *Polym. Eng. Sci.*, 45, 1152–1158.

Yen T F (1981), *The Future of Heavy Crude and Tar Sands*, New York, McGraw-Hill.

Yen T F (1991), *Encyclopedia of Polymer Science and Engineering*, New York, John Wiley & Sons.

Yen T F and Dickie J P (1968), 'The compactness of the aromatic systems in petroleum asphaltenes', *J. Inst. Pet.*, 54, 50–53.

Yen T F and Erdman J G (1962), 'Investigation of the structure of petroleum asphaltenes and related substances by infrared spectroscopy', *Prepr. Am. Chem. Soc., Div. Pet. Chem.*, 7, 5.

Yen T F and Erdman J G (1963), 'Asphaltenes and related substances: X-ray diffraction', *Encyclopedia of X-rays and Gamma Rays*, New York, Reinhold.

Yen T F, Erdman J G and Pollack S S (1961), 'Investigation of the structure of petroleum asphaltenes by X-ray diffraction', *Anal. Chem.*, 33, 1587–1594.

Yen T F, Erdman J G and Saraceno A J (1962), 'Investigation of the nature of free radicals in petroleum asphaltenes and related substances by electron spin resonance', *Anal. Chem.*, 34, 694–700.

Yen T F, Tynan E C and Vaughan G B (1970), 'Electron spin resonance studies of petroleum asphalts', in RA Friedel (editor), *Spectrometry of Fuels*, New York, Plenum.

You Z, Mills-Beale J, Foley J M, Roy S, Odegard G M, Dai Q and Goh S W (2011), 'Nanoclay-modified asphalt materials: Preparation and characterization', *Constr. Build Mater.*, 25, 1072–1078.

Yousefi A A (2003), 'Polyethylene dispersions in bitumen: the effects of the polymer structural parameters', *J. Appl. Polym. Sci.*, 90, 3183–3190.

Zerlia T and Pinelli G (1992), 'Asphaltenes determination in heavy petroleum products by partial least squares analysis of u.v. data', *Fuel*, 71, 559–563.

Polymer modified bitumen emulsions (PMBEs)

D. LESUEUR, Lhoist R&D, Belgium

Abstract: Polymer modified bitumen emulsions (PMBEs) are a special class of bituminous emulsions. There are several ways to prepare PMBEs. One possibility is to emulsify a PMB; another is to add a latex to a bitumen emulsion, either prior to the colloid mill or after. In all cases, the resulting PMBE shows improved rheological properties of the residue after breaking. Their design and manufacture differ in several ways from those of unmodified emulsions. In particular, emulsions of PMB are harder to manufacture than unmodified bitumen emulsions. However, PMBEs are characterized in the same way as unmodified emulsions. Their breaking behaviour is generally also similar to that of unmodified emulsions, but with a possibility, for latex-modified emulsions, of controlling the morphology in order to obtain a continuous polymer-rich phase with polymer content as low as 2–3% by weight of bitumen. This type of morphology can only be achieved by the hot process with polymer content above 6 wt%.

PMBEs have been successfully used for several decades in the road industry. They represent a class of high performance binders whose preferred application is in the form of chip seals and as microsurfacing for heavily trafficked pavements.

Key words: polymer modified bitumen, emulsion, chip seal, microsurfacing.

2.1 Introduction

Bitumen emulsions are by far the most commonly used binder in cold paving technologies, allowing numerous applications such as tack coats, microsurfacings and chip seals (Salomon, 2006; SFERB, 2006). So-called ‘cold technologies’ are generally regarded as environmentally friendly construction technologies (EFCT) because they help reduce energy spending thanks to lower operating temperatures and the use of wet aggregates, and they diminish fume and particle emissions to the atmosphere and therefore limit the impact on the environment. As quantified by the International Bitumen Emulsion Federation (IBEF), the production of a typical unmodified hot mix asphalt (HMA) represents 21 kg of equivalent CO₂ emissions per tonne of HMA and an energy cost of 277 MJ/t (Lebouteiller, 2008). In parallel, the production of cold mix asphalt (CMA) represents only 3 kg eq.CO₂/t and 36 MJ/t (Lebouteiller, 2008).

However, from the perspective of the end-user, cold technologies remain highly technical materials and therefore are thought to present some kind of technical risk. As a consequence, they are essentially used in a narrow application range and mostly on secondary roads. For example, gravel-emulsion is essentially used in France for reinforcement and reprofiling as its excellent fatigue resistance makes it a very interesting material for base courses, even for new constructions (Lesueur *et al.*, 2002). The situation is looking somewhat brighter in the case of microsurfacing, which constitutes a very specific type of cold mix used occasionally under heavy traffic but, however, far from represents the typical solution for wearing courses for highways.

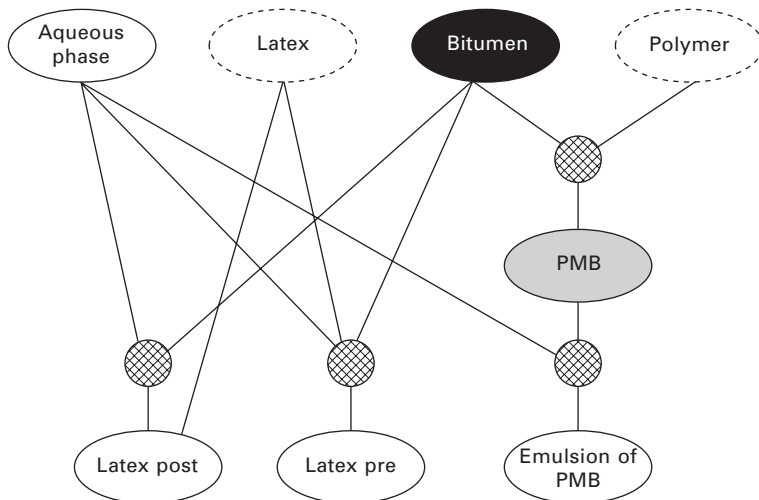
One way to improve the use of cold technologies under high traffic loads is through the use of high performance binders such as polymer modified bitumen emulsions (PMBEs). In fact, the microsurfacings applied on highways are always based on PMBE. Similarly, chip seals under high traffic loads are also based on PMBE. Indeed, the development of one of the best performing polymer-modified bitumens (PMBs) so far, i.e. the *in situ* crosslinking of styrene–butadiene block-copolymer sold under the Styrelf® and Stylink® trademarks, was initially developed in France for high performance chip seals in the late 1970s (LCPC, 2010).

Given this context, and in the absence of precise world statistics, a crude estimate of current PMBE production would be as follows. According to the International Bitumen Emulsion Federation, about 8 Mt of bitumen emulsions were used worldwide in 2005, meaning that almost 6% of the bituminous binders were used in this form (Lebouteiller, 2008). Since about 10% of the bituminous binders were PMB, we can roughly estimate that about 800,000 t of PMBEs were produced worldwide in 2005.

This chapter reviews our current knowledge of PMBEs, starting with their manufacturing and basic properties. In particular, we try to stress the differences between unmodified and modified emulsions, in order to highlight the key factors controlling this technology. Then, the breaking of PMBE is detailed, from which key aspects of their current use, especially for chip seal and microsurfacing applications, are discussed.

2.2 Manufacturing polymer modified bitumen emulsions (PMBEs)

When talking about PMBE, it is necessary to further separate them into three more categories (Fig. 2.1): emulsions of PMB, and latex modified emulsions by either post-addition or co-emulsification (Benedict, 1986; Johnston and King, 2008). Co-emulsification with a latex is also called latex pre-addition. Emulsions of PMB are also sometimes called ‘monophase’ PMBEs as opposed to latex modified emulsions which are then biphasic PMBEs (Johnston and King, 2008).



2.1 The three routes to PMBE: a latex (polymer emulsion) can be added to a bitumen emulsion (latex post), a latex can be added to the aqueous phase before bitumen emulsification (latex pre) or a PMB can be emulsified (emulsion of PMB).

Emulsions of PMB are made using a PMB as the starting material in the emulsion plant. All grades of PMB can potentially be used, but practical limitations explained in the next section generally limit the choice to PMB with polymer content of the order of 3 wt% based on total binder. Emulsions of PMB are somewhat more difficult to manufacture than emulsions of neat bitumen. They are still made using similar technology in the same plants, i.e. a colloid mill (Salomon, 2006; SFERB, 2006).

Two ways to manufacture PMBE from latex can be found. A latex is an emulsion of polymer, hence there is the possibility of mixing it with a bitumen emulsion. The first possibility consists in adding the latex directly inside the colloid mill (Fig. 2.1). This is generally known as latex co-emulsification or latex pre-addition if the latex is added to the aqueous phase. The second possibility is to add the latex directly into a regular bitumen emulsion, at the plant or just before use, and this is known as latex post-addition (Fig. 2.1).

Even if emulsions of PMB are more difficult to manufacture, especially for those that set rapidly, as detailed in the next sections, they are the preferred technology in France because of the intimate mixing of the polymer with bitumen. The properties of the recovered binder are not significantly different from that of the used PMB (King *et al.*, 1993), which makes it easy to anticipate the final properties.

Still, current latex technologies allow for very interesting control of morphology as discussed in the section on emulsion breaking (see Section

2.2.4). The technology is widely used in the USA; since polymer modification is obtained *in situ*, guidelines are provided by the suppliers in order to anticipate the properties of the recovered binder for different levels of latex modification.

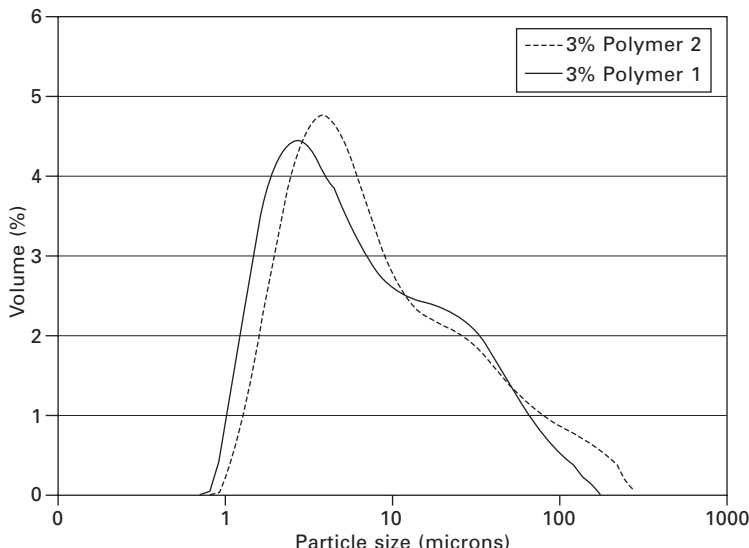
2.2.1 Formulation of PMBE

The formulation of PMBE has two aspects: firstly, the emulsion must be formulated in order to have a stable product; and second, the binder must be formulated in order to have the desired final properties.

The first step, i.e. emulsion formulation, is a classical emulsion formulation step. Depending on the chosen technology (i.e. emulsion of PMB or latex modification of a bitumen emulsion), the strategy will be somewhat different.

As explained in the next section, rapid-setting emulsions of PMB are somewhat more difficult to manufacture than their neat bitumen equivalents. In terms of final properties, the risk with emulsions of PMB is to have coarser particles and hence low storage stability and a high risk of clogging during pumping (Fig. 2.2).

In terms of formulation, this problem can be tackled by several means. Firstly, the nature and quantity of the fluxing agent can modify PMB emulsification.



2.2 Effect of polymer type on particle size distribution of the emulsion. With exactly the same emulsion formula (except for polymer type) and operating conditions, polymer 1 gives an emulsion with a residue on 800 micron sieve below 0.1%, where as polymer 2 gives an out-of-spec residue of 3%.

Therefore, a good recommendation would be that any modification in the formulation, including new polymer type, new bitumen source, new fluxing agent and/or new emulsifying agent, should be first validated at the laboratory or on a pilot scale before full-scale implementation.

Because of the difficulty in emulsifying PMB, the presence of additional emulsifying agent can help stabilize the most unstable emulsions, i.e. rapid-setting ones. As a matter of fact, rapid-setting unmodified emulsions are generally manufactured with 1–3 kg of emulsifying agent per tonne of emulsion (SFERB, 2006 – see Table 2.1). The emulsification of a PMB with a similar viscosity to that of an unmodified bitumen might necessitate 1–3 kg/t of excess surfactant. Surfactant suppliers even propose that specific co-emulsifiers are incorporated directly inside the PMB instead of inside the aqueous phase, as is usually done (Table 2.1). Note that slow-setting emulsions generally do not experience this problem, since they normally have sufficient amounts of surfactant added (generally above 5 kg/t) in order to stabilize a PMB.

Except for the difference in emulsifier content, the formulation of an emulsion of PMB is generally very similar to that of an unmodified bitumen (Table 2.1).

As for the formulation of PMBE using a polymer latex, there is no specific difficulty and the formula for the bitumen emulsion is generally unchanged, except for the addition of the latex (Table 2.1). The latex must be anionic or cationic in order to match the bitumen emulsion polarity. Several grades are commercially available, based on several polymers including styrene–butadiene random (SBR) copolymer, styrene–butadiene block copolymer, natural rubber and neoprene (Takamura, 2000; Ruggles, 2005; Johnston and King, 2008). They generally have a well-defined particle size of the order of 200 microns and a solids content of the order of 50–60%. The typical latex content in the emulsion is calculated so as to have generally 2–3 wt% of residual polymer in the final binder.

Table 2.1 Examples of emulsion formulas (kg per 1000 kg of rapid-setting emulsion with 65% binder)

	Bitumen emulsion	Emulsion of PMB	Latex emulsion
200 pen bitumen	630.0	611.1	580.0
Polymer (in bitumen)	–	18.9	–
Cationic latex (55 wt% solid content)	–	–	50.0
Water	346.2	344.2	346.2
HCl 36% in water	1.5	1.5	1.5
Cationic surfactant 1 (in water)	2.3	2.3	2.3
Cationic surfactant 2 (in bitumen)	–	2.0	–
Fluxing agent (in bitumen)	20.0	20.0	20.0

2.2.2 Manufacturing of PMBE

Manufacturing of PMBE is especially delicate with regard to emulsions of PMB. Firstly, the high viscosity of PMBs makes it necessary to process them at higher temperatures. Normal operating conditions for an unmodified emulsion are typically a bitumen temperature close to 140–150°C (in order to have a bitumen viscosity of 200 mPa.s) and an aqueous phase temperature of 50°C (Salomon, 2006). Using these conditions, and with the usual phase ratio close to 65 wt% bitumen, the emulsion exits the colloid mill at 90°C. The problem with binders requiring higher processing temperatures, which is the case for most PMBs but also the case for hard bitumens, is that the temperature must be increased, thereby creating a risk of reaching possibly 100°C at the colloid mill exit. Cooling systems are usually employed, but the proximity of the boiling point is detrimental to the emulsion and generates a larger proportion of big drops within the emulsion. This in turn affects storage stability and induces clogging problems during pumping. It is interesting to note that this problem is less seen with EVA-modified PMB, for which the viscosity at high temperature is generally lower than that of the parent bitumen. Therefore, EVA modification is very favourable for PMB emulsification. Secondly, the rheology of the PMB is distinct from that of neat bitumen (see Chapters 7 and 8 in this book, and Lesueur (2009) for an overview). Even if the exact mechanisms of bitumen droplet break-up and coalescence in a colloid mill are still not fully known (Ajour, 1977; Durand, 1994; Gingras *et al.*, 2005), PMB droplets are harder to deform than normal bitumen. As a matter of fact, the polymer-rich inclusions inside the PMB not only have elastomeric properties (Lesueur *et al.*, 1998) but also initially are larger in size (usually with a median particle diameter of 10–50 microns) than the final droplet size (typically having a median particle diameter of 5 microns). Therefore, the droplet-breaking step is more difficult. As a consequence, and in the absence of any change in the colloid mill operational conditions, the PMBE emulsion is generally coarser than the corresponding neat bitumen emulsion for the same binder content and viscosity. This again affects storage stability and increases the risk of pumps clogging.

Small changes that barely affect the rheological properties of the residual binder can still affect the emulsion formation process. Figure 2.2 illustrates the differences in particle size distribution for emulsions made with two polymers having identical rheological properties for the PMB, as measured with conventional testing (including viscosity at emulsifying temperature). However, polymer 1 gave a finer particle size distribution, easily passing the specifications limiting the amount of large particles (as measured by the residue on sieving using EN 1429 with an 800-micron sieve), where polymer 2 gave an emulsion out of specification (residue on sieving above 0.1%). It could be that elongational rheology (Malkin and Isayev, 2006)

of the PMB would capture differences between the materials that are not otherwise highlighted in the more classical shear rheology that is usually used to characterize PMB. As a consequence, polymer suppliers generally recommend specific polymer grades for emulsions of PMB that minimize these problems.

In all cases, commercial emulsions of PMB are formulated in order to take these effects into account and therefore have adequate particle size distribution and sufficient storage stability. Also, new emulsification technologies, based on high internal phase ratio technology consisting of laminar shearing of a concentrated emulsion, might allow for easier manufacturing of PMB emulsions (Lesueur *et al.*, 2009).

When PMBEs are manufactured by latex addition, all the difficulties observed for emulsions of PMB disappear. In the case of latex co-emulsification, the latex is generally stable, with a fine particle size (close to 200 microns) and in such a small quantity (typically 2–3 wt% of residual polymer based on the bitumen) that it is barely affected during mixing in the colloid mill. As a consequence, its presence does not significantly affect emulsion manufacture and the main advantage is good dispersion of the latex within the PMBE.

In the case of latex post-addition, the latex is added directly into a regular bitumen emulsion, at the plant or just before use. This last solution is very easy to implement but the dispersion of the latex is generally somewhat less efficient, and long storage times must be avoided in order to limit latex creaming. Also, mixing devices must be present in order to provide an acceptable homogeneity of the product.

2.2.3 Properties and specifications of PMBE

The emulsion is a carrier for the binder, and as such the properties of a PMBE are very similar to those of an unmodified emulsion, except of course for the properties of the residual binder. As a consequence, current specifications on emulsions are generally blind to the type of binder and directly apply to both PMBE and unmodified bitumen emulsions (Salomon, 2006). Only the specifications with regard to binder properties differ between PMBE and unmodified emulsion. Current specifications are described in ASTM D977 (anionic emulsions) and ASTM D2397 (cationic emulsions) in the USA and EN 13808 (cationic emulsions) for Europe.

As a result, the properties measured for specification purposes are as follows.

- Particle polarity, the emulsion being generally either anionic or cationic. Note that cationic emulsions are the most common and represent more than 95% of the current European market.
- Binder content, usually between 60 and 72 wt%.

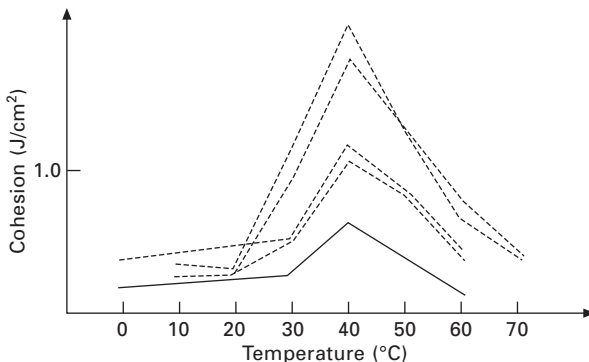
- Absence of large particles, quantified by the residue remaining on 125 and 850 micron sieves (ASTM) or 160 and 500 micron sieves (EN). In general, no more than 0.5 wt% of coarse particles are accepted, and the most severe specifications ask for less than 0.1 wt%.
- Storage stability, quantified by the difference in binder content in the top and bottom of a settled emulsion, generally after 7 days.
- Emulsion viscosity, generally through efflux time measurements (generally Saybolt–Furol, Engler or STV). Note that efflux time and dynamic or steady-state viscosity are related through complex formulas (Lesueur, 2003). Depending on the application, the viscosity must lie in the correct range. For example, in the case of cold mixes, too fluid an emulsion would drain from the aggregate, while too thick an emulsion would not allow for a good coating.
- Breaking index, in Europe, to quantify whether the emulsion is rapid or slow-setting. The test consists of measuring the mass of standard filler needed to agglomerate 100 g of emulsion (EN 13075-1). It is well documented that the breaking index increases with emulsifier content, hence making it relevant to assess emulsion breaking speed (Ajour, 1977; Boussad and Martin, 1996). Emulsions with a breaking index below 80 are generally considered rapid-setting while those with a breaking index higher than 120 are generally slow-setting.

As discussed earlier, the difference between PMBEs and unmodified emulsions essentially lies in the properties of the binder. In general, any binder testing can be performed on the recovered binder. However, a difficulty arises in finding an adequate method to recover the binder. Fast evaporation of water using ventilated ovens at temperatures above 60°C generally leads to a binder morphology that is not representative of the one observed in the field. This is especially true with latex modified emulsions, as detailed in the next section. As a consequence, the current EN specifications are based on binder testing after mild evaporation (24 hours at room temperature followed by 24 hours at 50°C – EN 13074).

In terms of residual binder testing, it is interesting to note that the French experience with PMBE for chip seals is based on the use of a pendulum test (EN 13588). With this test, cohesion values above 1 J/cm² can only be obtained through polymer modification (Fig. 2.3).

2.2.4 Breaking of PMBE

As stated in the former section, PMBEs and unmodified emulsions are very similar in terms of properties, except for the properties of the binder. This also applies to breaking properties, which are therefore treated in a similar theoretical framework for both types of emulsions. Still, differences coming



2.3 Recovered binder cohesion for unmodified (solid line) and polymer-modified emulsions (dotted lines). Adapted from PIARC (1999).

from the binder rheology and/or the special morphology (latex-modified emulsions) can still be found.

In order to understand the breaking of bitumen emulsions, it is necessary to define precisely what is meant by 'breaking'. The definition that will be used is that breaking of the emulsion represents the sum of all the events leading to the transformation of the initial binder emulsion to a final film of binder. Coalescence is then defined as that specific step of the breaking process where individual droplets of binder merge to form larger drops, as will be described in more detail later. These definitions for breaking and coalescence are in line with their accepted meaning by the International Union of Pure and Applied Chemistry (Everett, 1972).

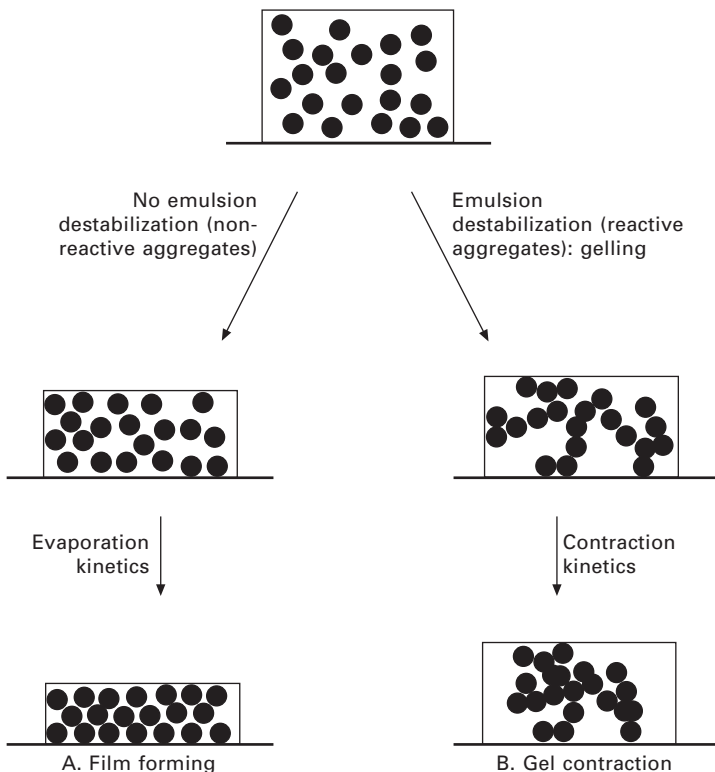
In order for an emulsion to break, it has to become somewhat unstable so that the initial droplets of binder have a restricted lifetime and tend to coalesce. Here, stability must be interpreted as thermodynamic stability and not as storage stability (Lesueur and Potti, 2004): an emulsion is said to be stable when the droplets retain their individuality as opposed to an unstable emulsion where the droplets tend to coalesce to form a final film of binder.

Hence, the breaking of the emulsion can be described in rational terms as a consequence of two events (Fig. 2.4):

- Disappearance of electrostatic repulsion between droplets (gel contraction)
- Very high bitumen concentration (film forming).

As far as PMBEs are concerned, and just like unmodified emulsions, the choice of emulsifier will govern the mechanism by which the droplets break.

The first case, leading to breaking by gel contraction, is the most common with cationic emulsions. A breaking agent is sometimes used in



2.4 Routes for break-up of bitumen emulsions. The gel contraction can be activated by reactive aggregates and/or the presence of a breaking agent (e.g. hydrated lime or cement). From Lesueur and Potti (2004).

order to promote destabilization, such as hydrated lime or cement (Cross, 1999; Niazi and Jalili, 2009). Note that very stable milk of lime with 45% solid fraction is now available and is being used as an emulsion breaking agent in microsurfacings or even tack coats. When the emulsion breaks by gel contraction, the kinetics of binder film formation is governed by three parameters (Bonakdar *et al.*, 2001):

- Binder viscosity: a soft binder or a binder softened by a fluxing agent coalesces more rapidly than a harder one. Similarly, a high temperature will also favour film formation because it decreases bitumen viscosity.
- Particle size: a larger particle size results in slower contraction kinetics.
- Binder–water interfacial tension: a higher tension means faster kinetics.

The presence of surfactants native to some specific bitumens, depending

on origin, is known to promote faster breaking kinetics (Chaverot *et al.*, 2008).

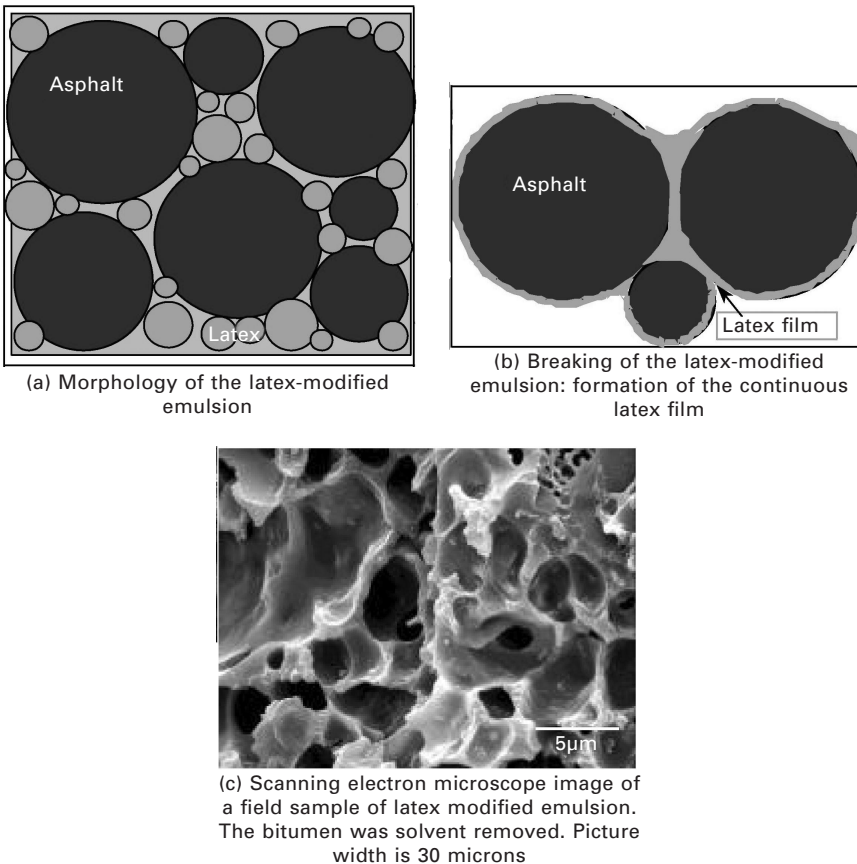
The second case, where evaporation is the driving force for breaking, is typical of anionic emulsions. Given the risk associated with relying on the action of climate in provoking emulsion breaking, current technologies are relying more and more on breaking by gel contraction. Still, favourable (i.e. dry and warm) weather generally accelerates breaking kinetics even for the gel contraction scheme. However, it should be noted that too fast an evaporation rate must be avoided, since water evaporation can induce the formation of a waterproof skin (Lesueur *et al.*, 2003). In such situations, the solution might be to decrease the emulsion film thickness (possible only for applications like chip seals) and/or to wait for milder conditions (i.e. avoid working during the hottest hours of the day).

In all cases, the morphology of the final binder film is temperature dependent. As explained in the previous section, accelerated drying procedures in the laboratory can lead to morphologies that are not representative of that observed in the field. This is especially true with latex-modified emulsions, for which the normal field breaking conditions should form a continuous latex film (Fig. 2.5). Any attempt to artificially accelerate the breaking process through inadequate 'too-fast' drying conditions would destroy the latex-modified emulsion morphology. This specific morphology is unique to latex-modified emulsions. As a consequence, a polymer content as low as 2 or 3 wt% can induce large differences in the rheological properties of the recovered binder, when amounts in excess of 6 wt% are needed for PMB made by the hot process in order to have a continuous polymer phase (Lesueur, 2009). This was clearly demonstrated in the work of Forbes and co-workers where different routes used in the manufacture of a PMBE were studied in terms of binder morphology (Forbes *et al.*, 2001). The same polymer was either used in latex form to obtain a co-emulsification or post-addition, or mixed with the bitumen in order to get an emulsion of PMB (Fig. 2.6). With 3 wt% of the same bitumen and polymer in all cases, a continuous polymer-rich phase was always obtained from latex-modified emulsions, regardless of the chosen route (i.e., post- or pre-addition), when the usual dispersion of polymer-rich nodules was found for the emulsion of PMB (Fig. 2.6 – Forbes *et al.*, 2001).

2.3 Uses of PMBE

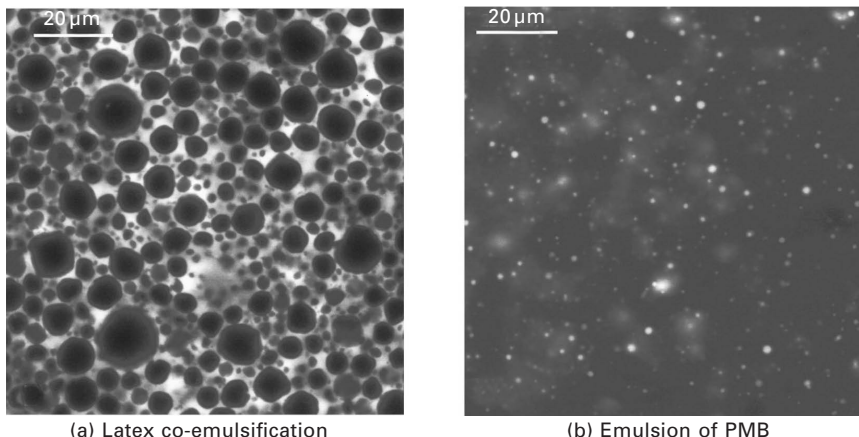
Given that PMBEs are emulsions with high performance binders, they are generally used under heavy traffic conditions. The most common applications are for chip seals and microsurfacing (Johnston and King, 2008).

A chip seal is a surface treatment consisting in applying separate but consecutive operations, one or various layers of emulsion at 500–2000 g/



2.5 Latex-modified emulsion breaking route. Upon breaking, the small latex particles are confined between the large bitumen particles (a). This eventually generates a continuous polymer network around the bitumen particles (b), as revealed by scanning electron microscopy of field samples (c). In this latter case, the samples were treated with OsO_4 in order to make the polymer insoluble and the bitumen was then extracted with MEK (methyl ethyl ketone). From Takamura (2002).

m^2 each and one or various layers of aggregate at 4–12 L/m^2 each. The resulting mosaic is called a chip seal (Salomon, 2006; SFERB, 2006). Its precise design must take into account several factors including traffic severity, climate, condition of the support (evenness, roughness, possible moderate defects such as bleeding or stripping, etc.). The use of PMBE in chip seals was thoroughly reviewed by Gransberg and James (2005) and Johnston and King (2008). PMBE emulsions for chip seals usually have a high binder content (up to 72 wt%), are rapid-setting and can have fluxing agent content

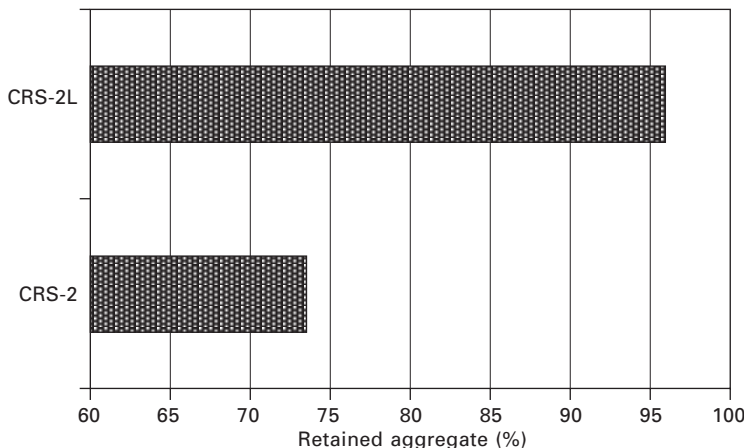


(a) Latex co-emulsification

(b) Emulsion of PMB

2.6 Effect of the chosen route on residual binder morphology. The polymer is the same in all cases and was added at 3 wt% to the same 180/220 pen bitumen. In the first case (a), the polymer was added in latex form and was co-emulsified with the bitumen. This way, a continuous polymer-rich network is formed. In the second case (b), the polymer was first added to the bitumen in order to form a PMB, which was then emulsified. The final morphology is typical for a PMB with a continuous asphaltene-rich phase with polymer-rich inclusions. Note that the particle size for the polymer-rich inclusions is smaller than that of the original PMB, because of the emulsion step which improves dispersion. From Forbes *et al.* (2001).

up to 10 wt% based on the binder. As a result, and from more than 30 years of field experience, polymer modification reduces temperature susceptibility, provides increased adhesion to existing surfaces, increases aggregate retention and flexibility, and allows the roadway to be opened to traffic earlier after application (Gransberg and James, 2005). Polymers are considered to be beneficial in minimizing bleeding, aiding chip retention, and enhancing the durability of the chip seal, and are recommended for roads having a high volume of traffic and for late season work, that is during unfavourable weather conditions for emulsions like early spring or late fall in continental climates (Gransberg and James, 2005). These benefits are quantified in Fig. 2.7 using a sweep test (ASTM D7000). The sweep test consists of applying a kind of 'brush' with a planetary motion onto the surface of a laboratory-prepared chip seal and measuring the amount of aggregates lost after abrasion. Aggregate retention after 5 hours curing at 35°C was greatly improved for eight different aggregates for a 3% latex added to a bituminous emulsion (Fig. 2.7). The same type of improvement was also obtained with emulsions of PMB (Serfass *et al.*, 1992). For these reasons, PMBEs are now used for chip seals under heavy traffic, and are for example recommended for traffic class T1 (between 300 and 750 heavy trucks per day) and above in France



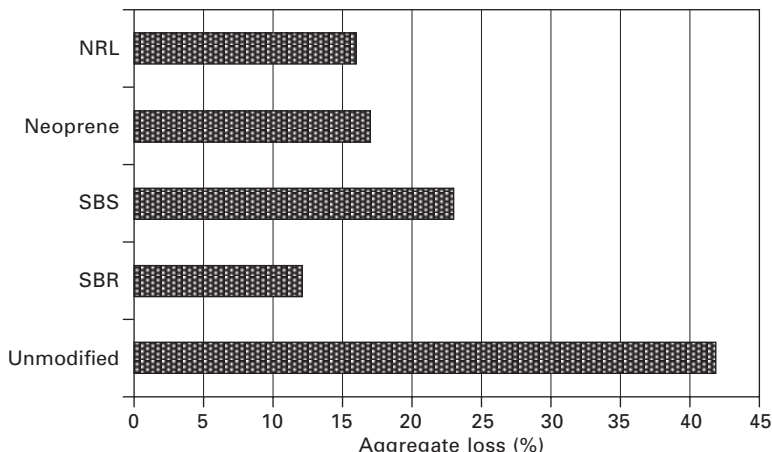
2.7 Average retained aggregate in the sweep test (ASTM D7000) for chip seals made of eight different aggregates and either an unmodified emulsion (ASTM classification CRS-2) or the same emulsion with 3% polymer (based on bitumen) pre-added to the aqueous phase in a latex form (CRS-2L). The chip seals were cured for 5 hours at 35°C before testing. Data from Takamura (2003).

(SETRA/LCPC, 1995) or for traffic class T1 (between 800 and 2000 heavy trucks per day) and above in Spain (DGC, 2000).

The same improved performance is also obtained in the case of microsurfacings and slurry seals (Johnston and King, 2008). A microsurfacing is a special cold mix manufactured and applied in-place using specific dedicated equipment (Salomon, 2006; SFERB, 2006). The mixture is generally laid at 10–20 kg/m². PMBEs for microsurfacings generally have a binder content between 60 and 65 wt%, are generally slow-setting and very seldom have fluxing agents. As illustrated in Fig. 2.8, the use of PMBE improves the wet abrasion resistance of microsurfacings. Again, a similar improvement is obtained when emulsions of PMB are used (Brûlé and Le Bourlot, 1993). In fact, the word ‘microsurfacing’ is now limited to slurry seals made with PMBE (ISSA, 2001). From more than 20 years of field experience, the use of PMBE in microsurfacings limits the risk of having stresses such as ravelling and bleeding (SETRA/LCPC, 1995). For these reasons, PMBEs are now used for microsurfacings under heavy traffic, and are for example recommended for traffic class T1 (between 800 and 2000 heavy trucks per day) and above in Spain (DGC, 2000).

2.4 Conclusions

PMBEs are a special class of bituminous emulsions. There are several ways to prepare PBMEs. One possibility is to emulsify a PMB. In this case,



2.8 Aggregate loss in the wet abrasion test after 6 days' soak (ISSA TB 100) for microsurfacings made with either an unmodified emulsion or a PMBE with 3% polymer added in latex form (NRL: natural rubber latex; SBR: styrene–butadiene random copolymer latex; SBS: styrene–butadiene triblock copolymer latex or neoprene latex). Data from Holleran (2006), cited in Johnston and King (2008).

the peculiarities of the binder might necessitate extra emulsifier addition, sometimes put in the binder phase, especially for rapid-setting emulsions. The properties of the original PMB are recovered once the emulsion has broken, and the polymer-rich inclusions are better dispersed than in the original PMB.

Another possibility is to add a latex to a bitumen emulsion, either prior to the colloid mill or after. In this case, emulsification can be achieved without any specific difficulty. The interest of this technology is that the latex can create a continuous polymer phase upon emulsion breaking even with polymer contents as low as 2 to 3 wt%.

In all cases, PMBEs show improved rheological properties of the residue after breaking when compared to unmodified bitumen emulsions, and this materializes for example in higher softening points or higher modulus at high operating temperatures (say in the 40–50°C range) which in turn imparts higher binder cohesion that generates a better resistance to traffic loads of the corresponding final application (chip seal, microsurfacing, etc.). Still, PMBEs are characterized in the same way as unmodified emulsions, with binder content, viscosity and particle size (especially the absence of coarse particles, i.e. from residue on sieves) being key properties. The main difference lies in the rheological properties of the residue.

Their breaking behaviour is generally also similar to that of unmodified emulsions, except for latex-modified emulsions where there is a possibility of controlling morphology in order to obtain a continuous polymer-rich phase

with polymer content as low as 2 to 3 wt%. This type of morphology can only be achieved by the hot process with polymer content above 6 wt%. Note that too extreme accelerated drying conditions (temperature above 50°C) must be avoided because they lead to unrepresentative morphology of the recovered binder.

Currently, PMBEs have been used successfully for several decades by the road industry. They represent a class of high performance binders whose preferred application is in the form of chip seals and microsurfacings for heavy trafficked pavements (i.e. more than 300 heavy trucks per day).

2.5 References

Ajour A. M. (1977), 'Chemical aspects of the formulation of bituminous emulsions', *Proc. 15th Int. Slurry Seal Assoc. (ISSA) Convention*, Madrid, 27–34

Benedict C. R. (1986), 'Experiments with cured cohesion testing of slurry seals and thin layered cold mixes', *Proc. 24th Int. Slurry Seal Assoc. (ISSA) Convention*, San Francisco, 55–70

Bonakdar L., Philip J., Bardusco P. *et al.* (2001), 'Rupturing of bitumen-in-water emulsions: experimental evidence for viscous sintering phenomena', *Colloids and Surfaces – A: Physicochem. Eng. Aspects*, 176, 185–194

Boussad N. and Martin T. (1996), 'Emulsifier content in water phase and particle size distribution: Two key-parameters for the management of bituminous emulsion performance', *Proc. 1st Eurasphalt and Eurobitume Congress*, Strasbourg, France, paper 6.159

Brûlé B. and Le Bourlot F. (1993), 'Gripfibre', *Revue Générale des Routes et Aérodromes*, 711

Chaverot P., Cagna A., Glita S. and Rondelez F. (2008), 'Interfacial tension of bitumen–water interfaces. Part 1: Influence of endogenous surfactants at acidic pH', *Energy and Fuels*, 22, 790–798

Cross S. A. (1999), 'Experimental cold in-place recycling with hydrated lime', *Transportation Research Record*, 1684, 186–193

DGC: Dirección General de Carreteras (2000), *Pliego de prescripciones técnicas generales para obras de carreteras y puentes (PG-3)*, Madrid (Spain), Ministerio de Fomento

Durand G. (1994), 'L'émulsion de bitume: la fabrication au service de son utilisation', *Revue Générale des Routes et Aérodromes*, 718, 53–55

Everett D. H. (1972), 'Definitions, terminology and symbols in colloid and surface chemistry', *Pure and Applied Chemistry*, 31, 579–638

Forbes A., Haverkamp R. G., Robertson T. *et al.* (2001), 'Studies of the microstructure of polymer-modified bitumen emulsions using confocal laser scanning microscopy', *J. Microscopy*, 204, 252–257

Gingras J.-P., Tanguya P. A., Mariotti S. and Chaverot P. (2005), 'Effect of process parameters on bitumen emulsions', *Chem. Eng. Proc.*, 44, 979–986

Gransberg D. and James D. M. B. (2005), *Chip Seal Best Practices*, NCHRP Synthesis 342, Washington, DC, Transportation Research Board

ISSA: International Slurry Seal Association (2001), *Recommended performance guidelines for micro-surfacing*, ISSA A143, Annapolis, MD.

Johnston J. B. and King G. N. (2008), 'Using polymer modified asphalt emulsions in surface treatments – a federal lands highway interim report', http://www.pavementpreservation.org/fhwa/pme09/Polymer_Modified_Asphalt_Emulsions.pdf

King G. N., Lesueur D., King H. W. and Planche J.-P. (1993), 'Evaluation of emulsion residues using SHRP binder specifications', *Proc. 1st World Congress on Emulsion*, Paris, vol. 2, article 3–30–122

LCPC: Laboratoire Central des Ponts et Chaussées (2010), *The LCPC: A key player in sustainable civil engineering*, Paris

Lebouteiller E. (2008), 'Asphalt emulsions world trends', *presented at the 4th Int. Seminar on Asphalt Emulsion Technol. (ISAET)*, Arlington, VA

Lesueur D. (2003), 'The rheological properties of bitumen emulsions. 1. Theoretical relationships between efflux time and rheological behavior', *Road Materials Pavement Design*, 4, 151–168

Lesueur D. (2009), 'The colloidal structure of bitumen: Consequences on the rheology and on the mechanisms of bitumen modification', *Adv. Colloid Interface Sci.*, 145, 42–82

Lesueur D. and Potti J. J. (2004), 'Cold mix design: A rational approach based on the current understanding of the breaking of bituminous emulsions', *Road Materials Pavement Design*, 5, 65–87

Lesueur D., Gérard J.-F., Claudy P. *et al.* (1998), 'Polymer modified asphalts as viscoelastic emulsions', *J. Rheol.*, 42, 1059–1074

Lesueur D., Kerzrého J.-P., Such C. *et al.* (2002), 'Bilan de l'expérimentation OPTEL sur le manège de fatigue du LCPC Nantes', *Revue Générale des Routes et Aérodromes*, 803, 69–76

Lesueur D., Coupé C. and Ezzarougui M. (2003), 'Skin formation during the drying of a bitumen emulsion', *Road Materials Pavement Design*, 2, 161–179

Lesueur D., Uguet Canal N., Hurtado Aznar J. *et al.* (2009), 'Nanoemulsiones de betún', *Carreteras*, 163, 33–46

Malkin A. Y. and Isayev A. I. (2006), *Rheology – Concepts, Methods and Applications*, Toronto, Chemtec Publishing

Niazi Y. and Jalili M. (2009), 'Effect of Portland cement and lime additives on properties of cold in-place recycled mixtures with asphalt emulsion', *Construction Building Materials*, 23, 1338–1343

PIARC: World Road Association (1999), 'Use of modified bituminous binders, special bitumens and bitumens with additives in road pavements', *Routes/Roads*, 303

Ruggles C. S. (2005), 'The efficient use of environmentally-friendly NR latex (NRL) in road construction – past, present and the future', *Natural Rubber*, 37, 2–4

Salomon D. R. (2006), *Asphalt Emulsion Technology*, TRC E-C102, Washington, DC, Transportation Research Board

Serfass J.-P., Joly A. and Samanos J. (1992), 'Modified asphalts for surface dressing – A comparison between hot-applied and emulsified binders', in *Polymer Modified Asphalt Binders*, Wardlaw K. R. and Shuler S., eds, ASTM STP 1108, Philadelphia, PA, 281–308

SETRA: Service d'Etudes Techniques des Routes et Autoroutes/LCPC: Laboratoire Central des Ponts et Chaussées (1995), *Enduits Superficiels d'Usure – Guide Technique*, Paris

SFERB: Section des Fabricants d'Emulsions Routières de Bitume (2006), *Bitumen Emulsions*, Paris, *Revue Générale des Routes et Aérodromes*

Takamura K. (2000), 'Morphology vs temperature: Comparison of emulsion residues

recovered by the forced airflow and RTFO drying', *Proc. 38th Int. Slurry Seal Assoc. (ISSA) Convention*, Amelia Island, FL, 1–18

Takamura K. (2002), 'Microsurfacing with SBR latex modified asphalt emulsion', Charlotte, NC, BASF (available from <http://worldaccount.bASF.com>)

Takamura K. (2003), 'Improved fatigue resistance of asphalt emulsion residue modified with SBR latex', Charlotte, NC, BASF (available from <http://worldaccount.bASF.com>)

Modification of bitumen using polyurethanes

P. PARTAL and F. J. MARTÍNEZ-BOZA,
Universidad de Huelva, Spain

Abstract: This work deals with reactive modification based on polymers containing functional groups, more specifically isocyanate-functionalised polymers of low molecular weight. A short-term modification, taking place during mixing, and a long-term bitumen modification, which develops over a long period of curing (up to several months), have been identified. However, the experimental results have shown that the degree of bitumen modification depends on bitumen reactivity and microstructure. Accordingly, the bituminous colloidal nature strongly affects the final properties of bitumen samples modified by isocyanate-based reactive polymers. Likewise, a reactive bitumen modification mechanism, involving a set of chemical reactions, has been identified. Thus, bitumen modification, by *in situ* formation of polyurethane/urea-based polymers in the bituminous matrix, has been described. Such a set of reactions between water and isocyanate-based modified bitumen has been used to promote its foaming at low processing temperatures, which could be used in novel applications where a foamed binder is required. The reactive foaming method proposed herein involves the reaction between water and free isocyanate groups, producing an amine and releasing carbon dioxide.

Key words: bitumen, modification, polymer, isocyanate, rheology, microstructure, foam.

3.1 Introduction

This introductory section will outline the main themes of the chapter and what the other sections will contain. Accordingly, Section 3.2 will introduce the need for bitumen modification and will compare the physical and chemical modification through non-reactive plastomers and elastomers, and reactive polymers.

Specifically dealing with reactive modification based on polymers containing functional groups, Section 3.3 will describe the modification ability of isocyanate-functionalised polymers of low molecular weight. A short-term modification, taking place during mixing, and a long-term bitumen modification, which develops over a long period of curing (up to several months), will be identified.

Then, Section 3.4 will focus on the influence that the bituminous colloidal

nature exerts on the final properties of bitumen samples modified by isocyanate-based reactive polymers. The results obtained will show that the degree of bitumen modification depends on bitumen reactivity and microstructure.

Furthermore, in Section 3.5, bitumen modification, by *in situ* formation of polyurethane/urea-based polymers in the bituminous matrix, will be described. A reactive bitumen modification mechanism, involving a set of chemical reactions, will be proposed.

Moreover, novel applications may arise from such chemical reactions, and among them Section 3.6 focuses on bitumen chemical foaming. Water addition to the isocyanate-based modified bitumen has been found to promote its foaming at low processing temperatures, which could be used in novel applications where a foamed binder is required. The reactive foaming method proposed herein involves the reaction between water and free isocyanate groups, producing an amine and releasing carbon dioxide.

Finally, a short descriptive section of sources of further information and advice will be addressed. This will provide a brief commentary on key books to consult (cross-referenced to full details given in the references), major trade/professional bodies, research and interest groups, websites, etc.

3.2 Bitumen modification by polymers

Bitumen is usually defined as a dark brown to black material, mainly obtained from crude oil distillation. It is widely used as a binder of mineral aggregates in road pavements (Airey 2003), as well as waterproofing material, as a joint sealant, and for roofing applications (Singh *et al.* 2003; Ait-Kadi *et al.* 1996).

Bitumen shows a high chemical complexity. It contains different types of molecular species, which are classified (in terms of solubility in *n*-heptane) into two major fractions, maltenes and asphaltenes. The asphaltenes consist of highly condensed planar and heteroatom polar groups, polar aromatic ring systems and large amounts of heteroatom polar functional groups (Dong *et al.* 2005). The maltenes fraction can be divided into three groups: saturates, aromatics and resins, based on differences in solubility and polarity (Redelius 2000).

Polymeric additives such as polyolefins, block copolymers, crumb rubber or recycled polymers have been widely used to enhance the in-service properties of bitumen (Ait-Kadi *et al.* 1996; Fawcett and McNally 2001; Navarro *et al.* 2004; García-Morales *et al.* 2004a). A bitumen additive should improve binder properties at both low and high in-service temperatures (Zanzotto *et al.* 2000). Consequently, it should be strong enough to withstand traffic loads at high temperature, which may cause rutting or permanent deformation, and be flexible enough to avoid excessive thermal stresses, at

low pavement temperatures. It also needs to be able to endure the thermal cycling of service without cracking or deforming (Ait-Kadi *et al.* 1996). Furthermore, a modifying agent of bitumen should be easily incorporated to yield a highly viscous mixture at in-service temperatures which remains homogeneous on storage, and should have a viscosity which permits its use in standard material manufacturing and paving equipment. Moreover, it should be highly resistant to ultraviolet light, thermal action and water, not leach deleterious substances into the environment, and be readily available (García-Morales *et al.* 2004b).

Polymers that have been commonly used to modify bitumen include styrene–butadiene–styrene copolymer (SBS), styrene–butadiene rubber (SBR), ethylene vinyl acetate (EVA), polyethylene (LDPE, HDPE, etc.) and waste polymers (plastic from agriculture, crumb tyre rubber, etc.) (Ait-Kadi *et al.* 1996; Blanco *et al.* 1996; Hesp and Woodhams 1991; Newman 1998; Yousefi 2003). For such polymers, the mixing process may have a significant effect on the technical properties of the resulting blend, as well as on the costs of the whole operation (Lu and Isaacsson 2001). Thus, high shear and processing temperatures (170–180°C) are necessary to reduce the viscosity differences between polymer and bitumen and to obtain suitable polymer dispersions. As a consequence, the final binder may undergo a ‘primary’ ageing, mainly due to the oxidation of maltene compounds, and polymer degradation, leading to a decrease in the expected mechanical performance of bituminous binders (Fawcett and McNally 2001; Lu and Isaacsson 2001; Airey 2003). Moreover, the use of high molecular weight polymers may yield thermodynamically unstable modified bitumens, and phase separation readily occurs during their storage at higher temperatures (García-Morales *et al.* 2004a).

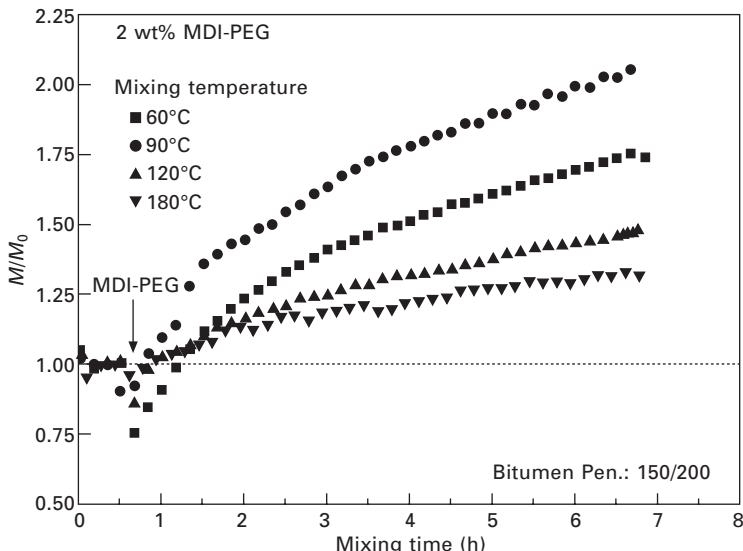
As an alternative, the use of reactive polymers as binder modifiers has been evaluated (Polacco *et al.* 2004a, 2004b; Sekar *et al.* 2002). These reactive polymers are cheaper, easier to mix and more compatible with bitumen than standard polymers, because they are able to form chemical bonds with some bitumen compounds and, as a result, they alter the structure and properties of the final binder. Consequently, the strength of the modified binder increases, its temperature susceptibility decreases and storage stability is improved (Trakarnpruk and Chanathup 2005). Examples of reactive polymers used for bituminous applications are polyethylene-*co*-methylacrylate (Trakarnpruk and Chanathup 2005), random terpolymers of ethylene, glycidyl methacrylate containing epoxy rings and an ester group, usually methyl, ethyl or butyl acrylate (Polacco *et al.* 2004a, 2004b; Engel *et al.* 1991; Pérez-Lepe *et al.* 2006; Sekar *et al.* 2002), isocyanate-based polymers (Singh *et al.* 2003, 2004), phenolic resins (Krivohlavek 1993), etc.

3.3 Modification by isocyanate-based reactive polymers

Reactive modification, based on polymers containing functional groups able to form chemical bonds with certain bitumen compounds, is therefore gaining great attention in academia and industry. In this sense, low-molecular-weight reactive isocyanate-terminated polymers have been proposed with this target in mind. Specifically, pre-polymers studied have been polypropylene glycol (PPG), or polyethylene glycol (PEG), functionalised by polymeric MDI, 4,4'-methylenebis(phenyl isocyanate), henceforth MDI-PPG or MDI-PEG, respectively. These polymers are synthesised by reaction of PPG or PEG and polymeric MDI, selecting a polyether/MDI molar ratio from 1:3 to 1:8, in N_2 atmosphere, at 40°C, for 48 h and under agitation. The resulting functionalised pre-polymer, typically with an average molecular weight between 700 and 2800 $g \cdot mol^{-1}$, is in liquid form having a light brownish colour and low viscosity (e.g. Newtonian viscosity of 182 mPa s at 25°C and 10.9 mPa s at 90°C).

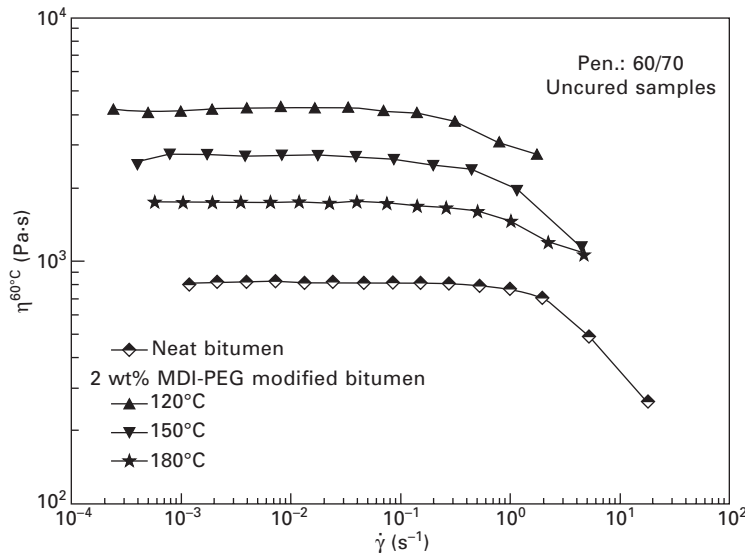
Such a liquid reactive polymer is therefore easily mixed with bitumen under gentle processing conditions. For instance, blends of MDI-PEG and bitumen have been prepared using low-shear stirring devices at temperatures between 60 and 180°C. Under such conditions, the kinetics of mixing were studied by means of an experimental setup consisting of a cup (40 mm diameter, 48 mm height) coupled with the motor of a controlled-strain ARES (Rheometric Scientific, USA), and a stirring device (anchor with 38 mm diameter) coupled with the transducer of the same rheometer. This tool allows for the monitoring of the evolution of torque with time.

The experiment consisted of pouring about 40 g of hot bitumen into the cup with the anchor placed 1 mm above the cup bottom. Prior to the bitumen–polymer blends, blanks of unmodified bitumen at different temperatures were seen to experience a torque increase during processing, in no case higher than 5% (not even for the highest processing temperature). Consequently, a constant torque value, M_0 , for neat bitumen at every temperature has been used to normalise the curves. Thus, the normalised torque (M/M_0), shown in Fig. 3.1, only gives information about polymer-induced changes during processing. As may be seen, a first region (with a constant value of the ratio M/M_0 of 1) can be observed where the base bitumen was stirred for 30 min to ensure that a constant temperature is reached. Polymer addition, carried out after the previous equilibration period, gives rise to a sharp drop in the value of the normalised torque for a very brief time interval followed by a continuous increase up to the end of the experiment. It is worth pointing out that the decrease in the values of the normalised torque is a consequence of the plasticising effect provoked by the addition of a liquid polymer having a much lower viscosity than neat bitumen (10.9 mPa s at 90°C).



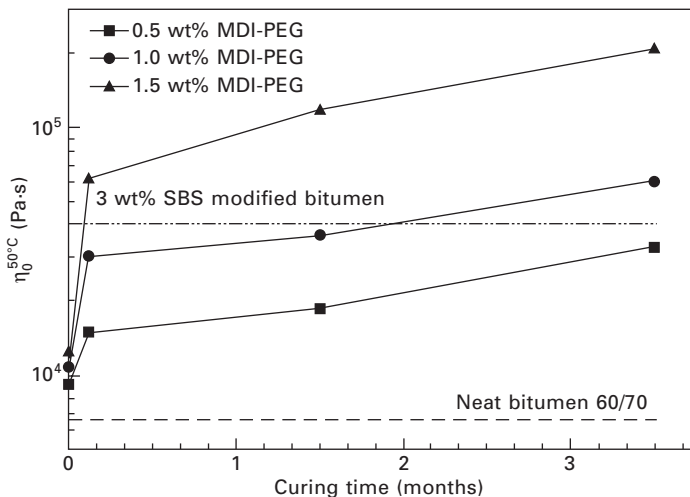
3.1 Evolution of M/M_0 (normalised torque) with time during the preparation of 2 wt% MDI-PEG modified bitumen at temperatures between 60 and 180°C. Adapted from Martín-Alfonso *et al.* (2009).

The torque increase recorded during the experiment may be used to give an insight into the short-term bitumen modification (occurring during processing). As shown in Fig. 3.1, low processing temperatures (e.g. 60°C) lead to remarkable normalised torque increases and slow modification kinetics (torque continues to increase significantly after 7 h of processing). On the contrary, higher mixing temperatures (e.g. 180°C) lead to a faster modification with a low increase of torque (values relatively steady after 7 h). In other words, high temperature seems to shorten reaction times. However, considering the final viscosity of the binder just after processing, different conclusions can be reached (Fig. 3.2). Thus, processing temperatures between 90°C and 120°C, depending on the selected bitumen, gave rise to the highest bitumen viscosity at 60°C (Martín-Alfonso *et al.* 2009). On the contrary, processing temperatures equal to or above 150°C, in addition to provoking bitumen ageing, have been found to lead to polymer thermal degradation and, therefore, to poorer viscosity enhancement (Fig. 3.2). Accordingly, results suggest the existence of an optimum processing temperature between 90 and 120°C (for which modification becomes higher) being the combination of positive (1 and 2) and negative (3) factors: (1) microstructural availability for the formation of a three-dimensional polymer–bitumen network, which increases as temperature becomes lower; (2) reaction ability, which increases with temperature; and (3) polymer degradation, which also increases with temperature.



3.2 Flow curves at 60°C for uncured samples of 2 wt% MDI-PEG modified bitumen mixed at temperatures between 120 and 180°C.
Adapted from Martín-Alfonso *et al.* (2009).

However, long-term modification (due to a slow curing process under room conditions) has been found to produce a much more significant enhancement in binder performance. Even though enhanced viscosity in MDI-PEG modified bitumen is observed immediately after processing (0 days curing) (Fig. 3.2), the most remarkable viscosity increase takes place after a certain curing period. Figure 3.3 shows the evolution of the zero-shear-rate-limiting viscosity, at 50°C, with curing time for modified bitumen samples containing 0.5, 1.0 and 1.5 wt% MDI-PEG. As already mentioned, polymer addition yields a small increase in non-cured binder viscosity compared to the viscosity of neat bitumen. After 7 days of storage at room temperature, the viscosity of the modified bitumen undergoes an important increase relative to the corresponding non-cured sample. In addition, the influence of MDI-PEG concentration on this viscosity increase with curing time is apparent. Thus, the differences in viscosity among samples with different polymer concentration increase with curing time (mainly for 1.5 wt% MDI-PEG modified bitumen). It can be noticed that the addition of 1 wt% MDI-PEG, and after 4 months curing, leads to a zero-shear-rate-limiting viscosity higher than that shown by a 3 wt% SBS-modified bitumen sample (Fig. 3.3). Moreover, a 0.5 wt% MDI-PEG modified bitumen reaches, after 7 months of curing, a value of viscosity (3.2×10^4 Pa s) close to that shown by a 3 wt% SBS modified bitumen (Navarro *et al.* 2006).

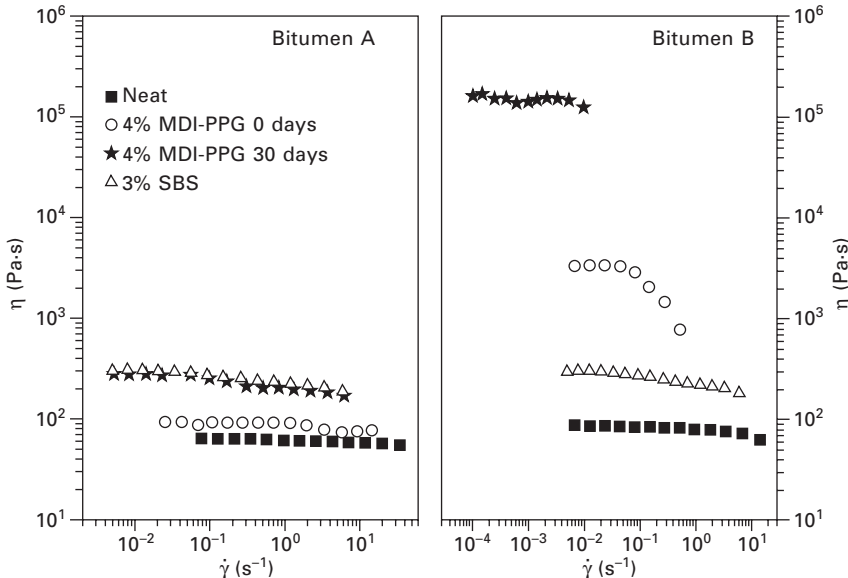


3.3 Evolution of zero-shear-limiting viscosity, at 50°C, with curing time at room temperature for 0.5, 1.0 and 1.5 wt% MDI-PEG modified bitumens. Adapted from Navarro *et al.* (2007).

3.4 The role of the bitumen colloidal nature

The effect of bitumen colloidal nature on the short-term (during processing) and long-term (during curing) modification of bitumen with an isocyanate-based reactive polymer should also be taken into account. Bitumen is a colloidal dispersion of asphaltenes into an oily matrix constituted by saturates, aromatics, and resins (which make up the maltene fraction). This composition is commonly known as SARAs fractions (Lesueur 2009). The chemical composition of bitumen depends primarily on its crude source and processing. The physico-chemical behaviour of bitumen depends on the relative concentration of its different fractions. Accordingly, a variation in its composition may strongly affect its mechanical properties and chemical reactivity (Becker *et al.* 2003; Iqbal *et al.* 2006). Regarding this concern, the selection of the bitumen to be reactively modified is a key factor in achieving successful binder modification. This fact, highlighted in Fig. 3.4, shows the different degree of modification reached by the MDI-PPG addition on two neat bitumens having similar penetration grade, within the 150–200 interval. The strong differences observed in the evolution of the extent of bitumen modification suggest that bitumen reactivity probably plays an important role in the degree of modification obtained (Martín-Alfonso *et al.* 2008a).

Bitumen modification by these pre-polymers is expected to take place by reaction of the isocyanate groups of the polymer with some bitumen compounds containing polar groups ($-OH$; $>NH$). Initially, reaction of isocyanate groups ($-NCO$) with those bitumen compounds takes place during



3.4 Viscous flow curves, at 60°C, for neat bitumen 150/200 and 3% SBS, and 4% MDI-PPG-modified binders (non-cured and 30-day-cured) from bitumens A and B. Adapted from Carrera *et al.* (2009).

processing, followed by a long-term modification process due to further chemical reactions during curing at room temperature. As a result, modified bitumen develops complex microstructures able to increase binder viscosity (and elasticity) at high in-service temperatures. Such a set of reactions seems to be strongly affected by bitumen type and source. Table 3.1 shows the evolution of the SARAs fractions, determined by thin layer chromatography coupled with a flame ionisation detector (TLC/FID), for two neat bitumens and 4 wt% MDI-PPG modified binders. As can be observed, the bitumen asphaltene fraction increases during binder processing (non-cured sample). Primarily, this increase should be attributed to the polymer reacting with the bitumen asphaltene fraction, and the remaining non-reacted polymer, which is not eluted by any of the solvents used in the chromatographic method. The latter seems to explain the results found for bitumen A, which experiences an increase close to 4 wt% (that is, the actual polymer concentration added) for the asphaltene fraction, after processing (Table 3.1).

On the contrary, modified bitumen B showed an asphaltene concentration increment close to 7% as compared with neat bitumen, much higher than that corresponding to the actual MDI-PPG added. This increase results from the reaction between some of the bitumen compounds being less polar than asphaltenes (e.g., aromatics and/or resins) and NCO groups during processing, and would explain the changes observed for the corresponding bitumen fractions (see Table 3.1). In addition, long-term curing reactions seem to

Table 3.1 SARAs fractions for neat bitumen, non-cured and cured modified binders

Compounds	Bitumen A			Bitumen B		
	Neat	4% MDI-PPG 0 days	4% MDI-PPG 30 days ^a	Neat	4% MDI-PPG 0 days	4% MDI-PPG 30 days ^a
Saturates (%) ^b	8.24	7.53	5.99	8.42	8.72	9.96
Aromatics (%) ^b	52.46	51.22	50.40	45.78	42.63	32.35
Resins (%) ^b	26.65	24.45	24.66	21.98	17.86	27.93
Asphaltenes (%) ^b	12.65	16.80	18.95	23.82	30.79	29.02

^aCuring under room conditions.

^bChromatographic peak percentage area.

Source: adapted from Carrera *et al.* (2009).

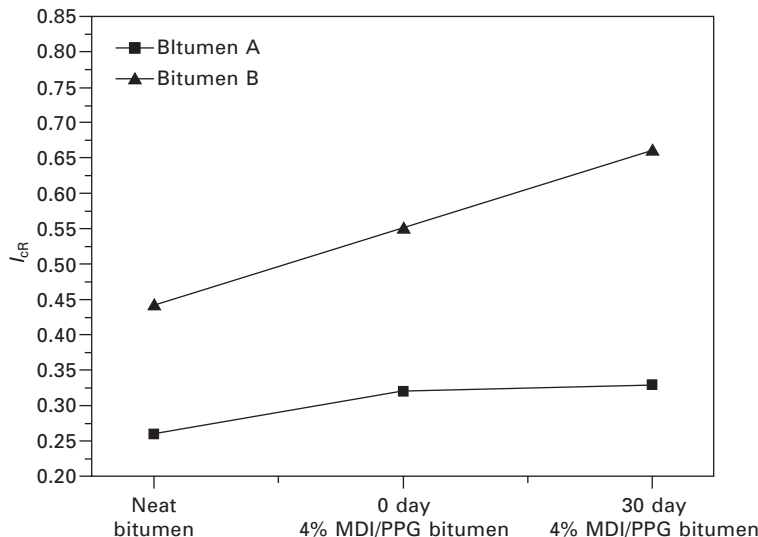
increase the concentration of the most polar groups (resins and asphaltenes), with slight changes in the saturate fraction.

This issue can be explored further by determining a modified Gaestel colloidal index (Gaestel *et al.* 1971; Baginska and Gawel 2004), I_{cR} , which accounts for chemical composition changes due to the reactive modification by MDI-PPG, and may be defined as follows:

$$I_{cR} = \frac{\text{saturates} + \text{asphaltenes} + \frac{\text{NCO}}{\text{polars}}}{\text{aromatics} + \text{resins}}$$

where NCO/polars refers to the resulting species formed by chemical reactions between reactive polymer and polar bitumen compounds, which cannot be eluted by any of the solvents employed in the chromatographic method. Figure 3.5 displays the evolution of the modified colloidal index, for the different bitumen samples studied, prior to and after reactive modification. According to the above-defined I_{cR} , a higher modified colloidal index would mean larger asphaltene clusters, leading to materials with more developed microstructures (i.e. with higher viscosity and elasticity). As may be seen, samples from bitumen B have the highest colloidal index values and, consequently, show the highest viscosities at high in-service temperatures (60°C) (Fig. 3.4).

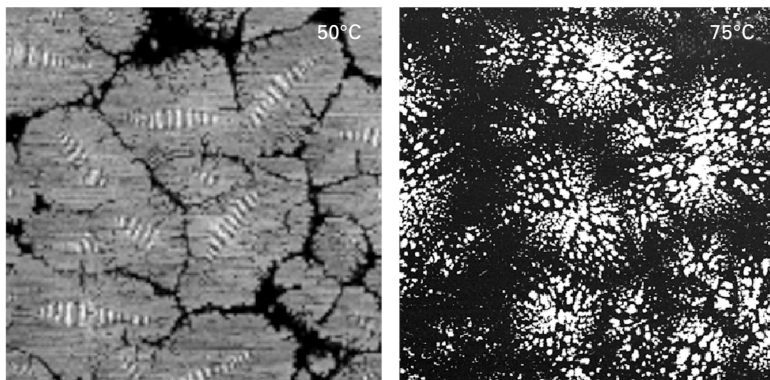
However, the modified colloidal index itself is not an adequate way to accurately predict the degree of modification expected for the resulting binders. In addition, bitumen microstructure must also be considered. In fact, the final degree of bitumen modification turns out to be a combination of two factors: firstly, bitumen reactivity with isocyanate-based polymers, and secondly, the ability of the bitumen microstructure to form a three-dimensional polymer-bitumen network, which develops further during binder curing (Carrera *et al.* 2009).



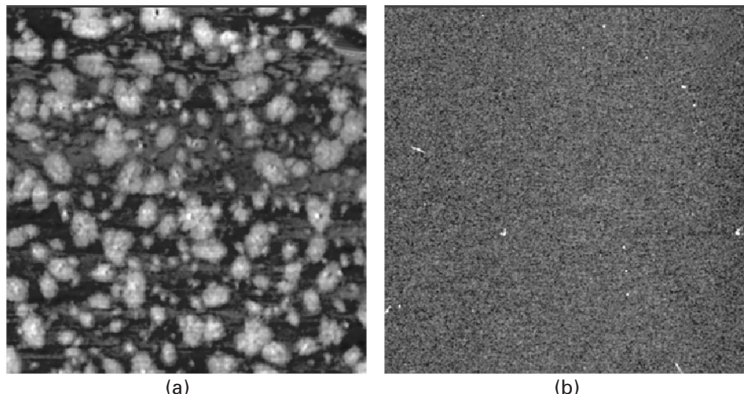
3.5 Colloidal index values for neat bitumen, non-cured and cured modified binders. Adapted from Carrera *et al.* (2009).

According to the bitumen colloidal model, aggregates formed by the association of several asphaltene particles are covered by a shell of resins that becomes thinner as temperature increases (Lesueur *et al.* 1996). The remaining resin molecules as well as saturates and aromatics make up the dispersing matrix. This model has been able to successfully explain most of the questions that arise in relation to bitumen microstructure. AFM observations in phase mode readily support this model and consequently help explain the observed bitumen softening at high in-service temperatures. Images in Fig. 3.6 were taken at 50 and 75°C on samples of neat bitumen (60/70 penetration grade). Two regions, dark and light, can be clearly distinguished. Each of them, which present very different mechanical response, corresponds to the maltenic and asphaltenic phases, respectively. Thus, asphaltene–resin micelles (light area) present a higher level of elasticity than the maltenic matrix, where micelles are dispersed (dark area). In this case, the bitumen sample is composed of ‘bee-like’ structures, attributed to large asphaltene domains (known to be formed by the association of round asphaltene particles with a diameter of about 100–200 nm), peptised by resins and surrounded by a smooth phase which corresponds to an oil phase (Loeber *et al.* 1996, 1998).

It can be observed that an increase in the testing temperature leads to an increase in the dark area because, as described by the colloidal model, a larger quantity of the resins covering the asphaltene micelles would remain dissolved. As a consequence, smaller asphaltene–resin domains would reduce their interaction with other neighbouring domains under high in-service



3.6 AFM pictures corresponding to a neat bitumen sample, with 60/70 penetration grade, at 50°C and 75°C. Window size: 25 $\mu\text{m} \times 25 \mu\text{m}$. Adapted from Martín-Alfonso *et al.* (2009).



3.7 AFM micrographs, at 30°C, for two neat bitumens with different microstructure: (a) 'flake-like' dispersion; (b) 'fine' dispersion. Window 25 \times 25 μm . Adapted from Carrera *et al.* (2009).

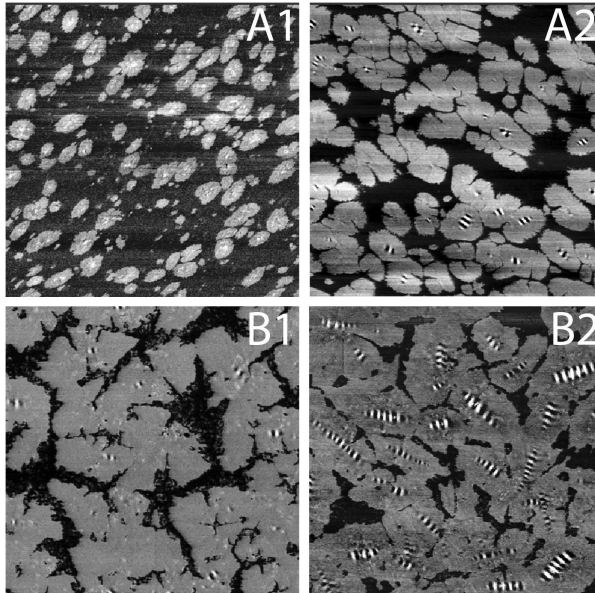
temperatures, significantly decreasing the bitumen viscosity and its elastic properties.

However, in addition to the above-described 'bee-like' structure, other possible bitumen structures have been identified: see Fig. 3.7. For instance, the bitumen sample shown in Fig. 3.7(a) matches what has been referred to as a 'flake-like' dispersion, and the bitumen sample in Fig. 3.7(b) corresponds to the so-called 'fine' dispersion (Masson *et al.* 2006). Among them, bitumen samples presenting 'bee-like' structures (e.g. bitumen B in Fig. 3.4) undergo higher degrees of modification than those showing 'flake-like' (bitumen A in Fig. 3.4) or 'fine' dispersions (Carrera *et al.* 2010a).

This behaviour arises from the modification mechanism found for isocyanate-

based pre-polymers. MDI-PEG addition may contribute to the development of a microstructural network formed by reaction of the polymer with some compounds of the asphaltene-rich region (i.e. polar resins and asphaltenes containing $-OH$ and $>NH$ groups). This hypothesis is supported by the AFM images shown in Fig. 3.8, taken at 50°C, for neat bitumen and 30-day-cured MDI-PPG modified binders A (Fig. 3.8A1 and 3.8A2, respectively) and B (Fig. 3.8B1 and 3.8B2, respectively). In general, the addition of 4 wt% MDI-PPG to bitumen yields larger light regions in both binders. However, quite different microstructures are observed in these modified binders: a well-developed three-dimensional network for binder B and a highly dispersed micelle microstructure for binder A. Polymer addition gives rise to a modified binder microstructure with lower thermal susceptibility. This would explain the improved viscosity of MDI-PEG modified bitumens found in the high temperature region (Fig. 3.4). Moreover, such a modification has found to lead to a macroscopic homogeneous material which does not show phase separation after storage at high temperature (Navarro *et al.* 2007).

As a result, the chemical composition of neat bitumen and its microstructure play relevant roles in bitumen modification by low-molecular-weight reactive polymers. The highest modification capability is obtained for neat bitumen that exhibits both a well-developed complex microstructure and a high chemical



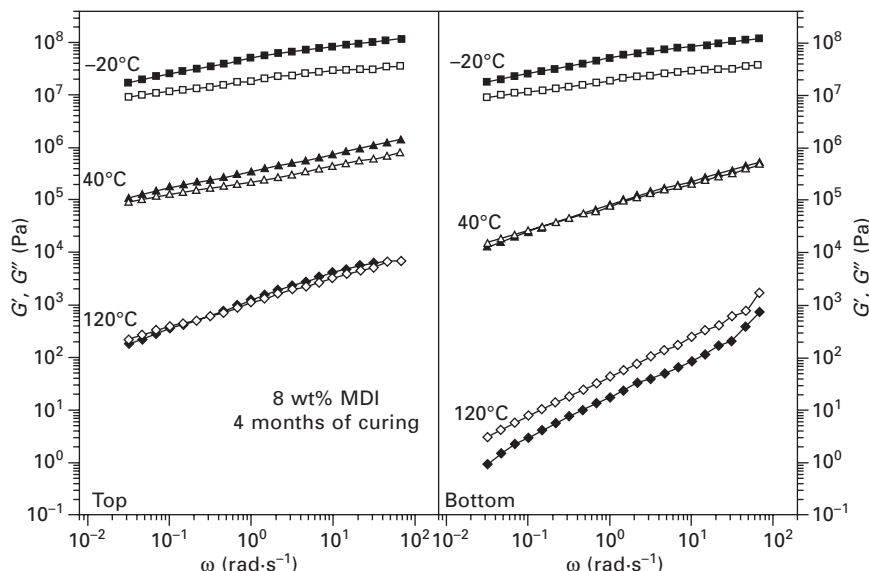
3.8 AFM micrographs (25 \times 25 μm), at 50°C, for neat (A1) and MDI-PPG modified (A2) bitumen A, and neat (B1) and MDI-PPG modified (B2) bitumen B.

reactivity with the isocyanate groups ($-NCO$). Accordingly, greater bitumen modification is obtained for neat bitumen samples with high concentrations of polar compounds (polar aromatics, resins, and asphaltenes) able to react with pre-polymer $-NCO$ groups, and with a well-developed asphaltene-rich colloidal microstructure (generally, neat bitumen having a high colloidal index and 'bee-like' microstructure).

3.5 Polyurethane/urea-based modified bitumen

In addition to short-term modification, long-term bitumen modification by MDI-based pre-polymers seems to be a complex process involving other factors previously not considered in reactive modification (i.e. modification results not only from a simple reaction between pre-polymer and some bitumen compounds).

The above-commented curing experiments consisted of a thin layer of modified bitumen that was exposed to the environmental conditions. Additional experiments were performed on a thicker layer placed into an opened container, taking samples from the top (exposed to air) and from the bottom (not exposed to air). Figure 3.9 shows the frequency dependence of the linear viscoelastic functions (elastic, G' , and viscous, G'' , moduli) at selected



3.9 Frequency dependence of the storage and loss moduli, at temperatures between -20 and $120^\circ C$, for 8 wt% MDI-PEG modified bitumen samples taken from the top and bottom of the container, after 4 months of storage under room conditions. Adapted from Martín-Alfonso *et al.* (2008b).

temperatures, ranging from -20 to 120°C , for PMB samples containing 8 wt% MDI-PEG taken from the top and bottom of the container. The binder was stored for 4 months. Hereinafter these samples will be referred to as 'top' and 'bottom' samples, respectively. For every temperature tested, G' and G'' curves corresponding to top samples exhibit higher values of G' and G'' than the bottom samples. However, the differences become smaller as temperature decreases, that is, near the glassy region. Furthermore, G' is higher than G'' in the whole range of temperatures studied for the top samples. The bottom samples show higher values of elastic modulus at temperatures below 10°C , with the viscous behaviour being predominant above 80°C . The terminal region, with G' and G'' being proportional to ω and ω^2 in a double-log plot, was not found in any case, not even at temperatures as high as 120°C . On the contrary, top samples showed improved elastic characteristics ($G' > G''$) in the whole temperature range studied, with a typical gel-like behaviour at 120°C (De Rosa and Winter 1994). As a result, polymer addition and the curing process lead to more complex materials with enhanced elastic behaviour and lower temperature susceptibility.

Hence, the modified bitumen in contact with the environment undergoes notable differences in its rheological response in relation to that of the bottom of the container, due most probably to a different curing mechanism. Air moisture (and bitumen oxidation) promotes polymer intermolecular reactions, which would considerably increase the molecular weight of bitumen polar compounds, leading to an increase in the viscoelastic moduli. This issue has also been suggested elsewhere for a SEBS functionalised with maleic anhydride (Becker *et al.* 2003). Long-term bitumen modification seems to be related to the reaction between reactive polymer and bitumen compounds and to the environmental conditions (probably due to air moisture). Under such conditions, water can slowly diffuse into the bitumen and react with the remaining free NCO groups, giving rise to an increase in the molecular weight of the polymer-bitumen molecules.

It is well known that there are two types of chemical reaction that occur during the reaction between NCO functionalised molecules and water. One is the reaction of isocyanate with water leading to an unstable carbamic acid, which decomposes to an amine and carbon dioxide. The other type of reaction leads to network formation and results from the reaction between isocyanate groups with the amine that was generated during the decomposition of carbamic acid, forming a disubstituted urea. Both types of reactions are exothermic and lead to an increase in the viscosity of the medium, due to the development of a polymer-bitumen network (Zeng 2002).

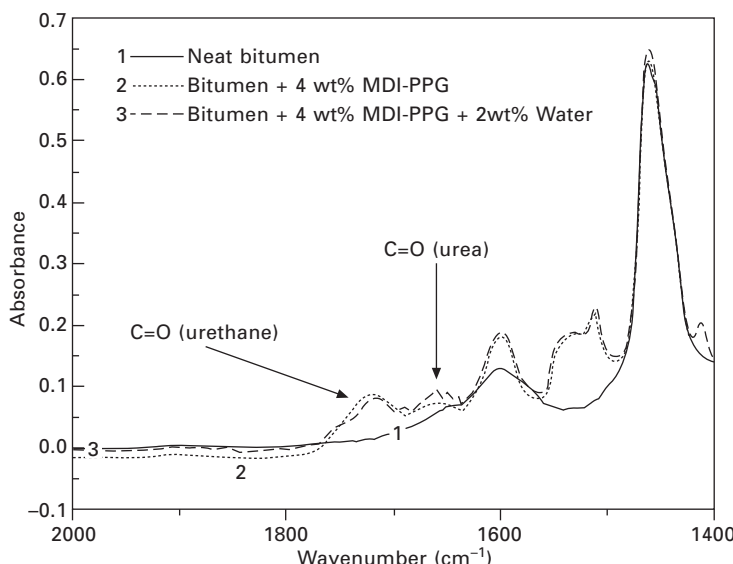
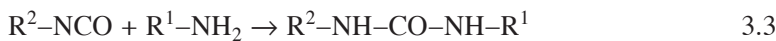
Therefore, a chemical modification mechanism via a set of three reactions has been proposed (Carrera *et al.* 2010b). Firstly, 'water-free' MDI-polymer modification of bitumen is expected to occur by reaction of $-\text{NCO}$ groups of the pre-polymer with functional groups containing active hydrogen atoms

(mainly $-\text{OH}$), typically present in the asphaltene micelles (Mondal and Khakhar 2004; Segura *et al.* 2005; Singh *et al.* 2003). This reaction can be written as follows:



Reaction 3.1 would lead to the formation of a higher number of urethane bonds (peak at 1725 cm^{-1} shown in Fig. 3.10) between polymer and certain bitumen groups (present in asphaltenes, resins and even aromatics) that occasionally might link asphaltene domains to each other. This first reaction would be responsible for the bitumen short-term modification.

Secondly, such large asphaltene domains might become even larger with the formation of urea linkages (peak at 1640 cm^{-1} shown in Fig. 3.10) after water addition by reaction with $-\text{NCO}$ groups available in these large asphaltene domains. But previously, added water yields an unstable carbamic acid which decomposes to an amine and carbon dioxide (reaction 3.2). Finally, the highly reactive amine is expected to react with isocyanate groups left in MDI-PPG chains, previously linked to bitumen compounds, with the formation of urea groups (reaction 3.3) (Mondal and Khakhar 2004; Segura *et al.* 2005). This set of reactions can be written as follows:

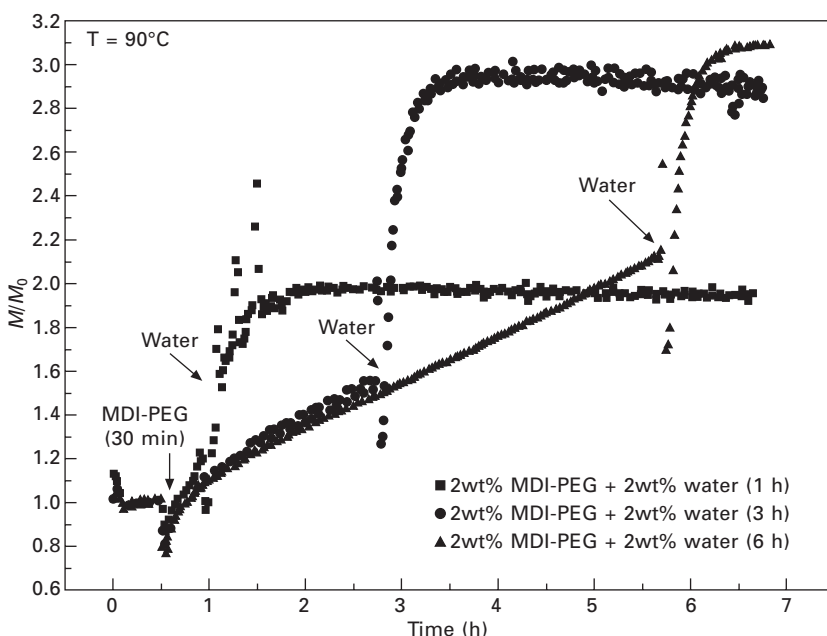


3.10 FTIR spectra showing C=O (urethane/urea) bands for neat and 4 wt% MDI-PPG modified bitumen B, before and after water addition. Adapted from Carrera *et al.* (2010b).

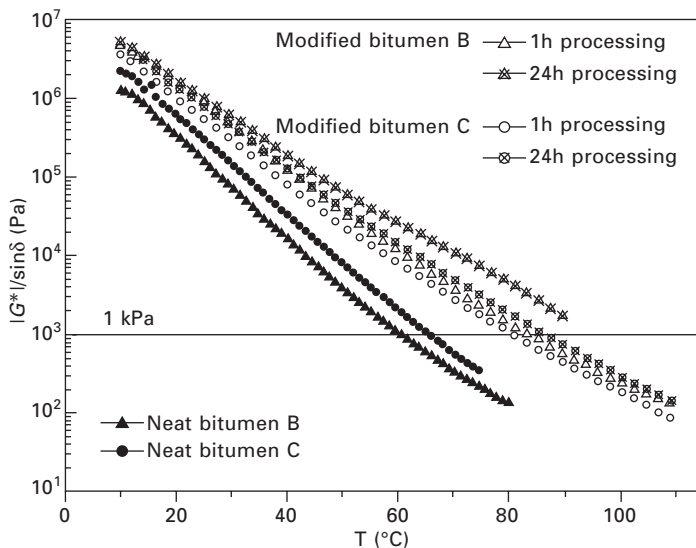
As a result, polymer addition (and its reaction with air moisture) contributes to the development of a new microstructure (during long-term bitumen modification) which has been proved to present a more satisfactory performance at increased temperatures, most probably due to the formation of chemical bonds between polymer and polar compounds within bitumen, as described above. So, water can slowly diffuse into bitumen and react with free remaining NCO groups, giving rise to an increase in the molecular weight of the polymer-bitumen molecules.

This approach may be used to increase the bitumen modification rate and, therefore, to prevent long-term bitumen modification. As deduced from the remarkable torque increase shown in Fig. 3.11, water addition during mixing seems to provoke an enhancement of the short-term modification, above all if water is added close to the end of the manufacturing process.

Accordingly, rigorous control of the processing conditions during the first reaction, which leads to the formation of a higher number of urethane bonds between polymer and certain bitumen groups, has turned out to be an additional key factor for the manufacture of these products. This result suggests that a much more remarkable bitumen modification can be achieved if MDI-PPG/bitumen reactions are favoured by using long processing times before water is added. In this sense, Fig. 3.12 shows the evolution of the 'rutting parameter',



3.11 Evolution with time of the normalised torque (M/M_0) during the processing of different bitumen/MDI-PEG/water blends, at 90°C and 60 rpm. Adapted from Martín-Alfonso *et al.* (2008b).



3.12 Temperature dependence of the 'rutting parameter', $|G^*|/\sin \delta$, for neat bitumen and MDI-PPG–water modified binders (from bitumen C and D) after 1 h and 24 h mixing at 90°C. Adapted from Carrera *et al.* (2010b).

$|G^*|/\sin \delta$, with temperature for different MDI-PPG–water modified bitumens. It can be seen that the rutting criterion outlined in AASHTO Designation MP1 (1993) (the temperature at which the binder has a value of $|G^*|/\sin \delta$, under certain testing conditions, equal to 1 kPa) is always satisfied within the temperature interval from 55°C to 65°C for the different neat bitumen samples studied in this work. Then, the addition of MDI-PPG and water to bitumen sample B produces a very significant enhancement, increasing the rutting critical temperature to values close to or above 90°C. Such an increase turns out to be more apparent for the longest reaction period between bitumen and the reactive polymer (i.e. before water addition) (Fig. 3.12). Similarly, MDI-PPG modified bitumen B was seen to undergo significant changes in penetration and ring and ball softening temperature after 24 h processing, leading to a much harder bituminous binder. For instance, after the addition of a 4 wt% MDI-PPG, penetration decreased from 150–200 to values within the 60–70 interval and the softening temperature increased to 64°C (Carrera *et al.* 2010b).

3.6 Bitumen foaming and future trends

Presently, foamed asphalt appears as an alternative to traditional hot-mix asphalt. Both low energy consumption and environmental side-effect-free paving technologies, which involve the mixing of mineral aggregates with a

bitumen emulsion or foamed bitumen, have emerged over the last decades. Cold in-place recycling, which has become an economical and sustainable paving practice, has been extensively used in the rehabilitation of pavements in many countries throughout the world (He and Wong 2006; Jenkins *et al.* 2000). Emulsification and foaming are competitive technologies in the asphalt pavement industry. Both techniques reduce the quantity of bitumen needed compared to traditional paving, because of an increase in the surface area and, consequently, a reduction in viscosity. However, a potential advantage of foamed bitumen is a shorter curing time before traffic gets back on the route, because foamed bitumen requires less water than an emulsion.

The physical bitumen foaming process, first proposed by Csanyi in the mid-1950s (Csanyi 1957) and further improved by a number of oil companies, consists of the injection of water into hot bitumen. As a result, the physical properties of the bitumen are temporarily altered when the injected water, in contact with the hot bitumen, is turned into vapour, which is trapped in thousands of tiny bitumen bubbles (Muthen 1998; Jenkins *et al.* 2000).

Recently, a new chemical foaming technology involving the use of foam-enhancing agents is being developed. The use of a poly(propylene glycol) functionalised with 4,4'-methylenebis(phenyl isocyanate) achieves a remarkable increase in the time taken for the foam to collapse and leads to a modified binder exhibiting significantly improved performance. The reactive foaming method involves the reaction between water and free -NCO groups, producing an amine and releasing carbon dioxide (reaction 3.2), which favours bitumen expansion. Consequently, bitumen modification is achieved via reactions 3.1 and 3.3.

In the standard physical procedure, foaming is promoted by the formation of tiny bubbles of steam after water comes into contact with hot bitumen (above 100°C and by a sudden pressure reduction), giving rise to foamed bitumen that resumes its original properties after the foam dissipates. Instead, the reactive process leads to both unstable and stable foams depending on the selection of the foaming agent and the processing conditions. Consequently, reactive bituminous foams may be applied as construction materials not only for the paving industry but also in buildings.

3.6.1 Bitumen foaming for pavement

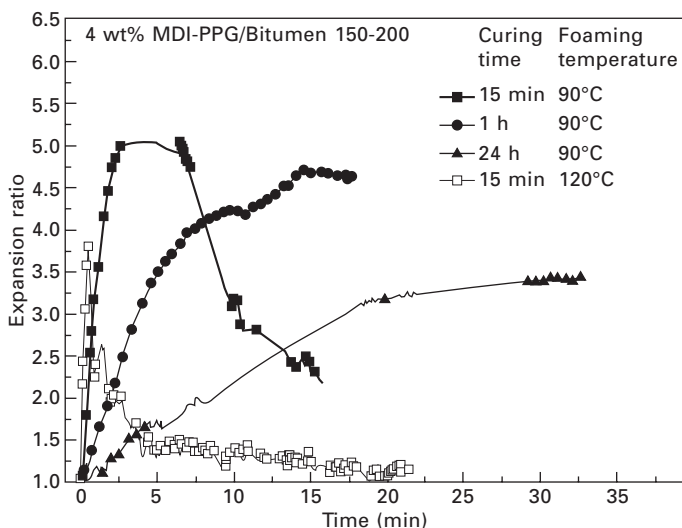
Some attempts have been made to develop a novel foamed asphalt technology involving polyurethane-modified bitumen (Carrera *et al.* 2010c). Normally, the polymer used has been a MDI-PPG. MDI-PPG polymers are synthesised following the procedure outlined in Section 3.3. Their main characteristics are molar ratio 1:3, functionality less than 3, average molecular weight about 3000 g/mol and low polydispersity (less than 1.5).

Blends for foamed pavement applications are formulated using a two-step

procedure. Firstly, modified bitumen is fabricated by mixing neat bitumen with 4 wt% MDI-PPG. In this step the processing conditions involve mixing times between 15 min and 1 h and temperatures ranging from 90 to 120°C. Secondly, this modified bitumen is foamed by adding water (1–2 wt%) in a low shear stirred tank for a short period so as to disperse the water.

The evolution of the expansion ratio (ER) (defined as the ratio of the volume of foam relative to the original volume of reactive polymer-modified bitumen), as a function of both time and processing temperature, is presented in Fig. 3.13 for a typical bitumen. At 90°C, ER suddenly increases up to a maximum value of 5 and then dramatically decreases, for a curing time less than 1 hour. This evolution may be explained when taking into consideration the large –NCO group content left in the reactive polymer, after 15 min of processing, that favours fast formation of bubbles (the first increase in ER) within a soft bituminous matrix, which then quickly collapses. For longer processing times a marked drop in both the foamability and the foaming rate is observed. Thus, regarding the maximum foamability, ER_{max}, the lowest values are obtained for the '24-h' sample. These results are directly related to a lower quantity of free –NCO groups being available after the 24 h reaction between MDI-PPG and some of the bitumen compounds (reaction 3.1) and the subsequent reduction in the volume of carbon dioxide released after water addition (reaction 3.2).

Increasing foaming temperature (120°C) leads to a slight reduction of the maximum foamability (ER_{max}). Thus, ER always shows a rapid increase



3.13 Evolution of foamed bitumen expansion ratio (ER) with time, at different foaming temperatures and curing times. Adapted from Carrera *et al.* (2010c).

within the first 1–2 min, up to a maximum ER value, which is then followed by an exponential decay. The highest values were reached for the ‘15-min’ and ‘1-h’ samples (between 3.75 and 4), whereas a slightly lower value was noticed for the ‘24-h’ sample (about 3.25) (Carrera *et al.* 2010c).

When foaming tests, at 90°C and 120°C, for the ‘15-min’ samples are compared, a delay in the ER overshoot with a decrease in the foaming temperature was observed (i.e. the foam collapses later at 90°C). As for standard bitumen foaming (He and Wong 2006), bubbles collapse when the elongation limit of the covering bitumen film is exceeded. The bitumen viscosity at 90°C is higher than that at 120°C. Accordingly, such an elongation limit would be more difficult to exceed in a matrix with a higher viscosity, that is, at lower temperature. Hence, a higher number of unbroken bubbles accumulate continually, giving rise to both higher values of ERmax and the elapsed time at the overshoot, resulting in a more stable foam (He and Wong 2006). On the other hand, the behaviour observed may also be the result of water loss, due to evaporation, when the water comes into contact with hot bitumen at 120°C (above the water boiling point). This may lead to a reduction in the volume of carbon dioxide produced.

Bitumen foams generally show values of ERmax either very close to or above 4, a value which has been reported to be the minimum value for appropriate mixing in paving practice (Jenkins and van de Ven 2001).

Also, an additional benefit of this reactive foaming, in comparison with the traditional practice, would be the longer time which elapses prior to the foam collapsing, which would allow for an in-place mixing with the aggregate (e.g. during cold-in-place asphalt recycling). As a result, using reactive isocyanate-based polymers may become a flexible way to obtain a wide variety of foamed binders with different foamability and stability characteristics, by merely changing the processing time and foaming temperature. Moreover, as previously seen, MDI-PPG-modified bitumen foaming (by reaction with added water) leads to a binding material with highly enhanced viscosity at 60°C, a fact that may improve its performance at high in-service temperatures (Carrera *et al.* 2010a).

3.6.2 Bitumen foaming for insulation

One of the first architectural design considerations is insulation, because of the high cost of air conditioning and heating of buildings, and thus the need for greater insulating efficiency. Polyurethane foams can be used for thermal insulation, as excellent energy savers, since the air trapped within the honeycomb-like structure confers quite low thermal conductivity. Examples in buildings applications are layers of floor and ceiling coverings, roofing boards, sheathing, perimeter insulation, sprayed walls/ceilings, industrial tanks, curtain wall panels, etc. (Szycher 1999; Guo *et al.* 2000). For such

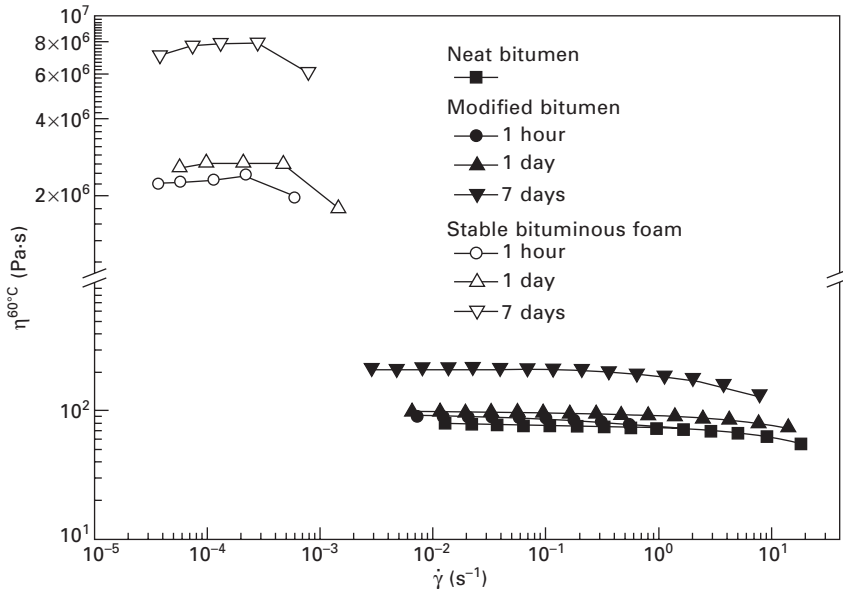
applications, stable bituminous foams may be considered as an emerging technology in the field of insulation.

Stable bituminous foams may be obtained by means of a process similar to that used for polyurethane foams (Eaves 2004). Firstly, during processing and high temperature curing, MDI-PPG reacts with bitumen compounds, leading to modified bitumens. The second step begins after water addition, and involves several stages (Izquierdo *et al.* 2010). Initially, since water solubility in bitumen is very low, the reacting system is immediately and severely stirred, for 30 s, to ensure an adequate dispersion of the reactants. Then, agitation is stopped and nucleation and growth of gas bubbles take place in a bituminous medium. These bubbles, dispersed in a liquid phase, are thermodynamically unstable and tend to escape from the dispersing medium. As pointed out in the previous section, at low polymer concentrations the resulting bituminous foam is unstable (since the bulk foamed blend expands up to a maximum volume and then decreases). On the contrary, at polymer concentrations large enough (e.g. 10 wt% MDI-PPG), the decrease in the foam final volume is not observed, as in the case for polyurethane foams. In this latter case, reactions involving water lead to a dramatic increase in MDI modified bitumen consistency, avoiding the collapse of bubbles.

It is important to underline that all bituminous foams have similar densities (350–400 kg/m³) and, consequently, their thermo-mechanical properties may be successfully compared. Taking into account that the approximate densities of bitumen and MDI-PPG are 1.0 and 1.2 g/ml, respectively, foaming yields a considerable reduction in material density.

Figure 3.14 shows the viscous flow curves, at 60°C, for modified bitumen having 10 wt% MDI-PPG and their corresponding bituminous foams, as a function of curing time, at 90°C, ranging from 1 hour (just after processing) up to 7 days. As can be observed, viscosity values corresponding to modified bitumen obtained just after processing (1 hour in Fig. 3.14) are similar to those for neat bitumen. Thereby, the expected viscosity reduction as a consequence of the addition of a low-viscosity liquid (pre-polymer) is damped by polymer-bitumen reactions occurring during mixing. However, a high curing temperature (at 90°C, and in the absence of water) causes a slight increase in viscosity, which is more important after 7 days of curing. Nevertheless, the addition of water yields the most significant changes in flow properties. Thus, a steep rise, of more than four orders of magnitude, in Newtonian viscosity is noticed, and the critical shear rate for the onset of the shear-thinning region is markedly shifted to much lower shear rates. These facts suggest the development of a highly structured system due to chemical reactions during the chemical blowing process.

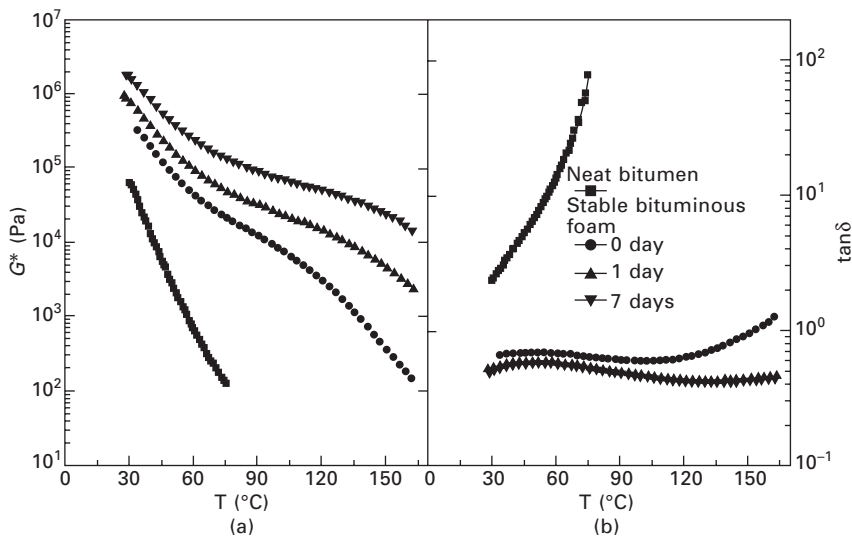
It is well known that linear viscoelastic properties of polymer-modified bitumen, over a wide range of in-service temperatures, can be determined by means of dynamic mechanical methods, consisting of temperature sweeps



3.14 Viscous flow curves, at 60°C, for 10 wt% MDI-PPG modified bitumen and bituminous foam (10 wt% MDI-PPG and 2 wt% water), as a function of curing time at 90°C. Adapted from Izquierdo *et al.* (2010).

in an oscillatory-shear type testing mode. The evolution of both complex shear modulus (stiffness and overall resistance to deformation), G^* , and the loss tangent, $\tan \delta$, (inversely proportional to the overall elasticity of the sample) with temperature is presented in Fig. 3.15(a) and 15(b) respectively, for typical foamed bitumen samples. As can be observed, complex modulus values significantly increase with curing time. Thus, the addition of 2 wt% water to 10 wt% MDI-PPG modified bitumen yields a dramatic increase in complex modulus values, mainly at temperatures above 60°C, even after a short curing time. These differences are larger as the testing temperature is raised. In addition, a flattening in the slope of G^* vs. temperature is noticed as curing time increases, denoting a significant reduction in material thermal susceptibility.

On the other hand, values of the loss tangent for bituminous foams are dramatically lower than those found for 10 wt% MDI-PPG modified bitumen, and remain always below 1. This indicates a predominantly elastic behaviour, which is even more pronounced after 1 day of curing. The maximum loss tangent, at a temperature of around 50°C, is related to deformation-relaxation processes of new structures which evolve as a result of bitumen–polymer reactions. However, this process occurs in a predominantly elastic medium for these bituminous foams. In fact, a loss tangent minimum value below 1

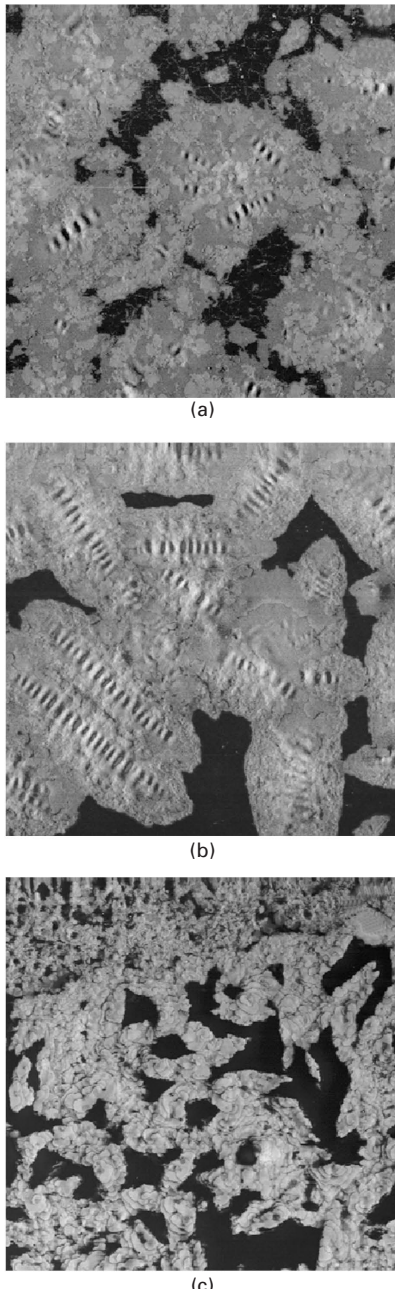


3.15 Temperature sweep tests in oscillatory shear, at 10 rad/s, for bituminous foam (10 wt% MDI-PPG; 2 wt% water): evolution of the complex shear modulus (a), and loss tangent (b) as a function of curing time at 90°C. Adapted from Izquierdo *et al.* (2010).

is indicative of a rubbery region, not observed in modified bitumens. This behaviour is a consequence of the development, during foam formation, of a chemically based three-dimensional network throughout the bitumen. Thus, a gel-like behaviour is observed in the experimental window studied and, consequently, the elastic characteristics of the binder are greatly improved.

Some of the thermo-rheological results shown may be additionally supported by means of atomic force microscopy (AFM) observations in phase mode. Figure 3.16(a) and (b) show AFM phase images corresponding to neat and modified bitumen after 7 days of curing at 90°C. Two regions, with two different intensity levels (light and dark), can be clearly distinguished. Thus, solid particles of asphaltenes (black and white streaks) appear covered by a solid shell of resins (light grey areas) surrounded by the maltenic matrix (darkest areas), in which asphaltene micelles (i.e. asphaltenes peptised by resins) are dispersed. For modified bitumen with 10 wt% MDI-PPG, Fig. 3.16(b), shows more compact asphaltic regions, as compared to neat bitumen. Consequently, polymer addition gives rise to the development of a highly structured bitumen matrix, due to the formation of chemical bonds between polymer and polar bitumen compounds.

Figure 3.16(c) shows a foamed bitumen AFM micrograph after 7 days of curing at 90°C. In contrast to the results shown in Fig. 3.16(a) and (b), a bitumen colloidal structure is not now apparent, because it vanishes as a result



3.16 AFM micrographs at 25°C for (a) neat bitumen, (b) modified bitumen after 7 days of curing at 90°C, and (c) foamed bitumen (window 25 × 25 μm). Adapted from Izquierdo *et al.* (2010).

of the reactions involving water discussed above. Thus, these micrographs show a continuous matrix of rigid phase (light areas), attributed to a three-dimensional network of high molecular weight polymer–bitumen compounds. In addition, dispersed soft regions are also clearly distinguished (dark areas), resulting from non-reacted bitumen phase or even from the presence of gas bubbles. Moreover, Fig. 3.16(c) shows a globular or ‘ball-like’ structure, which resembles the structure of polyurethane foams (Yontz *et al.* 2008).

These results suggest that the use of reactive polymer, synthesised by reaction of 4,4'-methylenebis(phenyl isocyanate) (MDI) with a low molecular weight poly(propylene glycol) (PPG), is a promising technique in the manufacture of bitumen-based coating materials and stable foamed bitumen. Specifically, it is possible to obtain stable foamed binders using conventional bitumen modified with 10 wt% MDI-PPG and 2 wt% water. These foams present a similar microstructure to that obtained for polyurethane foams. Viscous and linear viscoelastic properties of modified binders are dramatically improved when stable foamed binders are obtained.

3.7 Sources of further information and advice

Modification of bitumen with isocyanates is a new topic in the pavement and building construction fields. Few research groups are currently studying this topic, among others including those from the Complex Fluid Engineering Laboratory of the University of Huelva (www.complexfluidlab.com), and Professors Diogo and Bordado from the Technical University of Lisbon. Specifically on this topic, further reading can be found in articles from Navarro *et al.* (2006, 2007, 2009), Martín-Alfonso *et al.* (2008a, 2008b, 2009), Carrera *et al.* (2009, 2010a, 2010b, 2010c) and Izquierdo *et al.* (2010). It is worth pointing out that these articles describe the results from two research projects sponsored by a Spanish MEC-FEDER programme (Research Projects MAT2004-06299-C02-02 and MAT2007-61460).

In addition, there is a great variety of databases of scientific literature useful for researchers and technicians. The most common source of research papers is web databases such as Scopus (www.scopus.com) or Engineering Village (www.engineeringvillage.com), and scientific publisher websites such as Science Direct (www.sciencedirect.com), Springer (www.springerlink.com), John Wiley Interscience (www.interscience.wiley.com/) and American Chemical Society Publications (<http://pubs.acs.org/>).

A good source of information about diisocyanates and polyol technology is The European Diisocyanate and Polyol Producers Association (ISOPA) (www.isopa.org). This association is devoted to promoting the highest standards of best practice in the distribution and use of diisocyanates and polyols. The website contains information on the environmental, health and safety aspects of raw materials for polyurethanes.

Among the large number of suppliers of diisocyanates, BASF (www2.bASF.us/urethanechemicals) offers interesting links to the Company Handbook of Raw Chemicals (MDI and TDI). Similarly, Dow Polyurethanes (www.dow.com/polyurethane) offers online technical support on polyols and isocyanates.

Other sources dealing with foamed bitumen are:

- The Transportation Association of Canada (TAC) (www.tac-atc.ca/english). TAC is a neutral forum for gathering or exchanging ideas, information and knowledge on technical guidelines and best practices on roadways. TAC offers a wide range of products and services to members and non-members, among others on the topic of foamed bitumen with links to the TAC conference papers in PDF format.
- The National Center for Pavement Preservation (NCP) leads to collaborative efforts among government, industry and academia in the advancement of pavement preservation (www.pavementpreservation.org). A major goal for NCP is to maintain and expand its comprehensive, state-of-the-art resource library for pavement preservation practitioners. In this site there are interesting links, such as to the ARRA Basic Asphalt Recycling Manual (2001) (www.pavementpreservation.org/toolbox/links/1-124-BARM1.pdf). The Asphalt Recycling and Reclaiming Association (ARRA) (www.arra.org) is an association that edits the ARRA Basic Asphalt Recycling Manual.
- The Council for Scientific and Industrial Research (CSIR) in South Africa (asphalt.csir.co.za/foamasph/index.htm) presents result on foamed asphalt experience in South Africa.
- The Wirtgen Group (www.wirtgen.de) is a global company that offers a full range of mobile machines and high-quality services on everything relating to road construction, including foamed asphalt technologies.

3.8 References

AASHTO Designation MP1, 1993, American Association of Stage Highway and Transportation Officials, *Standard specification for performance graded binder*, Gaithersburg, MD.

Airey, G.D., 2003, 'Rheological properties of styrene–butadiene–styrene polymer modified road bitumens'. *Fuel* 82, 1709–1719.

Ait-Kadi, A., Brahimi, H., Bousmina, M., 1996, 'Polymer blends for enhanced asphalt binders'. *Polym. Eng. Sci.* 36, 1724–1733.

Baginska, K., Gawel, I., 2004, 'Effect of origin and technology on the chemical composition and colloidal stability of bitumens'. *Fuel Process. Technol.* 85, 1453–1462.

Becker, Y., Müller, A.J., Rodríguez, Y., 2003, 'Use of rheological compatibility criteria to study SBS modified asphalts'. *J. Appl. Polym. Sci.* 90(7), 1772–1782.

Blanco, R., Rodríguez, R., García-Garduño, M., Castaño, V.M., 1996, 'Rheological properties of styrene–butadiene copolymer-reinforced asphalt'. *J. Appl. Polym. Sci.* 61, 1493–1501.

Carrera, V., Partal, P., García-Morales, M., Gallegos, C., Páez, A., 2009, 'Influence of bitumen colloidal nature on the design of isocyanate-based bituminous products with enhanced rheological properties'. *Ind. Eng. Chem. Res.* 48, 8464–8470.

Carrera, V., Partal, P., García-Morales, M., Gallegos, C., 2010a, 'Novel bitumen/isocyanate-based reactive polymer formulations for the paving industry'. *Rheol. Acta* 49, 563–572.

Carrera, V., Partal, P., García-Morales, M., Gallegos, C., Pérez-Lepe, A., 2010b, 'Effect of processing on the rheological properties of poly-urethane/urea bituminous products'. *Fuel Process. Technol.* 91, 1139–1145.

Carrera, V., García-Morales, M., Navarro, F.J., Partal, P., Gallegos C., 2010c, 'Bitumen chemical foaming for asphalt paving applications'. *Ind. Eng. Chem. Res.* 49, 8538–8543.

Csanyi, L.H., 1957, 'Foamed asphalt in bituminous paving mixtures'. Bulletin 160. Highway Research Board, Washington, DC, pp. 108–122.

De Rosa, M.E., Winter, H.H., 1994, 'The effect of entanglements on the rheological behavior of polybutadiene critical gels'. *Rheol. Acta* 33, 220–237.

Dong, X.G., Lei, Q.F., Fang, W.J., Yu, Q.S., 2005, 'Thermogravimetric analysis of petroleum asphaltenes along with estimation of average chemical structure by nuclear magnetic resonance spectroscopy'. *Thermochim. Acta* 427, 149–153.

Eaves, D., 2004, *Handbook of Polymer Foams*. Shawbury, Shropshire, UK: Smithers Rapra.

Engel, R., Vidal, A., Papirer, E., Grosmanin, J., 1991, 'Synthesis and thermal stability of bitumen–polymer ionomers'. *J. Appl. Polym. Sci.* 43, 227–236.

Fawcett, A.H., McNally, T., 2001, 'Blends of bitumen with polymers having a styrene component'. *Polym. Eng. Sci.* 41, 1251–1264.

Gaestel, C., Smadja, R., Lamminan, K.A., 1971, 'Contribution à la connaissance des propriétés des bitumes routiers'. *Rev. Gen. Routes Aérodromes* 466, 85–95.

García-Morales, M., Partal, P., Navarro, F.J., Martínez-Boza, F.J., Gallegos, C., González, N., González, O., Muñoz, M.E., 2004a, 'Viscous properties and microstructure of recycled EVA modified bitumen'. *Fuel* 83, 31–38.

García-Morales, M., Partal, P., Navarro, F.J., Martínez-Boza, F., Gallegos, C., 2004b, 'Linear viscoelasticity of recycled EVA-modified bitumens'. *Energy Fuels* 18, 357–364.

Guo, A., Javni, I., Petrovic, Z., 2000, 'Rigid polyurethane foams based on soybean oil'. *J. Appl. Polym. Sci.* 77, 467–473.

He, G.-P., Wong, W.-G., 2006, 'Decay properties of the foamed bitumens'. *Constr. Build. Mater.* 20, 866–877.

Hesp, S.A., Woodhams, R.T., 1991, 'Asphalt–polyolefin emulsion breakdown'. *Colloid Polym. Sci.* 269, 825–834.

Iqbal, M.H., Hussein, I.A., Al-Abdul Wahhab, H.I., Amin, H.B., 2006, 'Rheological Investigation of the influence of acrylate polymers on the modification of asphalt'. *J. Appl. Polym. Sci.* 102(4), 3446–3456.

Izquierdo, M.A., Navarro, F.J., Martínez-Boza, F.J., Gallegos, C., 2010, 'Novel stable MDI isocyanate-based bituminous foams'. doi: 10.1016/j.fuel.2010.10.002.

Jenkins, K., van de Ven, M., 2001, 'Guidelines for the mix design and performance prediction of foamed bitumen mixes'. 20th South African Transport Conference, 'Meeting the Transport Challenges in Southern Africa'.

Jenkins, K.J., Molenaar, A.A.A., de Groot, J.L.A., van de Ven, M.F.C., 2000, 'Developments in the uses of foamed bitumen in road pavements'. *Heron* 45(3), 167–175.

Krivoohlavek, D., 1993, 'Method of producing, using and composition of phenolic-type polymer modified asphalts or bitumens'. US Patent 5,256,710.

Lesueur, D., 2009, 'The colloidal structure of bitumen: Consequences on the rheology and on the mechanisms of bitumen modification'. *Adv. Colloid Interface Sci.* 145, 42–82.

Lesueur, D., Gerard, J.F., Claudy, P., Létoffé, J.M., Planche, J.P., Martin, D.A., 1996, 'Structure related model to describe asphalt linear viscoelasticity'. *J. Rheol.* 40, 813–836.

Loeber, L., Sutton, O., Morel, J., Valletton, J.M., Muller, G., 1996, 'New direct observations of asphalts and asphalt binders by scanning electron microscopy and atomic force microscopy'. *J. Microsc.* 182, 32–39.

Loeber, L., Muller, G., Morel, J., Sutton, O., 1998, 'Bitumen in colloid science: a chemical, structural and rheological approach'. *Fuel* 73, 1443–1450.

Lu, X., Isacsson, U., 2001, 'Modification of road bitumens with thermoplastic polymers'. *Polym. Test.* 20, 77–86.

Martín-Alfonso, M.J., Partal, P., Navarro, F.J., García-Morales, M., Gallegos, C., 2008a, 'Use of a MDI-functionalized reactive polymer for the manufacture of modified bitumen with enhanced properties for roofing applications'. *Eur. Polym. J.* 44(5), 1451–1461.

Martín-Alfonso, M.J., Partal, P., Navarro, F.J., García-Morales, M., Gallegos, C., 2008b, 'Role of water in the development of new isocyanate-based bituminous products'. *Ind. Eng. Chem. Res.* 47, 6933–6940.

Martín-Alfonso, M.J., Partal, P., Navarro, F.J., García-Morales, M., Bordado, J.C.M., Diogo A.C., 2009, 'Effect of processing temperature on the bitumen/MDI-PEG reactivity'. *Fuel Process. Technol.* 90, 525–530.

Masson, J.F., Leblond, V., Margeson, J., 2006, 'Bitumen morphologies by phase-detection atomic force microscopy'. *J. Microsc.* 221, 17–29.

Mondal, P., Khakhar, D.V., 2004, 'Hydraulic resistance of rigid polyurethane foams III. Effect of variation of the concentration of catalysts on foam structure and properties'. *J. Appl. Polym. Sci.* 93, 2838–2843.

Muthen, K.M., 1998, 'Foamed asphalts mixes. mix design procedure'. Contract Report CR-98/077, prepared by CSIR TRANSPORTEK, Pretoria, South Africa.

Navarro, F.J., Partal, P., Martínez-Boza, F., Gallegos, C., 2004, 'Thermo-rheological behaviour and storage stability of ground tire rubber-modified bitumens'. *Fuel* 83, 2041–2049.

Navarro, F.J., Partal, P., Martínez-Boza, F., Gallegos, C., Bordado, J.C.M., Diogo, A.C., 2006, 'Rheology and microstructure of MDI-PEG reactive prepolymer-modified bitumen'. *Mech. Time-Depend. Mater.* 10, 347–359.

Navarro, F.J., Partal, P., García-Morales, M., Martínez-Boza, F., Gallegos, C., 2007, 'Bitumen modification with a low-molecular-weight reactive isocyanate-terminated polymer'. *Fuel* 86, 2291–2299.

Navarro, F.J., Partal, P., García-Morales, M., Martín-Alfonso, M.J., Martínez-Boza, F., Gallegos, C., Bordado, J.C.M., Diogo, A.C., 2009, 'Bitumen modification with reactive and non-reactive (virgin and recycled) polymers: A comparative analysis'. *J. Ind. Eng. Chem.* 15(4), 458–464.

Newman, J.K., 1998, 'Dynamic shear rheological properties of polymer-modified asphalt binders'. *J. Elast. Plast.* 30, 245–263.

Pérez-Lepe, A., Martínez-Boza, F.J., Attané, P., Gallegos, C., 2006, 'Destabilization mechanism of polyethylene modified bitumen'. *J. Appl. Polym. Sci.* 100, 260–267.

Polacco, G., Stastna, J., Vlachovicova, Z., Biondi, D., Zanzotto, L., 2004a, 'Temporary networks in polymer-modified asphalts'. *Polym. Eng. Sci.* 44, 2185–2193.

Polacco, G., Stastna, J., Biondi, D., Antonelli, F., Vlachovicova, Z., Zanzotto, L., 2004b, 'Rheology of asphalts modified with glycidylmethacrylate functionalised polymers'. *J. Colloid Interface Sci.* 280, 366–373.

Redelius, P.G., 2000, 'Solubility parameters and bitumen'. *Fuel* 79, 27–35.

Segura, D.M., Nurse, A.D., McCourt, A., Phelps, R., Segura, A., 2005, 'Chemistry of polyurethane adhesives and sealants'. In: Cognard, P. (ed.) *Handbook of Adhesives and Sealants*, Chapter 3. Amsterdam: Elsevier.

Sekar, V., Selvavathi, V., Sriram, V., Sairam, B., 2002, 'Modifications of bitumen by elastomer and reactive polymer. A comparative study'. *J. Petrol. Sci. Technol.* 20, 535–547.

Singh, B., Tarannum, H., Gupta, M., 2003, 'Use of isocyanate production waste in the preparation of improved waterproofing bitumen'. *J. Appl. Polym. Sci.* 90, 1365–1377.

Singh, B., Tarannum, H., Gupta, M., 2004, 'Evaluation of TDI production waste as a modifier for bituminous waterproofing'. *Constr. Build. Mater.* 18, 591–601.

Szycher, M., 1999, *Szycher's Handbook of Polyurethanes*. Boca Raton, FL: CRC Press.

Trakarnpruk, W., Chanathup, R., 2005, 'Rheology of asphalts modified with polyethylene-*co*-methylacrylate and acids'. *J. Met. Mater. Miner.* 15, 1–5.

Yontz, D.J., Hsu, S.L., Lidy, W.A., Gier, D.R., Mazor, M.H., 2008, 'Direct observation of morphological differences as a function of reaction temperature in model systems for polyurethane foams'. *J. Polym. Sci.* 36, 3065–3077.

Yousefi, A.A., 2003, 'Polyethylene dispersions in bitumen: The effects of the polymer structural parameters'. *J. Appl. Polym. Sci.* 90(12), 3183–3190.

Zanzotto, L., Stastna, J., Vacin, O., 2000, 'Thermomechanical properties of several polymer modified asphalts'. *Appl. Rheol.* 10, 134–144.

Zeng, J., 2002, 'Studies of PF resole/isocyanate hybrid adhesives'. Ph.D. thesis, Virginia State University, Petersburg, VA.

I. Gaweł, Wrocław University of Technology, Poland,
J. Piłat, P. Radziszewski, K. J. Kowalski,
and J. B. Król, Warsaw University of Technology, Poland

Abstract: Among several methods of waste rubber recycling, the reuse of crumb rubber for bitumen modification deserves special attention. The chapter includes a review of methods for bitumen modification with crumb rubber, a discussion of the types of bitumen–rubber interactions, and a description of the properties of rubber–modified bitumen and asphalt–rubber mixtures. It also summarizes the benefits from the use of asphalt rubber mixtures in road construction.

Key words: recycling of rubber wastes, bitumen modification with crumb rubber, asphalt–rubber mixture.

4.1 Introduction

Waste rubber forms a substantial part of the world's solid waste. Most of this waste consists of post-consumer tyres from passenger cars and trucks. Because of increasing production of cars and trucks, and on the other hand, a limited life period of the tyre, the amount of waste tyres generated in the world is increasing year on year. Each year about one billion tyres are discarded around the world (Heimbuch, 2009). In industrialized countries approximately 9 kg of waste tyres are generated annually per capita (Geiger *et al.*, 2008). Some of the tyres generated in the world are used for recycling, with the rest being stockpiled or landfilled (Airey *et al.*, 2003), which creates environmental problems and health hazards. Tyres stored in a dump or landfill generate a proliferation of rodents and insects (*Waste Management World*, 2010). The environmental hazard also includes a great fire risk. Due to their shape and long life span, ranging from a dozen to about 100 years, stored waste tyres occupy a large area. Therefore, most scrap tyres should be put to a new productive use.

An EU directive on prohibiting all dumping and landfill of discarded tyres presses us to intensify the search for the most promising methods of recycling this material. The European Tyre Recycling Association (ETRA) recommended in 1999 the use of recycled post-consumer tyres in asphalt pavement mixtures. This market can consume large numbers of discarded

tyres and seems to be an optimum environmental method of recycling waste rubber. Waste tyres have been used to produce crumb rubber for modification of bituminous binders.

4.2 Waste rubber recycling

Rubbers are crosslinked network polymers and are not easily processed into valuable products (Joseph *et al.*, 1994). The methods for recycling of scrap tyres consist of:

- Material recycling
- Energy recovery
- Reuse of waste tyres or their parts.

4.2.1 Material recycling

In material recycling, direct or processed waste rubber products are used. Recycling methods include retreading, waste rubber disposal through pyrolysis, grinding of tyres or other rubber products.

Retreading involves the removal of the remaining worn-out tread and the application of new tread. After retreading the tyre regains its original properties. There are two basic retreading methods: cold and hot. The hot method involves application of a belt of a raw rubber on a surface of milled tyre, followed by creation of a tyre tread in a hot mould and preservation via a vulcanization process. The cold method involves bonding the precured tread with the carcass. Both methods extend the life of tyres by an additional 150,000 km service.

Pyrolysis involves thermal decomposition of rubber in tyres. Pyrolysis is carried out at temperatures between 300 and 800°C in special reactors. In addition to valuable products (fuel oil, soot, steel), gaseous by-products are obtained under such temperature conditions. Pyrolysis of tyres, with the aim of obtaining oils that can be used as solvents in coal liquefaction, has been reported by Mastral *et al.* (1996). Recently a new method based on steam pyrolysis and gasification of waste tyres for the production of liquid fuels, chemical feedstocks and activated carbons was developed (Elbaba *et al.*, 2010). Steam pyrolysis-gasification of scrap tyres in the presence of Ni–Mg–Al catalyst produces a high yield of gas rich in hydrogen. It was suggested that the thermal decomposition of waste tyres at high temperature might be an alternative for production of hydrogen in future energy systems (Elbaba *et al.*, 2010). Disposal of waste tyres using pyrolysis is a very costly process and requires the use of additional devices to prevent environmental contamination.

Grinding of tyres to different granular sizes allows for a wide and varied use of rubber waste as a valuable component of composite materials in the

economy. It is particularly beneficial to use rubber from ground tyres in the road construction industry to modify the properties of asphalt mixtures. Crumb rubber from scrap tyres is a good alternative to polymers used as bitumen modifiers. Addition of ground rubber to bitumen results in an appreciable improvement in the performance-related properties of the binder (Beaty, 1992; Billiter *et al.*, 1997; Huang, 2008) and in the mechanical properties of the mixtures (Khedaywi *et al.*, 1993; Bahia and Davies, 1994; Hui *et al.*, 1994; Isacsson and Lu, 1995; Way, 2000). Field studies have shown improved performance of rubber asphalt pavements (Stroup-Gardiner *et al.*, 1996; Brown *et al.*, 1997; Way, 2000).

4.2.2 Energy recovery

Rubber is a good energy carrier, as it is characterized by a high calorific value. The calorific value of rubber is approximately 32 MJ/kg, which is close to the calorific value of coal (Gaweł and Slusarski, 1999). Waste tyres are used as fuel for combustion, mainly in cement kilns but also in power stations. Though combustion permits the use of the whole tyre, it is not an environmentally friendly way to utilize scrap tyres as it produces unwholesome materials. To avoid emission of toxic gases into the atmosphere, a precisely defined temperature distribution is required that ensures complete oxidation of gaseous products, and there must also be provided a system for desulphurization of waste gases (Slusarski, 1997). Combustion of post-consumer tyres excludes any use of their valuable polymeric components, which could be made useful for improving other materials, e.g. bitumen.

Waste tyres or their parts can be used for:

- Construction of lightweight road embankments
- Strengthening of subsoil
- Improving slope stability
- Construction of isolation and drainage layers
- Construction of retaining walls
- Verge strengthening
- Membranes and drainage layers
- Road culverts
- Construction of noise barriers.

Particularly noteworthy is the use of waste tyres to build lightweight road embankments. The shredded tyres are used for the construction of embankments to improve their functional characteristics. Water filtration conditions in embankments are improved and the structure is more resistant to frost damage. The embankment is significantly lighter and thus capable of being built on weaker ground. Furthermore, the rubber from waste tyres is not subjected to rapid biological decomposition.

The use of whole tyres or their parts in the above-mentioned forms is both economically beneficial and environmentally friendly. Only two available markets for waste tyres can consume the significant numbers available, i.e. fuel for combustion and material for civil engineering applications. Of the several methods for rubber scrap utilization, modification of bitumen with ground rubber seems to be a very promising application for these wastes.

Methods employed for waste tyre management are also dependent on national and regional government policies. In Europe, the main methods for waste tyre management are materials recovery (38.7%), energy recovery (32.3%), and retreading (11.3%) (ETRMA, 2008). In the US, the main methods used for tyre utilization are tyre-derived fuel (52.8%), ground rubber (16.8%), and civil engineering applications (11.9%) (US Rubber Manufacturers Association, 2009).

4.3 Shredding of scrap rubber from tyres

Shredding of scrap tyres can provide products with different properties. As a result of grinding tyres or other waste rubber products, rubber particles (with different granular size) and metal, and textile parts of reinforcement are obtained. The properties and usefulness of ground rubber depend on many factors including the type of rubber, method of grinding, particle size and shape and specific surface area of particles.

Two technologies are used to granulate the waste rubber: cryogenic technology and mechanical grinding at ambient temperature. Depending on the granular size and application, ground rubber can be divided into the following types:

- Rubber powder: <1.0 mm
- Crumb (or granulated) rubber: 1.0–15.0 mm
- Shredded rubber: >15.0–100 mm
- Cuts: >100.0–300 mm.

For the cryogenic method, the pre-treated waste tyres are subjected to cooling using liquid nitrogen. At low temperatures, rubber behaves like a brittle glass and can be easily ground when exposed to impact forces. In the case of the cryogenic method, whole tyres are subjected, continuously, to hammer mills where a broad spectrum of particle sizes is obtained. After the pre-crush stage, the material is transported to the cryogenic chamber in which, at between -80°C and -197°C , the main grinding in impact crushers takes place. Then, after the initial screening, waste removal and drying process, the rubber material is subjected to further separation of rubber from steel (in magnetic separators). Fibres are separated from rubber by air blowing. Next, ground rubber material is directed to a sorting screen and, using a pneumatic conveyor, to storage silos (Dantas Neto *et al.*, 2006). Using

cryogenic technology, the crumb rubber obtained has unchanged composition and structure and thus can be used in a wide range of applications. The process is environmentally friendly. The main disadvantage of this method is the relatively high cost of manufacturing, which depends mainly on the price of liquid nitrogen.

Mechanical grinding is the most popular and commonly used method. The grinding process consists of mechanical cutting and grinding material from the tyres. After initial shredding, using various devices (such as disintegrating knives), rubber material is ground to appropriate fractions (granulation). Grinding in mills allows rubber crumb of fine and very fine particle sizes to be acquired. Steel wire is removed from ground rubber material using electromagnetic sorting, and cord contamination through air separators. This environmentally friendly process is carried out at ambient temperatures. By means of mechanical grinding, rubber particles with large specific surface area are obtained, which is advantageous from the point of view of rubber application as a bituminous binder modifier.

Comparing the particle size obtained in the grinding process to the cryogenic method, it must be concluded that smaller particles can be obtained using the cryogenic process (particle size 0.1–0.4 mm). By means of the mechanical method, a lower degree of fragmentation is obtained with particle sizes ranging from 0.4 to 4 mm. In order to obtain a very fine granular size of crumb rubber with improved grain structure, a combination of both cryogenic and mechanical processes is possible (Putman and Amirkhanian, 2006).

4.4 Methods of bitumen modification with crumb rubber

There are two methods of adding the ground rubber from tyres to the asphalt mixture:

- Bitumen modification – ‘wet process’
- Using the ground rubber as a part of the asphalt mixture with partial bitumen modification – ‘dry process’.

In the first method, modified rubber-bitumen binder is obtained, while in the second, a modified asphalt mixture with rubber is created.

4.4.1 Wet process

To comply with the ASTM D8 (2002) standard, rubber-bitumen binder (or asphalt-rubber, according to US terminology) is defined as a mixture of bitumen binder, crumb rubber from waste tyres (at least 15% (by weight)) and additives lowering the viscosity, in which rubber components of modified binder ‘reacts’ with hot bitumen, significantly increasing its volume.

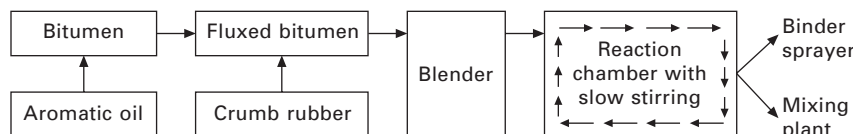
The first method for adding rubber to the bituminous binder was developed by Hancock in 1823. Cassell in 1844 reported the manufacturing process principles for binder containing natural rubber. The first application of this binder was the construction of a street in Cannes in 1960. McDonald developed an industrial technology for producing rubber-bitumen binder (McDonald, 1981).

In order to produce rubber-bitumen binder, crumb rubber of size up to 1 mm is used. The modification process is carried out at temperatures ranging from 170 to 220°C for 1–3 hours (Way, 2006). A higher temperature for this process reduces the flexibility of the binder. The optimum time of mixing bitumen with rubber is approximately 2 hours. A longer mixing time improves the properties of the rubber-bitumen binder but is not recommended due to the substantial increase in production costs. Crumb rubber added to hot bitumen swells by absorption of the light bitumen fractions and plasticizing additives. It was reported that crumb rubber when mixed with bitumen and stored at a temperature of about 200°C for 20 minutes approximately doubled its volume (Horodecka *et al.*, 2002).

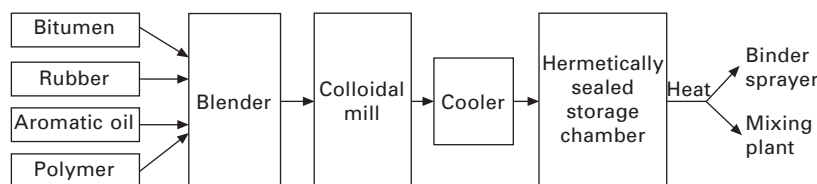
Depending on the production method, rubber-bitumen binder may be used to manufacture asphalt mixture immediately after production due to instability of the binder (non-storable binder) or may be stored. A production diagram for a non-storable rubber-bitumen binder is shown in Fig. 4.1, and for a storable binder in Fig. 4.2.

The production of a non-storable rubber-bitumen binder is as follows:

- Crumb rubber is placed into a special feeder.
- From the feeder, a certain amount of crumb rubber is added to the mixer with a bitumen (bitumen flux).



4.1 Production diagram of a non-storable rubber-bitumen binder (in accordance with Corté *et al.*, 1999; Way, 2006; CALTRANS, 2006).



4.2 Production diagram of a storable rubber-bitumen binder (in accordance with Corté *et al.*, 1999).

- Mixing the ingredients in the mixer takes about 1 hour.
- Maturation of the rubber-bitumen binder takes place in transport tanks.

Storable rubber-bitumen requires additional attention to provide a time-stable, homogeneous binder. Manufacture of the storable rubber-bitumen is carried out in special mixers and colloid mills at 175–185°C. Mixing of binder ingredients takes about 2 hours until the binder reaches a viscosity of 0.6 Pa·s. After completion of the mixing process, the temperature of the binder is reduced by 15–20°C and the binder is stored, without stirring, in a hermetically sealed container at 160°C. Rubber-bitumen binders can be stored without a significant change of properties for up to 2 weeks (Corté *et al.*, 1999).

4.4.2 Dry process

The dry method was developed in the 1960s in Sweden. In the dry method, the crumb rubber plays mainly the role of an aggregate and the rubber only partially modifies the bitumen binder. Although this method is technologically simpler, valuable properties of rubber are not fully used. Rubber is added to an intermittent grain size in the mineral mixture before it is mixed with a bitumen binder, and crumb rubber of grain sizes from 2 mm to 6 mm is mostly used. Ground rubber is added to warm mineral mix in an amount of 1–3% by weight of aggregate (CALTRANS, 2006; Dantas Neto *et al.*, 2009). The temperature of the aggregate is 160–180°C for a mixing time of 15–30 seconds. Then, after mixing of crumb rubber with the aggregate, the bitumen is added. The bitumen content is about 1% (by weight) higher than in the traditional asphalt mixtures. The total mixing time ranges from about 120 to 180 seconds. The asphalt mixture after addition of crumb rubber can be stored in a ready-mix container for 3–5 hours. During this time, bitumen is partially modified with rubber and the mixture gets improved viscoelastic properties.

Mixtures prepared by the dry process have more limited application compared to mixtures prepared by the wet process (Way, 2006). These mixtures are particularly used in cold climates, especially to reduce the slippage of tyres on ice-covered roads.

4.5 Rubber-bitumen interactions

It is generally believed that the rubber-bitumen interaction is a diffusion phenomenon and not a chemical reaction. When soaked in liquid bitumen, rubber particles absorb the components of similar solubility parameters and swell with increasing volume. They may swell to 3–5 times their original

volume (Massucco, 1994). It has been found, however, that swelling follows a linear rate for the first 90 seconds and then increases at a decreasing rate (Joseph *et al.*, 1994). The dimensions of the rubber particle increase until the concentration of liquid is uniform throughout the particle and equilibrium swelling is achieved (Blow, 1971).

The degree of swelling depends on blending temperature and duration, chemical nature and viscosity of bitumen, rubber composition and particle size. Compatibility of rubber and liquid is also an important factor that affects swelling.

The chemical nature of bitumen determines the equilibrium swelling whereas the viscosity of bitumen determines the rate of penetration into the bulk of the rubber (Stroup-Gardiner *et al.*, 1993). The penetration (diffusion) rate increases as the viscosity of the liquid decreases. As reported by Airey *et al.* (2003), the initial rate of bitumen absorption and possibly the amount of rubber swelling are related to the viscosity (penetration grade) of the binders, with the softer (less viscous) binders, having the highest rates of absorption. A study by Gaweł *et al.* (2006) has shown that the amount of rubber swelling in softer (higher penetration grade) bitumen is noticeably greater than in harder (lower penetration grade) bitumen (Table 4.1).

Rubber-bitumen interactions are a function of the molecular weight of the bitumen (Stroup-Gardiner *et al.*, 1993). Bitumens rich in low molecular weight components are more interactive with rubber. The lighter bitumen components penetrate more readily into the internal matrix of the polymer. HP-GPC analysis of bituminous binders before and after modification with crumb rubber has shown an increase in the large molecular size fraction and a decrease in the smaller molecular size fraction (Putman and Amirkhanian, 2010). It has been found that, of the non-polar components, *n*-alkanes and *n*-alkylbenzenes possess the highest propensity to penetrate into rubber particles (Gaweł *et al.*, 2006). Preferential absorption of the compounds with linear aliphatic chains into the rubber suggests that these components have good compatibility with the linear polymeric skeleton of the rubber.

Different data have been reported in the literature concerning the effect of the chemical composition of bitumen on the rate and amount of rubber

Table 4.1 Percent of rubber swelling in bitumen (rubber thickness 0.85 mm)

Percent of swelling ^a	Temperature (°C)			
	180	180	200	200
Rubber content (wt%)	5	10	5	10
Rubber swelling in bitumen of 70 dmm pen.	55	50	70	65
Rubber swelling in bitumen of 165 dmm pen.	70	65	80	75

^aSwelling is given as the percent of rubber mass increase.

Source: Gaweł *et al.* (2006).

swelling. According to Singleton *et al.* (2000), the composition of bitumen has no significant effect on the rate of interaction between rubber and bitumen if there are sufficient quantities of the low molecular weight fractions.

Bitumens differ in chemical composition depending on the type of the crude oil and the technology of production (Bagińska and Gaweł, 2004). Putman and Amirkhanian (2010) determined the interaction between rubber and bituminous binders from different sources by calculating the interaction effect (IE). The IE is defined as the change from the base to the drained binder for a given rubber modified binder to the base binder:

$$IE = \frac{\text{drained} - \text{base}}{\text{base}} \quad 4.1$$

The significant differences in the values of IE between bitumen of different origins demonstrate a substantial effect of binder source on rubber–bitumen interactions. The same conclusion was drawn by Frantzis (2004), who developed a method of determining the diffusion and solubility coefficients for rubber in bitumen. The increase in the mass of rubber soaked in the bitumen at 180°C for various durations was measured and a sorption curve generated. The diffusion coefficient was calculated from the slope of the linear region of the sorption curve. This study has shown that binders of different origins differ in diffusion coefficient values. For example, Venezuelan bitumen of a higher content of aromatics has a higher diffusion coefficient compared with Kuwaiti bitumen of a lower aromatics content. Among bitumens from the same crude source, higher penetration grade (softer) binders have higher diffusion coefficients (Frantzis, 2004).

The propensity of the components (generic fractions) of bitumen to penetrate into rubber particles was taken into account by some investigators when evaluating the interactions between rubber and bitumen (Singleton *et al.*, 2000; Gaweł *et al.*, 2006; Ould Henia and Dumont, 2008). Although a comparison of the results achieved under different experimental conditions may raise doubts about the conclusions drawn, it is essential to note (based on the data obtained by these researchers) that the changes in the generic composition of the bitumen depend on the composition of the base bitumen. For bitumen with an aromatics content (determined by the SARA method) ranging from about 50 to about 65 wt%, Singleton *et al.* (2000) reported a decrease in the saturate and aromatic fractions after curing with rubber. Ould Henia and Dumont (2008), using binders of a higher aromatics content (70–86 wt%, SARA method), concluded that the aromatic fraction of bitumen is the major component migrating into the rubber network. The bituminous binders used in their study had, however, a very low saturates content. A different pattern of change (determined by ASTM D4124 (2009b)) has been observed by Gaweł *et al.* (2006) in the composition of a bitumen from Russian crude, characterized by a much lower aromatics and a higher

saturates content (Table 4.2) as compared to the binders mentioned above. From the data in Table 4.2, it can be inferred that for bitumen of paraffin-naphthenic type (Russian), saturates are the major components penetrating into the rubber. The preferential penetration of saturates into the internal matrix of the polymer may be explained by the similarity in the solubility parameter of saturates and the solubility parameter of the rubber.

Compatibility of bitumen and rubber may be assessed by comparing the solubility parameters of the components. Bitumen components differ in solubility parameter (Yen and Chilingarian, 1994). For the bitumen of the composition described in Table 4.2, the solubility parameters of the components were the following: saturates $\delta = 17.5$, aromatics $\delta = 18.2$, resins $\delta = 19.5$, and asphaltenes $\delta = 22.3 \text{ MPa}^{1/2}$. However, for bitumen of a different chemical nature, the solubility parameters of these fractions may take values deviating from those given above (Rogel, 1997). Rubber from car tyres is predominantly a combination of styrene–butadiene rubber ($\delta = 17.5$) and natural rubber ($\delta = 14.8$) (Brandrup and Immergut, 1989). Comparison of solubility parameters of the components separated from the Russian bitumen with the solubility parameters of the rubber provides evidence that saturates possess the best compatibility with rubber.

The increase in the aromatics content of bitumen after rubber immersion (Table 4.2) can be explained in terms of both the reduction in saturates content and the migration of similar components from rubber to bitumen. Using the NMR technique in their study of rubber–bitumen interactions, Miknis and Michon (1998) observed that oils used in tyre manufacture and oils which are present in bitumen contain similar compounds. This observation prompted them to conclude that the oils most probably exchange during heating. GC-MS analysis of the molecular composition of some components extracted from crumb rubber before and after immersion in hot bitumen (of the generic composition specified in Table 4.2) has revealed a substantial decrease in acid content. Myristic, palmitic (dominant) and stearic acids were abundant in the rubber, as they are components of the curing system for the polymer, while the processed rubber contained only

Table 4.2 Generic composition of the 70/100 pen. grade bitumen (from Russian crude oil) before and after rubber soaking (rubber removed)

Fraction	Fraction content (wt%)	
	Before rubber soaking	After rubber soaking
Saturates	12.75	10.52
Naphthene-aromatics	33.88	37.46
Polar-aromatics (resins)	41.42	39.53
Asphaltenes	11.41	11.89

Source: Gawel *et al.* (2006).

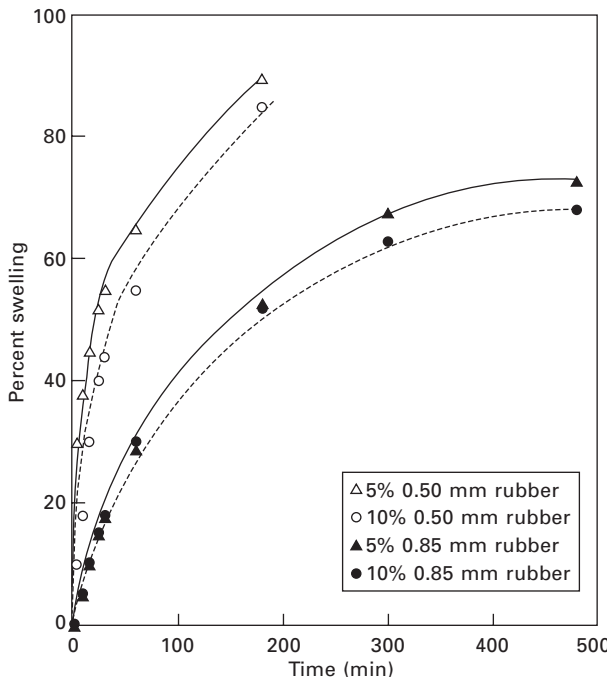
traces of those acids. This finding suggests that during immersion of the rubber in hot bitumen the acids penetrated from the rubber matrix into the bitumen. During separation of the residual binder into generic components, these acids probably concentrate in the naphthene-aromatic fraction, as can be inferred from the increase in the fraction content after modification with rubber (Table 4.2). It seems that naphthenic acids in bitumen also contribute to the interaction with rubber. Some Venezuelan bitumens displaying a higher acid content better interact with rubber. The decrease observed in the content of the polar-aromatic components (Table 4.2) can be attributed to the partial decomposition of polar-aromatics as a result of bitumen ageing at elevated temperature. The decomposition of polar-aromatics under ageing in the laboratory was observed with bitumen obtained from crudes of paraffin-naphthenic type, for example from Russian crude (Gaweł and Bagińska, 2004).

As follows from the literature review (Southern, 1967; Ould Henia and Dumont, 2008; Highways Agency, 2010), the rubber-bitumen interaction, expressed as the maximum amount of swelling, depends more on the nature of the crumb rubber than the chemical nature of the bitumen, provided that there are sufficient light fractions originally present in the binder. On the part of the rubber, the interaction depends on the crumb rubber content, particle size, rubber type (car tyre or truck tyre), processing method (mechanical grinding or cryogenic technology), and polymer composition (Billiter *et al.*, 1997; Bahia and Davies, 1995; Dias and Picado-Santos, 2008; Putman and Amirkhanian, 2010).

The rubber content of the binder was found to be an important contributory factor in rubber swelling (Gaweł *et al.*, 2006; Ould Henia and Dumont, 2008). Contrary to this finding, Airey *et al.* (2003) concluded that rubber swelling is independent of the rubber-bitumen ratio, provided that there are sufficient light bitumen fractions. This is the case for classical polymer swelling in solvent where the amount of solvent is large enough to obtain a swelling ratio independent of the quantity of the polymer added.

The effect of rubber particle size on the rate and amount of rubber swelling in hot bitumen is illustrated in Fig. 4.3. The rate of swelling was noticeably lower for thicker rubber samples. After 120 minutes' immersion in hot bitumen, the amount of swelling was approximately twice as high with 0.5 mm rubber samples as with 0.85 mm rubber samples. After 180 minutes' duration of the experiment, the cohesion of the thinner rubber samples dropped dramatically so that the procedure of swelling determination had to be discontinued.

It has been reported that the specific surface area of crumb rubber is an important property influencing the interaction between rubber and bitumen (Heitzman, 1992a; Dias and Picado-Santos, 2008). Owing to its rough shape and reticulated surface, the crumb rubber obtained by mechanical grinding



4.3 Swelling rate of rubber in 70/100 penetration grade bitumen, at 200°C.

interacts better with the bitumen than does the crumb rubber produced by the cryogenic method (cubic shape and smooth surface).

It is difficult to assess the chemical composition of the crumb rubber because of the large variability of tyres and the retreading processes (Airey *et al.*, 2003). In general, truck tyres have a larger content of natural rubber as compared to car tyres. The composition of rubber also differs between the tyre sections. Rubber types differ in their solubility parameter. The solubility parameter for rubber ranges from 17.8 to 20.8 MPa^{1/2} (Hansen and Smith, 2004). Similar solubility parameters of liquid and rubber ensure better compatibility of the components, and therefore better interaction between rubber and liquid (bitumen) is obtained. The molecular arrangement (crosslinks) of the polymer network affects significantly the degree of swelling (Airey *et al.*, 2003). The greater the number of crosslinks in the rubber, the shorter the average length of the rubber chains between crosslinks and the lower the rate of diffusion of lighter bitumen components into the rubber. The penetration of lighter bitumen components into the rubber may, however, degrade the colloidal stability of the bituminous binder. If bitumen is poor in light components, yet contains a high asphaltene content (heavy fraction), the addition of crumb rubber may lead to the coagulation of asphaltenes. To

prevent this, asphalts of a higher penetration grade are used. The pretreatment of the rubber with various organic compounds or their mixes also inhibits the penetration of light bitumen components into the rubber (Stroup-Gardiner *et al.*, 1993; Flanigan, 1995).

When mixed with hot bitumen, the rubber particles can be devulcanized and depolymerized. If the rubber is not partially devulcanized, it produces a heterogeneous binder with the rubber acting mainly as a flexible filler (Giavarini, 1994). However, excessive devulcanization accounts for the deterioration of binder properties. An improvement in the elasticity of the binder may be achieved by additional crosslinking of the polymer in the rubber-modified binder (Gaweł and Slusarski, 1999).

The interactions between rubber and bitumen affect the performance-related properties of the residual binder. The most pronounced effect of rubber swelling in liquid bitumen is an appreciable increase in the viscosity of the binder. Bitumen with a low content of lighter components and a high content of asphaltenes produces a high-viscosity binder (Ould Henia and Dumont, 2008). The considerable increase in stiffness and elastic behaviour of the residual binder is consistent with the loss of lighter bitumen components due to their diffusion into the rubber and oxidative ageing, as well as with the breakdown of the rubber (Huang, 2008).

The differences in the reported data on rubber-bitumen interactions (Joseph *et al.*, 1994; Massucco, 1994; Singleton *et al.*, 2000; Airey *et al.*, 2003; Gaweł *et al.*, 2006; Ould Henia and Dumont, 2008) are attributed to the following: different blending temperatures and durations, the use of bitumens differing in chemical nature or rubbers differing in particle size and chemical composition, and the change in solubility parameters of the components with a rise in temperature. Also, ageing of bitumen at a blending temperature of 160–210°C seems to be of importance to rubber-bitumen interactions (Singleton *et al.*, 2000; Ould Henia and Dumont, 2008).

4.6 Properties of rubber modified bitumen

The properties of rubber-bitumen binder depend on many factors such as the properties of the bitumen, the properties of the rubber, the duration and temperature of rubber-bitumen binder production, the manner and intensity of the mixing process, and the properties of the additives used. The consistency of the rubber-bitumen binder, its rheological behaviour and ageing resistance depend on the chemical composition of the bitumen as well as on the content and particle size of the crumb rubber. In addition, the specific surface of the rubber particles depends on the shredding method used. It should also be noted that the rubber chemical composition and impurity significantly affect the modification process and determine the final properties of the rubber-bitumen binder.

The amount of crumb rubber added varies in many countries and ranges from a low amount (5–12%) (Page, 1992) up to as high as 22% (CALTRANS, 2006) by weight of binder. A higher content of rubber in the bitumen causes a beneficial increase in the viscoelastic properties of the rubber–bitumen binder.

Granulation of the crumb rubber and its specific surface to a large extent determine the viscosity of a rubber–bitumen binder. Finer particles of rubber with a well-developed specific surface effectively swell in bitumen. The method of rubber shredding affects the surface characteristics of rubber particles. Rubber particles obtained by mechanical grinding have a developed surface (porous, jagged) and easily react with bitumen. Rubber particles obtained by cryogenic technology have a regular shape with smooth and glossy surfaces and resist the swelling process during the production of rubber–bitumen binder (Shen and Amirkhanian, 2005; Dantas Neto *et al.*, 2009).

The chemical composition of the rubber affects the quality of the rubber–bitumen binder. Components of the rubber derived from tyres are synthetic and natural rubbers, fillers, aromatic oils, sulphur and other chemical additives. A rubber tyre contains only about 50% rubber components. The most common contaminants of ground rubber are water, fibres and small metal parts (Hicks, 2002; Corté *et al.*, 1999). Extensive moisture in rubber crumb (more than 1% by weight) may cause bitumen to foam when the rubber is added. Therefore, crumb rubber dosed into the mixer should have moisture content below 0.75% (ASTM, 2009a).

Technical properties of rubber–bitumen binder depend on the crumb rubber with bitumen temperature and mixing time (Fanto *et al.*, 2003). A higher temperature of mixing is preferable, since it speeds up the interactions between bitumen and rubber particles. Also, a longer mixing time (more than 1 hour) increases the efficiency of modification. The mixing conditions of crumb rubber with bitumen affect the properties of rubber–bitumen binder. High-speed mixing, aside from increased swelling of rubber, causes fragmentation of soft rubber particles and enhances their dispersion in the liquid bitumen phase (Shen and Amirkhanian, 2005; Xiao *et al.*, 2006). In order to improve the modification process, various types of oils are used to soften and plasticize binder at low temperatures.

Rubber–bitumen binder is characterized by improved technical properties compared to conventional binders used in pavement construction. The improvement in properties includes:

- Increased softening point (increased resistance to permanent deformations)
- Reduced sensitivity to temperature (increased penetration index)
- Significant viscosity increase
- Extended temperature range of viscoelasticity
- Increased elasticity (increased elastic recovery)

- Improved binder properties at low temperatures
- Reduced binder susceptibility to ageing.

The softening point, a factor of rubber–bitumen binder which characterizes consistency at high service temperatures, favourably increases from 40 to 65°C (Radziszewski *et al.*, 2004). This temperature depends on the bitumen type used, the amount of rubber and the method of modification.

Thermal sensitivity is a measure of the viscoelastic properties of a binder. It is preferred that the binder shows low penetration changes as a function of temperature change. A measure of this is a penetration index, which for rubber–bitumen binder is above +1 (with a preferred value between 0 and +2) (Read and Whiteoak, 2003).

The viscosity of rubber–bitumen binder increases favourably at the high operating temperatures of road surfaces (60–80°C), while at technological (binder pumping, asphalt mixture production and compaction) temperatures (120–200°C) it increases adversely and uneconomically, since the binder requires additional heating.

Bitumen binder should be characterized by a wide temperature range of viscoelasticity. The value of the phase angle between stress and strain in a study of the complex modulus under cyclic loading gives an overview of the elastic or viscous behaviour of the material. In general, the loss factor ($\tan \delta$) for ideal asphalt should be as high as possible (and higher than 0) in low service temperatures and as low as possible (and lower than infinity) at high service temperatures. Rubber–bitumen binder has an extended temperature range of viscoelasticity compared to unmodified bitumen, up to about 90°C. This means that the rubber–bitumen binder will not become brittle ($\tan \delta > 0$) at low temperatures (−30°C), and at high temperatures (+60°C) the binder will not flow like a Newtonian liquid ($\tan \delta \neq \infty$) (Kalabińska *et al.*, 1999).

The elastic properties of modified binders are determined on a basis of elastic recovery studies. Assessment of bitumen elasticity involves determination of the elastic recovery of a modified binder sample, subjected to stretch during the ductility test. The results showed that the addition of crumb rubber to bitumen increases the elastic recovery from 5–10% up to about 75% compared to the initial elastic recovery (Piłat *et al.*, 2000).

Assessment of binder behaviour at low temperatures can be conducted according to various testing procedures: consistency studies (penetration test), ductility as a function of temperature, brittleness temperature (determined by the Fraass method) and creep stiffness (bending beam rheometer (BBR) test). It was found that rubber–bitumen binder at low temperature shows higher ductility (higher tensile strength and deformation energy) than unmodified bitumen. Brittleness (Fraass breaking-point temperature) of rubber–bitumen is about 7–10% beneficially lower than the breaking point for conventional bitumen.

As a result of ageing, bitumen binder gradually loses its viscoelastic properties and becomes an increasingly harder and brittle material. Changes as a result of ageing of bitumen binders are caused by evaporation of volatile bitumen components at high temperatures and oxidation during production of the mix and pavement service. The following changes in bitumen binder properties are caused by ageing:

- Hardening (resulting in penetration reduction as well as softening point and viscosity increase)
- Deterioration of the low temperature characteristics (e.g. higher stiffness at low temperature resulting in higher breaking point).

Rubber addition to bitumen delays ageing due to oxidation, because of the presence of oxidation inhibitors in rubber. Most evidence of improvement of the modified bitumen resistance to ageing can be observed in ductility tests with tensile force measurements. A beneficial effect of rubber-modified bitumen binder to improve its resistance to ageing is most evident in ductility studies with simultaneous measurement of the tensile force during the ductility test. On the basis of test results of ductility as a function of temperature, conducted for modified (e.g. SBS or EVA) and unmodified bitumens of different hardness, subjected to laboratory ageing (with RTFOT and PAV methods), it was found that rubber-bitumen binder exhibits the smallest, most favourable changes of ductility, maximum tensile force and deformation energy (Radziszewski, 2007).

4.7 Properties of asphalt-rubber mixture

Asphalt mixtures used in the road construction industry are complex mixtures of bitumen binder, aggregate and filler (aggregate with a particle size below 0.063 mm). By applying modifiers to asphalt mixtures, such as crumb rubber (using either the dry or wet methods), asphalt-rubber mixtures with improved properties, compared to conventional mixtures, can be obtained.

Many positive features, particularly concerning durability of asphalt-rubber mixtures, are due to the higher binder content in asphalt mixtures. Increased viscosity of rubber-bitumen can substantially increase the thickness of binder film on aggregate from 19 to 36 μm , compared with 5–9 μm in the case of unmodified binders (Heitzman, 1992b). In asphalt mixtures with low air void content and rubber-modified binder, the total binder content increased by about 20% (as compared to similar mixtures with unmodified binder); for porous mixtures there is an increase in the total binder amount of about 50–60% (and 40–50% for gap graded mixtures).

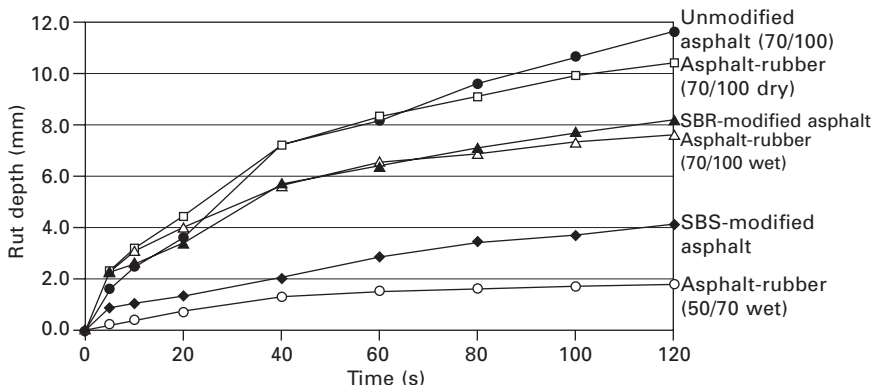
Asphalt-rubber mixtures are characterized by the following advantages compared to conventional asphalt mixtures:

- Increased resistance to permanent deformation
- Increased fatigue durability
- Improved viscoelastic properties
- Increased resistance to ageing.

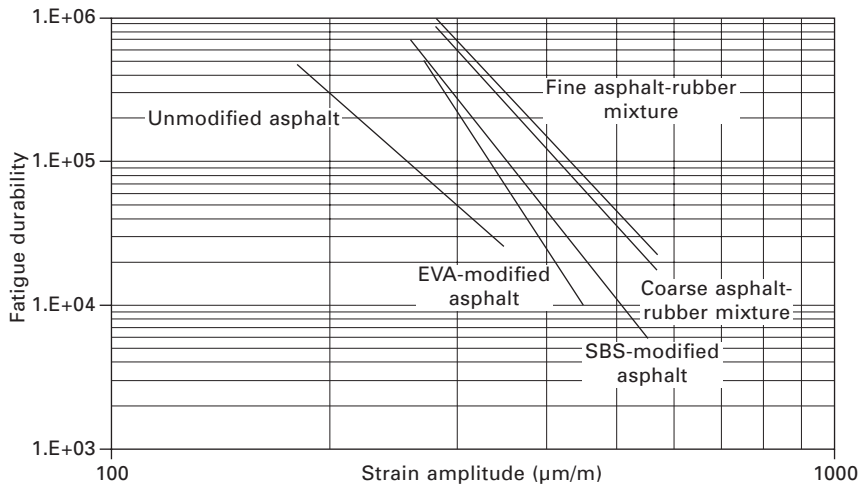
Resistance to permanent deformation tests conducted on a laboratory scale indicates a higher resistance to rutting of mixtures modified with rubber and polymers (Fig. 4.4). Resistance to permanent deformation of asphalt–rubber mixtures can be combined with a higher viscosity rubber–bitumen binder, compared to conventional binders. Studies by Martínez *et al.* (2006) and Fontes *et al.* (2009) showed that the use of the dry modification method and modification of soft binders by a wet method only marginally increase resistance to rutting. The greatest improvement in rutting resistance can be obtained with hard bitumen binder from 35–50 to 50–70 and with a wet modification method using over 15% rubber (Fontes *et al.*, 2009).

In fatigue tests held under laboratory conditions simulating fatigue *in situ*, it was found that the fatigue durability of samples of asphalt–rubber mixtures is better than that of asphalt mixtures containing conventional bituminous binders (Fig. 4.5). The chart of fatigue durability shows that for asphalt mixtures with modified binder there is a clear shift of fatigue life in the direction of higher values of fatigue life in the following order:

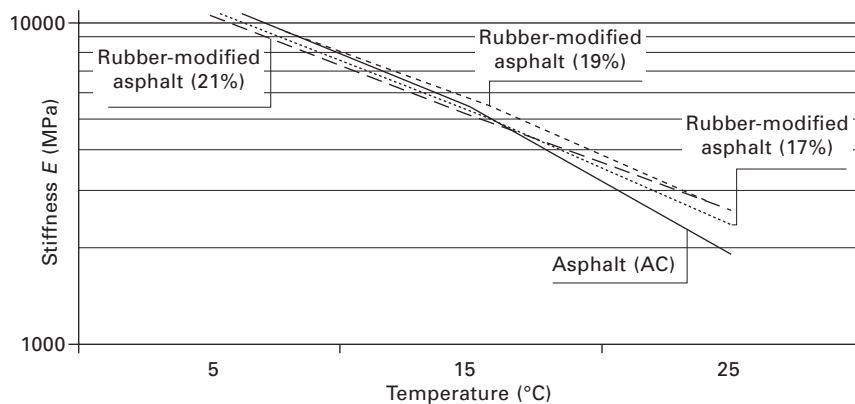
- Asphalt mixture with an unmodified bitumen binder
- Asphalt mixture with EVA modified bitumen
- Asphalt mixture with SBS modified bitumen
- Asphalt mixture with coarse-grained crumb rubber modified bitumen
- Asphalt concrete mixture with fine-grained crumb rubber modified bitumen.



4.4 Wheel tracking test versus time for various asphalt concrete mixtures (in accordance with Martínez *et al.*, 2006; Fontes *et al.*, 2009).



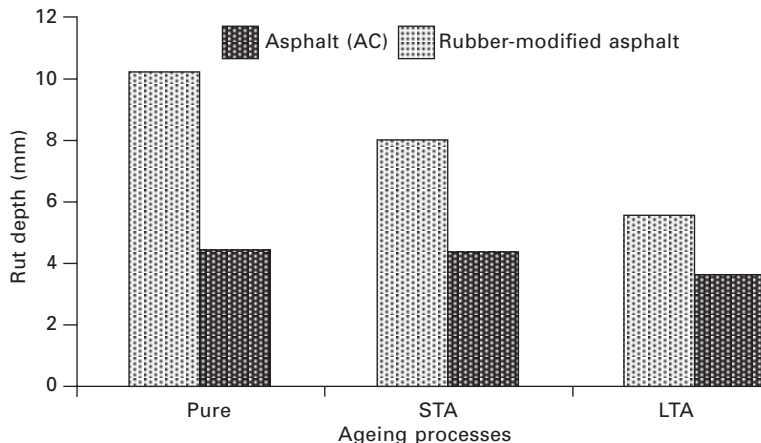
4.5 Fatigue life of various asphalt concrete mixtures (in accordance with Radziszewski, 1997).



4.6 Stiffness modulus E as a function of temperature (in accordance with Radziszewski, 2007).

For the same strain amplitude, fatigue life obtained for asphalt mixtures modified with crumb rubber was 15–20 times that of the fatigue life of asphalt mixture with unmodified binder.

The stiffness modulus of an asphalt mixture is defined as a function of temperature; it has particular importance to road surface durability and pavement design. In addition, it well characterizes the viscoelastic properties of asphalt mixtures. Figure 4.6 shows the stiffness modulus (E) for asphalt mixtures with crumb rubber-modified binder (17, 19, 21% by weight of crumb rubber) compared to an asphalt mixture with unmodified binder.



4.7 Changes in asphalt concrete rut depth as a result of short-term (STA) and long-term (LTA) ageing (in accordance with Radziszewski, 2007).

Based on data presented in Fig. 4.6 it should be noted that asphalt mixtures with rubber-bitumen have positively higher stiffness modulus at 25°C and also positive low values of stiffness modulus at 5°C. It can be concluded that modified mixtures are characterized by higher viscoelastic properties (extended viscoelastic range).

Asphalt mixtures undergo constant, adverse ageing changes. As a result of ageing, the mixture gradually loses its viscoelastic properties and the material becomes increasingly harder and more brittle, resulting in higher resistance to permanent deformation. As shown in Fig. 4.7, asphalt mixtures with a rubber-bitumen binder are more resistant to ageing than unmodified mixtures, which is reflected in the negligible changes in properties of the mixes in ageing studies (Radziszewski, 2007).

4.8 Performance of pavement with asphalt-rubber mixture

Crumb rubber from waste tyres is widely used as a bitumen modifier (in the wet process) or as a substitute of part of a mineral component (aggregate) in asphalt mixtures (in the dry process) for use in:

- Asphalt-rubber mixtures for construction of pavement layers
- SAM (Stress Absorbent Membrane) pavement coats and SAMI (Stress Absorbent Membrane Interlayer) membranes
- Sealings.

The first use of rubber-bitumen modified binders (25% of crumb rubber

by weight of bitumen) was surface repaving technology in so-called SAM layers to conduct maintenance operations. SAM can be used in sealing or as waterproof layers. A stress absorbent membrane exhibits high resistance to deformation and cracking. SAM coats with coarse aggregate or sand showed no damage after 12–15 years of service in various climatic conditions (Epps, 1994).

Another application of rubber–bitumen binder is to use it in SAMI layers as a stress-reducing layer. These are thin bitumen–rubber layers placed on damaged, fractured surfaces under new bitumen layers with a thickness of less than 10 cm (Way, 2006).

Rubber–bitumen binders, due to their viscous-elastic properties over a wide temperature range, are also used as a filling compound. They are used for sealing joints in pavement and other civil engineering structures. Fillers with rubber-modified bitumen are characterized by excellent adhesion to top surfaces of adjacent plates, traffic load resistance, weather conditions and chemical resistance (Epps, 1994).

Road surfaces made of asphalt–rubber mixtures are typically characterized by many advantages compared to conventional asphalt surfaces, such as:

- Improved anti-slip properties
- Increased ageing resistance of paving layers
- Increased durability (resistance to weather conditions)
- Increased resistance to reflective and low temperature cracking
- Improved rutting resistance
- Increased fatigue durability
- Lower maintenance costs of road paving.

Increased skid properties can be especially observed for surface layers constructed from asphalt mixtures with rubber produced by the dry method. Addition of crumb rubber to asphalt mixtures increases the mix resistance to frost action and increases the friction coefficient between tyres and the road surface: it is possible to reduce braking distance by about 25% (Epps, 1994).

Asphalt mixtures are subjected to ageing during production, paving, compaction and pavement service. The intensity of ageing depends primarily on temperature, access to oxygen (from the air), type of binder, and thickness of the binder layer covering the aggregate particles. In mixtures with a low content of binder, the bitumen film layer on the aggregate particles is thin (4–5 μm) and thus results in quicker ageing. According to Kandhal and Chakraborty (1996), ageing is slowed drastically when the thickness of binder film on the aggregate particles is greater than 9 μm . Increased viscosity of rubber-modified bitumen allows the use of a higher binder content in mixtures (Massucco, 1994; Gaweł and Slusarski, 1999), which leads to an increase in membrane thickness on the aggregate (19–25 μm). Increased thickness

of rubber–bitumen binder film on the aggregate particles contributes to a significant increase in ageing resistance of the pavement.

The use of rubber–bitumen binders in asphalt mixtures increases pavement durability. Surface layers with a rubber-modified binder exhibit increased stiffness modulus at high service temperatures and reduced stiffness modulus at low service temperatures. The viscoelastic nature of rubber–bitumen binders makes road pavement more resistant to cracking at low temperatures and more resistant to rutting at high temperatures. A thicker rubber–bitumen binder layer on the aggregate surface contributes to an increase in pavement durability.

Pavements subjected to multiple loads from the wheels of vehicles may crack due to fatigue. Pavement layers should not present fatigue cracking within the designed pavement life (they should provide ‘fatigue life’). Service experience of pavements shows that road structure layers of rubber–bitumen binder exhibit more than twice the fatigue resistance of pavement layers with unmodified binder (Epps, 1994).

Road pavements with asphalt–rubber mixtures are generally characterized by prolonged durability, and thus require fewer repairs. This has a significant impact on the reduction of service costs as compared to traditional pavement. Fewer disruptions for road users resulting from the reduced amount of repairs are also an important social aspect.

4.9 Economic benefits

In order to select an optimal paving technology, typically the following factors are taken into account: initial costs, rehabilitation costs and pavement life. Mixtures with rubber–bitumen binder allow for one of two scenarios: (a) thinner layers with unchanged pavement durability (resulting in up to 30% initial cost reduction), or (b) longer pavement life (and longer rehabilitation intervals) with unchanged layer thickness. In some cases, especially during rehabilitation work (placement of overlays), use of rubber-modified HMAs prevents using costly geotextiles.

In places with high volume use of asphalt–rubber technology, for example in Arizona, USA, approximately 50% of pavements have an asphalt–rubber surface (Zareh and Way, 2009). In fact, the primary purpose for using this technology is to reduce reflective cracking in rehabilitation overlays.

The typical cost of a mixture with rubber-modified bitumen is about 1.5–2.0 times higher than a conventional mixture (Jung *et al.*, 2002). However, a life cycle cost analysis (LCCA) proves the economic benefits of using asphalt–rubber mixtures. Moreover, in Arizona initial costs decreased when relevant patents expired and more contractors were in competition. As reported (Carlson and Zhu, 1999), initial construction costs for asphalt–rubber mixtures were lower when the thickness equivalency ratio could be utilized.

This means that less material can be used due to increased durability and strength in asphalt–rubber layers.

In order to extend pavement life (and rehabilitation intervals), maintenance action and proper pavement treatment applications have to be conducted (Sousa and Way, 2009). Due to their higher durability, for pavement maintenance where mixtures with rubber-modified bitumen binders are used, maintenance costs can be reduced (Sousa *et al.*, 2009). In most cases, significant differences in maintenance costs are visible after about five to six years; after about eight years double differences in maintenance costs can be recognized (Carlson and Zhu, 1999).

It can be expected that sustainable technological solutions, like the use of crumb rubber in HMA production, will be better supported by governments. Such support can be applied through, for example, tax deductions for companies using this technology.

4.10 Conclusions

Recycling of waste tyres is an important environmental issue. Among various methods of scrap tyre disposal, the use of crumb rubber to modify bitumen and asphalt mixtures can be considered the most efficient way to utilize this noxious waste. Rubber from tyre recycling can be a cheaper substitute for polymers used to modify bitumen.

The rubber–bitumen interaction is a diffusion phenomenon. Rubber particles absorb the bitumen components of similar solubility parameters and swell. The degree of swelling depends on the chemical nature and viscosity of bitumen, rubber content, particle size and polymer composition, and blending temperature and duration.

The interactions between rubber and bitumen affect the performance-related properties of the residual binder.

Rubber–bitumen binders and asphalt–rubber mixtures have good technological properties and extended lifetime. They can both be used in construction of high-traffic pavements, bridge waterproofing layers, sports field topcoats, cycle paths, etc.

Economic calculations take into account both ecological and technological aspects of rubber waste management and indicate the purposefulness of the use of bitumen and asphalt mixtures modified with crumb rubber from waste tyres.

4.11 References

Airey G D, Rahman M M and Collop A C (2003), ‘Absorption of bitumen into crumb rubber using the basket drainage method’, *Int J Pavement Eng*, 4, 105–119.

ASTM (2009a), ‘Standard Specification for Asphalt Rubber Binder’, American Society for Testing and Materials, D6114.

ASTM (2009b) 'Standard Test Method for Separation of Asphalt into Four Fractions', American Society for Testing and Materials, D4124.

ASTM (2002), 'Standard Terminology Related to Materials for Roads and Pavements', American Society for Testing and Materials, D8.

Bagińska K and Gaweł I (2004), 'Effect of origin and technology on the chemical composition and colloidal stability of bitumens', *Fuel Process Tech*, 85, 1453–1462.

Bahia H U and Davies R (1994), 'Effects of crumb rubber type and content on performance related properties of asphalt binders', *Proc Third Materials Engineering Conf, New Materials and Methods of Repair*, San Diego, CA, 449–466.

Bahia H U and Davies R (1995), 'Factors controlling the effect of crumb rubber on critical properties of asphalt binders', *J Ass Asphalt Paving Techn*, 63, 130–162.

Beaty A N (1992), 'Latex-modified bitumen for improved resistance to brittle fracture', *Highways Transportation*, 9, 32–41.

Billiter T C, Davison R R, Glover C J and Bullin J A (1997), 'Physical properties of asphalt–rubber binder', *Pet Sci Technol*, 15, 205–236.

Blow C M (1971), *Rubber Technology and Manufacture*, London, Institution of the Rubber Industry, IOM3.

Brandrup J and Immergut E H (1989), *Polymer Handbook*, New York, John Wiley & Sons.

Brown D R, Jared D, Jones C and Watson D (1997), 'Georgia's experience with crumb rubber in hot mix asphalt', *TRR Journal*, 1583, 45–51.

CALTRANS (2006), 'Asphalt rubber usage guide', Materials Engineering and Testing Services-MS #5, available from <http://www.dot.ca.gov/hq/esc/Translab/ope/Asphalt-Rubber-Usage-Guide.pdf> (accessed 30 September 2006).

Carlson D C and Zhu H (1999), 'Asphalt–rubber, an anchor to crumb rubber markets', *Third Joint UNCTAD/IRSG Workshop on Rubber and the Environment, International Rubber Forum*, Veracruz, Mexico, RPA.

Corté J F, Herbst G, Sybilski D, Stawiarski A and Verhée F (1999), 'Use of modified bituminous binders, special bitumens and bitumens with additives in road pavements', *World Road Association*, Paris, PIARC.

Dantas Neto S A, Farias M M and Pais J C (2006), 'Influence of crumb rubber gradation on asphalt-rubber properties', *Proc Asphalt Rubber 2006 Conf*, Palm Springs, CA, 679–692.

Dantas Neto S A, Farias M M and Pais J C (2009), 'Influence of cryogenic and ambient crushed rubber on the mechanical properties of hot mix asphalt', *Proc Asphalt Rubber 2009 Conf*, Nanjing, China, 341–354.

Dias J L F and Píscado-Santos L (2008), 'Characteristics of asphalt binders modified with the incorporation of recycled crumbled rubber', *Proc Third European Pavement and Asset Management Conf*, Coimbra, Portugal, 1–12.

Elbaba I F, Wu C and Williams P T (2010), 'Catalytic pyrolysis-gasification of waste tire and tire elastomers for hydrogen production', *Energy Fuel*, 24, 3928–3935.

Epps J (1994), 'Uses of Recycled Rubber Tires in Highways', *NCHRP Synthesis 198*, Washington, DC, TRB.

ETRMA (2008), *ELTs Treatment Data in 2007*, Brussels, ETRMA.

Fanto E, Durgo R, Biró S Z, Bartha L and Deak G Y (2003), 'Effect of storage time on rheological properties of crumb rubber modified bitumen', *Proc Asphalt Rubber 2003 Conf*, Brasilia, Brazil, 643–654.

Flanigan T P (1995), 'Process for producing tire rubber modified asphalt cement system and products thereof', US patent 5,397,818, 14 March 1995.

Fontes L P T L, Triches G, Pais J C and Pereira P A (2009), 'Evaluating permanent deformation in asphalt rubber mixtures', *Proc Asphalt Rubber 2009 Conf*, Nanjing, China, 269–284.

Frantzis P (2004), 'Crumb rubber–bitumen interactions: diffusion of bitumen into rubber', *J Mat Civil Eng*, 16, 387–390.

Gaweł I and Bagińska K (2004), 'Effect of chemical nature on the susceptibility of asphalt to aging', *Petroleum Sci Tech*, 22, 1261–1271.

Gaweł I and Slusarski L (1999), 'Use of recycled tyre rubber for modification of asphalt', *Progr Rubber Plast Tech*, 15, 235–248.

Gaweł I, Stepkowski R and Czechowski F (2006), 'Molecular interactions between rubber and asphalt', *Ind Eng Chem Res*, 45, 3044–3049.

Geiger A, Gergo P and Bartha L (2008), 'Chemically stabilized rubber bitumens', *MOL Scientific Magazine*, 3, 75–80.

Giavarini C (1994), 'Polymer-modified bitumen', in Yen T F and Chilingarian G V, *Asphaltenes and Asphalts*, vol. 1, 40, Amsterdam, Elsevier, 381–400.

Hansen C M and Smith A L (2004), 'Using Hansen solubility parameter to correlate solubility of C₆₀ Fullerene in organic solvents and polymers', *Carbon*, 42, 1591–1597.

Heimbuch J (2009), 'New technology hopes to boost tire recycling by 50%', *TreeHugger*, available from <http://www.treehugger.com/files/2009/05/new-technology-hopes-to-boost-tire-recycling-by-50.php> (accessed 5 November 2009).

Heitzman M A (1992a), 'Design and construction of asphalt paving materials with crumb rubber modifier', *TRR Journal*, 1339, 1–8.

Heitzman M A (1992b), 'State of the practice: Design and construction of asphalt paving materials with crumb rubber modifier Methods', Washington, DC, FHWA-SA-92-022, 17–20.

Hicks R G (2002), 'Asphalt rubber design and construction guidelines. Volume I – design guidelines', Northern California Rubberized Asphalt Concrete Technology Center and California Integrated Waste Management Board, Sacramento, CA.

Highways Agency (2010), 'Use of scrap rubber tyres in asphalt pavements', available from http://www.highways.gov.uk/knowledge_compendium/publications/AF9F5B741F03435286079A16016AA134.aspx (accessed 10 November 2010).

Horodecka R, Kalabińska M, Piłat J, Radziszewski P and Sybilska D (2002), 'Application of scrap tires at road building', Road and Bridge Research Institute Materials and Study, Report No. 54, Warsaw, Poland, 5–44.

Huang S-C (2008), 'Rubber concentration on rheology of aged asphalt binders', *J Mat Civil Eng*, 20, 221–229.

Hui J C, Morrison G R and Hesp S A (1994), 'Improved low-temperature fracture performance for rubber-modified asphalt binders', *TRR Journal*, 1436, 83–87.

Isacsson U and Lu X (1995), 'Testing and appraisal of polymer modified road bitumens – state of art', *Materials and Structures*, 28, 139–159.

Joseph T M, Li Z and Beatty C L (1994), 'The kinetics of the swelling of ground rubber tire particles', *Proc 52nd Annual Technical Conf ANTEC 94*, Part 2, San Francisco, CA, 1865–1866.

Jung J S, Kaloush K and Way G B (2002), 'Life cycle cost analysis: Conventional versus asphalt-rubber pavements', Report for the Rubber Pavements Association, August, Tempe, AZ.

Kalabińska M, Piłat J and Radziszewski P (1999), 'Rheological properties of Polish binders', no. 085, *Eurobitume Workshop*, Luxembourg.

Kandhal P S and Chakraborty S (1996), 'Effect of asphalt film thickness on short and long term aging of asphalt paving mixtures', *TRR Journal*, 1535, 83–90.

Khedaywi T S, Tamimi A R, Al-Masaeid H R and Khamaiseh K (1993), 'Laboratory investigation of properties of asphalt-rubber concrete mixtures', *TRR Journal*, 1417, 93–98.

Martínez G, Caicedo B, Gonzalez D and Celis L (2006), 'Mechanical properties of hot mixture asphalt with crumb rubber and other modifiers', *Proc Asphalt Rubber 2006 Conf*, Palm Springs, CA, 505–521.

Massucco J (1994), 'Asphalt rubber: a Federal perspective', *Proc Third Materials Engineering Conf, New Materials and Methods of Repair*, San Diego, CA, 467–474.

Mastral M A, Murillo R, Peres-Surio M J and Callen M S (1996), 'Coal hydroprocessing with tires and tire components', *Energy Fuels*, 10, 941–947.

McDonald C H (1981), 'Recollections of early asphalt-rubber history', presented at the National Seminar on Asphalt-Rubber, October, Kansas City, MO.

Miknis F P and Michon L C (1998), 'Some applications of nuclear magnetic resonance imaging to crumb rubber modified asphalts', *Fuel*, 77, 393–397.

Ould Henia M and Dumont A-G (2008), 'Effect of base bitumen composition on asphalt rubber binder properties', *ISAP*, 1–10.

Page G C (1992), 'Florida's initial experience utilizing ground tire rubber in asphalt concrete mixes', *J Ass Asphalt Paving Techn*, 61, 446–472.

Piłat J, Radziszewski P and Kalabińska M (2000), 'The analysis of visco-elastic properties of mineral–asphalt mixes with lime and rubber powder', *2nd Euroasphalt & Eurobitume Congress*, Barcelona, Spain, 648–654.

Putman B J and Amirkhanian S N (2006), 'Crumb rubber modification of binders: interaction and particle effect', *Proc Asphalt Rubber 2006 Conf*, Palm Springs, CA, 655–677.

Putman B J and Amirkhanian S N (2010), 'Characterization of the interaction effect of crumb rubber modified binders using HP-GPC', *J Mat Civil Eng*, 22, 153–159.

Radziszewski P (1997), *Fatigue life modelling of modified asphalt–aggregate mixtures. No. 45 Scientific Series*, Białystok, Poland, edited by Białystok University of Technology.

Radziszewski P (2007), *Aging caused changes in elastic–viscosity properties of modified binders and asphalt mixtures. No. 142 Scientific Series*, Białystok, Poland, edited by Białystok University of Technology.

Radziszewski P, Piłat J and Plewa A (2004), 'Influence of amount of crumb rubber of used car tires and heating time on rubber-asphalt properties', *Proc 19th Int Conf on Solid Waste Technology and Management*, Philadelphia, PA, S3C.

Read J and Whiteoak D (2003), *The Shell Bitumen Handbook*, London, Thomas Telford Publishing.

Rogel E (1997), 'Theoretical estimation of the solubility parameter distributions of asphaltenes, resins and oil from crude oil and related materials', *Energy Fuels*, 11, 920–925.

Shen J and Amirkhanian S (2005), 'The influence of crumb rubber modifier (CRM) microstructures on the high temperature properties of CRM binders', *Int J Pavement Eng*, 6, 265–271.

Singleton T M, Airey G D, Widyatmoko I and Collop A C (2000), 'Residual bitumen characteristics following dry process rubber–bitumen interaction', *Proc Asphalt Rubber 2000 Conf*, Vilamoura, Portugal, 463–482.

Slusarski L (1997), *Recycling of Polymers*, Warsaw, WNT.

Sousa J B and Way G B (2009), 'Optimum timing for pavement treatment application', *Proc Asphalt Rubber 2009 Conf*, Nanjing, China, 73–96.

Sousa J B, Way G B and Pais J (2009), 'Treatment performance capacity – A tool to predict the effectiveness of maintenance strategies', *Proc Asphalt Rubber 2009 Conf*, Nanjing, China, 47–72.

Southern E (1967), *Use of Rubber in Engineering*, London, McLaren.

Stroup-Gardiner M, Newcomb D E and Tanquist B (1993), 'Asphalt–rubber interactions', *TRR Journal*, 1417, 99–108.

Stroup-Gardiner M, Chadbourn B C and Newcomb D E (1996), 'Babbitt, Minnesota: Case study of pretreated crumb rubber modified asphalt concrete', *TRR Journal*, 1530, 34–42.

US Rubber Manufacturers Association (May 2009), *Scrap Tire Markets in the United States: 2007*.

Waste Management World (2010), 'Tyre recycling joint venture announced', available from <http://www.waste-management-world.com/index/display/article-display> (Accessed 9 November 2010).

Way G B (2000), 'Asphalt rubber – Research and development, 35 years of progress and controversy', *European Tire and Recycling Association Meeting*, Brussels.

Way G B (2006), 'Rubberised bitumen in road construction', *The Waste and Resources Action Programme*, Banbury, Oxfordshire, UK, The Old Academy.

Xiao F, Putman B J and Amirkhanian S N (2006), 'Laboratory investigation of dimensional changes of crumb rubber reacting with asphalt binder', *Proc Asphalt Rubber 2006 Conf*, Palm Springs, CA, 693–713.

Yen T F and Chilingarian G V (1994), 'Introduction', in Yen T F and Chilingarian G V, *Asphaltenes and Asphalts*, vol. 1, 40, Amsterdam, Elsevier, 1–6.

Zareh A and Way G B (2009), 'Asphalt–rubber 40 years of use in Arizona', *Proc Asphalt Rubber 2009 Conf*, Nanjing, China, 25–45.

The use of waste polymers to modify bitumen

F. J. NAVARRO DOMÍNGUEZ and
M. GARCÍA-MORALES, Universidad de Huelva, Spain

Abstract: This chapter deals with the modification of petroleum bitumen with different types of waste polymers: EVA, EVA/LDPE blend, PE, PP, crumb tyre rubber (CTR) and ABS, all of them coming from recycling plants of waste plastic materials. In addition, the influence of processing conditions (temperature, mixing device, etc.) on the rheological properties and microstructure is also summarised.

From the experimental results obtained, it can be deduced that CTR and polyolefins may enhance bitumen thermo-rheological behaviour. However, much more enhanced mechanical properties can be obtained using a combination of both CTR and polyolefin recycled polymers. In that sense, CTR would in the main improve material behaviour at low in-service temperatures and polyolefins would mainly improve high in-service temperature behaviour.

Regarding the processing conditions, the mixing device used (low or high shear) strongly affects the mechanical behaviour and microstructure of the blend obtained, especially in the case of polyolefins. For modified bitumen with CTR, no influence of the processing device was observed at temperatures equal to or below 180°C, since the processing conditions used are not able to break up the crosslinked network of the rubber.

Key words: modified bitumen, crumb tyre rubber, PE, PP.

5.1 Introduction

Bitumen can be defined as a dark brown to black cement-like material, whose compounds can be classified into two generic groups, maltenes and asphaltenes. Asphaltenes are the black-coloured fraction, insoluble in *n*-heptane, and having the highest polarity and molecular weight, whereas maltenes, also soluble in this solvent, are composed of saturated and aromatic compounds, and resins (Lesueur, 2009).

Bituminous binders have been widely used in construction applications, mainly for flexible road pavements, waterproofing, roofing, joint sealant, etc. In general, a binder must remain flexible enough to withstand sudden stresses without cracking at low temperatures during winter, but must also resist the permanent deformation or viscous flow at high in-service

temperatures. In that way, bitumen should resist stresses due to traffic loads and low temperatures in pavement application, as well as extensions and contractions in roof construction.

In order to achieve the desired mechanical properties, bitumens are modified mainly by using virgin polymers in order to change their natural rheological properties. In this sense, the extensive use of plastics and rubbers in all sectors of the industry, in agriculture, and also in everyday life, has led to a continuous increase of polymeric wastes creating an important environmental problem. The reutilisation of post-consumer or post-industrial polymeric materials, and their reuse in industry, could be a suitable way of solving environmental concerns, offering low-cost recycled resources. However, up to now, the reuse of polymeric wastes is of very limited potential because of the problems they entail. Currently, on average, only 7% are recycled to produce low-grade plastic (Mastral *et al.*, 2001).

On these grounds, new methods are being investigated to help relieve this problem. Thus, from an environmental and economic point of view, the use of recycled polymeric materials in the development of modified asphalts is an interesting alternative, since the resulting mixture may show similar performance to those containing virgin polymers (García-Morales *et al.*, 2004b).

In general, two major groups of recycled polymers may be considered: thermoplastics and thermosetting waste polymers. Here, we focus on the most interesting materials for bitumen modification, therefore those that can improve the mechanical properties of the resulting binder. Hence, different recycled thermoplastic polymers have been successfully used for modification of bitumen for paving purposes: polyethylene (González *et al.*, 2002), polypropylene (Murphy *et al.*, 2000) and EVA (García-Morales *et al.*, 2006b). The addition of such polymers to bitumen is known to enhance its in-service properties, yielding improved thermomechanical resistance, elasticity, and adhesion (Airey, 2003; González *et al.*, 2002).

Regarding thermosetting polymers, crumb tyre rubber (CTR) has been proven over the years to be the most important modifier of this category. Thus, crumb tyre rubber modified bitumen (CTRMB) is produced by using a wet process method, in which both components are processed at high temperatures (175–220°C) and stored until the resulting binder is mixed with mineral aggregates. Another technique, not considered here since it directly gives rise to an asphalt mixture, is the dry process which uses crumb rubber as a part of the aggregate in the hot mix. Even though the dry process enhances rutting resistance of mixtures at intermediate temperatures, it cannot inhibit cracking at low temperatures. In contrast, the binder prepared by the wet process has a high resistance to cracking and rutting as well (McGennis, 1995; Navarro *et al.*, 2002). As reported in the literature, the improvement of asphalt performance depends on many factors such as the crumb rubber

particle size, surface characteristics of the rubber particles, blending conditions, the manner in which crumb rubber devulcanises, and the chemical/physical properties of the bitumen, as well as the bitumen source (Bahia and Davies, 1994; Navarro *et al.*, 2002, 2004, 2005, 2007, 2010).

This chapter details some experimental results of bitumen modified by several thermoplastic recycled polymers (PE, PP, EVA) from agricultural and industrial origin, and crumb tyre rubber as elastic thermosetting polymer. In addition, the effect of both types of modifiers is also analysed, when jointly used as bitumen modifiers. Firstly, we focus on the influence of processing conditions, namely, the device characteristics, processing time and mixing temperature. Secondly, we present the effect of each single modifier on the thermomechanical, rheological and microstructural characteristics of the resulting modified bitumens.

5.2 Processing of waste polymer modified bitumens

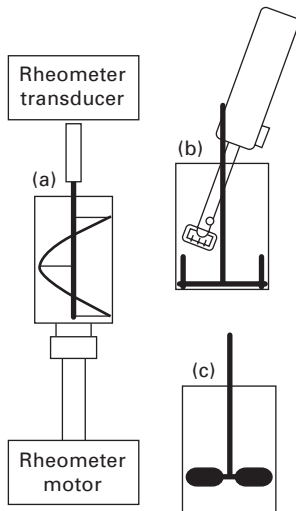
5.2.1 Processing of bitumens modified by waste thermoplastic polymers

Processing is well known to be of major importance in determining the thermomechanical properties of the final modified binder. On these grounds, it is necessary to establish optimum processing conditions, involving temperature and operation time, so that a bituminous binding material with excellent properties is attained. A large variety of mixing devices for polymer modified bitumen (PMB) processing, subdivided into any of low- or high-shear processing categories, have been traditionally used (García-Morales *et al.*, 2004a, 2004b, 2004c, 2006a, 2006b, 2007; González *et al.*, 2004, 2007). This subsection looks into both low- and high-shear processing kinetics of PMBs, which provides valuable information on the behaviour of the binder at different stages of the mixing operation (Belokon and Inozemtsev, 2002). A comparison among the thermomechanical properties of the modified binders resulting from using low- and high-shear processing devices will be further presented in Section 5.3.

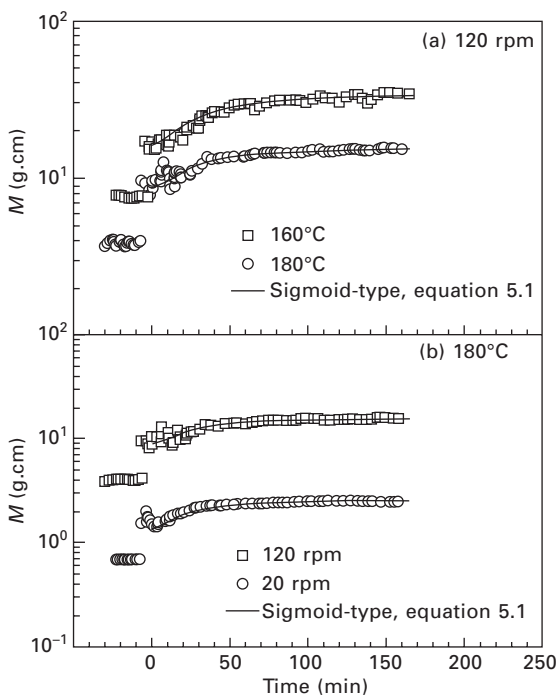
Low-shear processing

A low-shear processing device composed of a helical ribbon impeller inside a mixing vessel, coupled with a transducer and motor of a conventional controlled-strain rheometer, respectively (Fig. 5.1(a)), is considered in this subsection.

Figure 5.2 corresponds to the evolution of torque during the mixing of a 60 pen. bitumen (bit.1) with 5 wt% of a waste thermoplastic polyolefin (pol.1),



5.1 Different processing devices used in the manufacture of the PMBs studied.



5.2 Evolution of torque during processing of blends bit.1/pol.1 (5 wt%), manufactured with the low-shear device in Fig. 5.1(a), at (a) different temperatures, and (b) different agitation speeds.

which is a blend of ethylene vinyl acetate and low density polyethylene (ratio 2:1). Some characteristics of both bitumen and thermoplastic polyolefin are summarised in Table 5.1. Experiments were carried out at variable temperatures (160 and 180°C) for a constant agitation speed of 120 rpm (Fig. 5.2(a)), and at variable agitation speeds (20 and 120 rpm) for a constant temperature of 180°C (Fig. 5.2(b)).

Two different regions can always be observed in the evolution of torque with time. During the first stage, the neat bitumen was kept under stirring at the processing temperature, for about 20 minutes, with the aim of reaching thermal homogeneity throughout the bulk bitumen sample inside the mixing vessel. The second stage is characterised by a sharp increase in torque, as a consequence of polymer addition. For a short period of time after polymer addition, the torque data collected appear as a set of scattered points and a clear trend cannot be observed. Thus, the polymer has not reached its melting temperature yet and solid particles of polymer are dispersed into a continuous bituminous matrix; as a consequence, the torque cannot be accurately determined. A few minutes later, the temperature exceeds the

Table 5.1 Some characteristics of bitumens and waste polymers used

	Penetration (dmm)	Asphaltene content (wt%)	R&B temp. (°C)	Viscosity at 50°C (Pa·s)			
Bit.1	56	20.0	53.5	3.59×10^3			
Bit.2	150/200	22.5	–	1.27×10^3			
Bit.3	60/70	21.3	–	5.30×10^3			
<hr/>							
	M_w (g/mol)	M_w/M_n	VA content (wt%)	Melting temp. (°C)			
Pol.1	123 143	10.54	5	109 and 122			
Pol.2	–	–	2	112.5			
<hr/>							
	Average Sauter diameter (μm)	Specific surface area (m^2/g)	Total rubber hydrocarbon (wt%)	Carbon black (wt%)	THF extractable (wt%)	Ash (wt%)	Glass transition temp. (°C)
Rubber	211	0.0284	50 ± 5	32 ± 3	11 ± 3	4 ± 2	–
ABS	407	0.0147	–	–	–	–	95
<hr/>							
	MFI, 190°C and 2.16 kg (g/10 min)	MFI, 230°C and 2.16 kg (g/10 min)	Density (g/cm^3)	Ash (wt%)	M_w (g/mol)	M_w/M_n	
LDPE	0.80	–	0.930	0.80	223 080	5.59	
HDPE	0.33	–	0.964	1.44	231 792	9.09	
PP	–	3.96	0.910	3.05	402 537	6.00	

melting point of the polymer, which favours its blending with bitumen. The shear stresses originating from the rotation of the helical ribbon impeller enable the polymer to be dispersed into small droplets, throughout the bulk of the sample. In this way, the polymer domains start interacting with some of the bitumen compounds and, as a consequence, a slow increase in torque is observed over a long period of time, which depends on processing conditions, that is, agitation speed and temperature (Belokon and Inozemtsev, 2002). At the end of the mixing process, the blend achieves steady-state and torque becomes constant.

The evolution of torque with time can be represented by the following sigmoid-type equation:

$$\frac{M(t) - M_{\infty}}{M_0 - M_{\infty}} = \frac{1}{1 + (t/t_{1/2})^p} \quad 5.1$$

where M_0 and M_{∞} are the torque values for the polymer/bitumen blend right after polymer addition and at the final step of the process, respectively, while $t_{1/2}$ and p are fitting parameters. It is worth mentioning that models for torque increase based on exponential equations (Franco *et al.*, 2005) would not account for the short period of time prior to the polymer–bitumen interaction. Consequently, a sigmoid model is proposed.

Table 5.2 lists all the fitting parameters described, as well as the mixing time, t_{mix} , required by the bitumen–polymer blend to reach 95% of its steady-state torque value, M_{∞} (Tatterson, 1991). As can be observed, the model parameters $t_{1/2}$ and p , as well as the mixing time, t_{mix} , decrease as processing temperature increases. Agitation speed does not have any significant influence on mixing time, and the differences found should be attributed to inaccuracies in the experimental method used. An increase in agitation speed, however, leads to higher values of torque. Hence, temperature seems to have more influence on the rheological properties of the modified bitumen than agitation speed when samples are processed in a low-shear device.

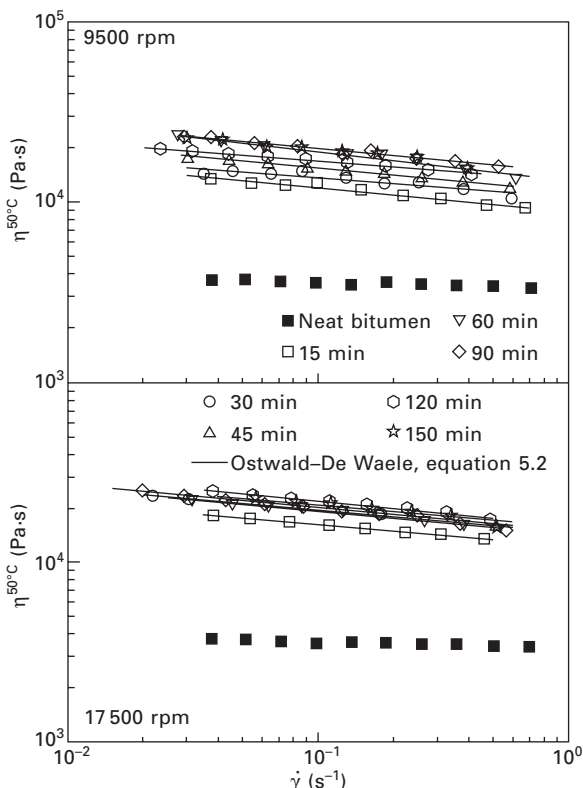
Table 5.2 Fitting parameters (equation 5.1) and t_{mix} values for blends of bit.1 and pol.1 (5 wt%) prepared with the low-shear mixer at two different temperatures (160 and 180°C) and agitation speeds (20 and 120 rpm)

	180°C		160°C
	120 rpm	20 rpm	120 rpm
M_0 (g·cm)	8.7	1.3	16.2
M_{∞} (g·cm)	15.7	2.6	34.3
$t_{1/2}$ (min)	29.0	25.7	35.4
p (–)	1.64	1.60	1.67
t_{mix} (min)	105.5	100	136.5

High-shear processing

A high-shear system composed of a high-shear homogeniser and an anchor impeller is considered in this subsection (Fig. 5.1(b)).

The mixing kinetics of a 60 pen. bitumen (bit.1, see Table 5.1) with 5 wt% of a waste thermoplastic polyolefin (pol.1, see Table 5.1) were followed by means of viscosity measurements of samples taken from the mixing device after different processing times. Figure 5.3 shows the viscous flow curves at 50°C for samples processed at different rotor speeds (9500 and 17 500 rpm), taken from the mixing vessel at 15-min intervals during the first 60 minutes of processing, and then at 30-min intervals up to the end of the test (150 minutes). The viscous flow curve at 50°C for the neat bitumen has also been included. The processing temperature was initially set to 150°C. However, due to the high level of heat generated by shear, the temperature rapidly increased up to 163 and 180°C for the two rotor speeds studied, respectively. After the first 15 minutes, the temperature remained steady.



5.3 Viscous flow curves, at 50°C, as a function of processing time, for blends bit.1/pol.1 (5 wt%) manufactured with the high-shear device in Fig. 5.1(c), at two different agitation speeds.

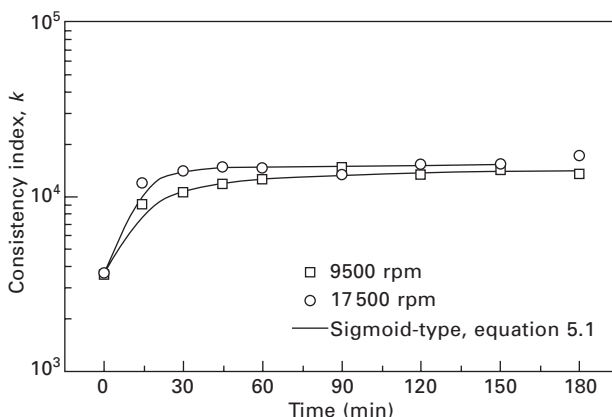
As can be seen in Fig. 5.3, polymer addition leads to a significant increase in viscosity, of about one order of magnitude higher at the last sampling time. In addition, this viscosity evolution depends on rotor speed. Thus, the PMB sample processed at 9500 rpm undergoes a progressive increase in viscosity. On the contrary, bitumen–polymer blends processed at 17 500 rpm show a much faster evolution of viscosity with processing time.

It is also worth pointing out that the shear-thinning behaviour shown by these modified bitumen samples at 50°C can be nicely described by a power-law equation, like that described by the Ostwald–De Waele model:

$$\eta = k \cdot \dot{\gamma}^{n-1} \quad 5.2$$

where k and n are the consistency and flow indexes, respectively.

Figure 5.4 shows the evolution of k , at 50°C, with processing time. As can be observed, the consistency index increases as processing time does. However, neither processing time nor rotor speed was seen to produce any significant effect on the flow index, which ranged between 0.85 and 0.90. As a result, the evolution of viscosity (and, therefore, torque) during processing can also be modelled by using the values of the consistency index instead of torque in equation 5.1, that is, replacing M_∞ and M_0 by k_∞ and k_0 , respectively. Table 5.3 shows that t_{mix} , calculated as the mixing time elapsed until reaching 95% of the steady-state value of the consistency index, k_∞ , largely decreases as rotor speed increases. Thus, a minimum processing time of about 45 minutes is required for binder processing at a rotor speed of 17 500 rpm. For longer processing times, the binder viscosity does not undergo any further significant change. However, mixing time increases up to 140 minutes when the binder is processed at a rotor speed of 9500 rpm



5.4 Evolution of the consistency index with processing time as a function of the agitation speed, for blends bit.1/pol.1 (5 wt%) manufactured with the high-shear device in Fig. 5.1(c).

Table 5.3 Fitting parameters (equation 5.1) and t_{mix} values for blends of bit.1 and pol.1 (5 wt%) prepared with the high-shear mixer at two different agitation speeds (9500 and 17 500 rpm)

	9500 rpm	17 500 rpm
k_{∞}	14 574	15 431
k_0	3630	3597
$t_{1/2}$ (min)	16.8	7.5
p (-)	1.27	1.55
t_{mix} (min)	139	43

and a temperature of 163°C, not far from the minimum mixing time in the low-shear mixer at 160°C. Nevertheless, the values of viscosity after t_{mix} remain quite similar no matter which rotor speed was applied.

5.2.2 Processing of bitumen modified by waste thermosetting polymers

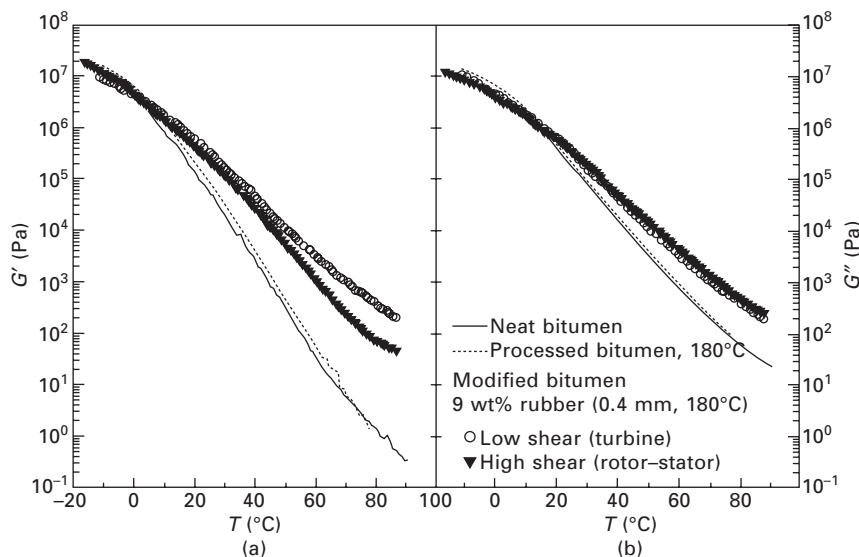
As has been previously reported, the thermo-rheological properties of CTRMBs are largely influenced by processing conditions. This subsection focuses on a study examining the influence that several processing devices and curing temperatures exert on the rheological and morphological characteristics of the resulting crumb tyre rubber-modified bitumen.

Here, we use a CTR concentration of 9 wt% (particle size 0.4 mm, 180°C) since previous results obtained by the authors demonstrated that this loading yielded similar rheological characteristics to those obtained by the addition of 3 wt% SBS, which is a general reference sample.

Influence of the processing device

Figure 5.5 shows the temperature dependence of the storage (G') and loss moduli (G'') of modified bitumen, obtained from oscillatory tests, at different processing devices. Results from blank samples (neat bitumen subjected to the same processing protocol as used for modification, but without polymer addition) have been also included in this figure. These thermo-rheological tests have been widely used as a tool to evaluate the end-use performance of polymer modified bitumen (Fawcett *et al.*, 1999; Fuentes-Audén *et al.*, 2008).

As can be observed, the evolution of neat bitumen linear viscoelastic behaviour demonstrates the well-known direct transition from the glassy to the Newtonian region with increasing temperature. In general, the addition of rubber leads to an increase in the elastic and viscous moduli in the high temperature region and a slight decrease in the low temperature



5.5 Evolution of (a) the storage modulus and (b) the loss modulus with temperature, at 1 Hz for unmodified bitumen and CTRMBs processed in different devices at 180°C.

Table 5.4 Solubilised rubber content in the modified bitumen samples studied

Sample	Processing device	Processing temp. (°C)	% solubilised
Raw rubber			11
CTRMB	Pilot plant	180	15
CTRMB	Laboratory 4-blade	180	15
CTRMB	Laboratory 4-blade	90	11
CTRMB	Laboratory 4-blade	120	11
CTRMB	Laboratory 4-blade	210	25
CTRMB	Laboratory 4-blade	250	45

zone. However, negligible differences in the values of the G'' function for CTRMBs processed in different devices are observed and only a slight drop in the elastic modulus is observed after high shear processing. These results can be explained taking into account that all the samples have the same amount of dissolved/dispersed rubber at 180°C during 1.5 h (see Table 5.4). The percentage of soluble components in raw rubber is around 11 wt%. Consequently, only about 4 wt% rubber is dissolved or dispersed in the bitumen due to partial depolymerisation (breaking of the backbone of the main chain) and devulcanisation (cleavage of the sulphur crosslink bonds) of the rubber particles. Consequently, the influence of the processing device was not significant because the temperature (180°C) was not high enough to produce rubber via depolymerisation or devulcanisation to any

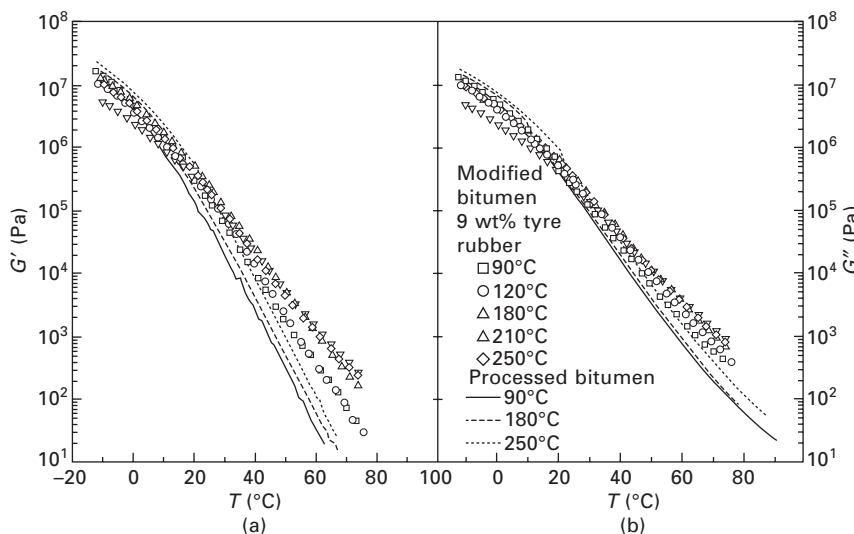
great extent (Billiter *et al.*, 1997; Zanzotto and Kennepohl, 1996; Navarro *et al.*, 2007).

In addition, rubber particle size used in this study ($>>5\text{ }\mu\text{m}$) can be considered large enough to exclude the possibility of any colloid-chemical activity and to neglect Brownian motion, so that the observed rheological behaviour must be explained in terms of hydrodynamic and/or mechanical interactions between particles in the bituminous phase. In this sense, a particle size reduction due to shear processing/temperature would explain the decrease in the storage modulus after processing in the pilot plant (Navarro *et al.*, 2002).

Influence of processing temperature on rheology of crumb tyre rubber modified bitumens (CTRMBs)

In order to study the effect of processing temperature, temperature sweep tests and flow curves have been performed on both unmodified bitumen and CTRMB samples, prepared at different temperatures, in a lab-scale device with a four-blade impeller.

Figure 5.6 shows elastic and viscous moduli from temperature sweep tests in the linear viscoelastic regime. Regarding unmodified bitumens (blank samples), an increase in processing temperature does not qualitatively change the linear viscoelastic behaviour, although both G' and G'' are raised in the whole temperature window tested. This rise in both moduli can be



5.6 Evolution of (a) the storage modulus and (b) the loss modulus with temperature, at 1 Hz for unmodified bitumen and CTRMBs processed at different temperatures.

considered as hardening, a consequence of processing (primary ageing). Bitumen ageing is a very complex process that produces a variation of both chemical composition and colloidal structure (García-Morales *et al.*, 2004b). The increase of asphaltene content, reported in Table 5.5, as a consequence of processing would explain these effects.

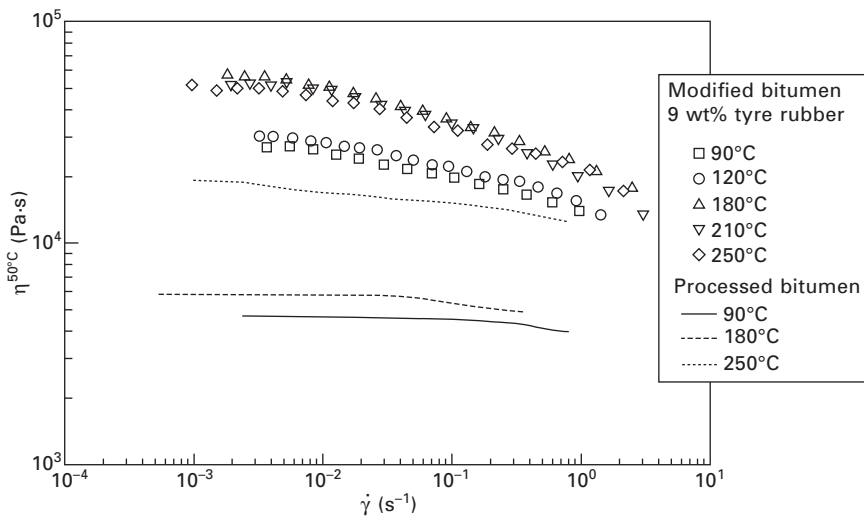
On the contrary, processing temperature has a more complex influence in the case of CTRMBs. Thus, in the high temperature region, an increase in processing temperature gives rise to an increase of both G' and G'' values, especially from 120 to 180°C, being clearly higher than all aged bitumens. By contrast, opposite behaviour is obtained in the low temperature zone, since all modified bitumens present lower values than their respective blank samples. Thus, unmodified bitumen processed at 250°C shows the highest moduli values, whilst they are a minimum for the CTRMB processed at 210°C.

From a technical performance point of view, in the high in-service temperature range, the observed increase in elastic and viscous moduli for all samples (aged bitumen and CTRMBs) causes enhanced rutting resistance of the resulting pavement (Navarro *et al.*, 2004). In addition, the same behaviour at low in-service temperatures makes the binder less flexible and more fragile, and so more susceptible to undergoing thermal cracking. Consequently, high processing temperatures cause negative effects on the performance of unmodified bitumen, whilst, on the contrary, the addition of crumb rubber induces better in-service properties at both low and high temperatures. The results obtained seem to indicate that the optimum CTRMB processing temperature, for the tyre rubber used in this study is 210°C.

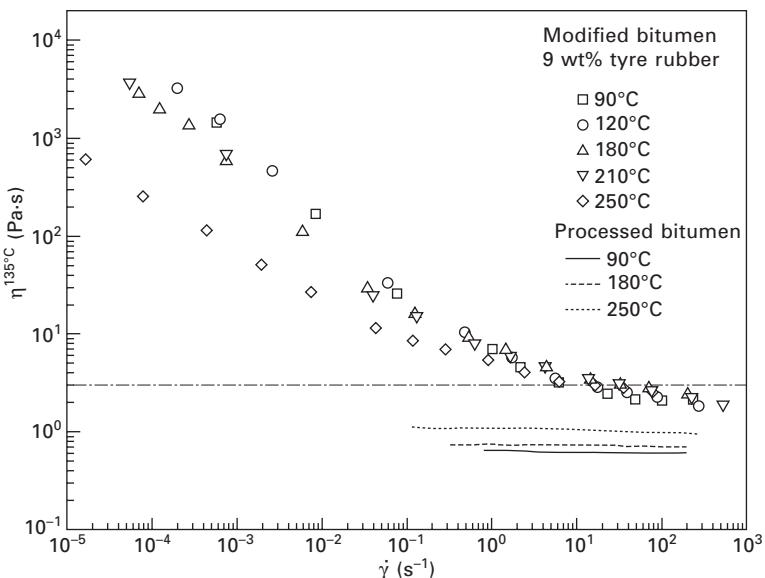
Figures 5.7 and 5.8 show the viscous flow behaviour, at 50°C and 135°C, for unmodified bitumen and CTRMBs manufactured at different processing temperatures. As expected, the data in Fig. 5.7 demonstrate that an increase in processing temperature always yields higher viscosity values, at 50°C, for unmodified bitumen, mainly at 250°C, although they are inferior to those corresponding to CTRMBs processed at any temperature between 90 and 250°C. Similarly, an increase in CTRMB processing temperature up to 180°C gives rise to higher viscosity values, at 50°C. However, viscous flow curves are slightly shifted to lower values for CTRMBs processed at higher processing temperatures.

Table 5.5 Asphaltene content for unmodified bitumen as a function of processing conditions

Processing temp. (°C)	Processing device	Wt% asphaltenes
Neat bitumen	–	20.2
180	Laboratory	21.2
250	Laboratory	23.8
180	Pilot plant	21.9



5.7 Viscous flow curves, at 50°C, of neat bitumen and CTRMBs, processed at different temperatures.



5.8 Viscous flow curves, at 135°C, of neat bitumen and CTRMBs, processed at different temperatures.

At 135°C (Fig. 5.8), unmodified bitumen always displays Newtonian behaviour, whereas CTRMBs show shear-thinning behaviour at low and intermediate shear rates, and a clear tendency to a high-shear-rate limiting

viscosity. Once again, CTRMBs exhibit higher viscosities than unmodified bitumen, as has been reported elsewhere (Airey, 2003; Navarro *et al.*, 2002). In addition, whereas all unmodified bitumen viscosity values, at 135°C, are well below 3 Pa·s (the limiting value required by AASHTO MP1, 1993), CTRMBs viscosities are above this limiting viscosity at low shear rates. Only at high shear rates, the viscous flow curves tend to approach this value. From an engineering standpoint, this last result is important since industrial operations such as pumping, handling and mixing of bitumen occur within the above high shear rate range. Thus, the AASHTO criterion, which has been developed for Newtonian bitumen, is not well defined for highly shear-thinning materials like CTRMBs and may be violated if the asphalt can be pumped and mixed at safe temperatures at high shear rates (Navarro *et al.*, 2002).

As demonstrated in this subsection, the final properties of CTRMBs are largely dependent on processing temperature. As reported in Table 5.4, the rubber solubilised in the bitumen phase remains constant and equal to the initial value for processing temperatures between 90 and 120°C, and, consequently, these conditions are not severe enough to break up the chemically crosslinked network. Thus, the observed rheological behaviour is a consequence of the presence of rubber particles swollen by light components of the maltenic fraction (Airey, 2003; Navarro *et al.*, 2005; Miknis and Michon, 1998). By increasing processing temperature, the dissolution/dispersion of rubber into the bitumen is clearly enhanced due to faster rates of breaking crosslink bonds. Then, two different effects influence the rheological properties of the resulting product. The first one is related to the bituminous phase, which is modified by an increased amount of soluble components (Navarro *et al.*, 2002). The second effect is associated with the remaining solid rubber, whose concentration decreases (Navarro *et al.*, 2005). Additionally, rubber particles are reduced in size, as a consequence of the disaggregation process, which also affects the rheological properties of CTRMBs (Navarro *et al.*, 2004).

5.3 Thermomechanical properties of waste polymer modified bitumens

5.3.1 Bitumen modification by waste thermoplastic polymers

Effect of polymer concentration and bitumen type

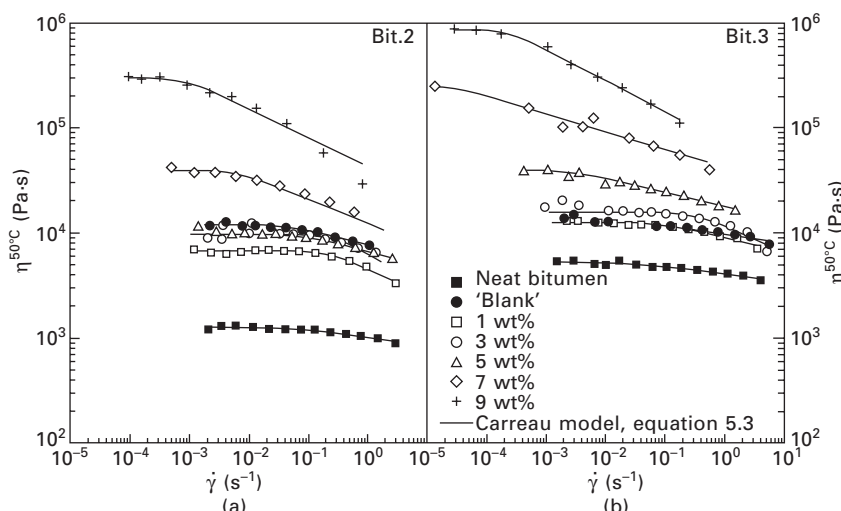
Blends of two bitumen samples with different penetration grades (150/200 pen. bit.2 and 60/70 pen. bit.3, in Table 5.1) and a waste ethylene vinyl acetate (pol.2, in Table 5.1), at polymer concentrations which ranged from 0 to 9 wt%, were prepared by using a low-shear device consisting of a mixing vessel and a 45°-pitched four-bladed turbine (Fig. 5.1(c)).

Figure 5.9 shows the experimental values of the steady-state viscosity versus shear rate at 50°C for the two bitumen samples, bit.2 and bit.3, and their corresponding modified binders with polymer contents between 0 and 9 wt%. Both neat and blank unmodified bitumens show a Newtonian behaviour over a wide range of shear rates. Likewise, PMBs after bitumen modification with waste polyolefin exhibit Newtonian behaviour at low shear rates. However, as the shear rate is raised, a decrease in viscosity, which corresponds to shear-thinning behaviour, may also be observed. This shear-thinning behaviour is more significant at the highest polymer concentration employed. It has been reported that the higher the extent of bitumen modification, the higher the deviation of the material behaviour from Newtonian flow (Filippova *et al.*, 2000). The flow behaviour observed can be described relatively well by the Carreau model:

$$\frac{\eta}{\eta_0} = \frac{1}{[1 + (\dot{\gamma}/\dot{\gamma}_c)^2]^s} \quad 5.3$$

where η_0 is the zero-shear-viscosity, $\dot{\gamma}_c$ is a critical shear rate for the onset of the shear-thinning region and s is a parameter related to the slope in this region.

The fitting parameters of the Carreau model, at 50°C, are presented in Table 5.6. As may be seen, 60/70 pen. bitumen exhibits higher values of zero-shear-viscosity than 150/200 pen. bitumen. In both blanks, it can be appreciated that there is a remarkable increase in viscosity after processing



5.9 Flow curves, at 50°C, of neat bitumen, and selected PMBs prepared with (a) bit.2 and (b) bit.3 with different concentrations of pol.2.

Table 5.6 Influence of polymer (pol.2) content on Carreau model parameters, at 50°C

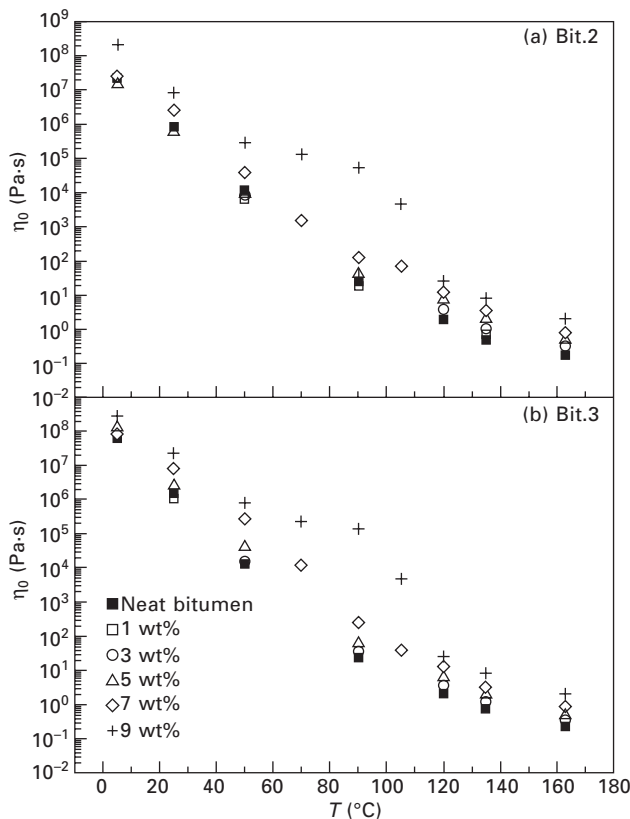
	Polymer content (wt%)							
	0	0 'blank'	1	3	5	7	9	
<i>Bit.2</i>								
$\eta_0 \times 10^{-3}$ (Pa·s)	1.273	12.040	6.856	9.700	9.795	39.240	303.7	
$\dot{\gamma}_c (s^{-1})$ s	0.042 0.036	0.036 0.064	0.202 0.129	0.127 0.088	0.076 0.075	0.004 0.083	0.001 0.137	
<i>Bit.3</i>								
$\eta_0 \times 10^{-3}$ (Pa·s)	5.296	12.710	12.580	15.920	39.510	256.5	871.5	
$\dot{\gamma}_c (s^{-1})$ s	0.208 0.085	0.023 0.044	0.084 0.066	0.284 0.123	$1.0 \cdot 10^{-3}$ 0.058	$2 \cdot 10^{-5}$ 0.084	$2.5 \cdot 10^{-4}$ 0.151	

(the so-called primary ageing, mentioned before), related to the increase in asphaltene concentration due to maltenic fraction oxidation and also to volatilisation of some bitumen light compounds. Such effects are more evident for the bitumen with the highest penetration grade, as may be deduced from Table 5.6.

On the other hand, polymer addition prompts an increase in bitumen viscosity above a critical polymer content. As may be observed from Fig. 5.9, the modification with this waste polyolefin would only be successful for loadings of polymer higher than 5 wt% in the 150/200 pen. bitumen and 1 wt% in the 60/70 pen. bitumen. Hence, oxidation by itself can produce the same or even more important effects on viscosity than addition of polymer at lower loadings than those mentioned above. A complete chemical characterisation carried out on the waste polyolefin showed the existence of degraded chains, with very low molecular weight and high vinyl acetate content (due to weathering during the polymer lifetime), which leads to a clear plasticising effect when added below a critical concentration. In contrast to that observed for viscosity, the critical shear rate for the onset of the shear-thinning region becomes lower as the amount of polymer in the sample increases (see Table 5.6). Moreover, PMBs obtained from 60/70 pen. bitumen have higher viscosities than those from 150/200 pen. bitumen. Consequently, higher polymer concentration or lower penetration grade bitumen leads to more structured binders with enhanced viscosity and higher sensitivity to shear.

When flow curves in Fig. 5.9 are ascertained at different temperatures and the data obtained are fitted to equation 5.3, the evolution of the zero-shear-viscosity (η_0) with temperature can be studied (Fig. 5.10). The temperature dependence of η_0 may be described by an Arrhenius-like equation:

$$\eta_0 = A e^{E_a/RT} \quad 5.4$$

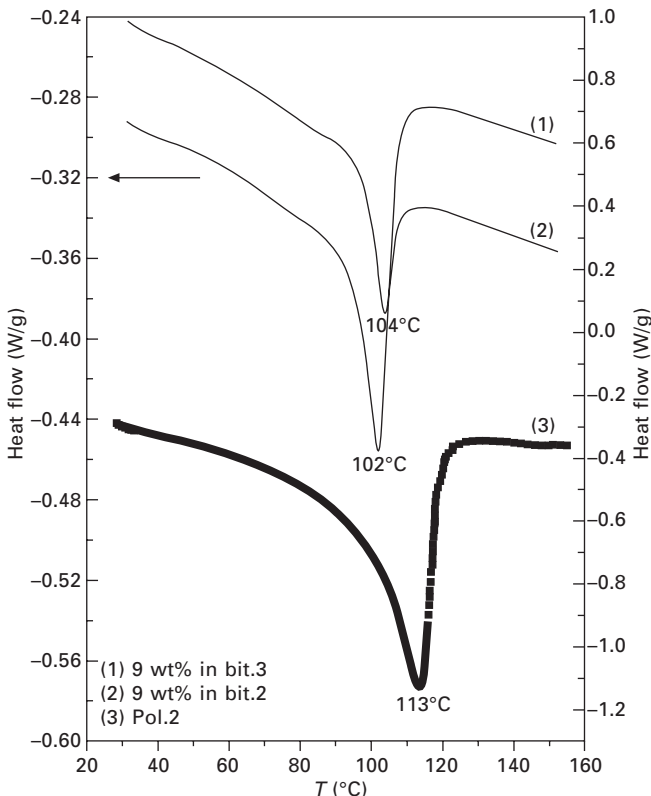


5.10 Temperature dependence of zero-shear-viscosity of neat bitumen, and selected PMBs prepared with (a) bit.2 and (b) bit.3 with different concentrations of pol.2.

where A is a pre-exponential parameter, R is the universal gas constant and E_a is the activation energy, a parameter which has been related to the binder thermal susceptibility (Ait-Kadi *et al.*, 1996).

It is worth noting that the temperature range over which results follow the Arrhenius model depends on polymer concentration. Thus, for PMBs having polymer content up to 7 wt%, this equation could fit the experimental results in the whole temperature range (5–163°C) studied. However, for blends containing 9 wt% polymer, the results do not obey the Arrhenius model beyond 90°C. This result suggests there has been microstructural changes in the bitumen, which significantly affect its rheological behaviour.

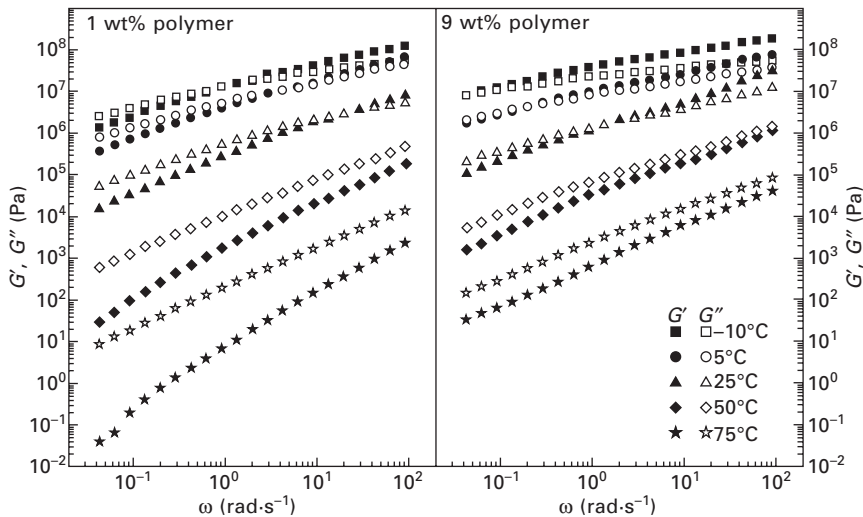
Differential scanning calorimetry studies can shed some light on this issue. Thus, Fig. 5.11 shows a characteristic peak, at 113°C, associated with the fusion of the waste polyolefin crystalline fraction (Champion *et al.*, 2001). However, the melting temperature of the waste polyolefin is further reduced down to



5.11 DSC curves of pol.2 (curve 3), and two selected PMBs prepared with bit.2 (curve 2) and bit.3 (curve 1), both at 9 wt% pol.2.

102 and 104°C (for 150/200 pen. and 60/70 pen. bitumens, respectively) due to polymer swelling by bitumen light compounds, a fact which results from bitumen disrupting the crystalline component of the polymer and yielding crystallites with a distribution of smaller sizes (Fawcett *et al.*, 1999; Fawcett and McNally, 2000). Hence, the binder rheology with 9 wt% polyolefin content seems to have a significant contribution from the polymer, with a marked drop in zero-shear-viscosity occurring at temperatures close to the melting point of the swollen polymer phase (see Fig. 5.10). These observations suggest that the rheological response of the binder containing 9 wt% waste polyolefin is governed by the polymer dispersed phase, though PMBs with lower polymer content behave similar to the straight run bitumen.

Likewise, studies of linear viscoelastic behaviour also reveal noticeable differences between PMBs with low and high waste polyolefin content. Figure 5.12 shows the frequency dependence of the linear elastic and viscous moduli in dynamic shear, as a function of temperature, for 60/70 pen. bitumen modified by addition of 1 and 9 wt% waste polyolefin. Figure 5.12 clearly



5.12 Frequency dependence of the linear elastic and viscous moduli in oscillatory shear, as a function of temperature, for blends bit.3/pol.2 at two different concentrations 1 and 9 wt%.

displays that both G' and G'' present higher values for the system having 9 wt% polymer, over the whole frequency range and for any temperature considered. Storage and loss moduli values become higher as temperature decreases. G'' is higher than G' at high temperatures in the whole frequency range. However, both moduli tend to reach similar values as temperature decreases, with a cross-over point at low temperature, which shifts to lower values of frequency as polymer concentration becomes larger. There is no plateau region at intermediate frequencies in any of the systems studied. As a consequence, entanglement effects are not significant and, therefore, a continuous transition from the elastic (glassy) to the Newtonian region occurs by decreasing the frequency (Partal *et al.*, 1999).

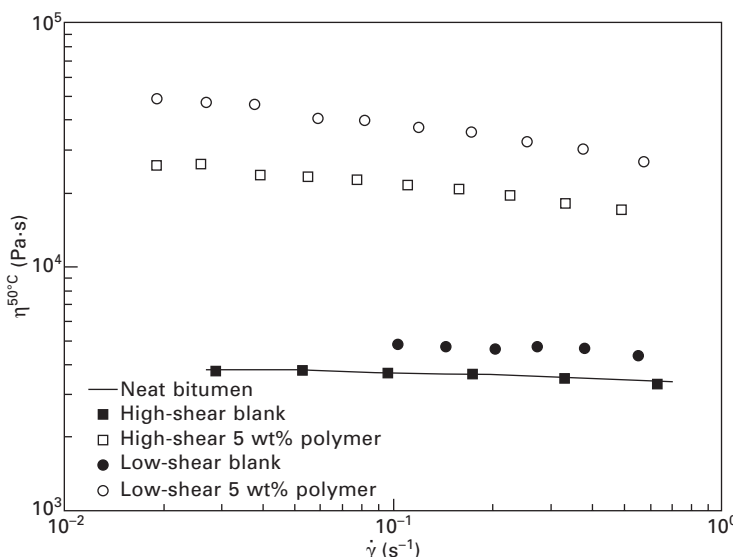
As can be observed in Fig. 5.12, at high temperatures, the difference between both moduli at 9 wt% polymer is smaller than that found at 1 wt% polymer. Furthermore, the sample with the lowest polymer content shows a viscous flow (or terminal) zone at high temperatures and low frequencies. Terminal behaviour is attained when the slopes of the loss and storage moduli versus frequency in log-log plots are, respectively, 1 and 2 (Ferry, 1980). Nevertheless, the above-mentioned terminal zone is not reached at 75°C for the highest polymer content. Thus, G' and G'' become parallel in the low frequency region, showing a typical behaviour of a critical gel (De Rosa and Winter, 1994).

Effect of processing

Figure 5.13 displays the viscous flow curves, at 50°C, of PMBs containing 5 wt% waste polyolefin (pol.1, see Table 5.1), prepared with bit.1 (see Table 5.1) by using two different, low- (Fig. 5.1(c)) and high-shear (Fig. 5.1(b)), processing devices. Optimum processing conditions were selected for any of the two processing methods, with the high-shear device presenting the shortest processing time.

A more significant increase in viscosity was observed after polymer addition for the modified binder processed using the low-shear device. However, if the viscosity curves for the corresponding blanks are taken into consideration, viscosity enhancement in the low-shear device should not be entirely attributed to polymer modification, but also to bitumen hardening during mixing (Fawcett *et al.*, 1999; Jiménez-Mateos *et al.*, 1996), and even to the oxidation of the waste polymer. As shown in Fig. 5.13, the blank sample processed in the high-shear device does not seem to be affected by any significant ageing process, and so presents the same value of viscosity as neat bitumen. This means that all the increase in viscosity is related to polymer modification, with the consequent benefits for the binder, mainly at low temperatures (later commented in Fig. 5.15).

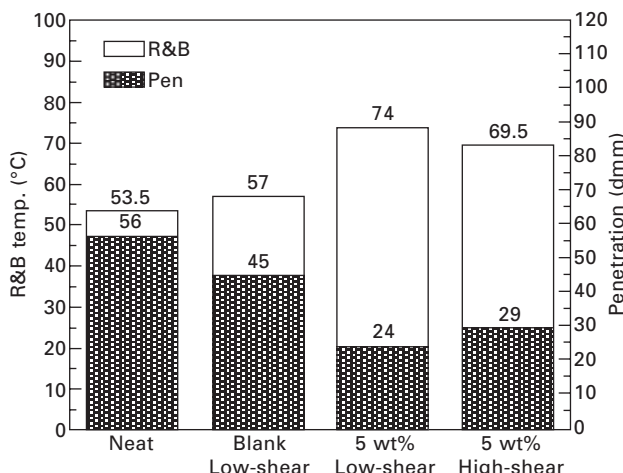
As previously seen from the viscous flow measurements, results of technological tests also reveal the existence of primary ageing after blending



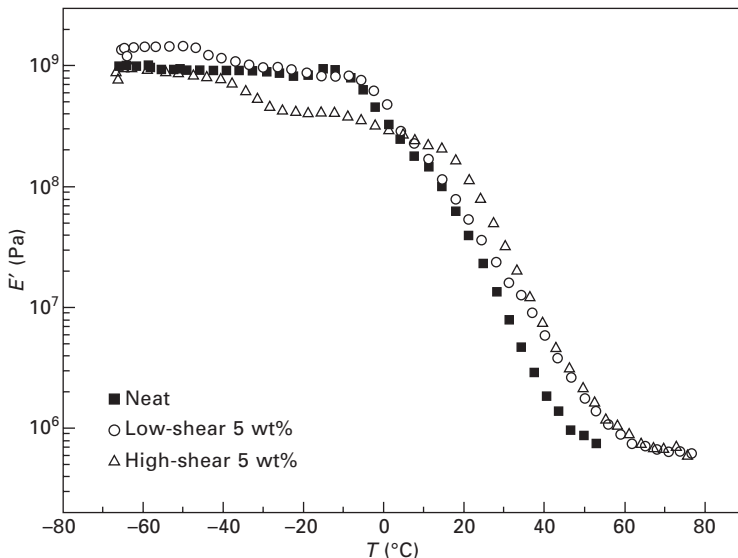
5.13 Viscous flow curves, at 50°C, for blanks and two blends of bit.1/pol.1 (5 wt%) manufactured with the low- and high-shear mixing devices in Figs 5.1(a) and 5.1(c), at the optimum processing conditions.

bitumen and polymer (Fig. 5.14). Thus, the low-shear blank shows increased value of softening temperature and a reduction of penetration, when compared to neat bitumen, which gives rise, after polymer addition, to a harder modified binder than that prepared by high-shear processing. However, Fig. 5.15, which presents the evolution with temperature of the linear elastic modulus in dynamic bending, makes clear that high-shear yields a notable shift in the temperature at which the glassy modulus appears, which might prevent pavements from thermal cracking. Instead, the low-shear sample does not present such a satisfactory behaviour, as the glassy region appears at much higher temperatures due to oxidation.

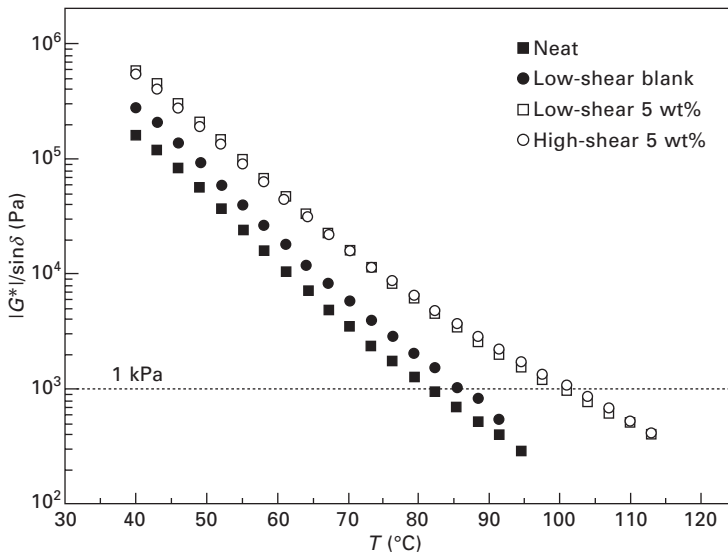
On the other hand, in the 1990s, the Strategic Highway Research Program (SHRP) presented the so-called 'rutting parameter', $|G^*|/\sin \delta$, as a way of efficiently classifying the rutting performance of bitumen. Some other parameters lately proposed (like zero-shear-viscosity) have proven to better correlate permanent deformation at high in-service temperatures in PMBs (Morea *et al.*, 2010). However, they are known to involve relatively time-consuming measuring methods. For instance, creep tests can take as long as or more than 5 hours to get to steady-state in modified bitumens. By contrast, the testing procedure proposed in SHRP is relatively easier and a more hands-on way to determine the degree of improvement attained, adequate for comparing the quality of different binders. Hence, Fig. 5.16 shows the evolution of the 'rutting parameter' with temperature for low- and high-shear binders. It can be seen that in both cases polymer addition



5.14 Results of penetration and softening temperature tests for neat bit.1 and two bit.1/pol.1 blends (5 wt%) manufactured with the low- and high-shear devices in Figs 5.1(a) and 5.1(c), at the optimum processing conditions.



5.15 Temperature dependence of the linear elastic modulus in dynamic bending for neat bit.1 and two bit.1/pol.1 blends (5 wt%) manufactured with the low- and high-shear devices in Figs 5.1(a) and 5.1(c), at the optimum processing conditions.



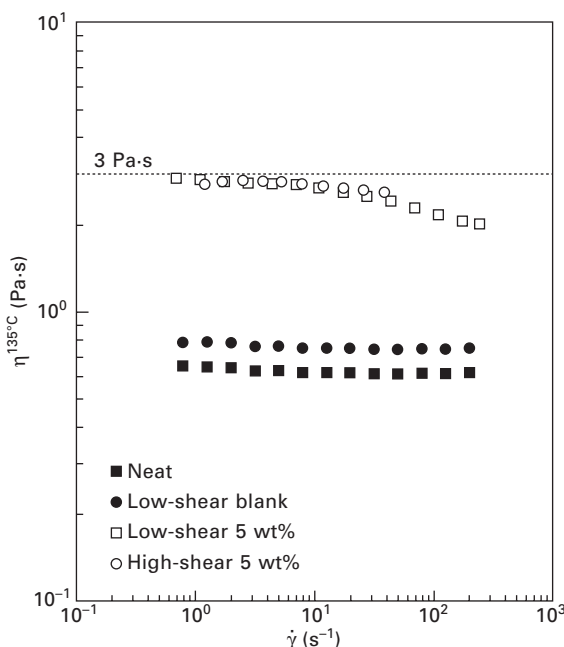
5.16 Evolution of the 'rutting parameter' with temperature for neat bit.1 and two bit.1/pol.1 blends (5 wt%) manufactured with the low- and high-shear devices in Figs 5.1(a) and 5.1(c), at the optimum processing conditions.

prompts an important rutting resistance enhancement (increase in temperature at which the binder has a value of $|G^*|/\sin \delta$ equal to 1 kPa, according to the rutting criterion outlined in AASHTO MP1, 1993), although no significant differences were found between the two processing methods studied.

In addition, hot mixing with mineral aggregates and lay-down operations are carried out at temperatures which fall within the interval 130–150°C. Consequently, the viscosity at 135°C should be less than 3 Pa·s, so that it can be assured that the asphalt will be pumped and mixed under safe conditions (AASHTO MP1, 1993). Figure 5.17 shows the steady-state viscous flow at 135°C, and makes clear that, on the one hand, both low- and high-shear binders fulfil the specifications required and, on the other hand, the processing method did not provoke any sensitive differences in the values of viscosity obtained.

Effect of polymer type

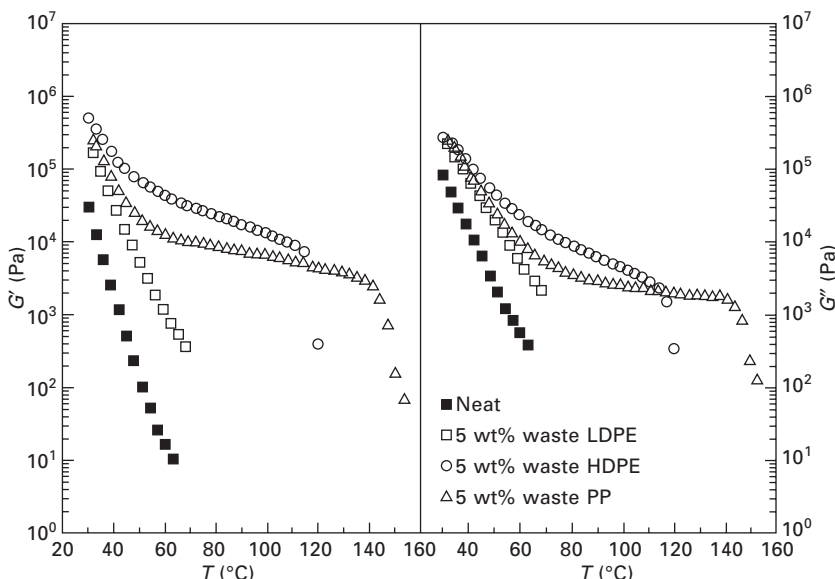
In order to study the influence of the polymer nature on the thermomechanical properties of the resulting bituminous binders, three different waste thermoplastic polyolefins will be considered: (a) waste LDPE; (b) waste HDPE; and (c) waste PP. Some physicochemical characteristics of the polyolefins



5.17 Viscous flow curves, at 135°C, for neat bit.1 and two bit.1/pol.1 blends (5 wt%) manufactured with the low- and high-shear devices in Figs 5.1(a) and 5.1(c), at the optimum processing conditions.

selected are presented in Table 5.1. Three different PMBs were prepared by blending bit.2 with the same content (5 wt%) of any of the polymers above, in the four-bladed turbine low-shear device shown in Fig. 5.1(c).

Figure 5.18 presents the evolution with temperature of the linear viscoelastic functions, G' and G'' , for the three different PMBs prepared. It can be observed that the addition of 5 wt% waste LDPE brings about a notable increase in the values of both elastic and viscous moduli, compared to the unmodified base bitumen. However, despite the polymer modification, the thermomechanical properties of this binder are seen to dramatically decrease with increasing temperature. Conversely, addition of 5 wt% waste HDPE or 5 wt% waste PP not only prompts an important enhancement in the G' and G'' values, but they also significantly enlarge the temperature interval before the viscous flow region appears. Thus, although the moduli enhancement is higher for the waste HDPE modified bitumen, waste PP addition shifts the onset of the terminal flow region up to 150°C (in comparison to 120°C for waste HDPE) which corresponds to the melting temperatures of the partially swollen polyolefins. It is worth mentioning that delays observed in the onset of the viscous flow suggest major differences between the microstructures of the different PMBs studied. Thus, for waste HDPE or waste PP modified bitumen, the viscoelastic behaviour found may relate to a swollen polymer



5.18 Temperature dependence of the linear elastic and viscous moduli in oscillatory shear, for neat bit.1 and selected PMBs prepared with bit.1 and three types of thermoplastic polyolefins (LDPE, HDPE and PP) at 5 wt%.

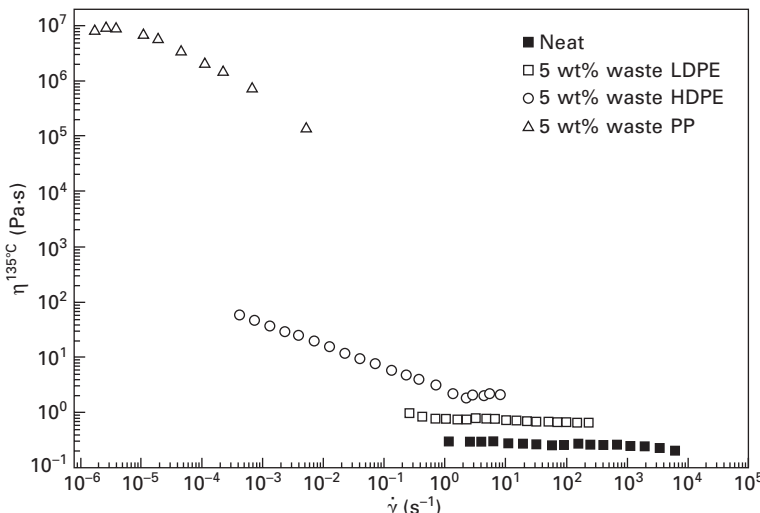
phase which largely extends throughout the binder, controlling its rheological response at small values of deformation. This does not occur when waste LDPE was employed as modifier.

Interestingly, the behaviour observed at intermediate temperatures (with HDPE showing higher values of G' and G'' than PP) reverses as testing temperature falls within the melting points of these polyolefins. Hence, the steady-state flow curves at 135°C in Fig. 5.19 clearly show that differences between HDPE and LDPE become smaller as their melting temperatures are exceeded. Consequently, major differences at 135°C are only noted for the waste PP modified bitumen, with a melting point corresponding to the swollen polymer phase which has not been reached and gives rise to viscosity values at low shear rates of about 10^7 Pa·s.

5.3.2 Bitumen modification by waste thermosetting polymers

Besides the processing conditions, the rheological, thermal and mechanical properties of CTRMBs are largely influenced by factors such as rubber concentration, particle size, rubber-grinding method and bitumen composition.

This subsection focuses on the most important factors affecting the final properties: particle size and rubber concentration.

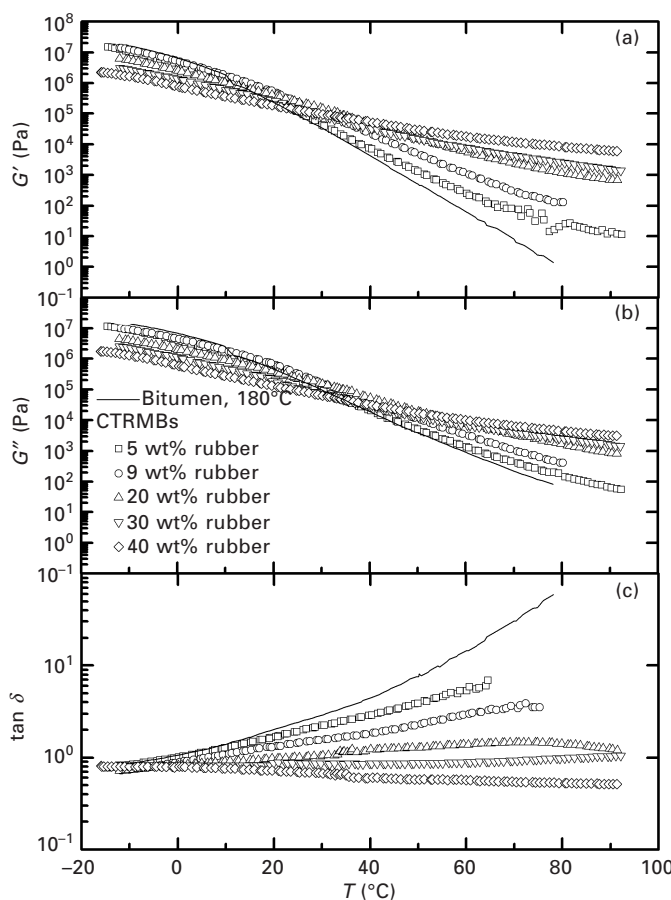


5.19 Viscous flow curves, at 135°C, for neat bit.1 and selected PMBs prepared with bit.1 and three types of thermoplastic polyolefins (LDPE, HDPE and PP) at 5 wt%.

Influence of rubber concentration

Figure 5.20 shows the evolution of storage and loss moduli with temperature, at constant frequency, for different rubber concentrations. As may be seen, the viscoelastic functions of neat bitumen display a direct transition from glassy to Newtonian behaviour. There is no 'plateau' region occurring at any of the temperatures studied, so that entanglement effects are not significant (Dongré *et al.*, 1996; Partal *et al.*, 1999).

The use of CRT as modifying agent of bitumen largely modifies material thermo-rheology at both low and high in-service temperatures. As can be observed, in the low temperature region, a remarkable reduction in moduli was observed with increasing polymer content. This reveals an increase in

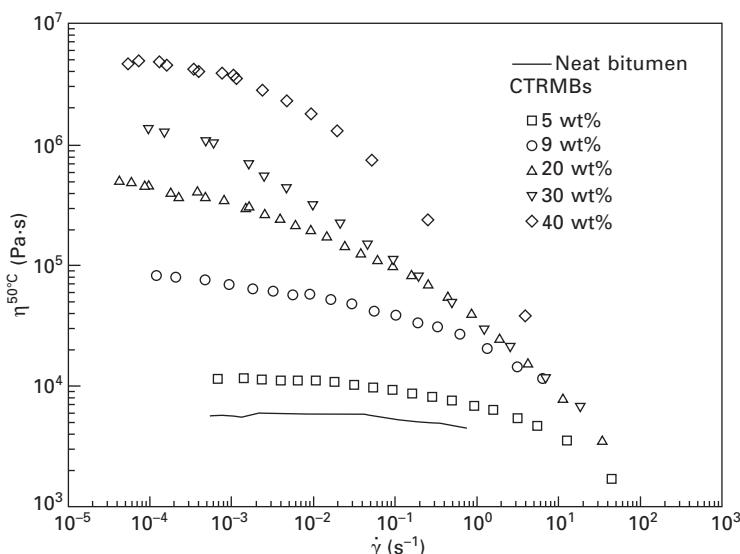


5.20 Evolution of (a) the storage modulus, (b) the loss modulus and (c) the loss tangent with temperature, at 1 Hz, for neat bitumen and CTRMBs with different rubber concentrations.

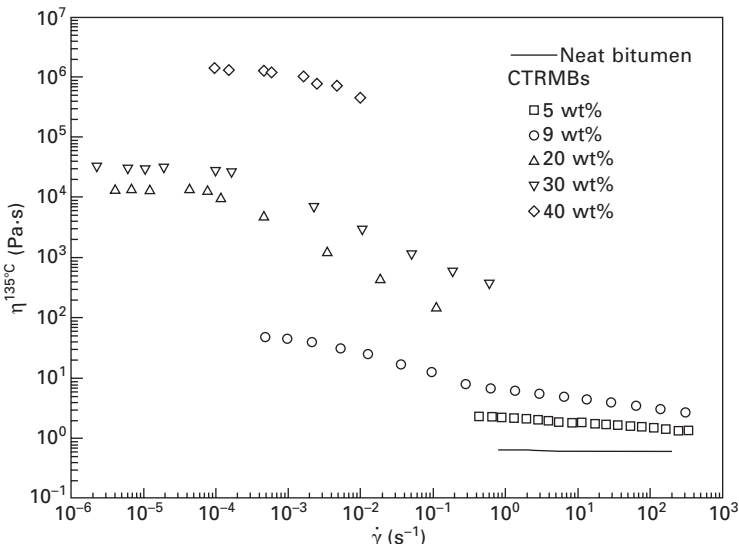
binder flexibility and, therefore, better thermal cracking resistance. On the contrary, in the high temperature region, a large increase in the storage and loss moduli values with rubber addition is clearly noticed. Consequently, a significant improvement of the rutting resistance of the resulting pavement is expected at these temperatures.

In addition, it is worth noting that a dramatic change in the rheological response is obtained by increasing the rubber content. Thus, at low rubber content, the samples display a predominantly viscous behaviour ($\tan \delta > 1$, except in the very low temperature region) whereas at high rubber concentration ($\geq 30\%$) the systems are mainly elastic ($\tan \delta < 1$). In addition, the loss tangent vs. temperature slope can be considered as a measure of material thermal susceptibility over the temperature range previously mentioned (20–70°C). As can be seen in Fig. 5.20(c), binder temperature susceptibility decreases with rubber addition and, consequently, an improved thermal resistance of the modified bitumen should be expected (Chebil *et al.*, 2000; Fuentes-Audén *et al.*, 2008; Navarro *et al.*, 2010).

The modification of rheological behaviour can also be deduced from flow measurements (Figs 5.21 and 5.22). The viscous flow response changes from Newtonian, in a wide range of shear rates, for neat bitumen 60/70, to shear-thinning for rubber-modified bitumen. This shear-thinning behaviour is more apparent as the rubber concentration increases and the zero-shear-rate-limiting viscosity is increased up to three orders of magnitude at 50°C and up to six orders at 135°C, relative to the unfilled bitumen. In this way, AASHTO



5.21 Viscous flow curves of neat bitumen and CTRMBs, as a function of rubber concentration, at 50°C.



5.22 Viscous flow curves of neat bitumen and CTRMBs, as a function of rubber concentration, at 135°C.

MP1 (1993) requires that the binder viscosity measured at 135°C should be less than 3 Pa·s. According to this limit, CTRMBs with rubber content higher than 5 wt% should not be used for road applications. Nevertheless, as pointed out above, this criterion may be violated if the asphalt can be pumped and mixed at safe temperatures.

As a result, viscous and viscoelastic results hint to microstructural changes at rubber content of 30 wt%. Since the particles used are large enough to exclude the possibility of any colloid-chemical activity, the rheological behaviour observed is due to hydrodynamic and/or mechanical interactions between swollen rubber particles. Consequently, an increase in rubber addition leads to a physical gelation process, and 30 wt% rubber can be considered a critical rubber concentration for a sol-gel transition in a wide range of temperatures, i.e. a state of matter between liquid and solid described by a three-dimensional macromolecular network consisting of aggregates of particles (Navarro *et al.*, 2005).

On the other hand, from these results, rubber addition also seems to move the glassy region of the mechanical spectrum to lower temperatures and, hence, thermal cracking would appear at lower temperatures. These outcomes are also in good agreement with those obtained from modulated differential scanning calorimetry (MDSC) – see page 126. In this sense, two glass transition temperatures can be determined, at lower temperatures, from the maximum of the derivative of the reversing heat capacity with respect to temperature (Table 5.7), which results from the overlapping of two glass

Table 5.7 Glass transition temperatures of selected samples, determined by MDSC

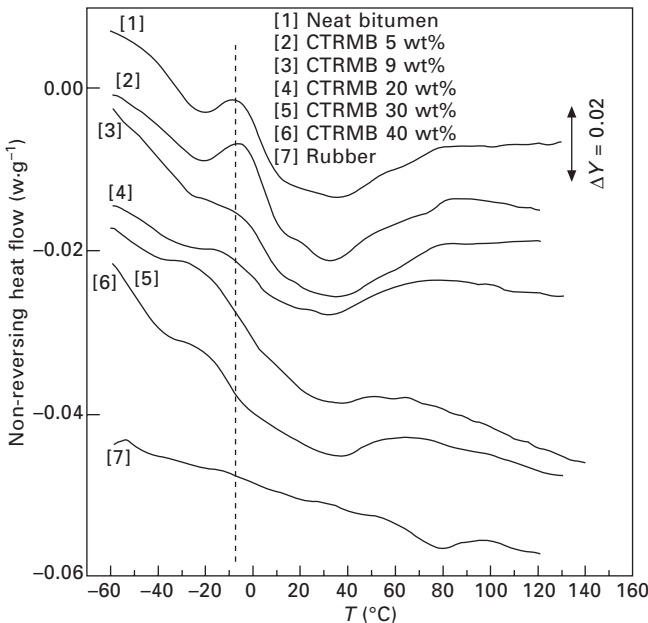
Sample	CTR (wt%)	$T_{g1}^{\text{DSC}} (\text{°C})$	$T_{g2}^{\text{DSC}} (\text{°C})$
Neat bitumen	–	–28.2	–13.3
CTRMB	5	–28.1	–13.9
CTRMB	9	–28.5	–14.3
CTRMB	20	–30.3	–16.7
CTRMB	30	–36.7	–16.2
CTRMB	40	–43.0	–17.4

transition processes corresponding to saturates and aromatics in the maltenic fraction (Masson *et al.*, 2002). As may be seen in Table 5.7, both glass transition temperatures, T_{g1} and T_{g2} , decrease as rubber content increases and, consequently, the glassy region which leads to brittle behaviour is also shifted to lower temperatures.

As reported elsewhere (Billiter *et al.*, 1997; Navarro *et al.*, 2005, 2007), at a processing temperature of 180°C, only 4% of the structural network of the rubber added was dissolved or disintegrated during sample digestion. Hence, the mechanical properties of the modified bitumen are mainly influenced by the remaining particles of rubber and, to a lesser extent, by the dissolved/dispersed fraction, and also by the bituminous phase. Moreover, the swelling process of the rubber particles by some light components of the bitumen may modify both the elastic characteristic of the filler and the bitumen colloidal microstructure. In this sense, the absorption of some bitumen compounds by the polymer causes modification in the glass transition temperature region (Table 5.7).

The above-mentioned swelling process and its effect on the thermal behaviour of the modified bitumen have been analysed by means of modulated differential scanning calorimetry (MDSC), a technique which allows the separation of reversing (cyclic component) and non-reversing heat flow (difference between the total heat flow and the reversing component), providing important information on bitumen composition and microstructure (Navarro *et al.*, 2002; García-Morales *et al.*, 2006b; Fuentes-Audén *et al.*, 2008). Thus, the non-reversing component of the heat flow curves, shown in Fig. 5.23, suggests some degree of compatibility between tyre rubber and bituminous compounds.

Therefore, a broad endothermic background from –60 to 80°C, approximately, is clearly noticeable for all the bituminous samples. This event arises from crystallisation of saturates and from the ordering of simple aromatic structures. On the other hand, a second observable thermal event, an exotherm centred around –7°C, arises from the cold-crystallisation of low molecular weight saturated segments in saturates and other maltenic compounds (García-Morales *et al.*, 2006b; Fuentes-Audén *et al.*, 2008).

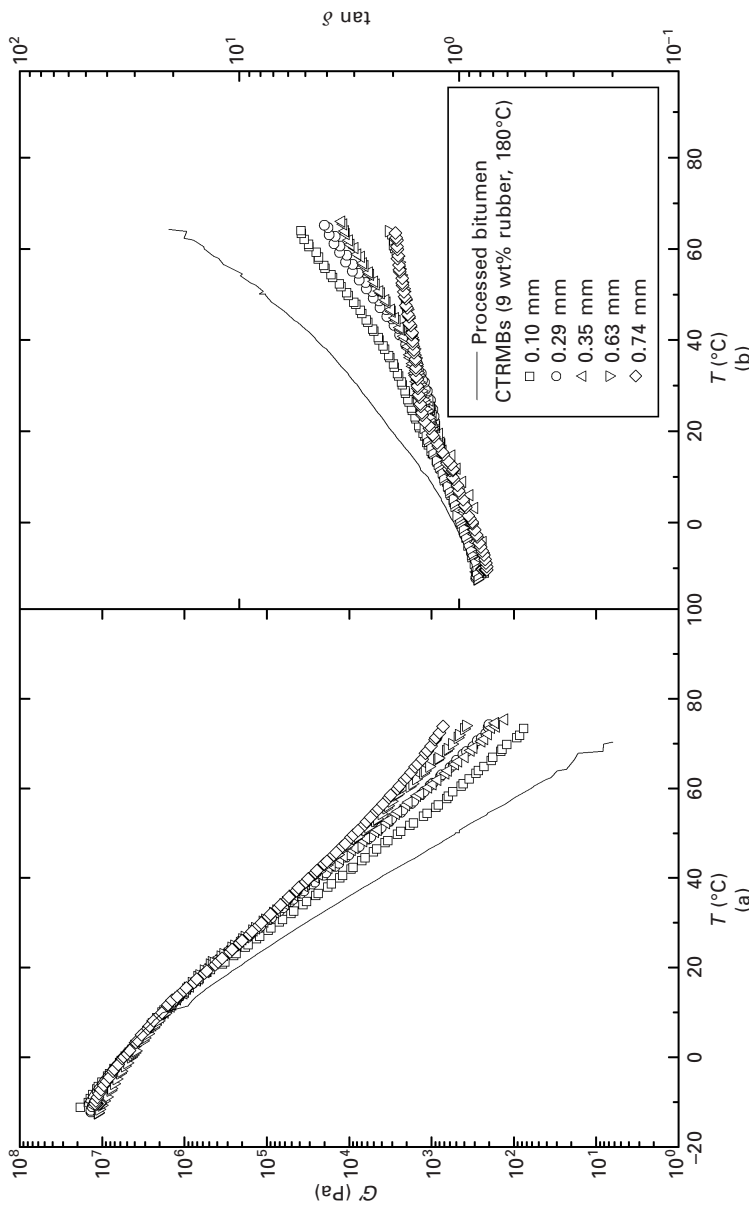


5.23 Non-reversing heat flow curves from modulated differential scanning calorimetry (MDSC) tests carried out on neat bitumen, crumb rubber and CTRMBs.

Further thermal events can be found in the high temperature region, i.e. between 20 and 80°C, probably due to the slow diffusion of relatively large and high molecular weight structures (asphaltenes, multi-rings and multi-arm structures) to form independent domains. As can be deduced from Fig. 5.23, the extension of the first and second thermal events is reduced by the presence of CTR, a fact that has been associated with the absorption of some components of the maltene fraction. In addition, the temperature at which the second event appears is shifted to lower values as tyre rubber concentration increases. This behaviour could be related to lower T_g values after rubber addition, as there is an increase in chain mobility which allows cold crystallisation to begin at lower temperatures.

Influence of particle size

Figure 5.24 shows the effect of particle size on the elastic modulus and loss tangent, at a constant frequency, of selected ground tyre rubber-modified bitumens with the same concentration (9 wt% rubber). In the low temperature region, rubber addition gives rise to a decrease of G' but similar values of $\tan \delta$. As mentioned before, it yields positive effects on the performance of a



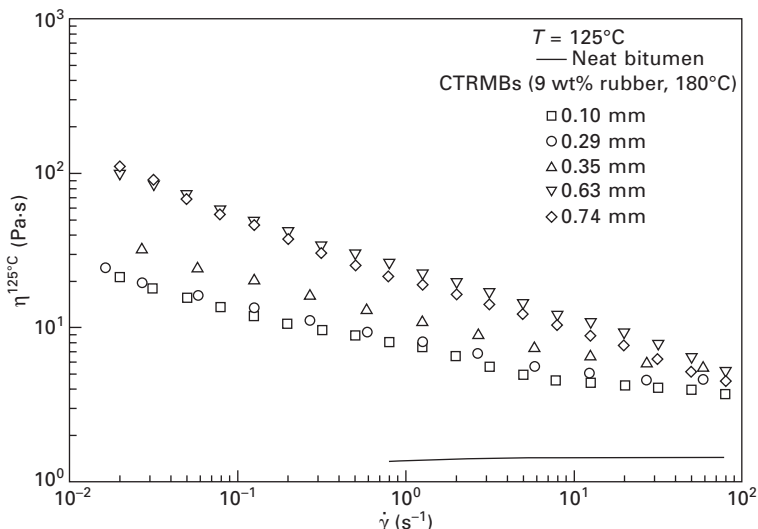
5.24 Evolution of (a) the storage modulus and (b) the loss modulus with temperature, at 1 Hz, for neat bitumen and CTRMBs having different particle size.

road asphalt binder, since higher flexibility, at low temperatures, is expected and so thermal cracking would occur at lower temperatures.

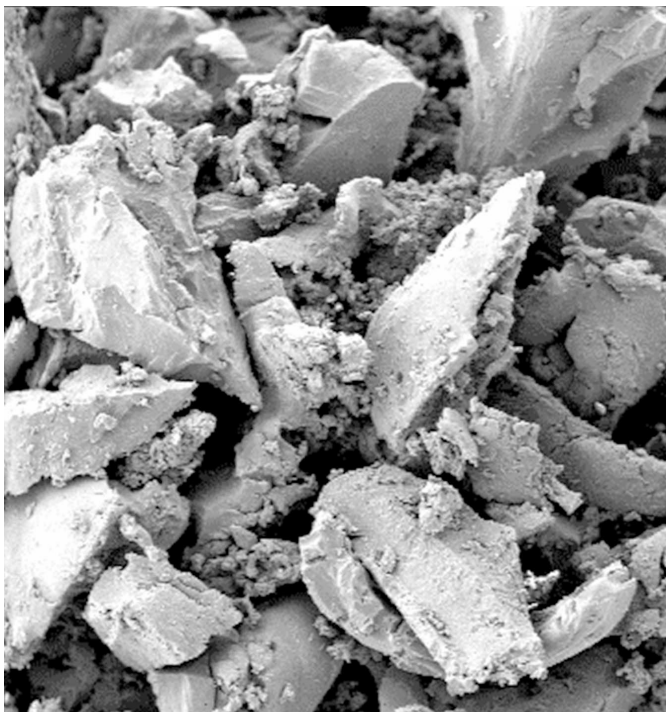
However, tyre rubber addition effects are more apparent as testing temperature rises, yielding an increase in storage modulus and a decrease of the loss tangent with respect to unmodified bitumen. In this region, larger rubber particle sizes give rise to more pronounced effects and, consequently, enhanced elastic properties are obtained.

Flow curves, at 125°C, also show that CTRMB viscosity increases with crumb rubber particle size, especially at low shear rates (Fig. 5.25). In addition, as can be easily deduced by observation of the slopes in Fig. 5.25, the shear-thinning nature of these binders becomes more pronounced.

As commented previously, at 180°C only 4 wt% of the added rubber is dissolved/disintegrated and 85 wt% insoluble rubber remains after processing and, therefore, the solid volume fraction remains almost constant, independent of particle size. In principle, an increase in particle size would lead to a decrease in viscosity, since the specific surface area of particles decreases as well. However, particle shape must also be taken into consideration. Thus, different authors found a dependence of the particle aspect ratio (length/ diameter) on the viscosity of polymeric fluids so that higher aspect ratios lead to higher viscosities (Metzner, 1985). Hence, the increase in viscosity observed with increasing particle size is related to an increase in the aspect ratio of the rubber. This assumption is confirmed from the data presented in Fig. 5.26, which shows an example of the shapes of rubber particles (mean



5.25 Viscous flow curves of neat bitumen and CTRMBs, as a function of particle size, at 125°C.



5.26 SEM of a ground tyre rubber sample having different mean particle size of 0.4 mm.

particle size of 0.4 mm) which are not spherical. In addition, as was reported elsewhere (Navarro *et al.*, 2002), aspect ratio increases with particle size (from an approximate value of 1.2 for sample 0.29 mm to 2.9 for sample 0.74 mm), affecting the final viscosity of the PMB.

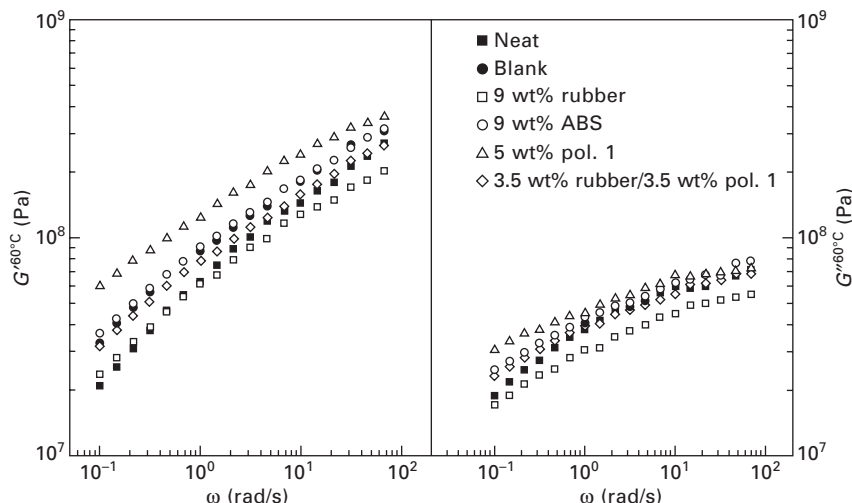
5.3.3 Combined bitumen modification by both waste thermoplastic and thermosetting polymers

In order to benefit from the properties of different waste polymers so as to obtain enhanced mechanical characteristics at both low and high in-service temperatures, PMBs can be prepared by blending bitumen with more than one additive. A combination of two other types of waste polymers (not polyolefins) with pol.1 (see Table 5.1) will be considered: (a) crumb tyre rubber (see Table 5.1), a waste thermosetting polymer which acts as a 'soft' filler; and (b) crumb ABS from waste electronics (see Table 5.1), which due to its high melting temperature acts as a 'hard' filler. Samples were prepared with a four-bladed turbine low-shear device (Fig. 5.1(c)).

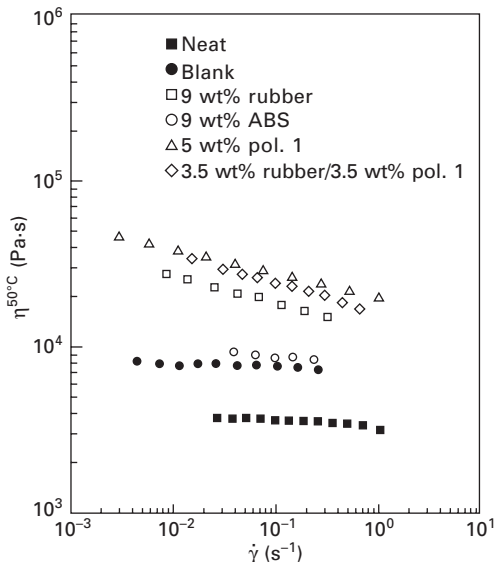
Firstly, the performance of each of these two polymers by itself will

be quantified. Figure 5.27 shows the frequency dependence of the linear viscoelastic functions, G' and G'' , at -20°C , for PMBs with 9 wt% rubber or 9 wt% ABS (from bit.1). Compared to the blank sample, the binder with 9 wt% rubber exhibits an enhanced rheological response at low temperatures, because G' values become significantly lower than those for the neat bitumen as frequency increases. This result suggests that tyre rubber is an efficient additive for bitumen modification in cold climates, as it endows the binder a larger flexibility and prevents it from thermal cracking (Navarro *et al.*, 2002). On the contrary, addition of 9 wt% ABS seems to be unable to improve the mechanical characteristics of the resulting bituminous binder. In fact, some authors have pointed out that this type of 'hard' filler may behave like a Griffith cracking initiator, because cracking is likely to initiate in the points where the filler particles are located (Hesp and Woodhams, 1992).

In addition, the viscous flow curves at 50°C shown in Fig. 5.28 show that 9 wt% ABS does not produce any significant increase in binder viscosity, compared to the viscosity of the blank. On the other hand, 9 wt% rubber leads to a viscosity increase of five times the blank sample, although this is lower than for the corresponding PMB with only 5 wt% waste polyolefin. Based on the above results, the combined modification by addition of 3.5 wt% waste polyolefin (pol.1) and 3.5 wt% rubber is proposed, and its effect on linear viscoelastic behaviour and viscous flow is shown in Figs 5.27 and 5.28, respectively. Thus, the PMB with rubber and waste polyolefin presents improved viscoelastic behaviour at low in-service temperatures, compared



5.27 Evolution of the linear elastic and viscous moduli in oscillatory shear, at 60°C , for neat bit.1 and selected PMBs prepared with bit.1 and different polymer types and contents of polymers.



5.28 Viscous flow curves, at 50°C, for neat bit.1 and selected PMBs prepared with bit.1 and different polymer types and contents of polymers.

to the sample with only 5 wt% waste polyolefin, with lower values of G' as frequency increases (see Fig. 5.27). On the other hand, Fig. 5.28 illustrates that the binder with both rubber and waste polyolefin (3.5 wt% of each) has values of viscosity very similar to the sample with only 5 wt% waste polyolefin and which exceed the viscosity of the 9 wt% rubber sample.

Consequently, previous results demonstrate that polyolefins mainly improve the asphalt performance at high in-service temperature, while the addition of this elastic polymeric filler, such as crumb rubber, provides the best results in the low temperature regime. The effectiveness of 'hard' filler-type waste polymers should be studied further.

5.4 Future trends

An increasing amount of waste polymeric materials are generated each year from the plastics industry. For economic and environmental reasons it is necessary that as much of this waste as possible is recycled instead of being disposed of in landfill sites. From the viewpoint purely of energy balances, physical recycling is preferable to energetic recycling (incineration, pyrolysis, gasification, etc.). As shown in this chapter, bitumen modification with waste polymers is an interesting alternative, since the resulting mixture may show similar performance to those containing virgin polymers.

In general, all modified bitumens included in this summary can be applied using traditional techniques at high temperatures, i.e. hot-mix asphalt (HMA). However, effect of waste polymer addition is unknown in the case of new techniques for lower-temperature application, aiming to reduce energy consumption and principally associated with reclaimed asphalt pavement (RAP). In our opinion, a strong emphasis must be put on new bituminous products, including the incorporation of waste polymers, with lower mixing, lay-down and compacting temperature which give rise to high-performing, long-lasting, durable and cost-effective pavements. Consequently, to achieve this, efforts must be focused on the development of new bituminous products containing recycled polymers, such as:

- Bitumen emulsions, for cold mix techniques
- Modified bitumen for half-warm or warm mix techniques
- Foamed bitumen.

5.5 Sources of further information and advice

The experimental data included in this chapter are part of several research projects sponsored by:

- CICYT, Spain (research project with reference MAT99-0545)
- MCYT-FEDER programme (research project MAT2001- 0066-C02-02)
- MEC-FEDER programme (MAT 2004-06299-002-02)
- MMA programme (research project 5,1-212/2005/3B, Ministerio de Medio Ambiente, Spain)
- MEC-FEDER programme (research project MAT2007-61460).

The authors gratefully acknowledge the financial support of the Spanish government.

5.6 References

AASHTO (1993), Standard specification for performance graded binder (Designation MP1), Gaithersburg, MD, Association of Stage Highway and Transportation Officials.

Airey G D (2003), 'Rheological properties of styrene butadiene styrene polymer modified road bitumens', *Fuel*, 82, 1709–1719.

Ait-Kadi A, Brahimí B and Bousmina M (1996), 'Polymer blends for enhanced asphalt binders', *Polym Eng Sci*, 36, 1724–1733.

Bahia H U and Davies R (1994), 'Effect of crumb rubber modifiers (CRM) on performance related properties of asphalt binders', *J Assoc Asphalt Paving Technol*, 63, 414–441.

Belokon N Y and Inozemtsev K A (2002), 'Rheokinetic characteristics of high-temperature dispersion of elastomers in oxidized asphalt', *Chem Technol Fuel Oil*, 38, 188–191.

Billiter T C, Davison R R, Glover C J and Bullin J A (1997), 'Investigation of the curing variables of asphalt-rubber binder', *Petrol Sci Technol*, 15, 205–236.

Champion L, Gerard J F, Planche J P, Martin D and Anderson D (2001), 'Low temperature fracture properties of polymer-modified asphalts: relationships with the morphology', *J Mater Sci*, 36, 451–460.

Chebil S, Chaala A and Roy C (2000), 'Use of softwood bark charcoal as a modifier for road bitumen', *Fuel*, 79, 671–683.

De Rosa M E and Winter H H (1994), 'The effect of entanglements on the rheological behavior of polybutadiene critical gels', *Rheol Acta*, 33, 220–237.

Dongré R, Youtcheff J and Anderson D (1996), 'Better roads through rheology', *Appl Rheol*, 6, 75–82.

Fawcett A H and McNally T (2000), 'Blends of bitumen with various polyolefins', *Polymer*, 41, 5315–5326.

Fawcett A H, McNally T, McNally G M, Andrews F and Clarke J (1999), 'Blends of bitumen with polyethylenes', *Polymer*, 40, 6337–6349.

Ferry J D (1980), *Viscoelastic Properties of Polymers*, New York, John Wiley & Sons.

Filippova A G, Kirillova L G, Okhotina N A, Dvoyashkin N K, Filippov A V, Vol'fson S I, Liakumovich A G and Samuilov Y D (2000), 'Viscosity of polymer-bitumen binders', *Colloid J*, 62, 755–758.

Franco J M, Delgado M A, Valencia C, Sánchez M C and Gallegos C (2005), 'Mixing rheometry for studying the manufacture of lubricating greases', *Chem Eng Sci*, 60, 2409–2418.

Fuentes-Audén C, Sandoval J A, Jerez A, Navarro F J, Martínez-Boza F, Partal P and Gallegos C (2008), 'Evaluation of thermal and mechanical properties of recycled polyethylene modified bitumen', *Polym Test*, 27, 1005–1012.

García-Morales M, Partal P, Navarro F J, Martínez-Boza F J, Gallegos C, González N, González O and Muñoz M E (2004a), 'Viscous properties and microstructure of recycled EVA modified bitumen', *Fuel*, 83, 31–38.

García-Morales M, Partal P, Navarro F J, Martínez-Boza F and Gallegos C (2004b), 'Linear viscoelasticity of recycled EVA-modified bitumens', *Energy Fuel*, 18, 357–364.

García-Morales M, Partal P, Navarro F J, Martínez-Boza F J, Mackley M R and Gallegos C (2004c), 'The rheology of recycled EVA/LDPE modified bitumen', *Rheol Acta*, 43, 482–490.

García-Morales M, Partal P, Navarro F J, Martínez-Boza F J and Gallegos C (2006a), 'Process rheokinetics and microstructure of recycled EVA/LDPE modified bitumen', *Rheol Acta*, 45, 513–524.

García-Morales M, Partal P, Navarro F J, Martínez-Boza F J and Gallegos C (2006b), 'Effect of waste polymer addition on the rheology of modified bitumen', *Fuel*, 85, 936–943.

García-Morales M, Partal P, Navarro F J, Martínez-Boza F J and Gallegos C (2007), 'Processing, rheology and storage stability of recycled EVA/LDPE modified bitumen', *Polym Eng Sci*, 47, 181–191.

González O, Peña J J, Muñoz M E, Santamaría A, Pérez-Lepe A, Martínez-Boza F and Gallegos C (2002), 'Rheological techniques as a tool to analyze polymer-bitumen interactions: Bitumen modified with polyethylene and polyethylene-based blends', *Energy Fuel*, 16, 1256–1263.

González O, Muñoz M E, Santamaría A, García-Morales M, Navarro F J and Partal P (2004), 'Rheology and stability of bitumen/EVA blends', *Eur Polym J*, 40, 2365–2372.

González O, Muñoz M E, Santamaría A, García-Morales M, Navarro F J and Partal P (2007), 'New routes for roads: using recycled greenhouse films to modify bitumens', *Int J Environ Technol Manage*, 7, 218–227.

Hesp S A and Woodhams R T (1992), 'Stabilization mechanisms in polyolefin-asphalt emulsions', in Wardlaw K R and Shuler S, *Polymer Modified Asphalt Binders*, ASTM STP 1108, American Society for Testing and Materials, Philadelphia, PA.

Jiménez-Mateos J M, Quintero L C and Rial C (1996), 'Characterization of petroleum bitumens and their fractions by thermogravimetric analysis and differential scanning calorimetry', *Fuel*, 75, 1691–1700.

Lesueur D (2009), 'The colloidal structure of bitumen: Consequences on the rheology and on the mechanisms of bitumen modification', *Adv Colloid Interface Sci*, 145, 42–82.

Masson J F, Polomark G M and Collins P (2002), 'Time-dependent microstructure of bitumen and its fractions by modulated Differential Scanning Calorimetry', *Energy Fuel*, 16, 470–476.

Mastral A M, Murillo R, Navarro M V, Callen M S and Garcia T (2001), 'Assessment of schemes for the processing of organic residues from the interior car decoration industry', *Ind Eng Chem Res*, 40, 1119–1124.

McGennis R B (1995), 'Evaluation of physical properties of fine crumb rubber modified binders', *Transport Res Rec*, 1488, 62–71.

Metzner A B (1985), 'Rheology of suspensions in polymeric liquids', *J Rheol*, 29, 739–775.

Miknis F P and Michon L C (1998), 'Some applications of nuclear magnetic resonance imaging to crumb rubber modified asphalts', *Fuel*, 77, 393–397.

Morea F, Agnusdei J O and Zerbino R (2010), 'Comparison of methods for measuring zero shear viscosity in asphalts', *Mater Struct*, 43, 499–507.

Murphy M, O'Mahony M, Lycett C and Jamieson I (2000), 'Bitumens modified with recycled polymers', *Mater Struct*, 33, 438–444.

Navarro F J, Partal P, Martínez-Boza F, Valencia C and Gallegos C (2002), 'Rheological characteristics of ground tire rubber-modified bitumens', *Chem Eng J*, 89, 53–61.

Navarro F J, Partal P, Martínez-Boza F and Gallegos C (2004), 'Thermo-rheological behaviour and storage stability of ground tire rubber-modified bitumens', *Fuel*, 83, 2041–2049.

Navarro F J, Partal P, Martínez-Boza F and Gallegos C (2005), 'Influence of crumb rubber concentration on the rheological behaviour of a crumb rubber modified bitumen', *Energy Fuel*, 19, 1984–1990.

Navarro F J, Partal P, Martínez-Boza F and Gallegos C (2007), 'Influence of processing conditions on the rheological behaviour of crumb tire rubber-modified bitumen', *J Appl Polym Sci*, 104, 1683–1691.

Navarro F J, Partal P, Martínez-Boza F and Gallegos C (2010), 'Novel recycled polyethylene/ground tire rubber/bitumen blends for use in roofing applications: Thermo-mechanical properties', *Polym Testing*, 29, 588–595.

Partal P, Martínez-Boza F J, Conde B and Gallegos C (1999), 'Rheological characterization of synthetic binders and unmodified bitumens', *Fuel*, 78, 1–10.

Tatterson G B (1991), *Fluid Mixing and Gas Dispersion in Agitated Tanks*, New York, McGraw-Hill.

Zanzotto L and Kennepohl G J (1996), 'Development of rubber and asphalt binders by depolymerization and devulcanization of scrap tires in asphalt', *Transport Res Rec*, 1530, 51–58.

Polypropylene fiber-reinforced bitumen

S. TAPKIN, Ü. UŞAR and Ş. ÖZCAN, Anadolu University, Turkey and A. ÇEVIK, University of Gaziantep, Turkey

Abstract: This chapter discusses the physical and mechanical behaviour of polypropylene fiber-reinforced modified asphalt mixtures. The chapter first reviews a general introduction to polypropylene modification of asphalt concrete. Then dry basis modification with polypropylene fibers and fatigue life improvement of asphalt concrete are discussed. Wet basis modification of asphalt with polypropylene fibers and repeated creep behaviour of bituminous concrete are introduced next. The utilisation of artificial neural networks for the prediction of Marshall test results of polypropylene modified dense bituminous mixtures is also investigated. Then a novel approach utilising closed-form solutions and parametric studies to predict the strain accumulation of polypropylene-modified Marshall specimens in repeated creep tests is proposed. Determination of optimal polypropylene fiber modification of asphalt concrete and the relevant mechanical and optical tests to fulfil this aim are also utilised. Finally, conclusions and a short commentary on likely future trends are introduced.

Key words: polypropylene fibers, asphalt concrete, bitumen modification, repeated creep, static creep, fluorescence microscopy, artificial neural networks, parametric study.

6.1 Introduction to polypropylene modification of asphalt concrete

Research into permanent deformation such as rutting in flexible pavements began in the early 1970s (Hofstra and Klomp 1972; Uge and Van de Loo 1974; Van de Loo 1974; Hills *et al.* 1974; De Hilster and Van de Loo 1977; Van de Loo and De Hilster 1978; Bolk and Van de Loo 1979). To solve the rutting problem in flexible pavements (and other problems such as fatigue and low-temperature cracking), scientists developed 'asphalt (bitumen) modification'. To this end, novel binders with improved rheological characteristics are continuously being developed (Brule 1996; Brown *et al.* 1990; Collins *et al.* 1991; Goodrich 1991; King *et al.* 1993; Isacsson and Lu 1995). The best known form of bituminous binder improvement is by means of polymer modification, traditionally used to improve the temperature susceptibility of bitumen by increasing binder stiffness at high service temperatures and reducing the stiffness at low service temperatures

(Airey 2004). The polymers that are used for bituminous binder modification can be divided into two broad categories mainly known as plastomers and elastomers. Plastomers tend to modify bitumen by forming a tough, rigid, three-dimensional network within the binder to resist deformation, while elastomers have a characteristically high elastic response and, therefore, resist permanent deformation by stretching and recovering their initial shape.

The main applications of polymer fiber reinforcement in the modern era began in the early 1990s. Brown *et al.* (1990) noted the potential of some fibers in improving tensile and cohesive strength of asphaltic concrete when compared to bitumen. Some researchers believe that fibers create physical changes to modifiers which have a positive effect on drain-down reduction (Maurer and Malasheskie 1989; Wu 2006). Yi and McDaniel (1993) used polypropylene fibers in an attempt to reduce reflection cracking in an asphalt overlay with mixed results, improving rutting resistance but resulting in rapid decreases in pavement strength and ride ability. In another study, Jenq *et al.* (1993) assessed the effects of fiber-reinforced asphalt concrete (using polypropylene and polyester fibers) on resistance to cracking, showing increased toughness values but no significant improvement in tensile strength and elasticity. Simpson and Kamyar (1994) conducted another study in which polypropylene, polyester fibers and some other polymers were used to modify a bituminous binder. The mixtures were found to have higher tensile strengths and resistance to cracking but no resistance to moisture-induced freeze-thaw damage or stripping potential. Polypropylene-modified samples were shown to decrease the potential for rutting.

Huang and White (1996) conducted research on asphalt overlays modified with polypropylene fibers. They found that the fibers increased the fatigue life of the overlay mixture. The Ohio Department of Transportation (1998) also carried out extensive research on the addition of polypropylene fibers to asphalt mixes. In a study carried out by Clevén (2000), fibers (polypropylene, polyester, asbestos and cellulose) appeared to increase the stiffness of the asphalt binder, resulting in stiffer mixtures with decreased binder drain-down and increased fatigue life. Mixtures containing fibers showed less decrease in void content and increased resistance to permanent deformation. The tensile strength and related properties of mixtures containing fibers were found to improve, especially for polypropylene, but not for all of the fiber types.

Tapkin (2008a) has found that addition of polypropylene fibers into asphalt concrete on a dry basis alters the behaviour of the mixture in such a way that Marshall stability values increase, flow values decrease and the fatigue life increases significantly. Tapkin *et al.* (2009a, 2009b, 2010) have also worked on the addition of polypropylene fibers to asphalt concrete on a wet basis, and have shown that the most favourable and suitable polypropylene type is multifilament, 3 mm long (M-03 type), which increased the Marshall stability values by 20% as well as the stiffness of the asphalt concrete. Repeated load

creep tests under different loading patterns have also shown that the time to failure of fiber-modified asphalt specimens under repeated creep loading at different loading patterns increased by 5–12 times versus reference specimens, a very significant improvement. In another accompanying study, it was found that polypropylene modification of bituminous binders developed the physical and mechanical properties of the mixture and substantially improved its resistance to permanent deformation. Polypropylene modification also results in a saving of 30% in the amount of bitumen, resulting in considerable cost savings (Özcan 2008). There are also a number of other studies in the literature on different applications of polypropylene fiber modification of asphalt concrete in the last decade which deserve attention (Lee *et al.* 2005; Ghaly 2008; Hejazi *et al.* 2008; Zhou *et al.* 2008, 2009; Al-Hadidy and Tan 2009; Zhang *et al.* 2010a, 2010b; Othman 2010).

6.2 Using polypropylene fibers to improve the fatigue life of asphalt concrete

The concept of using different types of fibers as reinforcing agents in the construction industry is not new (Hongu and Phillips 1997). The term fiber-reinforced concrete is defined by ACI 116R-00, Cement and Concrete Terminology, as concrete containing randomly dispersed oriented fibers (ACI 116R-00, 2000). In the early 1960s, Romualdi and his colleagues published the papers that brought fiber-reinforced concrete to the attention of academic and industry research scientists around the world (Romualdi and Batson 1963, Romualdi and Mandel 1964). A more detailed discussion and a general overview were provided in the pioneering paper by Zollo (1997).

Concrete is a weak construction material under tensile loading patterns and is particularly prone to cracking. These cracks generally develop and enlarge gradually with time and stresses penetrate the concrete, thereby impairing the waterproofing properties and exposing the interior of the concrete to destructive substances containing moisture, bromine, acid sulphate, etc. (Song *et al.* 2005). Polypropylene fibers also provide three-dimensional reinforcement of the concrete. In asphalt concrete there is a reaction between the hot aggregate and the cold polypropylene fibers when mixed together for a suitable period before adding hot bitumen to this blend and obtaining the asphalt mixture (dry process). The ‘sticking’ of polypropylene fibers with the aggregate-bitumen matrix forms a completely new generation of paving products. Although this is not a totally new technique (Brown *et al.* 1990; Ohio Department of Transportation 1998), using multifilament 3 mm long fibers (M-03 type) in pavement engineering applications is a new concept (Tapkin 2008a; Özcan 2008; Tapkin *et al.* 2009a, 2009b, 2010).

Polypropylene fibers have been used officially as a modifier for asphalt concrete in the United States. The Ohio State Department of Transportation

(ODOT) has published a standard for the use of polypropylene fibers in high-performance asphalt concrete (Ohio Department of Transportation 1998). In this standard, detailed instructions are provided on the production, laying out and compaction of asphalt concrete composed of aggregates, bitumen and polypropylene fibers. The fibers are required to meet the requirements stated in Table 6.1. Based on the extensive research carried out by the Ohio Department of Transportation, the polypropylene fibers should be added to the asphalt mix in a ratio of approximately 3.0 kg/ton. However, this ratio can be adjusted in order to satisfy the desired mechanical properties of the asphalt pavement. For mixtures incorporating polypropylene fibers, the mixing temperature should not exceed 143°C (290°F) (Ohio Department of Transportation 1998).

6.3 Experiments used to enhance the physical and mechanical properties of polypropylene fiber-reinforced asphalt mixtures

Marshall specimens were prepared in laboratory conditions according to ASTM D 1559-76. For mixtures incorporating polypropylene fibers, the mixing temperature was controlled in a manner to be less than 143°C. Controlling this temperature is important in the sense that polypropylene fibers cannot be heated at temperatures above 146°C because they will soften and melt, rendering them ineffective in the preparation of dense bituminous mixtures (Prowell 2000). Marshall stability and flow tests were done on the reference and polypropylene-modified asphalt samples. These tests might have been considered to be adequate to clarify the positive effects of polypropylene fibers on asphalt concrete, but in order to be able to calculate the fatigue life of these specific mixtures, repeated load indirect tensile tests (in other words, split tension tests) were also carried out by utilising the Universal Materials Testing Apparatus for Asphalt and Unbound Specimens (UMATTA) tester (ELE-UMATTA 1994).

Table 6.1 Physical properties of polypropylene fibers specified by Ohio Department of Transportation

Characteristic	Value	Standard
Denier	4 ± 1	ASTM D-1577
Length, mm	9.91 ± 2.0	–
Crimps	None	ASTM D-3937
Tensile strength, minimum, MPa	276	ASTM D-2256
Specific gravity, kg/m ³	910 ± 40	–
Melting temperature, minimum, °C	160	–

Source: Ohio Department of Transportation (1998).

The material properties of polypropylene fibers used throughout the dry basis modification studies are summarised in Table 6.2. Calcareous aggregates obtained from a native quarry and 60/70 penetration bitumen obtained from a nearby refinery were used in the preparation of all specimens. The physical properties of the bitumen are given in Table 6.3. The physical properties of the coarse and fine aggregates are shown in Tables 6.4 and 6.5. Aggregate

Table 6.2 The material properties of polypropylene fibers used throughout the dry basis modification studies

Characteristic	Value	Standard
Homogeneity, %	100%	–
Colour	Transparent	–
Length, mm	3–50	–
Melting temperature, °C	164	ASTM D-3418
Maximum operating temperature, °C	82	–
Thermal conductivity, 10^{-4} cal/cm-s-°C	2.6–2.8	ASTM C-177
Specific gravity, kg/m ³	905	ASTM D-792
Fire point, °C	590	–
Glass transition temperature, °C	–18	–
Alkali resistance as % of strength retained after treatment in 40% NaOH solution at 20°C for 1000 hours	99.5	–
Water absorption, %	0.01	ASTM D-570
Moisture retention, at 20°C and 65% relative humidity	<0.1%	ASTM D-265
Rupture resistance, MPa	31–41	ASTM D-638
Elongation, %	≥33	–
Elongation at rupture, %	100–600	ASTM D-638
Tensile strength, MPa	33	ASTM D-638
Compressive strength, MPa	48	ASTM D-695
Compressive modulus, MPa	–	–
Bending strength, MPa	41–55	ASTM D-790
Tensile modulus, MPa	1345	ASTM D-638
Tensile elongation at yield, %	12	ASTM D-638
Flexural strength, MPa	48	ASTM D-790
Flexural modulus, MPa	1241	ASTM D-790
Izod notched impact, J/m	101	ASTM D-256
Hardness, Rockwell, R	92	ASTM D-785
Coefficient of thermal expansion, linear, m/m/°C, 10^{-5}	6	ASTM D-696
Heat deflection temperature, °C (at 0.46 MPa and 1.82 MPa)	99/52	ASTM D-648
Dielectric strength (V/mil) short time, 0.32 cm thick	500–660	ASTM D-149
Dielectric constant at 1 kHz	2.25	ASTM D-150
Dissipation factor at 1 kHz	0.0005–0.0018	ASTM D-150
Volume resistivity (ohm-cm) at 50% RH	8.5×10^{14}	ASTM D-257
Arc resistance (s)	160	ASTM D-495

Table 6.3 Physical properties of bitumen

Property	Test value	Standard
Penetration at 25°C, 1/10 mm	63.5	ASTM D 5-97
Penetration index	+1.2	–
Ductility at 25°C, cm	>100	ASTM D 113-99
Loss on heating, %	0.06	ASTM D 6-80
Specific gravity at 25°C, kg/m ³	1036	ASTM D 70-76
Softening point, °C	57.2	ASTM D 36-95
Flash point, °C	230	ASTM D 92-02
Fire point, °C	270	ASTM D 92-02

Table 6.4 Physical properties of coarse aggregates

Property	Test value	Standard
Bulk specific gravity, kg/m ³	2695	ASTM C 127-04
Apparent specific gravity, kg/m ³	2715	ASTM C 127-04
Water absorption, %	0.29	ASTM C 127-04

Table 6.5 Physical properties of fine aggregates

Property	Test value	Standard
Bulk specific gravity, kg/m ³	2683	ASTM C 127-04
Apparent specific gravity, kg/m ³	2534	ASTM C 127-04
Water absorption, %	1.02	ASTM C 127-04

Table 6.6 Type 3 wearing course gradation according to the General Directorate of Highways of Turkey (2000)

Sieve size (mm)	Gradation limits (%)	Passing (%)	Retained (%)
12.7	100	100	0
9.52	87–100	93.5	6.5
4.76	66–82	74	19.5
2.00	47–64	55.5	18.5
0.42	24–36	30	25.5
0.177	13–22	17.5	12.5
0.074	4–10	7	10.5
Pan			7

gradation for the bituminous mixtures tested in the laboratory has been selected as an average of the wearing course type 3 gradation limits given by the General Directorate of Highways of Turkey (2000). The mixture gradation and gradation limits can be seen in tabulated form in Table 6.6. The apparent specific gravity of filler is 2602 kg/m³.

Preliminary experiments on Marshall specimens (prepared with 50 blows on each face representing medium traffic conditions) established the

proportion of bitumen and aggregates used in the dry basis modification of dense bituminous mixtures with polypropylene fibers. In these experiments, the optimum bitumen content (obtained by averaging maximum stability and unit weight, 4% air voids and 80% voids filled with asphalt values (General Directorate of Highways of Turkey 2000)) was determined as 5.5% by carrying out several series of Marshall designs (Tapkin 2008a). In this research, asphalt concrete prepared with 0.3%, 0.5% and 1% of polypropylene fibers by aggregate weight was investigated at the optimum bitumen content value of 5.5%, determined as approximately the same for the reference specimens (Tapkin 2008a).

Different types of polypropylene fibers were utilised in preparing the modified dense bituminous mixtures. These were M-03 (multifilament 3 mm long), M-09 (multifilament 9 mm long) and waste fibers: see Fig. 6.1(a), (b) and (c). It was found difficult to mix M-09 and waste fibers thoroughly after the introduction of bitumen to the aggregate–fiber mixture. The most important problem encountered with the M-09 fibers in particular was ‘balling’ (the clustering of individual particles into ball-like shapes because of the excessive length of the 9 mm fibers during thorough mixing with aggregate and bitumen). A further problem encountered was the non-uniform and unstable end mixtures of waste fibers. M-03 type fibers were found to be the best type of fibers to process and, due to the consistency of the test results with Marshall specimens (both physical and mechanical), 1% fiber content addition by aggregate weight was determined as the optimal amount of fiber addition. Over several years, many testing series were performed on the same aggregate and bituminous materials so a considerable amount of data has been obtained (Tapkin 2008a and other unpublished studies by the lead author). The most important physical and mechanical properties of Marshall specimens at 0.3%, 0.5% and 1% polypropylene fibers by aggregate weight (namely unit weight (kg/m^3), voids in mineral aggregate (VMA), voids filled with asphalt (V_f)%, air voids (V_a)%, stability (kg), flow (mm) and Marshall Quotient (kg/mm)) are shown in Figs 6.2–6.8.

As can be visualised from Fig. 6.2, the unit weight of Marshall specimens decreases in a regular manner by increasing the amount of polypropylene fibers used in the modification process. Specimens modified with 1% polypropylene (the optimum modification amount) were 6.46% lighter than the reference specimens. This is an important phenomenon in the sense that lighter asphalt mixtures can be obtained, resulting in lower handling and transport costs in the long term. From Fig. 6.5, it can be seen that polypropylene fiber modification increases the total air voids (V_a) in the resulting mixtures by 479%. This increase is important for pavements designed for use in ‘hot’ regions where asphalt is subjected to flushing and bleeding problems. In these conditions increased air voids can provide extra room for the displaced bituminous binder.



(a)

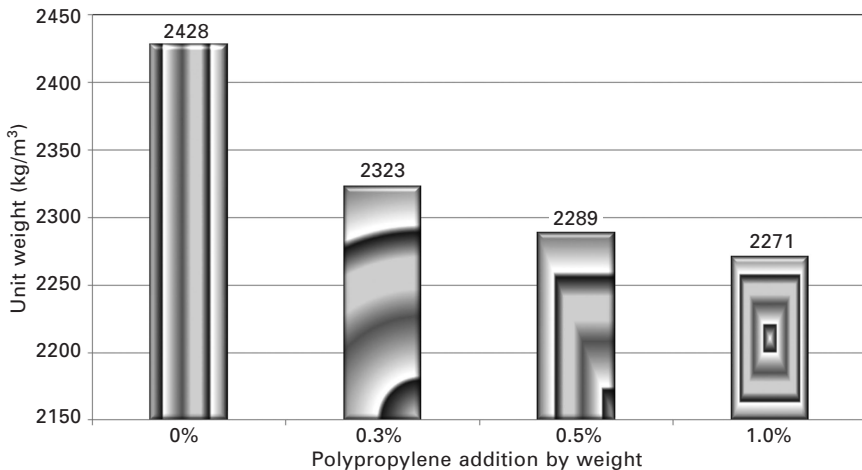


(b)

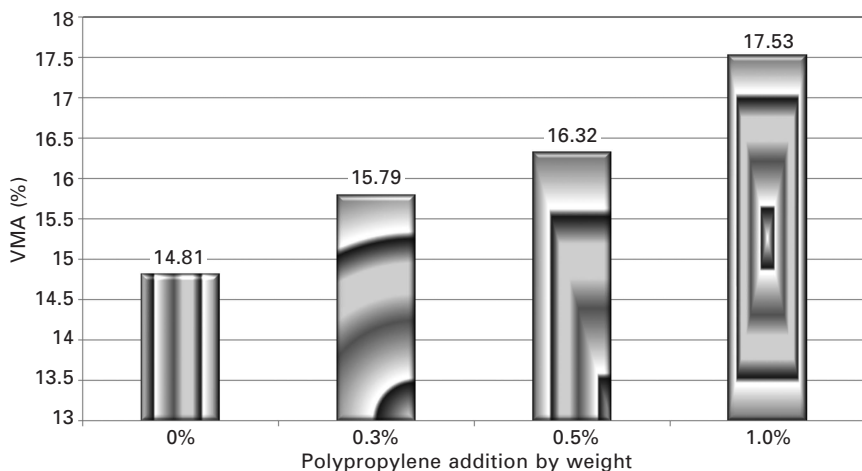


(c)

6.1 Types of polypropylene fibers: (a) M-03 (multifilament 3 mm long); (b) M-09 (multifilament 9 mm long); (c) waste polypropylene fibers.

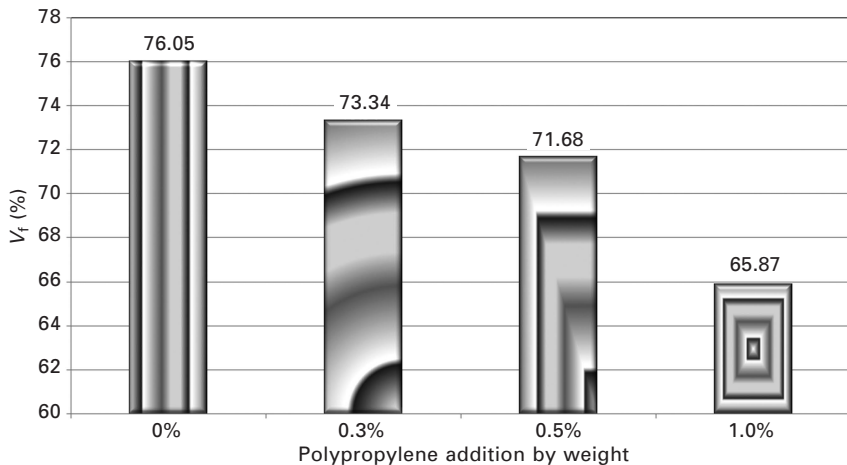


6.2 Effect of polypropylene fiber addition on unit weight values.

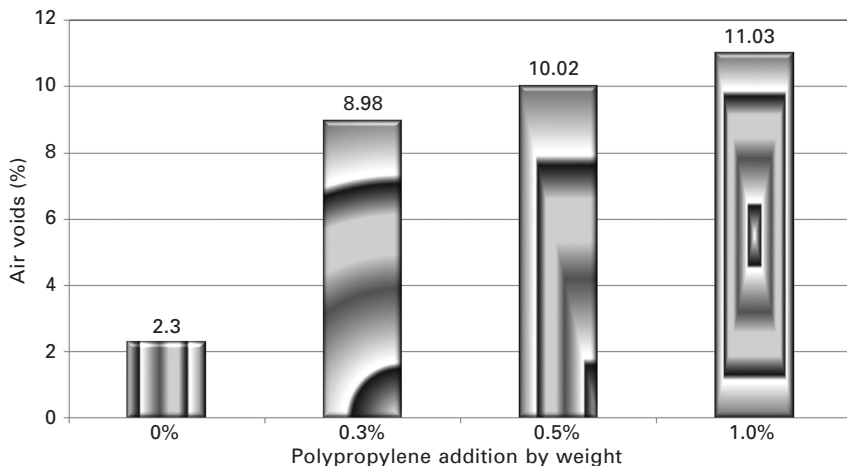


6.3 Effect of polypropylene fiber addition on voids in mineral aggregate (VMA) values.

With regard to mechanical behaviour, stability values increase by 158% and flow values decrease by 36%, which is a clear indication of the dry basis M-03 type polypropylene fiber modification. From the pseudo-stiffness point of view, which is giving some clues about the stiffness modulus of asphalt specimens before carrying out real mechanical testing, Marshall Quotient values increase by 245%, which is a perfect indication of the increase in the elastic modulus values of the Marshall specimens.



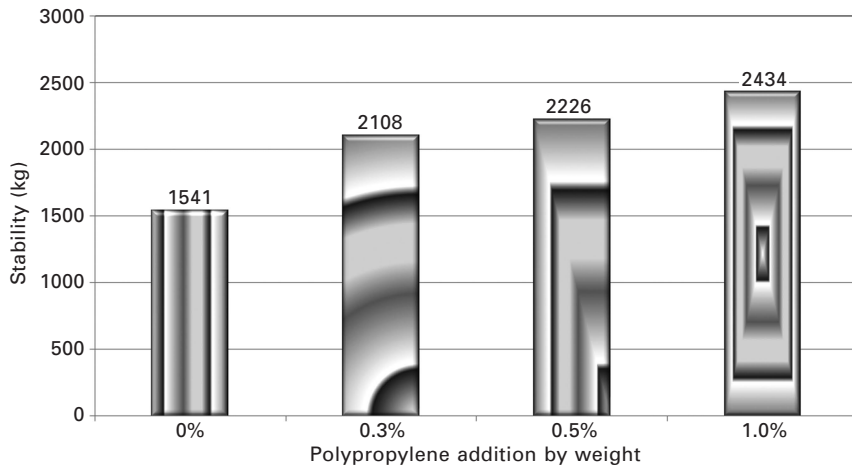
6.4 Effect of polypropylene fiber addition on voids filled with asphalt (V_f) values.



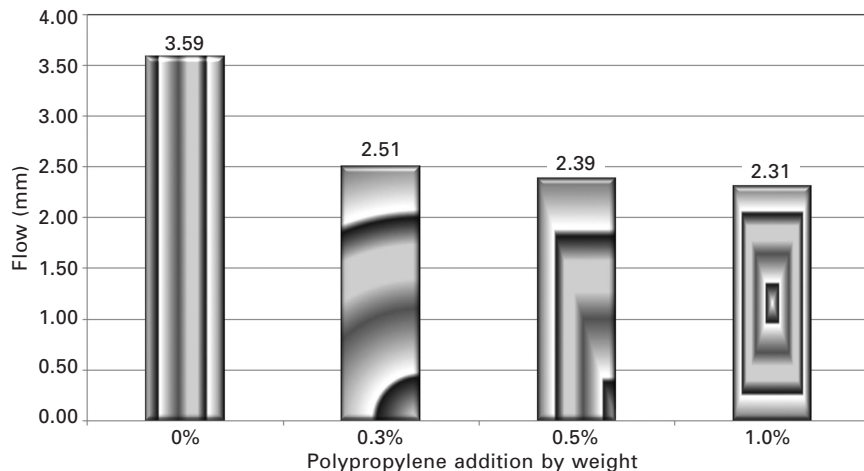
6.5 Effect of polypropylene fiber addition on air voids (V_a) values.

6.4 Analysing the fatigue life of bituminous concrete

Fatigue can be defined as the ‘phenomenon of fracture under repeated or fluctuating stress having a maximum value generally less than the tensile strength of the material’ (Austin and Gilchrist 1996). Another definition of fatigue is that ‘it is a process of progressive localised permanent structural change occurring in a material subjected to conditions that produce fluctuating stresses and strains at some point or points and which may culminate in cracks

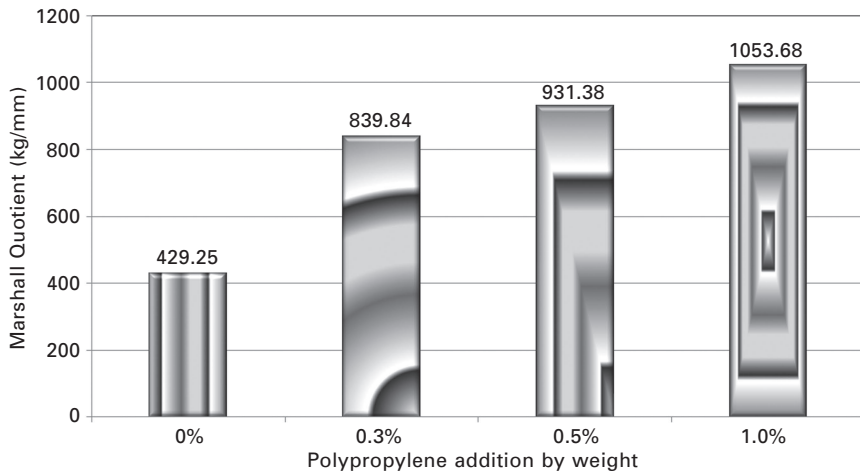


6.6 Effect of polypropylene fiber addition on stability values.



6.7 Effect of polypropylene fiber addition on flow values.

or complete fracture at a sufficient number of fluctuations' (ASTM 1963). The repeated load indirect tensile test is a commonly used tensile test (Austin and Gilchrist 1996; Whiteoak 1990). The UMATTA tester (ELE-UMATTA 1994) is a testing system that is used to find both the elastic modulus and the permanent and elastic deformation of specimens (Wallace and Monismith 1980). The aim of such experiments using these test methods is to model fatigue or alligator cracking on the pavement structure. In this study, repeated indirect loadings were applied on Marshall specimens and lateral deformations were measured. The criterion to terminate the experiments was when a visible crack occurring on the specimen surface was observed.



6.8 Effect of polypropylene fiber addition on Marshall Quotient values.

In the repeated load indirect tensile test, the tensile stress, elasticity modulus and strain are calculated using the following equations (Bonnaure *et al.* 1980):

$$\sigma_T = \frac{2P}{\pi t D} \quad 6.1$$

$$S_m = \frac{P(\mu + 0.273)}{Ht} \quad 6.2$$

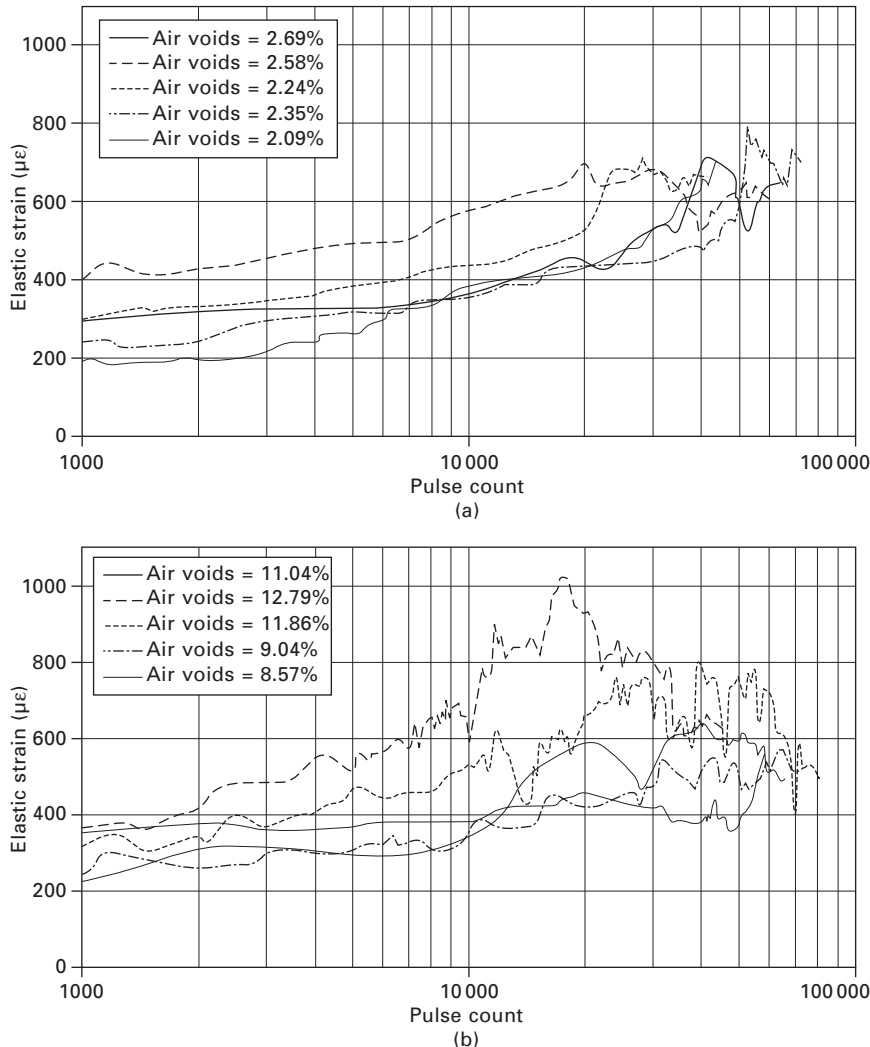
$$\varepsilon = \frac{H}{D} \quad 6.3$$

where σ_T is the tensile stress (N), S_m the elasticity modulus (MPa), ε the total strain, P the maximum value of the applied vertical load (N), t the thickness of the specimen (mm), D the diameter of the specimen (mm), H the total horizontal deformation that arises during the loading (mm), and μ the Poisson's ratio.

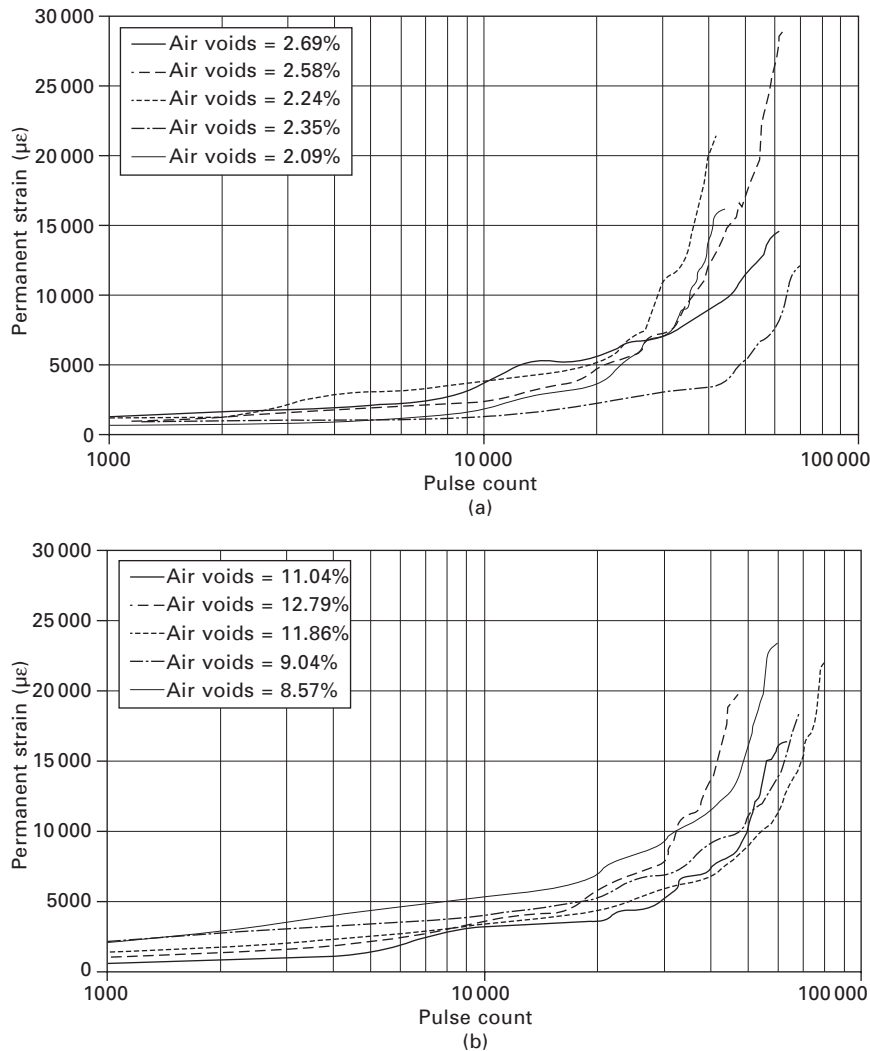
Based on the experimental results, the fatigue life of asphalt pavements was modelled to investigate the effect of adding polypropylene fibers. The test temperature was chosen as 50°C in order to resemble the *in situ* conditions which initiate fatigue cracking. The Poisson's ratio was assumed to be 0.35. The pulse period was selected as 500 ms. Loading time was chosen as 100 ms and the applied load was set to 1000 N. All of the tests were carried out with these testing parameters. This testing temperature (which seems much higher than the usual temperatures where fatigue cracking initiates in real asphalt concrete pavements on site) and loading pattern were chosen

on purpose in order to speed up the failure mechanisms in the laboratory environment (Tapkin 1998, 2008a, 2008b).

The resultant elastic strain–pulse count and elastic modulus–pulse count graphs visualise the ability of the specimens to carry the load. The graphs shown in Figs. 6.9–6.12 represent the fatigue life of the reference and fiber-reinforced specimens (with optimal fiber addition of 1% by weight) under the stress-controlled tests. In order to determine the effect of addition

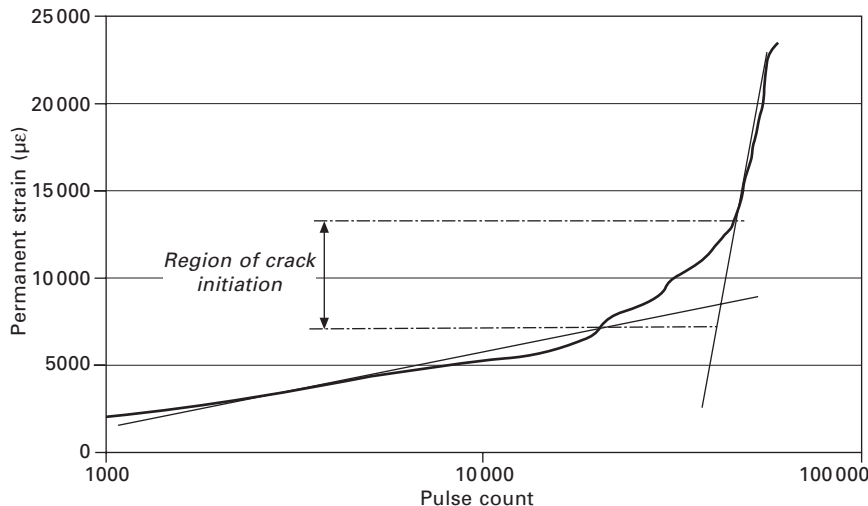


6.9 Elastic strain versus pulse count for (a) reference specimens and (b) fiber-reinforced specimens (with optimal fiber addition of 1% by weight).



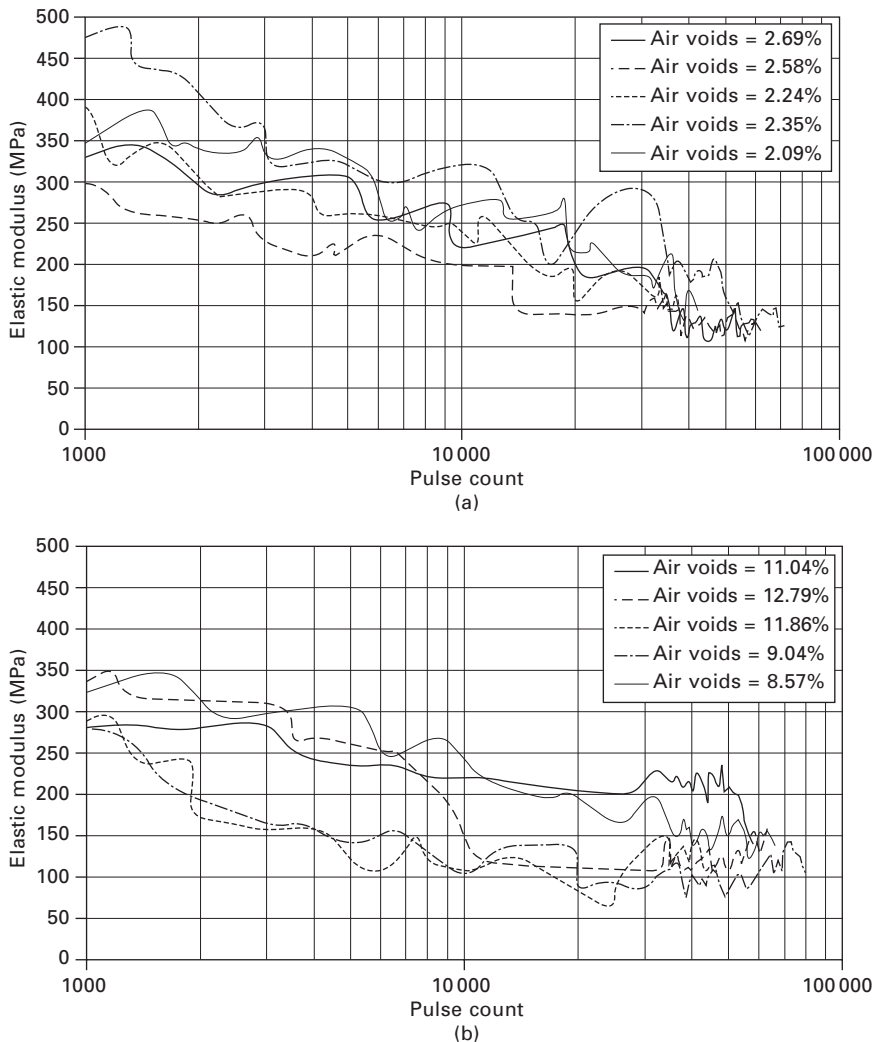
6.10 Permanent strain versus pulse count for (a) reference specimens and (b) fiber-reinforced specimens (with optimal fiber addition of 1% by weight).

of polypropylene fibers on fatigue life, the fatigue test results have been evaluated for fatigue life and elastic-permanent deformation response. The samples investigated show completely different fatigue life behaviour between specimens with and without M-03 type polypropylene fibers (Figs 6.9(a) and (b)). It can clearly be observed that addition of polypropylene fibers provides a longer fatigue life (Tapkin 2008a). When failure points are reached, the elastic deformation of the specimens with polypropylene



6.11 Region of crack initiation for permanent strain versus pulse count (Tapkin 1998).

added drops below the level of the reference specimens. This explains the much longer fatigue lives observed for the polypropylene-modified Marshall specimens. Permanent strains recorded during the tests show that as the number of repeated loadings increases, permanent strain values also increase. In the initial stages of the test, this increase is gradual and nearly linear. This is shown in Figs 6.10(a) and (b) for the permanent strain versus pulse count relations. It is believed that crack initiation starts before the pulse count reaches the point where the rate of increase in the permanent strain is at its maximum (Tapkin 1998, 2008b). When Fig. 6.11 is examined, it can be observed that, after a number of load repetitions, the rate of increase in permanent strain gets higher and, at later stages, again drops. Before visible cracks are observed on the samples, the increase in permanent strain with repeated loading again becomes nearly linear. Crack initiation, which is not visible and not easily detectable, most probably occurs in between the two linear portions of permanent strain plots (Tapkin 1998, 2008b). The permanent strain records of the fiber-reinforced specimens are higher than those for the reference specimens (Figs 6.10(a) and (b)), suggesting higher deformation-absorbing capacity (in other words toughness). The fatigue life corresponding to the 50% elastic modulus drop of the polypropylene fiber-based specimens increased by 27% when compared with reference specimens (Figs 6.12(a) and (b)). When the first crack initiation criterion was set as the fatigue life limit, the specimens with polypropylene fiber added also had a 17–24% higher fatigue life than the reference specimens (Figs 6.9(a) and (b)). The minimum value of the resilient modulus is believed to occur



6.12 Elastic modulus versus pulse count for (a) reference specimens and (b) fiber-reinforced specimens (with optimal fiber addition of 1% by weight).

at the end of the fatigue life. The fatigue life of fiber-reinforced specimens, calculated from the drop in the elastic modulus values, is again 27% longer than that of reference specimens (Figs 6.12(a) and (b)).

Marshall tests and repeated load indirect tensile tests have shown that the addition of polypropylene fibers considerably alters the behaviour of asphalt concrete, but in a very beneficial manner. The specimens with 1% polypropylene added (optimum modification amount) are 6.46% lighter than the reference

specimens. This is an important result in the sense that after modification, one can obtain lighter asphalt mixtures by utilising polypropylene fibers, reducing hauling expenditure in the long term. Polypropylene modification increases the total air void content in the resulting mixtures by up to 479%. This is a drastic increase from a pavement engineering point of view. Also this increase is important for pavements designed for use in 'hot' regions where asphalt is suspected to flushing and bleeding problems where highly increased air void content can facilitate displaced bituminous binder. V_f values decrease and VMA values increase in a similar manner related to the above discussions. From the mechanical behaviour point of view, Marshall stability values increase by 158% and flow values decrease by 36%, confirming the very positive effect of M-03 type polypropylene fiber modification. Finally, from the pseudo-stiffness point of view, Marshall Quotient (stability/flow) values increase by 245%, a clear indication of the increase in the elastic modulus of the Marshall specimens. From the fatigue testing results, the addition of 1% of polypropylene fibers prolongs the fatigue life by approximately 27%, an important indication of the effect of polypropylene modification. Polypropylene fibers have a different specific gravity and size distribution, and certain physical changes in the asphalt concrete matrix can explain the behavioural differences between modified and reference specimens. Also, from polypropylene fiber-bitumen interactions, differences in elasto-plastic and adhesive behaviour are observed when compared with natural calcareous filler-bitumen paste.

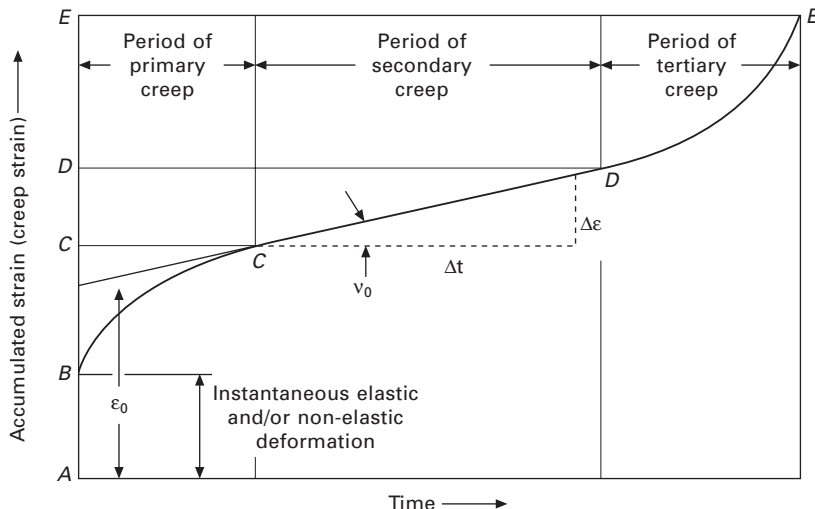
6.5 Analysing the repeated creep behaviour of bituminous concrete by utilising wet basis modification

Creep is defined as time-dependent deformation that is characteristic of a viscoelastic material subjected to load. In addition to its viscoelastic behaviour, asphalt concrete demonstrates elastoplastic and thermoplastic properties, so deformation characteristics of asphalt concrete depend also on temperature. Therefore, creep of asphalt concrete is the combination of elastic, plastic and viscoelastic behaviour.

The universal testing machine UTM-5P (5 kN, pneumatic) can carry out static and repeated creep tests (also elastic modulus and repeated load indirect tensile tests) (Feeley 1994). This apparatus allows the testing of asphalt concrete to determine the ability of the specimen to withstand repeated axial loading. The UTM-5P software can model varying road conditions through increases in frequency and force of applied axial loads. The UTM-5P comprises a loading frame, fitted with a closed loop servo-controlled pneumatic actuator assembly, control, and data acquisition system (CDAS). The CDAS has eight transducer inputs and houses an additional module that controls a servo valve.

The system can operate and control force, displacement or strain (using an on-specimen transducer) or a combination of all three (Feeley 1994).

Asphalt concrete under a constant stress condition exhibits a typical deformation characteristic which can be explained in four stages as shown in Fig. 6.13. Throughout the study, continuous aggregate gradation has been used to fit the gradation limits for wearing course Type 2 set by the General Directorate of Highways of Turkey (2006). The aggregate was a calcareous-type crushed stone obtained from a local quarry. 50/70 penetration bitumen obtained from a local refinery was also used in the preparation of the Marshall specimens. The physical properties of the bitumen samples are given in Table 6.7. The physical properties of the coarse and fine aggregates are given in Tables 6.8 and 6.9. The specific gravity of the filler is 2790 kg/m³. The mixture gradation and gradation limits are given in Table 6.10. Three types of polypropylene fibers, M-03, M-09 and waste fibers, were again used in this study. For M-03 type fibers, fiber contents of 3%, 4.5% and 6% by weight of aggregate were premixed with bitumen and were used in the preparation of standard Marshall specimens (Uşar 2007; Tapkin *et al.* 2009a, 2009b, 2010). The polypropylene-modified bitumen samples were prepared by means of a low-shear laboratory-type mixer rotating at 500 rpm for 2h at 170°C (Chen and Lin 2005). The physical properties of the polypropylene fiber-based bitumen samples with 3% fiber content are given in Table 6.11. The addition of 3% M-03 type fibers clearly results in a decrease in temperature susceptibility of the reference bitumen (as shown by the increase in the penetration index of the polypropylene-modified bitumen



6.13 Typical repeated creep curve for asphalt concrete.

Table 6.7 Physical properties of reference bitumen

Property	Test value	Standard
Penetration at 25°C, 1/10 mm	55.4	ASTM D 5-97
Penetration index	-1.2	-
Ductility at 25°C, cm	>100	ASTM D 113-99
Loss on heating, %	0.057	ASTM D 6-80
Specific gravity at 25°C, kg/m ³	1022	ASTM D 70-76
Softening point, °C	48.0	ASTM D 36-95
Flash point, °C	327	ASTM D 92-02
Fire point, °C	376	ASTM D 92-02

Table 6.8 Physical properties of coarse aggregates

Property	Test value	Standard
Bulk specific gravity, kg/m ³	2703	ASTM C 127-04
Apparent specific gravity, kg/m ³	2730	ASTM C 127-04
Water absorption, %	0.385	ASTM C 127-04

Table 6.9 Physical properties of fine aggregates

Property	Test value	Standard
Bulk specific gravity, kg/m ³	2610	ASTM C 128-04
Apparent specific gravity, kg/m ³	2754	ASTM C 128-04
Water absorption, %	1.994	ASTM C 128-04

Table 6.10 Type 2 wearing course gradation according to the General Directorate of Highways of Turkey (2006).

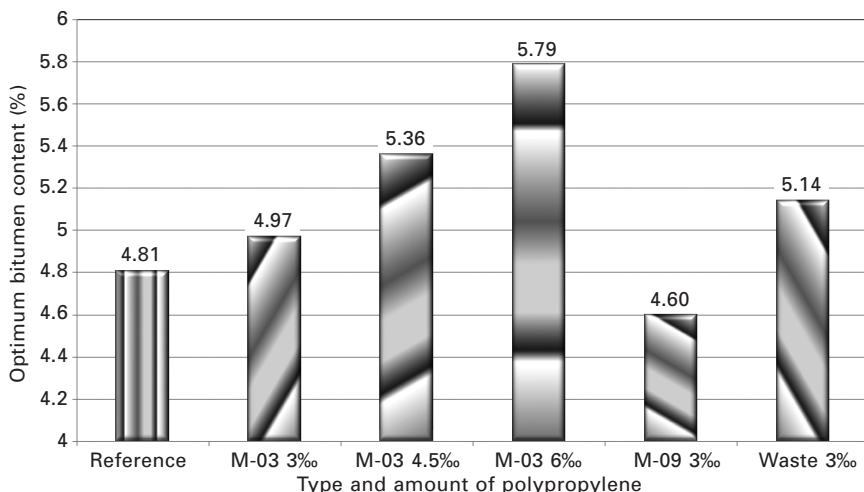
Sieve size (mm)	Gradation limits (%)	Passing (%)	Retained (%)
12.7	100	100	0
9.52	80–100	90	10
4.76	55–72	63.5	26.5
2.00	36–53	44.5	19.0
0.42	16–28	22	22.5
0.177	8–16	12	10.0
0.074	4–10	7	5
Pan	–	–	7

samples) improving the properties of the resultant asphalt concrete mixtures with an increase in the stiffness at very high ambient temperatures (Uşar 2007; Tapkin *et al.* 2009a).

The relevant physical and mechanical test results are given in the relevant literature (Tapkin *et al.* 2010). The optimum bitumen content is represented in Fig. 6.14. Based on previous studies, M-03 polypropylene fibers at dosage of 3% by weight of aggregates were selected to give the

Table 6.11 Physical properties of the M-03 type polypropylene fiber-modified bitumen samples

Property	Test value	Standard
Penetration at 25°C, 1/10 mm	45.5	ASTM D 5-97
Penetration index	-0.8	-
Ductility at 25°C, cm	>100	ASTM D 113-99
Loss on heating, %	0.025	ASTM D 6-80
Specific gravity at 25°C, kg/m ³	1015	ASTM D 70-76
Softening point, °C	52.1	ASTM D 36-95
Flash point, °C	292	ASTM D 92-02
Fire point, °C	345	ASTM D 92-02



6.14 Optimum bitumen contents for different types and amounts of polypropylene fibers.

optimal polypropylene addition amount. The optimum bitumen content for reference and test specimens with 3% M-03 fibers are 4.81% and 4.97%, respectively (Fig. 6.14). For the next set of experiments, these two values were taken as 5% for ease of preparation of the reference and polypropylene fiber-reinforced asphalt specimens (Uşar 2007; Tapkin *et al.* 2009a).

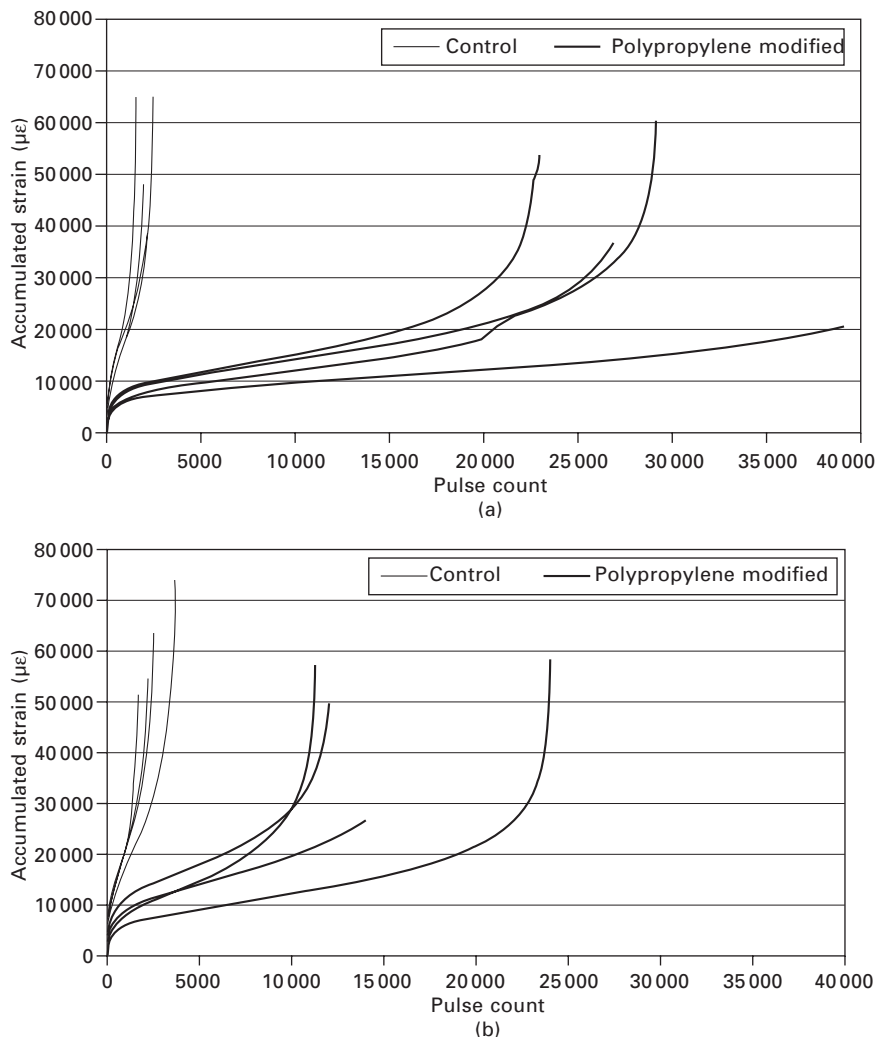
Repeated creep tests have been performed in order to log the accumulation mechanisms of the developing strains in the specimen body, or in other words permanent deformations. The creep deformation of standard Marshall specimens was measured as a function of pulse counts, i.e. time. The load on the specimens was uniaxial and dynamic, representative of the repeated application of axle loads on the pavement structure. The dimensions of asphalt specimens were approximately the same for nearly all test samples. Therefore, a unity in the dimensions was standardised. Prior to testing, the

specimens were put into a chamber for 24 hours in order to have a uniform temperature distribution and all of the tests were carried out at 50°C. For controlled temperature testing, the specimen's skin and core temperatures were estimated by transducers inserted in a dummy specimen and located near the specimen under test.

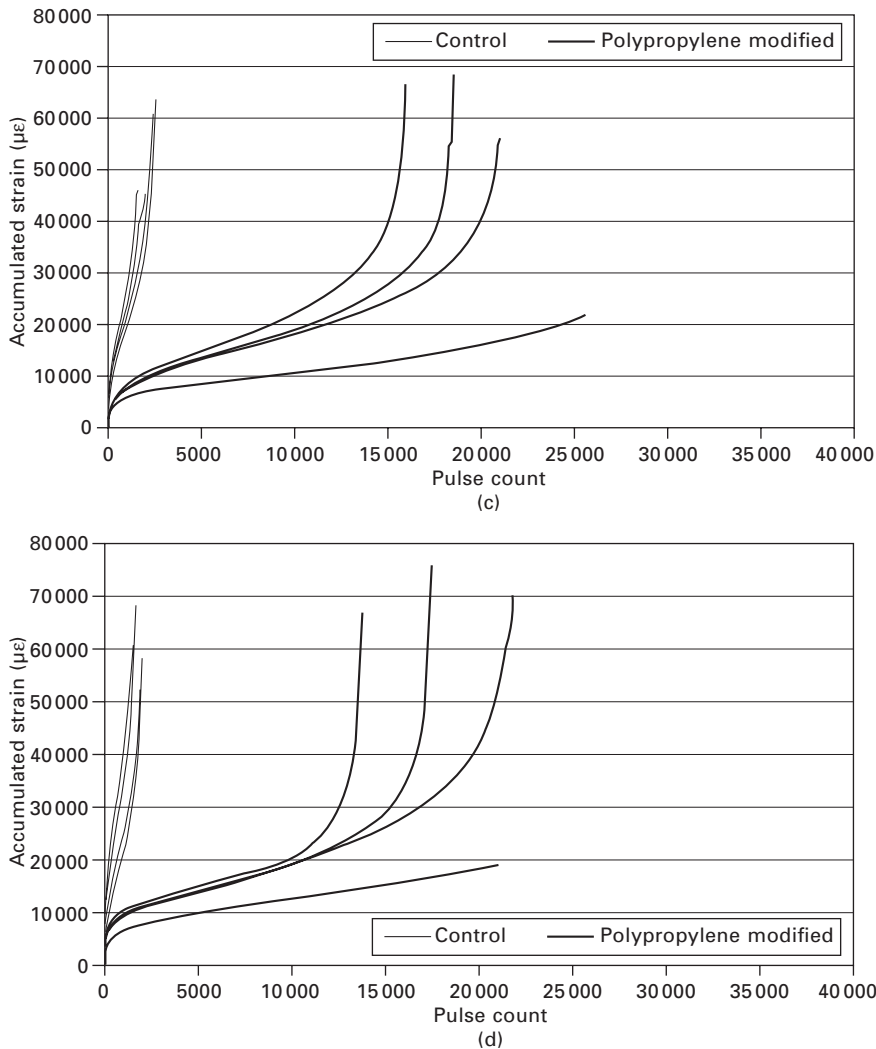
To understand the behaviour of the asphalt specimens under different loading patterns, different constant stress values were chosen. These values were 100, 207 and 500 kPa. As polypropylene modification was carried out, utilising lower stress values like 100 and 207 kPa was not feasible, since under such loading the tertiary creep region could not be observed within a reasonable period of time. Therefore, in order to be able to differentiate between the reference and fiber-reinforced samples, a real destructive loading level of 500 kPa (approximately 73 psi) was chosen as the standard stress value. This is a departure from the published pioneering literature of the 'rule of thumb' with regard creep testing (Hofstra and Klomp 1972; Uge and Van de Loo 1974; Van de Loo 1974; Hills *et al.* 1974; De Hilster and Van de Loo 1977; Van de Loo and De Hilster 1978; Bolk and Van de Loo 1979). This value very well represents the actual tyre pressure of the tyres on a loaded truck. Also it has to be mentioned that, in today's modern pavement engineering practices, there are also other modifying agents like polypropylene fibers which need to be tested in actual stress levels (like 500 kPa of loading level in repeated creep test, not 207 kPa like the older practices) in order to show the very positive contribution of these modifiers to the genuine mechanical behaviour of dense bituminous mixtures. The specimen strain during the pulsed loading stage of the test was measured in the same axis as the applied stress using two linear variable displacement transducers (LVDTs). The applied force was open loop controlled and rectangular in shape (Uşar 2007; Tapkin *et al.* 2009a, 2009b). Load periods were chosen as 500 ms for all of the specimens and the rest periods were 500, 1000, 1500 and 2000 ms, respectively. Four specimens were tested for each loading pattern. The reference specimens were prepared with 5% bitumen content. The fiber-reinforced (M-03 type with dosage of 3% by weight of aggregate) specimens were also prepared with 5% bitumen content.

The repeated creep test results are shown in Figs 6.15 and 6.16. As can be clearly seen in Figs 6.15(a) and 6.16(a) (500 ms load followed by 500 ms rest), fiber-reinforced specimens under repeated creep tests show a time-to-failure-point pattern which is approximately 12 times longer than for the reference specimens under the same loading pattern and temperature (this value is given as an average for four different specimens in two separate groups). When the reader analyses Fig. 6.15(a), he or she can see that the reference specimens are entering the tertiary stage of creep at around 2000 pulse counts. This point corresponds only to the primary creep stage for the polypropylene fiber-modified specimens (see Fig. 6.13). Fiber-modified

specimens reach the tertiary creep stage only for a pulse count of 20 000, which is a clear indication of the start of failure of these specimens. When the reference specimens collapsed, the fiber-reinforced specimens did not show any sign of failure (they are in fact just in their primary stages of creep). Creep stiffness values naturally drop to a certain level through the



6.15 Accumulated strain versus pulse count for (a) specimens with loading pattern of 500 ms load and 500 ms rest period, (b) specimens with loading pattern of 500 ms load and 1000 ms rest period, (c) specimens with loading pattern of 500 ms load and 1500 ms rest period, and (d) specimens with loading pattern of 500 ms load and 2000 ms rest period.

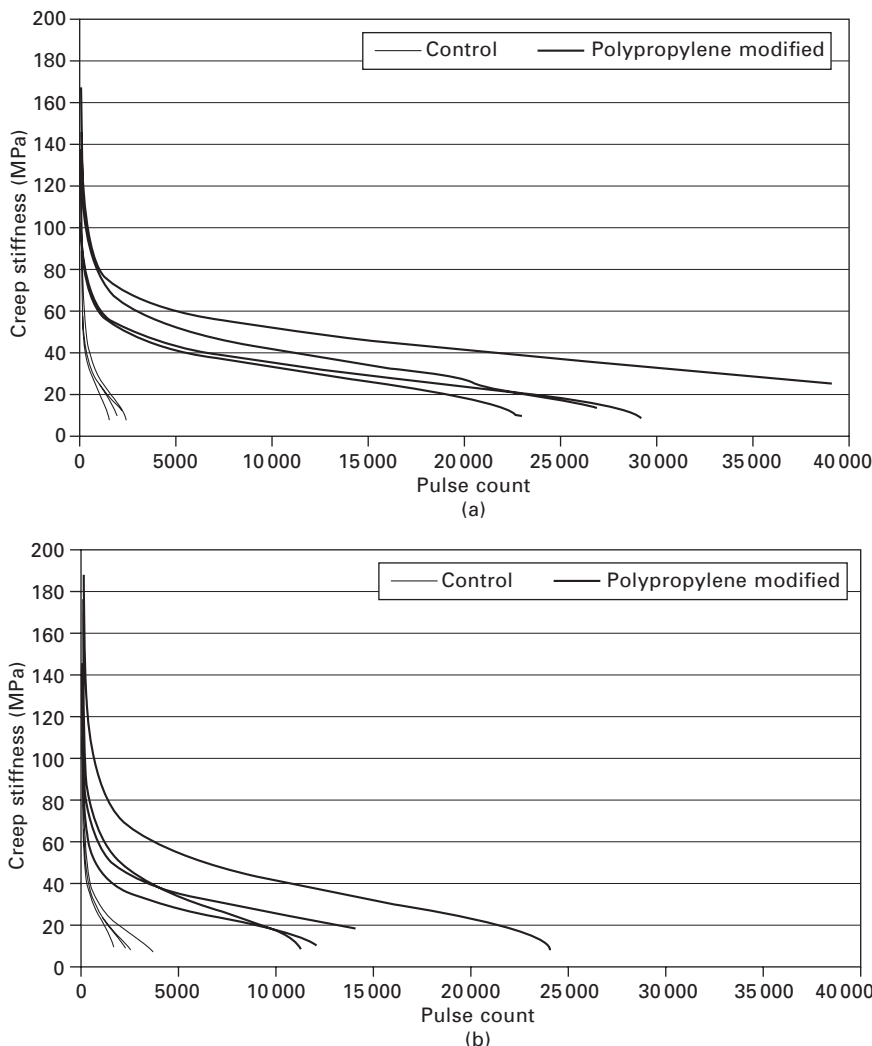


6.15 Continued

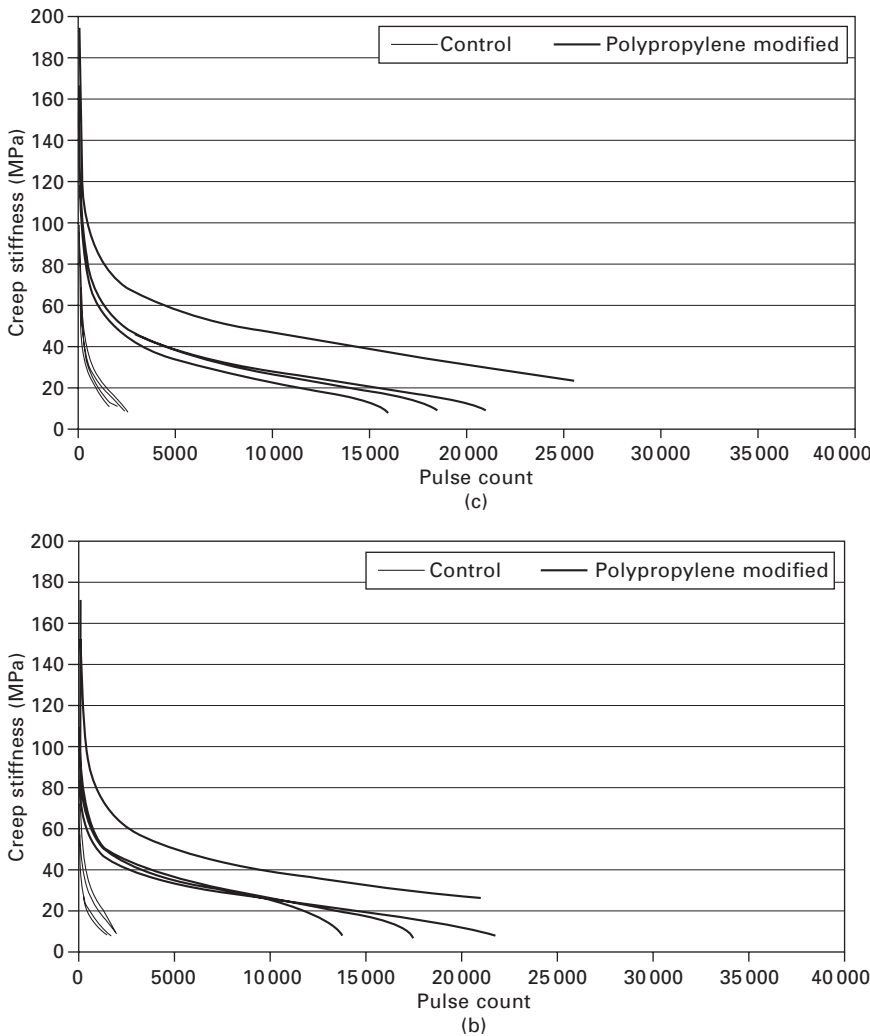
tests to around 10 MPa. This level can be accepted as the termination level for these tests. For both kinds of specimens, the termination stiffness values are the same, but the pattern of decrease in these values shows a marked difference (see Fig. 6.16(a)). When the reference specimens fail, the values of creep stiffness of the fiber-reinforced specimens have only dropped to 50% of their initial values (i.e. the time required to fail for these specimens is considerably longer). In addition, the initial creep stiffness values of the fiber-modified specimens are correspondingly higher compared to the reference specimens, but because of the operating conditions of the UTM-5P system,

an exact figure cannot be determined. Therefore, 200 MPa was selected as the maximum point of their creep stiffness upper range.

Figures 6.15(b) and 6.16(b) show graphs of the reference and fiber-modified specimens for 500 ms load followed by 1000 ms rest periods. In these two graphs, it can be seen that the service life of the modified specimens



6.16 Creep stiffness versus pulse count for (a) specimens with loading pattern of 500 ms load and 500 ms rest period, (b) specimens with loading pattern of 500 ms load and 1000 ms rest period, (c) specimens with loading pattern of 500 ms load and 1500 ms rest period, and (d) specimens with loading pattern of 500 ms load and 2000 ms rest period.



6.16 Continued

is approximately five times longer than for the reference specimens. With respect to the creep stiffness values, it can be stated that while the reference specimens fail, the fiber-modified specimen's creep stiffness values have only dropped by 50% of their original values (Fig. 6.16(b)). This is in agreement with the data presented in Fig. 6.16(a). Fiber-reinforced specimens under repeated creep tests show a point-to-failure pattern approximately 7.5 times higher than that of the reference specimens under a 500 ms load followed by 1500 ms rest period loading pattern (Fig. 6.15(c)). Similar to the previous loading patterns, when the reference specimens reach their tertiary creep

stage, the fiber-modified specimens are again in their primary creep stage, as expected. Also, accumulated strain versus pulse counts of fiber-reinforced specimens conform very well to the typical creep curve of a viscoelastic, elastoplastic and thermoplastic material such as asphalt concrete (see Fig. 6.13).

Accumulated strain versus pulse counts and creep stiffness versus pulse counts of the reference and modified specimens for the 500 ms load followed by 2000 ms rest period loading pattern are given in Figs 6.15(d) and 6.16(d), respectively. The main difference between this loading pattern and the 500 ms load followed by 500 ms rest loading pattern is related to the considerably longer rest periods. When the reference specimens fail, the creep stiffness of the modified specimens has dropped to the only 44% of its original value. This conforms very well to the behaviour under previous loading patterns.

These results show that the most suitable polypropylene fiber for asphalt concrete modification is the M-03 type, and that 3% addition of fibers by weight of aggregates has been determined as the optimal addition amount. The introduction of the polypropylene fibers into the asphalt mixture increased Marshall stability values by 22%. The stiffness of the Marshall specimens also increased significantly. It can be concluded that the time-to-failure of the fiber-modified asphalt specimens under repeated creep loading for different loading patterns increased by 5–12 times relative to the reference specimens. This is a very significant improvement from a pavement engineering viewpoint. The repeated creep tests resulted in the primary creep stage in polypropylene-modified specimens, while the reference specimens reached their tertiary creep stages at the same loading pulse counts. Similar behaviour was also obtained for creep stiffness. While the reference specimens are failing, the creep stiffness values for the fiber-reinforced specimens have dropped to only 50% of their original values. The results from the analysis of the tested specimens show that the addition of polypropylene fibers improves the creep behaviour of the specimens in a pronounced manner by increasing the time-to-failure of the samples under repeated creep testing (Uşar 2007; Tapkı *et al.* 2009a).

6.6 Using artificial neural networks to predict physical and mechanical properties of polypropylene-modified dense bituminous mixtures

The Marshall design procedure is a very well-known and standard technique for dense bituminous mixture design (Asphalt Institute 1994). But this testing procedure to determine the precise optimum bitumen content is very time-consuming and needs skilled workmanship. The unit weight, voids in mineral aggregate (VMA), voids filled with asphalt (V_f) and air voids (V_a) are obtained

through extra calculations that are carried out as routine physical property analyses throughout pavement laboratories around the world. Therefore, if researchers can obtain stability and flow values of a standard mixture with the help of mechanical testing, the remaining calculations will just be mathematical manipulation. Artificial neural networks can be a suitable means to predict the stability and flow values obtained at the end of the Marshall test procedure without carrying out destructive testing. Marshall Quotient values, which are in fact of 'pseudo-stiffness', are also related to stability and flow values, therefore their prediction is also very important.

Detailed knowledge about the applications of artificial neural networks in transportation and pavement engineering can be found in the relevant literature (Tapkin 2004; Ritchie *et al.* 1991; Kaseko and Ritchie 1993; Gagarin *et al.* 1994; Eldin and Senouci 1995; Cal 1995; Razaqpur *et al.* 1996; Roberts and Attoh-Okine 1998; Owusu-Ababia 1998; Alsugair and Al-Qudrah 1998; Kim and Kim 1998; Shekharan 1998; Attoh-Okine 2001, 2005; Lee and Lee 2004; Mei *et al.* 2004; Bosurgi and Trifiro 2005; Zeghal 2008; Xue *et al.* 2009; Alavi *et al.* 2011; Mirzahosseini *et al.* 2011). Throughout this part of the study, artificial neural networks were utilised in order to predict the stability, flow and Marshall Quotient values of asphalt concrete specimens obtained from a series of Marshall designs, based on experimental results described above. The ranges for these test results are shown in Table 6.12. The data set is properly divided into 80% training and 20% testing sets for the neural network training process and these sets are randomly selected from the experimental database. The optimal neural network architecture for stability, flow and Marshall Quotient was found to be 8–5–1 (five hidden neurons). The optimum training algorithm was found to be Levenberg–Marquardt back-propagation. Hyperbolic tangent sigmoid and log-sigmoid transfer functions were utilised for the hidden layer and output layer, respectively.

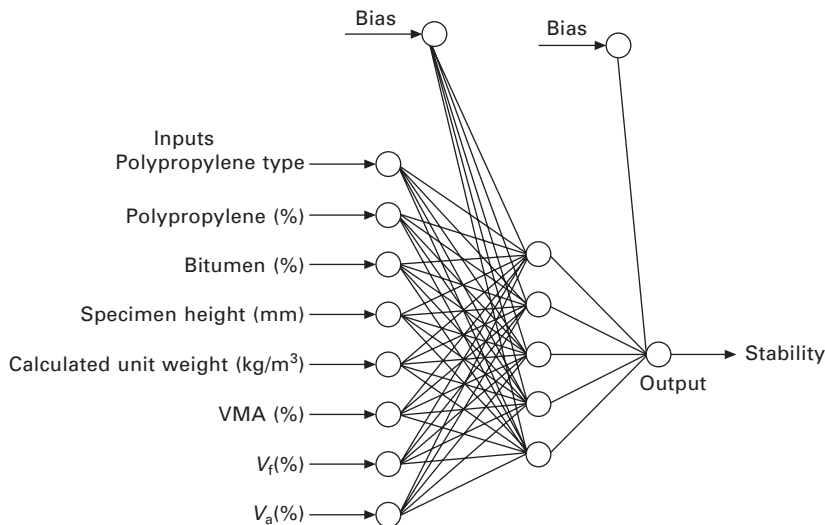
Statistical parameters of the training and testing sets and overall results of neural network models are presented in Table 6.13. As can be visualised from Table 6.13, the obtained neural network results are observed to be markedly close to actual test results. This is a perfect indication of the good training of the data set. Artificial neural network applications are treated as 'black-box' applications in general. However, this study opens this 'black box' and introduces the neural network application in a closed-form solution (Çevik 2006). This study aims to present the closed-form solutions of proposed neural network models for stability, flow and Marshall Quotient based on the trained NN parameters (weights and biases) as a function of polypropylene type, polypropylene percentage, bitumen percentage, specimen height (mm), calculated unit weight (kg/m^3), voids in mineral aggregate (VMA)%, voids filled with asphalt (V_f)% and air voids (V_a)%. These analyses were carried out separately for three different outputs, namely stability, flow and Marshall Quotient. In Fig. 6.17, the reader may find the neural network architecture

Table 6.12 Ranges of experimental database used throughout the study

Polypropylene type	Polypropylene percentage	Bitumen (%)	Specimen height (mm)	Calculated unit weight (kg/m ³)	VMA (%)	V _f (%)	V _a (%)	Marshall Quotient (kg/mm)	Stability (kg)	Flow (mm)
Maximum	3.00	6.00	7.00	62.00	2470.24	19.78	89.45	10.76	886.77	2289.4
Minimum	0.00	0.00	3.50	58.00	2311.26	14.47	40.70	1.48	92.77	689.52
Mean	1.15	2.78	5.24	59.86	2408.41	16.98	68.62	5.00	412.64	1396.6
Std. deviation	1.00	2.05	1.15	1.00	37.63	1.25	14.07	2.51	201.45	387.8

Table 6.13 Statistical parameters of neural network models utilised throughout the study

		Mean	Cov	R^2
Flow	Neural network training set	1.00	0.11	0.93
	Neural network testing set	0.98	0.25	0.71
	Neural network total set	0.99	0.16	0.81
Marshall Quotient	Neural network training set	1.00	0.12	0.94
	Neural network testing set	0.97	0.24	0.81
	Neural network total set	0.99	0.17	0.87
Stability	Neural network training set	1.00	0.03	0.99
	Neural network testing set	1.02	0.08	0.94
	Neural network total set	0.99	0.05	0.97



6.17 The neural network architecture related to stability analyses that have been carried out.

related to stability analyses that have been carried out. The other architectures for flow and Marshall Quotient are the same as in Fig. 6.17 except for the outputs.

Using weights and biases of the trained neural network model, the closed form of stability can be given as follows:

$$\text{Stability} = \frac{2290}{1 + \exp(9 - 0.386 \tanh H1 + 9.7 \tanh H2 + 0.55 \tanh H3 + 0.285 \tanh H4 - 0.92 \tanh H5)}$$

6.4

where

$$H1 = 4.4 \text{ PPTType} + 1.73 \text{ PP\%} + 1.47 \text{ Bit\%} - 0.41 \text{ SpecHeight} \\ + 0.0135 \text{ UW} - 0.366 \text{ VMA} - 0.237V_f - 0.91V_a - 1.875$$

$$H2 = 2.46 \text{ PPTType} - 0.035 \text{ PP\%} + 0.58 \text{ Bit\%} + 0.0476 \\ \text{SpecHeight} + 0.0113 \text{ UW} - 0.22 \text{ VMA} - 0.004V_f \\ + 0.39V_a - 39.5$$

$$H3 = -0.81 \text{ PPTType} - 0.165 \text{ PP\%} + 4.75 \text{ Bit\%} + 0.012 \\ \text{SpecHeight} + 0.011 \text{ UW} + 0.73 \text{ VMA} - 0.235V_f \\ - 1.41V_a - 39.9$$

$$H4 = -11.47 \text{ PPTType} - 0.356 \text{ PP\%} - 5.43 \text{ Bit\%} + 0.31 \\ \text{SpecHeight} + 0.0044 \text{ UW} - 0.34 \text{ VMA} - 0.0048V_f \\ + 2.3V_a - 6.58$$

$$H5 = -0.009 \text{ PPTType} + 0.18 \text{ PP\%} + 1.0316 \text{ Bit\%} - 0.058 \\ \text{SpecHeight} + 0.012 \text{ UW} - 0.77 \text{ VMA} + 0.0117V_f \\ + 0.756V_a - 22.9$$

Similarly, flow can be given as follows:

$$\text{Flow} = \frac{7.92}{1 + \exp(-5.88 + 5 \tanh H1 + 1.32 \tanh H2 + 1.39 \tanh H3 \\ + 0.25 \tanh H4 + 1.06 \tanh H5)}$$

6.5

where

$$H1 = 7.046 \text{ PPTType} - 1.464 \text{ PP\%} - 1.699 \text{ Bit\%} - 1.922 \\ \text{SpecHeight} + 0.012 \text{ UW} + 1.707 \text{ VMA} + 0.358V_f \\ + 2.728V_a + 33.14$$

$$H2 = -0.443 \text{ PPTType} - 0.95 \text{ PP\%} + 0.482 \text{ Bit\%} + 0.005 \\ \text{SpecHeight} + 0.004 \text{ UW} - 0.405 \text{ VMA} - 0.273V_f \\ - 0.880V_a + 18.37$$

$$H3 = -1.2 \text{ PPTType} + 0.068 \text{ PP\%} - 3.637 \text{ Bit\%} + 0.72 \\ \text{SpecHeight} - 0.014 \text{ UW} - 0.806 \text{ VMA} + 0.39V_f \\ + 2.5V_a - 6.31$$

$$H4 = -9.41 \text{ PPTType} + 3.43 \text{ PP\%} - 4.078 \text{ Bit\%} + 1.73$$

$$\text{SpecHeight} - 0.005 \text{ UW} - 2.25 \text{ VMA} - 0.39V_f - 3.22V_a + 2.74$$

$$H5 = 2.364 \text{ PPTType} + 1.69 \text{ PP\%} - 0.764 \text{ Bit\%} - 0.391$$

$$\text{SpecHeight} - 0.002 \text{ UW} + 0.167 \text{ VMA} - 0.033V_f + 0.445V_a + 23.81$$

In a similar fashion, the Marshall Quotient (MQ) can be given as:

$$\text{MQ} = \frac{887}{1 + \exp(0.915 - 4.14 \tanh H1 - 8.35 \tanh H2 - 1.17 \tanh H3 + 1.98 \tanh H4 + 3.25 \tanh H5)}$$

6.6

where

$$H1 = 0.809 \text{ PPTType} - 0.558 \text{ PP\%} + 0.18 \text{ Bit\%} - 0.294$$

$$\text{SpecHeight} + 0.011 \text{ UW} + 0.031 \text{ VMA} - 0.055V_f + 0.068V_a - 7.32$$

$$H2 = -0.503 \text{ PPTType} + 0.086 \text{ PP\%} + 0.053 \text{ Bit\%} + 0.205$$

$$\text{SpecHeight} - 0.004 \text{ UW} - 0.097 \text{ VMA} - 0.017V_f - 0.2V_a + 1.65$$

$$H3 = -0.47 \text{ PPTType} + 0.21 \text{ PP\%} - 0.545 \text{ Bit\%} - 0.367$$

$$\text{SpecHeight} + 0.0005 \text{ UW} - 0.34 \text{ VMA} + 0.046V_f - 0.494V_a + 29$$

$$H4 = 0.034 \text{ PPTType} - 0.103 \text{ PP\%} + 0.38 \text{ Bit\%} + 0.145$$

$$\text{SpecHeight} + 0.005 \text{ UW} - 0.4 \text{ VMA} + 0.001V_f - 0.067V_a - 15.1$$

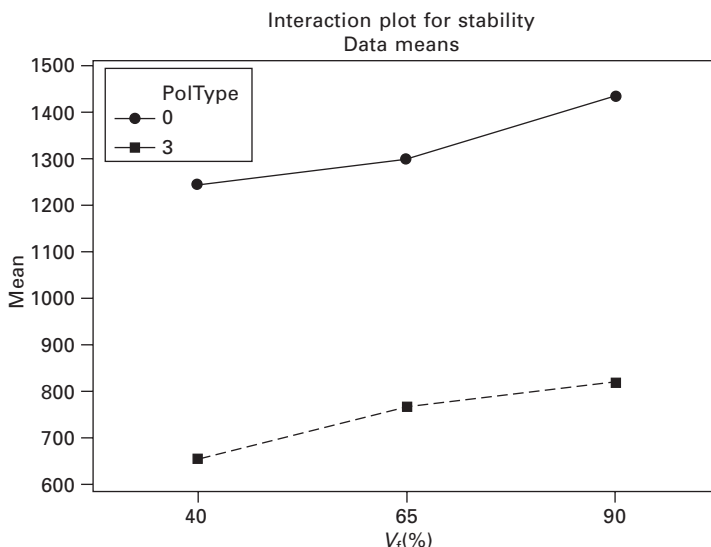
$$H5 = -1.922 \text{ PPTType} + 0.035 \text{ PP\%} + 0.3 \text{ Bit\%} + 0.28$$

$$\text{SpecHeight} + 0.006 \text{ UW} + 0.017 \text{ VMA} + 0.041V_f + 0.244V_a - 34$$

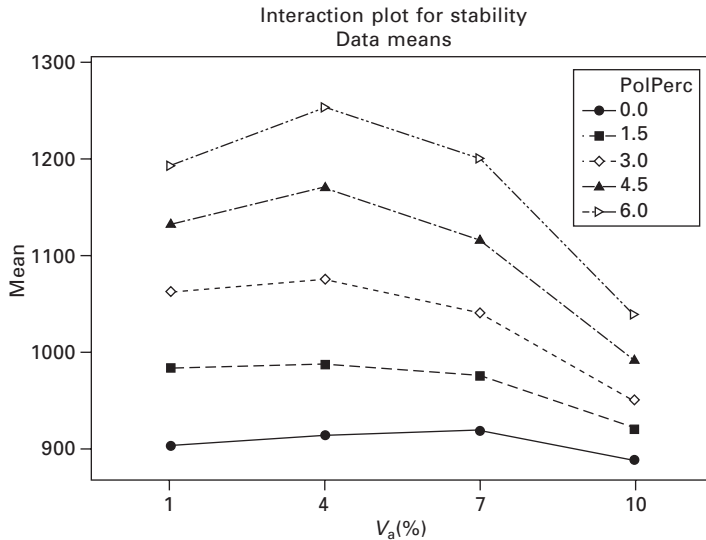
The main effects plot is an important graphical tool to visualise the independent impact of each variable utilised in the analyses carried out on stability, flow and Marshall Quotient values. This tool allows the reader to

visualise a better and much simpler snapshot of the overall significance of variable effects on the outputs and will provide a general overview. The main effects plot will also help researchers to perform further studies on stability, flow and Marshall Quotient values for the very well-known Marshall design procedure, without carrying out destructive tests for similar and specific type of aggregate sources, bitumen, aggregate gradation, mix proportioning, modification technique and laboratory conditions.

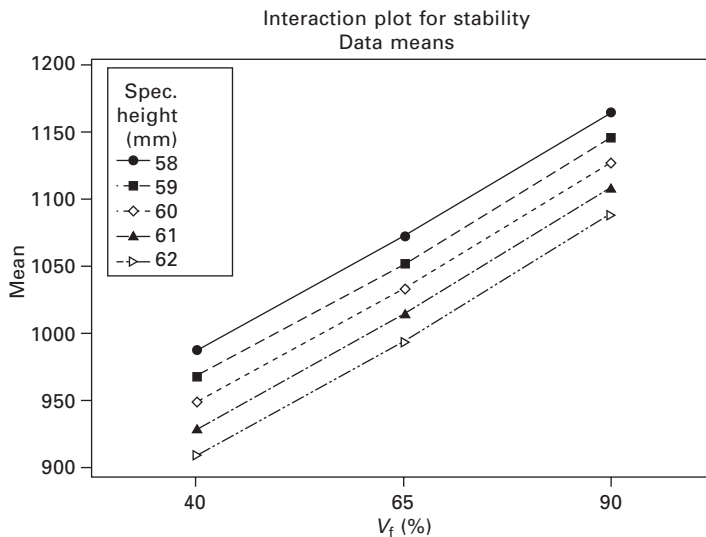
The maximum load the specimen will carry before failure is known as the Marshall stability. In Fig. 6.18 and for the other similar figures throughout the rest of this section, the y-axis relates to the output values that have been analysed. The mean stability values in this case increase in a noticeable manner with increase in voids filled with asphalt (V_f) values. This is an expected increase, as more bituminous material present in the voids of the total mixture means a more stable mixture. But the reader has to be aware of the fact that the range of stability values for the reference and polypropylene-modified specimens changes between a band of approximately 200 kilograms. After this band, one must bear in mind that the behaviour of the Marshall specimens is completely different from that stated in Fig. 6.18. Also, noticeable mean stability differences can be observed in Fig. 6.18 due to the polypropylene modification of the samples (here in the legend box, PolType 0 stands for polypropylene-modified specimen results). The mean stability values tend to increase first and then start to decrease in a noticeable manner as air voids start to increase, as can be clearly visualised from Fig. 6.19. In addition, when the polypropylene fiber content in the mixture increases, the mean



6.18 Polypropylene type vs. voids filled with asphalt (V_f) values.



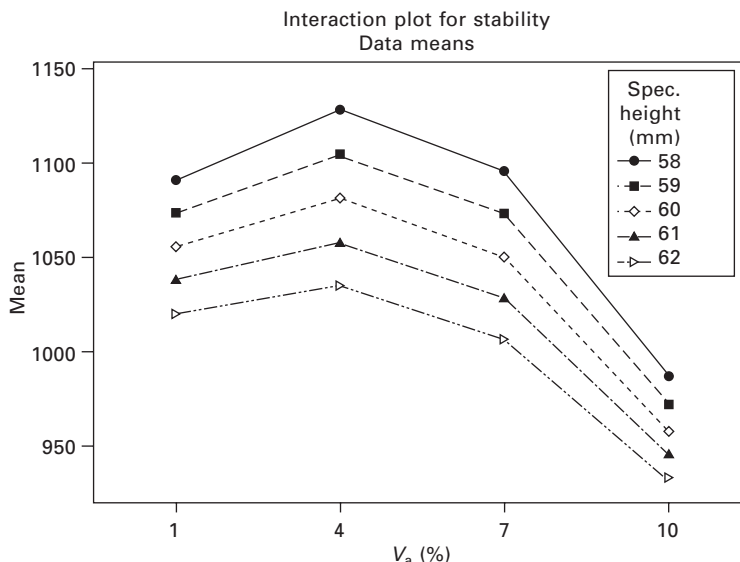
6.19 Polypropylene percentage vs. voids filled with asphalt (V_f) values.



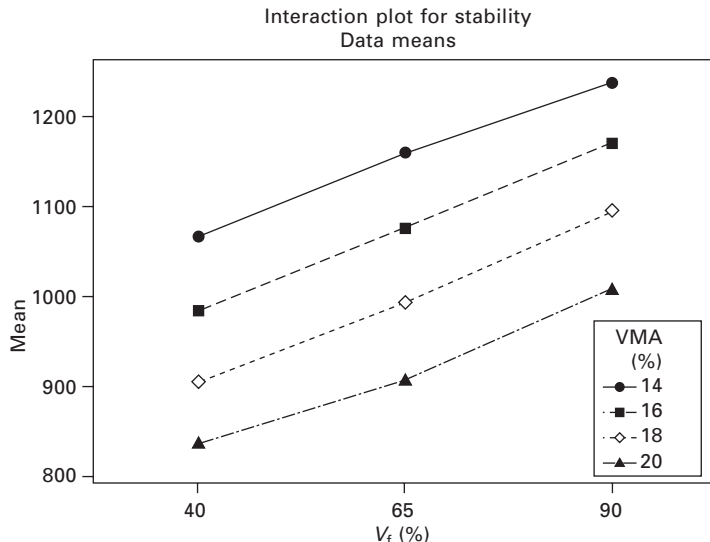
6.20 Specimen height vs. voids filled with asphalt (V_f) values.

Marshall stability values also increase. In Fig. 6.20, as specimen height (or thickness) increases, obviously the values of voids filled with asphalt (V_f) increase. This arises because of the nature of dense bituminous mixtures. Moreover, as the specimen height values increase, the stability values also decrease. This is because the thicker the specimen is, the more air voids the

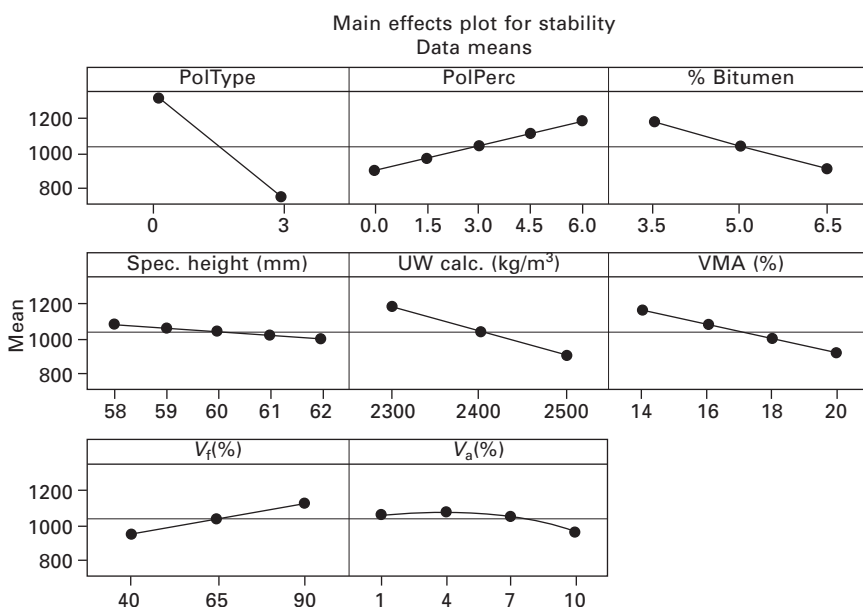
specimens have, so the lesser load carrying capacity they have. From Fig. 6.21, one can observe that as the air void values increase, the mean stability values tend to increase first and then decrease as can be expected from the above discussions. Also the mean stability values decrease with increasing specimen height, but the pattern is somewhat different for the polypropylene fiber modified system. When Fig. 6.22 is analysed, it is clear that when VMA (voids in mineral aggregate) values start to increase, mean stability values tend to decrease noticeably from Marshall specimen properties. Also when V_f values increase, the mean stability values increase correspondingly. In Fig. 6.23, whole trends for the parametric studies of mean effects of stability analysis that have been carried out on the well-trained neural network model can be clearly seen. In fact, this figure is an overall snapshot of the whole analysis. The amount of deformation of the specimen before failure occurs is known as flow. As we utilise polypropylene modification in this study, it is visualised from Fig. 6.24 that the mean flow values increase in a manner just as the bitumen content increases, as expected from a materials science perspective (PolType 0). As specimen height increases, air voids increase, therefore mean flow values also increase. In addition, as bitumen content increases, mean flow values further increase, as can be visualised from Fig. 6.25. Therefore one can visualise this doubled effect of both bitumen content and specimen height from the same graph. Overall, from Fig. 6.26, all the trends for the parametric study of mean effects of flow analysis that have been carried out on the well-trained neural network model can be clearly seen.



6.21 Specimen height vs. air voids (V_a) values.

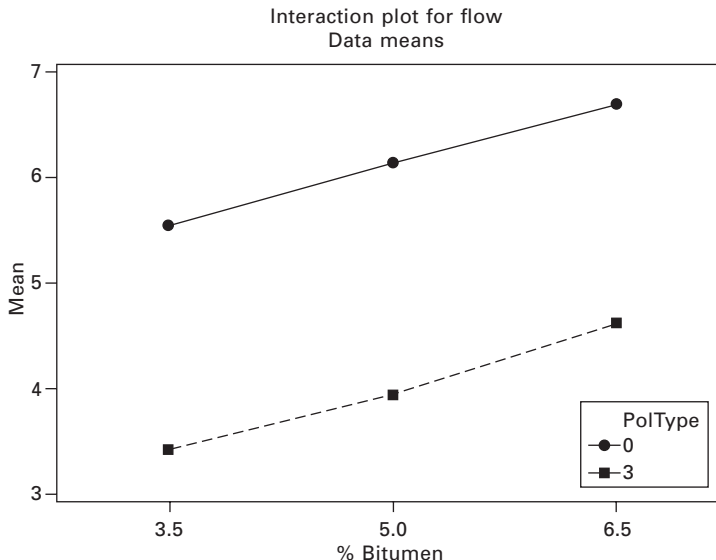


6.22 Voids in mineral aggregate (VMA) vs. voids filled with asphalt (V_f) values.

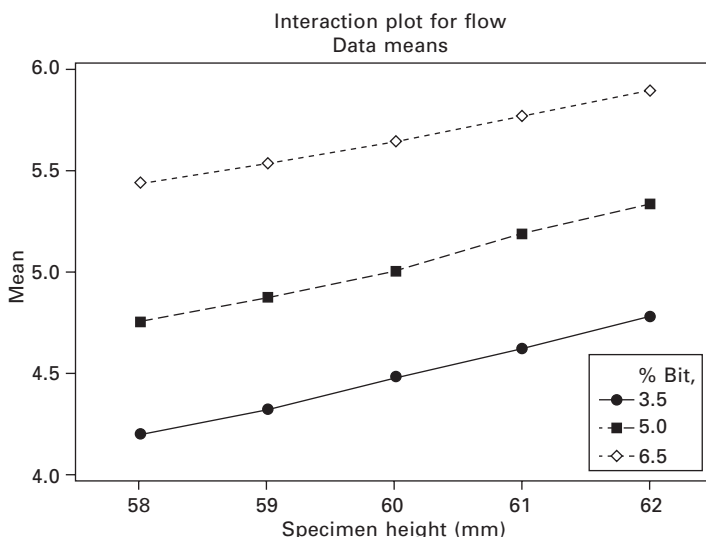


6.23 Whole trends for the parametric study of mean effects of stability analysis.

As air voids increase, the Marshall Quotient values decrease in a noticeable manner (Fig. 6.27). This is mainly because flow values increase abruptly when air void values increase. Also, for a fixed air voids value, as bitumen



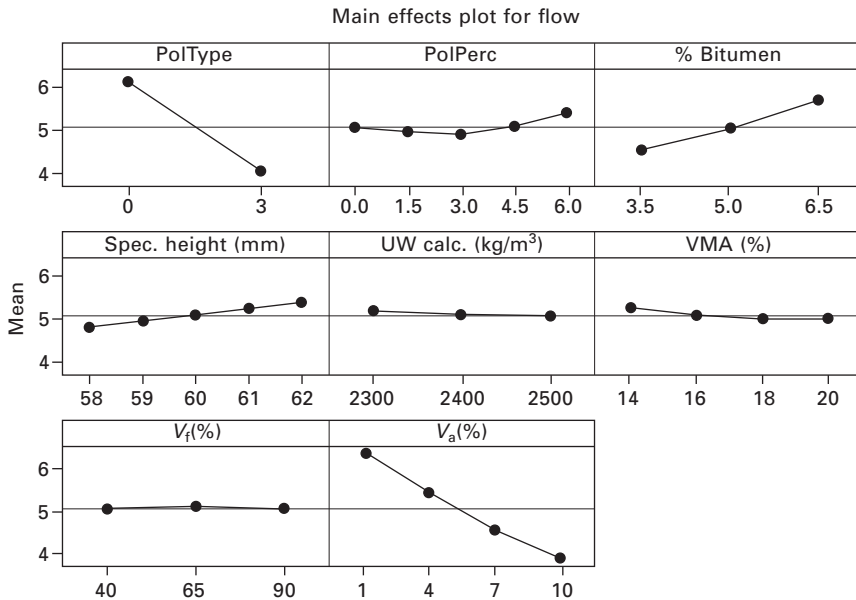
6.24 Interaction plot for polypropylene type versus % bitumen.



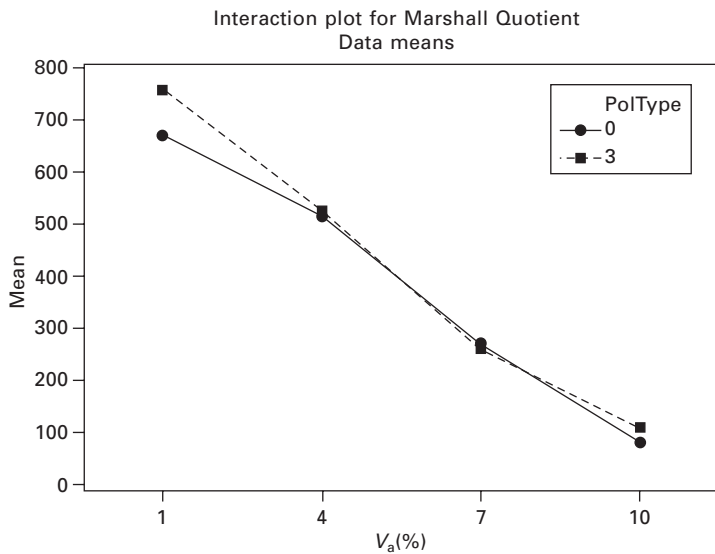
6.25 Interaction plot for % bitumen versus specimen height.

content increases, Marshall Quotient values decrease because of the sharp increase in flow values (Fig. 6.28). Finally, from Fig. 6.29, the overall trends for the parametric study of the mean effects of Marshall Quotient analysis can be visualised.

In this part of the study, a new and efficient approach to enable the prediction

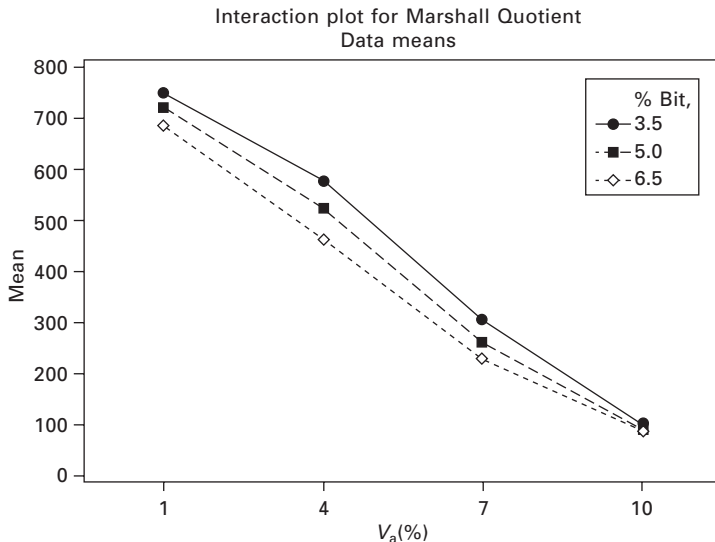
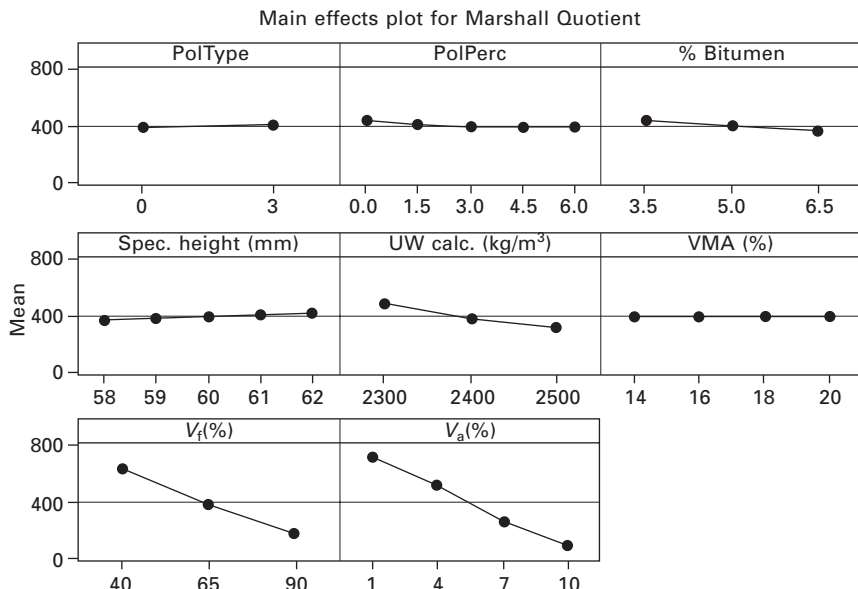


6.26 Whole trends for the parametric study of mean effects of flow analysis.



6.27 Interaction plot for polypropylene type versus air voids (V_a) values.

of mechanical properties such as stability, flow and Marshall Quotient without carrying out real destructive tests (obtained from Marshall designs) has been presented utilising artificial neural networks. Back-propagation

6.28 Bitumen percentage vs. air voids (V_a) values.

6.29 Whole trends for the parametric study of mean effects of Marshall Quotient analysis.

neural networks have been utilised for the neural network training process. The proposed neural network models for stability, flow and Marshall Quotient have shown very good agreement with experimental results

($R^2 = 0.97$, $R^2 = 0.81$, $R^2 = 0.87$) but it should be noted that this neural network model is valid only for the ranges of the experimental database used for neural network modelling. The explicit formulation of stability, flow and Marshall Quotient based on the proposed neural network model is also obtained and presented for further use by researchers. To obtain the main effects of each variable on stability, flow and Marshall Quotient, a wide range of parametric studies have been performed by using this neural network model. As a consequence, the proposed neural network model and formulation of the available stability, flow and Marshall Quotient of asphalt samples is quite accurate, fast and practical for use by other researchers studying in this field.

No rational model to predict rutting has been developed yet that encompasses all the relevant variables. In this part of the study, a neural network model has been proposed to predict the accumulated strains developed in the body of polypropylene-modified Marshall specimens during repeated load creep tests, in order to estimate the rutting potential of dense bituminous mixtures. This study is novel in the sense that, to date, no similar studies have been carried out for the prediction of the repeated creep test results to simulate tests carried out in the laboratory environment utilising a universal testing machine (UTM-5P) and artificial neural networks.

The main focus of this study is the prediction of repeated creep behaviour of polypropylene-modified bituminous mixtures using artificial neural networks based on experimental results described in Section 6.5. The range of experimental results obtained is given in Table 6.14. The optimal neural network architecture was found to be 8–15–1 (15 hidden neurons) as shown in Fig. 6.30. The optimum training algorithm was found to be Levenberg–Marquardt back-propagation. Hyperbolic tangent sigmoid and log-sigmoid transfer functions were used for the hidden layer and output layer, respectively. Statistical parameters of the testing and training sets and overall results from the neural network models are presented in Table 6.15. Comparisons of typical test set results and neural network results were observed to show very close agreement with actual test results.

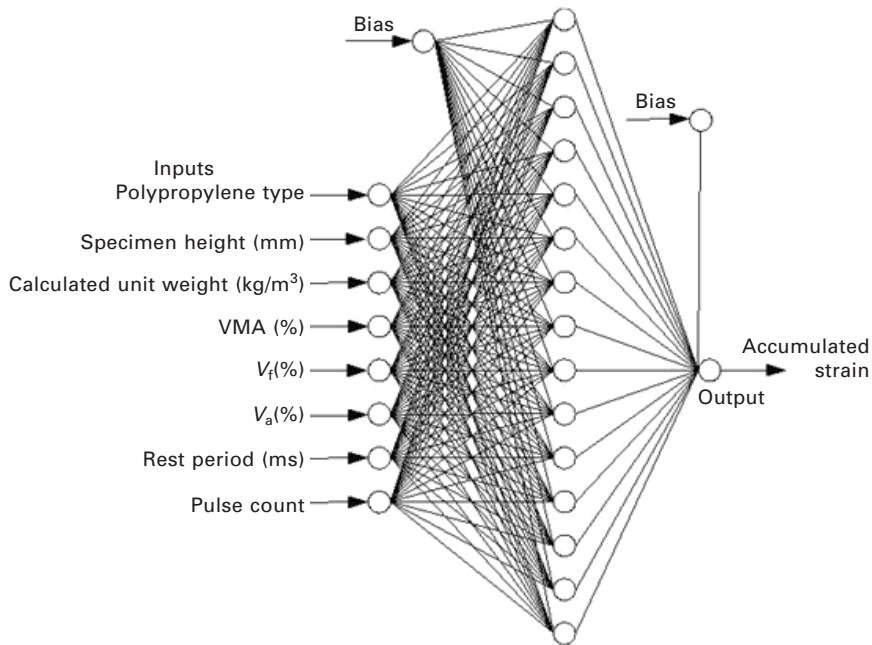
This study aims to present the closed-form solutions of the proposed artificial neural network model for accumulated strain based on the trained neural network parameters (weights and biases) as a function of polypropylene type, specimen height (mm), calculated unit weight (kg/m^3), voids in mineral aggregate (VMA)%, voids filled with asphalt (V_f)%, air voids (V_a)%, rest period (ms) and pulse count. Using weights and biases of the trained neural network model, accumulated strain can be expressed as follows:

$$\text{Accumulated strain} = \frac{75840}{1 + e^{-k}}$$

where:

Table 6.14 Ranges of experimental database used throughout this part of the study

	Polypropylene type	Specimen height (mm)	Calculated unit weight (kg/m ³)	VMA (%)	V _f (%)	V _a (%)	Rest period (ms)	Pulse count	Accumulated strain (με)
Maximum	3.00	60.00	2469.54	16.41	77.79	4.86	2000.00	39104.00	69937.00
Minimum	0.00	58.00	2419.80	14.69	68.24	2.90	500.00	2.00	459.70
Mean	1.45	58.80	2445.68	15.53	72.75	3.84	1217.86	5732.18	21681.79
Std. deviation	1.50	0.81	17.00	0.60	3.52	0.67	563.29	7052.19	11984.52



6.30 The optimal neural network architecture.

Table 6.15 Ranges of experimental database used throughout this part of the study

	Cov	RMSE	R^2
Neural network training set	0.28	1907	0.98
Neural network testing set	0.43	2355	0.96
Neural network total set	0.31	1995	0.97

$$\begin{aligned}
 k = & 12.4 \tanh H1 + 10.0 \tanh H2 - 15.1 \tanh H3 + 43.3 \tanh H4 \\
 & - 36.5 \tanh H5 + 30.8 \tanh H6 - 4.0 \tanh H7 - 6.0 \tanh H8 \\
 & + 11.6 \tanh H9 - 6.1 \tanh H10 - 21.6 \tanh H11 + 30.2 \tanh H12 \\
 & - 38.5 \tanh H13 + 19.4 \tanh H14 + 24.2 \tanh H15 + 9.16
 \end{aligned}$$

and

$$\begin{aligned}
 H1 = & -0.3 \text{PPTtype} - 0.418 \text{ SpecHeight} - 0.034 \text{ UW} \\
 & - 0.044 \text{ VMA} + 0.391 \text{ Vf} - 1.275 \text{ Va} + 0.00254 \text{ Rest} \\
 & - 0.00007 \text{ Pulse} + 82.7
 \end{aligned}$$

$$\begin{aligned}
 H2 = & -0.26 \text{ PPTtype} + 0.382 \text{ SpecHeight} - 0.019 \text{ UW} \\
 & - 0.609 \text{ VMA} + 0.066 \text{ Vf} + 1.364 \text{ Va} - 0.00040 \text{ Rest} \\
 & - 0.00004 \text{ Pulse} + 32.6
 \end{aligned}$$

$$\begin{aligned}
 H3 = & 2.107 \text{ PPTType} - 0.781 \text{ SpecHeight} - 0.029 \text{ UW} \\
 & + 0.078 \text{ VMA} - 0.356V_f - 4.057V_a - 0.00156 \text{ Rest} \\
 & + 0.00008 \text{ Pulse} + 149.5
 \end{aligned}$$

$$\begin{aligned}
 H4 = & -1.234 \text{ PPTType} - 0.544 \text{ SpecHeight} + 0.025 \text{ UW} \\
 & + 0.301 \text{ VMA} + 0.429V_f - 6.028V_a + 0.00218 \text{ Rest} \\
 & + 0.00004 \text{ Pulse} - 50.3
 \end{aligned}$$

$$\begin{aligned}
 H5 = & -2.438 \text{ PPTType} + 0.129 \text{ SpecHeight} + 0.035 \text{ UW} \\
 & + 0.192 \text{ VMA} - 0.191V_f + 2.193V_a + 0.00104 \text{ Rest} \\
 & - 0.00013 \text{ Pulse} - 88.4
 \end{aligned}$$

$$\begin{aligned}
 H6 = & 4.020 \text{ PPTType} - 1.285 \text{ SpecHeight} - 0.011 \text{ UW} \\
 & + 1.753 \text{ VMA} - 0.625V_f - 0.089V_a + 0.00076 \text{ Rest} \\
 & + 0.00008 \text{ Pulse} + 101.9
 \end{aligned}$$

$$\begin{aligned}
 H7 = & -0.791 \text{ PPTType} + 0.450 \text{ SpecHeight} + 0.031 \text{ UW} \\
 & - 0.288 \text{ VMA} + 0.222V_f - 0.023V_a - 0.00021 \text{ Rest} \\
 & - 0.00027 \text{ Pulse} - 115.5
 \end{aligned}$$

$$\begin{aligned}
 H8 = & 0.860 \text{ PPTType} - 1.528 \text{ SpecHeight} + 0.028 \text{ UW} \\
 & + 0.172 \text{ VMA} + 0.508V_f + 1.254V_a + 0.00176 \text{ Rest} \\
 & + 0.00001 \text{ Pulse} - 25.3
 \end{aligned}$$

$$\begin{aligned}
 H9 = & 0.401 \text{ PPTType} - 0.391 \text{ SpecHeight} - 0.036 \text{ UW} \\
 & - 0.852 \text{ VMA} + 0.098V_f + 0.707V_a + 0.00034 \text{ Rest} \\
 & + 0.00007 \text{ Pulse} + 122.1
 \end{aligned}$$

$$\begin{aligned}
 H10 = & -2.530 \text{ PPTType} - 0.901 \text{ SpecHeight} - 0.016 \text{ UW} \\
 & - 0.567 \text{ VMA} + 0.170V_f - 3.311V_a + 0.00586 \text{ Rest} \\
 & - 0.00012 \text{ Pulse} + 103.2
 \end{aligned}$$

$$\begin{aligned}
 H11 = & -0.757 \text{ PPTType} + 0.027 \text{ SpecHeight} - 0.031 \text{ UW} \\
 & - 2.162 \text{ VMA} + 0.012V_f - 3.493V_a - 0.00121 \text{ Rest} \\
 & - 0.00096 \text{ Pulse} + 124
 \end{aligned}$$

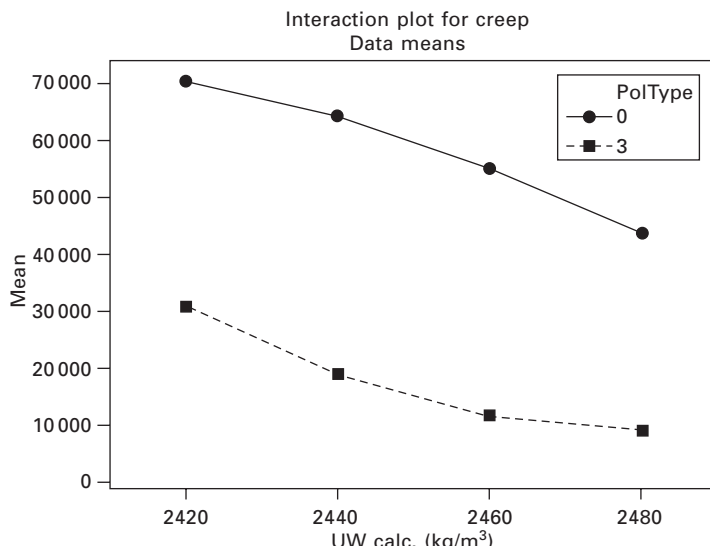
$$\begin{aligned}
 H12 = & -4.870 \text{ PPTType} - 0.581 \text{ SpecHeight} - 0.016 \text{ UW} \\
 & + 2.675 \text{ VMA} - 0.109V_f + 3.636V_a + 0.00207 \text{ Rest} \\
 & - 0.00014 \text{ Pulse} + 30.7
 \end{aligned}$$

$$\begin{aligned}
 H13 = & 2.130 \text{ PPTType} - 0.613 \text{ SpecHeight} + 0.042 \text{ UW} \\
 & - 0.306 \text{ VMA} + 0.414V_f - 5.908V_a + 0.00236 \text{ Rest} \\
 & + 0.00007 \text{ Pulse} - 79
 \end{aligned}$$

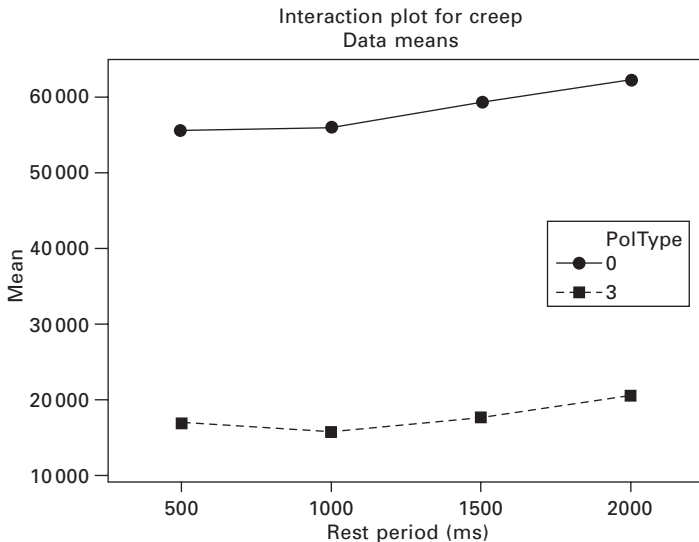
$$\begin{aligned}
 H14 = & 1.312 \text{ PPTType} + 0.899 \text{ SpecHeight} + 0.029 \text{ UW} \\
 & - 0.738 \text{ VMA} - 0.218V_f - 4.259V_a + 0.00047 \text{ Rest} \\
 & + 0.00009 \text{ Pulse} - 85.2
 \end{aligned}$$

$$\begin{aligned}
 H15 = & -0.717 \text{ PPTType} - 0.860 \text{ SpecHeight} - 0.029 \text{ UW} \\
 & - 0.326 \text{ VMA} + 0.010V_f - 1.862V_a - 0.00002 \text{ Rest} \\
 & + 0.00006 \text{ Pulse} + 134.6
 \end{aligned}$$

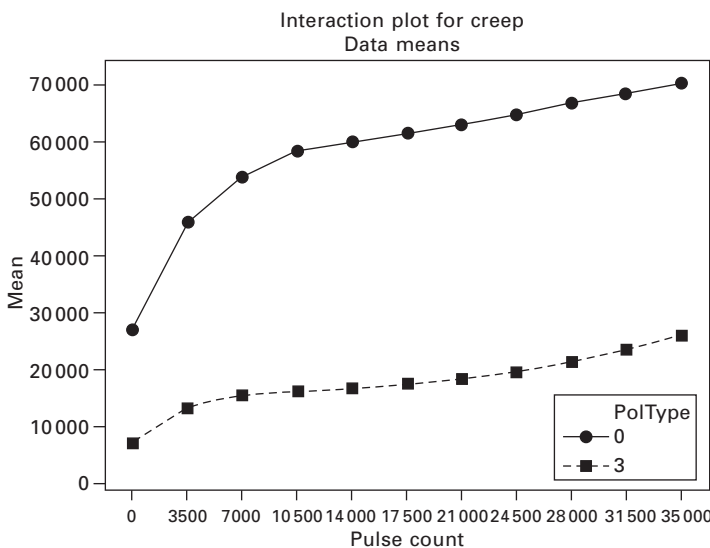
In Figs 6.31 – 6.35, *y*-axes represent the accumulated strain values in $\mu\epsilon$. In Fig. 6.31, it can be seen that as unit weight increases (which means less air voids and more Marshall stability values up to a certain degree), the accumulated strain values decrease considerably. This is as expected from a materials engineering point of view. Besides, as one moves from the reference (PolType 0) to the polypropylene fiber modified (PolType 3) specimens, accumulated strain values decrease in a noticeable manner. Figure 6.32 is a very exciting interaction plot from the mechanical evaluation point of view of dense bituminous mixtures. It also gives very important visual information for the repeated load creep test. As the rest period increases from 500 ms to 2000 ms for the Marshall specimens tested in the UTM-5P system, accumulated



6.31 Interaction plot for polypropylene type versus unit weight.

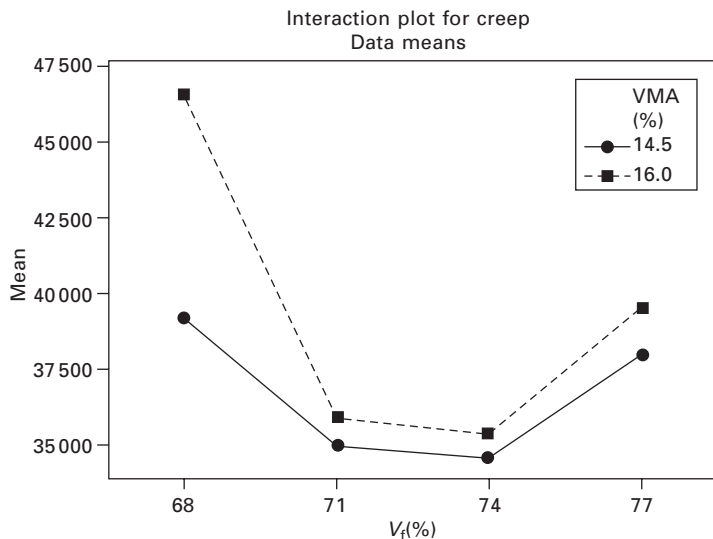


6.32 Interaction plot for polypropylene type versus rest period.

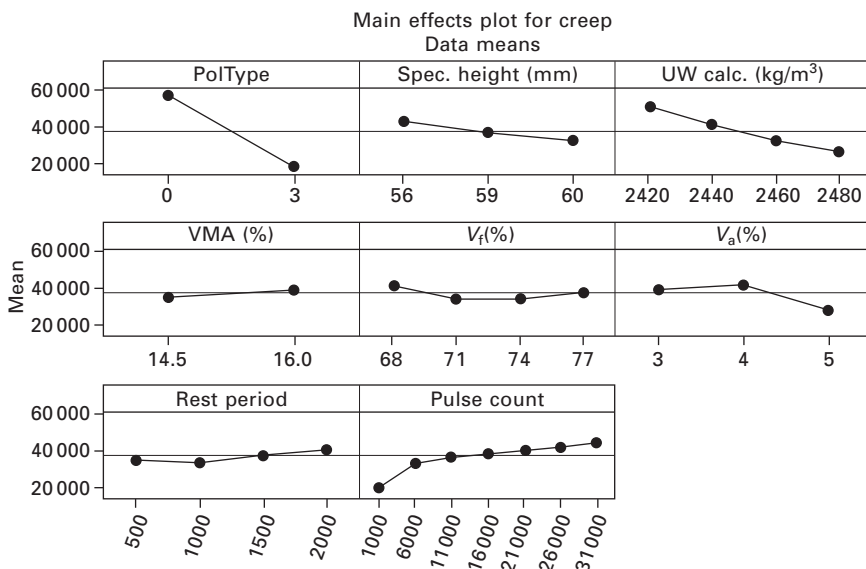


6.33 Interaction plot for polypropylene type versus pulse count.

strains increase little by little as seen in Fig. 6.15(a)–(d). As the asphalt mixture is modified by utilising polypropylene fibers, accumulated strains developed in the Marshall specimen bodies should decrease considerably for both kinds of specimens (please refer to Fig. 6.31).



6.34 Voids in mineral aggregate vs. voids filled with asphalt.



6.35 Whole trends for the parametric study of mean effects of accumulated strain analysis.

One can observe immediately the trend followed in the accumulated strain versus pulse count graphs in Fig. 6.15(a)–(d). In Fig. 6.33, the primary, secondary and tertiary creep regions can be easily seen (Fig. 6.13). The rapid increase of accumulated strain for the reference specimens can also

be visualised. Also, the shift between the two plots for the reference and polypropylene-modified mixtures, in the *y*-direction, shows the evolving nature of the specimens.

To a certain extent, as voids filled with asphalt values increase, the accumulated strain values decrease and thereafter accumulated strain values start to increase. This is an expected case and is in agreement with the trend seen in the VMA values. As VMA values increase, accumulated strain values also increase (please refer to Fig. 6.34). In Fig. 6.35, the general snapshot for the parametric study of mean effects of accumulated strain analysis can be visualised in a compact manner.

A novel approach has been proposed for the prediction of mechanical properties such as accumulated strain development at the end of repeated load creep tests carried out using experimental testing (UTM-5P) and utilising artificial neural networks. This approach is very important in the sense that for a certain type of asphalt mixture and for predetermined testing conditions, the accumulated strains at the end of repeated load creep tests can be estimated without carrying out destructive tests with UTM-5P or any similar testing equipment. This allows the rutting potential to be estimated. The proposed artificial neural network models for accumulated strain estimation have shown perfect agreement with experimental results ($R^2 = 0.97$). This model is valid for the range of the experimental database used for modelling. The explicit formulation of accumulated strain on the proposed artificial neural network model is also obtained through extensive analyses and presented for further use by researchers. To obtain the main effects of each variable on accumulated strain, a wide range of parametric studies have been performed by using the very well-trained artificial neural network model. As a result, the proposed artificial neural network model and formulation of the available accumulated strain development of Marshall specimens are quite accurate, fast and practical for use by other researchers studying in the experimental pavement engineering field.

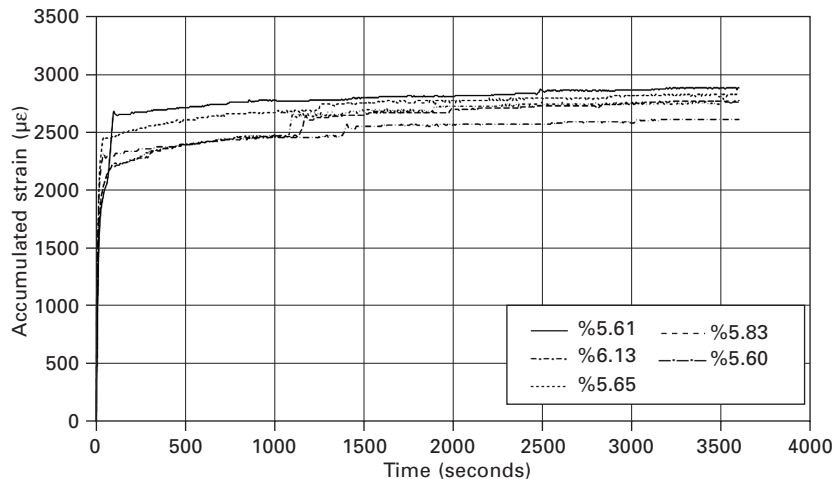
6.7 Determining the optimal polypropylene fiber modification of asphalt concrete utilising static creep tests, Marshall tests and fluorescence microscopy analyses

Extensive studies using the unconfined creep test (also known as simple creep test or uniaxial creep test) as a basis of predicting permanent deformation have been conducted to date. It has been found that the creep test must be performed at relatively low stress levels (not usually exceeding 30 psi (206.9 kPa)) and low temperature (not usually exceeding 104°F (40°C)), otherwise the sample fails prematurely (Hills 1973; Van de Loo 1974, 1976). The test conditions consist of a static axial stress, σ , of 100 kPa being applied to a

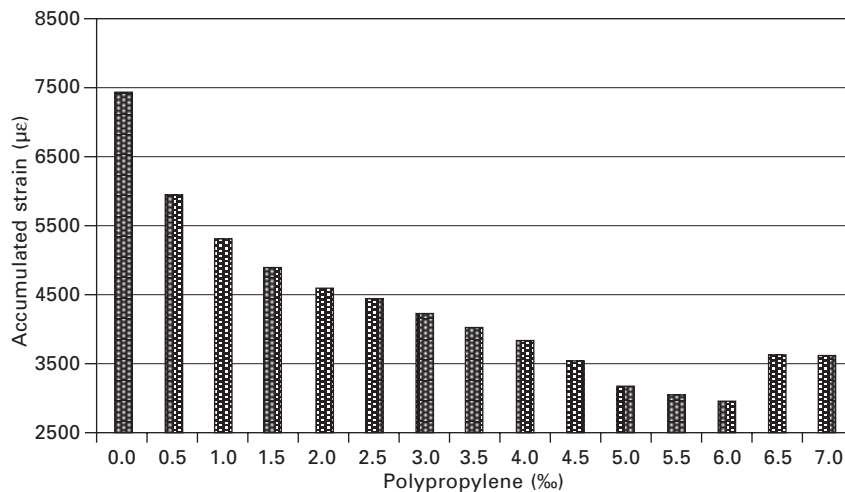
specimen for a period of 1 hour at a temperature of 40°C (Zurich 1977). This test is inexpensive and easy to conduct but the ability of the test to predict performance is extremely questionable. In-place asphalt mixtures are typically exposed to truck tyre pressures of approximately 120 psi (828 kPa) and maximum temperatures of 140°F (60°C) or higher (Roberts *et al.* 1996). Therefore, the conditions of this test do not closely simulate in-place conditions.

The main outcome of this part of the study was the major drawback of the static creep tests and those that have been carried out worldwide to date (Özcan 2008). Therefore, a completely different loading pattern and testing temperature were adopted. In this study, first the test temperature was chosen as 50°C, again just as in the repeated creep testing regime to simulate actual *in situ* conditions. To determine the optimum bitumen content for unmodified specimens, two Marshall designs were utilised. The height of the asphalt specimens was approximately the same for all samples. Prior to testing, the specimens were put in an environmental chamber for 24 hours to give them a uniform temperature distribution. Then, the static axial stress, σ , of 100 kPa was applied to the specimens as a preloading for 10 minutes, and afterwards 500 kPa of loading was applied to the specimens for 1 hour to simulate in-place conditions in a realistic manner (Özcan 2008). Also it has to be mentioned that, in today's modern pavement engineering practices, there are also other modifying agents like polypropylene fibers which need to be tested under actual stress levels (such as 100 kPa of preloading and 500 kPa loading level in the repeated creep test, not 10 kPa preloading and 100 kPa loading level as in older practices) in order to show the very positive contribution of these modifiers to the genuine mechanical behaviour of dense bituminous mixtures. In this manner, the rutting potential of dense bituminous mixtures can be explored in a more complete fashion coupled with the previous researches described in Section 6.6.

Starting with control specimens (a total of nine), Marshall specimens were prepared at the optimum bitumen content (5%) with polypropylene contents varying between 0.5% and 7.0% by aggregate weight in 0.5% increments. For each polypropylene content, a total of six specimens were fabricated. Therefore, a total of 84 (14 × 6) modified specimens were tested under the static creep test conditions stated above. In order to give an example of the change in accumulated strain versus time graphs of the specimens subjected to creep loading, curves for 5.5% modified specimens are given in Fig. 6.36. In Fig. 6.37, it can be clearly seen that the accumulated strain at the end of 1 hour of static loading decreases in a noticeable manner due to the addition of polypropylene fibers. Another interesting point is that, after 6% polypropylene addition with respect to the total weight of aggregate, the accumulated strains start to increase again. This allows for the determination of the optimal polypropylene content to the designated mixture. The initial



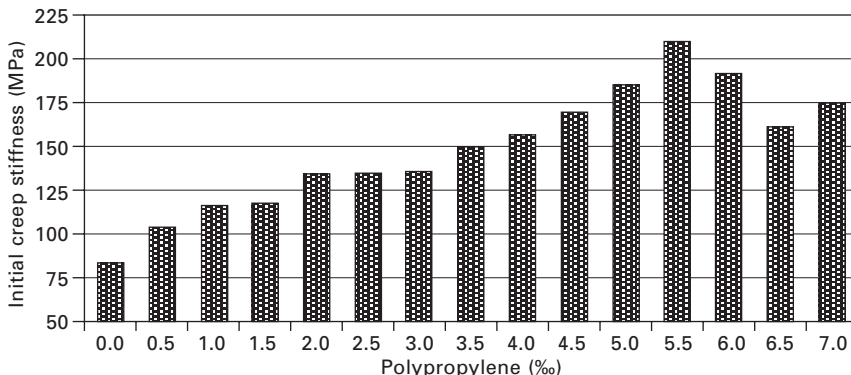
6.36 Accumulated strain versus time graphs for 5.5% polypropylene-modified specimens by weight of aggregate (legend representing total air voids).



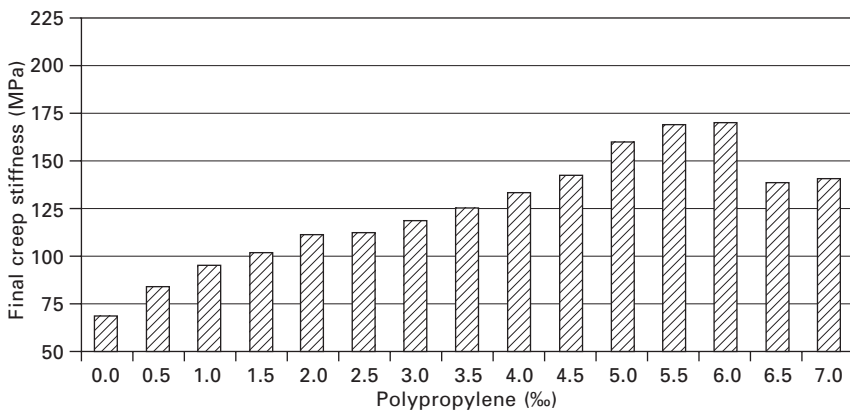
6.37 Accumulated strain values for 15 sets of specimens at the end of static creep tests.

(at the end of 100 seconds of 500 kPa loading) and final creep stiffness values for the 15 different sets of specimens are shown correspondingly in Figs 6.38 and 6.39. In these graphs, it can again be clearly seen that 5.5% polypropylene modification is an optimal amount to significantly change creep stiffness.

It can be readily observed from Figs 6.37–6.39 that the addition of polypropylene enhances the mechanical mixture properties in a very favourable



6.38 Initial creep stiffness versus time graphs for 15 different sets of polypropylene-modified specimens.



6.39 Final creep stiffness versus time graphs for 15 different sets of polypropylene-modified specimens.

manner. For example, the control specimens have a final accumulated strain value of $7433.89\mu\epsilon$. On the other hand, the 6% polypropylene-modified specimens have a final accumulated strain value of $2964.50\mu\epsilon$. This corresponds to a decrease of approximately 60% and is most significant. On the other hand, the initial and final stiffness (creep stiffness) values are 83.46 and 67.99 MPa, respectively. When the 6% polypropylene-modified specimens were investigated, these values were 191.65 and 169.15 MPa, respectively. These values correspond to an increase of 129% in the initial and 149% in the final creep stiffness values, and again are very significant.

In order to give more insight to the investigated problem of determining the optimal polypropylene fiber modification of dense bituminous mixtures, Marshall stability and flow tests were performed on 90 further specimens (six

for the control and six for each of the proposed amounts of polypropylene addition of 0.5% to 7.0% in 0.5% increments). By carrying out these tests, another value for the determination of the optimum polypropylene amount is sought. To show this, the stability, unit weight, air voids, voids filled with asphalt, voids in mineral aggregate, flow and Marshall Quotient values have been determined and averaged accordingly for the 15 sets of specimens, and are listed in Table 6.16. From Table 6.16, it can be observed that the average stability values of the control specimens increase up to 70% when 7% polypropylene modification is carried out. This is a dramatic increase when viewed from a pavement engineering viewpoint. The unit weight values drop by 2.9% until 5.5% polypropylene amount is added and from this point on they tend to increase again. The air voids increase by 80% until 5.5% polypropylene amount, but start to decrease from thereon. Voids filled with asphalt values show a similar trend (16.5% decrease) up to 5.5% polypropylene addition. The voids in mineral aggregate values increase by 16.4% up to 5.5% addition of polypropylene and then start to decrease from this point on. The behaviour for flow values is similar (i.e. a 23% decrease). Finally, Marshall Quotient values increase by 92%, which is an indication of pseudo-stiffness. At the end of the Marshall stability and flow tests, the physical and mechanical properties of the 15 sets of specimens reveal that optimal polypropylene addition is 5.5%.

A fluorescence microscope was used to investigate the morphology of the various polymer-modified bitumen samples (in this study M-03 type polypropylene fibers). A distinction can be made between the polypropylene-

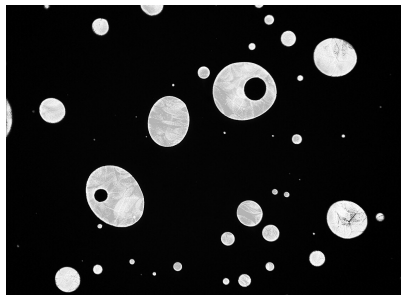
Table 6.16 Average physical and mechanical values obtained for 15 sets of specimens

Polypropylene amount (%)	Unit weight (kg/m ³)	V _f (%)	VMA (%)	Air voids (%)	Stability (kg)	Flow (mm)	Marshall Quotient (kg/mm)
0.0	2465	76.990	14.919	3.443	1294.355	3.463	376.899
0.5	2462	76.337	15.029	3.569	1355.712	3.416	400.559
1.0	2459	75.828	15.114	3.665	1378.510	3.408	405.166
1.5	2452	74.449	15.365	3.949	1391.292	3.388	411.593
2.0	2446	73.148	15.581	4.195	1453.083	3.233	463.103
2.5	2437	71.555	15.873	4.526	1500.593	3.081	490.412
3.0	2432	70.710	16.033	4.707	1542.140	2.982	523.329
3.5	2430	70.188	16.131	4.818	1626.905	2.826	588.954
4.0	2419	68.340	16.500	5.237	1703.500	2.788	618.161
4.5	2406	66.112	16.961	5.761	1837.763	2.748	680.879
5.0	2402	65.546	17.080	5.895	1971.715	2.628	755.850
5.5	2394	64.261	17.360	6.214	1917.643	2.678	724.647
6.0	2414	67.429	16.681	5.443	1989.972	2.984	682.360
6.5	2416	68.804	16.607	5.359	2113.038	3.169	678.393
7.0	2421	68.760	16.412	5.138	2186.930	3.211	683.755

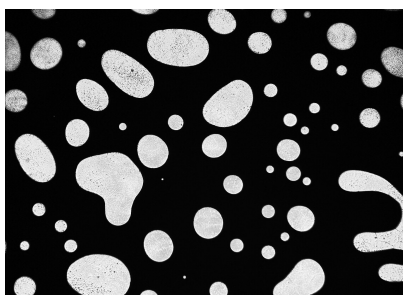
modified bitumen whose continuous phase is a bitumen matrix with dispersed polymer particles and samples whose continuous phase is a polymer matrix with dispersed bitumen globules. In the images obtained, the swollen polymer phase appears light while the bitumen phase appears dark. As depicted in Figs 6.40–6.46, the images show a clear change in morphology of the polypropylene-based polymer-modified bitumen as the polymer content increases. At polymer content below 5.5% by weight of aggregate, small polymer globules that are swollen by the base bitumen-compatible fractions are spread homogeneously in a continuous bitumen phase. At polymer content above 5.5% by weight of aggregate, a continuous polymer phase with a dispersed bitumen phase is observed. In this situation, the properties of the mixture are mainly determined by the polymer phase and therefore by the amount of polypropylene added.



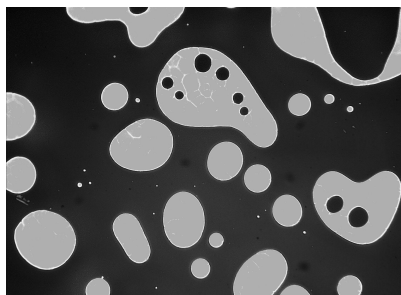
6.40 Concentrations of polypropylene in the base bitumen (0.5% by weight of aggregate).



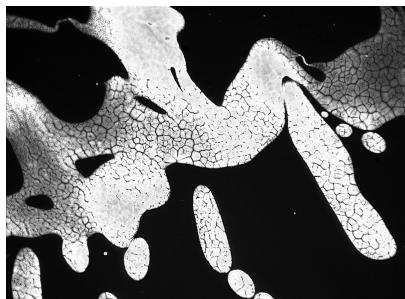
6.41 Concentrations of polypropylene in the base bitumen (1.5% by weight of aggregate).



6.42 Concentrations of polypropylene in the base bitumen (2.5% by weight of aggregate).



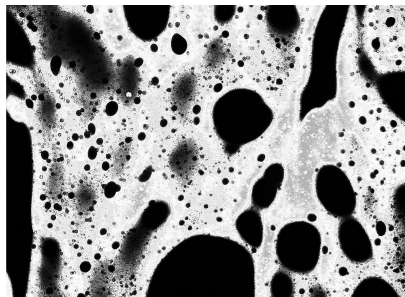
6.43 Concentrations of polypropylene in the base bitumen (3.5% by weight of aggregate).



6.44 Concentrations of polypropylene in the base bitumen (4.5% by weight of aggregate).



6.45 Concentrations of polypropylene in the base bitumen (5.5% by weight of aggregate).



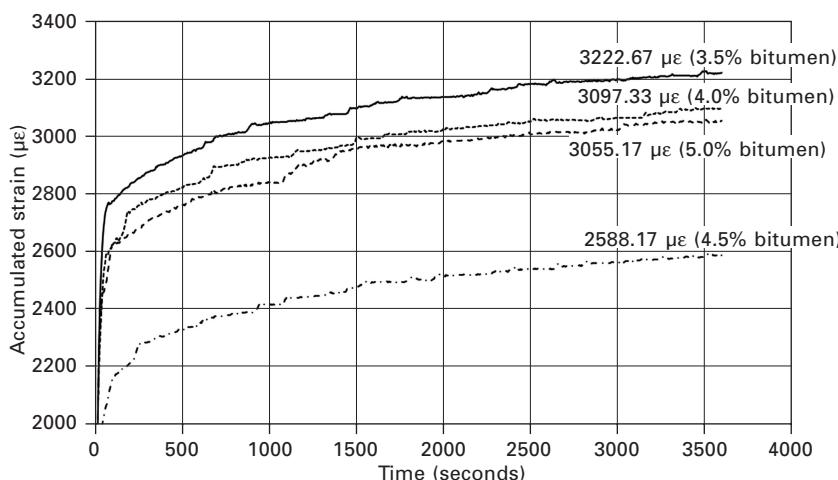
6.46 Concentrations of polypropylene in the base bitumen (6.5% by weight of aggregate).

6.7.1 Economic analysis of polypropylene-modified specimens prepared by utilising different percentages of bitumen

The optimum bitumen content has been determined as 5.38%. This value is only 7.6% more than the optimum bitumen content of the control specimens. While preparing the modified specimens, because of the swelling of polypropylene by different bitumen fractions, more bitumen is needed to prepare the same kind of specimens. Therefore, when preparing specimens for economic analysis, with the optimum bitumen percentage and optimal polypropylene addition amount (5.5%), the bitumen content can be taken as 5.0 wt%. This is a very realistic design approach. To carry out an economic analysis, with the optimum bitumen percentage and optimal polypropylene addition amount (5.5%), new sets of Marshall specimens have been fabricated and again static creep, Marshall stability and flow tests were completed on these specimens. In order to be able to investigate the economic concerns, four different sets of specimens with 3.5%, 4.0%, 4.5% and 5.0% were prepared

(six specimens repeated for each content) and subjected to static creep tests with the same testing regime.

To further understand the variation in the different properties, for the six different curves, the values at each time interval were averaged accordingly and a single set of curves was drawn once more with the final accumulated strains plotted on the corresponding graph (Fig. 6.47). As can be seen from Fig. 6.47, the permanent accumulated strain that is developed in the specimen body is measured as $3055.17\mu\epsilon$ for specimens prepared with 5.0% bitumen content (5.5% polypropylene modification). This value is only 5.20% less than the accumulated strain values of specimens prepared with 3.5% bitumen, 1.36% less than the accumulated strain values of specimens prepared with 4.0% bitumen, and 18% higher than the accumulated strain values of specimens prepared with 4.5% bitumen. In the first instance, it could be concluded that the specimens prepared with 4.5% bitumen behave in a very favourable manner when compared to specimens consisting of 5.0% bitumen. But in this case, the saving is only 10%. Therefore, the specimens with a bitumen content of 3.5% are of interest. These specimens, when viewed with regard to physical properties, have 43% less average air void contents, 2.7% less average specific gravity values, 5.75% less average voids in mineral aggregate values and finally 53% less voids filled with asphalt values (Özcan 2008). But they behave in a very similar fashion under static creep tests when compared to specimens prepared with 5.0% bitumen content. This deserves great attention, since 3.5% specimens are lighter, have more voids and have much less bitumen than 5.0% specimens. This is a significant



6.47 Average accumulated strain versus time graphs for optimum bitumen percentage and optimal polypropylene addition amount (5.5%) for polypropylene-modified specimens.

step in the development of a new generation of paving products. Altogether, there is a saving of 30% in the amount of bitumen used by utilising 3.5% bitumen in the design. Altogether the extra cost of using polypropylene fibers as a modifier is only 9.3% (for research purposes only, with no addition of technology and know-how, of course) but this cost is becoming much less, notwithstanding the dependency on expensive imported modifiers and know-how. This is a very important consideration for developing countries like Turkey.

The physical test results for specimens prepared with optimal polypropylene content for cost saving are given in the relevant literature (Özcan 2008). The physical and mechanical properties of the specimens prepared with 3.5% bitumen content compared with 5.0% bitumen content specimens are as follows: they are lighter, have more air voids and have less asphalt in their structures. Also, the Marshall Quotient (a kind of pseudo-stiffness) values are approximately 17% higher than for the 5.0% bitumen samples. In the light of these facts, it can be concluded that 3.5% bitumen specimens can be utilised in pavement design in a very favourable way.

6.8 Conclusions

To date, significant efforts have been made to investigate the physical and mechanical properties of polypropylene-modified asphalt specimens utilising the Marshall design. In the autumn of 2009, the principal author started to use an IPC Servopac Gyratory compactor in his laboratory to be able to get more insight into the actual compaction simulation in laboratory conditions (IPC 2009). In the 18 months since that time, more than 2000 kg of asphalt have been compacted and tested mechanically and by the UTM-5P, and this extensive testing scheme is continuing with great enthusiasm to resolve some of the unknown problems concerning this subject. In addition, extensive testing is being conducted in the principal author's laboratory to explore the effect of polypropylene modification on bituminous binder by newer testing equipment. In the light of all of the above discussions throughout the chapter and after 12 years of extensive research, he can say in a very determined manner that, using the multifilament 3 mm (M-03) type of polypropylene fibers as a modifier, on both a dry and a wet basis, will solve the distresses occurring at both moderate and high temperatures (such as fatigue cracking and rutting) in a perfect manner with very little extra cost (especially with an unpatented modifier). The total prevention of flushing and bleeding problems with the help of especially a wet-basis modification is another very attractive outcome of this kind of modification, especially for countries subjected to very high ambient temperatures during spring, summer and autumn months. But it has to be borne in mind that the engineers working on site must be aware of the benefits of polypropylene modification and stop persisting in

using 'expensive' modifiers and their accompanying 'sales' techniques. Only in this manner might the superb laboratory investigations about polypropylene fiber-reinforced bitumen will solve the asphalt modification problem for both developing and developed countries that are prone to the above-mentioned pavement problems.

6.9 References

ACI 116R-00 (2000), 'Cement and Concrete Terminology, Reported by ACI Committee 116', American Concrete Institute.

Airey, G.D. (2004), 'Fundamental binder and practical mixture evaluation of polymer modified bituminous materials', *International Journal of Pavement Engineering*, 5(3), 137–151.

Alavi, A.H., Ameri, M., Gandomi, A.H. and Mirzahosseini, M.R. (2011), 'Formulation of flow number of asphalt mixes using a hybrid computational method', *Construction and Building Materials*, 25(3), 1338–1355.

Al-Hadidy, A.I. and Tan, Y.-Q. (2009), 'Mechanistic approach for polypropylene-modified flexible pavements', *Materials and Design*, 30(4), 1133–1140.

Alsugair, A.M. and Al-Qudrah, A.A. (1998), 'Artificial neural network approach for pavement maintenance', *Journal of Computing in Civil Engineering*, 12(4), 249–255.

Asphalt Institute (1994), *Mix Design Methods for Asphalt Concrete and Other Hot-Mix Types*, Manual Series No. 2, Sixth edition, Asphalt Institute, Lexington, KY.

ASTM (1963), 'A guide for fatigue testing and the statistical analysis of fatigue data', ASTM Special Publication 91-A, American Society for Testing and Materials, Philadelphia, PA.

Attoh-Okine, N.O. (2001), 'Grouping pavement condition variables for performance modeling using self-organizing maps', *Computer-Aided Civil and Infrastructure Engineering*, 16(2), 112–125.

Attoh-Okine, N.O. (2005), 'Modeling incremental pavement roughness using functional network', *Canadian Journal of Civil Engineering*, 32(5), 899–905.

Austin, R.A. and Gilchrist, A.J.T. (1996), 'Enhanced performance of asphalt pavements using geocomposites', *Geotextiles and Geomembranes*, 14, 175–186.

Bolk, H.J.N.A. and Van de Loo, P.J. (1979), *The Creep Test: A Routine Method for the Design of Stable Asphalt Mixes*, Koninklijke/Shell-Laboratories, Amsterdam.

Bonnaire, F., Gravois, A. and Udrone, J. (1980), 'A new method for predicting the fatigue life of bituminous mixes', *Journal of the Association of Asphalt Paving Technologists*, 49, 499–524.

Bosurgi, G. and Trifiro, F. (2005), 'A model based on artificial neural networks and genetic algorithms for pavement maintenance management', *International Journal of Pavement Engineering*, 6(3), 201–209.

Brown, S.F., Rowlett, R.D. and Boucher, J.L. (1990), 'Asphalt modification', *Proceedings of the Conference on US SHRP Highway Research Program: Sharing the Benefits*, ICE, 181–203.

Brule, B. (1996), 'Polymer-modified asphalt cements used in the road construction industry: basic principles', *Transport Research Record*, 1535 (National Research Council, Washington, DC), 48–53.

Cal, Y. (1995), 'Soil classification by neural network', *Advances in Engineering Software*, 22, 95–97.

Çevik, A. (2006), 'A new approach for elastoplastic analysis of structures: neural networks', PhD thesis, Mechanical Engineering Department, University of Gaziantep, Gaziantep, Turkey.

Chen, J. and Lin, K. (2005), 'Mechanism and behavior of bitumen strength reinforcement using fibers', *Journal of Materials Science*, 40(1), 87–95.

Cleven, M.A. (2000), 'Investigation of the properties of carbon fiber modified asphalt mixtures', MS thesis in Civil Engineering, Michigan Technological University, Houghton, MI.

Collins, J.H., Bouldin, M.G., Gelles, R. and Berker, A. (1991), 'Improved performance of paving asphalts by polymer modification', *Journal of the Association of Asphalt Paving Technologists*, 60, 43–79.

De Hilster, E. and Van de Loo, P.J. (1977), *Influence of Test Parameters*, Koninklijke/Shell-Laboratories, Amsterdam.

Eldin, N.N. and Senouci, A.B. (1995), 'A pavement condition rating model using backpropagation neural network', *Microcomputers in Civil Engineering*, 10(6), 433–441.

ELE-UMATTA (1994), 'Universal materials testing apparatus for asphalt and unbound specimens', reference and operating manual, ELE International Ltd, Hemel Hempstead, Hertfordshire, UK.

Feeley, A.J. (1994), 'UTM-5P, Universal testing machine, hardware reference manual', Industrial Process Controls Ltd, Boronia, Australia.

Gagarin, N., Flood, I. and Albrecht, P. (1994), 'Computing truck attributes with artificial neural networks', *Journal of Computing in Civil Engineering*, ASCE, 8(2), 179–200.

General Directorate of Highways of Turkey (2000), 'Highway technical specifications, Item No. 170/2', General Directorate of Highways of Turkey, Ankara, Turkey.

General Directorate of Highways of Turkey (2006), 'Highway technical specifications', General Directorate of Highways of Turkey, Ankara, Turkey.

Ghaly, N.F. (2008), 'Combined effect of polypropylene and styrene-butadiene styrene on asphalt, and asphalt mixture performance', *Journal of Applied Sciences Research*, 4(11), 1297–1304.

Goodrich, J.L. (1991), 'Asphaltic binder rheology, asphalt concrete rheology and asphalt concrete mix properties', *Journal of the Association of Asphalt Paving Technologists*, 60, 80–120.

Hejazi, S.M., Abtahi, S.M., Sheikhzadeh, M. and Semnani, D. (2008), 'Introducing two simple models for predicting fiber reinforced asphalt concrete (FRAC) behavior during longitudinal loads', *Journal of Applied Polymer Science*, 109(5), 2872–2881.

Hills, J.F. (1973), 'The Creep of asphalt concrete mixes', *Journal of the Institute of Petroleum*, 59, 247.

Hills, J.F., Brien, D. and Van de Loo, P.J. (1974), 'The correlation of rutting and creep tests on asphalt mixes', *Journal of the Institute of Petroleum*, Paper IP 74–001.

Hofstra, A. and Klomp, A.J.G. (1972), 'Permanent deformation of flexible pavements under simulated road traffic conditions', *Third International Conference on the Structural Design of Asphalt Pavements*, University of Michigan, Volume I.

Hongu, T. and Phillips, G.O. (1997), *New Fibers*, Woodhead Publishing, Cambridge, UK.

Huang, H. and White, T.D. (1996), 'Dynamic properties of fiber-modified overlay mixture', *Transportation Research Record*, 1545, 98–104.

IPC (2009), 'IPC Servopac Gyratory Compactor', IPC Global, Boronia, Australia.

Isacsson, U. and Lu, X. (1995), 'Testing and appraisal of polymer modified road bitumens – state of the art', *Materiaux et Constructions*, 28(177), 139–159.

Jenq, Y.S., Chwen-Jang, L. and Pei, L. (1993), 'Analysis of crack resistance of asphalt concrete overlays. A fracture mechanics approach', *Transportation Research Record*, 1388, 160–166.

Kaseko, M.S. and Ritchie, S.G. (1993), 'A neural network based methodology for pavement crack detection', *Transportation Research Record, Part C*, 1C, 275–291.

Kim, Y. and Kim, Y.R. (1998), 'Prediction of layer moduli from FWD and surface wave measurements using artificial neural network', presented at Transportation Research Board, 77th Annual Meeting, Washington, DC.

King, G.N., King, H.W., Chaverot, P., Planche, J.P. and Harders, O. (1993), 'Using European wheel-tracking and restrained tensile tests to validate SHRP performance-graded binder specifications for polymer modified asphalts', *Proceedings of the 5th Eurobitume Congress*, Stockholm, vol. 1A (1.06), 51–55.

Lee, B.J. and Lee, H.D. (2004), 'Position-invariant neural network for digital pavement crack analysis', *Computer-Aided Civil and Infrastructure Engineering*, 19(2), 105–118.

Lee, S.J., Rust, J.P., Hamouda, H., Kim, Y.R. and Borden, R.H. (2005), 'Fatigue cracking resistance of fiber-reinforced asphalt concrete', *Textile Research Journal*, 75(2), 123–128.

Maurer, D.A. and Malasheskie, G. (1989), 'Field performance of fabrics and fibers to retard reflective cracking', *Transportation Research Record*, 1248, 13–23.

Mei, X., Gunaratne, M., Lu, J.J. and Dietrich, B. (2004), 'Neural network for rapid evaluation of shallow cracks in asphalt pavements', *Computer-Aided Civil and Infrastructure Engineering*, 19(3), 223–230.

Mirzahosseini, M.R., Aghaeifar, A., Alavi, A.H., Gandomi, A.H. and Seyednour, R. (2011), 'Permanent deformation analysis of asphalt mixtures using soft computing techniques', *Expert Systems with Applications*, 38(5), 6081–6100.

Ohio Department of Transportation (1998), 'Item 400HS, Standard specification for asphalt concrete – high stress using polypropylene fibers', Construction and Materials Specifications, Ohio Department of Transportation, Columbus, OH.

Othman, A.M. (2010), 'Impact of polypropylene application method on long term ageing of polypropylene modified HMA', *Journal of Materials in Civil Engineering*, 22(10), 1012–1018.

Owusu-Ababia, S. (1998), 'Effect of neural network topology on flexible pavement cracking prediction', *Computer-Aided Civil and Infrastructure Engineering*, 13(5), 349–355.

Özcan, S. (2008), 'The investigation of the effect of polypropylene fiber addition to the static creep behavior of bituminous mixtures', MS thesis, Anadolu University, Civil Engineering Department, Eskişehir, Turkey (in Turkish).

Prowell, B.D. (2000), 'Design, construction, and early performance of hot-mix asphalt stabilizer and modifier test sections', Interim Report (VTRC 00-IR2), Virginia Transportation Research Council, Charlottesville, VA.

Razaqpur, A.G., Abd El Halim, A.O. and Mohamed, H.A. (1996), 'Bridge management by dynamic programming and neural networks', *Canadian Journal of Civil Engineering*, 23, 1064–1069.

Ritchie, S.G., Kaseko, M. and Bavarian, B. (1991), 'Development of an intelligent system for automated pavement evaluation', *Transportation Research Record*, 1311, 112–119.

Roberts, C.A. and Attoh-Okine, N.O. (1998), 'A comparative analysis of two artificial

neural networks using pavement performance prediction', *Computer-Aided Civil and Infrastructure Engineering*, 13(5), 339–348.

Roberts F.L., Kandhal, P.S. and Brown, E.R. (1996), *Hot Mix Asphalt Materials, Mixture Design and Construction*, NAPA Education Foundation, Lanham, MD.

Romualdi, J.P. and Batson, G.B. (1963), 'Mechanics of crack arrest in concrete', *Proc. ASCE*, 89 EM3, 147–168.

Romualdi, J.P. and Mandel, J.A. (1964), 'Tensile strength of concrete affected by uniformly distributed closely spaced short lengths of wire reinforcement', *ACI J. Proc.*, 61(6), 657–671.

Shekharan, A. R. (1998), 'Effect of noisy data on pavement performance prediction by artificial neural networks', presented at Transportation Research Board, 77th Annual Meeting, Washington, DC.

Simpson, A.L. & Kamyar C. M. (1994), 'Case study of modified bituminous mixtures', *Proceedings of the Third Materials Engineering Conference*, ASCE, Somerset, KY, 88–96.

Song, P.S., Hwang, S. and Sheu, B.C. (2005), 'Strength properties of nylon and polypropylene-fiber-reinforced concretes', *Cement and Concrete Research*, 35(8), 1546–1550.

Tapkin, S. (1998), 'Improved asphalt aggregate mix properties by portland cement modification', MSc thesis, Middle East Technical University, Civil Engineering Department, Ankara, Turkey.

Tapkin, S. (2004), 'A recommended neural trip distribution model', PhD thesis, Middle East Technical University, Civil Engineering Department, Ankara, Turkey.

Tapkin, S. (2008a), 'The effect of polypropylene fibers on asphalt performance', *Building and Environment*, 43(6), 1065–1071.

Tapkin, S. (2008b), 'Mechanical evaluation of asphalt–aggregate mixtures prepared with fly ash as a filler replacement', *Canadian Journal of Civil Engineering*, 35(1), 27–40.

Tapkin, S., Uşar, Ü., Tuncan, A., and Tuncan, M. (2009a), 'Repeated creep behavior of polypropylene fiber-reinforced bituminous mixtures', *Journal of Transportation Engineering*, 135(4), 240–249.

Tapkin, S., Çevik, A. and Uşar, Ü. (2009b), 'Accumulated strain prediction of polypropylene modified marshall specimens in repeated creep test using artificial neural networks', *Expert Systems with Applications*, 36(8), 11186–11197.

Tapkin, S., Çevik, A. and Uşar, Ü. (2010), 'Prediction of Marshall test results for polypropylene modified dense bituminous mixtures using neural networks', *Expert Systems with Applications*, 37(6), 4660–4670.

Uge, P. and Van de Loo, P.J. (1974), *Permanent Deformation of Asphalt Mixes*, Canadian Technical Asphalt Association, Volume 19.

Uşar, Ü. (2007), 'Investigation of rheological behaviours of dense bituminous mixtures with polypropylene fiber in repeated creep test', MSc thesis, Anadolu University, Eskişehir, Turkey (in Turkish).

Van de Loo, P.J. (1974), *Creep Testing, A Simple Tool to Judge Asphalt Mix Stability*, Association of Asphalt Paving Technologists, Volume 43.

Van de Loo, P.J. (1976), 'Practical approach to the prediction of rutting in asphalt pavements: the shell method', *Transportation Research Record*, 616, 15–21.

Van de Loo, P.J. and De Hilster, E. (1978), *Creep Data of Samples Cored from Pavements*, Shell International Petroleum Co. Ltd, London.

Wallace, K., and Monismith, C.L. (1980), 'Diametral modulus testing on nonlinear pavement materials', *Proceedings of the Association of Asphalt Paving Technologists*, 49, 633–652.

Whiteoak, D. (1990), *The Shell Bitumen Handbook*, Shell Bitumen UK, Chertsey, Surrey.

Wu, S.-P. (2006), 'Effect of fiber types on relevant properties of porous asphalt', *Transactions of Nonferrous Metals Society of China*, 16, 791.

Xue, Y, Hou, H., Zhu, S., and Zha, J. (2009), 'Utilization of municipal solid waste incineration ash in stone mastic asphalt mixture: Pavement performance and environmental impact', *Construction and Building Materials*, 23(2), 989–996.

Yi, J. and McDaniel, S. (1993), 'Application of cracking and seating and use of fibers to control reflection cracking', *Transportation Research Record*, 1388, 150–159.

Zeghal, M. (2008), 'Modeling the creep compliance of asphalt concrete using the artificial neural network technique', *Geotechnical Special Publication, Proceedings of Sessions of GeoCongress 2008 – GeoCongress 2008: Characterization, Monitoring, and Modeling of GeoSystems, GSP 179*, 910–916.

Zhang, S.L., Zhang, Z.X., Xin, Z.X., Pal, K. and Kim, J.K. (2010a), 'Prediction of mechanical properties of polypropylene/waste ground rubber tire powder treated by bitumen composites via uniform design and artificial neural networks', *Materials and Design*, 31(4), 1900–1905.

Zhang, S.L., Zhang, Z.X., Pal, K., Xin, Z.X., Suh, J. and Kim, J.K. (2010b), 'Prediction of mechanical properties of waste polypropylene/waste ground rubber tire powder blends using artificial neural networks', *Materials and Design*, 31(8), 3624–3629.

Zhou, L., Li, P., Zhang, Z. and Chen, H. (2008), 'Analysis of effect of fiber on high temperature performance of asphalt mixture', *Journal of Wuhan University of Technology*, 30(11), 58–61.

Zhou, L., Li, P. and Zhang, Z. (2009), 'Investigation of high temperature properties of asphalt mixture containing fibers', *Material Design, Construction, Maintenance, and Testing of Pavements: Selected Papers from the 2009 GeoHunan International Conference (Geotechnical Special Publication 193)*, ASCE, 139–144.

Zollo, R.F. (1997), 'Fiber-reinforced concrete: an overview after 30 years of development', *Cement and Concrete Composites*, 19(2), 107–122.

Zurich (1977), 'Recommendation for the performance of unconfined static creep test in asphalt specimens' *Proceedings of the International Symposium on Plastic Deformability of Bituminous Mixes*, Zurich, 335–359.

Rheology of polymer-modified bitumens

C. GALLEGOS and M. GARCÍA-MORALES,
Universidad de Huelva, Spain

Abstract: Since 1987, when the Strategic Highway Research Program (SHRP) arose, rheometry has rapidly gained acceptance as a powerful technique for measuring mechanical properties of bitumen, which can be directly related to in-service performance. Neat bitumen and polymer-modified bitumen rheology is highly dependent on temperature. Thus, these binders should have low viscosity when handled and mixed with mineral aggregates at high temperatures. At intermediate temperature, binder linear viscoelastic behaviour is related to its resistance to traffic loading. Finally, at or below the glass transition temperature, thermal cracking is likely to occur under certain loading conditions. In this regard, this chapter first presents detailed information on general rheology and its application to the study of polymer-modified bitumen, which readers might find of great interest for the understanding of some other chapters in this book. In addition, two illustrative case studies are also envisaged. On the one hand, the rheological characterisation, and modelling, of bitumen modified by different elastomers and plastomers is described. On the other hand, the rheological behaviour of synthetic binders, mixtures of oil, resin and polymer with similar characteristics to bitumen but easily pigmented, is reviewed.

Key words: polymer, modified bitumen, binder, rheology, viscoelasticity.

7.1 Introduction

‘Rheology’, a term invented by Professor Eugene Bingham of Lafayette College in Easton (Pennsylvania, USA), is defined as ‘the study of the deformation and flow of matter’ (Walters, 2010).

Nowadays, it is well accepted that a given material can behave as a solid or a liquid depending on the time scale of the deformation process (Gallegos and Walters, 2010). In other words, the mechanical properties of all materials are time-dependent, i.e., they vary with time in response to an applied load or deformation. This phenomenon is simply a consequence of the Second Law of Thermodynamics, according to which a portion of the imparted energy of deformation is always dissipated as heat by viscous forces even while the rest may be stored elastically. The dissipation is neither instantaneous nor infinitely slow and is therefore a rate process. It is this that renders the physical properties time-dependent (Emri, 2010). Material rheological

behaviour goes from virtually purely elastic (no dissipation) to virtually purely viscous (instantaneous dissipation), or shows both elastic and viscous properties in-between. The behaviour of many materials, such as polymer-modified bitumen, typically falls between the extremes and they are defined as viscoelastic (at least in a wide temperature range). The behaviour may be expressed suitably by the Deborah number, De , the ratio of the characteristic time of the material, λ , on which molecular rearrangements take place, and the characteristic time of the deformation process, T (Reiner, 1964):

$$De = \frac{\lambda}{T} \quad 7.1$$

High Deborah numbers correspond to solid-like behaviour and low Deborah numbers to liquid-like behaviour. A material can appear solid-like either because it is, i.e. it has an infinite characteristic time, or because the deformation process that is in use is very fast. One obvious consequence of this is that even mobile liquid systems with very low characteristic times can behave like elastic solids when exposed to a very fast deformation process (viscoelastic liquids). On the contrary, solid-like materials will be able to flow for a time (viscoelastic solids).

It is generally assumed that bitumen is a complex colloidal system in which the asphaltenes are dispersed into a matrix of the remaining components, the maltenes (Lesueur *et al.*, 1996; Lesueur, 2009). The relationship between the complex colloidal structure of bitumen and its thermo-mechanical properties has been a subject of scientific and technical interest, due to the fact that bitumen has been widely used for road paving applications (Martín-Alfonso *et al.*, 2008b; Carrera *et al.*, 2009, 2010a, 2010b, 2010c). Although it is added in a very low concentration (5 wt%), bitumen controls the final properties and the performance of the asphalt mixture, since it is the only deformable component and forms a continuous matrix (Lewandowski, 1993; Adedeji *et al.*, 1996; Dongré *et al.*, 1996). From a material engineering point of view, bitumen can be classified as thermoplastic materials with thermally reversible properties (Carreau *et al.*, 2000). Thus, at high temperature, bitumen melts and can be easily pumped and mixed with stones. At ambient temperature, bitumen solidifies so that asphalt mixtures can sustain the stresses due to traffic.

Two main limitations, yielding poor road performance, observed in pavements are directly associated to the bitumen matrix that surrounds the mineral aggregates at high and low temperatures. The first problem, permanent deformation (rutting), occurs at service temperatures higher than 40°C, leading to channels in the direction of travel, and can be related to the viscosity of the bitumen matrix. The second appears at low temperatures (below 0°C) and can produce cracking of the road pavement, as a result of brittle fracture of the bituminous component of the asphalt (Adedeji *et al.*, 1996; Dongré *et al.*, 1996; Navarro *et al.*, 2002).

There has been a major interest in relating road low performance to the rheological behaviour of bitumen at different temperatures (King *et al.*, 1992). As reported by Dongré *et al.* (1996), bitumen shows a predominantly solid-like (glassy) behaviour at temperatures below the bitumen glass transition temperature T_g (temperature at which thermal cracking occurs). At sufficiently high temperatures, bitumen shows Newtonian behaviour (typically at $T_g + 100^\circ\text{C}$, the temperature at which bitumen is handled and mixed with mineral aggregates). In the intermediate temperature range (the behaviour in this region defines binder resistance to rutting), bitumen shows linear viscoelastic behaviour at small deformations, and non-linear viscoelastic behaviour (non-Newtonian viscous flow) at sufficiently large deformation rates.

As a consequence of the Strategic Highway Research Program (SHRP) carried out in the USA (Anderson and Kennedy, 1993; Anderson *et al.*, 1994), a set of performance-related specifications were developed for bitumen binders, where rheology plays a crucial role. Thus, different rheological tests, and rheometers, should be used to carry out a wide binder rheological characterisation aiming to set the above-mentioned binder performance-related specifications. Thus, rotational viscometry (to measure bitumen Newtonian viscosity at high temperature), small-amplitude oscillatory shear (to characterise bitumen linear viscoelastic properties at intermediate temperatures), flexural creep tests in the linear viscoelastic region at low temperatures, and uniaxial tension tests at low temperatures have been proposed.

Presently, tightening of binder specifications, in order to get longer repairing periods and reduce the total cost of road maintenance, and factors such as the increased traffic, heavier loads, etc., have forced the industry to develop new bituminous materials, for instance by adding different polymers. Polymers are usually used in a concentration range between 3% and 7% by weight for road applications (Polacco *et al.*, 2006a). The purpose of bitumen modification is to achieve the desired engineering properties to protect asphalt from the main pavement defects. In this sense, many authors have described the beneficial effects of polymer modification of binders, at high and low temperatures, so that polymer-modified asphalts increase the resistance of the bitumen to traffic loading, reducing permanent deformation at high temperature and thermal cracking at low temperature (Hesp and Woodhams, 1991; Ait-Kadi *et al.*, 1996; Lesueur *et al.*, 1998; González *et al.*, 2002).

A wide spectrum of polymers can significantly modify the properties of bitumens (Fawcett *et al.*, 1999; Fawcett and McNally, 2000; Pérez-Lepe *et al.*, 2003; 2005, 2006; Becker *et al.*, 2003; García-Morales *et al.*, 2004a, 2004b, 2006, 2007; Navarro *et al.*, 2002, 2005a, 2007a, 2007b, 2009, 2010; Vlachovicova *et al.*, 2005; Polacco *et al.*, 2006a, 2006b; Martín-Alfonso *et al.*, 2008a, 2008b). Among them, it is worth mentioning:

- Natural or synthetic rubbers (elastomers)

- Thermoplastic block copolymers, such as styrene–butadiene copolymers
- Ethylene–vinylacetate copolymers (EVA)
- Polyolefins, such as polyethylenes (PE) and polypropylenes (PP), also known as plastomers
- Reactive polymers.

Polymer-modified bitumen is a multiphase system. Usually, such bitumens contain a polymer-rich phase, an asphaltene-rich phase and a maltene-rich phase (Stastna *et al.*, 2003). The mechanical properties of polymer-modified bitumen depend on the nature and concentration of the polymer used.

7.2 Rheological characterisation of polymer-modified bitumen at in-service temperatures

7.2.1 Linear viscoelastic behaviour

As stated above, at temperatures above the bitumen glass transition temperature, bituminous binders are considered to behave as viscoelastic materials in a wide temperature range.

Viscoelastic materials possess both viscous and elastic properties in varying degrees. For a viscoelastic material, internal stresses depend not only on the instantaneous deformation, but also on the whole past history of deformation. When a material is deformed, thermodynamic forces immediately begin to operate to restore the minimum-energy state. Movement from the rest state represents storage of energy. If a material is submitted to deformations or stresses small enough so that its rheological functions do not depend on the value of the deformation or stress, the material response is said to be in the linear viscoelasticity range (Gallegos and Martínez-Boza, 2010).

Consider the function $\gamma(t)$ as representative of some action (shear strain) on a given material, and the shear stress, $\sigma(t)$, as the effect resulting from this action (Dealy and Wissbrun, 1995). A variation in shear strain occurring at time t_1 will produce a corresponding effect at some time later, t , which can be expressed as:

$$\sigma(t) = G(t - t_1) \delta\gamma(t_1) \quad 7.2$$

$G(t - t_1)$ is known as the relaxation function, or relaxation modulus, which is a property of the material and relates cause and effect. It is a function of the time delay between cause and effect.

A series of N changes in shear strain, each occurring at a different time, will all contribute cumulatively to the stress at some later time (Boltzmann superposition principle). Thus:

$$\sigma(t) = \sum_{i=1}^N G(t - t_i) \delta\gamma(t_i) \quad 7.3$$

If the change in strain occurs continuously, the sum may be replaced by an integral:

$$\sigma(t) = \int_{-\infty}^t G(t-t')\delta\gamma(t') \quad 7.4$$

This linear constitutive equation is appropriate to describe the behaviour of materials submitted to shear deformations, which is the most relevant type of deformation concerning bitumen in-service performance.

However, this equation can be generalised for any type of deformation that can be applied on the material. Thus, if the shear strain is replaced by the strain tensor, and the shear stress by the stress tensor, different forms of the Boltzmann superposition principle are obtained:

$$\sigma_{ij}(t) = \int_{-\infty}^t G(t-t')\delta\gamma(t') \quad 7.5$$

or

$$\sigma_{ij}(t) = \int_{-\infty}^t G(t-t')\gamma_{ij}(t')dt' \quad 7.6$$

In order to gain information on the influence function that relates cause and effect, a number of small strain experiments are used in rheology. Some of the more common techniques are stress relaxation, creep, and sinusoidal oscillations (Ferry, 1980; Macosko, 1994; Dealy and Wissbrun, 1995; Barnes, 2000). Different experimental methods are used because they may be more convenient for a particular material or because they provide data over a particular time range.

Stress relaxation

Stress relaxation after a step strain is the fundamental way in which the relaxation modulus is defined. In this experiment, a sample is suddenly deformed at a given strain, γ_0 , and the resulting stress is measured as a function of time. The relaxing stress data can be used to determine $G(t)$:

$$G(t) = \frac{\sigma(t)}{\gamma_0} \quad 7.7$$

Knowledge of the evolution of the linear relaxation modulus with time is essential to model the non-linear viscoelastic behaviour of polymer-modified bitumen, as stated by Polacco *et al.* (2006a).

Creep

Creep experiments are particularly useful for studying certain practical applications where long times are involved. In a creep experiment, a constant

stress, σ_0 , is instantaneously applied on a sample, and the resulting strain is recorded versus time. The strain values obtained as a function of time can be used to calculate the compliance, $J(t)$, as follows:

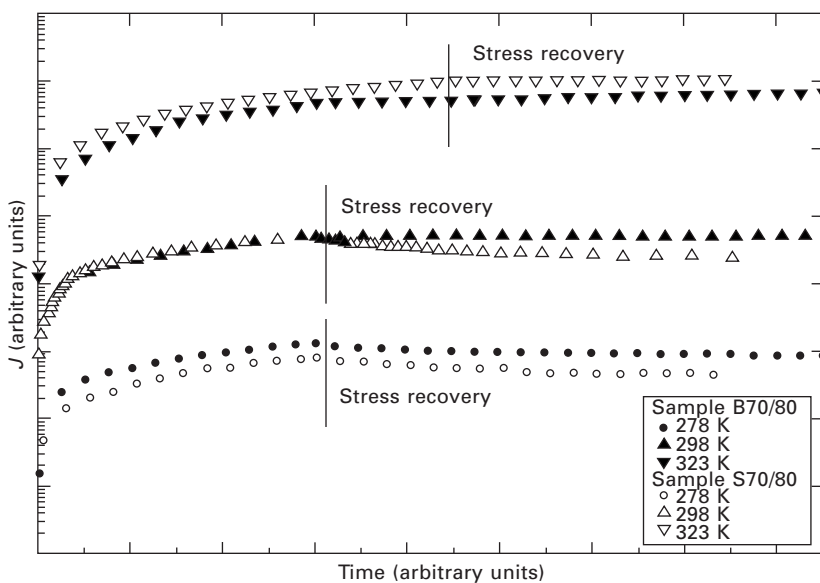
$$J(t) = \frac{\gamma(t)}{\sigma_0} \quad 7.8$$

This creep compliance function is independent of the shear stress applied in the linear viscoelasticity range.

Different authors have characterised the linear viscoelastic behaviour of polymer-modified bitumen by performing creep and recovery tests (Carreau *et al.*, 2000; Partal *et al.*, 1999). For instance, Fig. 7.1 shows typical semi-log curves of the evolution of the creep compliance with time for an unmodified bitumen and a synthetic binder. As can be observed, when a constant stress is applied on a sample, there is an instantaneous rise in compliance, after which $J(t)$ slowly rises with time until the stress applied on the sample is removed.

Small amplitude oscillatory shear

The most common type of test to characterise the linear viscoelastic behaviour of bitumen and polymer-modified bitumen is the small amplitude oscillatory shear (SAOS).



7.1 Linear creep and recovery compliance data versus time, for unmodified bitumen (B70/80) and a synthetic binder (S70/80), at different temperatures. Adapted from Partal *et al.* (1999).

In a similar way to performing relaxation or creep tests over a range of time, oscillatory tests over a range of frequency can be carried out. It is obvious that short times correspond to high frequencies, and long times to low frequencies.

In this test, the material is submitted to a simple shearing deformation, by applying a sine-wave-shaped input of stress or strain (Macosko, 1994; Dealy and Wissbrun, 1995; Barnes, 2000). If a sinusoidal strain is applied, the shear strain as a function of time would be given by:

$$\gamma(t) = \gamma_0 \sin(\omega t) \quad 7.9$$

where γ_0 is the strain amplitude and ω is the frequency.

By differentiating, the evolution of shear rate with time is given by:

$$\dot{\gamma}(t) = \gamma_0 \omega \cos(\omega t) = \gamma_0 \cos(\omega t) \quad 7.10$$

where γ_0 is the shear rate amplitude.

The resulting stress is measured as a function of time:

$$\sigma(t) = \sigma_0 \sin(\omega t + \delta) \quad 7.11$$

where σ_0 is the stress amplitude and δ is a phase shift, also known as loss angle. The amplitude ratio, G_d , defined from the ratio between σ_0 and γ_0 , and the loss angle, δ , are functions of frequency, although they are independent of strain amplitude in the linear viscoelasticity range. However, they do not have a direct relationship with the material functions traditionally used to characterise the linear viscoelasticity behaviour of a given material.

For this reason, the stress data can also be analysed by decomposing the stress wave into two waves of the same frequency, one in phase with the strain wave ($\sin \omega t$) and the other 90° out of phase with this wave ($\cos \omega t$):

$$\sigma = \sigma' + \sigma'' = \sigma' \sin \omega t + \sigma'' \cos \omega t \quad 7.12$$

Two dynamic moduli can be defined:

$$G' = \frac{\sigma_0'}{\gamma_0} \quad 7.13$$

(elastic, storage, or in-phase modulus) and

$$G'' = \frac{\sigma_0''}{\gamma_0} \quad 7.14$$

(viscous, loss, or out-of-phase modulus). Also, the loss tangent is given by

$$\tan \delta = \frac{G''}{G'} \quad 7.15$$

In addition, a complex modulus, G^* , can be defined as:

$$\sigma_0 = |G^*| \gamma_0 \quad 7.16$$

where G' and G'' are its real and imaginary parts, respectively:

$$G^*(\omega) = G'(\omega) + iG''(\omega) \quad 7.17$$

For a purely elastic material, there is no viscous dissipation and no phase shift, and the loss modulus is zero. On the contrary, there is no energy storage for a purely viscous liquid, as the storage modulus is zero and the loss angle is 90° .

In fact, G'' is a measure of the energy dissipated per cycle of deformation per unit volume:

$$E_d = \int_0^{2\pi/\omega} \sigma \gamma dt = \pi G'' \gamma_0^2 \quad 7.18$$

Another way to interpret the results obtained from small amplitude oscillatory shear tests is in terms of a sinusoidal strain rate. Two new material functions are then defined:

$$\sigma(t) = \gamma_0 [\eta'(\omega) \cos(\omega t) + \eta''(\omega) \sin(\omega t)] \quad 7.19$$

where:

$$\eta' = \frac{\sigma_0''}{\dot{\gamma}_0} = \frac{\sigma_0}{\dot{\gamma}_0} \sin \delta = \frac{G''}{\omega} \quad 7.20$$

and

$$\eta'' = \frac{\sigma_0'}{\dot{\gamma}_0} = \frac{\sigma_0}{\dot{\gamma}_0} \cos \delta = \frac{G'}{\omega} \quad 7.21$$

The complex viscosity is:

$$\eta^*(\omega) = \eta'(\omega) - i\eta''(\omega) \quad 7.22$$

and its magnitude:

$$|\eta^*| = \frac{\sigma_0}{\dot{\gamma}_0} \sqrt{(\eta')^2 + (\eta'')^2} \quad 7.23$$

The reciprocal of the complex modulus is also defined as an additional oscillatory material function, the complex compliance, J^* :

$$J^*(\omega) = \frac{1}{G^*(\omega)} = J'(\omega) + iJ''(\omega) \quad 7.24$$

where the real and imaginary components of the complex compliance are related to those of the complex modulus by:

$$J'(\omega) = \frac{G'(\omega)}{G'^2(\omega) + G''^2(\omega)} \quad 7.25$$

$$J''(\omega) = -\frac{G''(\omega)}{G'^2(\omega) + G''^2(\omega)} \quad 7.26$$

Time-temperature superposition principle (TTSP)

Without any doubt, the most important aspect of the rheological properties of unmodified and polymer modified bitumen is their dependence on temperature. For example, the sensitivity to temperature of the storage modulus, G' , can be described by what is known as the elastic thermal susceptibility (Carreau *et al.*, 2000):

$$G'_T = \frac{G'(30^\circ\text{C}, 10 \text{ Hz})}{G'(60^\circ\text{C}, 10 \text{ Hz})} \quad 7.27$$

However, most efforts have been dedicated to applying the time-temperature superposition principle to bituminous binders.

The time-temperature superposition principle states that the effect of increasing the loading time (or decreasing the frequency) on the mechanical properties of a material is equivalent to that of raising the temperature. Bitumen thermo-rheological simplicity (in other words, suitability of an empirical time-temperature superposition method for obtaining a master curve of bitumen mechanical spectra measured at different temperatures), reported by different authors, has become quite controversial (Lesueur *et al.*, 1996; Stastna and Zanzotto, 1999a, 1999b; Zanzotto *et al.*, 2000). In this sense, Lesueur (2009) proposes that, in some cases, the elastic (G'') and loss (G') moduli appear to be superimposable, but the phase angle (or loss tangent) shows some scattering at low frequencies. Thus, so-called Black diagrams seem to be a useful method to study the applicability of the time-temperature superposition principle (Becker *et al.*, 2003). When plotting the phase angle against G^* , the effect of shifting the curves along the frequency axis is eliminated, and temperature-independent curves can be obtained when the material holds the TTSP.

It has been reported that high asphaltene content asphalts do not conform to the TTSP, as a consequence of the temperature dependence of bitumen microstructure (Polacco *et al.*, 2006a). Thus, the non-applicability of the TTSP to bitumen is limited to high temperatures (above room temperature) because, at lower temperatures, the glass transition slows down structural changes and no more evolutions are observed in the time scale in which rheological tests are performed (Lesueur, 2009).

However, many researchers sustain that the mechanical spectrum of many modified bituminous products can be represented reasonably well by master curves of their linear viscoelastic material functions, G' and G'' (Stastna and Zanzotto, 1999a; Partal *et al.*, 1999; Zanzotto *et al.*, 2000; Anderson *et al.*,

1994), providing useful information about the effects studied (Yousefi *et al.*, 2000; Yousefi, 2003).

On the above-mentioned basis, the linear viscoelastic functions obtained at different temperatures can be empirically superposed onto master curves at a reference temperature (Partal *et al.*, 1999; Navarro *et al.*, 2007b). Accordingly, master curves of the storage (G') and loss (G'') moduli using an empirical shift-factor, a_T , which multiplies frequency, $\omega_T \cdot \omega$, may be obtained:

$$a_T = \frac{\omega_T}{\omega_{T_0}} \quad 7.28$$

where the correction for density changes is negligible.

Different equations may be used to describe the temperature dependence of the shift factors, a_T , used to obtain the superposed master curves:

- Arrhenius' equation:

$$a_T = \exp\left[\frac{E_a}{R} \left(\frac{1}{T} - \frac{1}{T_0}\right)\right] \quad 7.29$$

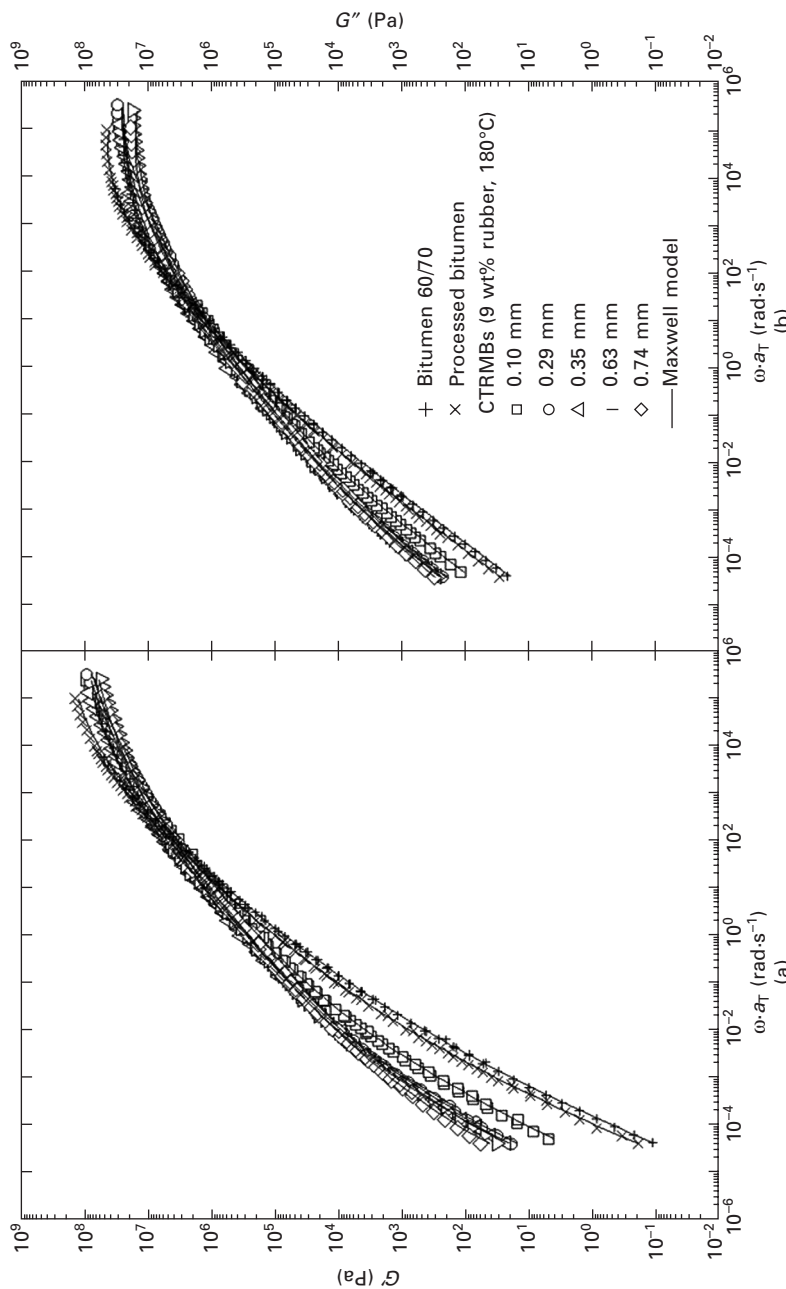
where T_0 is the reference temperature, and E_a is the activation energy, related to binder thermal susceptibility (Partal *et al.*, 1999; Ait-Kadi *et al.*, 1996).

- Williams–Landel–Ferry's equation. This model correlates bitumen viscosity as a function of the temperature and two characteristic constants:

$$\log a_T = \frac{-C_1(T - T_0)}{C_2 + (T - T_0)} \quad 7.30$$

where T_0 is the temperature of reference, and C_1 and C_2 are material constants (Carreau *et al.*, 2000).

It is well known that three different regions appear in the mechanical spectrum (master curves) of unmodified bitumen. Thus, the transition to the glassy region is mainly observed at high frequencies, whose onset is associated with the maximum in the G'' curves. At low frequencies, modified bituminous binders present values of G'' much higher than G' , and slopes close to 1 and 2 respectively, characteristic of the terminal or flow region of the mechanical spectrum. At intermediate frequencies, a crossover between both linear viscoelasticity functions occurs. In the case of modified bitumen, these three regions are usually still present (Dongré *et al.*, 1996). However, the overall qualitative behaviour clearly depends on the type of polymer used. Thus, as can be seen in Fig. 7.2, where master curves of the linear viscoelasticity functions are presented for crumb tyre rubber-modified bitumen, the qualitative evolution of the linear viscoelasticity



7.2 SAOS master curves ((a) for G' , (b) for G'') of the elastic and viscous moduli curves for unmodified bitumens and CTRMBs (reference temperature of 25°C). Adapted from Navarro *et al.* (2004).

functions with frequency does not significantly change (up to 9 wt% crumb tyre rubber concentration). Similar results have been obtained for bitumen 60/70 modified with 3 wt% SBS (Martínez-Boza *et al.*, 2001a). On the other hand, Polacco *et al.* (2006a) reported major differences in the shape of SAOS master curves in the intermediate frequency region for a radial SBS-modified bitumen. According to these authors, the loss tangent shows a non-monotone evolution, usually found in linear, highly entangled polymers with a narrow molecular weight distribution. Figure 7.3 reveals quite similar behaviour for EVA/LDPE modified bitumens (up to 9 wt%) to that shown in Fig. 7.2 for crumb tyre rubber-modified bitumen, with a direct transition from the glassy to the terminal region. No plateau was found at any of the concentrations employed, which demonstrates the non-existence of entanglements. Some differences with respect to crumb tyre rubber-modified bitumen can be found in the high frequency (or low temperature) region, where values of G' corresponding to EVA/LDPE modified bitumens still remain larger than those for neat bitumen.

Modelling linear viscoelastic behaviour

Most of the linear viscoelastic models used to describe the SAOS behaviour of modified bitumen are based on the applicability of the TTSP. Lesueur (2009) has recently reviewed the main linear viscoelastic models used to describe the linear viscoelastic behaviour of unmodified bitumen.

Concerning modified binders, their dynamic linear viscoelastic behaviour can be described by a generalised Maxwell model:

$$G' = G_e + \sum_{i=1}^N G_i \frac{(\omega \lambda_i)^2}{1 + (\omega \lambda_i)^2} \quad 7.31$$

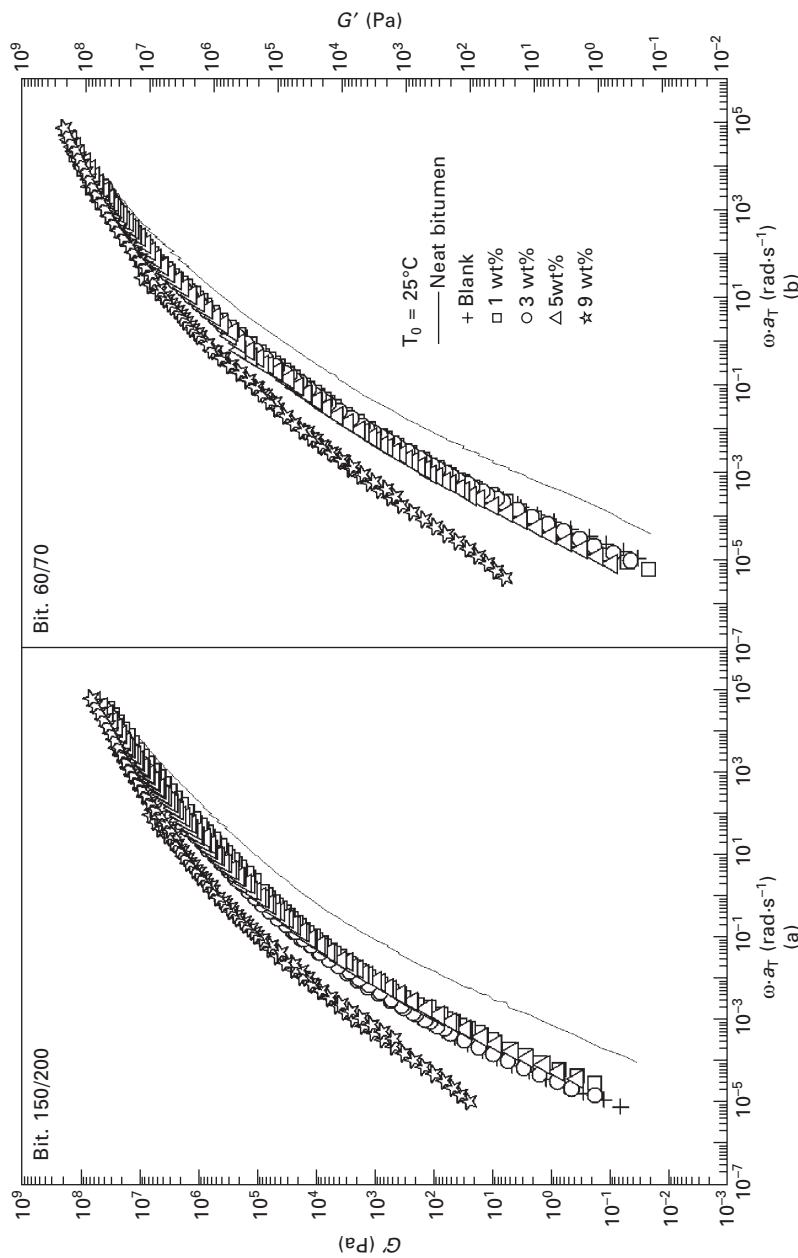
$$G'' = \sum_{i=1}^N G_i \frac{\omega \lambda_i}{1 + (\omega \lambda_i)^2} \quad 7.32$$

where G_e is the elastic modulus. This model considers a superposition of a series of N independent relaxation processes, each process having a relaxation time λ_i and a relaxation strength G_i . The resulting distribution or spectrum of relaxation times can be used to compare the mechanical behaviour of these binders.

On the other hand, in the case of the linear relaxation modulus:

$$G(t) = \sum_{i=1}^N G_i [\exp(-t/\lambda_i)] \quad 7.33$$

However, other authors (Carreau *et al.*, 2000, Stastna *et al.*, 2003) have used a continuous relaxation, or retardation, spectrum, $H(\lambda)$, to represent the linear



7.3 SAOS master curves ((a) for 150/200, (b) for 60/70) of the elastic modulus curves for unmodified bitumens and EVA/LDPE modified bitumens (reference temperature of 25°C). Adapted from García-Morales *et al.* (2004b).

viscoelasticity data of modified bitumens, which provides a continuous function of relaxation times, λ , rather than a discrete set. Thus, the linear relaxation modulus and the dynamic viscoelastic functions are now defined as:

$$G(t) = \int_{-\infty}^{\infty} H(\lambda) [\exp(-t/\lambda)] d(\ln \lambda) \quad 7.34$$

$$G'(\omega) = G_e + \int_{-\infty}^{\infty} H(\lambda) \frac{\omega^2 \lambda^2}{1 + \omega^2 \lambda^2} d(\ln \lambda) \quad 7.35$$

$$G''(\omega) = \int_{-\infty}^{\infty} H(\lambda) \frac{\omega \lambda}{1 + \omega^2 \lambda^2} d(\ln \lambda) \quad 7.36$$

As the spectra cannot be directly obtained from experimentation, the problem that generally arises is the calculation of these spectra from experimental data of a given linear viscoelasticity function. This, of course, implies inverting the corresponding integral equation relating the spectrum with the selected material function. However, it is a well-known fact that the resolution of these equations is an ill-posed problem, as small changes in rheological functions give rise to strong oscillations in the spectra. For that reason, many approximation methods have been developed to perform such calculations (Madiedo and Gallegos, 1997a, 1997b).

A different approach has been proposed by Stastna *et al.* (1994, 1996) and Zanzotto *et al.* (1996). Thus, they proposed the following fractional form of the complex modulus:

$$G^*(\omega) = i\eta_0 \omega \left[\frac{\prod_{k=1}^m (1 + i\omega\mu_k)}{\prod_{k=1}^m (1 + i\omega\lambda_k)} \right]^\beta \quad 7.37$$

where $i^2 = -1$, ω is the frequency, η_0 is the zero-shear viscosity and $\mu_k > 0$, $\lambda_k > 0$, $1 > \beta > 0$, $m < n$, $\eta_0 > 0$ are the fitting parameters. This model is flexible enough to describe the behaviour of modified bitumen with a relatively small number of parameters.

Likewise, in relation to the mechanical modelling of polymer-modified binders, it is worth mentioning the attempts carried out by Hadrzynski and Such (1998) and Lesueur *et al.* (1998). Detailed information on these models will be given in Section 7.3.1.

7.2.2 Non-linear viscoelastic behaviour

At sufficiently large deformations, modified bitumen shows non-linear viscoelastic characteristics. This behaviour is clearly observed, for instance,

by applying increasing deformation during relaxation tests or by characterising the viscous flow behaviour of these binders in a wide range of shear rates.

Modelling non-Newtonian viscous flow

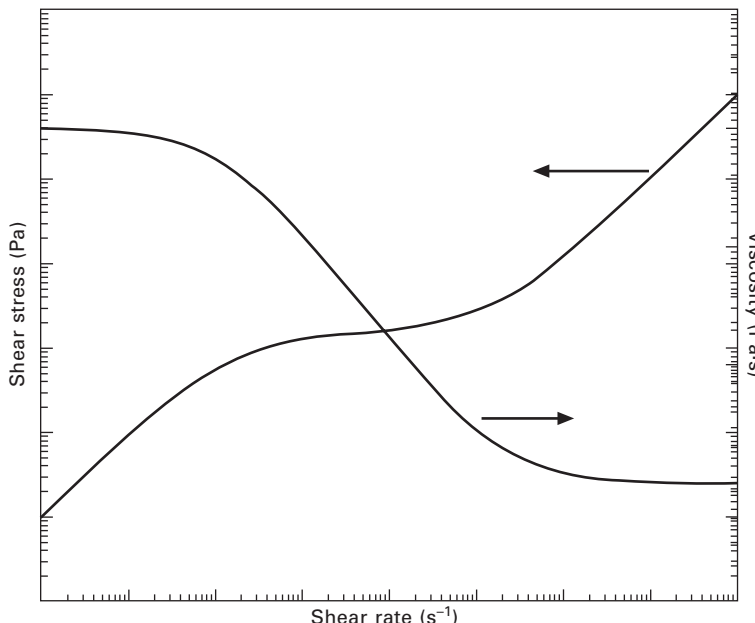
In the intermediate temperature range at which bitumen shows linear viscoelastic characteristics at sufficiently small deformations, it also displays non-Newtonian viscous response in a certain range of shear rates. The flow curve of a non-Newtonian fluid shows an apparent viscosity, shear stress divided by shear rate, which depends on flow conditions, i.e. shear rate, etc., and sometimes even on the kinematic history of the fluid element under consideration.

Complex materials may show different types of non-Newtonian behaviour. However, the most common one found in bitumen rheology is shear-thinning behaviour. This viscous response is characterised by a continuous decrease in apparent viscosity as shear rate increases (Partal and Franco, 2010).

However, most shear-thinning fluids with a complex microstructure also exhibit Newtonian regions at low and high shear rates. The resulting constant viscosity values at very low and high shear rates are known as the zero-shear-rate-limiting viscosity, η_0 , and the high-shear-rate-limiting viscosity, η_∞ . Thus, the apparent viscosity of a shear-thinning fluid decreases from η_0 to η_∞ , with increasing shear rate. These fluids are known as 'structured fluids', because shear rate affects material microstructure and their viscous behaviour changes according to the evolution of their microstructure. Data in a sufficiently wide range of shear rates may illustrate this complete viscous behaviour (see Fig. 7.4).

The viscous flow behaviour of polymer-modified bitumen has been extensively studied (see, for instance, Lesueur *et al.*, 1998; Polacco *et al.*, 2004, 2005, 2006b). Some examples of viscous flow behaviour found for modified bitumen are shown in Figs 7.5 (García-Morales *et al.*, 2006) and 7.6 (Navarro *et al.*, 2007b). They depend on binder composition, measurement temperature and shear rate range studied.

Thus, a typical viscous flow curve, at intermediate temperature, for polymer-modified bitumen is characterised by a zero-shear-rate-limiting viscosity and, after a critical shear rate, a shear-thinning behaviour in a wide range of shear rates (see Fig. 7.6(a)). This critical shear rate for the onset of the shear-thinning behaviour depends on different variables, for instance measurement temperature, binder ageing (Pérez-Lepe *et al.*, 2003), etc. On the other hand, Navarro *et al.* (2007b) have reported a quite different viscous behaviour for crumb tyre rubber-modified bitumen at high temperature (i.e. 135°C). Thus, this behaviour is characterised by a shear-thinning response in a wide shear rate range followed by a tendency to reach a high-shear-rate-limiting viscosity (see Fig. 7.6(b)).



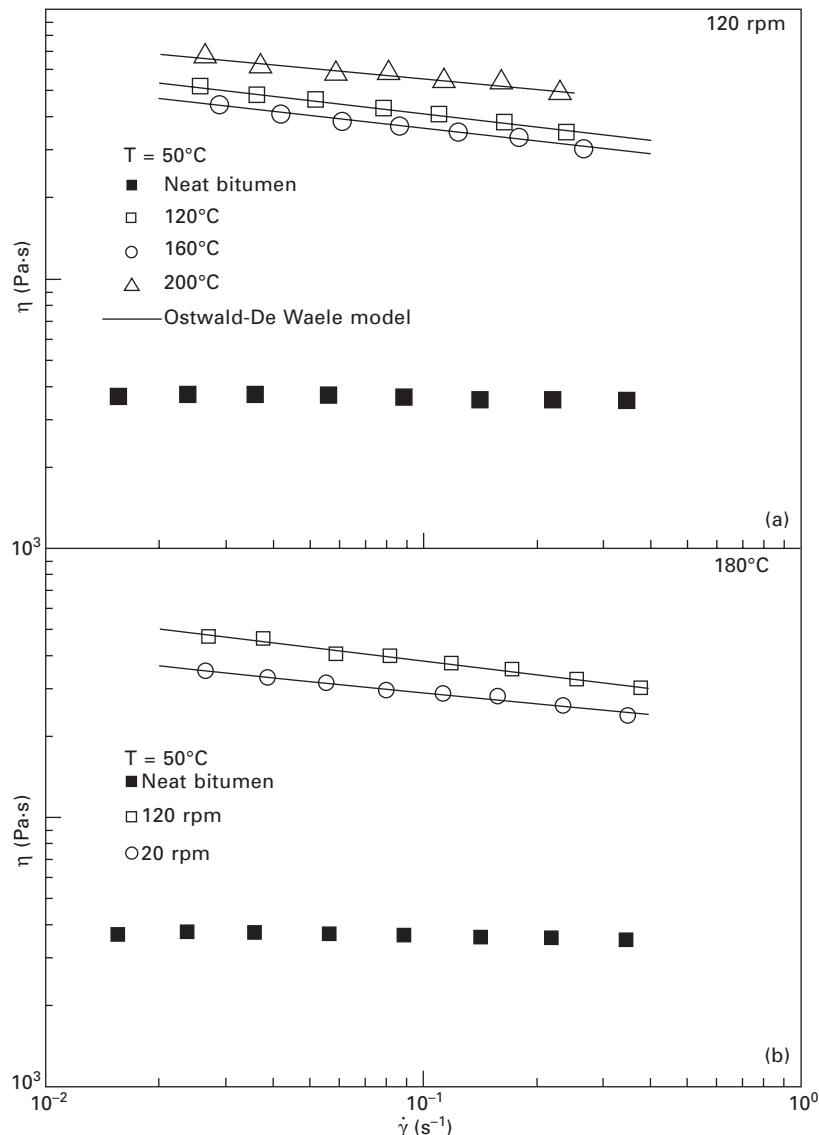
7.4 Log-log scale plot of the flow behaviour of 'structured' fluids.

However, Polacco *et al.* (2004, 2006a) contend that up to four different shapes of viscous flow curves can be found. Thus, for instance, a type of flow curve showing two distinct shear-thinning regions separated by a plateau was observed for SBS-modified binders (Stastna *et al.*, 2003; Polacco *et al.*, 2004). Based on analogies with other structured fluids, these authors concluded that there seems to be a 'rigid' rearrangement of polydomain structures, together with temporary detachment of flexible chains that 'jump' from one domain to another, thus confirming a temporary nature of the formed network.

Several equations have been proposed to model the non-Newtonian flow behaviour of modified bitumen. Some of them have a theoretical basis, while others utilise curve fitting which provides empirical relationships for shear stress (or apparent viscosity) versus shear rate curves (Bird *et al.*, 1987; Carreau *et al.*, 1997; Chhabra and Richardson, 1999). The more widely used viscosity models that may represent the 'structured' fluid response of these binders are as follows.

Ostwald–de Waele's or power-law model

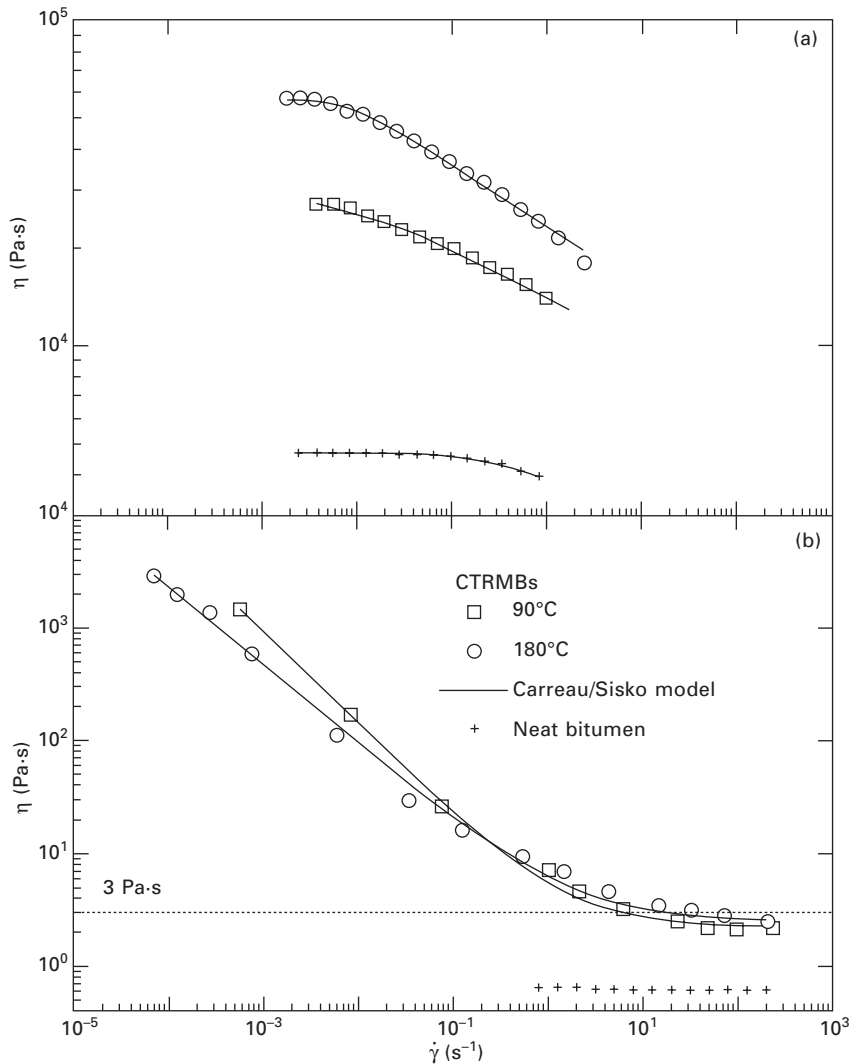
The relationship between shear stress and shear rate (plotted on log-log scale) for a shear-thinning fluid can often be approximated by a straight line over an experimental range of shear rate (or stress). For this part of the flow curve, an expression of the following form can be fitted:



7.5 Viscous flow curves, at 50°C, for EVA/LDPE modified bitumen, processed (a) at different temperatures (120–200°C) and 120 rpm, or (b) at different agitation speeds (20–120 rpm) and 180°C. Adapted from García-Morales *et al.* (2006).

$$\sigma = k\dot{\gamma}^n \quad 7.38$$

where k is the consistency index and n is the flow index. Thus, the apparent viscosity for the so-called power-law (or Ostwald–de Waele) fluid is given by:



7.6 Viscous flow curves, at (a) 50°C and (b) 135°C, for model crumb tyre rubber-modified bitumen, processed at different temperatures.
Adapted from Navarro *et al.* (2007b).

$$\eta = k\dot{\gamma}^{n-1} \quad 7.39$$

For $n < 1$, the fluid exhibits shear-thinning behaviour; for $n = 1$, the fluid shows Newtonian behaviour. For a shear-thinning fluid, the index n ranges from 0 to 1, so that the smaller the value of n , the greater the degree of shear-thinning. It should be noted that the dimensions of the flow consistency coefficient, k , depend on the numerical value of n . On the other hand, the value of k can be viewed as the value of apparent viscosity at the shear rate of unity.

This model has been used to fit the experimental results obtained, for instance, with EVA/LDPE-modified bitumen in a given range of shear rates (see Fig. 7.5).

Sisko's model

This three-parameter model predicts a shear-thinning region at intermediate shear rates and a Newtonian viscosity, η_∞ , at high shear rates:

$$\eta = \eta_\infty + k\dot{\gamma}^{n-1} \quad 7.40$$

where η_∞ is a high-shear-rate-limiting viscosity and k and n are parameters related to the consistency and flow indexes. It should be noted that the dimensions of k depend upon the value of n . With the use of the third parameter, this model provides a somewhat better fit to some experimental data, and is particularly recommended to describe the material flow behaviour in the high-shear-rate region.

This model has been used to fit the experimental results obtained, for instance, with model crumb tyre rubber-modified bitumen, at high temperature, in a range of shear rates between 10^{-5} and 10^3 s $^{-1}$ (see Fig. 7.6(b)).

Carreau's model

As shown in Fig. 7.4 for structured fluids, it is necessary to use a model which takes into account a power-law region at intermediate shear rates and two limiting viscosities, the zero-shear-rate-limiting viscosity, η_0 , and the high-shear-rate-limiting viscosity, η_∞ . Based on the molecular network considerations, Carreau (1972) proposed the following viscosity model which incorporates both shear-rate-limiting viscosities η_0 and η_∞ :

$$\frac{\eta - \eta_\infty}{\eta_0 - \eta_\infty} = \frac{1}{[1 + (\lambda\dot{\gamma})^2]^s} \quad 7.41$$

Parameter $\lambda = 1/\dot{\gamma}_c$, where $\dot{\gamma}_c$ is a critical shear rate for the onset of the shear-thinning region, and s is a parameter related to the slope of the power-law region. This model can describe shear-thinning behaviour over a wide range of shear rates but only at the expense of the added complexity of four parameters.

This equation has been used to fit the experimental results obtained, for instance, with model crumb tyre rubber-modified bitumen, at intermediate temperature (50°C), in a range of shear rates between 10^{-3} and 10 s $^{-1}$ (see Fig. 7.6(a)). However, the high-shear-limiting viscosity was suppressed, as a tendency to a second viscosity plateau was not observed at this temperature in the shear rate range studied.

In the case of viscous flow curves with two shear-thinning regions, a two-mode Carreau's viscosity model has been proposed (Stastna *et al.*, 2003):

$$\eta(\dot{\gamma}) = \frac{a - c}{(1 + (\lambda_1 x)^2)^b} + \frac{c}{(1 + (\lambda_2 x)^2)^d} \quad 7.42$$

where a and c are the values of the two viscosity plateaus, b and d are the power-law indexes, and λ_1 and λ_2 are two characteristic times related to the evolution of an oriented structure and bitumen–polymer interactions.

Modelling non-linear viscoelasticity

One approach to describing non-linear behaviour of complex materials is based on continuum mechanics principles, aiming to establish a rheological constitutive equation to replace the Boltzmann principle.

Wagner (1979) proposed the introduction of a non-linear memory function in the constitutive equation for non-linear viscoelasticity. Taking into account that the relaxation of stress following a large step strain can often be separated into time-dependent and strain-dependent factors, Wagner proposed the use of a memory function defined as the product of the linear memory function and the 'damping function'. Wagner's model can then be written as follows:

$$\sigma_{ij}(t) = \int_{-\infty}^t m(t - t')h(I_1, I_2)B_{ij}(t, t')dt' \quad 7.43$$

where $B_{ij}(t, t')$ is the Finger tensor, $h(I_1, I_2)$ is the damping function, an empirical function whose parameters are determined by fitting experimental data, and $m(t - t')$ is the memory function, related to the linear relaxation modulus by differentiation:

$$m(t - t') = \frac{dG(t - t')}{dt'} \quad 7.44$$

This model predicts material shear-thinning characteristics. However, it has been reported that the factorisation of the non-linear memory function into strain- and time-dependent components is not possible for many polymer-modified bitumens. In this case, an empirical equation for the non-linear relaxation modulus has been proposed:

$$G(t, \gamma) = c \exp\left\{-\left[\left(\frac{t}{a}\right)^b + \left(\frac{t\gamma^2}{g}\right)^h\right]\right\} + d \exp\left\{-\left[\left(\frac{t}{e}\right)^f + \left(\frac{t\gamma^2}{i}\right)^j\right]\right\} \quad 7.45$$

where a to j are fitting parameters. This equation assumes that the linear viscoelastic behaviour of polymer-modified bitumen can be described by two

stretch exponential modes, and that each relaxation mode is ‘attenuated’ by another simple stretch exponential factor (Polacco *et al.*, 2006a).

If the time-strain influence on the non-linear relaxation modulus can be factorised into two separate functions, and considering only the simple shear component of the stress tensor, the Wagner model yields:

$$\sigma(t, \dot{\gamma}) = - \int_{-\infty}^t \frac{dG(t-t')}{dt'} h(\gamma) \gamma(t, t') dt' \quad 7.46$$

where $\sigma(t, \dot{\gamma})$ is the transient shear stress and $h(\gamma)$ is the damping function, which can be easily calculated from the ratio between the non-linear relaxation modulus, $G(\gamma, t-t')$, and the linear relaxation modulus, $G(t-t')$:

$$h(\gamma) = \frac{G(\gamma, t-t')}{G(t-t')} \quad 7.47$$

Different types of damping functions have been proposed. According to Wagner:

$$h(\gamma) = \exp(-k\gamma) \quad 7.48$$

However, a more complex damping function, as the sum of two exponential functions, has been proposed by Polacco *et al.* (2006a) to fit the viscous flow curve of a 70/100 bitumen modified with 7.2 wt% SBS:

$$h(\gamma) = a [\exp(-k_1\gamma)] + (1-a)[\exp(-k_2\gamma)] \quad 7.49$$

and assuming that the evolution of the linear relaxation modulus with time can be described by a generalised Maxwell model:

$$G(t) = \sum_{i=1}^n g_i e^{-(t-t')/\lambda_i} \quad 7.50$$

The steady-state viscosity will result:

$$\eta(\dot{\gamma}) = \sum_{i=1}^n \frac{g_i \lambda_i}{(1 + k\lambda_i \dot{\gamma})^2} \quad 7.51$$

for a single exponential damping function, or

$$\eta(\dot{\gamma}) = a \sum_{i=1}^n \frac{g_i \lambda_i}{(1 + k_1 \lambda_i \dot{\gamma})^2} + (1-a) \sum_{i=1}^n \frac{g_i \lambda_i}{(1 + k_2 \lambda_i \dot{\gamma})^2} \quad 7.52$$

for a sum of two exponential damping functions. This last equation has been used by Polacco *et al.* (2006a) to fit the experimental flow curve of a 70/100 bitumen modified with 7.2 wt% SBS.

7.3 Case studies

7.3.1 Polymer-modified bitumen rheology: plastomers and elastomers

It is well known that the purpose of bitumen modification using polymers is to achieve desired engineering properties, such as increased shear modulus and reduced viscous flow at high temperatures and/or increased resistance to thermal fracture at low temperatures. There are a broad range of commercial polymer modifiers available that can be employed to reach these goals. Polymer modifiers for asphalts can be classified into two general categories, 'passive' polymers and 'active' polymers. Passive polymers, which are the most common modifiers used, are often further classified into elastomers and plastomers.

Of the four main groups of thermoplastic elastomers (polyurethane, polyether–polyester copolymers, olefinic copolymers and styrenic block copolymers), the styrenic block copolymers have proved to present the greatest potential when blended with bitumen (Read and Whiteoak, 2003). Styrenic block copolymers, also termed thermoplastic rubbers or thermoplastic elastomers, are normally produced by a sequential operation of successive polymerisation of styrene–butadiene–styrene (SBS). However, not only linear copolymers but also multi-armed copolymers, often referred to as radial or branched copolymers, can be produced. Thermoplastic elastomers derive their strength and elasticity from a physical crosslinking of the molecules into a three-dimensional network. This is achieved by the agglomeration of the polystyrene end-blocks into separate domains, which provide the physical crosslinks for a three-dimensional polybutadiene rubbery matrix.

In some instances, elastomers in the form of vulcanised rubbers (e.g. reclaimed tyre crumb) have been used for bitumen modification, although they are difficult to disperse. So, successful dispersion requires high temperatures and long digestion times and can result in a heterogeneous binder with the rubber acting mainly as a flexible filler (see Chapter 5, 'The use of waste polymers to modify bitumen').

On the other hand, polyethylene, polypropylene, poly(vinyl chloride), polystyrene and ethylene vinyl acetate (EVA) are the principal plastomers that have been examined as modified road binders. As thermoplastics, they are characterised by softening on heating and hardening on cooling. These polymers tend to influence the penetration more than the softening point, which is the opposite tendency of thermoplastic elastomers. Addition of plastomers increases the viscosity of the resulting modified binder, although they do not significantly increase its elasticity.

In general, when mixed with a bituminous binder, a typical polymer can either dissolve in the binder as a solute or phase-separate into a polymer-rich phase and a bitumen-rich phase. When a polymer completely dissolves,

an increase in binder viscosity is the only effect observed. On the contrary, if the polymer and bitumen are completely chemically incompatible with different densities, phase separation occurs on a macro-scale, resulting in gross separation of both phases, which hinders its application. In the middle, if they have some degree of compatibility and similar densities, separation may occur on a micro-scale, in which the polymer phase becomes swollen with some bitumen components. In that case, a further enhancement in the viscoelastic behaviour of the binder can be attained, mainly for high polymer contents. Since a modified binder consists of two distinct phases, three different cases must be considered (Becker *et al.*, 2001):

1. Low polymer content. Optical observations carried out by different researchers (Lesueur *et al.*, 1998; Airey, 2003; Fawcett and McNally, 2003; Lu and Isacsson, 2001) have shown that, if a polymer content below 4 wt% is used, the mechanical mixing leads to a two-phase structure with the bitumen being the continuous phase and the polymer being dispersed through it. In the polymer-rich phase, the polymer is swollen by the maltenes of the original bitumen and this phase may reach a volume fraction of up to 30%. Accordingly, the final bituminous matrix consists of the original bitumen with a decreased content in maltenic components. This process has been described as a physical distillation (Lesueur *et al.*, 1998). In relation to material rheological behaviour, at high service temperatures of around 60°C, the stiffness modulus of the polymer phase is higher than that of the matrix, with a consequent improvement in the mechanical performance of the binder. At low temperatures, the stiffness modulus of the dispersed phase is lower than that of the matrix, which reduces binder brittleness. In other words, polymer addition extends the useful temperature range of the asphalt.
2. Polymer content around 5 wt%. These binders present microstructures in which the two phases are continuous and interlocked.
3. Sufficiently high polymer content. Likewise, when the polymer concentration is increased further (more than 7 wt% polymer, in general), a phase inversion has been reported, e.g. for atactic poly(propylene), α -olefin copolymer (Fawcett and McNally, 2003), and SBS (Airey, 2003; Lu and Isacsson, 2001). In that case, the polymer phase is the matrix of the system. This is in fact not a bitumen, but a polymer plasticised by the oils in the bitumen in which the heaviest fractions of the initial binder are dispersed. These materials are usually employed for roofing applications.

Rheological properties of polymer-modified bitumens (PMBs) may vary with the base bitumen and the polymer type and content. For a given polymer concentration, it has been shown that the rheological behaviour of binders containing SBS differs widely from that of those containing EVA (Lu and

Isacsson, 2001). In the same way, Airey (2003) has shown that paraffinic bitumen shows a larger change in properties by SBS polymer modification compared to naphthenic bitumen.

In that sense, modelling of the rheological behaviour of PMBs has been successfully applied to some bituminous binders at low temperature. However, a satisfactory prediction of the behaviour of binders in the high temperature region, at which manufacture of a modified binder is carried out, remains a difficult issue. In order to be able to optimise the mixing process involved and thus the final binder's properties, it is of major importance to predict the properties of PMBs from the characteristics and relative concentrations of the bitumen and polymer of interest.

In relation to the mechanical modelling of polymer-modified binders, it is worth mentioning the attempts carried out by Hadrzynski and Such (1998) and Lesueur *et al.* (1998). In both cases, the authors sustain that the blend properties result from the phase properties. Thus, the phases involved are not neat bitumen and pure polymer, but those obtained from polymer/bitumen blends after centrifugation or by natural creaming at high temperature.

Hadrzynski and Such (1998) proposed a homogenisation model. In this type of model, when a biphasic material presents a repetitive volume unit, the blend behaviour can be mathematically represented from the properties of the two phases (matrix and inclusions) by changing the heterogeneous biphasic system into an equivalent homogeneous medium, that is, by putting all the inclusions together into one larger inclusion. The homogenisation model used by Hadrzynski was the self-consistent model originally described to predict the complex modulus of a biphasic viscoelastic material (Zaoui *et al.*, 1991).

From the complex modulus values of the bituminous matrix and the polymeric inclusions, the complex modulus of the blend can be obtained from the following expression:

$$3G^{*2} + [(2 - 5\phi_i) G_i^* + (5\phi_m - 3) G_m^*] - 2G_i^*G_m^* = 0 \quad 7.53$$

where G^* is the complex modulus of the blend, G_i^* and G_m^* are the complex moduli of the inclusions and the matrix, and ϕ_i and ϕ_m are the volumetric fractions of the inclusion and the matrix, respectively. As can be deduced, interfacial tension plays no role in this model.

The complex modulus values of a SBS-modified bituminous blend were adequately predicted within a temperature range from -20°C to 60°C , at 7.8 Hz. However, the frequency dependence of the complex modulus was not studied by Hadrzynski.

A mechanical model satisfactorily applied by Lesueur *et al.* (1998), in a wide temperature range, to predict the viscoelastic behaviour of a SBS-modified bitumen, is the Palierne model (Palierne, 1990), originally proposed for emulsions of viscoelastic spherical inclusions in a viscoelastic matrix,

especially for polymer blends. It has been applied successfully to a number of polymer blends (Brahimi *et al.*, 1991; Graebling *et al.*, 1993; Cassagneau *et al.*, 1995; Kim and Seo, 2003), foams (Chen *et al.*, 2004) and oil-in-water emulsions (Romoscanu *et al.*, 2003). The complex modulus of an emulsion can be calculated from the complex modulus of each phase, the interfacial tension and the size of the inclusions (Palierne, 1990). Thus,

$$G^* = G_m^* P^* (\lambda^*, \text{Ca}^*, \phi) \quad 7.54$$

where G^* is the complex modulus of the blend, G_m^* is the modulus of the matrix, P^* is a function of λ^* , the ratio between the modulus of the inclusion and the modulus of the matrix, Ca^* is the capillary number, and ϕ is the volumetric fraction of the dispersed phase, where λ and Ca^* are given by:

$$\lambda^* = \frac{G_i^*}{G_m^*} \quad 7.55$$

$$\text{Ca}^* = G_m^* \frac{a}{\gamma} \quad 7.56$$

where γ is the interfacial tension, and a is the radius of the spherical inclusion. The capillary number represents the equilibrium between the interfacial forces (due to the Laplace pressure $a/2\gamma$) and the mechanical forces exerted on the drops by the matrix (G_m^*).

In the case of polymer-bitumen blends, the function P^* is described as:

$$P^* = \frac{1 + 1.5\phi_i \frac{E^*}{D^*}}{1 - \phi_i \frac{E^*}{D^*}} \quad 7.57$$

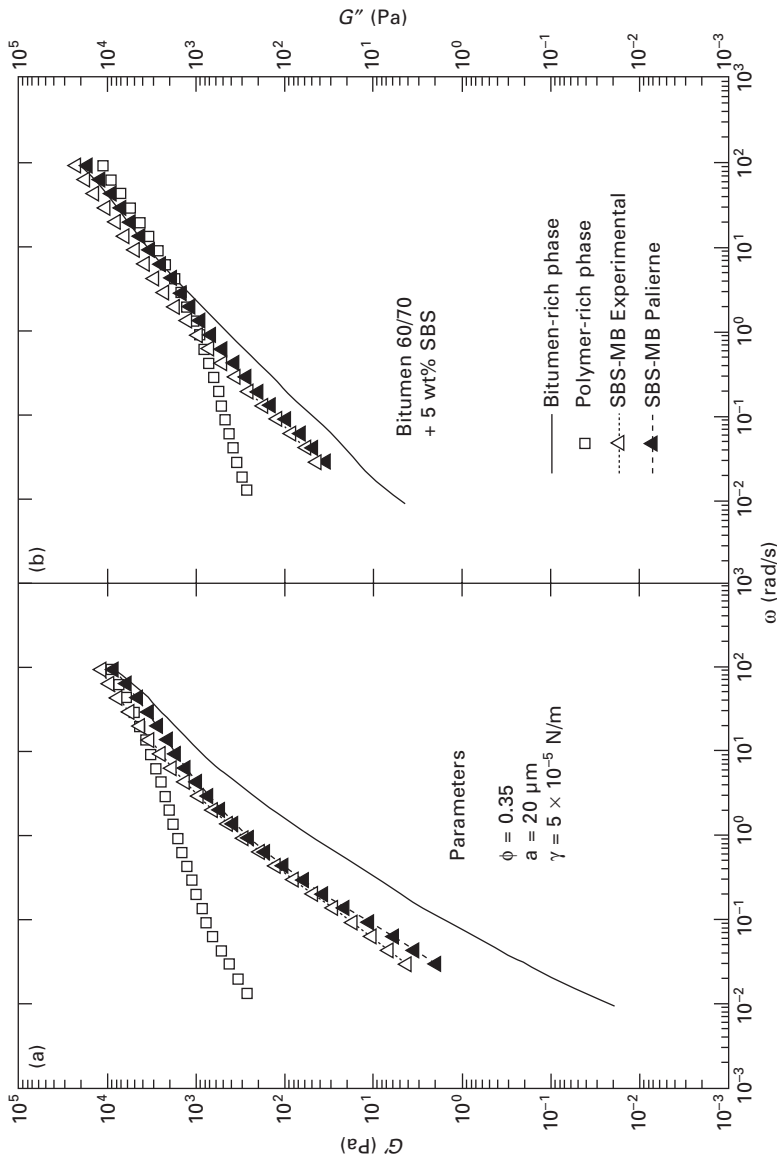
where

$$E^* = 2(\lambda^* - 1)(19\lambda^* + 16) + 8 \frac{5\lambda^* + 2}{\text{Ca}^*} \quad 7.58$$

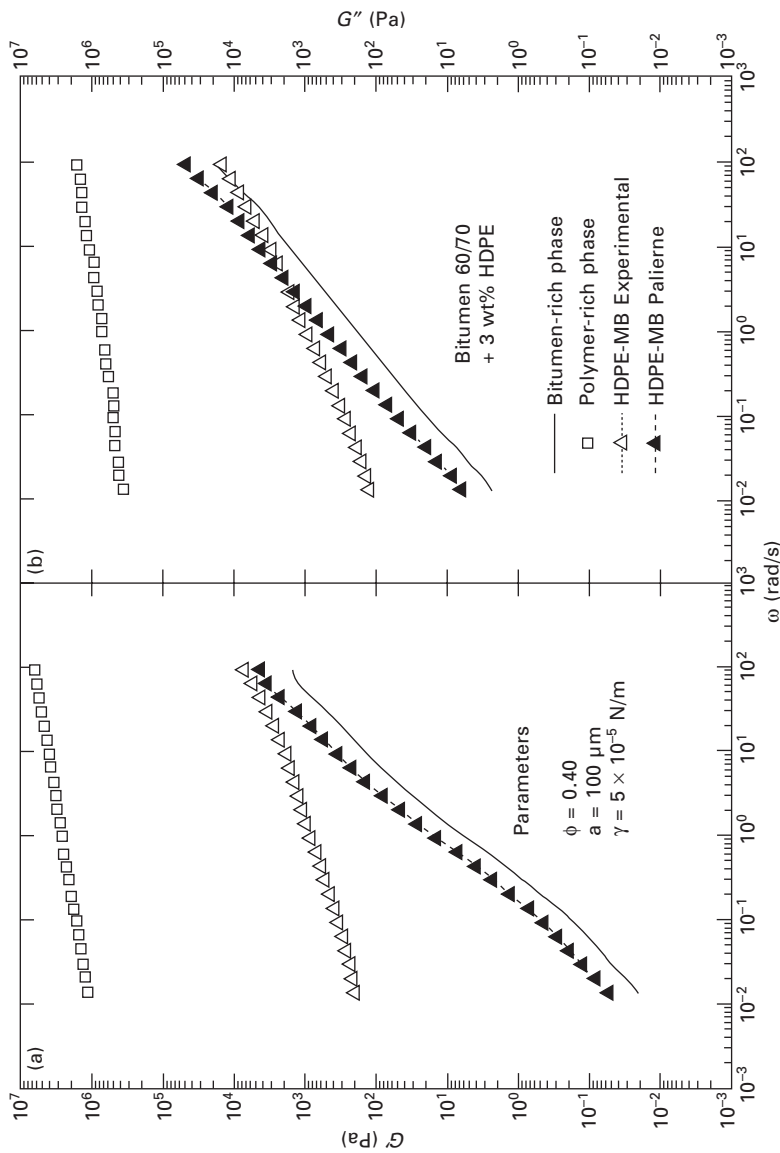
$$D^* = (2\lambda^* + 3)(19\lambda^* + 16) + 40 \frac{\lambda^* + 1}{\text{Ca}^*} \quad 7.59$$

Hence, the radius of the inclusion, the volume fraction of the polymer and the interfacial tension are required. Interfacial tension values of bitumen-polymer blends are not available, although values of interfacial tension of ternary polymer blends have been proposed to be of the same order to those of polymer-bitumen blends (Lesueur, 2002). The radius of the inclusion and the volume fraction could be determined from microscopic observations.

Applications of Palierne's model to two selected PMBs containing 5 wt% SBS and 3 wt% HDPE are presented in Figs 7.7 and 7.8, respectively. The



7.7 Experimental and Palierne model-predicted values (a) for G' , (b) for G'' of the frequency dependence of the linear storage and loss moduli in oscillatory shear, at 75°C, for a 5 wt% SBS-modified bitumen.



7.8 Experimental and Palierne model-predicted values ((a) for G' , (b) for G'') of the frequency dependence of the linear storage and loss moduli in oscillatory shear, at 75°C, for a 3 wt% HDPE-modified bitumen.

experimental values of the frequency dependence of the linear viscoelasticity functions (G' and G'') at 75°C for a 5 wt% SBS-modified binder are presented in Fig. 7.7. In this figure, the values of the moduli of the polymer-rich and bitumen-rich phases are also shown. Values of interfacial tension for SBS-bitumen blends were predicted by Lesueur *et al.* (1998) to be of the same order than those for ternary blends (asphaltenes/polymer/maltenes). Thus, a value of 5×10^{-5} N/m was assumed. Also, a microscopic characterisation, including image analysis, carried out on the sample allowed both inclusion average radius and volume fraction to be determined (20 μm and 0.35, respectively). As can be observed, the agreement between the experimental values of the SBS-modified binder and those predicted by Palierne's model is somewhat acceptable, although some differences are noticeable (Pérez-Lepe, 2004).

In the same way, Palierne's model was applied to describe the linear viscoelastic properties of a 3 wt% HDPE-modified binder, at 75°C (see Fig. 7.8). The interfacial tension was set at 5×10^{-5} N/m, with the equivalent average radius and volume fraction being 100 μm and 0.40, respectively. For this HDPE, even at the low polymer content considered, the binder does not present morphology with dispersed polymer particles. Figure 7.8 reveals that Palierne's model (derived for emulsions) does not apply to this incipient bi-continuous system, as can be deduced from the comparison between experimental and predicted values of the linear viscoelasticity functions.

In conclusion, Palierne's model is not able to predict the rheological behaviour of the binder when large and interconnected aggregates are formed within the bitumen matrix.

7.3.2 Rheology of synthetic binders

Research into a binder with similar characteristics to bitumen but which can be easily pigmented has forced the oil industry to develop a new material. This binder should not be considered as a bitumen from the point of view of its chemical composition, although its physical characteristics have been considered as a goal and on several occasions improved (Brule *et al.*, 1993). This new product, called synthetic binder, is basically a mixture of oil, resin and polymer (Brule *et al.*, 1993; Partal *et al.*, 1999). Of course, the dark-coloured asphaltenes should be omitted in the formulation of a synthetic binder. Pigmentable synthetic binders are used for coloured pavement applications. Coloured pavements can fulfil several functions: alert traffic to special situations, indicate differences in pavement functions, improve the effect of illumination, etc. (Schellenkens and Korenstra, 1987; Gustafsson, 1988).

In relation to the type of polymer used for these binders, block copolymers such as styrene–butadiene–styrene (SBS) have usually been selected, as they

proved to be very effective modifiers for bitumen due to their thermoplastic elastomeric properties (Collins *et al.*, 1991; Vonk and van Gooswilligen, 1991).

It has also been reported that synthetic binders containing SBS are multiphase systems that exhibit, at least, a polymer-rich phase and a resin-rich phase (Partal *et al.*, 1999; Martínez-Boza *et al.*, 2000, 2001a, 2001b). The first results from the absorption of some components of the oil fraction, with which the SBS would extend (Ho *et al.*, 1997), and the second would consist of the remaining oil/resin fraction.

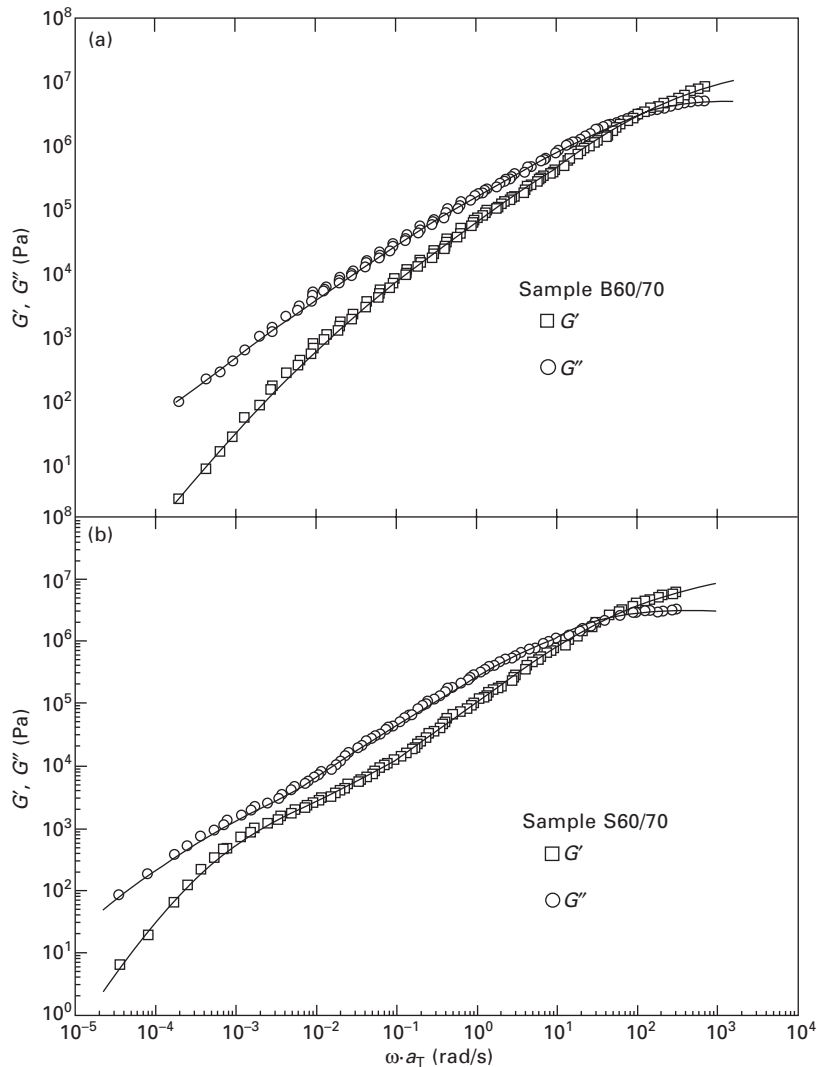
Partal *et al.* (1999) have studied the rheological behaviour of two pigmentable synthetic binders (S60/70 and S80/100, Shell Bitumen, UK) in the range 5–50°C. Figure 7.9 shows the master curves of the storage and loss moduli versus frequency for selected unmodified bitumen and synthetic binder samples. Within the temperature range studied, the temperature dependence of the shift factor for the systems studied was described by an Arrhenius-type equation fairly well.

As can be observed, both binders show a crossover point at high frequencies for a storage modulus value of the order of 10^6 Pa. In the low-frequency region, the rheological behaviour of the synthetic binder presents remarkable differences from that of the unmodified bitumen. The former is characterised by an apparent shift of the terminal zone to lower frequencies, corresponding to longer relaxation times. This fact may be influenced by a slight tendency to the appearance of a 'pseudo-plateau' region in G' . It has been related to the development of entanglements among the macromolecular components of the synthetic binder.

The loss tangent master curves for selected unmodified bitumen and synthetic binder samples are shown in Fig. 7.10. As may be seen, the synthetic binder S60/70 is characterised by a minimum in $\tan \delta$ in the low-frequency region. The unmodified bitumen B60/70 does not present such behaviour in the loss tangent, whose values continuously decrease when frequency is raised. On the other hand, the synthetic binder presents lower values of $\tan \delta$ in the low-frequency region (corresponding to the highest temperatures studied) than the unmodified bitumen, and, therefore, more elastic characteristics at high temperatures. The local minimum at low frequencies found in the synthetic binder (S60/70) is also characteristic of bitumen modified by SBS copolymers (Stastna *et al.*, 1994; Zanzotto *et al.*, 1996).

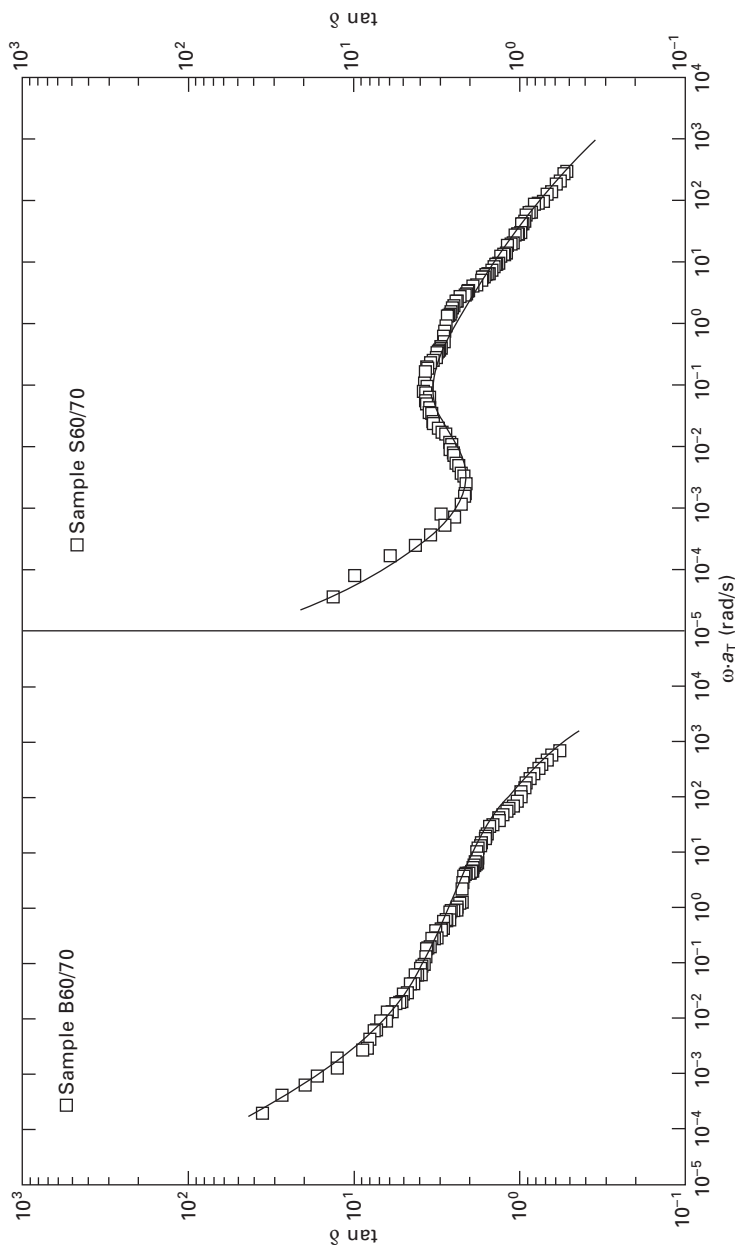
The same authors (Navarro *et al.*, 2005b) have studied the influence that composition and processing variables exert on the linear viscoelastic properties of model synthetic binders, for a wide range of temperature and frequency. Model synthetic binders were prepared by blending a non-modified colophony resin (40–65 wt%), a process aromatic oil, and a styrene–butadiene–styrene (SBS) triblock copolymer (5–15 wt%).

As can be observed in Figs 7.11 and 7.12, three different regions appear

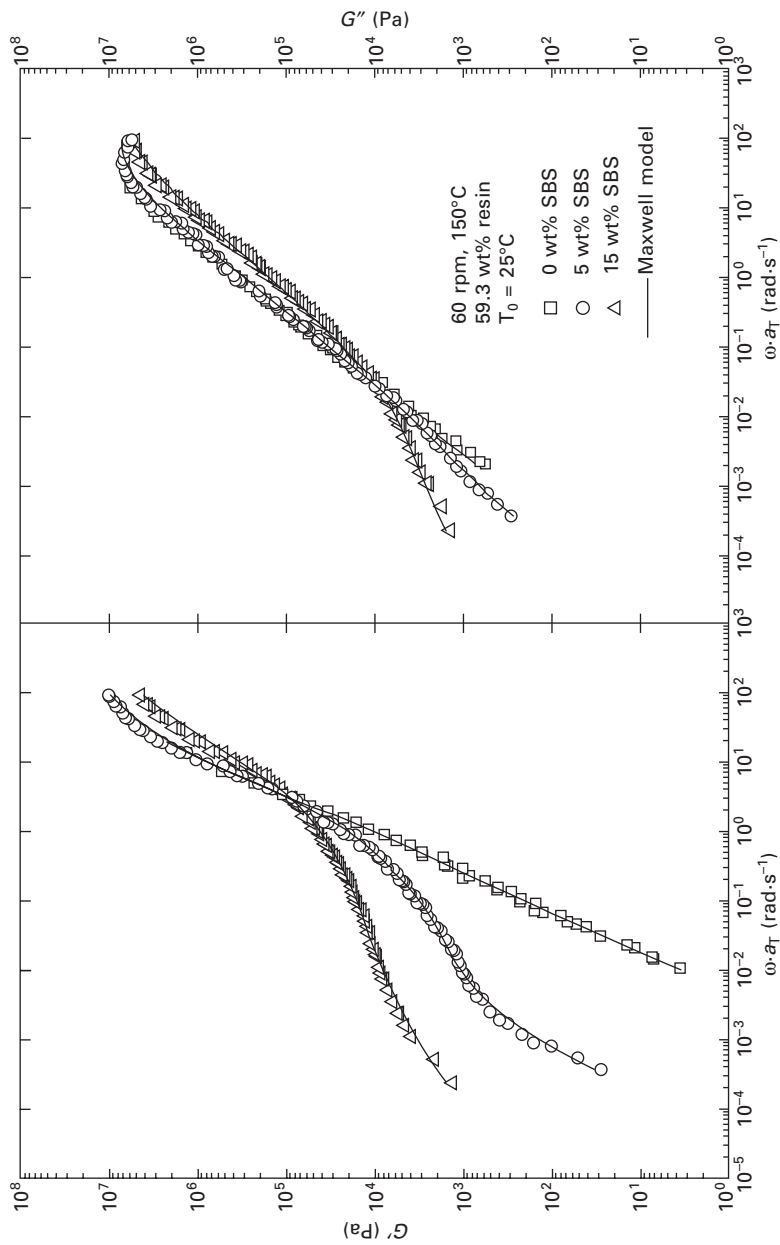


7.9 Master curves of the storage and loss moduli, G' , G'' , for (a) an unmodified bitumen, and (b) a synthetic binder, at a reference temperature of 25°C. Adapted from Partal *et al.* (1999).

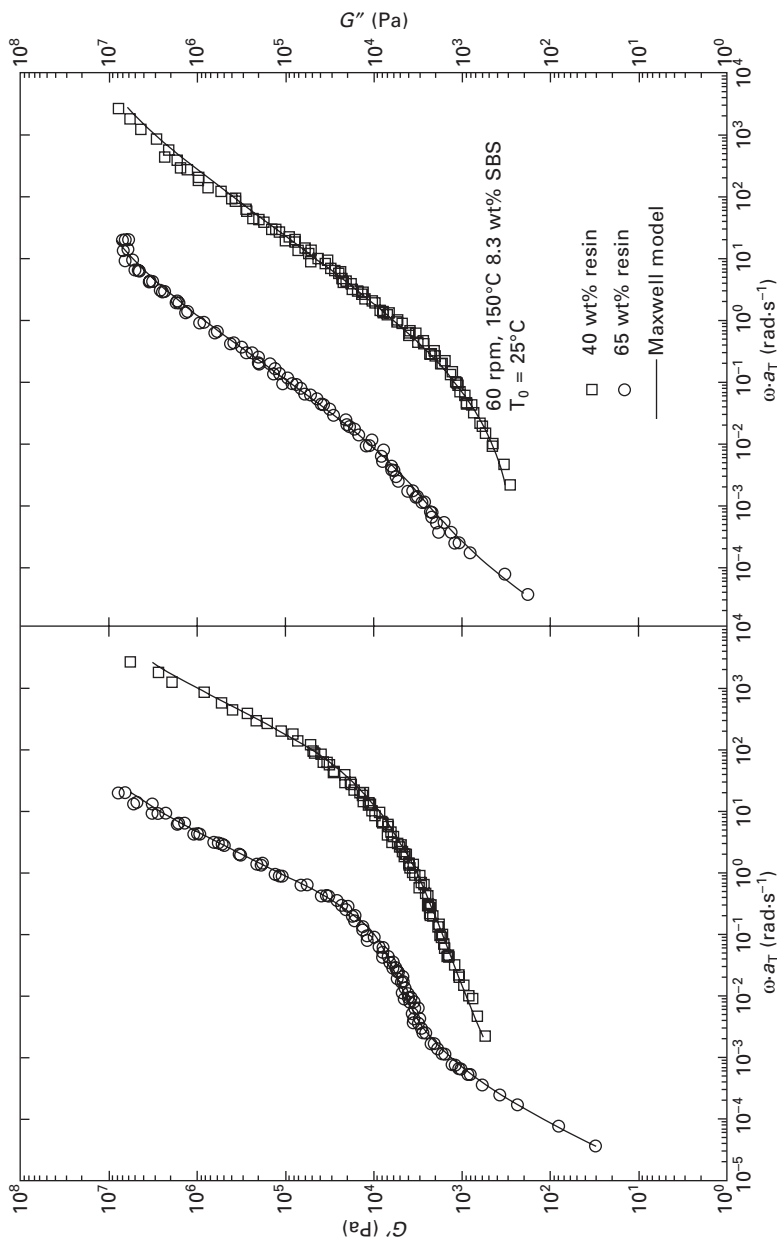
in the SAOS master curves obtained after application of an empirical time-temperature superposition method, depending on SBS and resin content. Thus, the transition to the glassy region is observed mainly at high frequencies. At low frequencies, the binder containing the lowest SBS content presents values of G'' much higher than those of G' , and slopes close to 1 and 2, respectively, characteristic of the terminal or flow region of the mechanical



7.10 Master curves of the loss tangent, $\tan \delta$, for selected bitumen and synthetic binder samples, at a reference temperature of 25°C. Adapted from Partal *et al.* (1999).



7.11 Master curves of the storage and loss moduli, G' , G'' , for synthetic binders, with constant resin concentration, at a reference temperature of 25°C. Adapted from Navarro *et al.* (2005b).



7.12 Master curves of the storage and loss moduli, G' , G'' , for synthetic binders, with constant polymer concentration, at a reference temperature of 25°C. Adapted from Navarro *et al.* (2005b).

spectrum. The most important differences between the samples were found at intermediate frequencies. The binder with the highest SBS concentration (15 wt%) develops a plateau region, showing values of G' higher than G'' , whereas only a shoulder in G' is found for the binder containing the lowest SBS content (5 wt%), the storage modulus having lower values than the loss modulus. On the other hand, an increase in resin concentration yields larger storage and loss moduli values in the higher frequency range.

An Arrhenius-like equation described the dependence on temperature of the shift factors calculated for the different model synthetic binders studied. The activation energy values obtained were seen to decrease by either decreasing resin content or increasing polymer concentration, yielding samples with lower thermal susceptibility.

The authors have explained these results on the following basis. At low polymer content (i.e. 5 wt%, 150°C) the polymer-rich phase is dispersed in a continuous resin-rich phase matrix, and its rheological response is similar to that predicted by the emulsion model (Bousmina, 1999). Thus, the shoulder of G' shown by some binders is due to the deformation relaxation process of the SBS-rich dispersed phase (Bousmina, 1999). On the contrary, when polymer content is sufficiently high (i.e. 15 wt% SBS obtained at 150°C and 1200 rpm) a phase inversion occurs, the polymer-rich phase is continuous, and a structural network is formed. In this case, a plateau region is detected in the mechanical spectrum of the material. SEM micrographs demonstrated the existence of a three-dimensional network of a polymer-rich phase and a dispersed resin-rich phase for the binder containing 15 wt% SBS, whereas dispersed polymer-rich microdomains in a continuous resin-rich phase clearly appeared for the binder containing 5 wt% SBS.

The presence of the above-mentioned phases clearly influences the relaxation spectra of these synthetic binders. Thus, the lowest relaxation time of the binder is related to the transition to the glassy region and is characterised by the presence of a local maximum in its weighted spectrum. As expected, the synthetic binders and the oil/resin sample having constant resin concentration show similar values of this characteristic relaxation time in the transition to the glassy region of the relaxation spectrum. On the contrary, at constant polymer concentration, this region is shifted to higher relaxation times as resin concentration is raised. On the other hand, the transition from the plateau to the terminal region is characterised by the terminal relaxation time, which may be calculated from the maximum of the weighted spectrum, at high relaxation times. This characteristic relaxation time moves to higher values as polymer concentration increases. As reported by Martínez-Boza *et al.* (2001b), these results are clear evidence that the viscoelastic behaviour observed at low relaxation times (high frequency) is closely related to the resin-rich phase, whilst the behaviour observed at intermediate relaxation times should be mainly attributed to the polymer-rich phase.

Under severe processing conditions (180°C and high agitation speed) and low polymer concentration, the polymer influence is damped and a continuous transition from the glassy region to the terminal region is observed. At high polymer concentration, where SBS forms a continuous network, a phase inversion can be induced by processing. Navarro *et al.* (2005b) have explained these changes in rheology/microstructure on the basis of a combined effect of resin oxidation and SBS degradation.

7.4 Conclusions and future trends

For many years, the thermo-mechanical characterisation of bitumen was based on various empirical tests, at both high and low temperatures, which served industrial needs quite well. For example, bitumen contribution to the permanent deformation process (rutting) has traditionally been handled by looking at bitumen consistency based on penetration and softening point tests (ASTM D5 and D36, respectively). However, these results are difficult to interpret and the need for rational specifications led to fundamental studies on the rheological behaviour of bitumen. Thus, in 1987, the Strategic Highway Research Program (SHRP) began developing new tests for measuring physical properties of bitumen that can be directly related to field performance. The Superpave performance-graded binder specifications (AASHTO MP1) arising from this study provided a performance-related specification based on the rheological properties of the binder, and the climate and loading conditions of the pavement where it is to be placed. Among many others, the document gave special relevance to the oscillatory shear test in the linear viscoelastic region. Thus, the importance of knowledge of the rheological behaviour of bitumen is apparent. Bitumen is a Newtonian fluid when handled and mixed with mineral aggregates at high temperatures. The linear viscoelastic region describes the resistance of bitumen to traffic loading (rutting and cracking due to fatigue). Finally, at or below the glass transition temperature, thermal cracking is likely to occur under certain loading conditions. As a result, understanding bitumen rheology is of major concern, as the mechanical properties of this binder are linked to the in-service performance of the actual asphalt pavements.

The relationship found between the results of the proposed rheological tests and expected bitumen performance has been validated in numerous studies. However, they do not appear to adequately determine the performance characteristics of modified binders. Many industry experts questioned whether AASHTO MP1 was able to correctly characterise the performance benefits of modified binders. Industrial researchers decided to take a look at those modified binder characteristics. So, a National Cooperative Highway Research Program (NCHRP) project, NCHRP 9-10, was begun in 1996 to address their performance benefits. The goal of NCHRP 9-10 was twofold.

First, it investigated whether changes to the AASHTO MP1 specifications and supporting test methods might permit better characterisation of all asphalt binders, including modified binders. Second, NCHRP 9-10 focused on producing recommended practices detailing the proposed test procedures for characterising modified binders.

New parameters and specifications have arisen since then. For example, the ‘rutting parameter’, $|G^*|/\sin \delta$, presented by AASHTO MP1 as a means to efficiently classify the rutting performance of bitumen, has been lately questioned. It has proven to underestimate bitumen resistance to permanent deformation. Thus, other parameters, like zero-shear-viscosity obtained from creep or oscillatory shear (in the linear viscoelasticity interval) tests under certain specific conditions for PMBs, have shown to better correlate permanent deformation at high in-service temperatures (see, for instance, Morea *et al.*, 2009).

In that sense, continuous efforts are currently being devoted to the development of models and test procedures able to guarantee accurate predictions of the performance of a selected PMB in a given application.

7.5 Sources of further information and advice

Some experimental data included in this chapter are part of several research projects sponsored by:

- CICYT, Spain (Research Project with reference MAT99-0545)
- MCYT-FEDER programme (Research Project MAT2001- 0066-C02-02)
- MEC-FEDER programme (MAT 2004-06299-002-02)
- MMA programme (Research Project 5,1-212/2005/3B, Ministerio de Medio Ambiente, Spain)
- MEC-FEDER programme (Research Project MAT2007-61460).

The authors gratefully acknowledge the financial support of the Spanish government.

7.6 References

Adedeji A., Grunfelder T., Bates F.S., Macosko C.W., Stroup-Gardiner M., Newcomb D.E. (1996). Asphalt modified by SBS triblock copolymer: structures and properties. *Polym. Eng. Sci.* 36, 1707–1723.

Airey G.D. (2003). Rheological properties of styrene butadiene styrene polymer modified road bitumens. *Fuel* 82, 1709–1719.

Ait-Kadi A., Brahimi B., Bousmina M. (1996). Polymer blends for enhanced asphalt binders. *Polym. Eng. Sci.* 36, 1724–1733.

Anderson D.A., Kennedy T.W. (1993). Development of SHRP binder specification. *J. Assoc. Asphalt Paving Technol.* 62, 481–507.

Anderson D.A., Christensen D.W., Bahia H.U., Dongré R., Sharma M.G., Antle C.E., Batton J. (1994). *Binder Characterization and Evaluation – Physical Characterization*. Strategic Highway Research Program, National Research Council, Washington, DC (Vol. 3).

Barnes H.A. (2000). *A Handbook of Elementary Rheology*. Institute of Non-Newtonian Fluid Mechanics, University of Wales, Aberystwyth, UK.

Becker Y., Mendez M.P., Rodriguez Y. (2001). Polymer modified asphalt. *Vision Tecnologica* 1, 39–50.

Becker Y., Müller A.J., Rodriguez Y. (2003). Use of rheological compatibility criteria to study SBS modified asphalts. *J. Appl. Polym. Sci.* 90, 1772–1782.

Bird R.B., Armstrong R.C., Hassager, O. (1987). *Dynamics of Polymeric Liquids, Vol. 1, Fluid Dynamics*, 2nd edn. Wiley, New York.

Bousmina M. (1999). Rheology of polymer blends: linear model for viscoelastic emulsions. *Rheol. Acta* 38, 73–83.

Brahimi B., Ait-Kadi A., Ajji A., Jérôme R., Fayt R. (1991). Rheological properties of copolymer modified polyethylene/polystyrene blends. *J. Rheol.* 35, 1069–1091.

Brule B., Le Bourlot F., Potti J.J. (1993). Synthetic binder emulsions. Application. *First Congress on Emulsion*, Vol. 3, EDS, Paris, 4–11–193/01–05.

Carreau P.J. (1972). Rheological equations from molecular network theories. *Trans. Soc. Rheol.* 16, 99–127.

Carreau P.J., Dekee D., Chhabra, R.P. (1997). *Rheology of Polymeric Systems: Principles and Applications*. Hanser, Munich, Germany.

Carreau, P.J., Bousmina M., Bonniet F. (2000). The viscoelastic properties of polymer modified asphalts. *Can. J. Chem. Eng.* 78, 495–502.

Carrera V., Partal P., García-Morales M., Gallegos C., Páez A. (2009). Influence of bitumen colloidal nature on the design of isocyanate-based bituminous products with enhanced rheological properties. *Ind. Eng. Chem. Res.* 48, 8464–8470.

Carrera V., García-Morales M., Partal P., Gallegos C. (2010a). Novel bitumen/isocyanate-based reactive polymer formulations for the paving industry. *Rheol Acta* 49, 563–572.

Carrera V., Partal P., García-Morales M., Gallegos C., Pérez-Lepe A. (2010b). Effect of processing on the rheological properties of poly-urethane/urea bituminous products. *Fuel Processing Technology* 91, 1139–1145.

Carrera V., García-Morales M., Navarro F.J., Partal P., Gallegos C. (2010c). Bitumen chemical foaming for asphalt paving applications. *Ind. Eng. Chem. Res.* 49, 8538–8543.

Cassagneau P., Espinasse I., Michel A. (1995). Viscoelastic and elastic behaviour of polypropylene and ethylene copolymer blends. *J. Appl. Polym. Sci.* 58, 1393–1399.

Chen X., Heuzey M.C., Carreau P.J. (2004). Rheological properties of injection molded LDPE and mPE foams. *Polym. Eng. Sci.* 44, 2158–2164.

Chhabra R.P., Richardson, J.F. (1999). *Non-Newtonian Flow in the Process Industries*. Butterworth-Heinemann, Oxford, UK.

Collins J.H., Boulding M.G., Gelles R., Berker A. (1991). Improved performance of paving asphalts by polymer modification. *Proc. Assoc. Asphalt Paving Technol.* 60, 43–79.

Dealy J.M., Wissbrun K.F. (1995). *Melt Rheology and its Role in Plastic Processing*. Chapman & Hall, London.

Dongré R., Youtcheff J., Anderson D. (1996). Better roads through rheology. *Appl. Rheol.* 6, 75–82.

Emri I. (2010). Time-dependent behaviour of solid polymers. In: *Rheology* (C. Gallegos and K. Walters, eds), *Encyclopedia of Life Support Systems*. UNESCO.

Fawcett A.H., McNally T. (2003). Polystyrene and asphaltene micelles within blends with a bitumen of an SBS block copolymer and styrene and butadiene homopolymers. *Colloid. Polym. Sci.* 281, 203–213.

Fawcett A.H., McNally T. (2000). Blends of bitumen with various polyolefins. *Polymer* 41, 5315–5326.

Fawcett A.H., McNally T., McNally G.M., Andrews F., Clarke J. (1999). Blends of bitumen with polyethylenes. *Polymer* 40, 6337–6349.

Ferry J.D. (1980). *Viscoelastic Properties of Polymers*. Wiley, New York.

Gallegos C., Martínez-Boza F.J. (2010). Linear viscoelasticity. In: *Rheology* (C. Gallegos and K. Walters, eds), *Encyclopedia of Life Support Systems*. UNESCO.

Gallegos C., Walters K. (2010). Rheology. In: *Rheology* (C. Gallegos and K. Walters, eds), *Encyclopedia of Life Support Systems*. UNESCO.

García-Morales M., Partal P., Navarro F.J., Martínez-Boza F., Gallegos C., González N., González O., Muñoz M.E. (2004a). Viscous properties and microstructure of recycled EVA modified bitumens. *Fuel* 83, 31–38.

García-Morales M., Partal P., Navarro F.J., Martínez-Boza F., Gallegos C. (2004b). Linear viscoelasticity of recycled EVA modified bitumens. *Energy & Fuels* 18, 357–364.

García-Morales M., Partal P., Navarro F.J., Martínez-Boza F., Gallegos C. (2006). Process rheokinetics and microstructure of recycled EVA/LDPE-modified bitumen. *Rheol. Acta* 45, 513–524.

García-Morales M., Partal P., Navarro F.J., Martínez-Boza F., Gallegos C. (2007). Processing, rheology, and storage stability of recycled EVA/LDPE modified bitumen. *Polym. Eng. Sci.* 47, 181–191.

González O., Peña J.J., Muñoz M.E., Santamaría A., Pérez-Lepe A., Martínez-Boza F., Gallegos C. (2002). Rheological techniques as a tool to analyze polymer–bitumen interactions: bitumen modified with polyethylene and polyethylene-based blends. *Energy & Fuels* 16, 1256–1263.

Graebling D., Müller R., Palierne J.F. (1993). Linear viscoelastic behaviour of some incompatible polymer blends in the melt. Interpretation of data with a model of emulsion of viscoelastic liquids. *Macromolecules* 26, 320–329.

Gustafsson P. (1988). Shell Mexphalte C: Liseberg amusement park in Gothenburg. *Shell Bitumen Review* 63, 12–14.

Hadrzynski F., Such C. (1998). Modélisation du comportement rhéologique des bitumes polymères. Le modèle autocohérent. *Bull. Lab. Ponts et Chaussées* 214, 3–18.

Hesp S.A.M., Woodhams R.T. (1991). Asphalt–polyolefin emulsion breakdown. *Colloid Polym. Sci.* 269, 825–834.

Ho R., Adedeji A., Giles D.W., Hajduk D.A., Macosko C.W., Bates F.S. (1997). Microstructure of triblock copolymers in asphalt oligomers. *J. Polym. Sci. B: Polym. Phys.* 35, 2857–2877.

Kim H.J., Seo Y. (2003). Effect of surface modification on the interfacial tension between the melts of high-density polyethylene and Nylon 66. Correlation between rheology and morphology. *Langmuir* 19, 2696–2704.

King G.N., King H.W., Harders O., Chaverot P., Planche J.P. (1992). Influence of asphalt grade and polymer concentration on the high temperature performance of polymer modified asphalt. *J. Am. Assoc. Paving Technol.* 61, 1–19.

Lesueur D. (2002). La rhéologie des bitumes: principes et modification. *Rhéologie* 2, 1–30.

Lesueur D. (2009). The colloidal structure of bitumen: Consequences on the rheology and on the mechanisms of bitumen modification. *Adv. Colloid Interf. Sci.* 145, 42–82.

Lesueur D., Gérard J.F., Claudy P., Létoffé J.M. (1996). A structure-related model to describe asphalt linear viscoelasticity. *J. Rheol.* 40, 813–836.

Lesueur D., Gérard J.F., Claudy P., Létoffé J.M., Martin D., Planche J.P. (1998). Polymer modified asphalts as viscoelastic emulsions. *J. Rheol.* 42, 1059–1074.

Lewandowski L.H. (1993). Polymer modification of asphalt paving binders. *Rubber Chem. Technol.* 67, 447–480.

Lu X., Isacsson U. (2001). Modification of road bitumens with thermoplastic polymers. *Polymer Testing* 20, 77–68.

Macosko C.W. (1994). *Rheology: Principles, Measurements and Applications*. VCH Publishers, New York.

Madiedo J.M., Gallegos C. (1997a). Rheological characterization of oil-in-water emulsions by means of relaxation and retardation spectra. *Recent Res. Dev. Oil Chem.* 1, 79–90.

Madiedo J.M., Gallegos C. (1997b). Rheological characterization of oil-in-water food emulsions by means of relaxation and retardation spectra. *Appl. Rheol.* 7, 161–167.

Martín-Alfonso M.J., Partal P., Navarro F.J., García-Morales M., Gallegos C. (2008a). Use of a MDI-functionalized reactive polymer for the manufacture of modified bitumen with enhanced properties for roofing applications. *Eur. Polym. J.* 44, 1451–1461.

Martín-Alfonso M.J., Partal P., Navarro F.J., García-Morales M., Gallegos C. (2008b). Role of water in the development of new isocyanate-based bituminous products. *Ind. Eng. Chem. Res.* 47, 6933–6940.

Martínez-Boza F.J., Partal P., Conde B., Gallegos C. (2000). Influence of temperature and composition on the linear viscoelastic properties of synthetic binders. *Energy & Fuels* 14, 131–137.

Martínez-Boza F.J., Partal P., Navarro F.J., Gallegos C. (2001a). Rheology and microstructure of asphalt binders. *Rheol. Acta* 40, 135–141.

Martínez-Boza F.J., Partal P., Conde B., Gallegos C. (2001b). Steady-state flow behaviour of synthetic binders. *Fuel* 80, 357–365.

Morea F., Agnusdei J.O., Zerbino R. (2009). Comparison of methods for measuring zero shear viscosity in asphalts. *Mater. Struct.* 43, 499–507.

Navarro F.J., Partal P., Martínez-Boza F.J., Valencia C., Gallegos C. (2002). Rheological characteristics of ground tyre rubber-modified bitumens. *Chem. Eng. J.* 89, 53–61.

Navarro F.J., Partal P., Martínez-Boza F.J., Gallegos C. (2004). Thermo-rheological behaviour and storage stability of ground tire rubber-modified bitumens. *Fuel* 83, 2041–2049.

Navarro F.J., Partal P., Martínez-Boza F.J., Gallegos C. (2005a). Influence of crumb rubber concentration on the rheological behaviour of a crumb rubber modified bitumen. *Energy & Fuels* 19, 1984–1990.

Navarro F.J., Partal P., Martínez-Boza F.J., Gallegos C. (2005b). Effect of composition and processing on the linear viscoelasticity of synthetic binders. *Eur. Polym. J.* 41, 1429–1438.

Navarro F.J., Partal P., García-Morales M., Martínez-Boza F.J., Gallegos C. (2007a). Bitumen modification with a low-molecular weight reactive isocyanate-terminated polymer. *Fuel* 86, 2291–2299.

Navarro F.J., Partal P., Martínez-Boza F.J., Gallegos C. (2007b). Influence of processing conditions on the rheological behaviour of crumb tyre rubber-modified bitumen. *J. Appl. Polym. Sci.* 104, 1683–1691.

Navarro F.J., Partal P., García-Morales M., Martín-Alfonso M.J., Gallegos C., Bordado J.C., Diogo A. (2009). Bitumen modification with reactive and non-reactive (virgin and recycled) polymers: a comparative analysis. *J. Ind. Eng. Chem.* 15, 458–464.

Navarro F.J., Partal P., Martínez-Boza F.J., Gallegos C. (2010). Novel recycled polyethylene/ground tire rubber/bitumen blends for use in roofing applications: thermo-mechanical properties. *Polymer Testing* 29, 588–595.

Palierne J.F. (1990). Linear rheology of viscoelastic emulsions with interfacial tension. *Rheol. Acta* 29, 204–214.

Partal P., Franco J.M. (2010). Non-Newtonian fluids. In: *Rheology* (C. Gallegos and K. Walters, eds), *Encyclopedia of Life Support Systems*, UNESCO.

Partal P., Martínez-Boza F.J., Conde B., Gallegos C. (1999). Rheological characterisation of synthetic binders and unmodified bitumens. *Fuel* 78, 1–10.

Pérez-Lepe A. (2004). PhD thesis, University of Huelva, Spain.

Pérez-Lepe A., Martínez-Boza F.J., Gallegos C., González O., Muñoz M.E., Santamaría A. (2003). Influence of the processing conditions on the rheological behaviour of polymer-modified bitumen. *Fuel* 82, 1339–1348.

Pérez-Lepe A., Martínez-Boza F.J., Gallegos C. (2005). Influence of polymer concentration on the microstructure and rheological properties of high-density polyethylene (HDPE)-modified bitumen. *Energy & Fuels* 19, 1148–1152.

Pérez-Lepe A., Martínez-Boza F.J., Attané P., Gallegos C. (2006). Destabilization mechanism of polyethylene-modified bitumen. *J. Appl. Polym. Sci.* 100, 260–267.

Polacco G., Stastna J., Vlachovicova Z., Biondi D., Zanzotto, L. (2004). Temporary networks in polymer modified asphalts. *Polym. Eng. Sci.* 44, 2185–2193.

Polacco G., Berlincioni S., Biondi D., Stastna J., Zanzotto L. (2005). Asphalt modification with different polyethylene-based polymers. *Eur. Polym. J.* 41, 2831–2844.

Polacco G., Stastna J., Biondi D., Zanzotto L. (2006a). Relation between polymer architecture and nonlinear viscoelastic behaviour of modified asphalts. *Current Opinion in Colloid & Interface Science* 11, 230–245.

Polacco G., Muscente A., Biondi D., Santini S. (2006b). Effect of composition on the properties of SEBS modified asphalt. *Eur. Polym. J.* 42, 1123–1121.

Read J., Whiteoak D. (2003). *The Shell Bitumen Handbook*, 5th edn. Thomas Telford, London.

Reiner M. (1964). The Deborah number. *Physics Today* 17, 62.

Romoscanu A.I., Sayir M.B., Hausler K., Burbidge A.S. (2003). Rheological behaviour of low-viscous emulsions and interpretation with a theoretical model. *Colloids Surf. A: Physicochem. Eng. Aspects* 223, 113–133.

Schellenkens J.C.A., Korenstra J. (1987). Shell Mxpathalte C bring colour to asphalt pavements. *Shell Bitumen Review* 62, 22–25.

Stastna J., Zanzotto L. (1999a). Linear response of regular asphalt to external harmonic fields. *J. Rheol.* 43, 719–734.

Stastna J., Zanzotto L. (1999b). Response to ‘letter to editor’: on the thermorheological complexity and relaxation modes of asphalt cements. *J. Rheol.* 43, 719–734.

Stastna J., Zanzotto L., Ho K. (1994). Fractional complex modulus manifested in asphalts. *Rheol. Acta* 33, 344–354.

Stastna J., Zanzotto L., Kennepohl G. (1996). Dynamic material functions and the structure of asphalts. *Transp. Res. Rec.* 1535, 3–9.

Stastna J., Zanzotto L., Vacin O.J. (2003). Viscosity function in polymer-modified asphalts. *J. Colloid Interf. Sci.* 259, 200–207.

Vlachovicova Z., Stastna J., MacLeod D., Zanzotto L. (2005). Shear deformation and material properties of polymer-modified asphalt. *Pet. Coal* 47, 38–48.

Vonk W.C., van Gooswilligen G. (1991). *Report 8.18*, pp. 1–14. Shell Laboratorium, Amsterdam, Netherlands.

Wagner M.H. (1979). Zur Netzwerktheorie von Polymer-Schmelzen. *Rheol. Acta* 18, 33–50.

Walters K. (2010). History of rheology. In: *Rheology* (C. Gallegos and K. Walters, eds), *Encyclopedia of Life Support Systems*, UNESCO.

Yousefi A.A. (2003). Polyethylene dispersions in bitumen: the effects of the polymer structural parameters. *J. Appl. Polym. Sci.* 90, 3183–3190.

Yousefi A.A., Ait-Kadi A., Roy C. (2000). Composite asphalt binders: effect of modified RPE on asphalt. *J. Mater. Civ. Eng.* 12, 113–123.

Zanzotto L., Stastna J., Ho K. (1996). Characterization of regular and modified bitumens via their complex modulus. *J. Appl. Polym. Sci.* 59, 1897–1905.

Zanzotto L., Stastna J., Vacin O. (2000). Thermomechanical properties of several polymer modified asphalts. *Appl. Rheol.* 10, 185–191.

Zaoui A., François D., Pineau A. (1991). *Comportement Mécanique des Matériaux, Volume I: Élasticité et Plasticité*. Hermès, Paris.

Factors affecting the rheology of polymer modified bitumen (PMB)

G. D. AIREY, University of Nottingham, UK

Abstract: This chapter describes the alterations to the rheological characteristics of bitumen modified with typically used plastomeric and elastomeric polymers. The rheological properties of these polymer modified bitumens (PMBs) have been measured through a combination of empirically based tests as well as fundamental, rheological techniques using a dynamic shear rheometer (DSR). In addition, the influence of ageing on the rheological properties of plastomeric and elastomeric PMBs has been investigated. Finally, the performance of asphalt mixtures incorporating these PMBs has also been assessed by means of standard asphalt mixture laboratory tests. The performance criteria have concentrated on the two main distress modes associated with flexible asphalt pavements, namely permanent deformation and fatigue cracking.

Key words: PMBs, rheological properties, dynamic shear rheometer, ageing, asphalt mixtures, permanent deformation, fatigue cracking.

8.1 Introduction

Polymer modification of bitumen (PMB) offers one solution to overcome the inherent deficiencies of conventional asphalt materials in pavement situations where they are subjected to excessive load and environment demands. The enhanced properties associated with both plastomeric and elastomeric PMBs provide the means to improve the mechanical performance of these modified pavement materials and allow them to fulfil their design requirements (Brown *et al.*, 1990; Isacsson and Lu, 1995). Traditionally, polymer modification has been accomplished by improving the temperature susceptibility of the modified bitumen with increased binder stiffness at high service temperatures and reduced stiffness at low service temperatures (Brule *et al.*, 1988; Collins *et al.*, 1991; Goodrich, 1991).

The use of synthetic polymers to modify the performance of conventional bituminous binders dates back to the early 1970s, with these binders subsequently having not only decreased temperature susceptibility but also increased cohesion and modified rheological characteristics (Brown *et al.*, 1990; Isacsson and Lu, 1995; Brule *et al.*, 1988; Collins *et al.*, 1991; Goodrich, 1991). Globally, approximately 75% of modified binders can be classified as

elastomeric and 15% as plastomeric, with the remaining 10% being either rubber or miscellaneous modified (Diehl, 2000; Bardesi, 1999). Within the elastomeric group, styrenic block copolymers, such as the thermoplastic rubber, styrene–butadiene–styrene (SBS) block copolymer, have shown the greatest potential when blended with bitumen (Bull and Vonk, 1984). In terms of plastomers, the semi-crystalline copolymer, ethylene vinyl acetate (EVA), can be considered to be the principal polymer used in pavement applications (Cavaliere *et al.*, 1993; Goos and Carre, 1996).

In this chapter the effect of polymer modification on the rheological properties of various EVA and SBS PMBs is presented based on measurements undertaken by conventional methods as well as more fundamental rheological tests using a dynamic shear rheometer (DSR). In addition to the rheological properties of the unaged binders, the effect of both short-term and long-term ageing has been investigated. Finally, the permanent deformation and fatigue performance of modified asphalt mixtures have been determined using a suite of tests associated with the Nottingham Asphalt Tester (NAT).

8.2 Polymer modification

It is generally accepted that polymer modification improves the temperature susceptibility of bitumen and, in addition, can improve its resistance to permanent deformation, thermal and fatigue cracking. These improvements are based on the fact that small amounts of polymer, of appropriate constitution and structure, can transform the rheology of standard bitumen. There are a number of aspects that determine the effectiveness of polymer as a modifier. These include the similarity in solvent parameters, without which dissolving of the two components is almost impossible with resulting interactions with bitumen being minimal. There is also an advantage if the polymer is able to form a three-dimensional network structure within the modified bitumen. Finally, there is a need for the polymer to re-establish its characteristics after each heating cycle during handling and processing as demonstrated by the thermoplastic nature of the polymer network.

Both SBS and EVA are polymers that fulfil the above requirements, creating strongly extended networks in the bitumen that disappear upon heating, enabling easy processing, while re-establishing their microstructure after cooling. Such networks could also be established using chemical crosslinking, but these would be irreversible due to the inability to break these links on heating. Crosslinking therefore has to be limited to prevent excessively high viscosities during processing, application and ultimately recycling of the modified binder.

In order to assess the effect of polymer modification, the rheological and mechanical properties of a range of unmodified bitumens and PMBs were compared in their pure binder state as well as after being incorporated

into asphalt mixtures. Three base bitumens (Bitumens A, B and C) from different crude sources were used to produce a number of laboratory blended, semi-crystalline EVA and block copolymer SBS PMBs (Airey, 2002, 2003). All three base bitumens have similar consistencies (penetrations between 60 and 81 dmm and softening points between 46.8 and 48.8°C) and differ only slightly in their chemical composition (SARA fractions) as shown in Table 8.1. The Colloidal Indices (CIs) of the three base bitumens were calculated in order to determine the potential compatibility of these bitumens to polymer modification. Serfass *et al.* (1992) are of the opinion that no precise CI borderline exists between what will be a 'compatible' and what will be an 'incompatible' bitumen. However, what is clear is that the different percentages of SARA fractions mean that the CIs of the three base bitumens differ considerably, and inevitably this will result in differences in compatibility and rheological performance of the EVA and SBS PMBs. In general, a lower CI value (i.e. a greater percentage of aromatics) will lead to a more compatible system with a higher degree of solvency for the EVA and SBS polymers.

In total, 15 EVA and SBS PMBs were produced at polymer contents ranging from low polymer modification at 3 wt% to intermediate polymer modification at 5 wt% to high degrees of modification at 7 wt%. Nine EVA PMBs were produced by mixing an EVA 20/20 semi-crystalline copolymer, containing 20% vinyl acetate with a melt flow index of 20, with each of the base bitumens at three polymer contents by mass. Six SBS PMBs were produced by mixing a linear SBS copolymer (31% styrene content) with Bitumens B and C at three polymer contents by mass. All the PMBs were prepared with a Silverson high shear laboratory mill at temperatures between 170°C and 185°C (depending on the viscosity of the PMB) until steady-state conditions were achieved.

When a polymer (elastomer or plastomer) is blended with bitumen, it absorbs portions of the maltenes (oil fractions) from the bitumen and can swell up to nine times its initial volume (Isacsson and Lu, 1995). Highly effective polymers are therefore present in bitumen/polymer blends as extended polymers and at high temperatures often occur in a single phase

Table 8.1 SARA analysis of the three base bitumens

Binder	Saturates (%) ^a	Aromatics (%) ^a	Resins (%) ^a	Asphaltenes (%) ^a	Colloidal index ^b
Bitumen A	5	69	15	11	0.190
Bitumen B	4	68	19	9	0.149
Bitumen C	11	58	17	14	0.333

^alatroscan thin film chromatography SARA analysis.

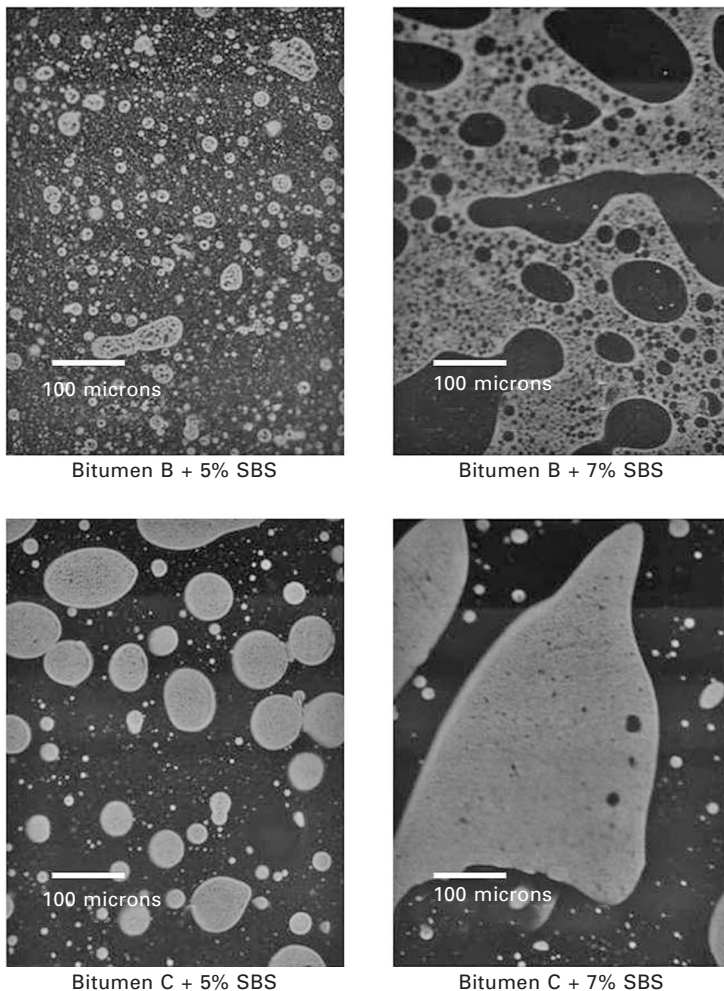
^bColloidal index (I_c) = (asphaltenes + saturates)/(resins + aromatics).

with the base bitumen. However, bitumen and polymer are still too different in their molecular parameters to remain in a single phase at ambient temperatures. Hence at ambient temperatures, all PMB blends consist of more than one phase and each of these phases has properties different from those of the base bitumen. In general, the chemical dissimilarity between the two components (base bitumen and polymer) will result in at least two distinct phases following mechanical mixing (Brule, 1996). This two-phase structure consists of a 'polymer-rich phase' and an 'asphaltene-rich phase', also known as the polymer and bitumen phases. The polymer phase consists of the polymer swollen by light, compatible fractions of the bitumen (e.g. aromatic oils), while the heavy fractions (mainly asphaltenes) are concentrated to form the bitumen phase. The distribution, continuity and homogeneity of the different phases have a significant effect on the performance of the PMB. In addition, the stability of these two phases, in terms of phase separation or incompatibility, must also be maintained during production and storage of the PMB to ensure optimum performance of the product.

At suitably high polymer concentrations, a continuous polymer network (phase) is formed throughout the PMB, significantly modifying the bitumen properties. The establishment of this continuous and dominant polymer phase allows the nature of the polymer to dictate the properties of the PMB rather than the base bitumen and can lead to substantial improvements in the mechanical and rheological performance of the binder. Under these conditions, the product tends to behave more as a polymer than conventional bitumen. One technique that can be used to identify the development and distribution of the different polymer and bitumen phases is fluorescent microscopy imaging (Airey, 2003).

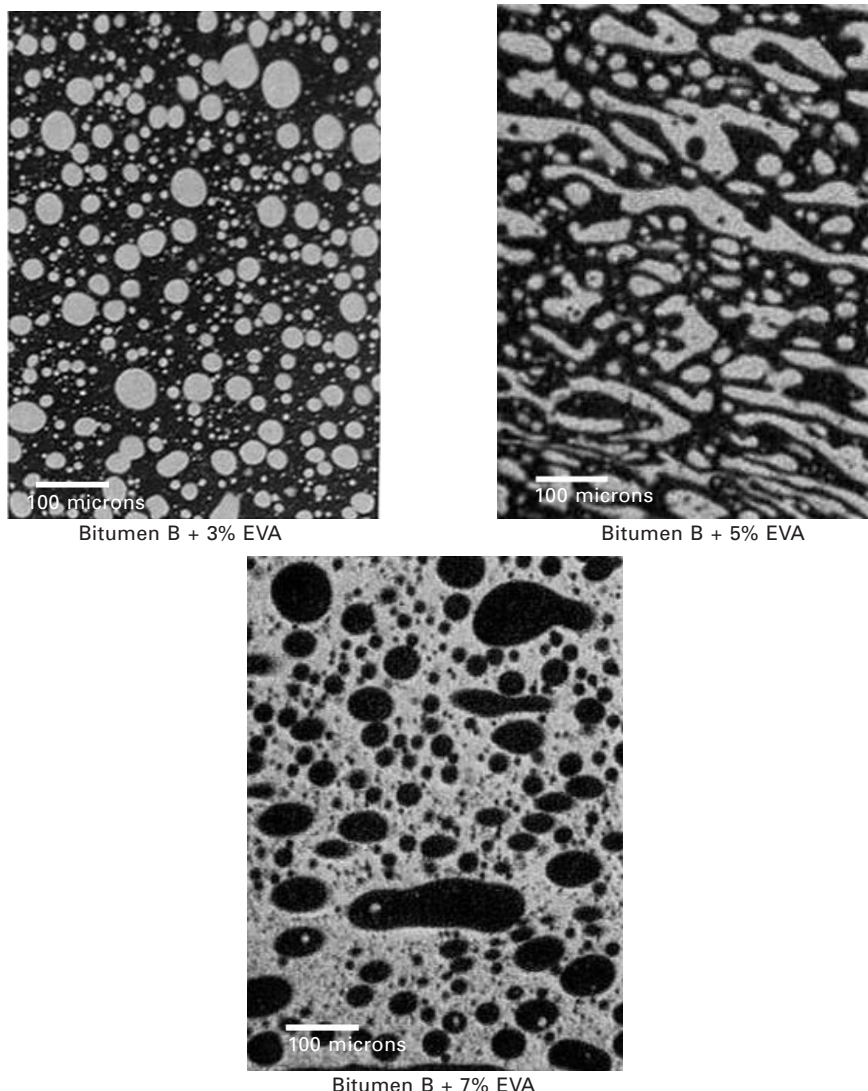
Fluorescent microscopy images of 5 wt% and 7 wt% SBS PMBs with Bitumens B and C, obtained using a Leitz Medilux microscope with incident UV light (wavelength between 420 and 490 nm) generated from a high-pressure 75 W Xenon lamp, are shown in Fig. 8.1. The images are typically produced at 25 \times to 400 \times magnification depending on the polymer structure (Wegan and Brule, 1999). The images clearly demonstrate the differences in the morphology of the SBS PMBs as a function of base bitumen type and polymer content. Fluorescent microscopy images of the EVA PMBs with Bitumen B at 100 \times magnification are also shown in Fig. 8.2. The fluorescent images show a change in the morphology of the PMBs as the polymer content increases. The image for the 3 wt% EVA PMB shows a continuous bitumen-rich phase with a dispersed polymer-rich phase, while the image for the 7 wt% EVA PMB shows the opposite with a continuous polymer phase with a dispersed bitumen phase. The image for the 5 wt% EVA PMB displays a relatively unstable, intertwined phase structure with neither phase dominating the overall system.

The different morphologies seen in Figs 8.1 and 8.2 are a function of the



8.1 Morphology of SBS PMBs.

swelling potential of the polymer (nature of the polymer), the nature of the base bitumen (composition of the maltene fraction), the polymer content of the PMB and the bitumen-polymer compatibility. The different morphological nature of PMBs will inevitably affect the rheological characteristics of these modified binders. PMBs that have a continuous polymer-rich phase generally produce polymeric-type modification rather than filler-type (stiffening) modification generally seen for continuous bitumen-phase PMBs.



8.2 Fluorescent images of EVA modified Bitumen B.

8.3 Conventional physical property tests

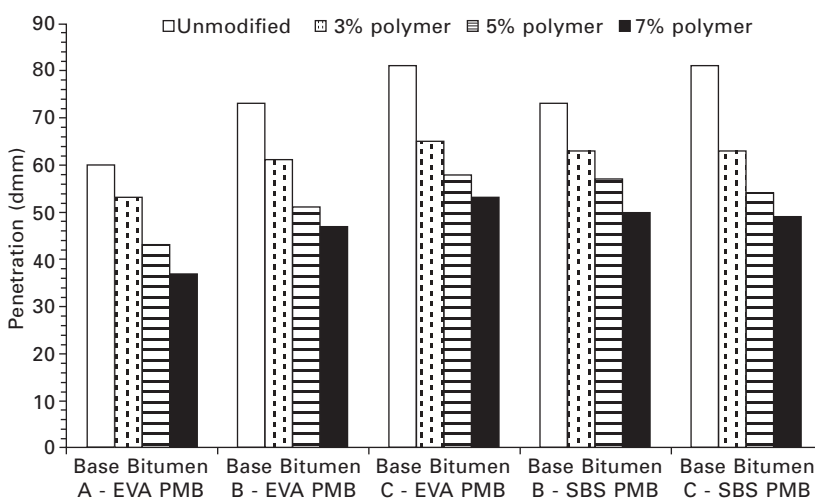
8.3.1 Penetration and softening point

Although penetration and softening point are empirically based tests, specifically used to determine the consistency of unmodified bitumens, they are still being used in practice to quantify the effects of polymer modification. The effects of polymer modification on various base bitumens in terms of

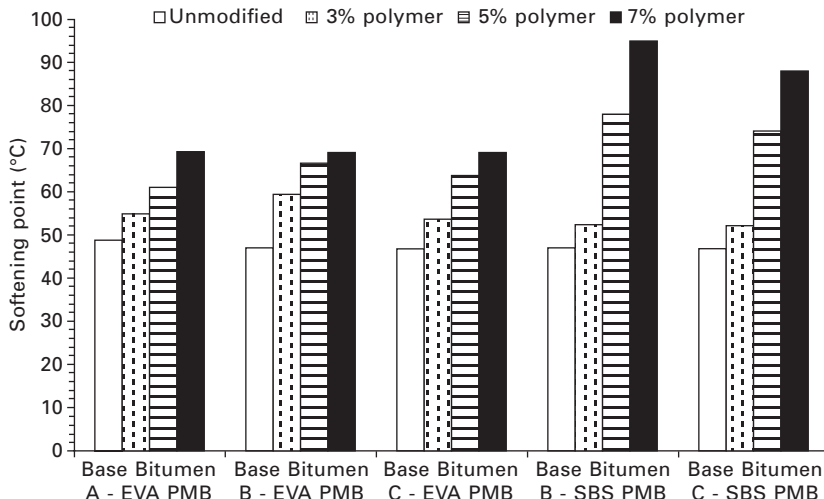
penetration (BS EN 1426) and softening point temperature (BS EN 1427) are shown in Figs 8.3 and 8.4. The results show very clearly that for all five PMB groups there is a decrease in penetration and an increase in softening point with increasing polymer content and subsequent polymer modification. This increase in binder hardness (decrease in penetration and increase in softening point) can be directly attributed to the stiffening effect caused by the addition of both the plastomeric polymer (EVA) as well as the elastomeric polymer (SBS) (Airey and Rahimzadeh, 2003).

Figure 8.3 illustrates that, although there are variations in the actual penetration values between the five PMB groups, no distinctive trends can be identified. The penetration test is therefore relatively insensitive to the morphology of the EVA and SBS PMBs, indicating a stiffening effect that could be accomplished through the addition of any 'filler'-type material, or even ageing of the base bitumen.

The information obtained from the softening point test provides a better insight into the relative effects of polymer modification. The results shown in Fig. 8.4 highlight differences in the increase in softening point for the EVA and SBS PMBs. The EVA PMBs show a relatively consistent increase in softening point as polymer content increases from 3 wt% to 7 wt%. However, for the SBS PMBs, the increase is relatively minor, approximately 10%, at the low polymer content, but shows a sharp increase at the 5 wt% level by approximately 60% and doubly when the polymer content is increased to 7 wt%. This 'S'-shaped curve for the two SBS PMBs indicates that below a certain SBS content, there is no continuous polymer network in the binder and the polymer simply acts as a filler, while at higher polymer contents



8.3 Penetration values of EVA and SBS PMBs.



8.4 Softening point values of EVA and SBS PMBs.

the polymer forms a complete network and the bitumen simply acts as an extender (Serfass *et al.*, 1992).

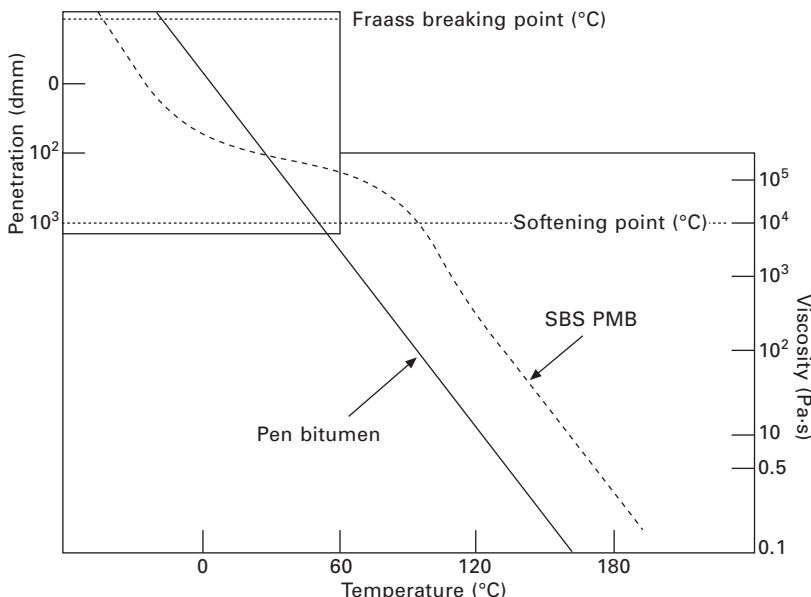
In addition to the increase in bitumen stiffness (decrease in penetration, increase in softening point), there is a significant reduction in temperature susceptibility with polymer modification as shown by an increase in penetration index (PI) (Pfeiffer and Van Doormal, 1936) in Table 8.2. However, it is important to note that unlike conventional, unmodified bitumen, the temperature susceptibility of PMBs is not constant over the entire temperature range normally associated with bituminous binders. This is illustrated in Heukelom's (1969) Bitumen Test Data Chart (BTDC) in Fig. 8.5, where the viscosity-temperature relationship for a typical SBS PMB can be compared to the linear relationship shown for a 'normal' penetration-grade bitumen. PI should therefore only be used as an indicator of the inherent temperature susceptibility of PMBs.

8.3.2 Empirical performance parameters

The low temperature fracture properties, cohesion and elasticity of the PMBs can be assessed by means of the Fraass breaking point (BS EN 12593), ductility (BS EN 13587) and elastic recovery (BS EN 13398) tests respectively. For the plastomeric polymers, the Fraass breaking point results show a reduction in low temperature flexibility with increasing modification, although the results for the Bitumen B EVA PMBs show consistent Fraass results before and after modification. All the ductility results show a decrease in ductility with EVA modification.

Table 8.2 Changes in conventional binder properties following EVA and SBS modification

Binder	Penetration Index (PI)	Fraass (°C) (BS EN 12593)	Ductility at 10°C (cm) (BS EN 13587)	Elastic recovery at 10°C (%) (BS EN 13398)
Bitumen A	-1.1	-18	21	-
3% EVA	0.1	-	13	-
5% EVA	0.9	-12	8	-
7% EVA	2.0	-11	5	-
Bitumen B	-1.1	-12	63	-
3% EVA	1.5	-	16	-
5% EVA	2.3	-13	20	-
7% EVA	2.5	-13	19	-
Bitumen C	-0.9	-28	130	-
3% EVA	0.4	-	22	-
5% EVA	2.2	-14	10	-
7% EVA	2.9	-10	12	-
Bitumen B	-1.1	-12	63	-
3% SBS	-0.1	-16	95	68
5% SBS	4.4	-15	99	76
7% SBS	6.1	-14	101	81
Bitumen C	-0.9	-28	130	-
3% SBS	-0.1	-18	81	71
5% SBS	3.7	-16	90	78
7% SBS	5.3	-14	81	80



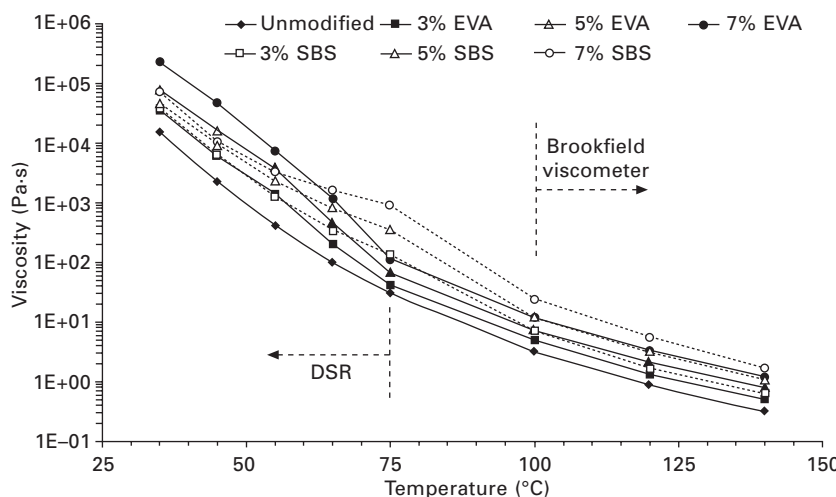
8.5 Idealised viscosity-temperature relationship for a polymer modified bitumen.

In terms of low temperature performance, the Bitumen B SBS PMBs show a slight improvement of low temperature flexibility as shown by a decrease in Fraass temperature. However, the opposite trend can be seen for the Bitumen C SBS PMBs. It is important to note that although the behaviour of the SBS PMBs relative to their respective base bitumens is different, the actual Fraass breaking point temperatures for each polymer content PMB pair are almost identical.

With regard to ductility and elastic recovery at 10°C, the results are again similar for the SBS PMB pairs, although the ductilities of the Bitumen B SBS PMBs are approximately 10–25% greater than those of Bitumen C. The Fraass and ductility results show the considerable influence of the base bitumen, the nature of the polymer and the base bitumen–polymer compatibility on the intermediate and low temperature physical properties of PMBs.

8.3.3 Viscosity of PMBs

Viscosities between 35°C and 140°C were obtained from DSR and rotational viscometer (Brookfield) measurements for Bitumen B EVA and SBS PMBs (Airey, 2001). These viscosity values measured were plotted against temperature, see Fig. 8.6, and show a consistent increase in viscosity with increasing polymer content for the EVA and SBS PMBs. As with the penetration and softening point tests, the viscosities give a clear indication of the stiffening effect of polymer modification. However, the wider temperature range of this viscosity–temperature plot allows a better rheological characterisation of the different PMBs than that available from the penetration and softening point tests.



8.6 Viscosity–temperature relation for EVA and SBS PMBs.

The viscosity-temperature relationships for the EVA and SBS PMBs show that polymer modification occurs at lower temperatures for the plastomeric EVA PMBs compared to the elastomeric SBS PMBs and at slightly lower magnitudes. The viscosity curves for the three EVA PMBs clearly indicate the melting (fusion) region of the EVA copolymer between 55°C and 75°C. Compared to the plastomeric, semi-crystalline EVA polymer, the melting range of the SBS copolymer occurs at higher temperatures between 75°C and 100°C (Isacsson and Lu, 1995; Airey and Brown, 1998) and therefore produces a distinctly different rheological behaviour. The presence of the SBS polymer network allows for a ‘plateau-like’ viscosity behaviour to be seen between 55°C and 75°C.

8.4 Advanced rheological characterisation

Empirical tests, such as penetration and softening point, and even the more fundamental tests such as Brookfield viscosity, do not provide a complete rheological characterisation of bitumen as they do not quantify the time-dependent response of the binder. This has led to the use of dynamic mechanical methods using oscillatory-type testing to fully characterise the rheological properties of bitumen. These tests are generally conducted under linear viscoelastic (LVE) conditions where the rheological response of the bitumen can be considered to be independent of stress and strain level.

These advanced rheological tests are undertaken using DSRs, which apply oscillating, sinusoidal shear stresses and strains to samples of bitumen sandwiched between parallel plates at different loading frequencies and temperatures. The sinusoidal stress and strain readings are then used to calculate various stiffness, viscosity and viscoelastic parameters that are used to build a complete picture of the rheological properties of the bitumen as a function of temperature and time of loading (or loading frequency).

The principal viscoelastic parameters that are obtained from the DSR are the complex shear modulus, G^* , and the phase angle, δ . G^* is defined as the ratio of maximum stress to maximum strain and provides a measure of the total resistance to deformation of the bitumen when subjected to loading. The phase angle is a measure of the viscoelastic balance of the bitumen behaviour. If δ equals 90° then the bitumen can be considered to be purely viscous in nature, whereas δ of 0° corresponds to purely elastic behaviour. Between these two extremes the material behaviour can be considered to be viscoelastic in nature with a combination of viscous and elastic responses.

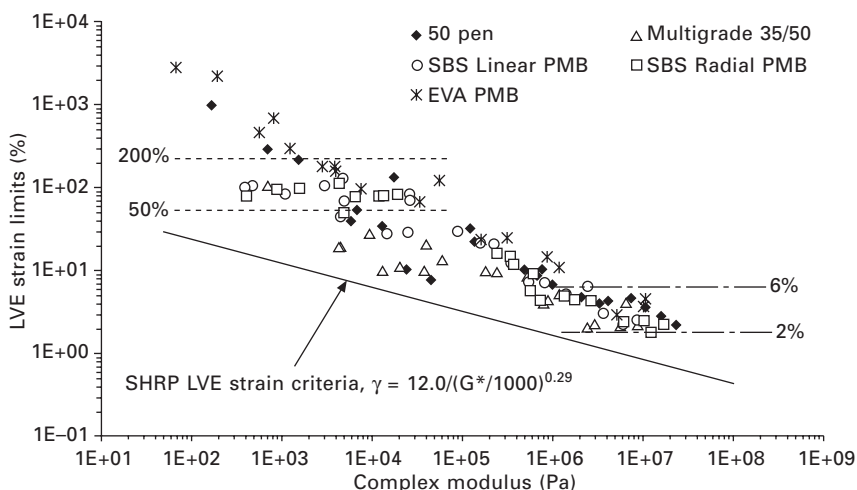
8.4.1 Linear viscoelastic response

In general, conventional bitumen possesses a relatively wide linear range (where the response is independent of the stress/strain magnitude). However,

due to the increased polymeric nature of PMBs, there is a possibility that the linear range for modified bitumen, particularly high polymer content PMBs, will show a narrower linear range. This assumption can be checked by subjecting the binders to a series of stress/strain sweeps at different temperatures and loading frequencies using DSR (Airey *et al.*, 2002). Using these stress/strain sweeps, the linearity limits for penetration-grade bitumen as well as different PMBs can be determined as a function of a percentage reduction in initial complex modulus. These LVE strain limits can then be plotted against the complex modulus to establish the boundary between linear and non-linear viscoelastic response.

The linear viscoelastic behaviour for both penetration-grade bitumens as well as EVA and SBS PMBs is shown in Fig. 8.7. As a function of complex modulus, the strain limits for the binders are all very similar. As would be expected, there is a general increase in the strain limit with a decrease in stiffness. The results show that for all the binders, including plastomeric EVA PMB and elastomeric SBS PMBs, there is a strain-dependent LVE criterion between 2% and 6% at high G^* values (>10 MPa). In addition, there is a second strain criterion between 50% and 200% for the SBS PMBs due to the presence of the dominant elastomeric polymer matrix at high temperatures which can be seen by the bifurcation of the data.

The linearity results provide clear evidence that sensibly engineered modified binders (softer base bitumens with higher modifier content) do not show narrower linear ranges and therefore lower linearity limits. The presentation of the LVE strain limits as a function of complex modulus removes any stiffening effect on the narrowing of the linear range so that



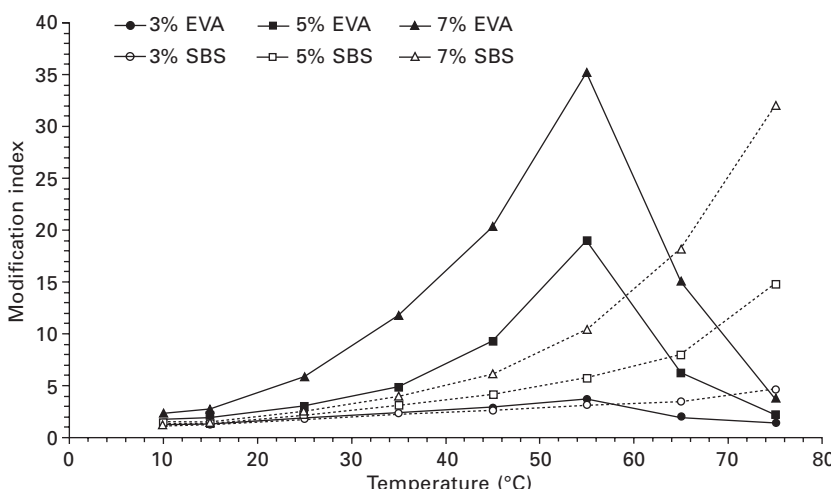
8.7 LVE strain limits as a function of G^* for conventional bitumens and PMBs.

any reduction in the linear limit can be attributed solely to the effect of modification.

8.4.2 DSR rheological parameters

Using G^* measurements at 0.02 Hz over a range of temperatures, modification indices ($G^*_{\text{modified}}/G^*_{\text{unmodified}}$) can be determined for Bitumen B EVA and SBS PMBs as shown in Fig. 8.8. The modification indices for the EVA PMBs show a peak modification at 55°C while the SBS PMBs show a continued increase in modification up to the maximum temperature of 75°C used with the DSR tests. The significance of 55°C for the EVA PMBs corresponds to the onset of crystalline melting of the EVA copolymer which reduces the impact of polymer modification, as seen by the reduction in modification index.

This thermal behaviour and melting of the EVA copolymer can also be characterised by means of differential scanning calorimetry (DSC) (Shutt *et al.*, 1993; Brule and Gazeau, 1996). A Mettler DSC 30 analyser, performed in its heating mode using a heating rate of 5°C per minute from 0 to 120°C, was used to determine the temperatures of the endothermic reactions linked to first-order transitions, associated with melting of the crystalline fractions of the EVA copolymer. Table 8.3 shows the temperature of fusion range for the nine EVA PMBs. The results show that the melting temperatures are dependent on the type of polymer and base bitumen but are generally insensitive to polymer content (Gazeau *et al.*, 1996). In addition, the DSC results support the DSR findings in terms of the melting range of the EVA PMBs and the associated maximum polymer modification.



8.8 Modification indices based on G^* at 0.02 Hz for EVA and SBS PMBs.

Table 8.3 Variations in DSC thermal ranges due to EVA modification

Binder	Temperature fusion range		
	Low temp (°C)	Peak temp (°C)	High temp (°C)
Bit A + 3% EVA	41	69.7	81
Bit A + 5% EVA	46	69.9	82
Bit A + 7% EVA	47	69.9	86
Bit B + 3% EVA	44	66.7	80
Bit B + 5% EVA	44	69.6	83
Bit B + 7% EVA	43	69.9	85
Bit C + 3% EVA	43	61.9	77
Bit C + 5% EVA	42	61.5	81
Bit C + 7% EVA	42	65.4	82

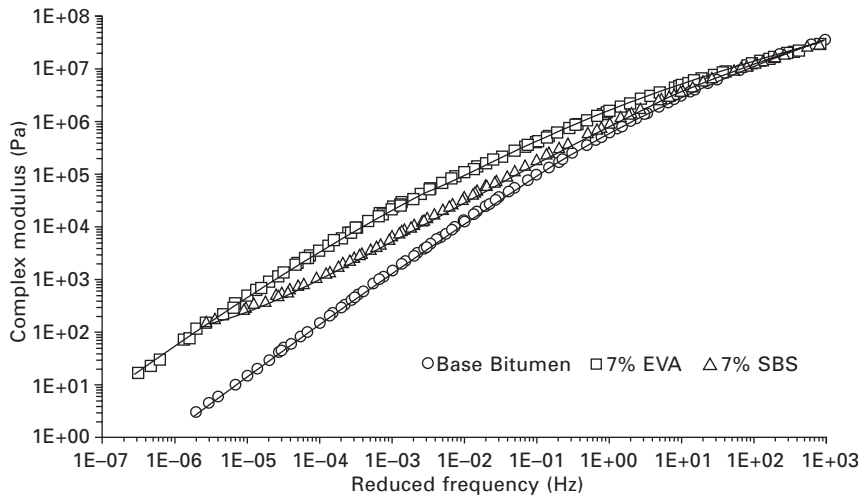
The pattern of modification for both the EVA and SBS PMBs in Fig. 8.8 agrees with that of Lenoble *et al.* (1993), where at low temperatures (<10°C), the complex moduli for a pure bitumen and various PMBs (EVA, EMA, SBS, etc.) are very similar and that most binders tend towards the same complex modulus at these low temperatures irrespective of the polymer and bitumen grade. As temperatures increase above 10°C, the influence of the polymer begins to appear and PMBs tend to show superior thermal susceptibility and enhanced rheological properties compared to pure bitumen.

Rheological data generated from the DSR can also be presented in the form of complex modulus and phase angle master curves (i.e. several isothermal plots shifted along the frequency axis to produce a smooth curve). The construction of master curves relies on the ability to shift rheological data through the equivalency between time and temperature (known as thermo-rheological simplicity) using a concept known as the time-temperature superposition principle (Ferry, 1980).

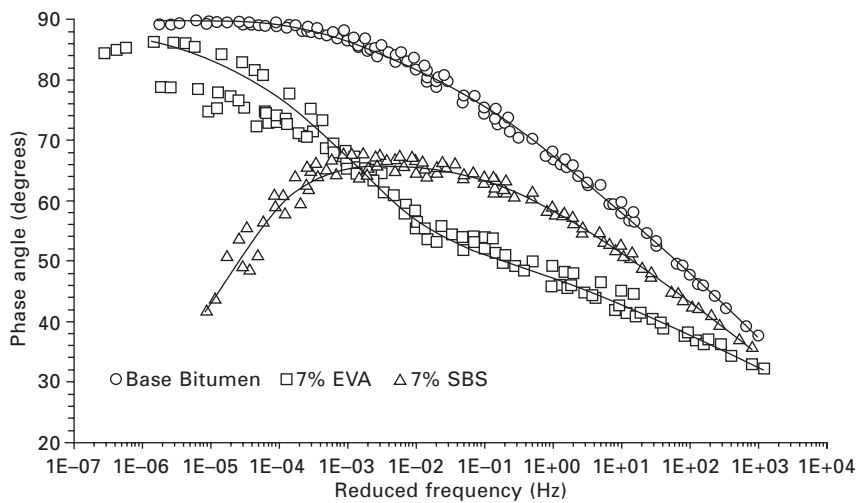
Master curves of complex modulus and phase angle for a base bitumen and EVA and SBS PMBs are shown in Figs 8.9 and 8.10. The graphs clearly show the increase in 'stiffness' (increased G^* values) as well as elastic response (decrease in δ values) for the PMBs. In addition, the graphs show the considerable differences in the precise rheological properties of the EVA and SBS PMBs. The increased elastic response of the PMBs (plastomers and elastomers) in terms of the rheological, viscoelastic balance of the binders should not be confused with the empirical, elastic recovery or elasticity (the ability of the binder to stretch and recover elastically) found only for the elastomeric SBS PMBs.

8.5 Ageing

Bitumen, like many other organic substances, is affected by the presence of oxygen, ultraviolet radiation and changes in temperature. These external



8.9 Complex modulus master curves at 25°C for EVA and SBS PMBs.



8.10 Phase angle master curves at 25°C for EVA and SBS PMBs.

influences result in the phenomenon known as 'ageing' and cause changes in the chemical composition and therefore the rheological and mechanical properties of bitumen (Petersen, 1984). Ageing is primarily associated with the loss of volatile components and oxidation of the bitumen during asphalt mixture production (short-term ageing) and progressive oxidation of the in-place material in the road (long-term ageing). Both factors cause an increase in viscosity (or stiffness) of the bitumen and consequential stiffening of the asphalt mixture.

Tests related to ageing of bitumen can be broadly divided into two categories, namely tests performed on neat bitumen and tests performed on asphalt mixtures. Much of the research into the ageing of bitumen utilises thin film oven ageing to age the bitumen in an accelerated manner. Typically, these tests are used to simulate the relative hardening that occurs during the mixing and laying process (i.e. short-term ageing). To include long-term hardening in the field, thin film oven ageing is typically combined with pressure oxidative ageing.

The most commonly used short-term ageing test is the rolling thin film oven test (RTFOT), standardised in BS EN 12607-1 and ASTM D2872. In the RTFOT, eight glass cylinders each containing 35 g of bitumen are fixed in a vertically rotating shelf. During the test, the bitumen flows continuously around the inner surface of each container in relatively thin films of 1.25 mm (Hveem *et al.*, 1963). The method ensures that all the bitumen is exposed to heat and air and the continuous movement ensures that no skin develops to protect the bitumen. The conditions in the test are not identical to those found in practice, but experience has shown that the amount of hardening in the RTFOT correlates reasonably well with that observed in a conventional batch mixer.

Long-term ageing of bitumen can be achieved using the pressure ageing vessel (PAV) developed to simulate the in-service oxidative ageing of bitumen in the field (Christensen and Anderson, 1992). The method involves hardening of bitumen in the RTFOT followed by oxidation of the residue in a pressurised ageing vessel. The PAV procedure (detailed in AASHTO R28-06) entails ageing 50 g of bitumen in a 140 mm diameter pan (approximately 3.2 mm binder film thickness) within the heated vessel, pressurised with air to 2.1 MPa for 20 hours at temperatures between 90 and 110°C. One of the main problems with the PAV procedure is the high temperature used with the test and the effect it may have on PMBs, particularly SBS modified products that undergo a phase transition (polystyrene block melting) at these temperatures (Phillips, 1997). An alternative long-term ageing procedure, known as the high pressure ageing test (HiPAT), developed from the PAV but with a lower temperature of 85°C and a longer exposure at 2.1 MPa of 65 hours compared to 20 hours, has been recommended to overcome the high temperature problems of the PAV (Hayton *et al.*, 1999). The HiPAT protocol has therefore been used to simulate long-term ageing of the base bitumens, EVA and SBS PMBs.

8.5.1 Ageing of conventional bitumen

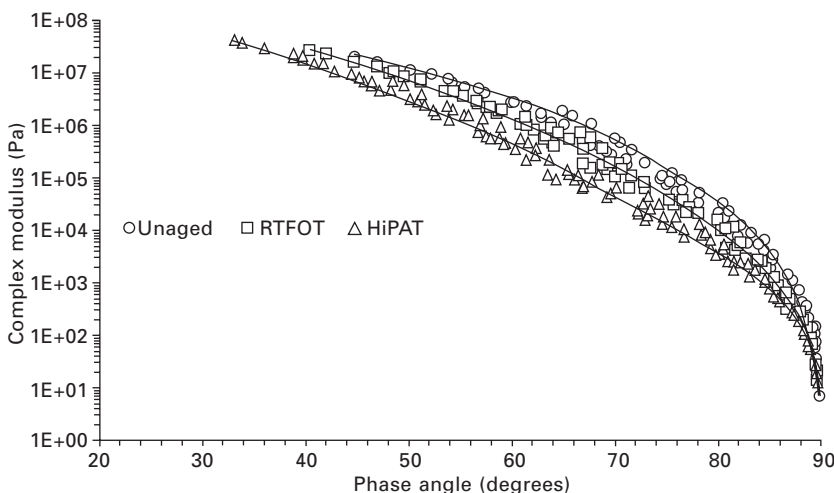
The three base bitumens were subjected to the RTFOT and HiPAT ageing protocols and showed a progressive hardening of the binders through a decrease in penetration and an increase in softening point temperature (Airey

and Brown, 1998). DSR tests were also performed on the short-term and long-term aged binders and the rheological data represented in the form of a Black diagram.

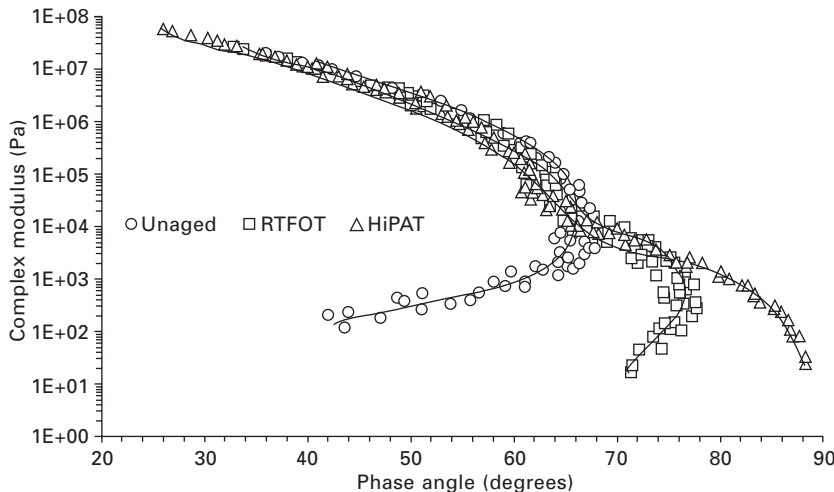
Figure 8.11 shows the unaged, RTFOT and HiPAT aged Black diagram for Bitumen C. The rheological data show a continuous shift of the curves towards lower phase angles after ageing. The shift in the Black diagram curves is caused by the dual action of an increase in complex modulus, indicating hardening of the bitumen, and a decrease in phase angle, indicating an increase in the elastic behaviour of the bitumen. The different magnitudes of these two actions result in the shifting of the Black diagram curves towards lower phase angle values for a given complex modulus. This very standard change in rheological performance following ageing can be compared to the changes experienced by the EVA and SBS PMBs.

8.5.2 Ageing of SBS PMBs

The effect of ageing on the rheological properties of SBS PMBs differs from that seen for conventional bitumens. The changes in the rheological characteristics of the 7 wt% SBS PMB with Bitumen B after ageing are also shown in the form of a Black diagram in Fig. 8.12. The rheological behaviour of the unaged, RTFOT and HiPAT aged SBS PMB can be divided into two areas above and below a complex modulus value of 10 kPa. At high stiffness values, corresponding to low temperature and high frequency tests, the Black diagram curves show a shift towards lower phase angles indicating the hardening (ageing) of the PMB. This phenomenon is similar to the hardening effect seen for penetration-grade bitumens.



8.11 Black diagram for unaged, RTFOT and HiPAT aged Bitumen C.



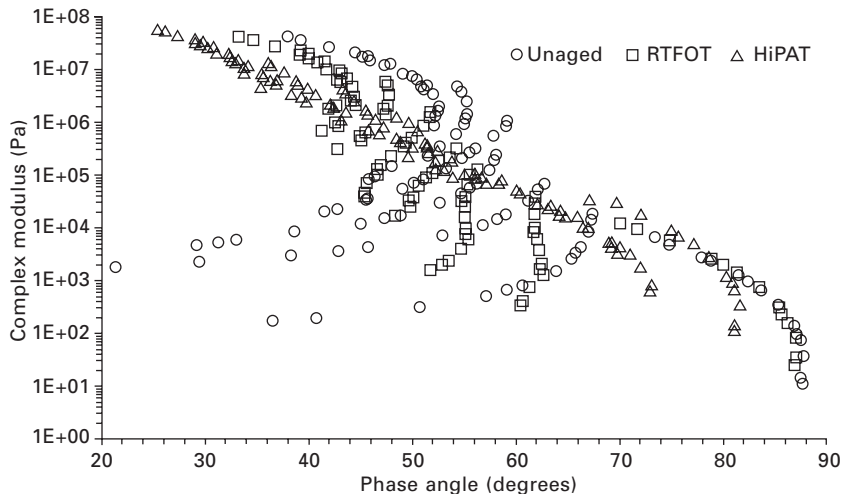
8.12 Black diagram for unaged, RTFOT and HiPAT aged 7 wt% SBS – Bitumen B.

The second area occurs below the complex modulus value of 10 kPa and shows an opposite shift of the curve towards higher phase angles rather than lower phase angles, thereby indicating a change towards a more viscous rather than a more elastic response after ageing. This change towards a more viscous response after ageing ('softening' of the PMB) can be attributed to the degradation of the SBS polymer during ageing.

This degradation, or change in the molecular weight of the SBS polymer, can be quantified by gel permeation chromatography (GPC) (Airey and Brown, 1998; Linde and Johansson, 1992; Kuppens, 1995) and is associated with the oxidation of the sensitive double bonds in the butadiene part of the copolymer. GPC analysis allows changes in the molecular weight distribution of both the polymer and bitumen phases to be identified. Generally, the SBS copolymer degrades to a lower molecular size after RTFOT ageing, with a further degradation after HiPAT ageing. The opposite is true for the bitumen phase, which shows an increase in the larger molecular size fractions (asphaltenes) after ageing. Another factor that may be responsible for the changes in rheological properties of SBS PMBs after ageing is alterations to the compatibility between the base bitumen and polymer after oxidation.

8.5.3 Ageing of EVA PMBs

The rheological data for the unaged, RTFOT and HiPAT aged 7 wt% EVA PMB with Bitumen B are shown in the form of a Black diagram in Fig. 8.13. Unlike the regular shifting of the Black diagram curves towards lower phase angles for the unmodified bitumens after ageing, the changes in the Black

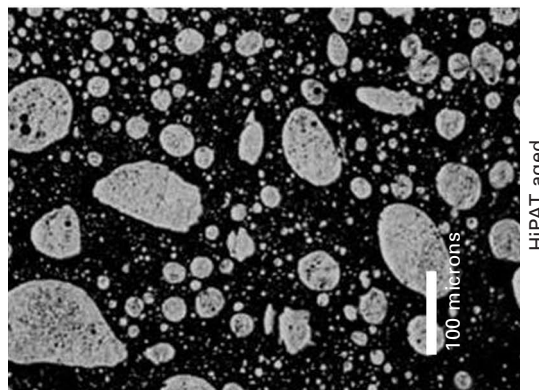


8.13 Black diagram for unaged, RTFOT and HiPAT aged 7 wt% EVA – Bitumen B.

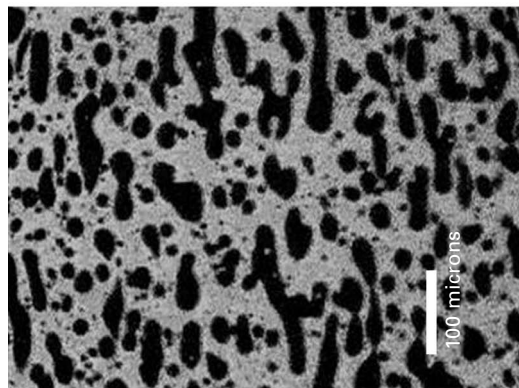
diagram with ageing for the EVA PMB are considerably more complex. Similar shifts towards lower phase angles after ageing do occur at G^* values greater than 10 MPa where the bitumen phase can be considered to have a greater influence on the rheological character of the PMB. However, at G^* values less than 10 MPa, the Black diagram curves show a significant alteration in the rheological behaviour of the EVA PMB. These rheological changes consist of the G^* versus δ waves, associated with different EVA crystalline structures at different temperatures, changing their shape and orientation with ageing. Fluorescent microscopy images for the unaged, RTFOT and HiPAT aged binders in Fig. 8.14 show changes in the morphology of the EVA PMBs with laboratory ageing. These changes in phase structure manifest themselves as alterations in the rheological characteristics of the aged EVA PMBs which differs from that seen for penetration-grade bitumens.

8.6 Asphalt mixture performance

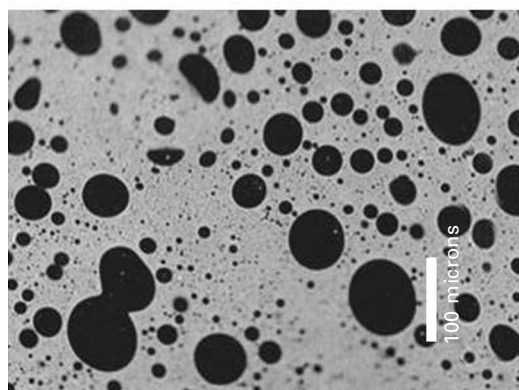
Performance improvements, in terms of reduced permanent deformation and increased fatigue cracking resistance, of asphalt mixtures incorporating PMBs can be demonstrated using standard asphalt mixture laboratory tests. In the UK, this means using either wheel tracking (permanent deformation) and flexural beam (fatigue) tests or the permanent deformation and fatigue testing modules associated with the Nottingham Asphalt Tester (NAT). The NAT was developed in the mid 1980s at the University of Nottingham in response to the need for rapid, economical test methods to measure key mechanical properties of asphalt mixtures under repeated loading conditions



HiPAT aged



RTFOT aged



Unaged

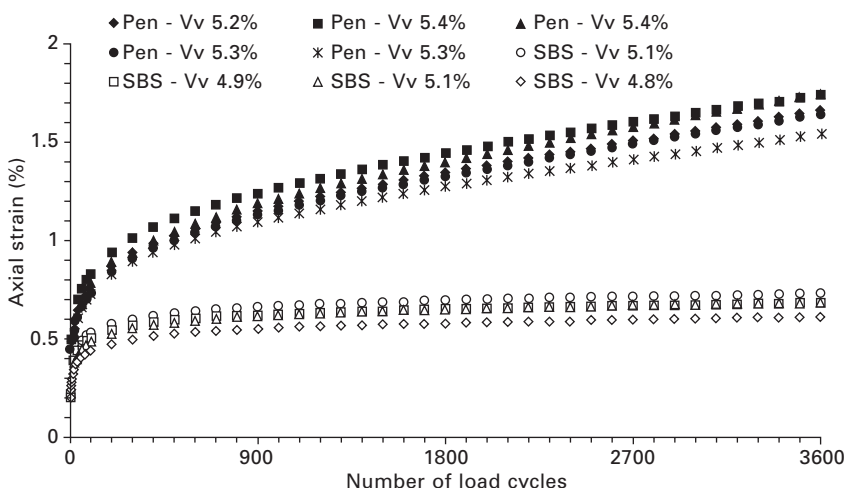
8.14 Morphology of unaged, RTFOT and HiPAT aged 7 wt% EVA - Bitumen B.

(Cooper and Brown, 1989; Brown and Cooper, 1993). It was designed to carry out tests on either 100 mm or 150 mm diameter specimens which could be produced either by moulding (compaction) in the laboratory or by coring from pavements. The NAT comprises a pneumatic loading system, a rigid test frame manufactured from stainless steel and a series of sub-systems (loading modules) that can be used to perform indirect tensile and direct compression tests (Brown and Cooper, 1993; Brown *et al.*, 1994). Data acquisition and control are computerised and the entire system is located in a temperature-controlled unit.

8.6.1 Permanent deformation response

The permanent deformation responses of two asphalt mixtures, using the direct, uniaxial compression configuration of the repeated load axial test (RLAT), are shown in Fig. 8.15. The two asphalt materials consist of a stone mastic asphalt (SMA) aggregate gradation with an unmodified, control 40/60 penetration-grade bitumen and a 7 wt% SBS PMB. The RLA tests were performed under the following test conditions:

- Test temperature: 50°C
- Test duration: 7200 seconds (3600 cycles)
- Load pattern: 1 second loading followed by 1 second rest period
- Axial stress: 100 kPa
- Conditioning stress: 10 kPa for 600 seconds.



8.15 RLAT axial strain versus load applications for unmodified and SBS modified asphalt mixtures at 50°C.

The plots in Fig. 8.15 show the accumulation of permanent strain for five SMA 40/60 pen test specimens and four SMA SBS PMB asphalt specimens and clearly indicate a superior resistance to permanent deformation for the SBS modified asphalt mixture (Airey, 2004). In addition to the comparison of ultimate percentage strain after 3600 load cycles, the slopes (micro-strain or percent strain per cycle) associated with axial strain versus load cycles between 900 and 3600 cycles can be used to compare the relative performance between the control and SBS polymer modified asphalt mixture. The mean strain rate ($\mu\text{e}/\text{cycle}$) is generally considered to be a more reliable measure of the rutting performance of the asphalt mixtures as this parameter, unlike the ultimate strain, is independent of the initial strain experienced during the RLAT test. The results in Fig. 8.15 clearly show the superior rutting resistance of the modified asphalt mixture as demonstrated by lower values of ultimate strain and strain rate (slope) compared to the control mixture.

8.6.2 Fatigue cracking resistance

The fatigue properties of the unmodified and SBS polymer modified asphalt mixtures were determined using the NAT indirect tensile fatigue test (ITFT) with the following test parameters:

- Test temperature: 20°C
- Loading condition: controlled stress
- Loading rise-time: 124 milliseconds
- Load pulse rate: 40 pulses/minute (1500 ms between pulses)
- Failure indication: 9 mm vertical deformation.

The maximum tensile strain $\varepsilon_{\text{xmax}}$ determined as a function of maximum tensile stress at the centre of the specimen, σ_{xmax} , Poisson's ratio, ν , and the indirect tensile stiffness modulus at σ_{xmax} , S_m , is defined as:

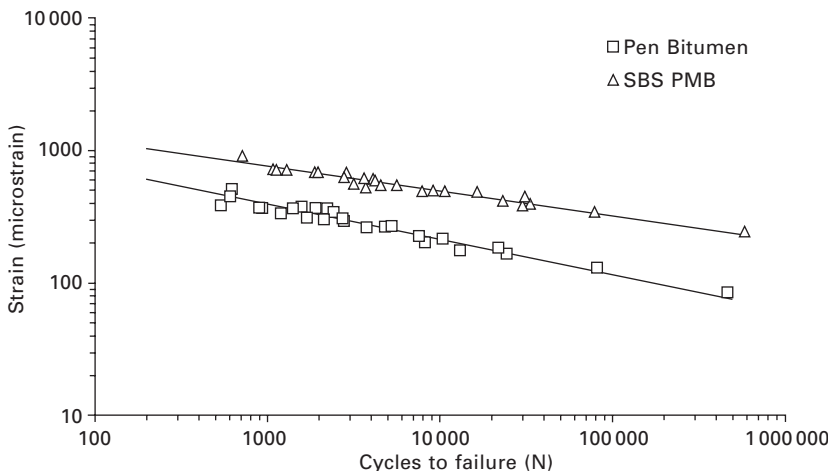
$$\varepsilon_{\text{xmax}} = \frac{\sigma_{\text{xmax}}(1 + 3\nu)}{S_m} \times 1000 \quad 8.1$$

Using linear regression analysis of the ITFT results, fatigue functions for the control and SBS modified asphalt mixtures can be determined in the following form:

$$N_f = a\varepsilon_0^{-b} \quad 8.2$$

where N_f is fatigue life, ε_0 is the initial tensile strain (micro-strain), and a and b are experimentally determined coefficients.

The fatigue functions, together with the raw fatigue data, for SMA 40/60 pen and SMA SBS PMB mixtures are presented in Fig. 8.16. In terms of the fatigue performance of the different asphalt mixtures, the fatigue functions



8.16 Fatigue functions for unmodified and SBS modified asphalt mixtures.

clearly show the superior fatigue performance of the polymer modified asphalt mixture.

8.7 Conclusions

Whether conventional binder tests or more advanced rheological methods are used, the conclusions are the same in that polymer modification enhances the rheological properties of bitumen by increasing viscosity, complex modulus and elastic response. Conventional penetration, softening point, Fraass, ductility, elastic recovery and high-temperature viscosity tests have shown increased stiffness and improved temperature susceptibility of both elastomeric and plastomeric PMBs. However, dynamic shear rheometry, differential scanning calorimetry, gel permeation chromatography and fluorescent imaging have been required to identify the complex changes in morphology, chemistry and rheology associated with semi-crystalline EVA PMBs and styrenic block SBS PMBs. With regard to polymer modification, the results have shown the changes in morphology with increasing modification from bitumen phase-dominant systems to polymer phase-dominant systems. The DSR results have identified the formation of different crystalline structures at different temperatures for the semi-crystalline EVA PMBs and the enhanced high temperature/low frequency elastic response of the SBS PMBs.

The effects of laboratory simulated ageing have been shown to differ amongst the penetration-grade bitumens, EVA and SBS PMBs. The effect of oxidative ageing for the penetration-grade bitumens has been seen as an increase in stiffness and elastic response. However, the effects of laboratory

ageing for the EVA and SBS PMBs consist of a considerably more complex change in the binder's chemical nature, morphology and, consequently, rheological characteristics. The extent of these changes is dictated not only by the type and nature of the polymer but also by the polymer content and the compatibility between the polymer and base bitumen.

Using both elastomeric and plastomeric PMBs in asphalt mixtures provides a means of increasing the resistance of the mixture to the distress mechanisms of both permanent deformation and fatigue cracking.

8.8 Sources of further information and advice

Forde, M. (ed.) (2009) *ICE Manual of Construction Materials, Volume 1, Asphalts in Road Construction*, Thomas Telford, ISBN: 978-0-7277-3642-0.

This book gives an excellent coverage of asphalts in road construction, including recent developments in asphalt technology such as stone mastic asphalt, thin surfacings, and high modulus bases. As well as covering the materials themselves, it deals with the design and maintenance of asphalt mixtures, production, laying and compaction of asphalt, and cold and warm asphalt mixtures.

Read, J.M. and Whiteoak, C.D. (2003) *The Shell Bitumen Handbook*, Shell UK Oil Products Limited, ISBN: 0 7277 3220 X.

Essential reading if you want to get to grips with the fundamentals of bitumen. It deals with the structure and constitution of bitumen, as well as polymer modified bitumens, and goes on to link this to the engineering properties. The book also covers the design and testing of asphalt mixtures as well as pavement design.

Thom, N.H. (2008) *Principles of Pavement Engineering*, Thomas Telford, ISBN: 978-0-7277-3480-8.

This excellent book sets out the material needed to equip practising engineers as well as students with the fundamental understanding needed to undertake the design and maintenance of all pavement types. The book contains theoretical concepts that are presented in a way that is easily understood together with quantitative material to illustrate the key issues.

Domone, P. and Illston, J. (ed.) (2010) *Construction Materials: Their Nature and Behaviour*, Spon's Press, Taylor & Francis, ISBN: 0-415-46515-X.

A comprehensive textbook on all aspects of bituminous materials, including polymer modified bitumens and sustainable issues surrounding recycling of road pavements.

8.9 References

Airey GD (2001), 'Viscosity-temperature effects of polymer modification as depicted by Heukelom's bitumen test data chart', *International Journal of Pavement Engineering*, 2, 223–242.

Airey GD (2002), 'Rheological evaluation of ethylene vinyl acetate polymer modified bitumens', *Construction and Building Materials*, 16, 473–487.

Airey GD (2003), 'Rheological properties of styrene butadiene styrene polymer modified road bitumens', *Fuel*, 82, 1709–1719.

Airey GD (2004), 'Fundamental binder and practical asphalt mixture evaluation of polymer modified bituminous materials', *International Journal of Pavement Engineering*, 5, 137–151.

Airey GD and Brown SF (1998), 'Rheological performance of aged polymer modified bitumens', *Asphalt Paving Technology*, 67, 66–100.

Airey GD and Rahimzadeh B (2003), 'Empirical and fundamental rheological properties of polymer modified bitumens', *Proc. 6th International RILEM Symposium on Performance Testing and Evaluation of Bituminous Materials*, Zurich, 102–109.

Airey GD, Rahimzadeh B and Collop AC (2002), 'Linear viscoelastic limits of bituminous binders', *Asphalt Paving Technology*, 71, 89–115.

Bardesi A (1999), 'Use of modified bituminous binders, special bitumens and bitumens with additives in pavement applications', Technical Committee Flexible Roads (C8), World Road Association (PIARC), 3.

Brown SF and Cooper KE (1993), 'Simplified methods for determination of fundamental material properties of asphalt mixes', *Proc. International Conference on SHRP and Traffic Safety on Two Continents*, The Hague, 87–105.

Brown SF, Rowlett RD and Boucher JL (1990), 'Asphalt modification', *Proc. Conference on US SHRP Highway Research Program: Sharing the Benefits*, ICE, London, 181–203.

Brown SF, Cooper KE, Gibb JM, Read JM and Scholz TV (1994), 'Practical tests for mechanical properties of hot mix asphalt', *Proc. 6th Conference on Asphalt Pavements for Southern Africa*, Cape Town, 2, IV-29–IV-45.

Brule B (1996), 'Polymer-modified asphalt cements used in the road construction industry: basic principles', *Transportation Research Record 1535*, National Research Council, 48–53.

Brule B and Gazeau S (1996), 'Characterisation of rheological and thermal behaviour of asphalt cements modified by ethylene copolymers', *Proc. ACS Symposium on Modified Asphalts*, Orlando, FL, 131–147.

Brule B, Brion Y and Tanguy A (1988), 'Paving asphalt polymer blends: relationship between composition, structure and properties', *Asphalt Paving Technology*, 57, 41–64.

Bull AL and Vonk WC (1984), 'Thermoplastic rubber/bitumen blends for roof and road', Shell Chemical Technical Manual TR 8, 15.

Cavaliere MG, Diani E and Vitalini Sacconi L (1993), 'Polymer modified bitumens for improved road application', *Proc. 5th Eurobitume Congress*, Stockholm, 1A, 138–142.

Christensen DW and Anderson DA (1992), 'Interpretation of dynamic mechanical test data for paving grade asphalt cements', *Asphalt Paving Technology*, 61, 67–116.

Collins JH, Bouldin MG, Gelles R and Berker A (1991), 'Improved performance of paving asphalts by polymer modification', *Asphalt Paving Technology*, 60, 43–79.

Cooper KE and Brown SF (1989), 'Developments of a simple apparatus for the measurement of the mechanical properties of asphalt mixes', *Proc. Eurobitume Symposium*, Madrid, 494–498.

Diehl CF (2000), 'Ethylene–styrene interpolymers for bitumen modification', *Proc. 2nd Eurasphalt and Eurobitume Congress*, Barcelona, 2, 93–102.

Ferry JD (1980), *Viscoelastic Properties of Polymers*, John Wiley & Sons, New York, 271.

Gazeau S, Maze M, Brule B and Perret P (1996), 'Application of differential scanning calorimetry (DSC) to the characterisation of ethylene copolymers modified bitumen', *Proc. Eurasphalt and Eurobitume Congress*, Strasbourg, 142–151.

Goodrich JL (1991), 'Asphaltic binder rheology, asphalt concrete rheology and asphalt concrete mix properties', *Asphalt Paving Technology*, 60, 80–120.

Goos D and Carre D (1996), 'Rheological modelling of bituminous binders: a global approach to road technologies', *Proc. Eurasphalt and Eurobitume Congress*, Strasbourg, 39–51.

Hayton B, Elliott RC, Airey GD and Rayner CS (1999), 'Long term ageing of bituminous binders', *Proc. Eurobitume Workshop on Performance Related Properties for Bituminous Binders*, Paper 126, Luxembourg.

Heukelom W (1969), 'A Bitumen Test Data Chart showing the effect of temperature on the mechanical behaviour of asphaltic bitumens', *Journal of the Institute of Petroleum Technologists*, 55, 404–417.

Hveem FN, Zube E and Skog J (1963), 'Proposed new tests and specifications for paving grade asphalts', *Asphalt Paving Technology*, 32, 247–327.

Isacsson U and Lu X (1995), 'Testing and appraisal of polymer modified road bitumens – state of the art', *Materials and Structures*, 28, 139–159.

Kuppens EAM (1995), 'Ageing resistance of bitumen', *Proc. Rheology of Bituminous Binders European Workshop*, Eurobitume, Paper No. 49, Brussels.

Lenoble C, Vercoe T and Soto T (1993), 'Rheology as a performance indicator for modified bitumen', *Proc. 5th Eurobitume Congress*, Stockholm, 71–75.

Linde S and Johansson U (1992), 'Thermo-oxidative degradation of polymer modified bitumen', in *Polymer Modified Asphalt Binders*, editors K.R. Wardlaw and S. Shuler, ASTM STP 1108, 244–253.

Petersen JC (1984), 'Chemical composition of asphalt as related to asphalt durability: State of the art', *Transportation Research Record* 999, National Research Council, 13–30.

Pfeiffer JPh and Van Doornal PM (1936), 'The rheological properties of asphaltic bitumens', *Journal of the Institute of Petroleum*, 22, 414.

Phillips MC (1997), 'Developments in specifications for bitumens and polymer modified binders, mainly from a rheological point of view', *Proc. 2nd European Symposium on the Performance and Durability of Bituminous Materials*, Leeds, 3–18.

Serfass JP, Joly A and Samanos J (1992), 'SBS-modified asphalts for surface dressing – a comparison between hot-applied and emulsified binders', in *Polymer Modified Asphalt Binders*, editors K.R. Wardlaw and S. Shuler, ASTM, STP 1108, 281–308.

Shutt R, Turmel C and Touzard B (1993), 'Differential scanning calorimetry analysis and rheological properties of bitumens modified by semi-crystalline polymers', *Proc. 5th Eurobitume Congress*, Stockholm, 1A, 76–80.

Wegan V and Brule B (1999), 'The structure of polymer modified binders and corresponding asphalt mixtures', *Asphalt Paving Technology*, 68, 64–88.

Ageing of polymer modified bitumen (PMB)

J.-Y. YU, Z.-G. FENG and H.-L. ZHANG,
Wuhan University of Technology, P. R. China

Abstract: To realize the ageing of polymer modified bitumens (PMBs) correctly is of great significance for academicians and technicians. This chapter begins by discussing the main causes of ageing for PMBs. It then illustrates simulative ageing methods, ageing performance and characterization, as well as the means for improving the ageing resistance of PMBs. The chapter finally outlines a short commentary on likely future trends and provides some sources of further information and advice.

Key words: polymer modified bitumen, thermal-oxidative ageing, photo-oxidative ageing, simulative ageing methods, ageing performance and characterization.

9.1 Introduction

Polymer modified bitumens (PMBs) are widely used in many aspects of infrastructural construction, such as in pavements, waterproofing and protective coats. One of the most important uses of PMBs is for pavement construction due to their excellent road performance. However, the physical and chemical characteristics of PMBs are believed to be easily changeable during production, storage, transportation, mixing with aggregates, laying and compaction, and in-service life because of the inevitable contact with the natural environment (oxygen, heat and light, etc.). The interactions during these processes, such as bitumen oxidation, polymer degradation, dehydrogenation, loss of volatiles and physical hardening, may cause PMBs to become stiff, brittle and easily damaged. All these result in irreversible changes in physicochemical properties, mechanical performance and structural features, and all contribute to the ageing of PMBs.

Ageing of PMBs, consequently, may cause great damage to pavements and lead to many distresses, such as fatigue cracking, pot holes and so on. To prevent deterioration pavements need to be maintained and this costs a lot of money globally every year. Therefore, it is of much significance to comprehend the ageing of PMBs correctly, seek new insight so as to enhance the durability of PMBs and prolong the service life of pavements.

This chapter, for this purpose, mainly discusses why ageing of PMBs

occurs and how to simulate the ageing processes, and evaluate the ageing characteristics of PMBs under laboratory conditions, and what means can be used to improve the ageing resistance of PMBs. Moreover, a short commentary on likely future trends is also contained in this chapter. Finally, sources of further information and advice, including some key books and major trade/professional bodies, are provided.

9.2 Main causes of ageing for polymer modified bitumens (PMBs)

Ageing of PMBs can be classified into three stages: the period of storage and transportation, the mixing and laying process, and long-term in-service life. The ageing evolution of each stage can be judged by comparing the performance-related properties of aged PMBs with unaged PMBs. Heat, ultraviolet (UV) light, oxygen or a combination of these factors were the principal factors causing ageing of PMBs and deterioration of bituminous pavement (Lu and Isacsson, 2002; Mouillet *et al.*, 2008a; Wu *et al.*, 2010). In terms of what initiates ageing, PMBs can be classified into two main categories: thermal-oxidative ageing and photo-oxidative ageing.

9.2.1 Thermal-oxidative ageing

As a kind of organic material, PMBs are easily to be aged under the influence of heat and oxygen. The thermal-oxidative ageing takes place mostly during the first two stages (i.e. the period of storage and transportation, mixing and laying process). During the first stage, PMBs are kept in the storage tank. Though the temperature of the storage tank is high (about 170°C), the degree of ageing of PMBs is very weak at this stage because the storage tank is airtight and there is little oxygen contacting the surface of the PMBs (Anon., 1995). In the mixing and laying process, the aggregates are coated with a thin layer of PMB film that is about 5–15 µm thick. At the same time, the mixing temperature is often up to 160–180°C, which may cause the rapid oxidation of bitumen, as well as the degradation of some polymers. As a result, the properties of PMBs deteriorate significantly after the process of mixing and laying, which consequently can be recognized as one of the main stages of bitumen ageing.

It is believed by most researchers that the temperature as well as the duration of time plays an important role in determining the extent of ageing of PMBs (Ruan *et al.*, 2003a, 2003b). Lau *et al.* (1992) found that both hardening rate (r_η) and oxidation rate (r_{CA}) could be described by an Arrhenius equation:

$$r_a = A_a \exp\left(\frac{-E}{RT}\right) \quad 9.1$$

where A_a is the pre-exponential factor; E is the activation energy of the oxidation reaction (J/mol); $R = 8.314$ J/mol·K; T is the temperature (K); and subscript a = η or CA.

Table 9.1 shows the effect of temperature on the hardening rate or oxidation rate of base and modified bitumens. It can be easily observed that the value of r_η and r_{CA} increases with the rise of temperature, indicating a rapid hardening rate or oxidation rate at high temperatures. The bitumen modified by styrene–butadiene rubber (SBR) or styrene–butadiene–styrene (SBS) exhibits a slower hardening rate or oxidation rate than base bitumen with no relevance to temperature (Ruan *et al.*, 2003b).

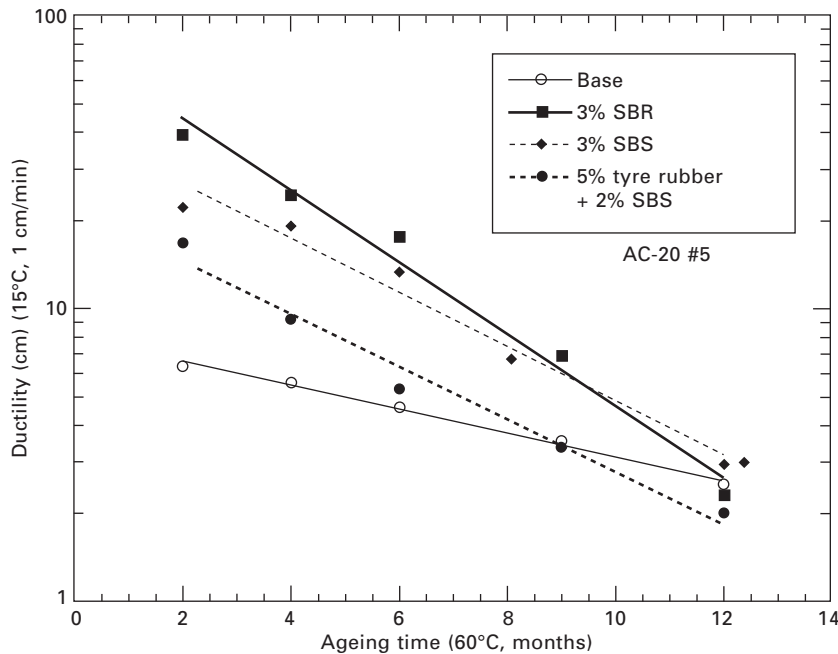
Ruan *et al.* (2003a) also conducted the experiment examining the effect of time on oxidative ageing of different PMBs as shown in Fig. 9.1. It can be found that the ductility of base bitumen and PMBs decreased obviously with the extension of ageing time. However, the ductility of modified bitumens decreased more dramatically than that of the base bitumen, and some modified bitumens showed lower ductility value than the base bitumen after 12 months of ageing.

From a chemical point of view, thermal-oxidative ageing is a very complex process in normal bitumens due to their high molecular weight and complex chemical composition; the complexity increases when polymers are incorporated into the bitumen (Lu and Isacsson, 1998). As for PMBs, the mechanisms of thermal-oxidative ageing are influenced by the characteristics of bitumen and polymer, as well as the molecular interactions between the two components. Studies indicated that the thermal-oxidative ageing of SBS modified bitumen was associated with the degradation of the SBS polymer and oxidation of bitumen, leading to a decrease in polymer molecular weight and an increase in the content of polar oxygen-containing molecules and bitumen molecular weight. Therefore, the general trend for SBS modified

Table 9.1 Effect of temperature on the hardening rate (r_η) or oxidation rate (r_{CA}) of base bitumen and PMBs

Property	Temperature (°C)	Base	2 wt% SBR	3 wt% SBR	3 wt% SBS
r_η	60	0.00821	0.00459	0.00372	0.00510
	204	22.752	9.984	13.080	11.688
r_{CA}	60	0.00153	0.00093	0.00093	0.00102
	204	1.330	0.912	1.661	1.388

Source: adapted with permission from Ruan Y H, Davison R R and Glover C J (2003), 'Oxidation and viscosity hardening of polymer-modified asphalts', *Energy and Fuels*, 17, 991–998. © 2003 American Chemical Society.



9.1 Decreases in ductility with ageing time.

bitumens was that the binders became more homogeneous upon ageing (Lu and Isacsson, 1998, 2000; Wu *et al.*, 2009). For ethylene vinyl acetate (EVA) modified bitumen, however, the binder became less homogeneous upon ageing due to lower compatibility between the EVA polymer chains and oxidized bitumen molecules. The main reason for the ageing of EVA modified bitumen was oxidative hardening of the base bitumen with the EVA polymer remaining stable under ageing (Mouillet *et al.*, 2008b).

9.2.2 Photo-oxidative ageing

Sunlight, especially the UV radiation, may affect the upper layer of a pavement surface, causing the bitumen to become harder and more brittle and to adhere less. Photo-oxidative ageing is a form of long-term ageing that occurs throughout the service life of pavements in which ageing happens a little faster during the first two to three years of use on the pavement and becomes much slower after this. The studies showed that the principal factors that influence photo-oxidative ageing of PMBs are the wavelength of light, PMB film thickness and the intensity of UV radiation (Wu *et al.*, 2010; Yamaguchi *et al.*, 2005).

It is well known that the wavelength of UV light ranges from 200 to 400 nm. Nevertheless, the wavelength of UV light reaching the surface of the

earth is often 290 to 400 nm due to the absorption of UV light (200–290 nm) by the aerosphere. Whether or not PMBs, exposed under the light radiation, suffer oxidation and degradation depends on the energy of chemical bonds and light of different wavelengths. The light energy at different wavelengths is shown in Table 9.2. The energy of different chemical bonds in bitumen is shown in Table 9.3. As can be seen from Tables 9.2 and 9.3, the energy of UV light (wavelength 290–400 nm) is higher than that of some of chemical bonds found in bitumen, and these can break such chemical bonds in PMBs. Therefore, PMBs are easily aged by the action of UV radiation.

The degree of photo-oxidative ageing is most severe at the surface of the bitumen layer and decreases with increasing depth. It was found that the degree of degradation worsened towards the surface of the bitumen layer, and rapidly increased in the thickness range below 200 μm (Yamaguchi *et al.*, 2005). Consequently, increasing the film thickness by increasing the bitumen content in asphalt mixtures, even if only slightly, would improve the durability of pavements due to the prevention of photo-degradation of bitumen.

The intensity of UV radiation is also a critical factor in determining the extent of bitumen ageing. Wu *et al.* (2010) investigated the influence of intensity of UV radiation on the viscosity of AH-70 bitumen (Table 9.4). The results showed that the degree of photo-oxidative ageing increased with a rise in UV intensity. Besides, environmental temperature also affects photo-oxidative ageing to some extent. Generally speaking, a rise of temperature can accelerate the degree of photo-oxidative ageing of bitumen.

The mechanism of photo-oxidative ageing can be explained using free radical theory. Some weaker chemical bonds in the bitumen molecule can be

Table 9.2 Energy of light at different wavelengths

Wavelength (nm)	200	300	420	470	530	580	620	700	1000
Energy (kJ/mol)	595.5	397.1	283.6	253.5	224.8	205.3	192.1	170.2	119.1

Table 9.3 Energy of different chemical bonds found in bitumen

Chemical bond	O–H	C–F	C–H	N–H	C–O	C–C	C–Cl	C–N	C=C
Energy (kJ/mol)	463.0	441.2	413.6	389.3	351.6	347.9	328.6	290.9	615.3

Table 9.4 Effect of the intensity of UV radiation on the viscosity of bitumen*

UV radiation intensity (W/m^2)	95	139	173
Viscosity (60°C Pa·s)	995	1246	1520

* The experiment was conducted at 60°C for 48 hours for a bitumen film thickness of 150 μm .

broken by UV radiation, which forms free radicals during the process. These free radicals initiated by UV light radiation may react with oxygen and form some oxygen-containing substances such as hydroperoxide, carbonyl groups and so on. These functional groups can further initiate oxidation reactions when subjected to UV light, which cause the degradation and oxidation of bitumen. With regard to the PMBs, however, the mechanism of photo-oxidative ageing is much more complex because the polymers used in PMBs may experience different changes from bitumen under the action of UV light radiation. In addition, the mechanism of different PMBs is also diverse due to the different polymers used in bitumen. As a result, the photo-oxidative ageing of different PMBs should be investigated respectively.

9.3 Simulative ageing methods of polymer modified bitumens (PMBs)

The simulative ageing methods used in laboratory conditions aim to simulate the environmental conditions observed during the manufacture and construction of pavements and later in the field during their service life. In these tests, bitumen ageing is accelerated by increasing temperature and light intensity, decreasing bitumen film thickness, increasing oxygen pressure, or various combinations of these factors. These simulative ageing methods can provide a quick and convenient way to understand the ageing behaviour of PMBs.

Various laboratory methods have been applied to simulate short- and long-term ageing of PMBs and some of them are standardized. At present, the most used simulative methods for short-term ageing are known as the thin film oven test (TFOT, ASTM D 1754) and the rolling thin film oven test (RTFOT, ASTM D 2872). As for the long-term ageing, the pressure ageing vessel (PAV, ASTM D 6521) is a standardized method designed to simulate the oxidative ageing that occurs in bitumen during pavement service. With the emphasis on UV radiation on bitumen ageing, some accelerated methods for UV ageing have also been performed in the laboratory. However, the standardized method for UV ageing has not been fully established.

9.3.1 TFOT

The TFOT covers the determination of the effects of heat and air on a thin film of bituminous materials. The effects of this treatment are determined from measurements of selected bitumen properties before and after the test. This method assesses changes in the properties of bitumen during conventional hot-mixing at about 150°C as indicated by viscosity, penetration or ductility measurements. It yields a residue which approximates the bitumen condition as incorporated in a pavement.

The TFOT is executed in an oven with a plate and axis, and the rotation

of the plate is carried out around the axis. Firstly, the bitumen is heated to liquid at proper temperature (no more than 150°C). Then the flowing bitumen (50 ± 0.5 g) is poured into stainless steel pans with an inner diameter of 140 mm, making the thickness of bitumen film about 3.2 mm. The bitumen for the TFOT is finally heated in the oven for 5 hours at $163 \pm 1^\circ\text{C}$.

This technique has been validated for some time for unmodified bitumen, whereas its validity is still open to doubt in the case of modified bitumen. The conditions used during the TFOT are somewhat limited for PMBs because the polymer modifiers and bitumen are not fully compatible, readily leading to phase separation when the PMBs are aged by TFOT. Therefore, the stability of PMBs is poor at elevated temperature. Furthermore, the surface of PMBs, at the same time, may be 'skinning' during the test, which prevents the development of ageing and thus weakens the normal ageing process (Jia *et al.*, 2005).

9.3.2 RTFOT

This test method is intended to measure the effect of heat and air on a moving film of bituminous material. The RTFOT, in which the conditions are similar to the actual short-term ageing that takes place at the site where the binder is applied, is used for estimating high-temperature short-term ageing in the laboratory. In this method, the glass containers are heated to 160°C before loading the sample. Then 35 ± 0.5 g of bitumen is poured into glass containers and aged at 163°C for 75 minutes with an air flow rate of 4 L/min. Afterwards the aged binders are evaluated by measuring their physical/rheological properties and chemical characteristics.

Similar to TFOT, the RTFOT method was originally developed to simulate ageing of unmodified binders. The film of PMB, however, may not flow efficiently within the rotating bottle during the RTFOT, meaning that the binders are not exposed to heated air as a continuously moving thin film, as intended in the test. As a result, the validity of this method when applied to PMBs is also open to doubt at present. However, in the absence of a viable alternative, it has been used with considerable success to compare different PMBs during laboratory studies.

The modified rolling thin film oven test (MRTFOT) presented by Lu and Isacsson (2000) was to add a stainless steel rod which was 6 mm in diameter and 127 mm long to the glass bottle. This modification was proposed so as to reduce the effect of high consistency PMBs on the rolling process. The other ageing conditions of MRTFOT were the same as for RTFOT (163°C and 75 minutes). This modified method, which may improve the current experimental status of bitumen ageing, may be very useful in developing new scientific and technical approaches to simulating ageing of PMBs.

9.3.3 PAV

The PAV test covers the accelerated oxidative ageing of bitumen by means of pressurized air and elevated temperature in a pressurized ageing vessel. This test method is intended to simulate in-service oxidative ageing of bitumen. Bitumen used in the PAV is first aged by RTFOT or TFOT in order to simulate the short-term thermal-oxidative ageing. A specified mass (50 ± 0.5 g) and thickness (about 3.2 mm) of residue from the RTFOT or TFOT is placed in stainless steel pans and aged at specified ageing temperatures (90°C , 100°C or 110°C) for 20 hours in the vessel pressurized with air to 2.1 ± 0.1 MPa. The ageing temperature is selected according to the grade of bitumen of interest. At the end of the test, the pan holder and pans are removed from the PAV, and placed in an oven set at 163°C . The bitumen is heated sufficiently until fluid to pour and stir gently to assist in the removal of air bubbles before further tests.

9.3.4 UV radiation test

The effect of UV radiation on degradation of bitumen has attracted much attention from both academic and industrial groups in recent years. However, it is often ignored in laboratory simulations due to the fact that UV radiation affects only the upper layers of the pavement surface. Though laboratory methods to simulate short- and long-term ageing of bitumen in a pavement are standardized, none of them takes into account the influence of UV radiation. In the published literature (Durrieu *et al.*, 2007; Mouillet *et al.*, 2008a; Wu *et al.*, 2010), many different tests have been applied to simulate UV ageing, but there was still no standardized method for this test.

To be close to the ageing conditions during pavement service life, all UV radiation tests are performed on binders previously submitted to RTFOT or TFOT. Mouillet *et al.* (2008a) deposited 25 μL of binder in a 170 g/L solution of dichloromethane on a slide and made a 10 μm thick film after the solvent was eliminated by evaporation in air. The slides prepared in this way were placed in an Atlas 2000 chamber and subjected to UV radiation (UVA-340C; 0.44 W/m^2 fluorescent lamps). UV exposure was carried out at 60°C for 60 hours during which infrared analysis of the slides was performed at different time intervals.

Wu *et al.* (2010) used a UV radiation oven to investigate the UV degradation of bitumen specimens. The UV radiation oven consisted of a cabinet vessel, a temperature-controlled system and an ultraviolet light source. The bitumen was spread on glass plates with film thicknesses of approximately 50 μm , 100 μm , 150 μm and 200 μm , respectively. The plates were then placed in the UV radiation oven for 48 hours. The exposure intensities of the UV lamp were set at 95 W/m^2 , 139 W/m^2 , 173 W/m^2 and 200 W/m^2 , respectively. The test temperatures were 45°C , 65°C and 80°C , respectively.

As mentioned above, many factors influence UV degradation of bitumen and it is hard to establish a laboratory condition which is relatively consistent with the actual environmental condition of various areas in which PMBs are used. Therefore, a standardized method for UV ageing of bitumen has not been achieved throughout the world. Nevertheless, it would be of much significance if a UV ageing method could be standardized. This would require intensive studies and global cooperation of both academic researchers and industrial technicians.

9.3.5 Natural exposure ageing (NEA)

The evaluation of bitumen ageing through field tests may provide interesting information on the evolution of bitumen properties. The advantages of NEA are the authenticity of environmental conditions, the comprehensiveness of environmental factors, the traceability of test data, and the reliability of test results. The main factors which influence NEA of PMBs are as follows:

- The place/site for the natural exposure experiment. The proper exposure field is one of the most critical factors for NEA. Generally, the choice of exposure field depends on the samples and purpose of the test.
- The cycle of the natural exposure experiment. The NEA often requires a long period of time and thus the efficiency of the experiment is very low.
- The role of pollutants. In the field test, the suspended particles, corrosive gas, acid rain and other kinds of pollutants will damage the samples used in the NEA. As a result, some protective measures must be adopted during the NEA test.

Because the environmental conditions can vary at different times, the field ageing of materials or products may not follow a scientific theory in a fixed pattern, and its performance will vary with climatic conditions. Therefore, the repeatability of NEA is not very good. In fact, several different methods are used simultaneously on the same tests to evaluate the physical or chemical properties of different PMBs.

9.4 Ageing performance and characterization of polymer modified bitumens (PMBs)

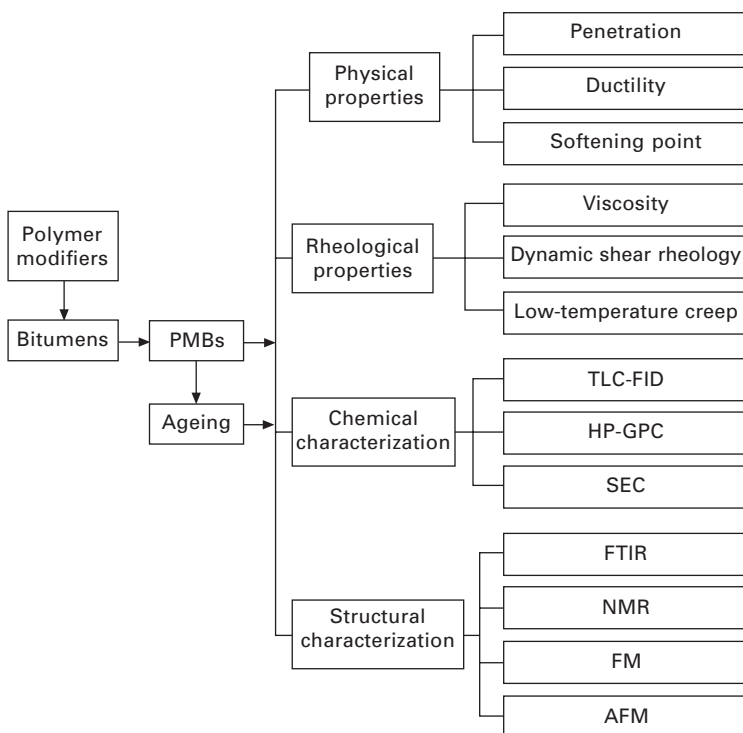
With the ageing process of PMBs, PMB chemical components are transformed and inevitably this results in changes of binder performance. The evaluation of ageing performance of PMBs is largely investigated by means of physical properties (i.e. penetration, ductility, softening point, etc.) and rheological properties (i.e. viscosity, dynamic shear rheology, low-temperature creep, etc.) of unaged and aged PMBs. The chemical characteristics of PMBs before

and after ageing can be compared by means of thin-layer chromatography with flame ionization detection (TLC-FID), high-pressure gel permeation chromatography (HP-GPC) and size exclusion chromatography (SEC). In order to correctly understand the ageing process of PMBs, some advanced testing methods have also been used, such as Fourier transform infrared (FTIR) spectroscopy, nuclear magnetic resonance (NMR), fluorescence microscopy (FM) and atomic force microscopy (AFM). A schematic diagram showing the techniques used to study ageing of PMBs is displayed in Fig. 9.2.

9.4.1 Physical properties

Changes in physical properties (penetration, ductility and softening point) are the most conventional parameters measured to evaluate the ageing of PMBs. Generally speaking, the ageing performance of PMBs is not only influenced by the nature of the base bitumen but also dependent on the polymer characteristics and content.

Zhang *et al.* (2010) investigated the physical properties of two modified bitumens (linear SBS modified bitumen and radial SBS modified bitumen)



9.2 Schematics of the techniques applied for the ageing evaluation of PMBs.

before and after TFOT and PAV ageing. Durrieu *et al.* (2007) studied the physical properties of SBS modified bitumen (PMB 2-4) before and after ageing (RTFOT, PAV, 12 months on road and 26 months on road). The results from their experiment are listed in Table 9.5. For linear and radial SBS modified bitumen, the changes in softening point and penetration values were slight after TFOT ageing. However, after PAV ageing, the changes were obvious for the two binders. The ductility exhibited a decrease after both TFOT and PAV ageing for the two binders, but the radial SBS modified bitumen showed a better low-temperature ductility than linear SBS modified bitumen. The penetration and softening point of PMB 2-4 after the different stages of laboratory or field ageing displayed an obvious decrease and increase, respectively. Based on these data, an interesting result was obtained in that the PAV simulation of PMB 2-4 corresponded to only 12 months of ageing of the pavement. However, for base bitumen, it has been established that the PAV simulation corresponds to a service life of four to five years (Harrigan *et al.*, 1994; Migliori *et al.*, 2000; Al-Azri *et al.*, 2006).

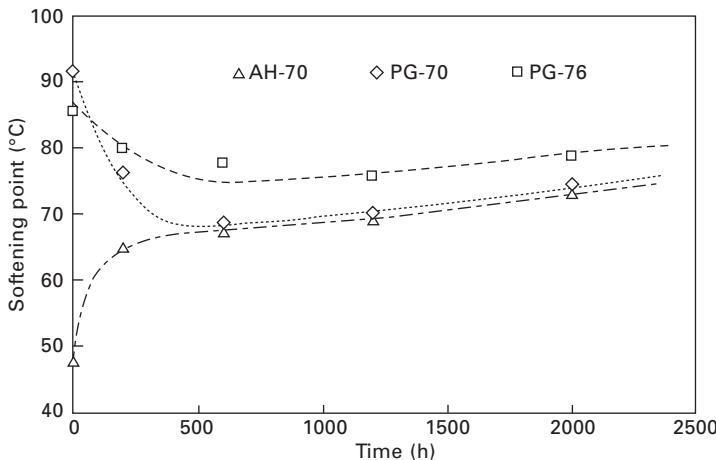
Wu *et al.* (2009) studied the effects of PAV ageing time on the softening point of base bitumen (AH-70) and SBS modified bitumens (PG-70 and PG-76), as shown in Fig. 9.3. Before PAV ageing, the softening points of the SBS modified bitumens were higher than that of base bitumen. With the increase in ageing time, the softening point of base bitumen increased dramatically below 500 hours while those of SBS modified bitumens decreased. Above 500 hours the softening point of all the bitumens increased gradually up

Table 9.5 Effect of ageing on physical properties of SBS modified bitumen

PMB	Ageing methods	Penetration (25°C, 0.1 mm)	Ductility (5°C, cm)	Softening point (°C)
SK-90 + 3.5 wt% linear SBS ^a	Unaged	49	39.1	53.2
	TFOT	50	20.1	53.0
	PAV	43	2.9	60.1
SK-90 + 3.5 wt% radial SBS ^a	Unaged	49	23.4	53.7
	TFOT	49	21.9	53.1
	PAV	47	3.4	58.0
PMB 2-4 ^b	Unaged	41	–	56.0
	RTFOT	30	–	62.0
	PAV	19	–	71.2
	12 months on road	19	–	69.2
	26 months on road	16	–	73.0

^a Adapted from Zhang F, Yu J Y and Wu S P (2010), 'Effect of ageing on rheological properties of storage-stable SBS/sulfur-modified asphalts', *J Hazard Mater*, 182, 507–517.

^b Adapted from Durrieu F, Farcas F and Mouillet V (2007), 'The influence of UV aging of a styrene/butadiene/styrene modified bitumen: comparison between laboratory and on site aging', *Fuel*, 86, 1446–1451.



9.3 Effects of PAV ageing time on softening point of base and SBS modified bitumens.

to 2000 hours. This behaviour may be explained as follows: for the base bitumen, more asphaltenes with high molecular weight were formed due to the oxidation during PAV ageing, leading to high softening points of the corresponding aged bitumen. For SBS modified bitumens, the degradation of the SBS modifier and the oxidation of the bitumen happened at the same time. The former tended to decrease the softening point while the latter tended to increase the softening point. Both of them determined the change of softening point, and the role of the former was more pronounced in the early stages of PAV ageing.

The penetration retention rate (PRR), ductility retention rate (DRR) and softening point increment (SPI) are usually used to compare the extent of ageing of different bitumens. These parameters can be computed as follows:

$$PRR = (P/P_0) \times 100\% \quad 9.2$$

$$DRR = (D/D_0) \times 100\% \quad 9.3$$

$$SPI = S - S_0 \quad 9.4$$

where P_0 , D_0 and S_0 are the penetration, ductility and softening point of unaged bitumen, and P , D and S are the penetration, ductility and softening point of the corresponding aged bitumen.

9.4.2 Rheological properties

PMBs are viscoelastic materials; their rheological properties are of great importance for both unaged and aged binders. The rheological properties

of PMBs may change during different ageing processes. As a result, many valuable and practical insights may be obtained from determining rheological indices to estimate ageing of PMBs (Valtorta *et al.*, 2007).

Viscosity

Viscosity is an important index to evaluate flowability and deformation of bitumen. With regard to PMBs, rotational viscosity is commonly measured, since they are relatively more viscous at the normal testing temperature. The rotational viscosity is usually measured using a Brookfield viscometer fitted with a thermosel temperature control system, meeting the requirements of the standard test method ASTM D 4402. It is useful to determine the flow behaviour of bitumen at high temperatures and to establish the viscosity-temperature profiles.

Zhang *et al.* (2010) investigated the viscosity changes of linear and radial SBS modified bitumen before and after TFOT and PAV ageing. Meanwhile, the effect of sulfur on viscosity changes of unaged and aged SBS modified bitumen was also evaluated, as shown in Table 9.6. The results showed that the viscosity, for both linear and radial SBS modified bitumen, reduced slightly after TFOT but increased after PAV ageing. The addition of sulfur made the change in viscosity of the aged PMBs smaller, indicating a more stable system of PMBs as a result of dynamic vulcanization.

The ageing index (AI), which can be calculated by formula 9.5, is also an important parameter to assess the ageing resistant properties of bitumen:

$$AI = \eta/\eta_0 \quad 9.5$$

where η_0 is the viscosity of unaged bitumen (Pa·s), and η is the viscosity of the aged bitumen (Pa·s). Ruan *et al.* (2003b) used the AI calculated from the zero-shear viscosity at 60°C to evaluate the RTFOT ageing of both base and modified bitumen (Table 9.7). The results indicated that polymer (SBR, SBS or tyre rubber) modified bitumen had lower values of AI than their

Table 9.6 Effect of ageing on the viscosity of SBS modified bitumen

PMB	Viscosity (135°C, Pa·s)		
	Unaged	TFOT	PAV
SK-90 + 3.5 wt% linear SBS	1.29	1.23	2.01
SK-90 + 3.5 wt% linear SBS + 0.1 wt% sulfur	1.40	1.38	1.93
SK-90 + 3.5 wt% radial SBS	1.34	1.13	1.83
SK-90 + 3.5 wt% radial SBS + 0.1 wt% sulfur	2.19	2.03	2.49

Source: adapted from Zhang F, Yu J Y and Wu S P (2010), 'Effect of ageing on rheological properties of storage-stable SBS/sulfur-modified asphalts', *J Hazard Mater*, 182, 507–517.

Table 9.7 Value of AI for base and modified bitumen

Bitumen/PMB	AI
AC-5	1.95
AC-5 + 1 wt% SBR	1.87
AC-5 + 2 wt% SBR	1.65
AC-10	1.66
AC-10 + 2 wt% SBR	1.54
AC-10 + 4 wt% SBR	1.36
AC-10 + 2 wt% SBS	1.36
AC-10 + 4 wt% SBS	1.24
AC-10 + 10 wt% tyre rubber	1.23
AC-10 + 18 wt% tyre rubber	1.12

Source: adapted with permission from Ruan Y H, Davison R R and Glover C J (2003), 'Oxidation and viscosity hardening of polymer-modified asphalts', *Energy and Fuels*, 17, 991–998. © 2003 American Chemical Society.

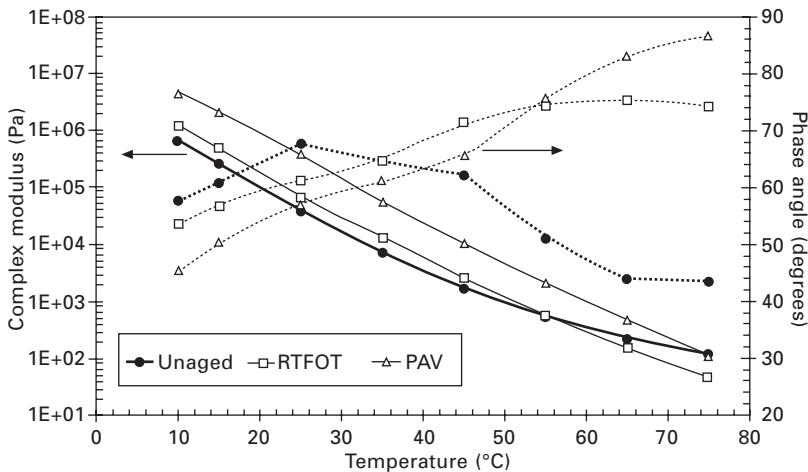
corresponding base bitumen. Moreover, the increase in modifier concentration caused a further decrease in the AI value of modified bitumen.

Dynamic shear rheology

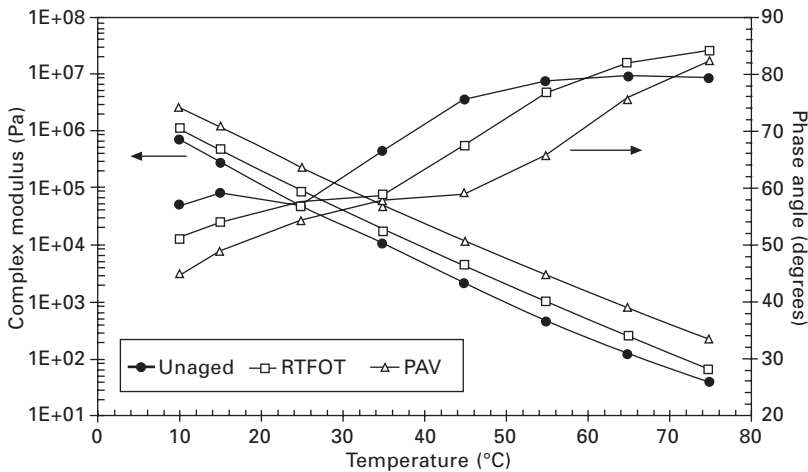
The dynamic shear rheometer (DSR) is used to measure the linear viscoelastic moduli and phase angle of bitumen in the sinusoidal (oscillatory) loading mode. Measurements may be obtained at different temperatures, strain and stress levels, and test frequencies. Thus, the device can be used to invoke time–temperature superposition and to construct linear viscoelastic master curves.

Airey (2003) measured the complex modulus and phase angle at 0.02 Hz for PMB-AS7 (7 wt% SBS modified bitumen A) and PMB-BS7 (7 wt% SBS modified bitumen B) in their unaged, RTFOT and PAV aged conditions, as shown in Figs 9.4 and 9.5. Both PMBs showed an increase in complex modulus between 10 and 55°C after RTFOT and PAV ageing, but the behaviour at temperatures greater than 55°C differed between the two PMBs. For PMB-AS7, instead of an increase there was a decrease in complex modulus after ageing, which could be attributed to degradation of SBS copolymer into lower molecular weight fragments after ageing. This phenomenon was not evident for PMB-BS7, as the rubber–elastic network did not dominate the rheological behaviour of the PMB to the same degree as that seen for PMB-AS7.

As shown in Figs 9.4 and 9.5, the phase angle of PMBs after RTFOT and PAV ageing displayed a decrease within the temperature domain of 10 to approximately 35°C. In the temperature domain greater than 40°C, where the SBS polymer network was rheologically dominant, the changes of phase



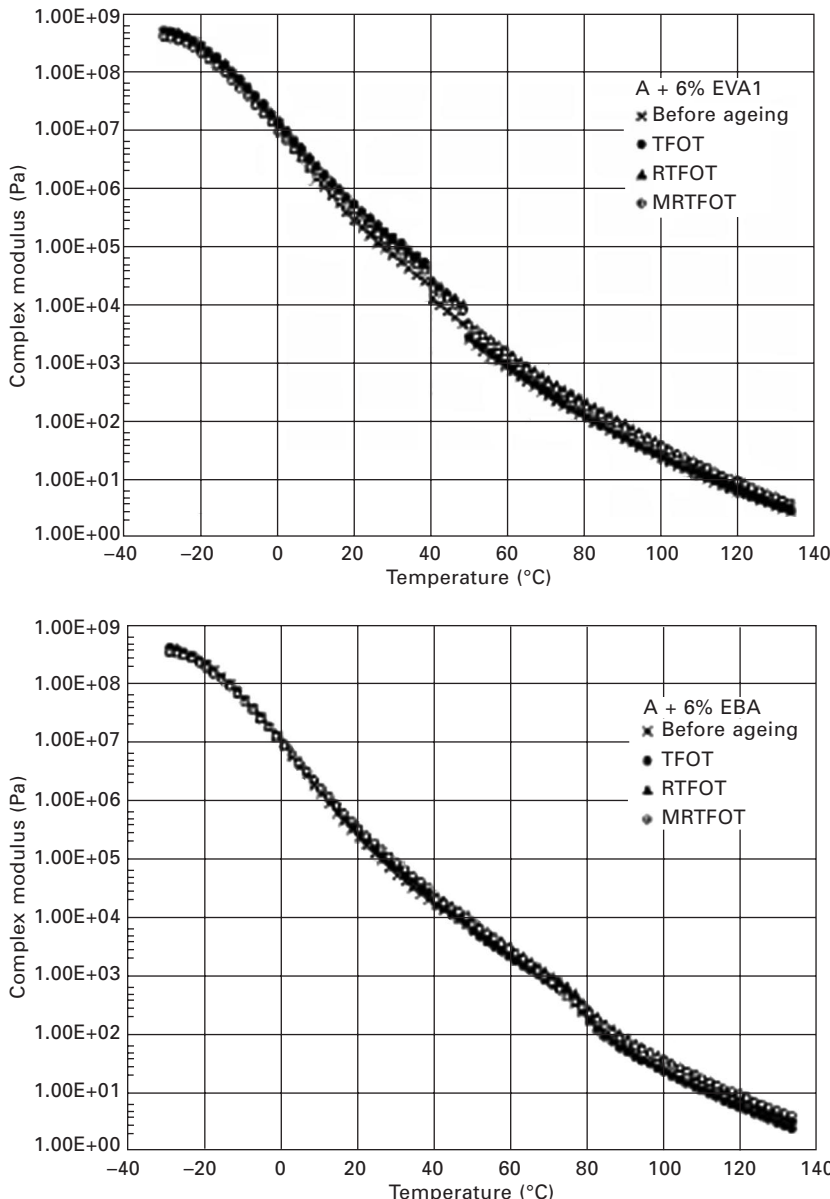
9.4 Complex modulus and phase angle at 0.02 Hz for PMB-AS7 (unaged, RTFOT and PAV).



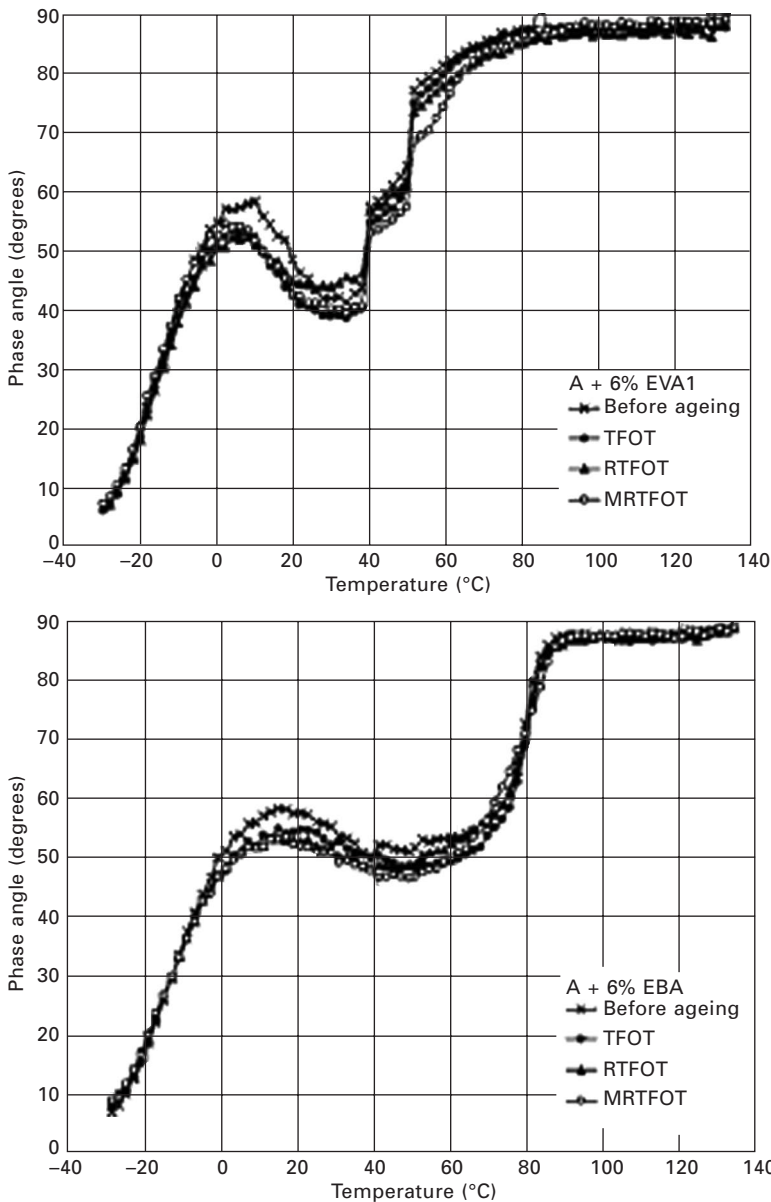
9.5 Complex modulus and phase angle at 0.02 Hz for PMB-BS7 (unaged, RTFOT and PAV).

angle after RTFOT and PAV ageing were different from those experienced for unmodified bitumens. Again the rheological behaviour for PMB-AS7 differed from that of PMB-BS7, particularly above 45°C. At these elevated temperatures there was an increase in phase angle after RTFOT and PAV ageing, indicating a more viscous response for PMB-AS7. This increase in viscous rather than elastic response after ageing was not evident for PMB-BS7, although the phase angle did increase slightly after RTFOT at temperatures greater than 65°C.

Lu and Isacsson (2000) studied the effects of ageing on the rheological properties of ethylene vinyl acetate (EVA) modified bitumens and ethylene butyl acrylate (EBA) modified bitumens (Figs 9.6 and 9.7). Evidently, the



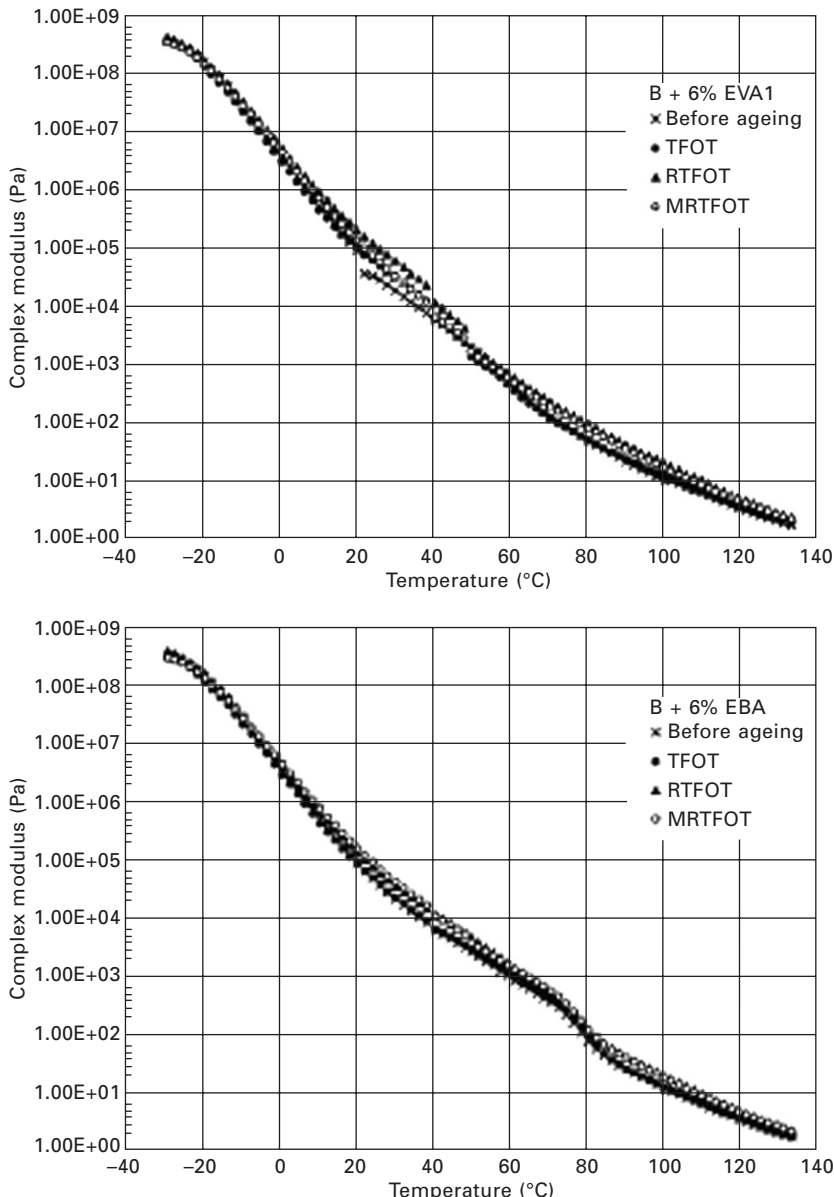
9.6 Effect of ageing on temperature dependence of complex modulus and phase angle (EVA1 and EBA modified bitumen A).



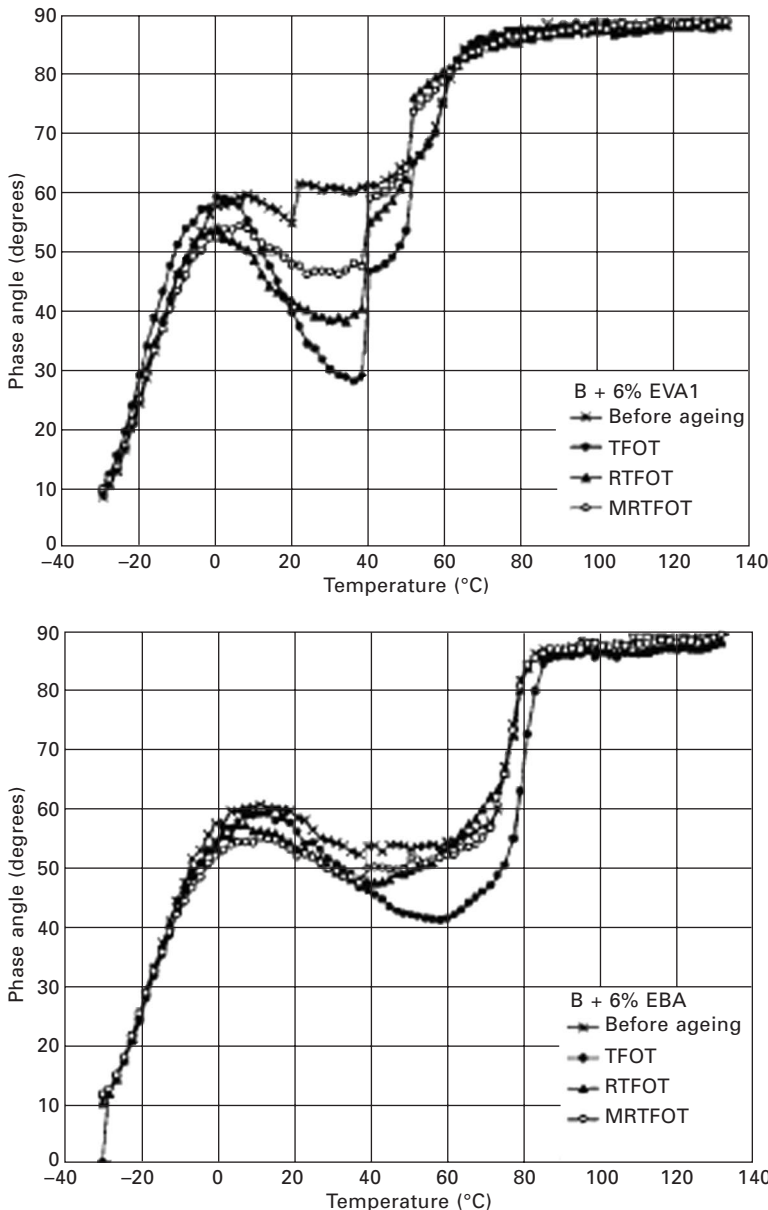
9.6 Continued

process of ageing increased the complex modulus and decreased the phase angle, and the degree of ageing was determined by the corresponding base bitumen to a great extent. The phenomena were mainly due to oxidative hardening of the bitumen. In other words, addition of plastomers probably did not alter the mechanism of bitumen ageing.

The master curves of rheological characterization can be built from the dynamic data taken in isothermal frequency sweep tests. Polacco *et al.* (2006) developed the master curves (reference temperature equal to 0°C)

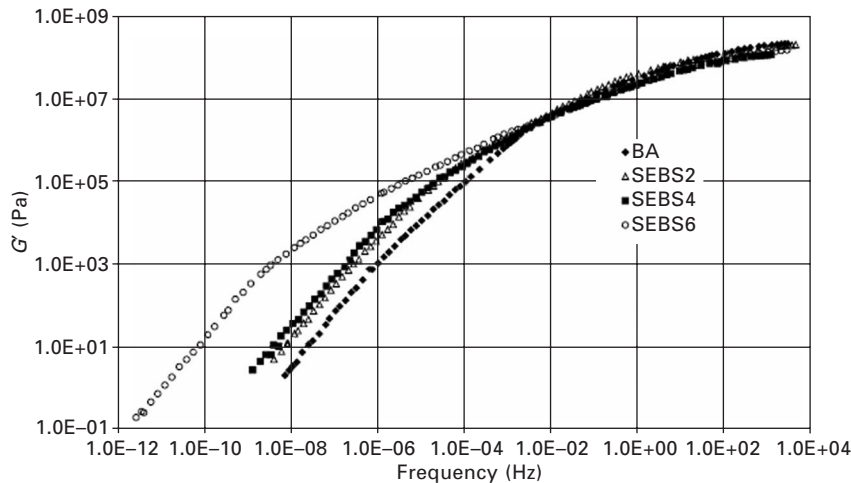


9.7 Effect of ageing on temperature dependence of complex modulus and phase angle (EVA1 and EBA modified bitumen B).

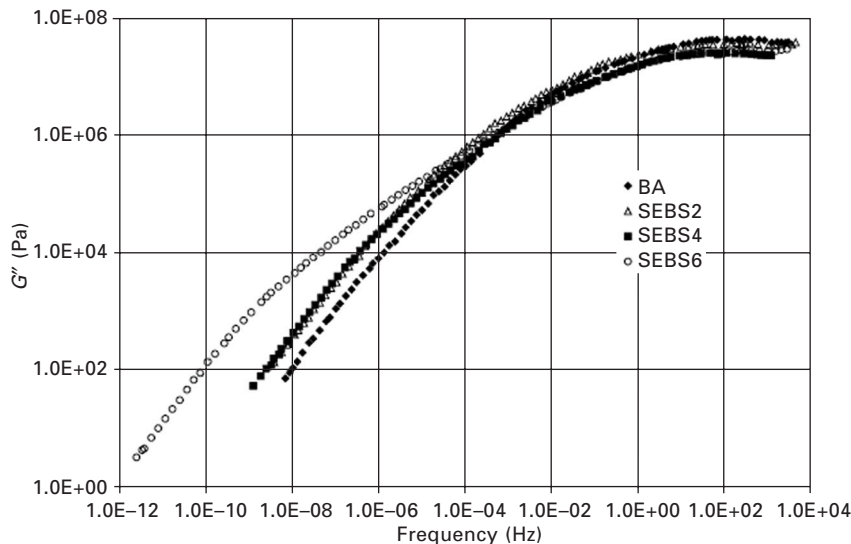


9.7 Continued

of storage modulus (G') and loss modulus (G'') for BA (base asphalt), SEBS2 (2 wt% SEBS modified bitumen), SEBS4 (4 wt% SEBS modified bitumen) and SEBS6 (6 wt% SEBS modified bitumen), as shown in Figs 9.8 and 9.9. At high frequencies, no significant differences were detectable



9.8 Master curves of storage modulus (G') for BA, SEBS2, SEBS4 and SEBS6.



9.9 Master curves of loss modulus (G'') for BA, SEBS2, SEBS4 and SEBS6.

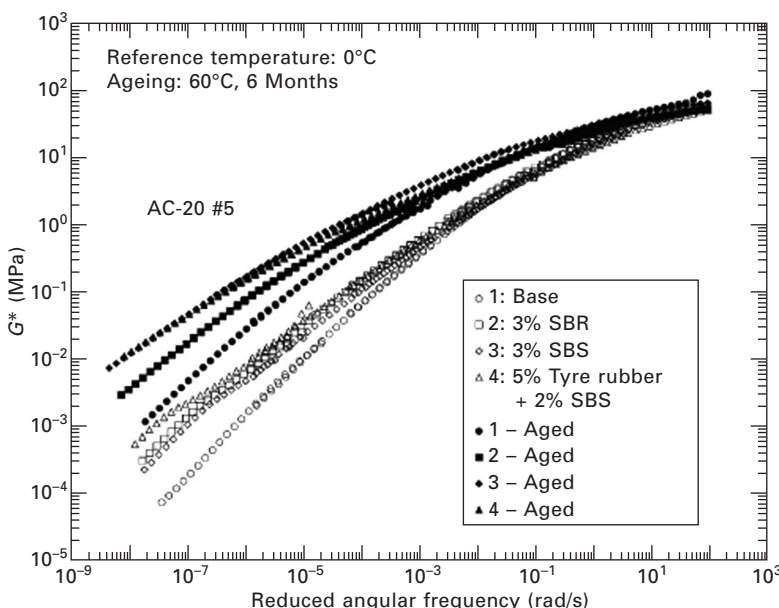
between the four materials. All the materials showed a maximum in G'' at 10^2 Hz, corresponding to a glass transition temperature of about -20°C . At lower frequencies the curves differentiated, but those relative to SEBS2 and SEBS4 remained very close to each other, and remained intermediate between those of BA and SEBS6. The behaviour of SEBS6 was qualitatively

different from that of the other materials. With a small polymer quantity, the PMB was similar to BA. The polymer dispersed in the asphalt matrix did not behave as a real modifier, but rather as a filler, and had an effect mainly on the modulus values. In the case of SEBS6, the polymer was not (or not completely) dispersed in isolated small islands, and some bridges between the polymer-rich zones appeared.

Ruan *et al.* (2003a) investigated the complex modulus (G^*) master curves for the base and modified bitumens at a reference temperature of 0°C (Fig. 9.10). Compared with the base bitumen, the modified binders showed a marked increase in G^* at low angular frequency and a slight decrease in G^* at high angular frequency. The results indicated that oxidative ageing (60°C, 6 months) increased G^* , especially at low frequency. At high frequency, the change in G^* with ageing was relatively small. For aged bitumen, there was still a significant difference in G^* between the base and modified binders, especially at low angular frequencies.

Low-temperature creep

The bending beam rheometer (BBR) is used to measure the low-temperature creep response of bitumen. Creep stiffness and the slope of the log stiffness versus log time curve are obtained at several loading times ranging from



9.10 Master curves of G^* for the base and modified bitumens at 60°C.

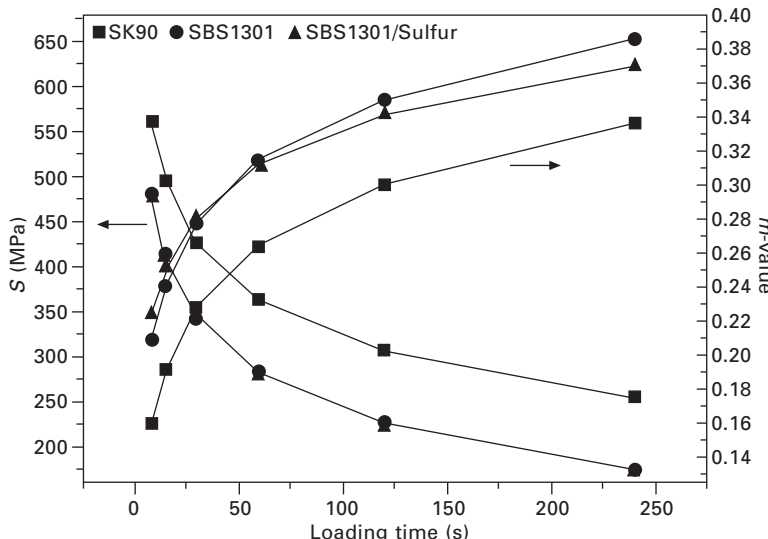
8 to 240 s. It is used to apply a constant load to a prismatic beam loaded in simple bending at its midpoint. The device is useful for measuring moduli ranging from 30 MPa to 3 GPa. These moduli typically occur in the temperature range from -40 to 25°C depending on the grade and ageing history of the binder.

Zhang *et al.* (2010) investigated the influence of TFOT ageing on the low-temperature creep behaviour of SBS modified binders with or without sulfur. The test temperature was chosen at -18°C . The results are shown in Figs 9.11 and 9.12. The base bitumen always had the highest creep stiffness (S) and lowest creep rate (m -value) before and after ageing. The addition of SBS improved the low-temperature cracking resistance of the base bitumen before and after ageing, as shown by the declined creep stiffness and increased creep rate. Moreover, the use of sulfur further improved the low-temperature cracking resistance of the aged binders.

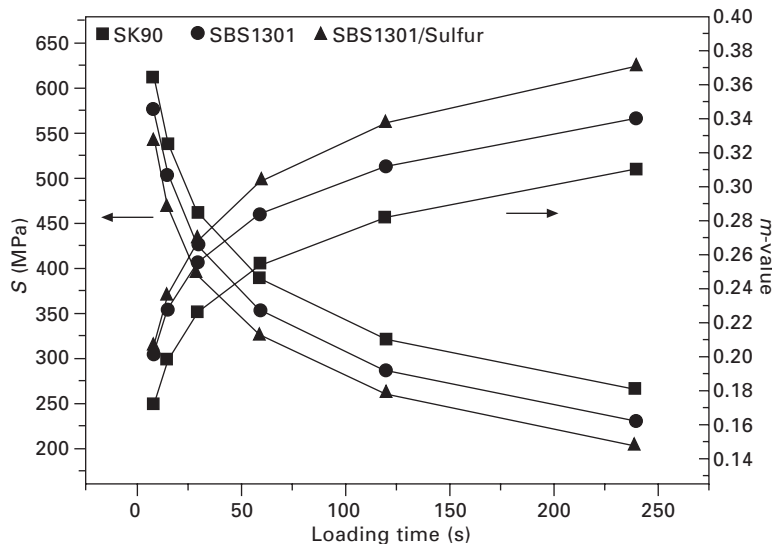
9.4.3 Chemical characterization of PMBs

Thin-layer chromatography with flame ionization detection (TLC-FID)

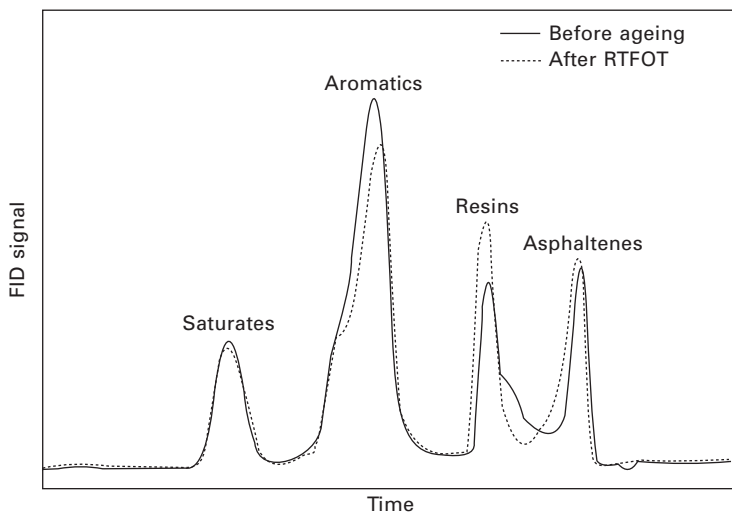
The generic fractions of bitumen can be separated and tested by TLC-FID. The common procedures for TLC-FID are according to the published literature (Ecker, 2001; Lu and Isacsson, 2002). Using this method, four generic fractions, namely saturates, aromatics, resins and asphaltenes, can be determined. The FID signal of base bitumen before and after ageing is



9.11 Curves of creep stiffness (S) and creep rate (m -value) versus loading time for base and SBS 1301 modified bitumens.



9.12 Curves of creep stiffness (S) and creep rate (m -value) versus loading time for base and SBS 1301 modified bitumens after TFOT ageing.



9.13 The FID signal of bitumen before and after ageing.

shown in Fig. 9.13 (Lu and Isacsson, 2002). The ratio of peak area represents the relative content of each fraction.

As for neat bitumen, ageing usually decreases aromatic content and at the same time increases the content of resins and asphaltenes. However,

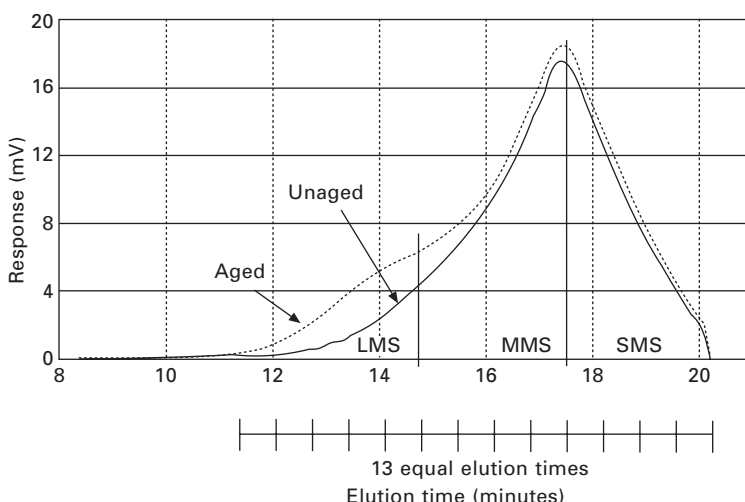
the content of saturates changes slightly due to their inert nature to oxygen. Since the fractionation of bitumen is mainly based on molecular polarity, the compositional changes should imply transformation of different fractions, i.e. aromatics → resins → asphaltenes (Lu and Isacsson, 2002). Hereby, the TLC-FID method may also be applicable for the evaluation of ageing of PMBs.

High pressure gel permeation chromatography (HP-GPC)

HP-GPC is a relatively easy way to detect change in molecular size distribution of bitumen during the ageing process. In general, an increase in large molecular size (LMS) leads to an increase in viscosity and stiffness of bitumen. The viscosity change of bitumen due to ageing may be predicted with some degree of accuracy by HP-GPC (Wahhab *et al.*, 1999; Kim *et al.*, 2001).

Lee *et al.* (2009) described the typical HP-GPC chromatograms of unaged and short-term aged (154°C oven ageing for 4 hours) bitumen (Fig. 9.14). In this figure, the chromatogram profile was partitioned into 13 slices (i.e. 13 equal elution times) and three parts: large molecular size (LMS; slices 1–5), medium molecular size (MMS; slices 6–9) and small molecular size (SMS; 10–13). Generally speaking, the LMS value of the chromatogram was used to evaluate ageing effects of PMBs. The change of LMS after short-term oven ageing indicated that the higher ageing temperature and longer ageing time may lead to a greater increase in the LMS ratio of bitumen.

In terms of binder types, the base and rubber modified binders were found



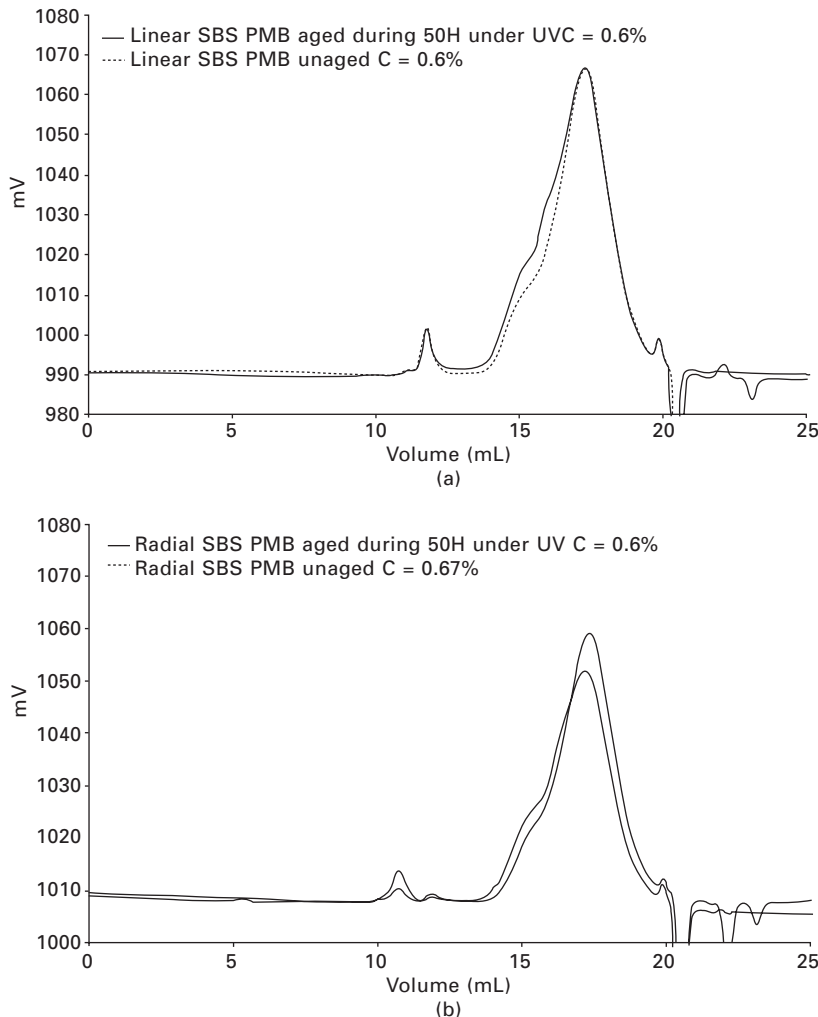
9.14 Typical GPC chromatograms of the unaged and short-term aged bitumen.

to be not significantly different, because the rubber in the bitumen was removed by a syringe filter for the GPC test. Therefore, the chromatogram of the rubberized binder was similar to that of the base binder. However, SBS modified bitumen which had a higher LMS value initially showed a smaller increase in the LMS ratios than the base bitumen after ageing, indicating a better resistance to ageing for SBS modified bitumen (Lee *et al.*, 2009).

Size exclusion chromatography (SEC)

The molecular weight distribution of bitumen can also be determined by SEC; experimental procedures have been described previously (Ruan *et al.*, 2003b; Mouillet *et al.*, 2008a). Mouillet *et al.* (2008a) developed the SEC chromatograms for unaged and UV-aged SBS modified bitumen (Fig. 9.15). The superposing of chromatograms for unaged and aged modified bitumen did not suggest elastomer modification by chain scission after ageing. Indeed, after 50 hours of UV exposure, there were always polymer peaks without molecular weight change of the major population. At the same time, the ageing of base bitumen was reflected with an increase in the peak area corresponding to the high molecular weight fraction. The intensity difference between unaged and aged radial SBS modified bitumen (Fig. 9.15(b)) was due to a concentration difference of analysed solutions: 0.67% (w/v) for the unaged PMBs and 0.6% (w/v) for the aged PMBs. According to the SEC analysis, it seems that, during UV ageing, the bituminous matrix had a protective effect with regard to chain scission of the elastomer.

Ruan *et al.* (2003b) studied the SEC chromatograms for SBR and SBS modified bitumen, as shown in Figs 9.16 and 9.17. In these figures, chromatograms from both the refractive index detector (RI) and the intrinsic viscosity detector were included. The three peaks (from left to right) for both chromatograms corresponded to modifiers (polymers), primary asphaltenes, and primary maltenes. Polymer molecules flowed out of the column before asphaltenes, which meant that both SBR and SBS molecules were larger than the asphaltenes. The SBS peak was narrower and higher than that of SBR, meaning that the molecular weight distribution of this SBS was narrower than that of the SBR. After 12 months of ageing at 60°C, two prominent differences in chromatograms between the unaged and aged bitumen were evident. First, the asphaltenes peak increased dramatically in size and shifted to an earlier elution time. This phenomenon was the result of the production of more asphaltenes from naphthenes and polar aromatics, and from an increase in the size of the asphaltene structures due to increasing interactions. Second, the polymer peak shifted to a later elution time, decreased in height and broadened, indicating that the large polymer molecules decomposed to smaller ones, thereby increasing the polymer molecular weight distribution.

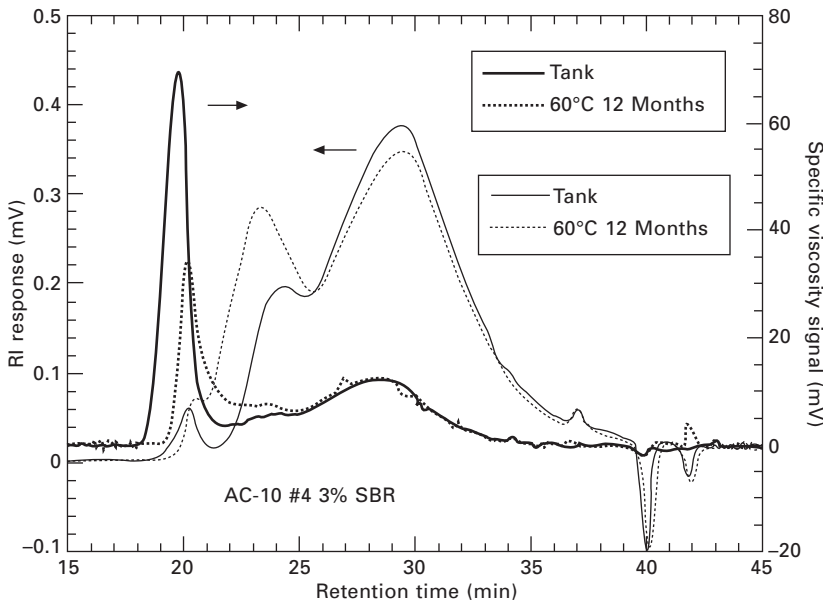


9.15 SEC chromatograms of the PMBs before and after 50 hours of UV exposure: (a) linear SBS modified bitumen, (b) radial SBS modified bitumen.

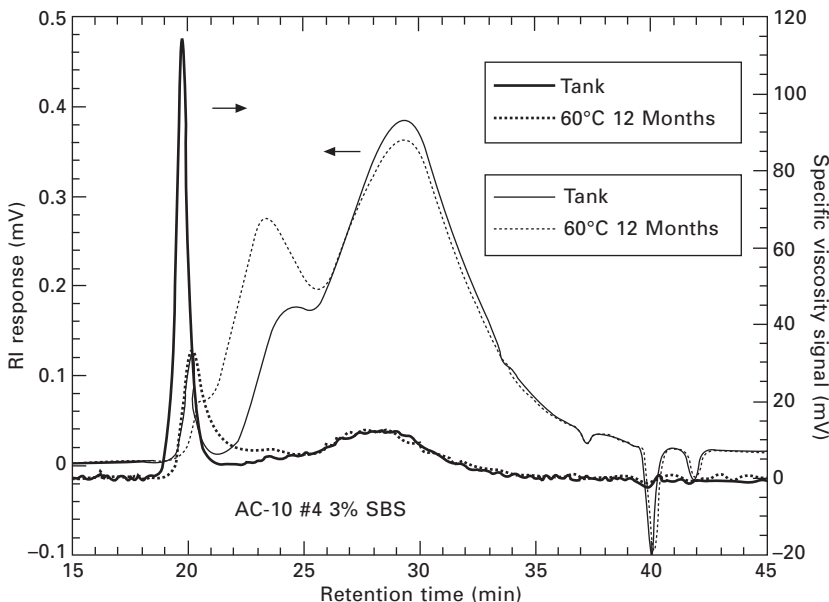
9.4.4 Structural characterization of PMBs

Fourier transform infrared (FTIR) spectroscopy

FTIR spectroscopy can be used to determine the functional characteristics of bitumen before and after ageing. It is able to offer quick and reliable information regarding aliphaticity, aromaticity and oxygenation rate. This technique can give more accurate data such as the average distribution length of aliphatic chains, oxygenation and substitution mode of aromatics (Lamontagne *et al.*,



9.16 SEC chromatograms for AC-10 + 3% SBR. Adapted with permission from Ruan Y H, Davison R R and Glover C J, 'Oxidation and viscosity hardening of polymer-modified asphalts', *Energy and Fuels*, 17, 991–998. © 2003 American Chemical Society.



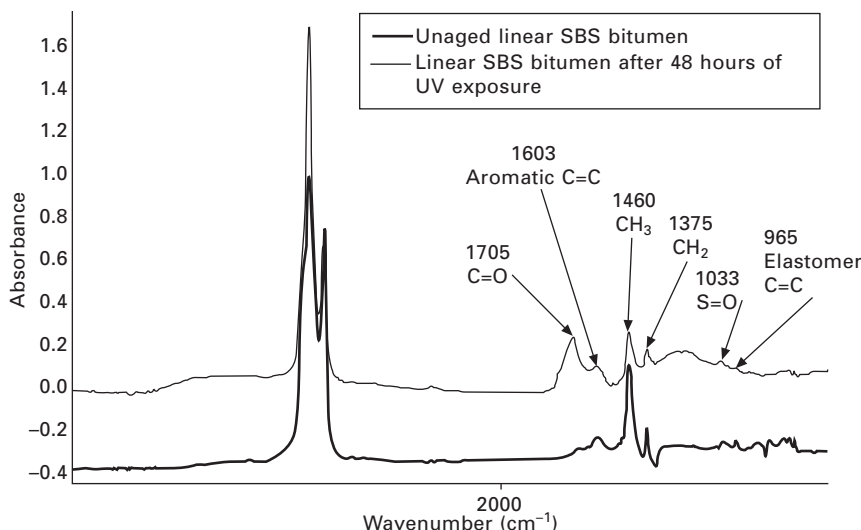
9.17 SEC chromatograms for AC-10 + 3% SBS. Adapted with permission from Ruan Y H, Davison R R and Glover C J, 'Oxidation and viscosity hardening of polymer-modified asphalts', *Energy and Fuels*, 17, 991–998. © 2003 American Chemical Society.

2001a). A structural description of unaged PMBs and those after conventional ageing can be made using the FTIR spectral technique. This monitoring can be performed either by considering the area of the functional bands or by calculating structural indices in order to avoid the effect of variables, such as the thickness of the film (Lamontagne *et al.*, 2001b).

The monitoring of ageing is performed by studying the changes in the spectra obtained, in particular those affecting two characteristic bands: carbonyl functional groups, C=O (centred around 1700 cm^{-1}) and butadiene double bonds C=C (centred around 965 cm^{-1}). Changes were clearly visible in the spectra of SBS modified bitumen before and after UV ageing; see Fig. 9.18 (Mouillet *et al.*, 2008a, 2008b). Examination of the C=O band provided a means of monitoring oxidation of the whole binder, and the determination of the C=C band permitted the monitoring of the deterioration of the SBS copolymer, as a result of modification of the butadiene copolymer by diminution of the double bond content.

Atomic force microscopy (AFM)

AFM is a very high-resolution form of scanning probe microscopy. The AFM images a structure by scanning a tiny tip over the sample surface. It is capable of measuring topographic features at the nanometre-scale or even at atomic-scale resolution. AFM has the advantage of imaging almost any type of surface, including polymers, ceramics, composites, glass, and



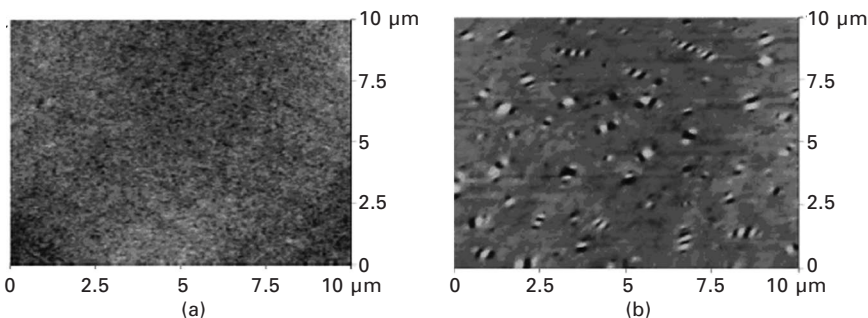
9.18 FTIR spectra of SBS modified bitumen before and after 48 hours of UV exposure at 340 nm and 0.44 W.

biological samples (Giessibl, 2003). Loeber *et al.* (1996) first used AFM for the observation of a heat-cast bitumen film, thus preserving the solid-state morphology without the extraction of its components with solvents. Ever since then, AFM has been used by more and more researchers to investigate the morphology of bitumen (Masson *et al.*, 2006; Baumgardner *et al.*, 2006). It allows one to visualize precise details of the nano- and superstructure of bitumen without special sample preparation.

Wu *et al.* (2009) investigated the structural characteristics of SBS modified bitumen before and after PAV ageing (at 60°C and 2.1 MPa air pressure for 1200 hours) by means of AFM (Fig. 9.19). It is known that two-dimensional AFM images can give us insight into the aggregate structure. For SBS modified bitumen, the 'bee-like' structure appeared on the surface of aged samples, and no 'bee-like' network structures were displayed on the surface of unaged samples. According to Loeber's study (Loeber *et al.*, 1996), the 'bee-like' structure was caused by the existence of asphaltene micelles in bitumen. Obviously, in the process of PAV ageing, oxidation occurs and more asphaltene micelles appeared. SBS was also degraded after PAV ageing, leading to the disappearance of the network structure and to the formation of asphaltene micelles in SBS modified binders.

9.5 Methods for improving the ageing resistance of polymer modified bitumens (PMBs)

Various methods for improving the ageing resistance of bitumen have been developed over the last few decades (Yamaguchi *et al.*, 2004, 2005; Yu *et al.*, 2007, 2010; Ouyang *et al.*, 2006; Zhang *et al.*, 2009). Some of them have been shown, to some extent, to improve the properties of PMBs after the ageing process, to enhance the in-service performance of pavement and to prolong pavement life (Ouyang *et al.*, 2005, 2006; Zhang *et al.*, 2009). Some additives (e.g. carbon black, titanium dioxide, caesium dioxide, ultraviolet



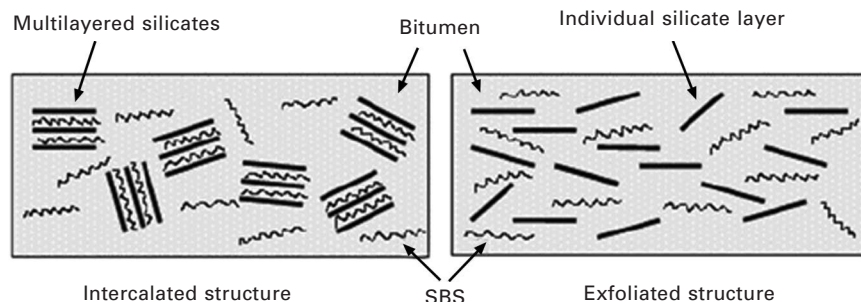
9.19 Two-dimensional AFM images of SBS modified bitumen (a) before and (b) after PAV ageing.

absorbent, montmorillonite, etc.) which are useful for base bitumen may also be advantageous when added to PMBs, and thus some attempts to modify PMBs with different modifiers have been investigated (Yu *et al.*, 2007).

Ouyang *et al.* (2006) evaluated the effects of two antioxidants, zinc dialkyl dithiophosphate (ZDDP) and zinc dibutyl dithiocarbamate (ZDBC), on the TFOT ageing properties of SBS modified bitumen. The result showed that ZDDP or ZDBC modified PMBs were resistant to the formation of carbonyl groups and degradation of butadiene to some extent, indicating the improvement of ageing resistance of SBS modified bitumen with the addition of antioxidants. The authors proposed that ZDDP and ZDBC retarded the oxidation of SBS modified bitumen through inhibition of peroxides and scavenging of radicals during the ageing process. Yu *et al.* (2007) investigated the thermal-oxidative ageing properties of SBS modified bitumen with different sodium montmorillonite (Na-MMT) and organophilic montmorillonite (OMMT) content. The results showed that Na-MMT/SBS modified bitumen formed an intercalated structure, whereas the OMMT/SBS modified bitumen formed a partially exfoliated structure. The addition of Na-MMT or OMMT both improved the ageing resistance of SBS modified bitumen, which was ascribed to the platelet and/or tactoid barrier of the intercalated or exfoliated structure to oxygen (Fig. 9.20), thus reducing the oxidation of bitumen and the degradation of SBS efficiently.

9.6 Future trends in research on polymer modified bitumen (PMB) ageing

The main causes of ageing, simulative ageing methods, ageing performance and characterization, as well as methods employed to improve the ageing resistance of PMBs, have been detailed in the previous sections, but further work and related aspects on research into PMB ageing still need to be addressed.



9.20 Schematic of structures of layered silicate/SBS modified bitumen.

The standard simulative ageing methods (TFOT and RTFOT), which have been validated for unmodified bitumen, are still open to doubt for PMBs. As a result, a programme of laboratory simulative ageing testing for various PMBs is necessary to validate the potential changes to the standard specification. Meanwhile, advanced appropriate methods need to be explored for the ageing simulation of PMBs. Furthermore, an intensive study should be carried out on the relationship between UV ageing and a field test in order to establish a standardized method for UV exposure ageing. For PMBs with different kinds of polymers, the laboratory simulative ageing method may be diverse to some extent. These appeal for a comprehensive study to fully evaluate a large, representative set of PMBs and seek for the best laboratory simulative ageing method for various PMBs.

As for the performance and characterization of PMBs, much attention should be paid to the effect of ageing on the changes in properties at low temperature, for the presented studies mostly focus on the ageing performance at high temperature but pay less attention to the low-temperature performance of aged PMBs. DSR and BBR can be applied to investigate the fatigue cracking and creep deformation at low temperature, respectively. However, the measurements are not restricted to these. A wide array of testing can be tried provided it is useful for the understanding of low-temperature performance of PMBs.

In order to prolong the service life of pavements dramatically, great efforts should be made to develop high-performance ageing-resistant PMBs with different additives (including organic polymers or inorganic particles, nano- or micro-materials, etc.) and/or new processing technology. On the one hand, new modifiers should be sought to improve the ageing resistance of PMBs. On the other hand, functional additives may be added to traditional PMBs to enhance their ageing resistance. These methods may increase the cost of PMBs, but this is reasonable if the new modified binders truly improve pavement performance and prolong service life of pavement to the degree expected.

9.7 Sources of further information and advice

Further information and a brief commentary on key books and reports to consult and major trade/professional bodies are provided in this section.

The Shell Bitumen Industrial Handbook (Anon., 1995)

This handbook contains extensive information that an engineer needs to know about bitumen, from the tarlike mixture of hydrocarbons derived from petroleum to the most commonly used bitumens for road surfacing and roofing applications.

Asphalt Science and Technology (Usmani, 1997)

This book is organized as follows: characterization, mechanical and rheological aspects, polymer modification, and performance-modification relationships of asphalt. Chemists and civil engineers involved in asphalt research, development and engineering will find this book useful. Professionals in highway departments and students of civil engineering should also benefit.

NCHRP Report 459: Characterization of Modified Asphalt Binders in Superpave Mix Design (Bahia *et al.*, 2001)

This report presents the findings of a research project to evaluate the applicability of the 'Standard Specification for Performance Graded Asphalt Binder' to modified asphalt binders. It will be of particular interest to materials engineers in state highway agencies as well as to materials suppliers and paving contractor personnel responsible for the production and use of modified asphalt binders for asphalt pavement construction.

The Shell Group

The Shell Group is a global group of energy and petrochemicals companies with around 101,000 employees in more than 90 countries and territories. Their innovative approach ensures they are ready to help tackle the challenges of the new energy future.

China Petroleum & Chemical Corporation

China Petroleum & Chemical Corporation is one of the largest integrated energy and chemical companies in China. The scope of its business mainly covers production, marketing, storage and transportation of petrochemicals, chemical fibres, chemical fertilizers and other chemical products; research, development and application of technology and information.

9.8 References

Airey G D (2003), 'Rheological properties of styrene butadiene styrene polymer modified road bitumens', *Fuel*, 82, 1709–1719.

Al-Azri N, Bullin J, Richard R *et al.* (2006), 'Binder oxidative aging in Texas pavements: hardening rates, hardening susceptibilities, and impact of pavement depth', *Transp Res Board*, 06, 2600.

Anon. (1995), *The Shell Bitumen Industrial Handbook*, Chertsey, Surrey, UK Shell Bitumen, 63–115.

Bahia H U, Hanson D I, Zeng M *et al.* (2001), *NCHRP Report 459: Characterization of Modified Asphalt Binders in Superpave Mix Design*, Washington, DC, National Academy Press.

Baumgardner G L, Masson J F, Hardee J R *et al.* (2006), 'Polyphosphoric acid modified asphalt: proposed mechanisms', *Proc Assoc Asphalt Paving Technologists*, 74, 283–305.

Durrieu F, Farcas F and Mouillet V (2007), 'The influence of UV aging of a styrene/butadiene/styrene modified bitumen: comparison between laboratory and on site aging', *Fuel*, 86, 1446–1451.

Ecker A (2001), 'The application of Iatroscan-technique for analysis of bitumen', *Petrol Coal*, 43, 51–53.

Giessibl F J (2003), 'Advances in atomic force microscopy', *Rev Mod Phys*, 75, 949–983.

Harrigan E T, Leahy R B and Youtcheff J S (1994), *The Superpave Mix Design System Manual of Specifications, Test Methods, and Practices*, Washington, National Research Council, 61–71.

Jia J, Zhang X N and Yuan Y (2005), 'Rolling thin film oven test investigation for polymer modified asphalt', *J Harbin Inst Tech*, 12, 635–638.

Kim K W, Ahn K A, Kim S W *et al.* (2001), 'Effect of PMA binder aging on strength characteristics of asphalt concretes', *J Adv Miner Aggr Compos*, 6, 20–28.

Lamontagne J, Dumas P, Mouillet V *et al.* (2001a), 'Comparison by Fourier transform infrared (FTIR) spectroscopy of different ageing techniques: application to road bitumens', *Fuel*, 80, 483–488.

Lamontagne J, Durrieu F, Planche J P *et al.* (2001b), 'Direct and continuous methodological approach to study the ageing of fossil organic material by infrared microspectrometry imaging: application to polymer modified bitumen', *Anal Chim Acta*, 444, 241–250.

Lau C K, Lunsford K M, Glover C J *et al.* (1992), 'Reaction rates and hardening susceptibilities as determined from POV aging of asphalts', *Transp Res Rec*, 1342, 50.

Lee S J, Amirkhanian S N and Kim K W (2009), 'Laboratory evaluation of the effects of short-term oven aging on asphalt binders in asphalt mixtures using HP-GPC', *Constr Build Mater*, 23, 3087–3093.

Loeber L, Sutton O, Morel J *et al.* (1996), 'New direct observations of asphalts and asphalt binder by scanning electron microscopy and atomic force microscopy', *J Microsc*, 182, 32–39.

Lu X H and Isacsson U (1998), 'Chemical and rheological evaluation of ageing properties of SBS polymer modified bitumens', *Fuel*, 77, 961–972.

Lu X H and Isacsson U (2000), 'Artificial aging of polymer modified bitumens', *J Appl Polym Sci*, 76, 1811–1824.

Lu X H and Isacsson U (2002), 'Effect of ageing on bitumen chemistry and rheology', *Constr Build Mater*, 16, 15–22.

Masson J F, Leblond V and Margeson J (2006), 'Bitumen morphologies by phase-detection atomic force microscopy', *J Microsc*, 221, 17–29.

Migliori F, Dumas P and Molinengo J C (2000), 'Use of pressure aging vessel (PAV) to study the aging of bituminous mixes with polymer modified bitumens', *Proc. 2nd Eurasphalt & Eurobitume Congress*, Technical session 2.

Mouillet V, Farcas F and Besson S (2008a), 'Ageing by UV radiation of an elastomer modified bitumen', *Fuel*, 87, 2408–2419.

Mouillet V, Lamontagne J, Durrieu F *et al.* (2008b), 'Infrared microscopy investigation of oxidation and phase evolution in bitumen modified with polymers', *Fuel*, 87, 1270–1280.

Ouyang C F, Wang S F, Zhang Y *et al.* (2005), 'Preparation and properties of styrene–butadiene–styrene copolymer/kaolinite clay compound and asphalt modified with the compound', *Polym Degrad Stabil*, 87, 309–317.

Ouyang C F, Wang S F, Zhang Y *et al.* (2006), 'Improving the aging resistance of styrene–butadiene–styrene tri-block copolymer modified asphalt by addition of antioxidants', *Polym Degrad Stabil*, 91, 795–804.

Polacco G, Muscente A, Biondi D *et al.* (2006), 'Effect of composition on the properties of SEBS modified asphalts', *Eur Polym J*, 42, 1113–1121.

Ruan Y H, Davison R R and Glover C J (2003a), 'The effect of long-term oxidation on the rheological properties of polymer modified asphalts', *Fuel*, 82, 1763–1773.

Ruan Y H, Davison R R and Glover C J (2003b), 'Oxidation and viscosity hardening of polymer-modified asphalts', *Energy and Fuels*, 17, 991–998.

Usmani A M (1997), *Asphalt Science and Technology*, New York, Marcel Dekker.

Valtorta D, Poulikakos L D, Partl M N *et al.* (2007), 'Rheological properties of polymer modified bitumen from long-term field tests', *Fuel*, 86, 938–948.

Wahhab H I A A, Asi I M, Ali F M *et al.* (1999), 'Prediction of asphalt rheological properties using HP-GPC', *J Mater Civ Eng*, 11, 6–14.

Wu S P, Pang L, Mo L T *et al.* (2009), 'Influence of aging on the evolution of structure, morphology and rheology of base and SBS modified bitumen', *Constr Build Mater*, 23, 1005–1010.

Wu S P, Pang L, Liu G *et al.* (2010), 'Laboratory study on ultraviolet radiation aging of bitumen', *J Mater Civil Eng*, 22, 767–772.

Yamaguchi K, Sasaki I and Meiarashi S (2004), 'Mechanism of asphalt binder aging by ultraviolet irradiation and aging resistance by adding carbon black', *J Jpn Petrol Inst*, 47, 266–273.

Yamaguchi K, Sasaki I, Nishizaki I *et al.* (2005), 'Effects of film thickness, wavelength, and carbon black on photodegradation of asphalt', *J Jpn Petrol Inst*, 48, 150–155.

Yu J Y, Wang L, Zeng X *et al.* (2007), 'Effect of montmorillonite on properties of styrene–butadiene–styrene copolymer modified bitumen', *Polym Eng Sci*, 47, 1289–1295.

Yu J Y, Wang X, Hu L *et al.* (2010), 'Effect of various organomodified montmorillonites on the properties of montmorillonite/bitumen nanocomposites', *J Mater Civil Eng*, 22, 788–793.

Zhang F, Yu J Y and Wu S P (2010), 'Effect of ageing on rheological properties of storage-stable SBS/sulfur-modified asphalts', *J Hazard Mater*, 182, 507–517.

Zhang J, Wang J L, Wu Y Q *et al.* (2009), 'Evaluation of the improved properties of SBR/weathered coal modified bitumen containing carbon black', *Constr Build Mater*, 23, 2678–2687.

Natural weathering of styrene–butadiene modified bitumen

J.-F. MASSON, P. COLLINS, J. R. WOODS and
S. BUNDALO-PERC, National Research Council of Canada,
Canada and I. L. AL-QADI, University of Illinois at
Urbana-Champaign, USA

Abstract: This chapter reports on the long-term weathering of 12 bituminous sealants that contain thermoplastic elastomers, namely block copolymers of polystyrene and polybutadiene. The goal of the work was to determine the rate and mechanisms of sealant weathering so that future accelerated aging tests could be developed. By means of physico-chemical analysis, much weathering was found to occur in the early years of service. Weathering pathways were found to be mass loss, oxidation, and copolymer degradation. Specific mechanisms include the loss of aromatics with time, the formation of sulfoxides, sulphones, and their acids, ketones, and carboxylic acids. Block copolymer degradation occurs mainly through a scission between polystyrene and polybutadiene blocks, and the crosslinking of polybutadiene fragments. The chapter ends with a brief discussion of the suitability of current accelerated aging tests to simulate the natural weathering of elastomeric sealants.

Key words: natural weathering, physico-chemical analysis, bituminous sealants, copolymers of polystyrene and polybutadiene.

10.1 Introduction

Weathering is the process of aging that occurs in service when a material is exposed to the elements: sunlight, rain, snow, brine, freezing and thawing, for instance. There are few studies of material weathering because they usually take several years to perform. In this chapter, we report on the weathering of bituminous sealants over a decade in the streets of Montreal, Canada. These sealants all contain block copolymers of polystyrene (PS or S) and polybutadiene (PB or B). After some background on bitumen and its properties, and the reason for its modification with polymers, this chapter continues with an overview of the physico-chemical methods adapted to study sealants and their composition. These include Fourier-transform infrared spectroscopy (FTIR), gel permeation chromatography (GPC) and high-resolution thermogravimetry (HRTG). On this basis, the chapter follows with

an analysis and a discussion of the most common weathering mechanisms in bituminous sealants. The chapter ends with a brief discussion on the future development of accelerated aging methods based on the weathering mechanisms reported.

10.2 Background

Asphalt is a mixture of bitumen with inorganic fines. Natural open-air deposits are found around the world and notably in the Middle East and Caribbean (Speight, 1999). As a result, asphalt has been used in construction applications since the dawn of time. Already in the Bronze Age, Sumerians and Assyrians used it to join materials and to waterproof wood pylons and walls (Jones, 1963; Speight, 1999; Lambert, 2005). Today there are almost 200 applications for asphaltic materials (Anon., 1989). The binder in these materials, bitumen, is obtained in large quantities as a residue of crude oil processing (Speight, 1999). Upon distillation and the removal of gases, fuels, and oils, the remaining crude oil residue is bitumen. Its composition and physico-chemical characteristics depend on the crude oil source and the process used to extract the more valuable commodity products. For classification purposes, bitumen is characterised by its viscosity, its penetration, or its modulus (Read and Whiteoak, 2003). In most cases bitumen is a viscoelastic material and its mechanical or flow characteristics depend on time and temperature. For instance, if a vessel filled with bitumen were punctured at the bottom, the flow of bitumen would be relatively rapid at high temperature, e.g., 170°C, but slow at sub-zero temperatures. In contrast, a perfect solid would not flow regardless of temperature and a perfect liquid would on the contrary flow at all temperatures. Hence, because of its viscoelastic nature, bitumen is sensitive to temperature and so are the properties of bituminous products. In service, these products can flow or deform at summer temperatures, and they can fracture at low temperatures, which can limit their application.

To reduce the temperature sensitivity of bituminous products and improve their properties, bitumen is often modified with ground tyre rubber (Shim-Ton *et al.*, 1980) or one of several polymers (Boutevin *et al.*, 1989; Giavarini, 1994; Lewandowski, 1994). Block copolymers of PS and PB are most common, and as will be seen later, a family of such copolymers is widely used to modify bitumen. For convenience, we henceforth refer to this family as SB-copolymers. The combination of PS and PB blocks is most interesting because the blocks can have respective glass transition temperatures (T_g) near 100°C and -95°C (Masson *et al.*, 2005). When SB-copolymers are mixed with bitumen, the temperature at which bitumen flows can be raised towards the T_g of PS, and the temperature at which bitumen is more sensitive to fracture can be lowered towards the T_g of PB. Hence, bitumen with SB-copolymers

can be used most advantageously in climates with both cold winters and warm summers, e.g., Canada, Switzerland, Scandinavia and Russia.

Bitumen modified with less than about 4% SB-copolymer by weight of bitumen is used for roadway applications, mostly as an aggregate binder in asphalt concrete mixtures. In these modified bitumens, the SB-copolymer is dispersed in the bitumen matrix (Kraus and Rollmann, 1981; Ajour and Brûlé, 1982; Brûlé *et al.*, 1984; Bouldin *et al.*, 1991). Bitumens modified with more than about 7 wt% SB-copolymer are common in waterproofing applications, including membranes, coatings, caulk, and sealants. In this case, the phase structure of the material is reversed; a discrete bitumen phase is dispersed into a continuous polymer phase (Kraus and Rollmann, 1981; Masson *et al.*, 2002). Co-continuous bitumen and copolymer phases are often obtained with copolymer concentrations between about 4 wt% and 7 wt%. In all cases, however, the degree of dispersion of one phase in the other depends on the composition of bitumen, the copolymer molecular weight, the S/B ratio, and the copolymer architecture (Kraus and Rollmann, 1981; Masson *et al.*, 2003).

This chapter discusses the long-term natural weathering of bituminous sealants that contain SB-copolymers. It provides data on the true aging of these materials, as opposed to that from accelerated aging; the latter may or may not provide an accurate representation of weathering (Frohnsdorff and Masters, 1980; Wypych, 2008). Given that bituminous sealants can have up to 20 wt% SB-copolymer (Masson *et al.*, 2001), this chapter also provides a perspective on the aging of SB-copolymers where the copolymer phase is continuous as opposed to discrete, and hence it may help to better understand similar materials, including waterproofing membranes and coatings. A clear focus is made on the change in sealant composition upon weathering, a subject barely studied before (Hean and Partl, 2004). Before the weathering of sealants is addressed, however, it is worthwhile to briefly review the general composition of these materials and the methods involved in the analysis of weathered sealants in our laboratories.

10.3 Bituminous sealants and methods of analysis

The composition of bituminous sealants, which is dictated by performance and economic imperatives, can be fairly complex. Bitumen, the main component, can be mixed with a block copolymer of PS and PB, ground tyre rubber (GTR), mineral filler, mineral oil, sulphur, and specialised additives (Table 10.1). The range of composition varies much and not all sealants are complex mixtures. Simple sealants contain bitumen, some GTR, and mineral oil. Figure 10.1 illustrates the microstructure of three sealants, from fluorescence optical microscopy. The upper microphotograph shows a sealant with 8 wt% SB-copolymer co-continuous with bitumen. The middle

Table 10.1 Typical components in bituminous sealants and their common range

Component	Content (wt%)
Bitumen	45–95
Block copolymer of PS and PB	0–20
Ground tyre rubber	0–25
Mineral oil	5–15
Mineral filler	0–35
Sulphur	0–0.5
Specialty additives	0–2

one shows a sealant with discrete GTR and copolymer, the darkest and the lightest phases, respectively. The bottom morphology is that of a sealant with GTR and low (1 wt%) copolymer content.

The properties of bituminous sealants can be investigated by a number of physico-chemical methods (Hugener and Hean, 1996; Masson *et al.*, 2002). The methods listed in Table 10.2 are those adapted or developed in our laboratories to study bituminous sealants. To study the rate and mechanisms of weathering in particular, three methods have proved invaluable, namely Fourier-transform infrared spectroscopy, gel permeation chromatography, and high-resolution thermogravimetry.

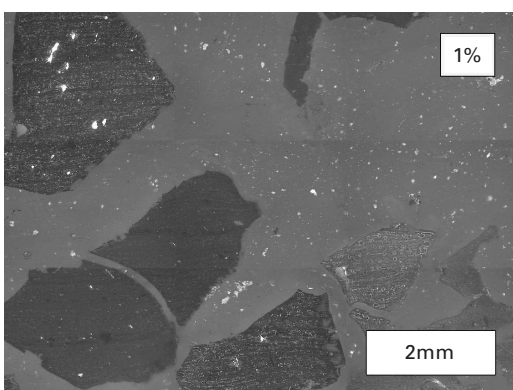
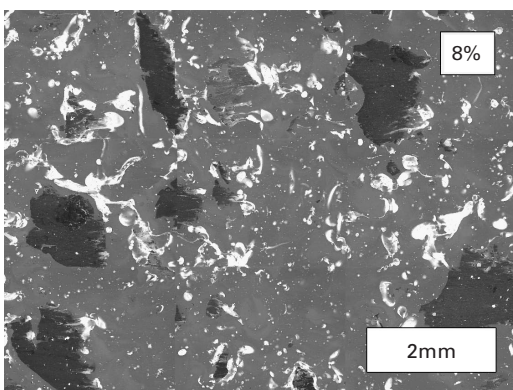
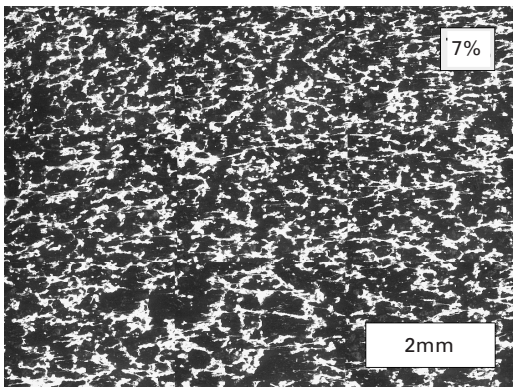
10.3.1 Fourier-transform infrared spectroscopy (FTIR)

FTIR is a most important method to identify and quantify polymers in sealants (Choquet and Ista, 1990; Masson *et al.*, 2001) and it has long been used to study bitumen oxidation (Campbell and Wright, 1964). The basics of the method can be found in several textbooks (Lambert *et al.*, 1976; Pavia *et al.*, 1979). To identify the polymer, transmission, photo-acoustic, or attenuated total reflectance methods can be used (Koenig, 1992). To date, all sealants investigated in our laboratory contained block copolymers of PS and PB. In the fingerprint region, between 400 cm^{-1} and 2000 cm^{-1} , the PB block shows an absorbance of medium intensity at 966 cm^{-1} and one of weak intensity at 911 cm^{-1} , whereas the PS block shows an absorbance of medium intensity at 699 cm^{-1} . The origin of these frequencies and that of other typical infrared absorbance bands from bituminous sealants are shown in Table 10.3.

In working with sealant solutions, transmission FTIR can be used to measure the content of SB-copolymer as the sum of the PB and PS weight contents:

$$C = W_{\text{PS}} + W_{\text{PB}} = A_{\text{PS}} F_{\text{PS}} / (a l s)_{\text{PS}} + A_{\text{PB}} F_{\text{PB}} / (a l s)_{\text{PB}} \quad 10.1$$

where C is the total copolymer content, W_i is the weight content of PS or PB, A_i is the infrared absorbance at either 699 cm^{-1} (PS) or 966 cm^{-1} (PB),



10.1 Morphology of bituminous sealants as obtained from fluorescence microscopy. The copolymer content is indicated in the upper right corner. Magnification is 100 \times . Width of white box is 2 mm.

Table 10.2 Methods to characterise bituminous sealants

Method ^a	Output	Use
UV-microscopy	Image of microstructure	Identification and semi-qualitative analysis of components: copolymer, ground tyre rubber, filler
FTIR	Spectrum of infrared absorbance	Oxidation; polymer and filler identification; polymer content
GPC	Separation of bitumen and polymer	Measure of molecular weights and copolymer architecture
HRTG	Mass loss upon heating	Contents of filler, and light, medium, and heavy hydrocarbons
DSR	Temperature dependence of stiffness and relaxation	Effect of temperature and aging on mechanical properties

^aUV, ultraviolet; FTIR, Fourier-transform infrared spectroscopy; GPC, gel permeation chromatography; HRTG, high-resolution thermogravimetry; DSR, dynamic shear rheometry.

Table 10.3 Common infrared fingerprinting absorbances from bituminous sealants

Bond	Group	Source ^a	Frequency (cm ⁻¹)
C—H	Methyl	Bitumen, oils, PS, PB	1450, 1376
	Methylene	Bitumen, oils, PS, PB	1465
	Alkene	Bitumen, PB	1000–650
	Aromatic	Bitumen, PS	900–690
C=C	Alkene	PB main chain	966
	Alkene	PB vinyl group	911
	Aromatic ring	PS	699
	Aromatics	Bitumen	1600, 1490
C=O	Ketone	Oxidation	1740–1700
S=O	Sulphoxide	Oxidation	1030
CO ₃	Carbonate	Filler	874, 712

^aPS: polystyrene; PB: polybutadiene.

F_i is the formula weight of the repeat unit in Dalton (1 Da = 1 g/mol), a is the molar absorbance (L/mol/cm), l is the cell thickness (cm), and s is the sealant concentration in solution (g/L). With equation 10.1 and the respective molar absorptivities of 277 L/mol/cm⁻¹ and 69 L/mol/cm⁻¹ for PS and PB blocks (Masson *et al.*, 2001), the calculated copolymer content is within 10% of that obtained by proton nuclear magnetic resonance. With equation 10.1, it is also possible to calculate the S/B weight ratio as $W_{\text{PS}}/W_{\text{PB}}$.

If the infrared spectrum of the sealant or SB-copolymer is obtained not from solution but from a solid film cast from solvent onto a KBr crystal, then the S/B ratio can be calculated by rearranging equation 10.1 to:

$$W_{PS}/W_{PB} = A_{PS} a_{PB} F_{PS}/A_{PB} a_{PS} F_{PB} \quad 10.2$$

With values of $F_{PS} = 104$ Da, $F_{PB} = 54$ Da and the above molar absorptivities, equation 10.2 is reduced to

$$S/B = 0.48A_{699}/A_{966} \quad 10.3$$

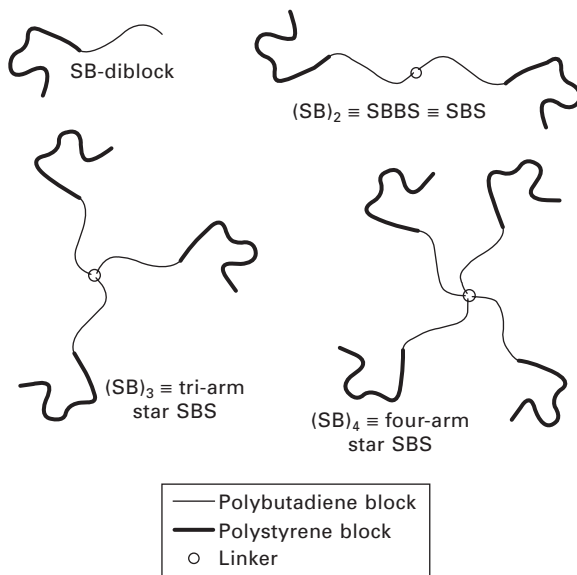
from which a ratio of 0.428, for instance, would translate to a 30/70 S/B weight ratio.

10.3.2 Gel permeation chromatography (GPC)

Polymer analysis

FTIR spectroscopy can provide positive identification of an SB-copolymer in bituminous sealants, but it is GPC that informs us of polymer size and of the extent of modification upon weathering. Indeed, GPC is a sieving method that allows for separating and analysing molecules of different weights and architectures (Bidlingmeyer, 1992; Wu, 1995).

The copolymer architecture, its linearity, depends on the link between the PS and PB diblocks. In the simplest case, PS and PB blocks are joined into a diblock SB-copolymer (Fig. 10.2). In other cases, a coupler links n diblocks into $(SB)_n$, where n is usually 2 to 4 (Legge, 1989). A most common

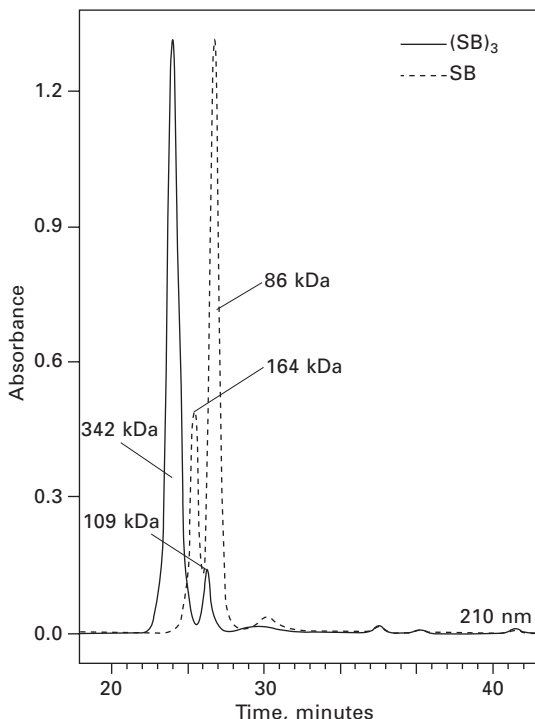


10.2 Some architectures of block copolymers of polystyrene (S) and polybutadiene (B).

copolymer is the linear SBS triblock copolymer, where $n = 2$, $(\text{SB})_2 \equiv \text{SB-BS} \equiv \text{SBS}$. With $n > 2$, the structure is that of an n -arm star.

GPC separates compounds based on molecular size, with the largest compounds being separated first, i.e., after shorter elution times. Consequently, a mixture of $(\text{SB})_n$ copolymers can be separated based on the values of n . As an example, Fig. 10.3 shows results for two copolymers of PS and PB. Both copolymers give rise to a pair of peaks, which demonstrates that each product is a mixture. The dotted trace shows maxima at 25.5 and 27.0 minutes. Based on a calibration curve that relates elution time to molecular weight, these elution times translate to molecular weights of 164 kDa and 86 kDa, respectively. Within experimental error, the 2:1 ratio of these weights reveals the copolymer architecture: $(\text{SB})_2$ in the first case and SB in the other. In contrast, the full trace in Fig. 10.3 shows maxima at 24.3 and 26.4 minutes for molecular weights of 342 kDa and 109 kDa. The respective intensities of these maxima and their 3:1 molecular weight ratio provide the key to a three-arm star block copolymer, $(\text{SB})_3$, that contains some SB diblock. Similar analysis can be applied to sealants.

In GPC analysis of bituminous sealants, we commonly use three UV-

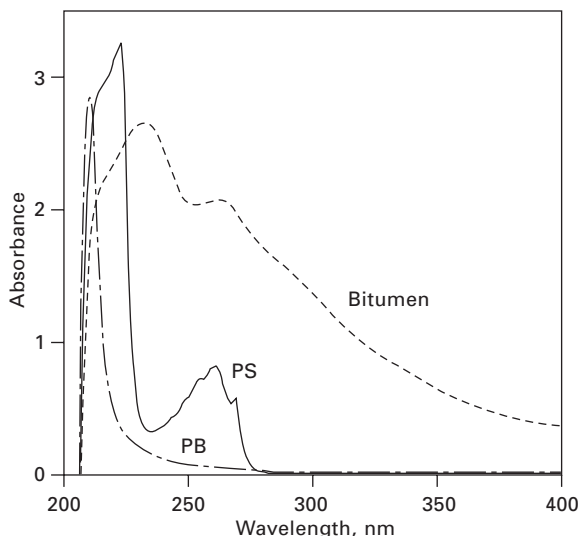


10.3 GPC responses from two commercial sources of block SB-copolymers. UV-light detection at 210 nm.

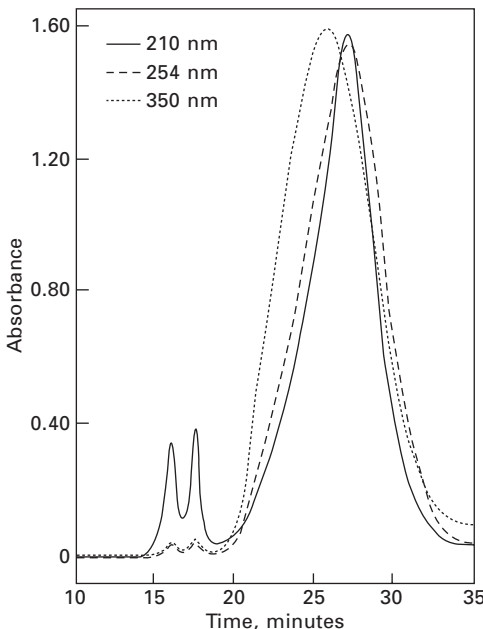
light detection wavelengths, namely 210 nm, 254 nm, and 350 nm. This is advantageous because of the UV chromophores in bitumen modified with SB-copolymers, namely the fused aromatics in bitumen, and alkene and phenyl groups in the copolymers. Figure 10.4 shows that at 350 nm the absorbance of bitumen is orders of magnitude greater than those of PS and PB. At 254 nm, bitumen and PS are preferentially detected, and at 210 nm they are all well detected. Consequently, the analysis of bituminous sealants at various wavelengths allows for some selectivity in detection. For bitumen (Fig. 10.5), the longer wavelength is more sensitive to high molecular mass fused aromatics (Pasto and Johnson, 1969; Pribanic *et al.*, 1989) whereas the 210 nm absorbance is typical of single aromatic systems such as alkyl benzenes and phenols (Lambert *et al.*, 1976; Pavia *et al.*, 1979).

Sulphur analysis

The performance of bituminous sealants partly depends on the stability of the copolymer-bitumen mixture. In general, the stability of these mixtures against segregation is controlled by thermodynamic factors; high polymer molecular weights reduce stability, whereas high alkene content in the polymer enhances stability (Kraus and Rollmann, 1981; Masson *et al.*, 2003). To prevent a possible segregation of the copolymer and bitumen, and to modify the elastic properties of sealant, sulphur is often used. Sulphur can



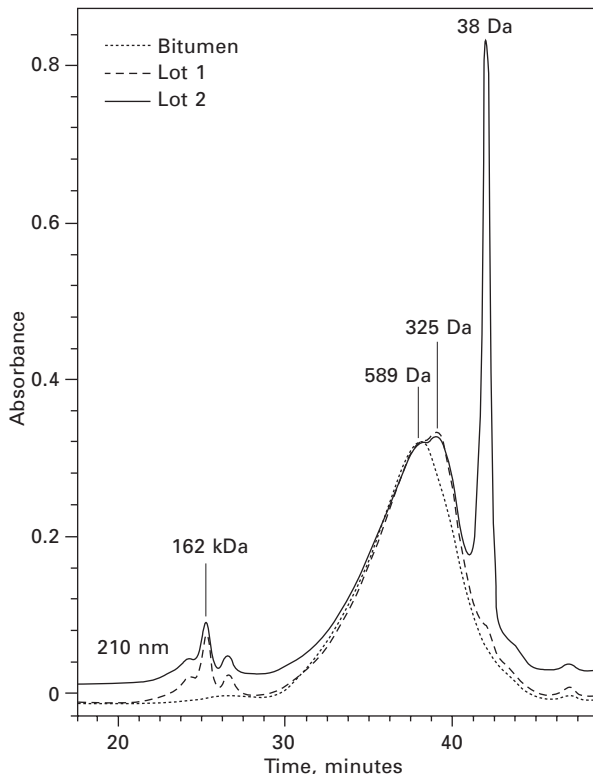
10.4 Ultraviolet absorbance of important sealant components: bitumen, polystyrene (PS) and polybutadiene (PB). Solution concentrations of 0.0625% in tetrahydrofuran (w/v).



10.5 GPC of a bituminous sealant with UV-light detection at 210 nm, 254 nm and 350 nm.

react with alkyl aromatics (Petrossi *et al.*, 1972) and crosslink unsaturated copolymers in a process similar to rubber vulcanisation (Maldonado *et al.*, 1979; Coran, 1994).

During vulcanisation, sulphur rings (S_8) open into linear sulphane bridges ($-S_x-$), $x = 1$ to 8 (Coran, 1994). Sulphanes have strong UV absorbance (Fehér and Münzner, 1963) and as a result they are easily visible with a UV-VIS chromatographic detector (Steudel, 2002). Figure 10.6 shows an example of this detection on two batches of the same bituminous sealant prepared on two different days in an industrial plant. Each batch was 7000 kg. As a reference, the base bitumen shows a single broad maximum near 38.5 min for a molecular weight of 589 Da. Lot 1, with 8% copolymer and 0.2% sulphur by weight of bitumen, showed the bitumen signal as a shoulder to a new maximum near 39.5 min for a molecular weight of 325 Da. With a molecular weight in excess of S_8 (256 Da), we attributed this new maximum to alkyl-aromatic sulphides. Lot 2 of the same sealant showed an additional signal, a spike at a molecular weight of 38 Da that can be attributed to hydrogen sulphide (H_2S , 34 Da), a gas readily produced during vulcanisation (Kemp and Malm, 1935; Tinyakova *et al.*, 1956; Petrossi *et al.*, 1972). With an analysis of the copolymer, bitumen, and sulphur peaks, GPC can thus be used to follow the extent of their reaction during manufacture, or to follow

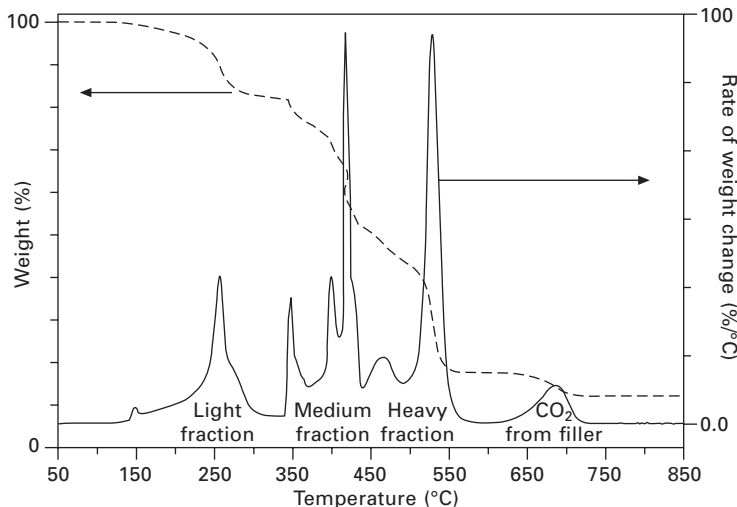


10.6 GPC with UV detection at 210 nm of base bitumen and two sealant batches produced on different days.

their change after weathering. The two lots in Fig. 10.6, for instance, were obviously produced under different conditions.

10.3.3 High-resolution thermogravimetry

Thermogravimetry (TG) is a method of controlled combustion that allows for measuring the temperature at which a material degrades (Hatakeyama and Quinn, 1999). When bitumen or bituminous materials are heated at a constant rate, this transformation is most often a cascade of irreproducible and poorly resolved mass losses. In efforts to use TG as a fingerprinting and quantitative tool, we developed a high-resolution TG method that allows for a clear separation of mass losses that arise from light, medium and heavy bitumen fractions (Masson and Bundalo-Perc, 2005). In this method, the rate of heating depends on the rate of sample weight loss. Figure 10.7 shows TG results for a bituminous sealant, where the mass loss and its derivative are presented. The derivative curve, which provides the rate of weight change



10.7 Mass loss and rate of mass loss upon heating a bituminous sealant by high-resolution thermogravimetry.

upon heating, shows a series of well-defined peaks that can be attributed to various components. In the analysis of bituminous sealants, four mass loss regions are clearly identified: 50–325°C, 325–500°C, 500–600°C, and 600–850°C. The first region captures the weight loss due to the boiling of light hydrocarbons. The second region highlights the degradation temperatures of PS and PB blocks, and alkyl aromatics in bitumen. The third region is more closely associated with heavy bituminous aromatics, like asphaltenes. Beyond 600°C, a temperature at which all the hydrocarbons have turned to gas, the mass loss arises from mineral fillers that evolve carbon dioxide. Limestone, the most common filler, shows a mass loss peak near 700°C and leaves a residue of calcium oxide 2.16 times the carbon dioxide weight loss.

The area under the derivative peaks provides the percent mass loss from various sealant components. With the high-resolution method, a coefficient of variation better than 5% by weight is typically obtained (Table 10.4). As we will see later, this method is useful to measure the loss of bituminous material upon aging.

10.4 Weathering of bituminous sealants

Twelve bituminous sealants were installed over 24 linear km of cracks found in asphalt pavements in Montreal, Canada. We reported earlier on the installation and performance of these sealants (Masson *et al.*, 1998, 1999, 2002). The virgin sealants were collected during installation, and the weathered sealants were collected after one, three, five, and nine years of service, a time during

Table 10.4 Typical variability in percent mass loss from sealant fractions as measured by HRTG

Sample ^a	Light fraction	Middle fraction	Heavy fraction	Total organics	CO ₂ from filler	Residue
	(50–325°C)	(325–500°C)	(500–600°C)	(50–600°C)	(600–900°C)	(900°C)
Bv1	16.6	39.4	26.0	87.5	5.5	12.6
Bv2	16.3	40.6	25.1	87.5	5.6	12.6
Bv3	17.7	39.0	25.5	87.7	5.5	12.3
Bv4	18.2	38.3	26.1	88.0	5.3	12.2
Average	17.2	39.3	25.7	87.7	5.5	12.4
COV (%) ^b	5.0	2.5	1.9	0.2	1.8	1.6

^aFrom the surface of as-received sealant, without remixing.

^bCoefficient of variation.

which winter air temperatures went down to –40°C on occasion and summer air temperatures attained 37°C. The retrieved specimens were typically 10 cm long with a cross-section 4 cm wide and 1 cm deep.

To determine the rate and mechanism of sealant aging, 60 specimens from 12 sealants were subjected to physico-chemical analysis. However, in efforts not to roll out a tedious product-by-product description of the effects of weathering, we highlight here the major aging mechanisms as obtained by FTIR, GPC, and HRTG. Sealants are labelled A to M and their aging state is labelled as v or wN, where v indicates the virgin (unaged) state and wN indicates weathering over N years. As examples, Sealant Av refers to the virgin state of Sealant A, and Sealant Cw5 refers to Sealant C weathered over 5 years. FTIR spectra of weathered sealants were acquired from sample cross-sections with a 15-bounce attenuated total reflectance accessory that allowed for an analysis of the entire depth of the specimen, 1 cm. GPC and HRTG results are those obtained on about 10 mg samples taken at mid-depth in the specimens. Further experimental details are found elsewhere (Masson *et al.*, 2002; Masson and Bundalo-Perc, 2005).

10.4.1 Carbon and sulphur oxidation

There are many infrared spectroscopy studies of bitumen oxidation (Campbell and Wright, 1964; Jemison *et al.*, 1992; Herrington *et al.*, 1994; Herrington and Ball, 1996) including polymer-modified bitumen (Ruan *et al.*, 2003). In most cases, accelerated laboratory methods of oxidation are used. In contrast, few field studies of bitumen natural weathering have been performed (Verhasselt and Choquet, 1993; Such *et al.*, 1997; Mallick and Brown, 2004) and even fewer have studied natural oxidation by means of infrared spectroscopy (Durrieu *et al.*, 2007). In working with bituminous sealants, Hean and

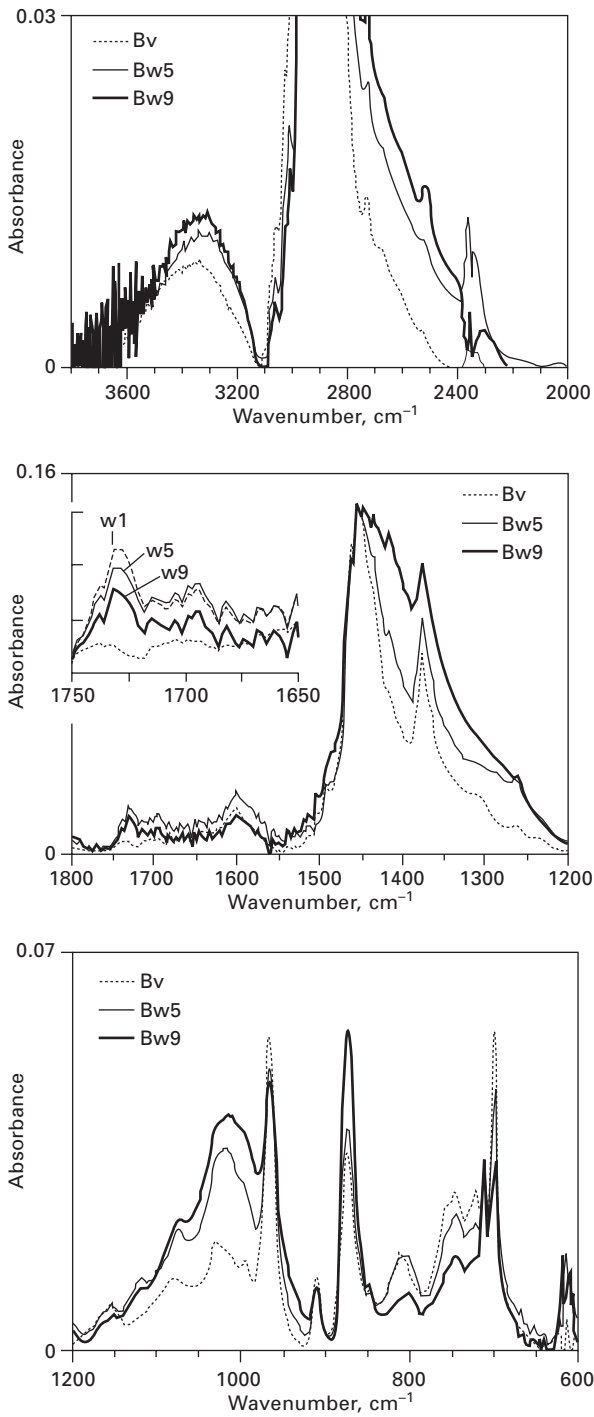
Partl (2004) have studied the evolution of the engineering properties of the materials after their weathering over five years in Switzerland, but they did not report on the effects of oxidation.

The weathering of Sealant B possibly represents the simplest case of carbon and sulphur oxidation. With this material, weathering leads to an increase in infrared absorbance centred near 3300 cm^{-1} , 2600 cm^{-1} , 1400 cm^{-1} and 1030 cm^{-1} (Fig. 10.8). Absorbances from C—O in aliphatic and aromatic carboxylic acids were observed between 1450 cm^{-1} and 1400 cm^{-1} , and between 1300 cm^{-1} and 1200 cm^{-1} , respectively (Lambert *et al.*, 1976). This assignment is consistent with the rise of the broad hydroxyl band near 3300 cm^{-1} . Sulphur oxidation is also recognised by the typical sulphoxide absorbance near 1030 cm^{-1} (Petersen, 1986; Lamontagne *et al.*, 2001). The rise in background between 2400 and 2800 cm^{-1} is further attributed to sulphur oxidation, the O—H stretching in sulphur acids, $-\text{SO}_x\text{OH}$ (Lambert *et al.*, 1976).

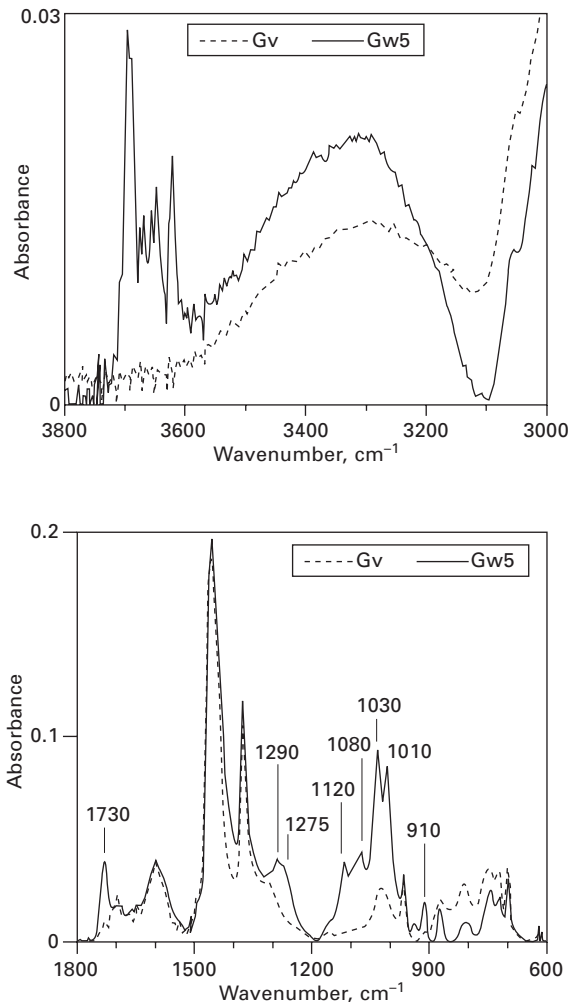
As shown in Fig. 10.8, hydroxyl and sulphoxide absorbance increase with weathering. In contrast, carbonyl absorbances decrease with weathering time; an initial step of oxidative weathering in the first year gives rise to carbonyl ($\text{C}=\text{O}$) absorbances, visible near 1730 cm^{-1} and 1700 cm^{-1} . Weathering beyond one year, however, causes a constant decrease, such that the lowest carbonyl absorbance is obtained after nine years of weathering. The reason for this decrease will be discussed later.

Except for the carbonyl region, the spectrum of Sealant B weathered for one year overlaps with that weathered for five years. Such an overlap indicates that oxidation can progress quickly once sealants are in-service, and then again only after several years of weathering. This first suggests that high-temperature installation is responsible for early oxidation, but it is already established that installation is not oxidative (Hugener and Hean, 1996; Masson *et al.*, 2007, 2008). Consequently, the FTIR results on Sealant B reveal that natural oxidative weathering can occur in steps, as opposed to the continuous oxidation obtained by laboratory accelerated aging methods (Liu *et al.*, 1996).

Another common pattern of sealant oxidation is shown in Fig. 10.9. For clarity, this figure only shows the virgin sealant (Gv) and the material weathered for five years (Gw5). Here the noteworthy feature pertains to sulphur oxidation, namely a series of sharp and intense absorbances between 1200 cm^{-1} and 900 cm^{-1} . In addition to the common $\text{S}=\text{O}$ peak at 1030 cm^{-1} , sulphone ($\text{O}=\text{S}=\text{O}$) and sulphonic acid ($-\text{SO}_2\text{OH}$) absorbances are quite apparent. Table 10.5 shows the multiple frequencies that arise from these groups. The intense absorbance at 1010 cm^{-1} in Fig. 10.9 was initially attributed to C—O, but after the observation of its synchronous rise or fall with the absorbance at 1030 cm^{-1} in several sealants, it was attributed to $\text{S}=\text{O}$ in heavy aromatics. Above 3000 cm^{-1} , the formation of sulphur and



10.8 Infrared spectra of Sealant B in its virgin state (Bv) and after 5 and 9 years of weathering (Bw5, Bw9). The inset shows the enlarged carbonyl region with 1 year of weathering (w1).



10.9 Infrared spectra of Sealant G before (Gv) and after 5 years of weathering (Gw5). Table 10.5 lists the labelled group frequencies.

carboxylic acids gives rise to signals like those shown in Fig. 10.8 for Sealant B, with the additional feature of sharp absorbances attributed to free hydroxyl groups between 3600 and 3800 cm⁻¹ (Fig. 10.9).

The prevalence of high oxides of sulphur upon weathering bituminous sealants is reminiscent of the sulphates obtained by accelerated photo-oxidation of bitumen (Huang *et al.*, 1995), an oxidation process that leads to water-soluble material (Streiter and Snone, 1936; Oliver and Gibson, 1972). It is thus not surprising that sealant mass loss is observed with FTIR and HRTG, as detailed below.

Table 10.5 Common infrared oxidation frequencies in weathered bituminous sealants

Bond	Functional group assignments ^a	Frequency (cm ⁻¹)
O—H	Free carboxylic acids, alcohols	3800–3700
	Bound carboxylic acids, alcohols	3250–3450
	Sulphonic and sulphinic acids	2800–2400
C=O	Aliphatic ketones	1730–1700
	Aromatic ketones	1700–1680
	Carboxylic acids	1720–1680
C—O	Aliphatic carboxylic acids	1440–1400
	Phenols	1360–1340
	Aromatic carboxylic acids	1300–1200
S=O	Sulphones	1290, 1120
	Sulphoxides	1030, 1010
	Sulphonic and sulphinic acids	1120, 1080, 910

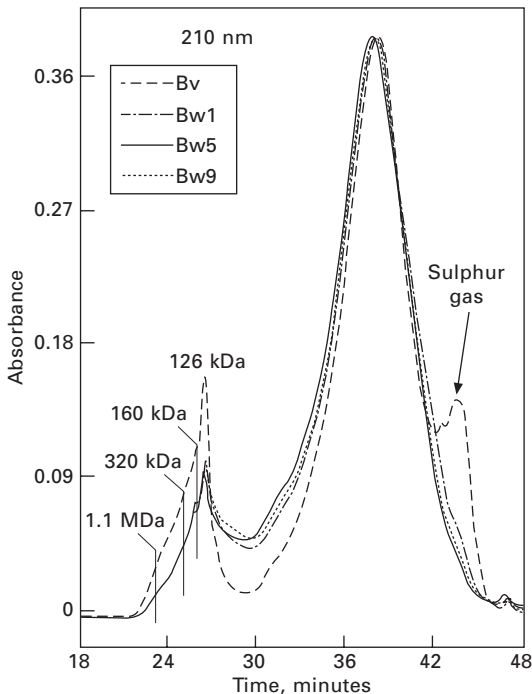
^aBased on Lambert *et al.* (1976), Lin-Vien *et al.* (1991), and Huang *et al.* (1995).

10.4.2 Reaction and loss of sulphur compounds

We have seen earlier in Fig. 10.6 that GPC can reveal the presence of sulphur compounds in bituminous sealants. Figures 10.10 to 10.12 show GPC curves for Sealant B at 210 nm, 254 nm and 350 nm, respectively. At all wavelengths, the unaged virgin sealant (Bv) shows sulphur gas between 42 and 46 min for molecular weights between 30 Da (H_2S) and 160 Da (H_2S_5). As seen at 210 nm, vulcanisation is also effective as the main SB-copolymer component at 126 kDa is crosslinked to higher molecular mass material. The crosslinking is such that at least three shoulders are detected, at 160 kDa, 320 kDa and 1.1 MDa, indicating that up to 10 crosslinks exist.

Figures 10.10 to 10.12 also show the change in sulphur gas content with time. The concentration of sulphur gas drops constantly upon weathering, more so in the first year of weathering, which is most easily seen at 210 nm and 254 nm. Beyond one year of weathering, small but regular depressions of the signal from sulphur gas are observed. The vast majority of the sealants investigated show a similar trend, but to a lesser degree, as the initial signal from sulphur gas is much lower.

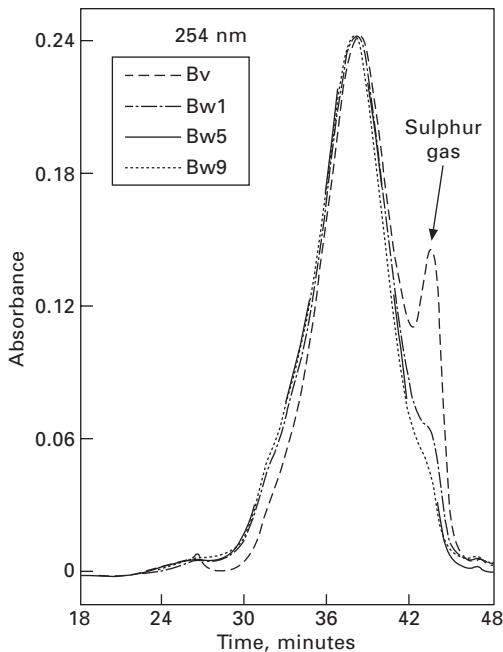
Figure 10.13 shows the GPC results on another sealant (C), where the noteworthy change is not so much the loss of sulphur gas with time, but the change in bitumen–sulphur compounds with weathering. At 254 nm, the main bitumen peak from Sealant C shows a molecular weight of 450 Da and a shoulder on the low molecular weight side at 320 Da. As we did earlier for the sealant batches in Fig. 10.6, we attributed the shoulder in Sealant C to sulphur–bitumen compounds. Upon weathering, the shoulder intensity



10.10 GPC at 210 nm of Sealant B in its virgin state (Bv) and after weathering for 1 to 9 years (Bw1, Bw5, Bw9).

decreases regularly until it becomes almost indistinguishable after nine years of weathering. The same trend is observed for the sulphur gas signal centred at 66 Da.

The loss in signal for sulphur compounds at 254 nm concurs with the rise of another signal at 210 nm (Fig. 10.14). At 210 nm, the virgin sealant (Cv) shows a maximum at 500 Da and a sharp but incompletely resolved shoulder at 1 kDa. Upon weathering, the intensity of this shoulder rises systematically until it reaches the same intensity as the main bitumen after nine years of weathering. The observation of this signal at 210 nm suggests that it affects the lighter and more paraffinic hydrocarbons in the sealant, confirmed by the constant rise in the boiling point of the lighter fraction during HRTG analysis (Fig. 10.15). This is concurrent with the rise in oxidation, as seen by FTIR (Fig. 10.16), and most notably with the rise in absorbance for sulphur oxides between 1200 cm^{-1} and 900 cm^{-1} . The combined FTIR, GPC and HRTG results thus indicate that light sulphides are preferentially oxidised during weathering.

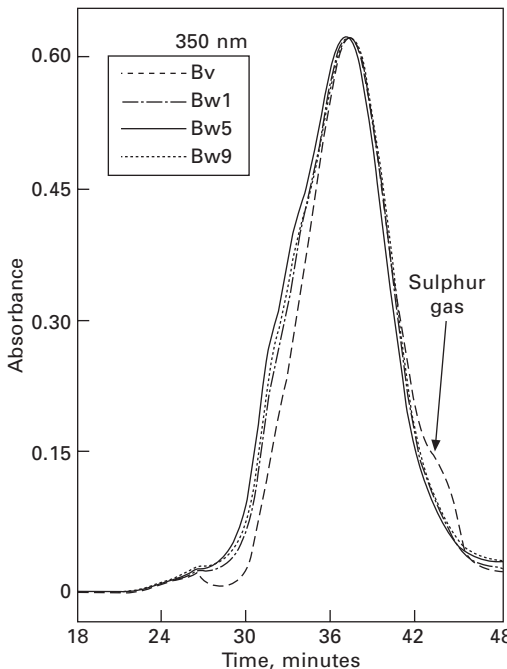


10.11 GPC at 254 nm of Sealant B in its virgin state (Bv) and after weathering for 1 to 9 years (Bw1, Bw5, Bw9).

10.4.3 Mass change and loss of aromatics

The FTIR spectra for sealants B, C and G have been shown in Figs 10.8, 10.16, and 10.9, respectively, and they all show that weathering leads to a decrease in absorbance between 850 cm^{-1} and 700 cm^{-1} , a region characteristic of substituted and fused aromatics (Lambert *et al.*, 1976; Lin-Vien *et al.*, 1991). This decrease can be fairly regular, but it is often greater after five years of weathering. From FTIR, it is clear that weathering leads to a general loss of aromatic fractions in bituminous sealants. This is sometimes concurrent with the decrease in carbonyl signal between 1700 and 1750 cm^{-1} as shown for sealants B and C in Figs 10.8 and 10.16, respectively.

In sealants with a carbonate signal at 873 cm^{-1} in the FTIR spectrum, including sealants B and C, the loss of aromatics upon weathering leads to an increase in the intensity of the carbonate signal. This relative increase in filler content is consistent with the results of HRTG, which shows a rising mass loss from the filler between 600 and 900°C . Sealant B is a good example of this (Table 10.6). As indicated in the rightmost column of the table, the increase in filler weight appears to occur stepwise. This should not be regarded as a stepwise loss in aromatics, but as the result of competing mass loss and oxidative mass gain. This is well shown in Table 10.6 with the

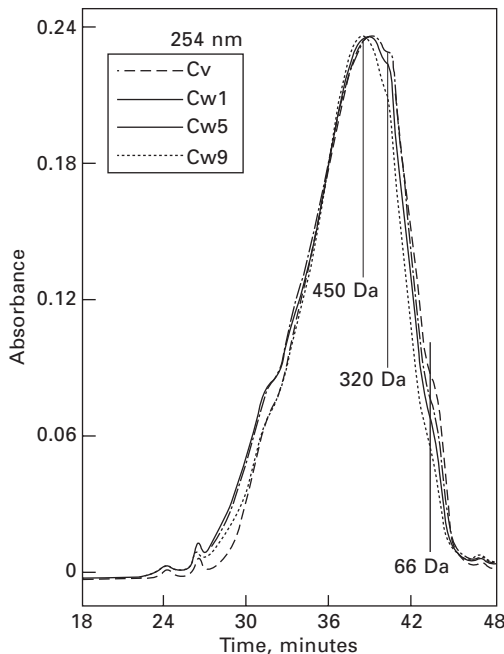


10.12 GPC at 350 nm of Sealant B in its virgin state (Bv) and after weathering for 1 to 9 years (Bw1, Bw5, Bw9).

change in mass loss below 600°C. The light, medium and heavy fractions are lost during the first three years of weathering, and more so with the middle fraction. Beyond three years, however, the heavy fraction gains weight due to oxidation, a fact consistent with the appearance of FTIR oxidation bands. The results shown for Sealant B in Table 10.6 are quite typical. For many sealants, the aromatics, that is, the middle and heavy HRTG fractions, gain weight upon weathering and most often this happens between one and five years in the field. The combination of FTIR and HRTG results thus generally indicates that sealant weathering occurs in part through oxidation followed by a loss of aromatic compounds.

10.4.4 Copolymer degradation

Maréchal and Brûlé were pioneers in the study of polymer degradation in mixtures with bitumen (Maréchal, 1980, 1983; Maréchal *et al.*, 1983; Brûlé *et al.*, 1984). In working with waterproofing materials, Maréchal showed that mixtures with 7 to 13% linear SBS exposed to oven aging at 70°C for up to six months were strongly affected by heat aging. The copolymer degraded until the SBS peak disappeared completely from the gel permeation chromatogram,



10.13 GPC at 254 nm of Sealant C in its virgin state (Cv) and after weathering for 1 to 9 years (Cw1, Cw5, Cw9).

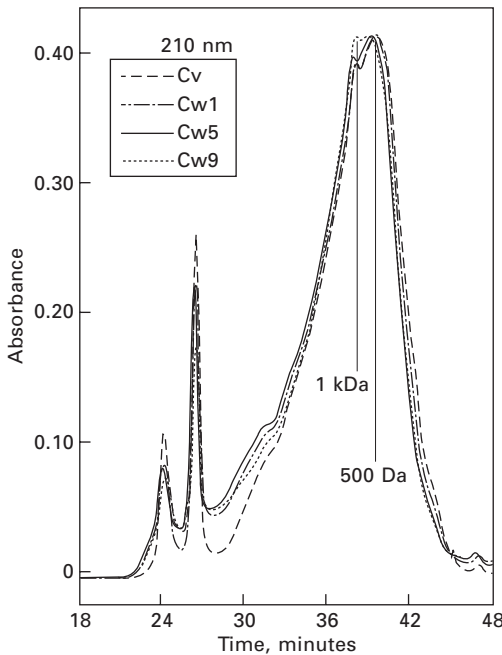
and the intensity of the peak associated with the double bond of the PB block was reduced significantly in the FTIR spectra, while the PS signal remained constant. In working with roadway materials, Brûlé *et al.* showed that the same accelerated aging leads to a 50% reduction in molecular weight. Similar results were later obtained by Linde and Johansson (1992).

The installation of bituminous sealant at 170–190°C can also lead to extensive degradation of the SB-copolymer (Masson *et al.*, 1998), although this process is non-oxidative (Hugener and Hean, 1996; Masson *et al.*, 2007, 2008).

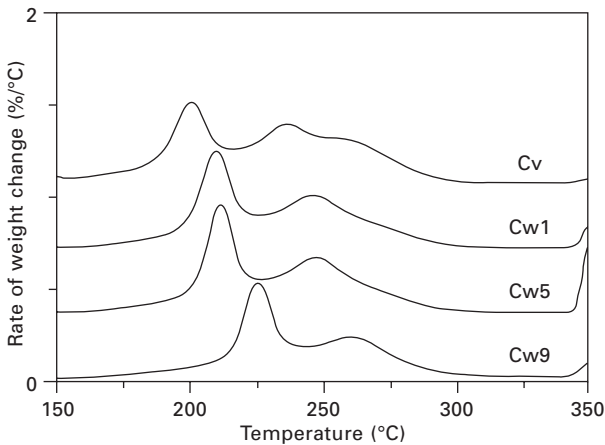
In their field study, Hean and Partl (2004) did not observe significant copolymer degradation in weathered sealants. As we will see below with Sealant K, however, this was likely because of extensive thermal degradation during installation, which leaves little copolymer to degrade during weathering.

Fragmentation and crosslinking

We have seen earlier with Sealant B that copolymers of PS and PB could be crosslinked during material production to achieve very high molecular weights (Fig. 10.10). Like Sealant B, one other sealant had crosslinked copolymers in its virgin state. In contrast, five sealants without crosslinked polymer in their virgin state were found to crosslink upon weathering.

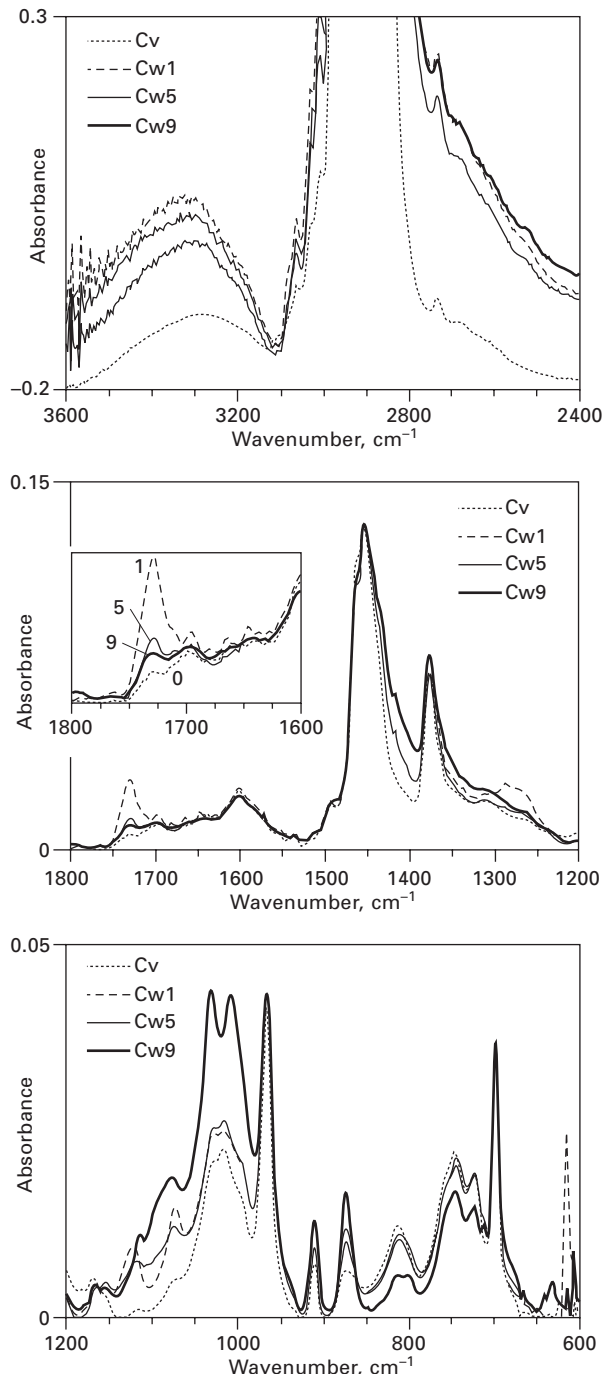


10.14 GPC at 210 nm of Sealant C in its virgin state (Cv) and after weathering for 1 to 9 years (Cw1, Cw5, Cw9).



10.15 HRTG of the light fraction in Sealant C before (Cv) and after weathering 1 to 9 years (Cw1, Cw5, Cw9).

Sealant F provides an example of copolymer degradation that leads to crosslinking (Fig. 10.17). The virgin material shows a major peak at 126 kDa and a shoulder at 224 kDa, which can be attributed to SB and SBS,

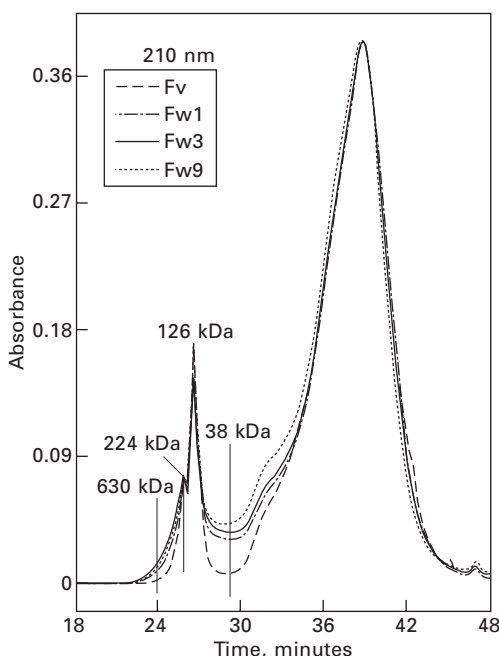


10.16 Infrared spectra of Sealant C in its virgin state (Cv) and after 1, 5, and 9 years of weathering (Cw1, Cw5, Cw9).

Table 10.6 Percent mass loss after the weathering of Sealant B as measured by HRTG

Sample	Light fraction (50–325°C)	Middle fraction (325–500°C)	Heavy fraction (500–600°C)	Total organics (50–600°C)	Carbonate filler ^a (600–900°C)
Bv	18.0	38.7	25.8	82.5	11.6
Bw1	17.9	33.1	25.6	76.6	16.2
Bw3	16.3	31.7	22.8	70.8	16.0
Bw5	16.4	31.0	24.4	71.8	18.4
Bw9	16.2	32.5	25.3	74.0	18.4

^a The carbonate content is 2.16 times larger than the CO₂ weight loss.



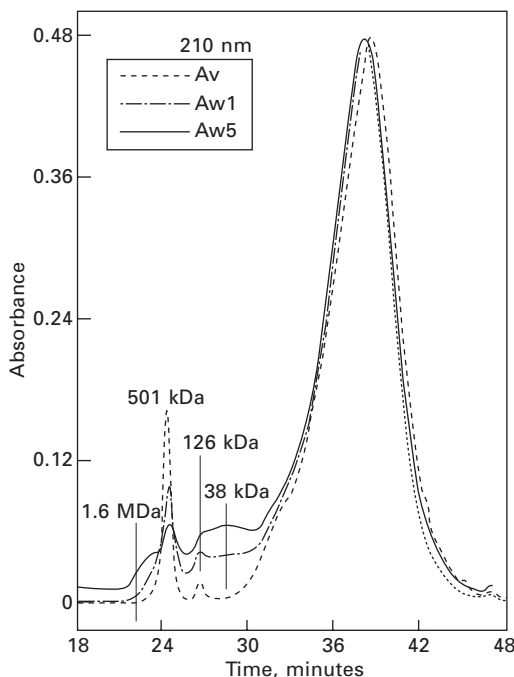
10.17 GPC of Sealant F in its virgin state (Fv) and after 1, 3, and 9 years of weathering (Fw1, Fw5, Fw9).

respectively. Upon weathering, the intensity of the SBS peak remains constant, but that of SB decreases. This is an obvious sign of its degradation, the result of which is two-fold: (a) an increase in the concentration of matter with molecular weights at 38 kDa, seen as a rise in background at 29 min in Fig. 10.17, and (b) a rise in the concentration of high molecular weight matter up to about 630 kDa, visible at 24 min.

The rise in background centred at 38 kDa is not the result of a statistical

degradation. From solution FTIR the copolymer in Sealant F is found to have an S/B ratio of 30/70, and simple calculations show that a breakdown of an SB diblock of 126 kDa into separate PS and PB blocks provides respective segments of 38 kDa and 88 kDa. The lower molecular weight PS fragments correspond to the rise in background, but no discrete rise is visible for PB fragments at 88 kDa. This is most likely because some PB fragments are crosslinked to produce the high molecular weight material. To produce material of 630 kDa, for instance, five PB fragments of 88 kDa must be crosslinked. Such crosslinking through the reaction of alkene groups represents a reaction yield of 0.3% normally not detectable by FTIR spectroscopy, and as expected no change in PB absorbance at 966 cm^{-1} or 911 cm^{-1} was detected with FTIR upon weathering, or in PS absorbance at 699 cm^{-1} for that matter.

Another example of copolymer breakdown into PS and PB fragments is illustrated by Sealant A in Fig. 10.18. The virgin material shows a major peak at 501 kDa and a minor one at 126 kDa, respectively, from SB_4 and SB. Upon weathering there is an important decrease in SB_4 , concurrent with the rise of a shoulder at 29 min, again from PS fragments of 38 kDa. This shoulder becomes more intense than the SB signal starting at five years of

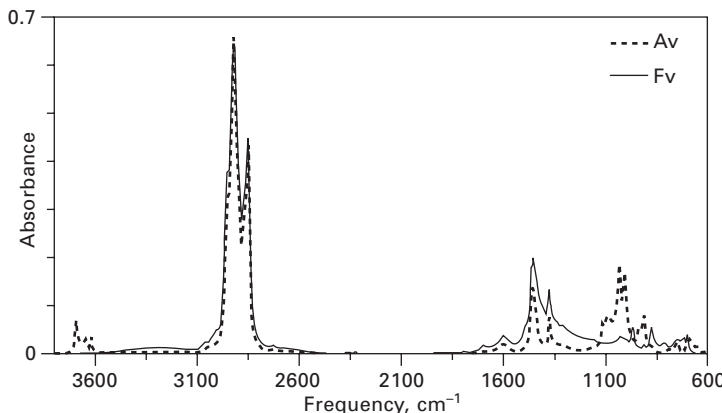


10.18 GPC of Sealant A before (Av) and after 1 and 5 years of weathering (Aw1, Aw5).

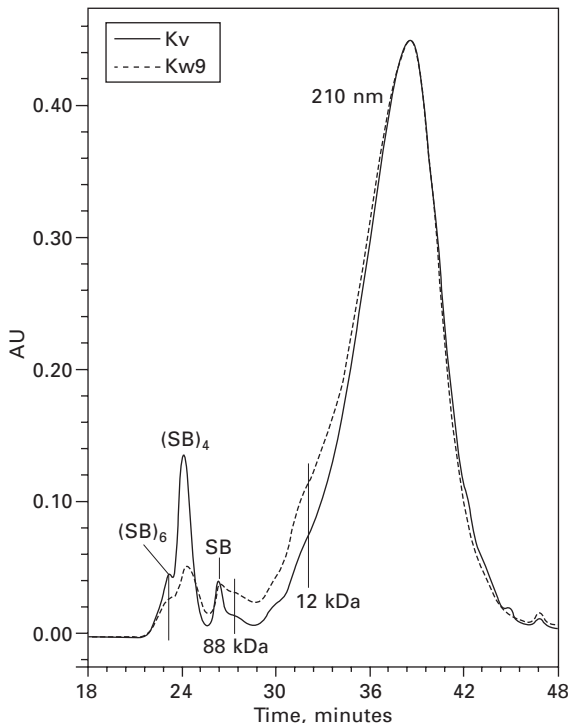
weathering. The rise of this shoulder hints to an apparent increase in the SB peak, but the true intensity of the SB signal remains constant, as the peak to valley distance on the high molecular weight side of this peak is constant regardless of weathering. In Sealant A, as with Sealant F shown earlier, it is the major copolymer component that degrades preferentially. This degradation leads to a rise in signal at 22.5 min for molecular weights near 1.6 MDa and can be attributed to the crosslinking of PB fragments, as above, which translates into the creation of about 18 crosslinks, or the reaction of 1% of the alkene groups in PB fragments of 88 kDa. The greater rate of crosslinking in Sealant A than in Sealant F is most likely due to its greater sulphur content, visible in the FTIR spectra of the virgin material as oxides of sulphur, whose very strong signals absorb near 1000 cm^{-1} , as shown in Fig. 10.19.

Fragmentation without crosslinking

Figure 10.20 shows the GPC results for Sealant K, a sealant overheated during its installation (Masson *et al.*, 1998). The figure only shows the virgin sealant (K_v) and that weathered for nine years (Kw9) because sealants weathered for one, five, and nine years overlap almost perfectly. In its virgin state, Sealant K contains a mixture of $(\text{SB})_6$, $(\text{SB})_4$ and SB as shown in Fig. 10.20, but upon installation and weathering a much reduced content of $(\text{SB})_6$ and $(\text{SB})_4$ is found. The lack of change upon weathering, be it for one, five or nine years, must result from the extensive thermal degradation during installation (Masson *et al.*, 1998), which reduced the average copolymer molecular weight to such an extent that no greater oxidative degradation was possible during weathering. Not surprisingly, Sealant K showed poor field performance (Masson *et al.*, 1999).



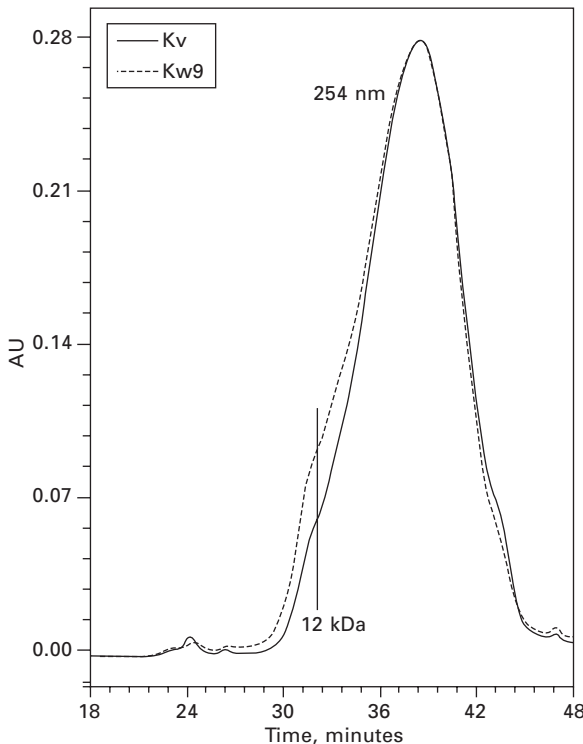
10.19 FTIR spectra of sealants A and F in their virgin (unaged) state.



10.20 GPC results at 210 nm for sealant K before (Kv) and after 9 years of weathering (Kw9).

The degradation of Sealant K is noteworthy in two other respects. Firstly, weathering did not lead to crosslinking of the degraded products, as no high molecular weight material is visible left of $(SB)_6$ in Fig. 10.20. Secondly, thermal degradation of the major components during installation did not lead to a shoulder at 38 kDa for PS, but to a shoulder at 88 kDa for PB. From these observations, it may be concluded that PB fragments are visible in the chromatogram of Sealant K because they did not crosslink. This is complementary to that shown for sealants A and F previously, where weathering produced high-molecular-weight material. It must therefore be concluded that crosslinking during weathering occurs due to oxidation, and that crosslinking does not occur during high-temperature installation because installation is non-oxidative (Hean and Partl, 2004; Masson *et al.*, 2007, 2008).

The second aspect of interest with Sealant K resides in the growth of a pair of unresolved peaks from new chemical species with molecular weights of 12 kDa and 6 kDa, whose UV absorptions are stronger at 254 nm and 350 nm than at 210 nm (Figs 10.20 to 10.22). The origin of these peaks must therefore be associated with aromatic compounds. Many sealants show

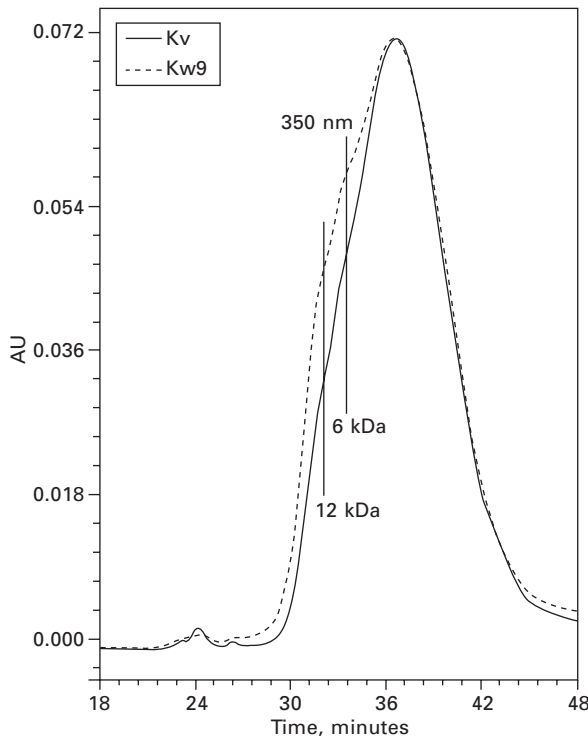


10.21 GPC results at 254 nm for sealant K before (Kv) and after 9 years of weathering (Kw9).

these twin peaks, but to a lesser degree, including Sealant B (Fig. 10.12). Whether they arise from oxidised bitumen aromatics or polystyrene fragments is uncertain. They are reminiscent of those observed with a refractive index detector on bitumen submitted to oxidative thin film oven aging (Kim and Burati, 1993), but unfortunately, no molecular weights were provided by these authors. In their use of GPC with UV detection at 340 nm to analyse SBS-modified bitumen heated from 200°C to 220°C, Brûlé *et al.* (1984) attributed newly detected masses near 10 kDa to copolymer fragments swollen with bitumen chromophores that absorb in the UV. In this work, we could not attribute the twin peaks visible most clearly in Fig. 10.22 to either the bitumen or the copolymer, and neither possibility helped to explain the 2:1 molecular weight ratio of these peaks.

10.4.5 Synthesis of weathering pathways

Our physico-chemical analysis of virgin and weathered bituminous materials has revealed that weathering rates are product dependent, but that weathering



10.22 GPC results at 350 nm for sealant K before (Kv) and after 9 years of weathering (Kw9).

mechanisms are often common. Hence, we have shown some representative examples of weathering pathways. To get a better overall view of weathering, however, it is helpful to provide a qualitative side-by-side product comparison of the various degradation factors and their relative importance. This comparison based on GPC, FTIR and HRTG is shown in Tables 10.7, 10.8 and 10.9, where short-term and long-term respectively mean within and beyond one year of weathering. This breakdown in time helps to provide a rate aspect to the various factors.

Table 10.7 shows the GPC results. It begins with a comparison of copolymer architecture, and the molecular weight of the major component as obtained at 210 nm on the virgin sealants. The architecture of the copolymer in sealant A, for instance, is shown as 3[1], which indicates the value of n in $(SB)_n$. The value in brackets shows the n value for the minor component(s). Hence, 3[1] stands for $(SB)_3$ and SB as the primary and secondary components, respectively. The secondary component generally represents 10% to 50% of the UV absorbance of the main component. Sealants B and J are shown as a range, e.g., 1–10, because they are crosslinked. The next characteristic in Table 10.7 is the molecular weight of the major copolymer component,

Table 10.7 Overview of GPC results for bituminous sealants and the relative effects of weathering

Sealant												
	A	B	C	D	E	F	G	H	J	K	L	M
Architecture, <i>n</i> -value in (SB) _n	3[1]	1-10	1[4]	2[1.3]	1[2.3]	1[1.5]	2[1]	1[4]	1-5	3[1.5]	1[2.3]	1[4]
Major polymer peak, kDa	355	126	126	252	126	126	178	126	126	417	126	126
Polymer degradation, short-term (210 nm, 100-1000 kDa) ^a	+++	++	+	++	+	+	++	+	++	+++	+	+
Polymer degradation, long-term (210 nm, 100-1000 kDa) ^a	+	+	+	0	0	+	0	0	0	0	+	0
Loss of sulphur gas (254 nm, 38 Da) ^a	+	+++	++	+	+	+	0	+	++	+	0	

^a 0, not detected; +, perceptible; ++, important; +++, very important.

Table 10.8 Overview of composition and weathering pathways for bituminous sealants as obtained by FTIR

Sealant	A	B	C	D	E	F	G ^b	H	J ^b	K ^b	L ^b	M
Copolymer content (wt%)	4.5	12.4	11.6	3.4	17.3	8.2	6.3	7.7	3.6	n.d.	n.d.	5.3
S/B ratio	56/44	29/71	29/71	41/59	27/73	29/71	31/69	33/67	34/66	n.d.	n.d.	29/71
Loss of PS (699 cm ⁻¹)	0	0	0	0	0	0	0	0	0	n.d.	n.d.	+
Loss of PB (911 cm ⁻¹) ^a	0	0	0	0	0	0	n.d.	0	n.d.	n.d.	n.d.	+
Sulphur oxidation (1200–1000 cm ⁻¹)	++	++	+	+	+	+	+++	+	n.d.	n.d.	n.d.	+
Carbon oxidation (1800–1200 cm ⁻¹)	++	++	+++	++	+	+	++	+	n.d.	n.d.	n.d.	+
Loss of carbon or sulphur oxides	++	0	++	0	0	+	0	0	n.d.	n.d.	n.d.	0
Loss of aromatics (825–700 cm ⁻¹)	+	++	+	0	0	+	+++	+	n.d.	n.d.	n.d.	+

^a From the absorbance at 911 cm⁻¹ because the stronger absorbance at 966 cm⁻¹ often overlaps with an oxidation band.

^bn.d., not determined.

See also the footnote to Table 10.7.

Table 10.9 Change of sealant mass upon weathering as obtained by HRTG

Sealant	A	B	C	D	E	F	G	H	J	K ^b	L ^b	M ^b
Loss of light fraction, short-term	++	0	++	++	0	0	++	++	0	n.d.	n.d.	n.d.
Loss of aromatics, short-term ^a	++	++	+	++	0	++	++	++	0	n.d.	n.d.	n.d.
Loss of light fraction, long-term	+	+	++	0	+	++	++	+	+	n.d.	n.d.	n.d.
Loss of aromatics, long-term ^a	+	+	+	0	0	+++	+++	+	0	n.d.	n.d.	n.d.
Oxidative weight gain	++	+	+	+++	+	+++	+++	++	0	+	n.d.	n.d.

^a For brevity, both the medium and heavy fractions are classified as aromatics (see Fig. 10.7).

^bn.d., not determined.

Each '+' indicates a change in mass between 0% and 2% by weight.

which shows that most sealants contain an $(SB)_n$ copolymer with molecular weights that vary according to $(126)_n$ kDa with n most often being equal to one. The table also highlights the effect of weathering on copolymer degradation, with a range from not detectable (0) to very important (+++), where each '+' represents a change in GPC signal intensity of about 15%. Half of the sealants showed more than a 30% reduction in the main copolymer signal in the first year of weathering, a time after which many sealants show little more polymer degradation. This highlights the prevalence of short-term weathering on copolymer degradation and a levelling of the effect of weathering with time.

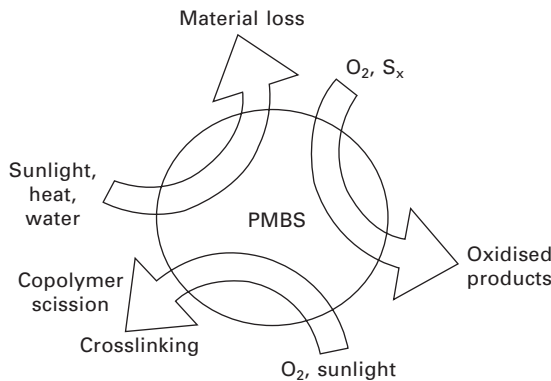
It must be emphasised that GPC measures copolymer molecular weight, not copolymer content. GPC may show that molecular weight is reduced after weathering, but it is FTIR that can show copolymer content, about 3% to 17% for the above samples, and its change over time (Table 10.8). Of the sealants studied with FTIR, only one sealant showed some loss in copolymer content, namely Sealant M. Otherwise, no decrease in PB or PS absorbance was measured, although GPC showed that 0.3% to 1% of the alkene groups could crosslink, a level of change below the detection limit of FTIR. The effect of natural weathering on PB is thus in stark contrast to that observed by FTIR after oven aging of SBS-modified bitumen, which leads to a large loss in alkene content (Maréchal, 1980).

Other FTIR results collected and shown in Table 10.8 reveal that seven of nine weathered sealants lost aromatics or oxidised compounds. Given the constant copolymer content, this loss is at the expense of bituminous components. Results from HRTG in Table 10.9 show that all fractions are lost over time, not only the aromatics, and that weight gain due to oxidation is most common.

The large amount of data collected on weathered bituminous sealants can be distilled down to four natural aging processes:

1. Oxidation of bituminous matter into ketones, carboxylic acids, sulphoxides, sulphones and their corresponding sulphinic and sulphonic acids
2. Scission of block copolymers into PS and PB fragments
3. Oxidative crosslinking of PB fragments
4. Loss of bituminous matter.

These processes can be combined into a coherent picture, as shown in Fig. 10.23, where oxidation may occur at any time, during either sealant manufacture, installation or weathering. Once the initial hydrophobic bituminous material is oxidised or fragmented, or both, the degradation products may be washed away by rain, snow, or brine, or even evaporate in warm weather. Repeated cycles lead to progressive copolymer degradation and material loss. Given that photo-oxidation of bitumen produces water-soluble oils (Streiter and Snone, 1936; Oliver and Gibson, 1972), it is likely that exposure to sunlight is a



10.23 Degradation cycle for polymer-modified bituminous sealants (PMBS).

Table 10.10 Year-to-year percent mass change in sealant total organic content as measured by HRTG

Sealant						
	B	C	D	E	F	G
Year 1	-6	-6	-7	-3	+7	-10
Year 3 ^a	-6	n.d.	+8	-5	n.d.	+7
Year 5	+1	+2	-2	+2	-3	-4
Year 9	+2	-8	-2	+2	-17	-14

key aspect in the weathering cycle. This degradation cycle is perhaps most easily detected in trends shown by HRTG in Table 10.10. Mass loss most often readily occurs in the first year of weathering, followed by oxidative mass gain. This would place the starting point of the degradation cycle in the upper left corner of Fig. 10.23.

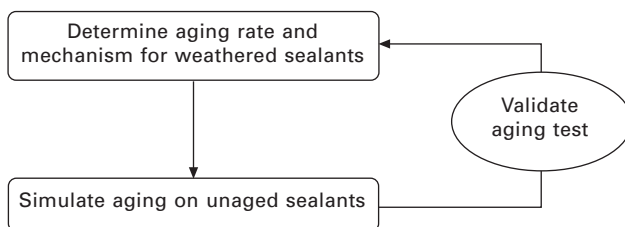
10.5 Future trends

In this work, 12 bituminous sealants were installed on streets of Montreal. After periodic service, weathered sealants were collected. The sealant performance in these cold urban conditions was previously evaluated and it was found not to correlate well with standard test results, as the better-performing sealants often failed to meet the standard requirements (Masson *et al.*, 1999). Obviously, the standard specification could not predict performance, one reason being the lack of an accelerated aging test.

There are many accelerated aging tests for bituminous materials (Read and Whiteoak, 2003; Wypych, 2008), but it is often unclear how well they

replicate natural weathering. Consider for instance a case known in most households, the heating of an egg, which contains proteins, a bio-material that can be used as adhesive. The heating of an egg after three different accelerated aging methods, the pan, boiling water, and the microwave oven, does not reproduce natural aging, which gives a chick. In this case, we know the result of natural aging. In contrast, this is not so with most construction materials, for which the lack of field data precludes the use of accelerated aging methods that truly simulate weathering.

The results reported in this chapter provide a basis on which an effective accelerated aging method can be developed. The results may apply not only to bituminous sealants with an SB-copolymer, but also to other materials of similar composition, including waterproofing membranes, caulks, and binders. Figure 10.24 shows the route to the development and validation of an appropriate accelerated aging test. Such a test must reproduce natural weathering as closely as possible, and in the case of sealants it must include material loss, oxidation, copolymer degradation and crosslinking. In this perspective, it is interesting to consider the potential suitability of long-term aging methods commonly applied to various types of bituminous materials, namely pressure aging (ASTM, 2008a), oven aging (ASTM, 2007), and UV aging (ASTM, 2008b, 2009). All these methods lead to oxidation, and may lead to polymer degradation, but not all of them may lead to material loss. Pressure aging is the case in point, where air pressure over the sample cannot lead to material loss, in this case by evaporation. More promising are methods like photo-oxidative aging and water spray, which lead to the loss of water-soluble material (Streiter and Snone, 1936; Oliver and Gibson, 1972). Hence, future efforts in developing an accelerated aging test for bituminous sealants would best concentrate on methods that may lead to mass loss. To follow the scheme in Fig. 10.24, it would then be a matter of exploring the correspondence of natural weathering with that obtained after various times and temperatures of accelerated aging.



10.24 Validation cycle for the development of an accelerated aging procedure for bituminous sealants.

10.6 References

Ajour, A.-M. and Brûlé, B. 1982. 'New bituminous binders' (in French). *Travaux Paris*, 572, 29–32.

Anon. 1989. *The Asphalt Handbook*. Lexington, KY: Asphalt Institute, 10–11.

ASTM 2007. 'Standard practice for dark oven heat exposure of roofing and waterproofing materials, ASTM D5869'. West Conshohocken, PA: ASTM International.

ASTM 2008a. 'Standard practice for accelerated aging of asphalt binder using a pressurized aging vessel (pav), ASTM D6521'. West Conshohocken, PA: ASTM International.

ASTM 2008b. 'Standard practice for accelerated weathering test conditions and procedures for bituminous materials (fluorescent uv, water spray, and condensation method), ASTM D4799'. West Conshohocken, PA: ASTM International.

ASTM 2009. 'Standard practice for accelerated weathering test conditions and procedures for bituminous materials (xenon-arc method), ASTM D4798'. West Conshohocken, PA: ASTM International.

Bidlingmeyer, B.A. 1992. *Practical HPLC Methodology and Applications*. New York: Wiley, 358–369.

Bouldin, M.G., Collins, J.H., and Berker, A. 1991. 'Rheology and microstructure of polymer/asphalt blends'. *Rubber Chemistry and Technology*, 64, 577–600.

Boutevin, B., Pietrasanta, Y., and Robin, J.-J. 1989. 'Bitumen-polymer blends for coatings applied to roads and public constructions'. *Progress in Organic Coatings*, 17, 221–249.

Brûlé, B., Druon, M., and Brion, Y. 1984. 'Micromorphology and mechanical properties of an SBS bituminous binder: The influence of preparation and aging' (in French). *Bulletin de Liaison des Laboratoires des Ponts et Chaussées*, 132, 65–72.

Campbell, P.G., and Wright, J.R. 1964. 'Ozonation of asphalt flux'. *Industrial and Engineering Chemistry Product Research and Development*, 3, 186–194.

Choquet, F., and Ista, E. 1990. 'Determination of SBS, EVA and APP polymers in modified bitumens'. In: Wardlaw, K.R., and Shuler, S. (eds) *Polymer Modified Asphalt Binders*, ASTM STP 1108. Philadelphia: American Society for Testing and Materials, 35–49.

Coran, A.Y. 1994. 'Vulcanization'. In: Mark, J.E., Erman, B., and Eirich, F.R. (eds) *Science and Technology of Rubber*, 2nd edn. San Diego, CA: Academic Press, 339–385.

Durrieu, F., Farcas, F., and Mouillet, V. 2007. 'The influence of uv aging of a styrene/butadiene/styrene modified bitumen: Comparison between laboratory and on site aging'. *Fuel*, 86, 1446–1451.

Fehér, F., and Münzner, H. 1963. 'Ultraviolet absorption spectra of sulphanes and derivatives' (in German). *Chemische Berichte*, 96, 1131–1149.

Frohnsdorff, G., and Masters, L.W. 1980. 'The meaning of durability and durability prediction'. In: Sereda, P.J., and Litvan, G.G. (eds) *Durability of Building Materials and Components*, ASTM STP 691. Philadelphia: American Society for Testing and Materials, 17–30.

Giavarini, C. 1994. 'Polymer-modified bitumen'. In: Yen, T.F., and Chilingarian, G.V. (eds) *Asphaltenes and Asphalts 1*. Amsterdam: Elsevier Sciences, 381–400.

Hatakeyama, T., and Quinn, F.X. 1999. *Thermal Analysis: Fundamentals and Applications to Polymer Science*. New York: Wiley, 38–64.

Hean, S., and Partl, M.N. 2004. 'Long-term behaviour of polymer bitumen joint sealants on a trial road section'. In: *Third Eurasphalt & Eurobitumen Congress*, Vienna, 546–559.

Herrington, P.R., and Ball, G.F.A. 1996. 'Temperature dependence of asphalt oxidation mechanism'. *Fuel*, 75, 1129–1131.

Herrington, P.R., Patrick, J.E., and Ball, G.F.A. 1994. 'Oxidation of roading asphalts'. *Industrial and Engineering Chemistry Research*, 33, 2801–2809.

Huang, J., Yuro, R., and Romeo Jr., G.A. 1995. 'Photooxidation of Corbett fractions of asphalt'. *Fuel Science and Technology International*, 13, 1121–1134.

Hugener, M., and Hean, S. 1996. 'Comparison of short-term aging methods for joint sealants'. In: Beech, J.C., and Wolf, A.T. (eds) *Durability of Building Sealants*. London: E & FN Spon, 37–47.

Jemison, H.B., Burr, B.L., Davison, R.R., Bullin, J.A., and Glover, C.J. 1992. 'Application and use of the atr, ft-ir method to asphalt aging studies'. *Fuel Science and Technology International*, 10, 795–808.

Jones, P.M. 1963. *Bituminous Materials*. Ottawa: National Research Council Canada, 1–4.

Kemp, A.R., and Malm, F.S. 1935. 'Hard rubber (ebonite)'. *Industrial & Engineering Chemistry*, 27, 141–146.

Kim, K.W., and Burati Jr, J.L. 1993. 'Use of GPC chromatograms to characterize aged asphalt cements'. *Journal of Materials in Civil Engineering*, 5, 41–52.

Koenig, J.L. 1992. *Spectroscopy of Polymers*. Washington, DC: American Chemical Society, 43–50.

Kraus, G., and Rollmann, K.W. 1981. 'Morphology and mechanical behaviour of bitumen modified with butadiene-styrene block copolymers' (in German). *Kautschuk und Gummi Kunststoffe*, 34, 645–657.

Lambert, J.B. 2005. 'The deep history of chemistry'. *Bulletin for the History of Chemistry*, 30, 1–9.

Lambert, J.B., Shurvell, H.F., Verbit, L., Cooks, R.G., and Stout, G.H. 1976. *Organic Structural Analysis*. New York: Macmillan, 225–309.

Lamontagne, J., Dumas, P., Mouillet, V., and Kister, J. 2001. 'Comparison by Fourier transform infrared (ftir) spectroscopy of different ageing techniques: Application to road bitumens'. *Fuel*, 80, 483–488.

Legge, N.R. 1989. 'Thermoplastic elastomers. Three decades of progress'. *Rubber Chemistry and Technology*, 62, 529–547.

Lewandowski, L.H. 1994. 'Polymer modification of paving asphalt binders'. *Rubber Chemistry and Technology, Rubber Reviews*, 67, 447–480.

Lin-Vien, D., Colthup, N.B., Fateley, W.G., and Grasselli, J.G. 1991. *The Handbook of Infrared and Raman Characteristic Frequencies of Organic Molecules*. Boston, MA: Academic Press, 45–306.

Linde, S., and Johansson, U. 1992. 'Thermo-oxidative degradation of polymer modified bitumen'. In: Wardlaw, K.R., and Shuler, S. (eds) *Polymer Modified Asphalt Binders*, ASTM STP 1108. Philadelphia: American Society for Testing and Materials, 244–253.

Liu, M., Lunsford, K.M., Davison, R.R., Glover, C.J., and Bullin, J.A. 1996. 'The kinetics of carbonyl formation in asphalt'. *AIChE Journal*, 42, 1069–1076.

Maldonado, P., Mas, J., and Phung, T.K. 1979. 'Process for preparing bitumen-polymer compositions'. US patent application 865,245.

Mallick, R.B., and Brown, E.R. 2004. 'An evaluation of superpave binder aging methods'. *International Journal of Pavement Engineering*, 5, 9–18.

Maréchal, J.-C. 1980. 'Elastomeric SBS-bitumen: Characteristics and degradation of bulk material' (in French). *Cahiers du Centre Scientifique et Technique du Bâtiment*, 1659, 1–17.

Maréchal, J.-C. 1983. 'Methods for the study of aging of bitumen-polymer SBS materials'. *Durability of Building Materials*, 1, 201–208.

Maréchal, J.-C., Ghaleb, M., and Bonnet, D. 1983. 'Aging of SBS-modified bituminous waterproofing membranes' (in French). *Cahiers du Centre Scientifique et Technique du Bâtiment*, 1831, 1–27.

Masson, J-F. and Bundalo-Perc, S. 2005. 'Solventless fingerprinting of bituminous materials: A high-resolution thermogravimetric method'. *Thermochimica Acta*, 436, 35–42.

Masson, J-F., Lauzier, C., Collins, P., and Lacasse, M.A. 1998. 'Sealant degradation during crack sealing of pavements'. *Journal of Materials in Civil Engineering*, 10, 250–255.

Masson, J-F., Collins, P., and Légaré, P.P. 1999. 'Performance of pavement crack sealants in cold urban conditions'. *Canadian Journal of Civil Engineering*, 26, 395–401.

Masson, J-F., Pelletier, L., and Collins, P. 2001. 'Rapid ftir method for quantification of styrene-butadiene type copolymers in bitumen'. *Journal of Applied Polymer Science*, 79, 1034–1041.

Masson, J-F., Collins, P., Margeson, J., and Polomark, G. 2002. 'Analysis of bituminous crack sealants by physicochemical methods: Relationship to field performance'. *Transportation Research Record*, 1795, 33–39.

Masson, J-F., Collins, P., Robertson, G., Woods, J.R., and Margeson, J. 2003. 'Thermodynamics, phase diagrams, and stability of bitumen–polymer blends'. *Energy and Fuels*, 17, 714–724.

Masson, J-F., Bundalo-Perc, S., and Delgado, A. 2005. 'Glass transitions and mixed phases in block sbs'. *Journal of Polymer Science, Part B: Polymer Physics*, 43, 276–279.

Masson, J-F., Collins, P., Bundalo-Perc, S., Woods, J.R., and Al-Qadi, I.L. 2007. 'Early thermodegradation of bituminous sealants resulting from improper installation: field study'. *Transportation Research Record*, 1991, 119–123.

Masson, J-F., Woods, J.R., Collins, P., and Al-Qadi, I.L. 2008. 'Accelerated aging of bituminous sealants: Small kettle aging'. *International Journal of Pavement Engineering*, 9, 365–371.

Oliver, J.W.H., and Gibson, H. 1972. 'Source of water-soluble photooxidation products in asphalt'. *Industrial and Engineering Chemistry Product Research and Development*, 11, 66–69.

Pasto, D.J., and Johnson, C.R. 1969. *Organic Structure Determination*. Englewood Cliffs, NJ: Prentice-Hall, 83–108.

Pavia, D.L., Lampman, G.M., and Kriz, G.S.J. 1979. *Introduction to Spectroscopy: A Guide for Students of Organic Chemistry*. Philadelphia: W. B. Saunders, 13–80.

Petersen, J.C. 1986. 'Quantitative functional group analysis of asphalts using differential infrared spectrometry and selective chemical reactions, theory and application'. *Transportation Research Record*, 1096, 1–11.

Petrossi, U., Bocca, P.L., and Pacor, P. 1972. 'Reactions and technological properties of sulfur-treated asphalt'. *Industrial & Engineering Chemistry Product Research and Development*, 11, 214–219.

Pribanic, J.S., Emmelin, M., and King, G.N. 1989. 'Use of a multiwavelength uv-vis detector with hp-gpc to give a three-dimensional view of bituminous materials'. *Transportation Research Record*, 1228, 168–176.

Read, J., and Whiteoak, D. 2003. *The Shell Bitumen Handbook*. London: Thomas Telford Publishing, 119–170.

Ruan, Y., Davison, R.R., and Glover, C.J. 2003. 'The effect of long-term oxidation on the rheological properties of polymer modified asphalts'. *Fuel*, 82, 1763–1773.

Shim-Ton, J., Kennedy, K.A., Piggott, M.R., and Woodhams, R.T. 1980. 'Low temperature dynamic properties of bitumen–rubber mixtures'. *Rubber Chemistry and Technology*, 53, 88–106.

Speight, J.G. 1999. *The Chemistry and Technology of Petroleum*. New York: Marcel Dekker, 1–34.

Steudel, R. 2002. 'The chemistry of polysulfanes'. *Chemical Reviews*, 102, 3905–3945.

Streiter, O.G., and Snoke, H.R. 1936. 'A modified accelerated weathering test for asphalts and other materials'. *Journal of Research of the National Bureau of Standards*, 16, 481–485.

Such, C., Ballié, M., Lombardi, B., Migliori, F., Ramond, G., Samanos, J., and Simoncelli, J.-P. 1997. 'Bitumen aging susceptibility: Experimentation A 08' (in French), Paris, Laboratoire Central des Ponts et Chaussées, 1–69.

Tinyakova, E.I., Khrennikova, E.K., and Dolgoplosk, B.A. 1956. 'Role of hydrogen disulfide in the vulcanization process'. *Russian Chemical Bulletin*, 5, 1179–1181.

Verhasselt, A.F., and Choquet, F.S. 1993. 'Comparing field and laboratory aging of bitumens on a kinetic basis'. *Transportation Research Record*, 1391, 30–38.

Wu, C.-S. (ed.) 1995. *Handbook of Size Exclusion Chromatography*. New York: Marcel Dekker, 1–24.

Wypych, G. 2008. *Handbook of Materials Weathering*, Toronto: ChemTec Publishing, 223–236.

Fuel resistance of bituminous binders

G. POLACCO, S. FILIPPI, M. PACI and
S. MARKANDAY, University of Pisa, Italy and F. MERUSI
and F. GIULIANI, University of Parma, Italy

Abstract: The solubility of bituminous binders in oil-derived products is a primary cause of pavement damage in airport systems, filling stations, parking lots and industrial plants, where fuel spillage may occur. The chapter first introduces the solutions proposed and adopted in order to overcome this problem and the tests normally employed to quantitatively describe and measure solubility. Then, the effect of three common bitumen modifiers, i.e. thermoplastic polymers, crumb tyre rubber and waxes, on bitumen solubility is broadly described. In each of the three cases, the mechanism by which the modifier influences the binder solubility is hypothesized and discussed.

Key words: fuel resistance, hydrocarbon oils, polymer modified bitumen, crumb rubber mixes, wax modified bitumen.

11.1 Introduction

11.1.1 Fuel resistance of bituminous binders

It is well known that mechanical performance, durability and failure mode of bitumen pavements strictly depends on bitumen origin and chemical composition. In particular, the solubility in oil-derived products, such as fuels, traditionally limits the use of hot-mix bitumen and bituminous pavements. Where a prolonged and repetitive condition of fuel spillage exists, the loss of adhesion at the interface of the mastic–aggregate systems determines premature pavement deterioration, such as surface softening, ravelling and other deeper damage. Fuel is therefore often identified as a primary cause of pavement damage occurring in airport systems, filling stations, parking lots and industrial plants. This is particularly important in the case of airfields, where kerosene spillage is a problem of decisive importance in pavement management.

11.1.2 Solutions proposed in the past

A drastic solution, widely used in airports, is the use of concrete pavements, which are insensitive to hydrocarbons and also characterized by a high load-

bearing capacity. However, even in airfields, the high construction costs can make such a solution not convenient and flexible pavements remain, in most cases, preferable. This is why coal-tar pitches were traditionally employed to achieve the desired fuel resistance (Yan, 1986). Nevertheless, the use of coal-tar derivatives was gradually reduced because of health and environmental risks associated with their high carcinogenic polycyclic aromatic compound content (Deneuvillers and Letaudin, 2003). As a consequence, the development of alternative and environmentally friendly materials for pavement or for bitumen pavement protection is nowadays a topic of great technological and practical interest.

Another approach that was proposed, as a possible alternative to coal tar pitches, is the application of polymer and resin-based layers over the binder surface (Newman and Shoenberger, 2002). Of course, in this case a fuel resistance better than that of a typical coal tar emulsion can be obtained and in some cases an almost total fuel impermeability was recorded (Newman and Shoenberger, 2002; Giuliani and Rastelli, 2006; Rushing and Tom, 2009). However, this solution has several drawbacks. Firstly, it involves the use of expensive materials and procedures. Moreover, it changes dramatically the surface characteristics and properties of the pavement and becomes ineffective when thermal or fatigue cracking damages the protective superficial layer.

11.1.3 What's going on: searching for new solutions

The preferable approach appears to be the use of appropriate modifiers to develop a material with improved fuel resistance that maintains the peculiar characteristics of classical bituminous binders and which can be processed with conventional techniques and equipment (Plug *et al.*, 2004). The further and quite obvious step is to analyse and evaluate the effect of conventional modifiers on fuel resistance. In this respect, the first candidates are polymeric modifiers, which are widely used to produce high-performance pavements. An allegedly small number of kerosene-resistant products based on polymer modification are produced and have been commercialized by different industrial groups (Corun *et al.*, 2006), but in all cases the composition is not specified. After addition to a base bitumen, polymers form a network swollen with the bitumen molecules, thus inducing profound changes to the binder structure and therefore in its performance and rheological properties. For the same reason, polymers may be expected to have a significant influence also on the solubility of bitumen in hydrocarbons.

Analogously, in recent years there is growing attention towards the use of waxes which allows the production of so-called warm bitumens. As is the case for polymers, waxes are also employed as modifiers for purposes completely different from those related to solubility. However, their crystalline nature was found to indirectly affect solubility.

Finally, a peculiar case is that of crumb tyre rubber, used for the production of so-called rubber bitumens. From a chemico-physical point of view, crumb rubber cannot be exactly classified as a modifier, because when mixed with a bitumen it gives a macroscopically biphasic material. On the other hand, crumb rubber cannot even be considered as an additive or as the aggregates which simply fill the binder without interacting with it. During the 'dry' or 'wet' method of mixing (Gawel and Slusarski, 1999), a partial swelling of the crumb rubber particles with some bitumen molecules occurs and the final result is a 'modified-loaded' material that can be used for the preparation of the external layer of pavements. Therefore, even if not exactly falling in the class of modifiers, crumb rubber somehow acts in a similar way as polymers do and has been shown to be another interesting candidate for the production of fuel-resistant pavements.

These three classes of modifiers are now evaluated in order to establish whether they can be useful to enhance fuel resistance and to understand the mechanisms that affect solubility in hydrocarbons.

11.2 Solubility of bituminous binders

11.2.1 How to measure fuel solubility: common and proposed techniques

The first important point to be underlined is that, at the moment, there is no readily available method to evaluate the fuel resistance of bituminous binders for asphaltic pavements. However, in the case of sealants, there is the US federal specification SS-S-1401-C for 'sealants, joints, jet-fuel resistant, hot applied, for tar cement and tar concrete pavements' that defines an immersion test and evaluates the changes in penetration and in dry mass after immersion for 24 hours at 49°C. The test fuel is a mixture composed of 70% isoctane and 30% toluene by volume, conforming to the requirements of ASTM reference Fuel B of ASTM D471.

Furthermore, specification CEN EN 12697-43, 2005, provides a measure of the fuel resistance of bituminous concretes by determining the weight loss of bitumen mixtures after immersion and the brush test. Therefore, this specification is not designed for the binder alone, but for concrete mixes whose fuel resistance depends on a number of factors, such as mixture permeability, bitumen film thickness, aggregate properties, mix design, etc., in addition to binder properties. Moreover, the test, which involves the recovery of bitumen after immersion in a fuel, does not provide results that are fully associated with the bitumen properties, and thus is inadequate in describing the real binder performance.

Other, not standardized, tests can be found in the scientific literature. Steernberg *et al.* (2000) suggested the use of Marshall specimens prepared

with Dutch aggregate and limestone filler. The specimens are fully immersed in fuel for controlled periods, then dried, and the weight loss is used as an indicator of fuel resistance. Also, this method was developed for concretes and it was used to establish a relation between different bitumen modifiers, such as coal-tar, resins and thermoplastic polymers. Moreover, the authors outlined some fundamental aspects of bitumen-fuel interactions. In particular, the dissolution process was associated with absorption of fuel in the bitumen. In fact, this is of crucial importance in defining the fuel resistance of bitumen, since the presence of fuel retained by the binder may induce several secondary effects on the final binder resistance. In this context, Giuliani and Merusi (2008) confirmed that the kerosene resistance of bituminous binders must be evaluated taking into account both bitumen solubility in kerosene and kerosene solubility in bitumen. The same consideration is applicable to bitumen mixtures, where, of course, the amount and size distribution of the aggregates must also be taken into account (Giuliani *et al.*, 2009a; Praticò *et al.*, 2008a).

Giuliani and Merusi (2008) proposed a procedure to evaluate the solubility of polymer modified bitumens (PMB) in a jet fuel and measured the variation of their viscoelastic properties after a dip in the fuel. Another approach was presented by Corun *et al.* (2006), who studied the rheological properties of binders recovered from mixtures previously immersed in fuel. However, in this case, it is not clear to what extent the results are influenced by the procedure employed to recover the bitumen. Other attempts to assess the fuel resistance of bitumens by comparing the properties recorded before and after immersion in the fuel were made by Seive *et al.* (2004), who used the mass loss during immersion and the Duriez stability of the recovered bitumen specimen, and by Praticò *et al.* (2008b).

11.2.2 A simple method to measure fuel solubility

The use of an experimental approach based on the binder alone seems to be preferable, in view of a correct interpretation of its fuel resistance when used in bituminous pavements or sealants. Thus, a simple test procedure was developed by Giuliani *et al.* (2009b). Solubility tests are done on cylindrical samples with 25.4 mm diameter and 10 mm height, at room temperature, using the following procedure: 300 mL of kerosene is poured at room temperature into a 500 mL beaker and agitated with a magnetic stirrer set at 100 rpm; the bitumen sample is weighed and placed on a metallic net, with mesh of 0.5 mm subsequently dipped in the liquid. At time intervals of 20 min, the net is removed from the beaker; the sample is wiped with a filter paper and weighed. The total time of dipping is 120 min. The weight loss of the samples is then taken as a measure of the tendency of the binder to dissolve in the fuel. In a preliminary study, the test was applied to five different bitumens (at least

20 samples for each bitumen) in order to evaluate its reproducibility. The statistical analysis showed that the percentage error was always below 10 and reporting the data as the average of at least two measurements granted sufficient reliability to the expected conclusions. It is important to note that, while the samples do completely disintegrate after immersion for a sufficiently long time (i.e. weight loss equal to 100%), a measurable amount of material is in fact insoluble and remains suspended or settles to the bottom of the beaker. Moreover, the recorded weights of the samples may be affected by both dissolved binder and soaked kerosene. Nevertheless, given the scope of the test, the binder weight loss is a meaningful indicator of the tendency of the bitumen pavement to degrade by the action of the fuel.

In order to get a standardized version of the test, it will be necessary to introduce a thermostatic bath that would allow an accurate control of the test temperature and unequivocally define the composition of the fuel. Moreover, temperature and residence time can be used as adjustable parameters to modulate the capability of the test to adequately discriminate between different binders and hydrocarbons.

The following results were obtained following the above procedure, with measurements performed at room temperature and with a total immersion time of 120 minutes in unleaded kerosene classified as Jet Fuel A-1.

11.3 Bitumen modification to enhance fuel resistance

11.3.1 Polymer modified bitumens

Introduction

As already stated, a possible way to improve the fuel resistance of bituminous binders is by the use of polymer modified bitumens. In this respect, three patents were published by Hendriks *et al.* (1997), Planche *et al.* (2002) and Thornton (2006) which address this issue. Hendriks proposed a highly modified PMB, based on the addition of both a thermoplastic block copolymer, such as poly(styrene-*b*-ethylene-*b*-styrene) (SBS), and a poly(ethylene vinyl acetate) (EVA) with vinyl content of at least 20% by weight; Planche *et al.* proposed the use of a crosslinkable elastomer and a functionalized polyolefin; and Thornton proposed the use of a methylene/methyl acrylate copolymer. The common characteristic of the approach described in these three patents is that a modification with a very high quantity of polymer is suggested. In order to develop a fuel-resistant PMB without adding an exaggerated quantity of polymer, accurate knowledge of the effect and mechanism through which the polymers may improve the fuel resistance is necessary.

It is quite obvious that the effectiveness of a polymer as anti-solubility agent will depend on its interaction with the base bitumen. Therefore,

although some consideration regarding the behaviour of different polymers may be generalized, the appropriate choice of type and quantity of polymer to be added will change depending on the bitumen composition. Moreover, the fuel resistance must be coupled with all the other properties that are required for pavement performance. This means that not all polymers that are effective in increasing fuel resistance may guarantee good performance and storage stability of the PMB. Furthermore, it is important to limit the required amount of polymer, otherwise both cost and operating difficulties may arise.

A comparative study of different polymeric modifiers

An extensive comparison based on several polymers and two different base bitumens, referred to hereinafter as A and B, allows one to establish a correlation between fuel resistance and binder characteristics. The main properties of the two base bitumens are reported in Table 11.1.

The polymers were first added in at loadings of 4% and 6% by weight, in order to have compositions that are commonly used in bitumen modification for road pavements. Then, the effects of higher, but still limited, polymer content for the most promising formulations were investigated.

The tested polymers were two ethylene–vinyl acetate copolymers, referred to herein as EVA14 and EVA28, with 14 wt% and 28 wt% vinyl acetate, respectively; two ethylene–acrylic acid copolymers, EAA6 and EAA11, with 6.2 wt% and 11.0 wt% acrylic acid, respectively; an ethylene–methyl acrylate copolymer, EMA25, with 25 wt% methyl acrylate; and two styrene–butadiene–styrene block copolymers, one linear, *ISBS*, with 31 wt% of bound styrene, and a radial one, *rSBS*, with 30 wt% of bound styrene. The rate of dissolution of base bitumens and PMBs when dipped in jet fuel was evaluated and coupled with a morphological and compositional analysis. The PMBs will now be coded as ‘base bitumen–polymer type–polymer content’. Thus, A-EVA14-6 is the PMB obtained from base bitumen A by addition of 6 wt% (with respect to the total mass) of EVA14.

Solubility tests were performed as described above, but the samples were

Table 11.1 Physical properties and chemical composition of bitumens A and B

Bitumen	S/A/R/A (wt%)	Penetration (dmm)	Softening point (°C)
A	2.2/59.1/23.3/15	77	49
B	5.3/43.7/25.4/25	48	83

Source: Giuliani *et al.* (2009b).

kept immersed in the fuel until complete disintegration occurred and no residue remained on the metallic net. Then, the base bitumen, the PMBs and the kerosene-insoluble part were characterized by thin layer chromatography, with flame ionization detector (TLC-FID) to measure the content of saturates, aromatics, resins and asphaltenes (S/A/R/A).

In order to better interpret the solubility data, it is useful to analyse the morphological and mechanical properties of the different PMBs. For the morphological analysis, bitumen samples taken directly from the mixing can were poured into small cylindrical moulds, preheated to the mixing temperature. The moulds were cooled to -30°C , and then the samples were removed from the moulds and fragile-fractured. Finally, the fractured surfaces were examined with a fluorescence microscope. Penetration and softening point of the PMBs are reported in Table 11.2, while the morphology of the PMBs is shown in Fig. 11.1, and Figs 11.2–11.5 show the weight loss vs. time curves of all mixes.

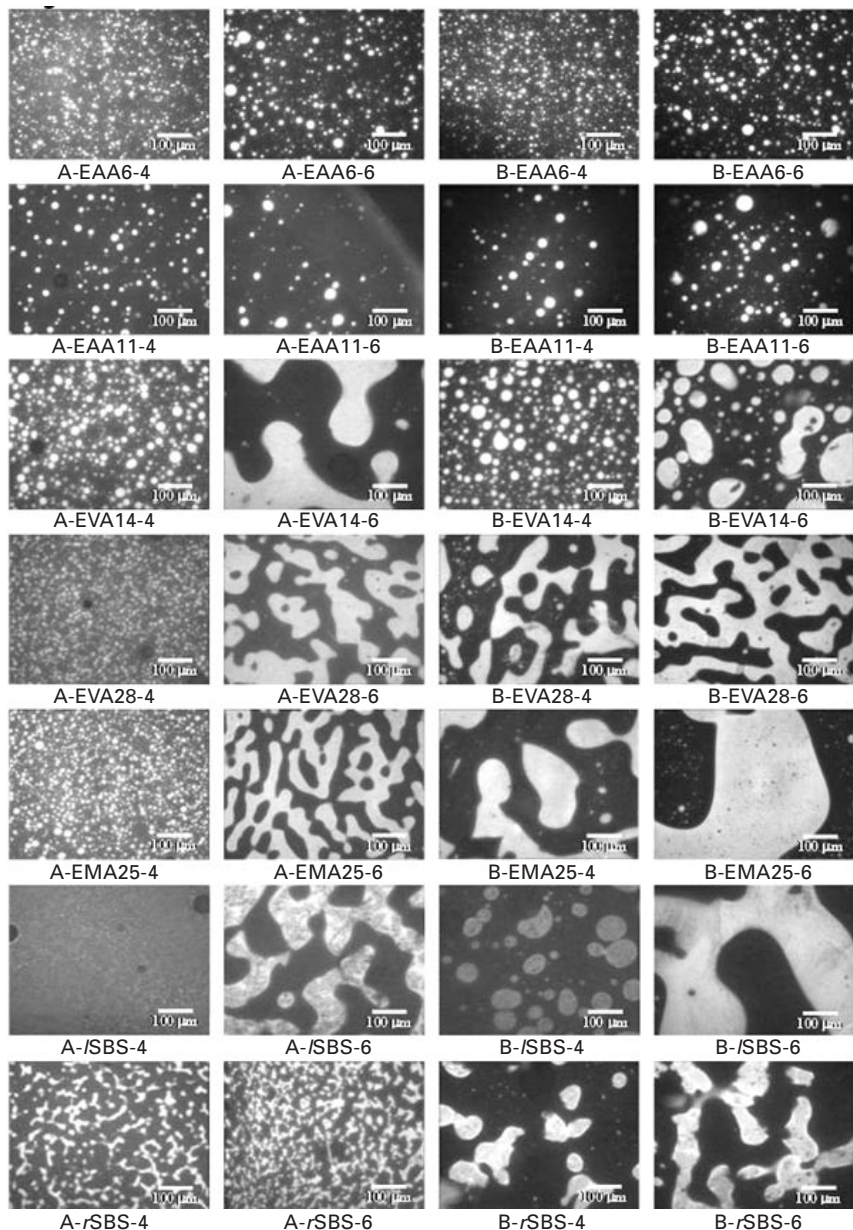
In Fig. 11.1, the white-grey areas represent the polymer domains (swollen by some of the bitumen components), whereas the dark areas indicate the asphaltene-rich phase. When the polymer-bitumen compatibility is high, swelling induces 'phase inversion' and the polymer-rich phase becomes the matrix, whereas for the incompatible asphaltene-rich fraction, it forms the dispersed phase. Such an outcome is highly desirable as it facilitates the strongest enhancement of PMB properties (Polacco *et al.*, 2006).

Figures 11.2–11.5 show that the fuel resistance of the PMBs containing either EAA copolymer is comparable to that of the unmodified bitumens.

Table 11.2 Penetration and softening point of the PMBs

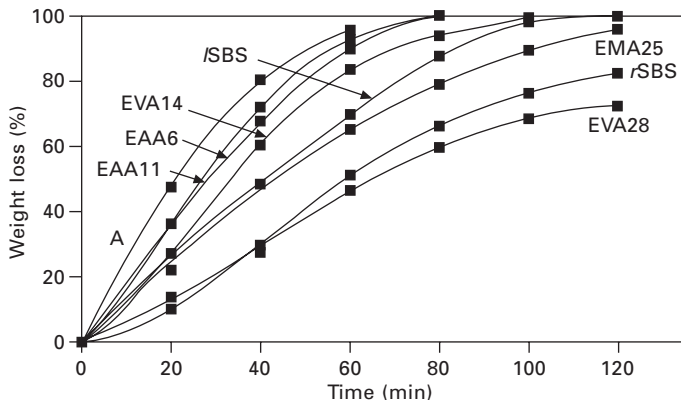
PMB	Penetration	Softening	PMB	Penetration	Softening
	(dmm)	($^{\circ}\text{C}$)		(dmm)	($^{\circ}\text{C}$)
A- <i>ISBS</i> -4	42	54.0	B- <i>ISBS</i> -4	56	73
A- <i>ISBS</i> -6	38	96.5	B- <i>ISBS</i> -6	49	94
A- <i>rSBS</i> -4	44	102.0	B- <i>rSBS</i> -4	54	91
A- <i>rSBS</i> -6	37	111.0	B- <i>rSBS</i> -6	45	104
A-EVA14-4	40	54.0	B-EVA14-4	44	58
A-EVA14-6	47	79.5	B-EVA14-6	39	76
A-EVA28-4	51	55.5	B-EVA28-4	55	56
A-EVA28-6	54	60.5	B-EVA28-6	47	62
A-EAA11-4	45	50.5	B-EAA11-4	53	50
A-EAA11-6	39	52.5	B-EAA11-6	49	53
A-EAA6-4	44	51.0	B-EAA6-4	47	52
A-EAA6-6	37	53.0	B-EAA6-6	38	54
A-EMA25-4	48	57.0	B-EMA25-4	50	67
A-EMA25-6	46	77.5	B-EMA25-6	37	74

Source: Giuliani *et al.* (2009b).

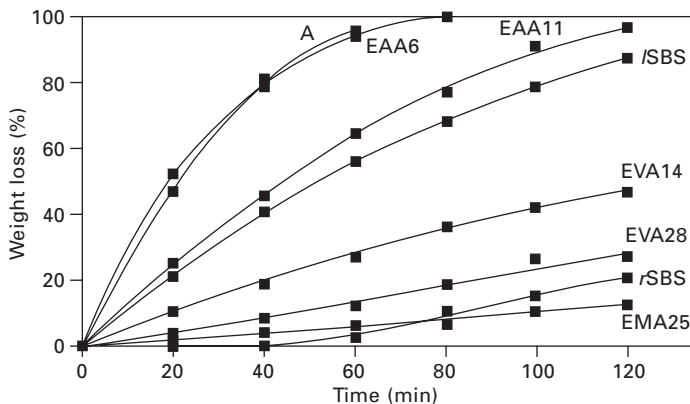


11.1 Fluorescence microscopy of the PMBs (from Giuliani *et al.*, 2009b).

At the same time, it can be seen from Table 11.2 and Fig. 11.1 that, in spite of the presence of polar acrylic acid units in their backbone, the EAA copolymers are poorly compatible with both A and B base bitumens. The

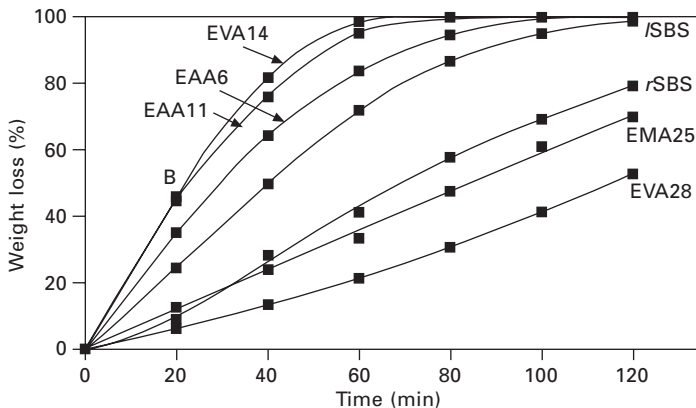


11.2 Solubility of base bitumen A and PMB with 4% of added polymer (from Giuliani *et al.*, 2009b).

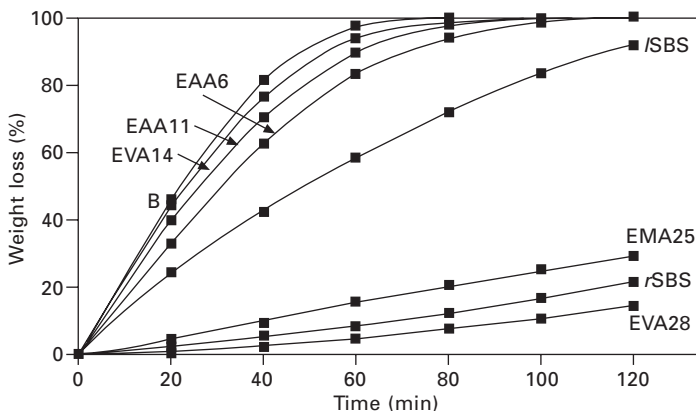


11.3 Solubility of base bitumen A and PMB with 6% of added polymer (from Giuliani *et al.*, 2009b).

softening point enhancement obtained on addition of these modifiers is marginal and the fluorescence micrographs show that the polymer forms a minor phase consisting of small, spherical droplets dispersed within the bituminous matrix. Therefore, there are no significant interactions between polymer and bitumen and the latter is not 'protected' from dissolution in the fuel. Probably, the concentration of acrylic units is too low to balance the highly apolar and bitumen-repulsive character of the ethylene sequences (Polacco *et al.*, 2005). In fact, the weight content of the polar $-\text{O}-\text{C}=\text{O}$ groups in the ethylene copolymers (Table 11.3) is lowest for the two EAAs. Thus, even considering that these groups are able to form hydrogen bonds with polar molecules, it may be concluded that the overall polarity of these



11.4 Solubility of base bitumen B and PMB with 4% of added polymer (from Giuliani *et al.*, 2009b).



11.5 Solubility of base bitumen B and PMB with 6% of added polymer (from Giuliani *et al.*, 2009b).

Table 11.3 Content of polar groups in the copolymers

Polymer	Comonomer (wt%)	O—C=O groups (wt%)
EAA6	6	3.67
EAA11	11	6.72
EVA14	14	7.16
EVA28	28	14.32
EMA25	25	12.79

Source: Giuliani *et al.* (2009b).

copolymers is too low to make them sufficiently compatible with the base bitumens.

The behaviour of EVA14, as a PMB additive, is intermediate between that of an ineffective modifier and that of the polymers that were found to strongly improve the fuel resistance of the base bitumens. As shown in Table 11.3, the content of $-\text{O}-\text{C}=\text{O}$ groups in EVA14 is close to that in EAA11, and the PMBs prepared from base bitumen B and these two polymers both have very poor fuel resistance. However, the morphology and the softening point of the B-EVA14-6 sample suggest that some, still weak, interactions between the components of this blend are present. Changing the base bitumen, from B to A, further emphasizes the peculiarity of EVA14. The fuel resistance of the PMB now depends very strongly on polymer loading. In fact the weight loss of the A-EVA14-6 sample was found to be only 45% at the end of the test. The blend morphology is highly concentration-dependent too, and an increase of additive loading from 4 wt% to 6 wt% results in the morphology of the polymer-rich fraction altering from that of a dispersion of small spherical droplets into that of an irregularly shaped co-continuous phase. The morphology of the A-EVA14-6 blend is therefore close to phase inversion. All these features indicate that significant interactions were active between EVA14 and bitumen A, whereas they were much weaker with bitumen B.

The different effect that EVA14 has on the two bases is due to their composition. EVA14 is composed of two kinds of monomeric units which have different polarity. The ethylene units have affinity only with saturates which are present in very small quantities in bitumens. The vinyl acetate groups are the main candidate to 'link' polymer and bitumen and they will preferably interact with resins and asphaltenes. Accordingly, the different aromatic and resin/asphaltene contents can be related to the different behaviour of bitumen A and bitumen B. For base bitumen A, the small amount of polar fractions is almost completely engaged to interact with the available vinyl acetate units of EVA14 when the polymer loading is relatively high (6 wt%). In contrast, such a favourable situation fails to prevail when the ratio between vinyl acetate units of the polymer and polar fractions of the bitumen is too low (i.e. either when A is loaded with 4 wt% of polymer or when base bitumen B is used).

The data obtained when EVA28 and EMA25 were added to the base bitumens help substantiate this hypothesis. EVA28, which has double the vinyl acetate content of EVA14, strongly increases the resistance to kerosene of both base bitumens. In this case also the addition of only 4 wt% is enough to observe this effect. The A-EVA28-4 blend is unexpectedly far from phase inversion and still shows the presence of spherical droplets. However, the dimensions of these droplets are smaller than those of A-EVA14-4 and this is evidence that stronger interactions are present in the blend when the vinyl

acetate content is higher. In B-EVA28-6 the phase inversion has almost taken place and the polymer-rich phase has become the matrix.

The last polymer containing polar oxygen groups, EMA25, had a positive effect on kerosene resistance, in almost all combinations. Also for this polymer, there was a remarkable change in morphology and solubility when the loading was increased from 4 wt% to 6 wt%. In particular, for base bitumen A the blend morphology changes from that of droplet dispersion to the already described intermediate situation where two clearly separated, almost isovolumetric, phases coexist.

A different situation appears in the case of the SBS copolymers. A first observation is that, even if the chemical composition is almost identical, radial and linear SBS have different effects on kerosene resistance, the radial copolymer being considerably more efficient. SBS chains consist of linked butadiene and styrene blocks. The two blocks are incompatible, and this leads to the formation of a biphasic material in which glassy styrenic domains are dispersed in a flexible polybutadiene matrix. In contrast to crystalline solids, block copolymers are characterized by fluid-like disorder on the molecular scale and by a high order at longer lengths (Hamley, 2004). The rigid domains, interconnected through the polybutadiene flexible chains, constitute the nodes of a physical elastomeric network whose configuration is somehow preserved after mixing with bitumen. The domains can have lamellar, spherical, cylindrical and gyroidal shape (Kotaka *et al.*, 2001) and can be arranged in a mesophase structure. The linear or radial configurations of these block copolymers lead to different molecular arrangements that confer different physico-mechanical properties to the polymer network and are responsible for differences in their swelling characteristics by the bitumen components. In fact, *l*SBS did not significantly improve the kerosene resistance of the base bitumens, whereas *r*SBS was very effective.

The morphologies of the two blends A-*l*SBS-4 and A-*l*SBS-6 differ considerably from each other and also from those of the oxygenated polymers. The 4 wt% blend shows a uniform dispersion where the polymer appears to be intimately mixed with the bitumen: the fluorescent zones are very small and the whole image has smooth grey-scale colours. A macroscopic separation can be seen in the 6 wt% blend, but a closer look at the image reveals that the polymer-rich zones contain a dispersion of dark spots due to asphaltene-rich droplets. The situation changes with base bitumen B, which has a lower aromatic content, and the morphology suggests lower compatibility. The 4 wt% blend has large polymer-rich islands which, however, do not assume a spherical shape but appear much more irregular and again contain internal black spots. With regard to the 6 wt% blend, the polymer-rich zones are large enough to coalesce and give rise to a continuous phase. When comparing the images obtained with *l*SBS and *r*SBS we have a clear picture of how much polymer architecture, not only chemical composition, may influence

the interaction with the bitumen components. The more aromatic bitumen A better interacts with SBS and leads to formation of small and irregularly shaped polymer-rich zones, while the second base does not give a satisfactory morphology. These differences in the morphology can be directly associated with the effect on mechanical properties, while they do not appear to be mirrored by differences of fuel resistance.

Relation between polymer structure and anti-kerosene effect

From the above considerations, it can be concluded that in the case of SBS a change in block co-polymer architecture, from linear to radial, strongly influences fuel resistance, while the bitumen composition seems not to be very important. On the contrary, with oxygenated polymers, differences in fuel resistance correlated with the bitumen composition can be better appreciated. This can be explained by analysing the different character of the two kinds of polymers. The oxygenated polymers have a random distribution of ethylene apolar units (which interact only with the aliphatic bitumen components) and $-\text{O}-\text{C}=\text{O}$ units which interact with the polar components. In contrast, for SBS copolymers, the polarity of the aromatic rings of the polystyrene blocks and the double bonds of the polybutadiene sequences will probably have stronger affinity with the aromatic and resin fractions. Therefore, all repeating units of SBS can actively interact with the two most important (from the quantitative point of view) bitumen fractions, while for oxygenated polymers only the polar functional groups create a link with the bitumen, thus making composition a very important parameter.

The above-described character of bitumen–polymer interactions is confirmed by TLC-FID analysis (Table 11.4) performed on the PMBs of base bitumen A with 6 wt% added polymer. Before analysing the results, some considerations are necessary. The first step of the procedure used for the analysis of such samples is the dissolution of PMBs in dichloromethane (DCM), but if the polymer used to modify the bitumen is not soluble or is only partially soluble

Table 11.4 TLC-FID analysis of the PMBs from base bitumen A

PMB	Saturates (%)	Aromatics (%)	Resins (%)	Asphaltenes (%)
A	2.2	59.1	23.3	15.4
A-EAA11-6	1.9	56.2	22.3	19.6
A-EVA28-6	2.0	52.5	27.4	18.1
A-EMA25-6	1.9	43.6	32.6	21.9
A-rSBS-6	2.0	56.0	27.0	15.0
A-rSBS-6	1.9	49.1	33.0	16.0

Source: Giuliani *et al.* (2009b).

in DCM, then also part of the binder may not dissolve, thus making analysis of the material impossible (as was the case for EAA6-6 and A-EVA14-6). The second point is that, when comparing the chromatographic data of the base bitumen with those of the PMBs, differences in the relative percentages of the S/A/R/A fractions before and after modification may be due to both the presence of the polymer in a particular fraction and the migration of bitumen molecules from one fraction to another. The latter phenomenon is induced by the polymer. The more a polymer influences the results of the TLC-FID analysis, the more it interacts with the bitumen molecules and the higher is the effect on kerosene resistance. The presence of a bond with the polymer chain limits the mobility of the bitumen molecules and therefore also the kinetics of dissolution. A preliminary test performed on the polymers alone shows that the SBS copolymers prevalently reside in the resins, while the oxygenated polymers mix preferably with the asphaltenes. Moreover, the solid residues recovered after 24 hours' immersion in the test fuel were subjected to chromatography. Due to the presence of polymer in the residue, some of the samples were not soluble in DCM and toluene was used to prepare the starting solution. In all cases (Table 11.5) these residues were entirely constituted of polymer, resin and asphaltene molecules.

In the TLC-FID analysis of PMB with the SBS copolymers, the main difference with respect to the unmodified base bitumens is the relative percentage of aromatics and resins. Due to their compatibility with the macromolecules, some of the aromatic components are entrapped in the polymeric network and thus counted with the polymer in the resin fraction. The higher variation observed for *r*SBS is coherent with the fact that with respect to *l*SBS, *r*SBS confers higher kerosene resistance thanks to its higher ability to entrap the aromatic molecules in its network.

Compared to SBS, the three oxygenated polymers, which preferably interact

Table 11.5 TLC-FID analysis of the residues

Bitumen	DCM		Toluene	
	Asphaltenes (%)	Resins (%)	Asphaltenes (%)	Resins (%)
A	85.1	14.9		
A- <i>l</i> SBS-6	95.2	4.8	91.9	8.1
A- <i>r</i> SBS-6	–	–	–	–
A-EVA14-6	–	–	94.8	5.2
A-EVA28-6	65.8	34.2	63.7	34.3
A-EAA11-6	94.9	5.1	93.4	6.6
A-EAA6-6	95.1	4.9	96.2	3.8
A-EMA25-6	–	–	93.7	6.3

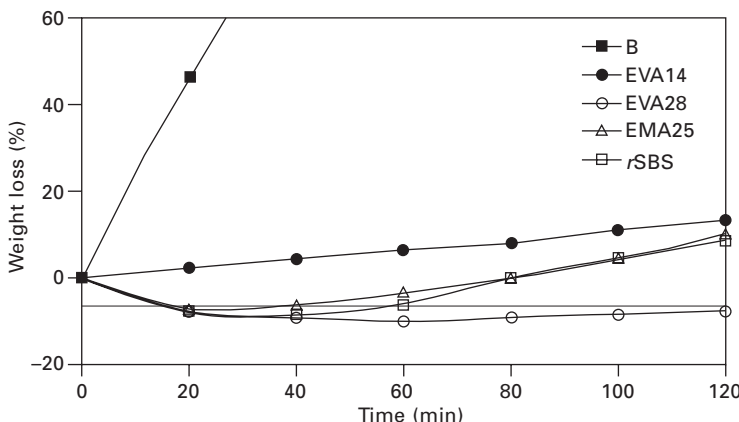
Source: Giuliani *et al.* (2009b).

with the polar fractions, strongly influence the asphaltene fraction. The EAA11 with lower O—C=O content alters significantly only the asphaltenic fraction, while the others have a strong influence also on the other three fractions. Supposing that all EAA11 ends up in the asphaltenic fraction, a recalculation of the bitumen fraction gives S/A/R/A = 2.0/58.6/23.7/14.5, which is very close to that of the base bitumen. Therefore, due to the modest interaction with the bitumen, EAA11 does not change the S/A/R/A composition and has a low effect on kerosene resistance.

Considering the case of EMA25 and EVA28, the latter contains the lower asphaltene fraction, as measured by TLC-FID. From the asphaltene content in A-EVA28-6 we can calculate that about 60% of the EVA is in such a fraction. Supposing that the remaining polymer is in the resins, the recalculated bitumen composition is S/A/R/A = 2.1/55.9/26.6/15.4. Therefore, the aromatics decrease and the resins increase with respect to bitumen A. Finally, the effect of EMA25 is qualitatively similar to that of EVA28, but quantitatively more pronounced, giving further confirmation of the high degree of interaction with the bitumen molecules and the strong effect on kerosene solubility.

PMBs with high polymer content

All the results discussed so far were obtained using polymer quantities equal to 4% and 6% by weight with respect to the total mass, typical loadings used in PMBs. However, in order to confirm the findings and better evaluate the potential of polymers in anti-kerosene formulations it is important to consider also binders containing higher polymer content. For this reason, base bitumen B was modified with 8% and 10% of the most promising polymers: EVA14, EVA28, EMA25 and *r*SBS. With respect to similar binders prepared with lower polymer content, in all cases a reduction in weight loss was recorded. Figure 11.6 shows the results in the case of PMBs prepared with 10 wt% of polymer, while the softening points are shown in Table 11.6. A couple of conclusions can be made from examining the solubility curves. The first is that the different efficacy of the four kinds of polymers can still be observed, but, at high contents, all the polymers provide a very good resistance to kerosene. This is not surprising, given that the resistance was supposed to be mainly influenced by the degree of interaction established within bitumen and between bitumen and polymer. The proposed mechanism may be reinforced only by increasing the presence of monomeric units able to engage with the bitumen components. The second point is that some of the weight loss curves have negative values. This simply means that the recorded weight of the samples dipped in the fuel was higher than the initial weight of the dry sample. Considering that the weight increase of the samples is definitively bigger than the experimental error, it is reasonable to assume that kerosene



11.6 Solubility of base bitumen B and PMB with 10% of added polymer.

Table 11.6 Softening point of the PMBs with high polymer content

PMB	Softening point (°C)
B-rSBS-8	106.0
B-rSBS-10	113.0
B-EVA14-8	85.0
B-EVA14-10	86.0
B-EVA28-8	63.0
B-EVA28-10	65.0
B-EMA25-8	79.0
B-EMA25-10	83.5

soaking prevails on the release of bitumen molecule in the solvent. This effect was not observed for EVA14, and was observed only in the first part of the test in the case of EMA25 and *r*SBS, while it persisted even after two hours of dipping in the case of EVA28. Of course, the results reported in Fig. 11.6 do not mean that the problem of kerosene resistance may be solved with any kind of polymer, just by increasing its content in the binder. It is necessary to keep in mind that the binder should meet other requirements, e.g. have a reasonable cost and be workable with conventional equipment. With respect to the latter point, the values of the softening points suggest that the binders with *r*SBS may be quite problematic, while those with EVA28 do not seem to be as sensitive to polymer content.

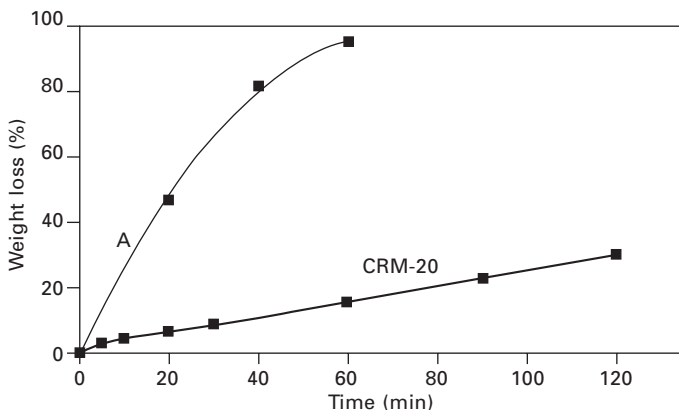
11.3.2 Rubber bitumens

Introduction

Considering the results related to the use of PMBs, it appears to be a logical consequence to test a non-conventional modifier, such as crumb rubber modifier (CRM), as additive to improve the fuel resistance of bituminous binders. CRM is a polymeric material with increasing importance in the pavement industry due to both the good performance that it guarantees and the advantage of promoting the recycling of a significant amount of end-of-life tyres. The use of CRM as bitumen modifier was first demonstrated several years ago and the American Society for Testing and Materials (ASTM D6114-97) defines bitumen rubber as a blend of bitumen, reclaimed tyre rubber and other additives, in which the rubber component is at least 15% by weight of the total blend and has reacted with hot bitumen cement sufficiently to cause swelling of the rubber particles. The high modifier concentration required and the ability to swell in the presence of bitumen, together with the consideration that CRM is not soluble in kerosene, suggests CRM maybe a potential modifier for bituminous materials which require improved intrinsic fuel resistance.

To evaluate the effect of CRM, base bitumen A was modified through a wet process with 20 wt% CRM, with respect to the total weight (Merusi *et al.*, 2010). The CRM was prepared by a cryogenic process yielding a particle diameter around 0.6 mm. Digestion time and methodology are described in ASTM D-6114. The modified binder is referred to as CRM-20. The solubility tests were performed in a similar way to that described in Section 11.2.2, with the difference that the ring and ball apparatus traditionally used for softening point measurements was utilized as an immersion device and the metallic net was large enough to allow the particles to fall to the bottom of the beaker. Again, the weight loss was measured at selected time intervals. Figure 11.7 shows that CRM-20 retains a considerable part of its mass after immersion in the jet fuel. Of course, in evaluating this result the fact that in CRM-20 the rubber is an intrinsically insoluble component should be taken into account. When the sample deaggregates, the CRM particles are released in kerosene and contribute to the weight loss which is a measure of the resistance of the whole binder and not of bitumen alone. The same results can therefore be reported after normalization that takes into account the rubber content. This would change only the quantitative representation of the fuel resistance, and not its qualitative interpretation.

The high modifier concentration and the ability to swell in presence of bitumen, together with the consideration that CRM is not soluble in kerosene, helps to interpret Fig. 11.7. The reduced solubility in CRM-20 is due to the rubber-bitumen interaction. As previously demonstrated by several studies (Airey *et al.*, 2004; Gawel *et al.*, 2006; Ould Henia and Dumont, 2008)



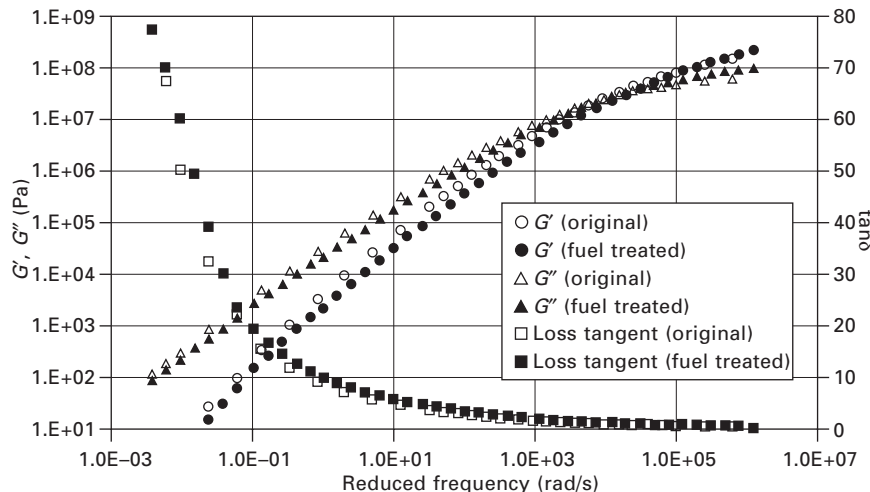
11.7 Solubility of base bitumen A and CRM-20 (from Merusi *et al.*, 2010).

the swelling process of the rubber particles is mainly due to a migration of aromatics and saturates from bitumen into the rubber network, commonly accepted for bitumen–polymer interaction (Polacco *et al.*, 2006). TLC-FID analysis confirms that particle swelling is mainly due to migration of the aromatic components into the rubber network (Ould Henia and Dumont, 2008). As already stated, only aromatics and saturates are completely soluble in kerosene, while resins are partially insoluble and asphaltenes almost totally insoluble. Therefore, we can suppose that the increase in kerosene resistance is due to the fact that a certain amount of the soluble fraction is retained and fixed by the CRM.

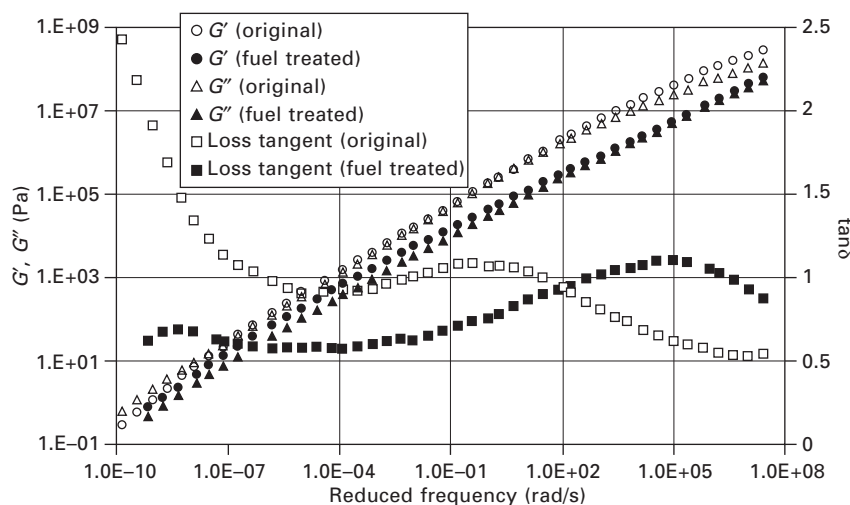
Effect of kerosene on the rheological properties

In addition to weight loss, fuel damage was also evaluated on the basis of the rheological differences between original and post-immersion recovered samples. The samples immersed for 120 minutes were subjected to a controlled drying period at room temperature, to provide test specimens for rheological investigation. Viscoelastic properties of original and fuel-treated binders were evaluated by performing stress-controlled frequency sweeps at various temperatures under linear viscoelastic conditions. The problem of having an appropriate comparison (it is not possible to test bitumen A after two hours of immersion) was bypassed by using CRM-20 immersed for two hours and bitumen A immersed for 30 minutes, corresponding to a 30% weight loss. Master curves, before and after the fuel treatment, of loss tangent ($\tan \delta$), elastic (G') and loss moduli (G'') of A and CRM-20 are reported in Figs 11.8 and 11.9 respectively.

Figure 11.8 shows that the original binder does not change significantly as



11.8 Master curves of base bitumen A (reference temperature 30°C) (from Merusi *et al.*, 2010).

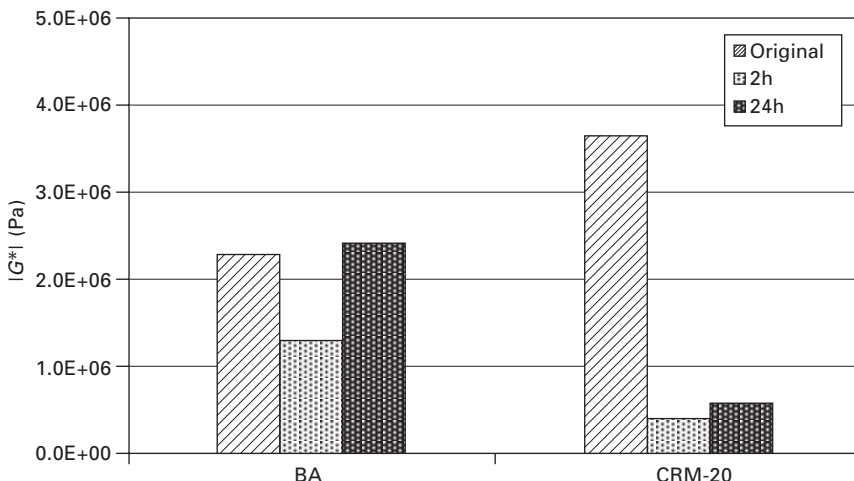


11.9 Master curves of CRM-20 (reference temperature 30°C) (from Merusi *et al.*, 2010).

a consequence of the fuel treatment. The main difference is a slight reduction in the absolute value of the moduli. On the contrary, CRM-20, when recovered after immersion in fuel, does not retain its initial rheological properties. Again, a reduction of the moduli was observed and this could be due to the presence of retained kerosene (this hypothesis will be discussed below). The master curves of $\tan \delta$ reveal important differences between the two materials,

showing effects related to a redistribution of the elastic, delayed elastic and viscous components of the binder. The loss tangent of the untreated binder has a classical trend, showing the tendency to a liquid state at low frequencies (high temperatures), an intermediate plateau zone, and a final decrease at high frequencies (low temperatures). The treated binder displayed different behaviour and shows a loss tangent which, except for the frequencies between 10^4 and 10^6 rad/s, is always lower than 1. These changes are compatible with the loss of light fractions: at high temperatures the bitumen matrix of the original binder shows the classic behaviour of a liquid. After fuel treatment, the reduction of aromatics and saturates increases the stiffness of the binder and, at the measured temperatures, the material still maintains a low $\tan \delta$ which fails to show the natural tendency to increase. The low molar mass molecules are too few to confer mobility on the asphaltene aggregates and the material shows non-Newtonian behaviour. G'' of the untreated binder is higher than G' in the low-frequency range, the two moduli are similar in the intermediate zone, and G' prevails at high frequencies. On the contrary, after fuel treatment, G' is higher than G'' practically at all frequencies, with the exception of a quite small window in the high-frequency, low-temperature zone.

Therefore, the original binder is 'homogeneously' dissolved in the fuel, while for the CRM binder the composition is considerably different when comparing the original and fuel-treated samples. As already mentioned, this difference may be due to both a selective dissolution in the fuel and a partial retention of the latter in the bitumen. The retention of kerosene in the bitumen can be seen as a 'temporary' effect, mainly linked to the methodology used in this study. In other words, this contribution could be reduced by using samples subjected to a longer drying period. Figure 11.10 shows on a linear scale the complex modulus $|G^*|$ measured at 20°C and 10 rad/s for the original binders and for the same after immersion in kerosene and a drying period of 2 or 24 hours. In both cases, $|G^*|$ of the binder immersed in kerosene and dried for 2 h is lower than $|G^*|$ of the untreated binder and this is due to the presence of non-evaporated fuel. An increase in the drying period (24 h) reduces the presence of kerosene in the sample and determines an increase in the magnitude of the complex modulus. For bitumen A the complex moduli of untreated and 24 h dried binder are almost identical, which means that the decay in $|G^*|$ recorded after a drying period of 2 h is a temporary effect that can be eliminated by a complete evaporation of the fuel. On the contrary, for CRM-20 the complex modulus of 24 h dried binder remains much lower than that of the untreated sample. After the drying, the treated binder does not have the same characteristics as the original one. Therefore, the immersion in fuel changes the overall composition. This can be due to a selective solubility, limited to the bitumen components that are not entrapped in the rubber, and/or to kerosene soaking.



11.10 Complex modulus of bitumen A and CRM-20 (from Merusi *et al.*, 2010).

In conclusion, the solubility tests show that bitumen modification with CRM strongly improves fuel resistance of the base bitumen. This reduction is a consequence of the absorption of the lighter, and essentially kerosene soluble, bitumen fractions into the rubber particles. However, the improvement observed in terms of weight loss is accompanied by significant changes in binder composition and consequently its rheological properties are altered.

11.3.3 Wax modified bitumens

Introduction

Production, laying and compaction of hot-mix bitumens require high temperatures during the whole process cycle. Therefore, the main goal of warm bitumen technologies is to reduce the process temperatures, which in turn results in a decrease in cost, consumption and atmospheric emissions, without affecting performance and durability of the mixtures. In addition to the environmental and economic advantages, the development of warm bitumen technology can induce a practical improvement: when the production temperature is the same as that adopted for the traditional hot mix bitumens, warm mixtures allow haulage of bitumen over longer distances, and a longer construction season, and facilitate the use of bitumen under Nordic climate conditions (Giuliani and Merusi, 2009; Edwards *et al.*, 2010).

Presently, warm bitumen technology involves a large group of very different technical solutions, including process technology modification, water-based technologies and organic additives. Some promising technical solutions involve procedures based on mixture modification with additives able to foam

bitumen, such as zeolite, or to reduce the bitumen viscosity, such as waxes. The latter have a crystalline structure and relatively low molecular weight and melting temperature. The aim of their addition to bitumen is to lower the viscosity at production temperatures without affecting the consistency at pavement service temperatures. For this reason, many technical investigations have recently focused on the use of commercial wax to develop warm-mix bitumen technologies.

Basically, waxes are already present in small quantities as natural constitutive components of all petroleum products, including bitumens (Lu and Redelius, 2006). Several studies have been carried out into the determination of wax content (Lu *et al.*, 2008) and crystallization properties and chemical structure (Michon *et al.*, 1999; Lu *et al.*, 2005; Redelius and Lu, 2006; Siddiqui *et al.*, 2002), but also into its influence on bitumen mixture properties (Edwards and Redelius, 2003; Edwards *et al.*, 2006; Lu and Redelius, 2006). With regard to the in-service performance, the presence of wax can be associated with different side-effects that negatively influence pavement quality and durability. In particular, it is traditionally assumed that the wax melting can soften bitumen at high service temperatures, affecting the rutting resistance of the pavement, and that wax crystals can increase mixture stiffness and sensitivity to fatigue and thermal cracking at low temperatures.

Therefore, we have two contradictory assumptions with regard to the effect of the addition of waxes to bitumen: from a performance point of view they have to be eliminated, while from the viscosity point of view they should be added. The key to interpreting this apparent inconsistency is associated with the definition of wax, which cannot be contained in a single unequivocal definition. Petroleum waxes include different types of waxes and also some aromatics and molecules with polar functional groups which may crystallize upon cooling. Petroleum wax can be classified as paraffin (or macrocrystalline) waxes and microcrystalline waxes. Paraffin waxes refer to *n*-alkanes with linear carbon backbone chains and low molecular weight (<C45), having a melting point generally lower than 70°C and forming a macrocrystalline structure upon cooling. Microcrystalline waxes are aliphatic hydrocarbon compounds with branched chains, chemically known as iso- and cyclo-alkanes. Moreover, microcrystalline petroleum waxes have a specific distribution of molecular weight where high molecular weight compounds with carbon backbone chain length >C45 prevail. Hence, the physical properties of microcrystalline waxes differ from those of paraffin waxes, and they have higher melting points (generally >70°C).

Waxes have been commercialized as bitumen flow improvers for use in WMB, e.g. Montan waxes, Fischer–Tropsch waxes and functionalized waxes. Montan waxes are a combination of non-glyceride long-chain carboxylic acid esters, free long-chain organic acids, long-chain alcohols and other organic compounds with complex structures. They are obtained by solvent

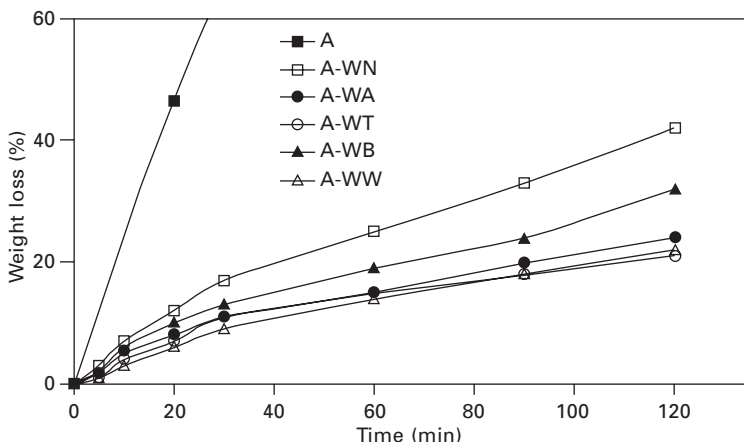
extraction from certain types of lignite and brown coal. Fischer–Tropsch waxes consist of a mixture of *n*-alkanes and iso-alkanes, where *n*-alkanes with carbon chain lengths ranging from C40 to C120 are predominant, and have a fine microcrystalline structure at low temperatures. Compared with paraffin waxes, Fischer–Tropsch waxes have higher melting points (generally $>90^\circ\text{C}$) due to their longer carbon chains, and reduced brittleness. Functionalized waxes are chemically modified hydrocarbon microcrystalline waxes, including waxy amides produced by amidation of fatty acids. Other modified waxes are produced through saponification or esterification of hydrocarbon waxes and can be recorded as bitumen modifiers. This kind of wax can have very different physical properties due to its different chemical structure. In particular, functionalized waxes generally have a melting point higher than 100°C and show specific crystallization properties.

In conclusion, in the list of waxes designed and proposed as bitumen modifiers there is extreme variability in structure and properties and all these waxes are nominally different from petroleum waxes. This makes their role in bitumen modification difficult to define and their effect on the final physical properties not easily predictable. Nevertheless, the almost complete insolubility of waxes in paraffinic hydrocarbons suggests that they could provide some advantage with regard to fuel resistance.

Effect of waxes on bitumen solubility

The effect of waxes on bitumen solubility was tested by modifying base bitumen A with five different waxes (Merusi *et al.*, submitted), referred to as WN (a Montan wax), WA and WB (mixes of Montan wax and high molecular weight hydrocarbons), WT (a mix of Montan wax and fatty acid derivatives) and WW (Fischer–Tropsch wax). All mixes contained 6 wt% of wax, added to a bitumen sample heated at 160°C for 30 minutes and subsequently mixed at 4000 rpm for 15 minutes.

The results of the solubility tests carried out for the above-described wax-modified bitumens (WMB) are reported in Fig. 11.11. All waxes impart a considerably high fuel resistance. As for polymers and CRM, the waxes are insoluble in kerosene, but in this case it is not possible to invoke the mechanism of selective migration. The waxes are scarcely soluble with bitumen and they basically maintain their crystalline nature after mixing with it (Lu *et al.*, 2005; Edwards and Isacsson, 2005; Edwards *et al.*, 2005). It is not realistic that the wax crystals could swell and entrap some of the bitumen components. In this case, we can suppose that the kerosene-insoluble wax crystals somehow constitute a physical barrier to the dissolution of the binder. In order to validate this hypothesis, it is useful to evaluate the residual crystallinity of the waxes after their mixing with the binder. Table 11.7 shows the melting temperature (T_m) and enthalpy of pure waxes ($\Delta H_{m,p}$) and



11.11 Solubility of base bitumen A and WMB with 6% of added wax (from Merusi *et al.*, submitted).

Table 11.7 DSC analyses of wax and WMBs

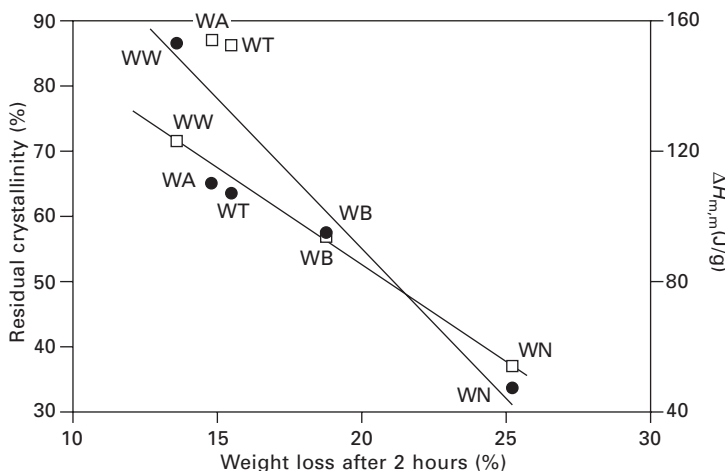
Pure wax	T_m (°C)	$\Delta H_{m,p}$ (J/g)	Mixes	T_m (°C)	$\Delta H_{m,m}$ (J/g)	$\Delta H_{m,m}/\Delta H_{m,p}$
T	146.7	124.0	L-6T	126.4	107	0.862
A	69	18.5	L-6A	68.5	16	0.865
	145	107.5		124.0	94	0.874
N	84.7	127.8	L-6N	78.6	47	0.371
B	–	168.3	L-6B	–	95	0.570
W	98.9	214.0	L-6W	84.8	153	0.715
	111			105.7		

Source: Merusi *et al.* (submitted).

relative mixes with bitumen ($\Delta H_{m,m}$). The two values reported for wax WA correspond to the melting of two well-separated peaks respectively, while the two T_m values reported for wax WW correspond to iso- and *n*-paraffins (in this case, a single global ΔH is reported, because the two melting peaks partially overlap). In the case of wax WB, the calorimetric spectrum is composed of several peaks and therefore just a single global melting enthalpy is reported. $\Delta H_{m,m}$ for the mixes is calculated by normalizing the integral of the melting peaks with respect to the wax content. The $\Delta H_{m,p}/\Delta H_{m,m}$ column basically represents the fraction of residual crystallinity of the waxes in the mixes. For all mixes, a reduction of the melting point of the wax crystals was observed, probably due to waxes having partial miscibility with some of the bitumen components. The decrease in T_m is particularly important (about 20°C) for the WT and WA waxes. Despite this, these two waxes display

fairly high values of $\Delta H_{m,p}/\Delta H_{m,m}$, suggesting that their crystalline fraction is predominantly preserved after mixing with the bitumen. As reported in Fig. 11.11, waxes WT and WA provide similar, and very high, fuel resistance.

Different levels of resistance are obtained with waxes WW, WB and WN. The residual crystallinity is very small ($\Delta H_{m,p}/\Delta H_{m,m} = 0.37$) for the Montan wax (WN), intermediate for the mixed wax WB, and fairly high ($\Delta H_{m,p}/\Delta H_{m,m} = 0.71$) for the Fischer-Tropsch wax (WW). For these paraffinic waxes, the change of $\Delta H_{m,p}/\Delta H_{m,m}$ parallels that of the starting melting enthalpies $\Delta H_{m,p}$, and is probably ascribable to the increased content of linear paraffinic hydrocarbons and to the increased length of the carbon chains: the Montan waxes (WN and WB) have carbon chain lengths ranging from C_{20} to C_{50} , while the Fischer-Tropsch waxes (WW) have a higher molecular weight (from C_{40} to C_{120}). In the same way, the fuel resistance of the mixes containing paraffinic waxes increases almost linearly with the crystalline fraction of the wax component, as measured by $\Delta H_{m,m}$. At first glance, for the paraffinic waxes there is a qualitative correlation between fuel resistance and both melting enthalpy and residual crystallinity in the mixes (Fig. 11.12). The mix A-WN is the one with the lowest crystallinity (37.1%) and the highest solubility. Samples A-WA, A-WT and A-WW have the highest crystallinity and higher resistance, A-WB displaying intermediate behaviour. In the graph, the symbols corresponding to the mixes with the other two waxes (WA and WT) do not fall on the same straight line drawn for the mixes A-WN, A-WB and A-WW. This is not surprising if we consider that WA and WT have different chemical structures, due to the presence



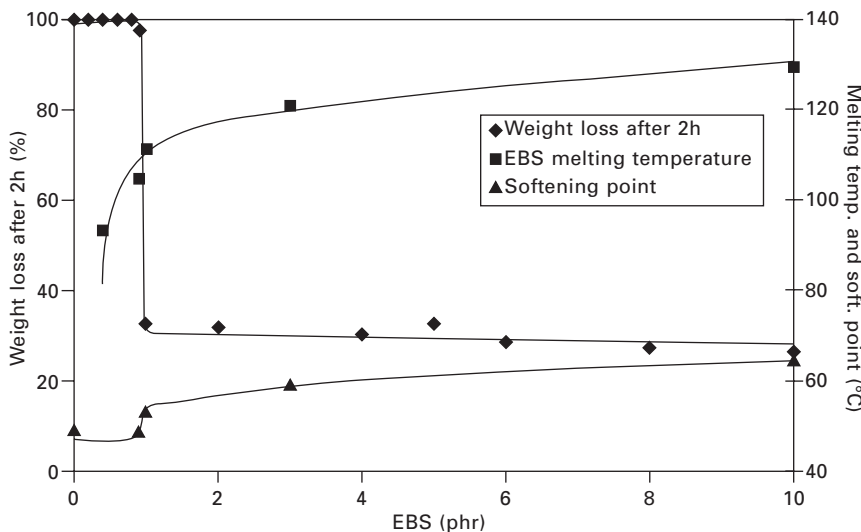
11.12 $\Delta H_{m,m}$ (●) and residual crystallinity (□) as a function of weight loss after 60 min of dipping in kerosene (from Merusi *et al.*, submitted).

of amidic bonds. The chemical composition of WA is almost identical to that of WT, while that of WW is almost identical to those of WB and WN. The crystal structures of the two types of substances (amidic and paraffinic) are different and, therefore, their degrees of crystallinity cannot be directly correlated with the corresponding melting enthalpies.

The results shown in Fig. 11.12 suggest that there is a correlation between the residual crystalline fraction of the wax additives and their beneficial effect on fuel resistance of the mixes. Of course, the solubility is not simply determined by the quantity, but also by the nature (i.e. chemical composition and dimensions) of the crystals. However, this confirms that the fuel resistance of WMBs probably derives from the presence of crystals and that, for a given category of waxes, the solubility can be directly correlated with the degree of residual crystallinity (for a fixed wax content).

Effect of wax concentration

As solubility is directly correlated with the presence of wax crystals, which constitutes a physical barrier for the diffusion process, it is particularly interesting to evaluate the effect of wax concentration on fuel resistance. This was done by adding to base bitumen A different quantities of ethylene-bis-stearamide (EBS) which is the main component of the amidic waxes. Figure 11.13 shows the weight loss (%) after two hours of immersion, as well as the softening point of the binders and the melting temperature of EBS crystals as



11.13 Weight loss, softening points and EBS melting temperature as a function of EBS content.

a function of wax content (expressed in phr). It is very interesting to observe that for the three quantities there is a sort of critical wax concentration that corresponds to a step change in the recorded value. When the EBS content is lower than or equal to 0.9 phr, the sample completely dissolves after two hours of immersion. Passing from 0.9 to 1.0 phr of EBS, the recorded weight loss is equal to about 33%. Higher concentrations of wax do not significantly change the solubility (the weight loss with 10 phr of EBS is equal to 27%). Analogously, the softening point changes from 48.5°C (almost identical to that of base bitumen A) to 53°C when the wax content is increased from 0.9 to 1.0 phr. Such big changes show that 1.0 phr of EBS corresponds to a situation where the crystal network reaches a sort of continuity, more or less analogous to the phase inversion of PMBs, which induces a macroscopic effect on the binder properties. The trend of the melting temperature of the EBS crystals suggests that the critical value may be strictly related to the ability of the asphalt components to disturb EBS crystallization.

11.4 Conclusions

The contribution of different modifiers to the fuel resistance of bituminous binders has been outlined and discussed in order to develop materials with an improved intrinsic resistance to hydrocarbon oils. The solubility tests showed that all the modifiers studied can increase the resistance of the base bitumen to fuel. Nevertheless, important differences were recorded between the three classes of modifiers and the different types of modifiers in each class. Polymers lead to a quite sensible improvement in that the final resistance is strongly dependent on polymer structure and compatibility with the bitumen. Several polymers were tested and some were shown to be very interesting from this point of view. However, not all the polymers that improved fuel resistance also guarantee storage stability of the PMB and, in some cases, the required amount of polymer can be quite high. The effect of crumb rubber is generally stronger than the effect of polymers, and the required amount of CRM can be maintained in the range usually adopted for this kind of modifier. However, the contact with kerosene may significantly alter the rheological properties of the binder. Waxes generally produce the most important improvement in fuel resistance.

With regard to the mechanisms involved in improving fuel resistance, it appears reasonable to associate the reduced solubility obtained with polymers and crumb rubber with a selective swelling, facilitated by the modifiers, which involves the bitumen components that are more soluble in kerosene. As a consequence, the soluble molecules are less accessible to the fuel. On the contrary, in the case of wax modifiers, the waxes form a physical barrier composed of a network of insoluble crystals well dispersed in the whole bituminous mass.

The future developments in this field may be related to the study of synergistic effects between two modifiers, for example addition of two polymers or a polymer and a wax.

11.5 References

Airey G, Rahman M and Collop A C (2004), 'Crumb rubber and bitumen interaction as a function of crude source and bitumen viscosity', *Road Materials and Pavement Design*, 5(4), 453–475.

Corun R, Van Rooijen R C and De Bondt A H (2006), 'Performance evaluation of jet fuel resistant polymer-modified asphalt for airport pavements', *Proceedings of the 2006 Airfield and Highway Pavement Specialty Conference*. American Society of Civil Engineers (ASCE), Atlanta, GA.

Deneuvillers C and Letaudin F (2003), 'Environmentally friendly fuel resistant surfacing', *Proceedings of the World Road Association (PIARC) Conference*, Durban, South Africa.

Edwards Y and Isacsson U (2005), 'Wax in bitumen', *Road Materials and Pavement Design*, 6(3), 281–309.

Edwards Y and Redelius P (2003), 'Rheological effects of waxes in bitumen', *Energy & Fuels*, 17(3), 511–520.

Edwards Y, Tasdemir Y and Isacsson U (2005), 'Influence of commercial waxes on bitumen aging properties', *Energy and Fuels*, 19, 2519–2525.

Edwards Y, Tasdemir Y and Isacsson U (2006), 'Influence of commercial waxes and polyphosphoric acid on bitumen and asphalt concrete performance at low and medium temperatures', *Materials and Structures*, 39, 725–737.

Edwards Y, Tasdemir Y and Butt A (2010), 'Energy saving and environmentally friendly wax concept for polymer modified mastic asphalt', *Materials and Structures*, 43(1), 123–131.

Gawel I and Slusarski L (1999), 'Use of recycled tire rubber for modification of asphalt', *Progress in Rubber and Plastics Technology*, 15(4), 235–248.

Gawel I, Stepkowski R and Czechowski F (2006), 'Molecular interactions between rubber and asphalt', *Industrial and Engineering Chemistry Research*, 45(9), 3044–3049.

Giuliani F and Merusi F (2008), 'Anti-kerosene asphalt binders designed for airfield pavements. A rheological approach to fuel resistance evaluation', *Proceedings of the Symposium on Asphalt Pavement and Environment*, ISAP, Zürich, Switzerland.

Giuliani F and Merusi F (2009), 'Flow characteristics and viscosity function in asphalt binders modified with wax', *International Journal of Pavement Research and Technology*, 2(2), 51–60.

Giuliani F and Rastelli S (2006), 'Test methods to evaluate fuel resistance of aprons asphalt pavements in airports and heliports', *Proceedings of the Second International Airports Conference: Planning Infrastructure and Environment*, São Paulo, Brazil.

Giuliani F, Merusi F and Rastelli S (2009a), 'Experimental evaluation of fuel damage in bituminous materials', *Proceedings of the 88th Annual Meeting of the Transportation Research Board*, TRB, Washington, DC.

Giuliani F, Merusi F, Filippi S, Biondi D, Finocchiaro M L and Polacco G (2009b), 'Effects of polymer modification on the fuel resistance of asphalt binders', *Fuel*, 88, 1539–1546.

Hamley I W (2004), *Developments in Block Copolymer Science and Technology*, New York, Wiley.

Hendriks H E J, Steernberg K, Terlouw T and Vonk W C (Shell International Research Maatschappij B.V.) (1997), *Bitumen compositions and a process for their preparation*, WO patent application 97/44397.

Kotaka T, Okamoto M, Kojima A, Kwon Y K and Nojima S (2001), 'Elongational flow-induced morphology change of block copolymers. Part 1. A polystyrene-block-poly(ethylene butylene)-block-polystyrene-block-poly(ethylene butylene) tetrablock copolymer with polystyrene spherical microdomains', *Polymer*, 42, 1207–1217.

Lu X and Redelius P (2006), 'Effect of bitumen wax on asphalt mixture performance', *Construction and Building Materials*, 21, 1961–1970.

Lu X, Langton M, Olofsson P and Redelius P (2005), 'Wax morphology in bitumen', *Journal of Materials Science*, 40, 1893–1900.

Lu X, Kalman P and Redelius P (2008), 'A new test method for determination of wax content in crude oils, residues and bitumens', *Fuel*, 87, 1543–1551.

Merusi F, Polacco G, Nicoletti A and Giuliani F (2010), 'Kerosene resistance of asphalt binders modified with crumb rubber: solubility and rheological aspects', *Materials and Structures*, 43, 1271–1281.

Merusi F, Giuliani F, Filippi S, Moggi P and Polacco G, 'Kerosene-resistant asphalt binders based on non-conventional modification', submitted to *Journal of Transportation Engineering*.

Michon L C, Netzel D A and Turner T F (1999), 'A ^{13}C NMR and DSC study of the amorphous and crystalline phases in asphalts', *Energy & Fuels*, 13, 602–610.

Newman K and Shoenberger J E (2002), 'Polymer concrete micro-overlay for fuel and abrasion resistant surfacing: laboratory results and field demonstrations', *Proceedings of the 2002 Federal Aviation Administration Airport Technology Transfer Conference*, FAA, Atlantic City, NJ.

Ould Henia M and Dumont A G (2008), 'Effect of base bitumen composition on asphalt rubber binder properties', *Proceedings of the ISAP Symposium on Asphalt Pavement and Environment*, ISAP, Zürich, Switzerland.

Planche J P, Chaverot P, Lapalu L and Ponsardin M (TotalfinaElf France) (2002), *Procédé de préparation de composition bitumen/polymère à résistance aux solvants pétroliers améliorée, compositions ainsi obtenues et leur utilisation comme liants bitumineux*. French patent application 2849047 A1, 20 December 2002.

Plug C, Srivastava A and De Bondt A H (2004), 'A durable jet fuel resistant pavement layer with the use of a polymer modified asphalt emulsion', *Proceedings of the 3rd International Symposium on Asphalt Emulsion Technology*, Washington, DC.

Polacco G, Berlincioni S, Biondi D, Stastna J and Zanzotto L (2005), 'Asphalt modification with different polyethylene-based polymers', *European Polymer Journal*, 41, 2831–2844.

Polacco G, Stastna J, Biondi D and Zanzotto L (2006), 'Relation between polymer architecture and nonlinear viscoelastic behavior of modified asphalts', *Current Opinion in Colloid & Interface Science*, 11(4), 230–245.

Praticò F G, Ammendola R and Moro A (2008a), 'Asphalt concrete for fuel-resistant roads', *Proceedings of the 4th Euroasphalt and Eurobitume Congress*, Copenhagen.

Praticò F G, Ammendola R and Moro A (2008b), 'Fuel resistance of HMAs. Theory and experiments', *International Journal of Pavement Research and Technology*, 1(4), 100–106.

Redelius P and Lu X (2006), 'Compositional and structural characterization of waxes isolated from bitumens', *Energy & Fuels*, 20, 653–660.

Rushing J F and Tom Jr J G (2009), 'Laboratory testing of asphalt surface treatments

for airfield pavements', *International Journal of Pavement Research and Technology*, 2(5), 196–204.

Seive A, Leroux C and Teurquetal F (2004), 'Fuel performance evaluation of asphalt pavements', *Proceedings of the 3rd Euroasphalt and Eurobitume Congress*, Vienna.

Siddiqui M N, Ali M F and Shirokoff J (2002), 'Use of X-ray diffraction in assessing the aging pattern of asphalt fractions', *Fuel*, 81, 51–58.

Steernberg K, Read J M and Seive A (2000), 'Fuel resistance of asphalt pavements', *Proceedings of the 2nd Euroasphalt and Eurobitume Congress*, Barcelona, Spain.

Thornton J (COLAS) (2006), *A bituminous binder and its manufacturing process, and a process for improving fuel resistance of such bituminous binder*, European patent application EP 1700887 A1, 10 March 2006.

Yan T Y (1986), 'Manufacture of road-paving bitumen using coal tar', *Industrial and Engineering Chemistry Product Research and Development*, 25(4), 637–640.

Physico-chemical techniques for analysing the ageing of polymer modified bitumen

V. MOUILLET, Centre d'Etudes Techniques de l'Equipement-Méditerranée, France and F. FARCAS and E. CHAILLEUX, Institut Français des Sciences et Technologies des Transports, de l'Aménagement et des Réseaux, France

Abstract: Road bitumen undergoes, during its service life, an ageing process that leads to a material's hardening. But, when a polymer modified bitumen (PmB) has been used, what happens after oxidation/ageing is very complex to analyse, due to the number of chemical parameters involved: the nature of the polymer (structure and chemistry), the chemistry of bitumen, and the type of blending. The chapter begins by describing the main physico-chemical and rheological methods that are the most appropriate to study PmB and also to follow their evolution during thermal or photo-ageing. It then presents a new way of characterizing these heterogeneous products by infrared microscopy without modifying the internal equilibrium between polymeric and bituminous phases. The chapter includes the results of an investigation, at the microscopic scale, of PmB ageing so as to understand how any changes in composition or processing affect PmB evolution with time.

Key words: polymer modified bitumen, photo-oxidation, thermal oxidation, physico-chemical methods, infrared microscopy.

12.1 Introduction

Increase in traffic volume has led to a wider use of polymer modified bitumens (PmB) in road construction. During the design phase of bituminous mixes for road pavements, it is fundamental to be able to predict or at least to estimate the evolution of physical properties of bituminous binders with respect to time, in order to ensure the durability of the whole infrastructure. Indeed, when bituminous materials are exposed to heat, air and ultraviolet (UV) radiation, a gradual degradation of physical and mechanical properties occurs (Wu *et al.*, 2008). That binders oxidize in pavements and thereby harden is accepted (Al-Azri *et al.*, 2006; Petersen, 2009). Indeed, because bituminous binder is a natural organic end product of the degradation of ancient living organisms, it is subject to chemical oxidation by reaction with atmospheric oxygen (Petersen, 2009). During the service life in a pavement, the bituminous

binder is exposed to the oxygen in air at ambient pressures that lead to the thermal oxidation of certain binder molecules (Lu and Isacsson, 1998; Mill, 1996; Petersen, 1998; Mouillet *et al.*, 2008a). This thermal oxidation takes place throughout the service life of the road and is divided into short-term ageing (which occurs during manufacturing and laying) and long-term ageing (which occurs over several years during service life). Ageing is already a very complex process in conventional bitumen and the complexity increases when polymer is added to modify bitumen. One of the most important issues is to describe the process involved: is PmB ageing a consequence of bitumen ageing, polymer ageing, or a combination of both at the same time?

The majority of physical and chemical techniques used to investigate pure bitumens can also be used to study modified binders, i.e. spectrophotometry, chromatography and differential scanning calorimetry. However, the use of these techniques and the interpretation of the results are usually not the same because of differing objectives. Additionally, most PmBs feature a two-phase structure made of polymer-rich areas along with polymer-poor regions, depending on the asphalt chemistry, the polymer nature and content. PmBs are usually multiphase systems, and appear heterogeneous when viewed at the optical microscopic level. It is therefore important to take this peculiar feature into consideration when trying to sort out the respective effect on ageing of the polymer and the bitumen. What happens after oxidation/ageing is even more complex, due to the number of chemical parameters involved: the nature of the polymer (structure and chemistry), the chemistry of the bitumen, and the type of blending. In order to answer this key question, several tests and methods have been used by researchers. This chapter is limited to a presentation of the main test methods, which are the most appropriate to the study of PmB and, in particular, with regard to ageing of these binders.

This chapter briefly describes, in the following order:

- Laboratory assessment of binder ageing
- Methods usually employed in the chemical and rheological characterization of PmB ageing
- Investigation at microscopic level of PmB ageing.

12.2 Usual methods for physico-chemical characterization of polymer modified bitumen (PmB) ageing

12.2.1 Laboratory ageing procedures

During the service life of a pavement, the bituminous binder is exposed to heat, air and ultraviolet (UV) radiation that lead to the gradual degradation of physical and mechanical properties of asphalt mixes. This ageing process is of pragmatic importance and consequently is simulated in the laboratory

by various accelerated ageing tests (Mouillet and Dumas, 2008). However, none of these takes into account the influence of UV radiation (Montepara and Giuliani, 2004; Verhasselt, 1999), although, in the real environment, solar radiation could affect the upper layers of the pavement surfacing and explain some of the divergences observed between the standardized laboratory simulations of ageing and observations made in the field (Durrieu *et al.*, 2007).

Thermal ageing

It is well known that the principal cause of ageing in service of bituminous binders is oxidation by oxygen from the air. Oxidation results in the formation of highly polar and strongly interacting oxygen-containing functional groups (Mill, 1996; Petersen, 1998). Thermal oxidation takes place throughout the life of the road and is divided into short-term ageing (which occurs during manufacturing and laying) and long-term ageing (which occurs over several years during in-service life).

At this time, several accelerated ageing methods have been developed and standardized at the European level to simulate binder ageing in the road (Migliori and Corté, 1998; Such *et al.*, 1997). It is generally accepted that the Rolling Thin Film Oven Test ('RTFOT', norm EN 12607-1), in part, simulates the changes that occur in an unmodified binder during mixing, transportation and laying of a hot mixed bituminous material, although this may need validating for some modified binders (Montepara and Giuliani, 2004). On the other hand, different methods exist to simulate the long-term changes (hardening) that occur in a bituminous mixture in service, but no one method is universally accepted. The Pressure Ageing Vessel ('PAV', norm EN 14769) is a potentially suitable ageing method developed during the American Strategic Highways Research Program (SHRP). This method has been adopted in the USA; in Europe, the corresponding procedure has been standardized because PAV is the most easily accepted long-term ageing test. It is currently in use to simulate field ageing, even though there is no available information about the equivalence of this test with the service years of a binder in a road. However, whether this test, or any other candidate test, is truly representative of years in-service will certainly never be solved. At this time, the laboratory simulation techniques of the action of ageing on modified bitumen are still a substantially open problem because they were developed for unmodified binders and need re-evaluation for polymer-modified bitumen (Mouillet *et al.*, 2008a). The following two conventional tests are well known and validated for neat bitumen, and are currently used to simulate PmB ageing:

- RTFOT (75 min, 163°C, air flow of 4 L/min) is claimed to simulate ageing at the jobsite (i.e. mixing and laying). This technique has been

validated for some time for unmodified bitumen (Migliori *et al.*, 2000) for which it is considered to be more severe than actual jobsite conditions (Such *et al.*, 1997). In the case of modified bitumen, its validity is still open to discussion because, among other things, the RTFOT reference temperature of 163°C is not representative of the actual temperature used in plant during the mixing of aggregates with modified binders. Usually, to avoid viscosity problems, the temperature of the modified binder in the hot plant is set between 163°C and 180°C. This is the reason why it is preferable to perform the RTFOT test at 175°C for modified bitumen (Mouillet and Dumas, 2008).

- PAV (20 h, 100°C, air pressure of 2.1 MPa) is claimed to simulate several years of ageing in field service conditions. This link has been established for unmodified bitumen, but how long this equivalence is depends on several parameters, such as void content, climate, and composition of the binder (Anderson, 1999; Verhasselt, 1999; Farcas, 1996). Recently, a study of several experimental pavements with unmodified binders found the Superpave RTFOT plus 20-hour PAV ageing test to be approximately equal to hot-mix ageing plus four years on the road (Al-Azri *et al.*, 2006). However, in the case of modified bitumen, no similar information is available because no clear correspondence between the long-term ageing simulation technique and field data can be established (Mouillet and Dumas, 2008). This is due to the fact that binders in pavement age at different rates depending upon climate, air voids, position of the asphalt layer in the pavement structure, modified binder oxidation kinetic parameters, initial ageing level when placed, and binder hardening susceptibility. One should also note that the influence of UV radiation action on superficial layer ageing is not taken into account by the RTFOT plus 20-hour PAV ageing procedure. This could explain some of the divergences noticed between the standardized laboratory simulations of ageing and observations in the field (Durrieu *et al.*, 2007).

UV ray ageing

The influence of solar radiation on bituminous binders has been known for some considerable time, as Niepce in 1822 developed a photo-etching technique based on the transformation of a thin layer of bitumen by the action of light (Durrieu *et al.*, 2007). Notwithstanding this, the influence of light on bitumen ageing is ignored in laboratory simulations of ageing as it is recognized that due to the high absorption coefficient of bitumen – particularly for ultraviolet (UV) radiation – solar radiation affects only the upper layers of the pavement surfacing (Verhasselt, 1999). In the 1950s, an ‘exposure test’ (Duriez and Arambide, 1962) was developed which showed that the effect of solar radiation depended on the nature of the bitumen

(Barth, 1962). Later, several other authors (Durrieu *et al.*, 2007; Airey, 2003) confirmed this observation and also observed that the photochemical reaction had a significant effect on bitumen films with a thickness of 3 mm, while thicker films showed a slight effect (Traxler, 1963). In the case of elastomer based PmB, the rate of photo-oxidation appears to depend on the nature of the base bitumen as well. However, one can note on the one hand that inside the bituminous matrix, the elastomer architecture does not influence its degradation when exposed to UV radiation and, on the other hand, the bitumen ‘protects’ the elastomer towards UV radiation (Mouillet *et al.*, 2008b).

12.2.2 Physico-chemical characterization methods

Bitumen is composed of an extremely large number of chemically diverse organic molecules; it is a complex mixture of molecules, ranging from rather non-polar hydrocarbons similar in composition to waxes to highly polar or polarizable hydrocarbon molecules containing condensed aromatic ring systems that incorporate heteroatoms such as oxygen, nitrogen and sulphur (Petersen, 2009). This complexity increases when a polymer is incorporated in bitumen using mechanical mixing and/or chemical reaction (Korhonen and Kellomäki, 1996). Nevertheless, the same physico-chemical methods can be used to analyse both polymer modified and neat bitumen, i.e. spectrophotometry, chromatography and differential scanning calorimetry. However, the use of these techniques and the interpretation of results are usually not the same because of differing objectives, in particular towards the ageing mechanism, as described below.

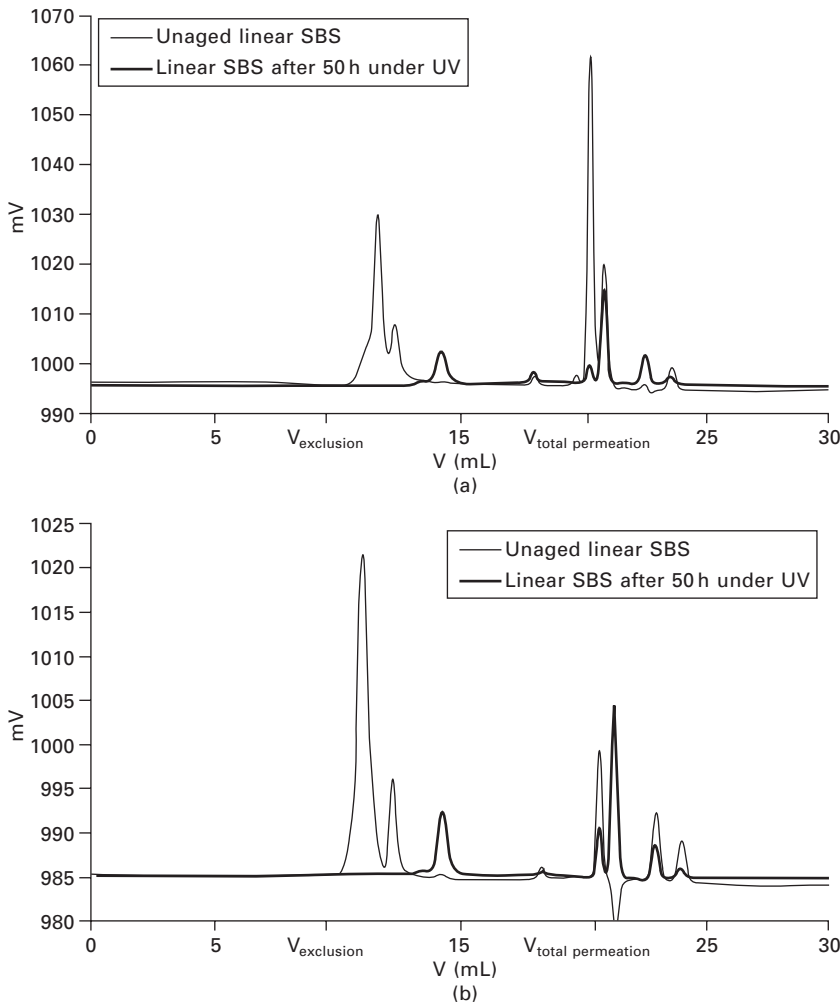
Characterization of the ageing of the polymer part by size exclusion chromatography (SEC)

Size exclusion chromatography (SEC) is a column liquid chromatographic technique that separates molecules according to their size. It is based on the partition of macromolecules (solute) dissolved in a mobile phase. The sample solution is introduced onto the column, which is filled with a porous gel (stationary phase), and is carried by solvent (mobile phase) through the column. The separating of molecules based on size takes place by repeated exchange of the solute molecules between the bulk solvent of the mobile phase and the stationary phase within the pores of the packing (Yau *et al.*, 1979). In a simplified case, this partition depends only on the size of macromolecules and pores (Holtzhauer and Rudolph, 1992). Usually, separated macromolecular fractions are detected by refractive index or viscosity detection.

SEC is a useful analytical technique for separating compounds with very different molecular sizes, such as bitumen and most polymers. As no chemical

reaction has taken place between the bitumen and the polymer, this technique can be used to separate the polymer fraction, which can then be precisely identified by infrared spectroscopy. Applied to linear SBS and radial SBS modified bitumen, SEC allows distinguishing between elastomer architectures in bitumen (Mouillet *et al.*, 2008b): the PmB chromatograms display, for the polymer part, a bimodal distribution in the case of radial SBS (major peak of $M_w = 144\,444$) and a monomodal distribution in the case of linear SBS ($M_w = 300\,000$). It can be noted that the lowest radial SBS molecular weight can be explained by a difference in interaction between the polymer and bitumen components (Mouillet *et al.*, 2008a; Marechal, 1982): indeed, the polymer is more or less swollen depending on the chemical nature of bitumen oil component and polymer structure. However, some polymers, such as styrene/isoprene/styrene (SIS), cannot be separated because they have a similar size as bitumen so they elute at the same volume.

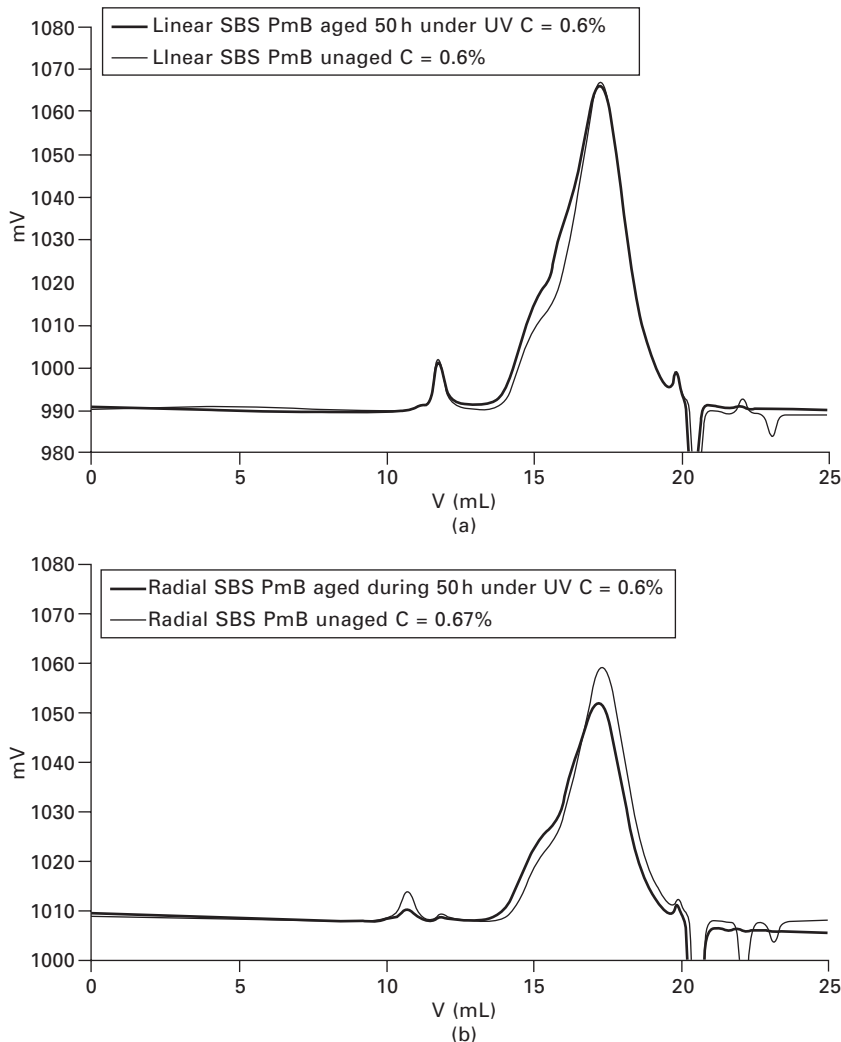
SEC is also a useful technique to monitor PmB ageing. Some authors have applied SEC to study the photo-ageing of linear and radial SBS based PmB (Mouillet *et al.*, 2008a; Durrieu *et al.*, 2007). Indeed, even if the impact of thermal ageing on the degradation of SBS elastomers in the bitumen has been extensively studied (Lu and Isacsson, 1998; Mouillet *et al.*, 2008b; Durrieu *et al.*, 2007; Marechal, 1982; Oliver and Tredrea, 1997), there are no studies dealing with photo-oxidation of these copolymers in a bituminous matrix. So, in order to study the effect of photo-oxidation on molecular size of SBS when added to bitumen, pure SBS elastomer and SBS modified bitumen have been submitted to photo-ageing in a UV paint chamber according to EN ISO 11341. The SEC analysis of pure elastomer, before and after 50 hours of UV exposure, presents an identical evolution of average molecular weight for the linear and radial SBS, namely scission of polymer chains leading to oligomer production that elute at 13 mL ($M_w = 44\,430$) and 18 mL ($M_w = 460$), respectively (see Fig. 12.1). However, the same approach applied to PmB does not suggest elastomer modification by chain scission after ageing (see Fig. 12.2). Indeed, after 50 hours of UV exposure, there are always polymer peaks without molecular weight change of the major population (144 444 for the linear SBS and 300 000 for the radial SBS). At the same time, the ageing of bitumen is reflected in peaks increasing in intensity, corresponding to the high molecular weight populations. It can be noted that the intensity differences between unaged and aged radial SBS modified bitumen (see Fig. 12.2) are due to a concentration difference of analysed solutions ($C = 0.67\%$ for the unaged PmB and $C = 0.6\%$ for the aged PmB). From the SEC analysis, it seems that, during photo-ageing, the bituminous matrix has a protective effect with regard to scission of elastomer chains.



12.1 SEC chromatograms of the linear SBS elastomer (a) and radial SBS elastomer (b) before and after 50 hours of UV exposure.

Follow-up of the degree of oxidation by Fourier transform infrared (FTIR) spectroscopy

Fourier transform infrared spectroscopy is a well-known analytical technique that can give information on the nature and the content of existing functional and structural groups in bitumen (Pieri, 1994). This technique can also be used to detect and analyse the oxygenated species contained in bitumen and that produced as a consequence of ageing mechanisms (Mouillet *et al.*, 2010). For example, FTIR spectroscopy has been applied by some authors (Mouillet *et al.*, 2008b) to follow PmB structural changes due to photo-ageing: for this



12.2 SEC chromatograms of the bitumen modified by either linear SBS elastomer (a) or radial SBS elastomer (b) before and after 50 hours of UV exposure.

purpose, two PmBs manufactured with the same 35/50 base bitumen and two different SBS (linear and radial SBS) have been tested. They were aged by RTFOT followed by UV exposure (Montepara *et al.*, 2000) in a weathering oven (Durrieu *et al.*, 2007). The UV exposure was performed at 60°C for up to 170 hours, and the slides on which the PmB films were placed were analysed by FTIR spectroscopy at intervals of one or two hours. Then, the selection of two characteristic absorption bands permits structural changes

occurring inside the PmB during this photo-ageing to be studied (see Fig. 12.3), namely:

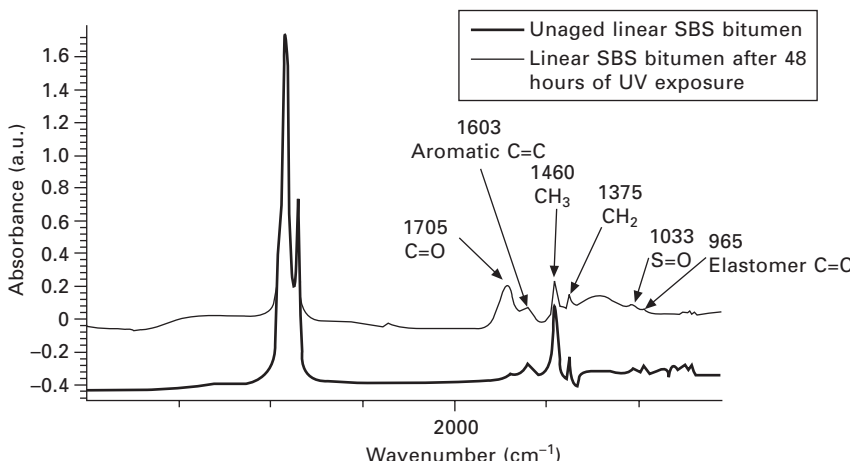
- the following-up of the C=O band (around 1700 cm⁻¹) for the monitoring of the oxidation of the whole binder,
- the following-up of the elastomer C=C band (around 965 cm⁻¹) for the monitoring of the deterioration of the SBS copolymer as a result of modification of the butadiene copolymer by diminution of the double bond content.

But, in order to avoid the effect of the analysed quantities, that is to say the thickness of the film sample, the monitoring of these two infrared bands is performed using a semi-quantitative approach (Lamontagne, 2002; Pieri, 1994; Lamontagne *et al.*, 2001b) based on the definition of the following two relative indices:

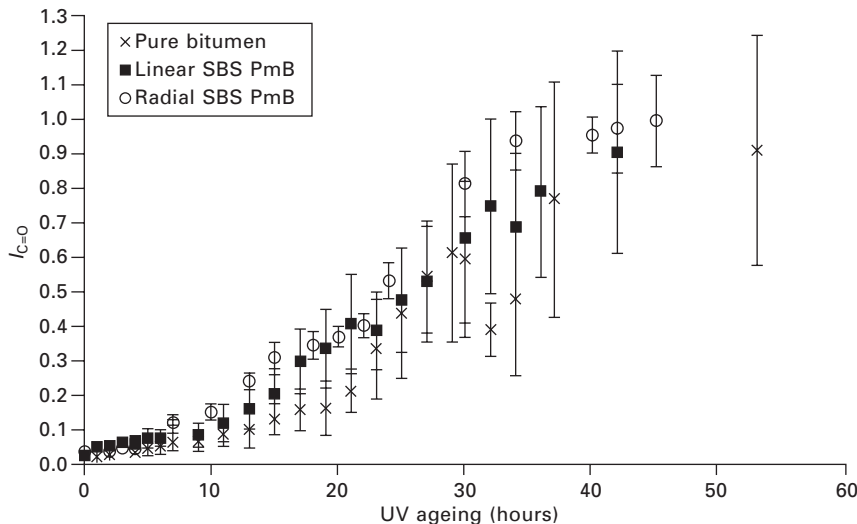
$$I_{C=O} = \frac{\text{Area of the carbonyl band centred around } 1700 \text{ cm}^{-1}}{\sum \text{Area of the spectral bands between } 2000 \text{ and } 600 \text{ cm}^{-1}}$$

$$I_{SBS} = \frac{\text{Area of the ethylene band centred around } 965 \text{ cm}^{-1}}{\sum \text{Area of the spectral bands between } 2000 \text{ and } 600 \text{ cm}^{-1}}$$

The evolutions of C=O index for the two PmBs studied are identical and correspond to that of the base bitumen (see Fig. 12.4); this observation is in good agreement with previous studies (Durrieu *et al.*, 2007) and seems to demonstrate that the carbonyl functional groups of the base bitumen hide



12.3 FTIR spectra (transmission mode) of linear SBS modified binder before and after 48 hours of UV exposure at 340 nm and 0.44 W of UV exposure.

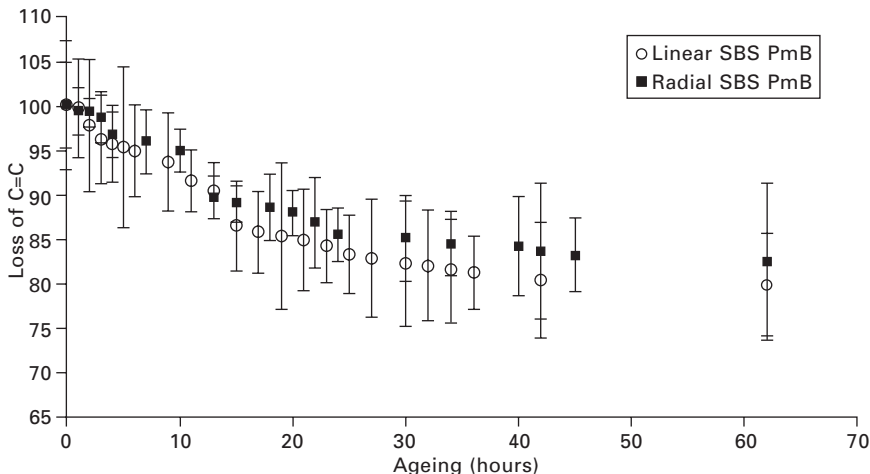


12.4 Evolution of C=O index for the base bitumen and the bitumens modified by linear or radial SBS exposed to UV radiation.

the carbonyls of the copolymers. Moreover, the similarity of the CO index curves underlines the fact that SBS copolymers do not provide a significant 'protective action' on the photo-oxidation of bitumen, in agreement with previous results obtained on other bituminous binders (Durrieu *et al.*, 2007).

The evolution of the elastomer C=C band index, expressed as a percent of loss in relation to the beginning of UV exposure, displays a similar behaviour for the two PmBs studied when exposed to UV radiation (see Fig. 12.5). But it has to be noted that the decrease of the C=C double bond of the polymer is much less important when a polymer is added to bitumen (Mouillet *et al.*, 2008b). Indeed, the loss of *trans*-butadiene double bonds is around 93% for pure linear SBS and 100% for pure radial SBS when exposed to UV, while for SBS added to the bituminous matrix the loss of double bonds is only 15% after 60 hours of UV exposure (see Fig. 12.5).

These results can be explained either by the anti-oxidizing effect of certain bitumen components (Cortizo *et al.*, 2004), or by the hydrogen donor character of bitumen resins that would have an inhibitory effect on elastomer oxidation. Indeed, some authors (Kubo *et al.*, 1994) have shown the inhibitory effect of hydrocarbon solvents containing hydrogen donor atoms on SBS degradation. Moreover, a study of the thermal degradation of acrylonitrile–butadiene–styrene polymer added to bean oil has demonstrated that the oil can capture macro-radicals (Dong *et al.*, 2001). As such, the oil molecules isolate the polymer chains, decreasing the possibility of



12.5 Evolution of C=C index for bitumen modified with linear and radial SBS and exposed to UV radiation.

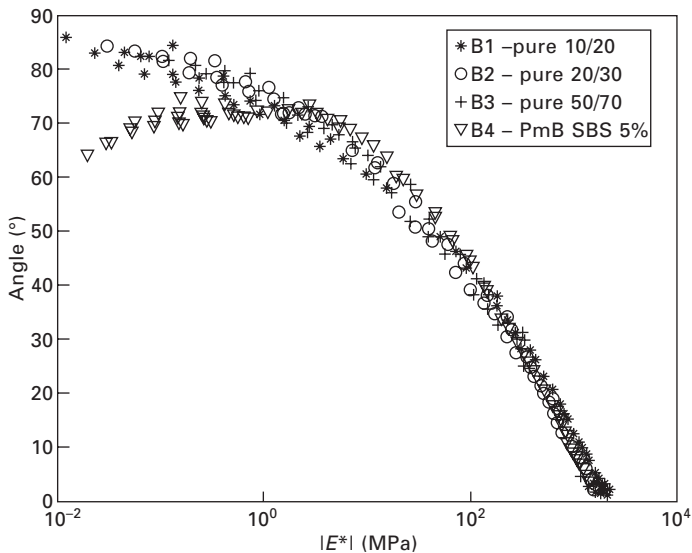
intermolecular transfer of macro-radicals. The same phenomenon has already been reported for polymer mixtures (Pospíšil *et al.*, 1999).

FTIR spectroscopy has confirmed that the nature of the elastomer added to bitumen does not influence the oxidation kinetics of PmB. For the same bituminous matrix, radial and linear SBS display exactly the same oxidation kinetics and the same decrease of the *trans*-butadiene double bond in SBS.

FTIR spectroscopy can also be used to identify and quantify polymers in PmBs (Farcas *et al.*, 2009) and to monitor the content of polymers during ageing. However, a quantitative analysis is only possible for polymers whose absorption bands do not overlap with those of bitumen itself.

Evolution of viscoelastic properties

Addition of polymers affects the mechanical properties of bitumen by increasing the elasticity or plasticity range (Isacsson and Lu, 1995). The complex modulus $|E^*| = E' + iE''$ (or $|G^*| = G' + iG''$ with $|E^*| = 3 \times |G^*|$) and the phase angle $\delta = \arg(E^*)$ (or $\delta = \arg(G^*)$) measured in the linear viscoelastic domain (Goodrich, 1991) can reflect the influence of the polymer on bitumen properties (Mouillet *et al.*, 2004; Airey, 2004). In case of an elastomeric modifier, like styrene–butadiene–styrene (SBS), the elasticity given by the polymer is especially visible on the linear viscoelastic properties of bitumen at high temperature or low frequency (Chailleux *et al.*, 2006) as shown on Black diagrams (see Fig. 12.6). Indeed, for the low modulus and high phase angle region, the rheological behaviour of PmB differs from that



12.6 Complex modulus of four bituminous binders plotted in a Black diagram.

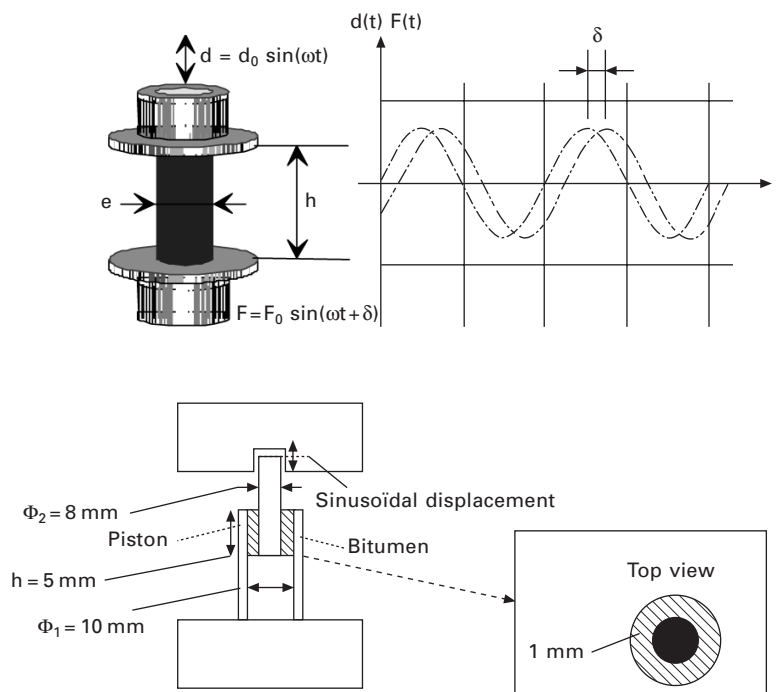
of pure bitumen (see Fig. 12.6): the phase angle of pure bitumen tends to 90° whereas a relaxation phenomenon was observed for PmB. A decrease of phase angle was observed for PmB at high temperature or low frequency, showing a more pronounced elastic behaviour (Lapalu *et al.*, 2004). This effect is due to the polymer strongly influencing the rheological properties as soon as the bituminous matrix becomes fluid. The phase angle decrease, at high temperature/low frequency, is more or less pronounced according to polymer content: rheological behaviour tends towards viscoelastic solid behaviour with a continuous polymeric network, while a simple 'plateau' is observed on the Black diagram with a polymer dispersed in the bituminous matrix (Ramond and Such, 2003).

The question addressed here deals with how this property given by the SBS polymer behaves during ageing. To check the durability of this rheological property with time in service, a comparison study of PmB on site with laboratory ageing procedures has been performed. The binder tested here is a PmB with 2.2 wt% of SBS (physical blend). It was used to prepare an asphalt concrete 0/6 surface course. The lane without traffic of this road was cored each year from 2004, which was the year of the road construction. Binder was extracted and recovered from pavement cores and the results compared to laboratory ageing (according to RTFOT and PAV procedures) of the same binder that was used for the hot-mix production at the mixing plant on site. Then the complex modulus was measured so as to understand the effect of ageing on the small-strain domain mechanical

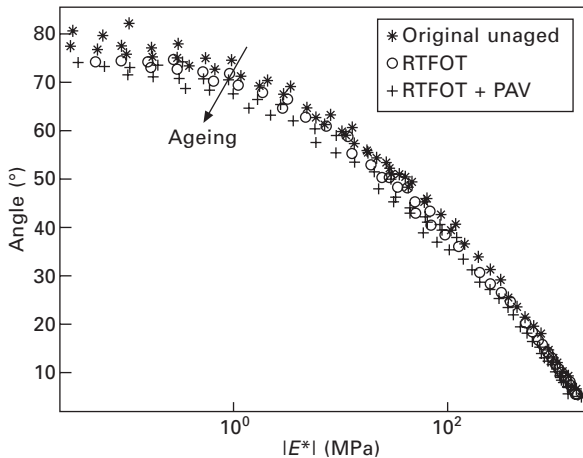
behaviour using a 'Metravib' viscoanalyser in displacement control mode in the linear domain at low strain. At low temperature (-20°C ; 20°C), viscoelastic characterization is performed in traction-compression mode of loading on a cylinder (see Fig. 12.7). An annular shearing mode of loading is employed at higher temperatures (20°C ; 80°C). At each temperature, the complex modulus is measured from 1 Hz to 100 Hz.

Conventional ageing tests and on-site ageing lead to a shift of the curves towards lower phase angle, especially in the low modulus and high angle region (see Figs 12.8 and 12.9, respectively). It has to be noted that the high modulus region seems not to be affected by laboratory ageing procedures but appears to be affected by field ageing. Moreover, this ageing in the field seems to have a more aggressive effect on the viscoelastic response.

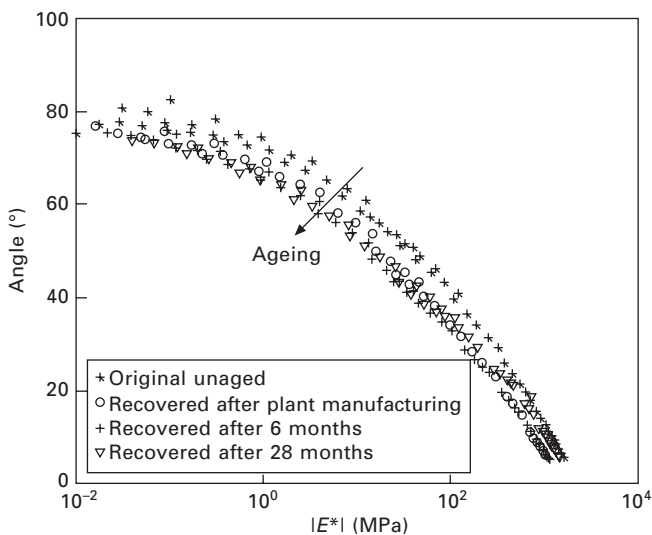
Based on the isochrones at 7.8 Hz (see Figs 12.10 and 12.11), it can be noted that the norm of the complex modulus above -10°C increases with increasing ageing time, irrespective of whether it is from laboratory procedures or *in situ* evolution. Nevertheless, hardening is more pronounced for the on-site ageing. Below -10°C , conventional ageing tests (namely RTFOT and PAV procedures) appear to have no effect on the modulus, whereas field ageing slightly reduces the complex modulus (in a significant way). Phase



12.7 Principle of the 'Metravib' viscoanalyser.

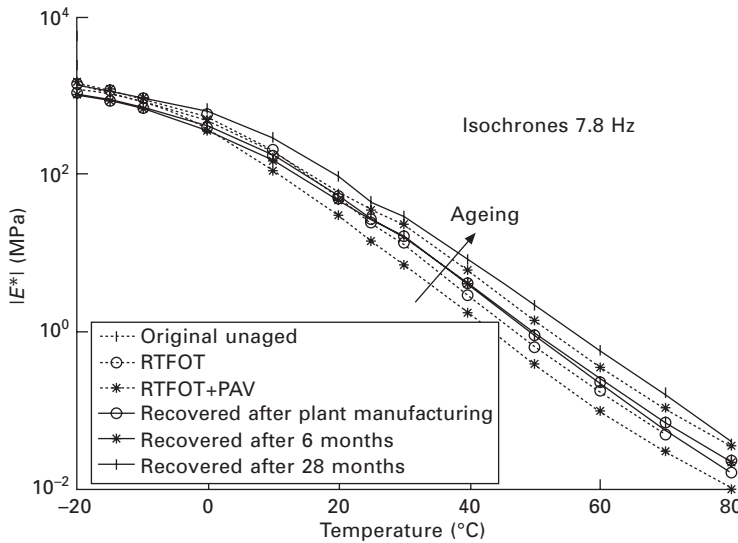


12.8 Black diagram of PmB before and after laboratory ageing procedures.

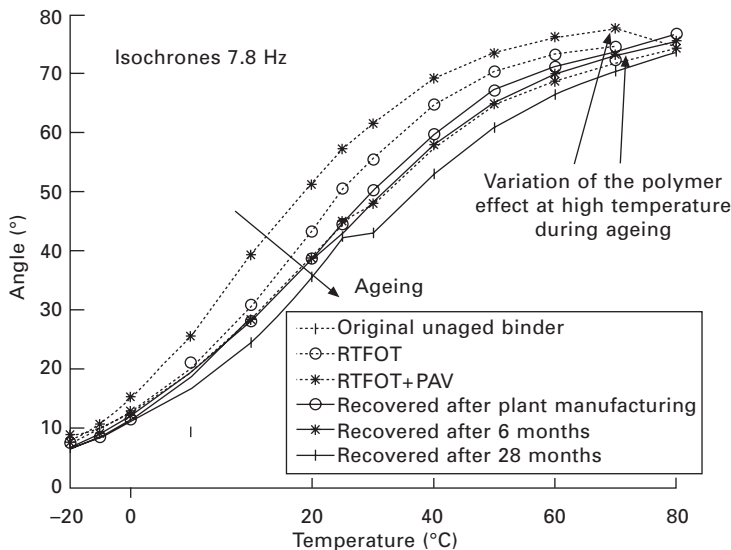


12.9 Black diagram of PmB before and after *in situ* ageing.

angle decreases with ageing over a large temperature range whatever the ageing procedure. But, at high temperature, the polymer effect on phase angle, which is visible for unaged and RTFOT aged binders (see Fig. 12.11), disappears for the binders aged by the RTFOT+PAV procedure and on site: the phase angle tends towards 90° instead of decreasing below 70°C. Hence, the elasticity effect given by the SBS polymer appears to decrease with this long-term ageing.



12.10 Isochrones of the norm of the complex modulus at 7.8 Hz.



12.11 Isochrones of the phase angle at 7.8 Hz.

In order to quantify the ageing effect, temperatures for which rheological properties of the PmB are equal to given values are determined. These isoproperty temperatures have been determined according to two rheological states: the first one corresponds to the rutting risk and is described by the temperatures needed to get $|G^*| = 0.1$ MPa and $\delta = 70^\circ\text{C}$ while the

second is the temperature needed to get $|G^*| = 20$ MPa and $\delta = 45^\circ\text{C}$, and corresponds to the risk of fatigue (see Table 12.1). The temperatures of iso-properties ($T@|G^*| = 0.1$ MPa, $T@|G^*| = 20$ MPa, $T@ \delta = 70^\circ$ and $T@ \delta = 45^\circ$) increase with ageing, showing that the binders become harder (modulus increase) and more elastic (phase angle decrease). It can be noted that considering $T@|G^*| = 0.1$ MPa and $T@|G^*| = 20$ MPa, the RTFOT procedure is equivalent with plant manufacturing, but this is not the case for $T@ \delta = 70^\circ$ and $T@ \delta = 45^\circ$. This means that the capacity of the material to relax stress (linked with the phase angle) does not evolve with the same ageing kinetic as the material stiffness (linked with the norm of complex modulus). Indeed, variations of iso-angle temperature during ageing steps are higher than variation of iso-modulus temperature (see Table 12.1). It is also observed that iso-angle temperatures increase more in the soft domain (at high temperature): indeed, the temperature for which $\delta = 70^\circ$ increases up to 27°C from its original state to 28 months' field ageing. Consequently, the correlations between laboratory ageing procedures (RTFOT or PAV) and field ageing depend on the property considered (modulus or phase angle) and on the chosen temperature range.

Then, to investigate how the property given by the SBS polymer behaves during ageing, the content of SBS (see Table 12.2) measured by infrared spectroscopy (Farcas *et al.*, 2009) has been compared to the rheological evolution of materials. This study has shown that the disappearance of the polymeric 'plateau' on the phase angle isochrones during ageing is in accordance with the decrease of polymer content observed by infrared spectroscopy. This decrease is significant according to the repeatability of the measurement (namely 0.1%) and is very important in the case of field

Table 12.1 Temperature of iso-angle and iso-modulus for elastomer modified binders aged in laboratory and on site

Material	$T@ G^* = 0.1$ MPa	$T@ \delta = 70^\circ$	$T@ G^* = 20$ MPa	$T@ \delta = 45^\circ$
PmB at origin	52.0°C	41.7°C	14.9°C	14.7°C
PmB after RTFOT	55.7°C	49.1°C	18.7°C	21.3°C
PmB after RTFOT + PAV	61.4°C	63.8°C	19.7°C	25.4°C
PmB recovered from asphalt cores after plant manufacture	57.8°C	56.7°C	19.4°C	25.2°C
PmB recovered from asphalt cores 6 months old	58.5°C	60.6°C	17.9°C	27.5°C
PmB recovered from asphalt cores 28 months old	65.0°C	68.7°C	22.8°C	32.2°C

Table 12.2 SBS content of elastomer modified binders aged in laboratory and on site

Material	Percent of SBS measured by infrared spectroscopy
PmB at origin	2.2%
PmB after RTFOT	2.1%
PmB after RTFOT + PAV	2.0%
PmB recovered from asphalt cores after plant manufacture	1.7%
PmB recovered from asphalt cores 6 months old	1.4%
PmB recovered from asphalt cores 28 months old	1.1%

Source: Farcas *et al.* (2009)

ageing (around a 50% loss). The same trend is also detected in phase angle isochrones (see Fig. 12.11).

Therefore, viscoelastic measurement in the linear domain can be relevant in evaluating the effect of polymer content during ageing. According to phase angle isochrones, the polymeric 'plateau' tends to disappear with ageing in the temperature range studied. Moreover, the evolution of phase angle is faster than that of modulus norm. Hence, this decrease of capacity of the material to relax stress with ageing could be the main problem with regard to pavement integrity. Nevertheless, this effect is also probably dominated by the ageing of the bituminous matrix.

12.3 Investigation at the microscopic scale of polymer modified bitumen (PmB) ageing

12.3.1 Analysis of PmB by infrared microscopy

The formation of a functional modified bitumen system is based on the dissolution and/or fine dispersion of polymer in bitumen and on the compatibility of the polymer-bitumen system. PmBs generally display a biphasic microstructure with polymer nodules dispersed in a continuous bitumen phase, or with a bitumen phase dispersed within a continuous polymer phase, or even with two interlocked continuous phases. So, microscopy techniques are indispensable in the analysis of such multiphase heterogeneous systems at the optical microscopic level. Current microscopy techniques such as UV fluorescence microscopy (Brûlé and Brion, 1986) can show PmB microstructure, but cannot inform on the structural and chemical changes occurring with polymer modification. Among other micro-spectroscopy techniques, infrared microscopy enables a local determination

of the structure (Clark, 1992) because it simultaneously allows visualizing the material microstructure and chemically characterizing the visualized micro-phases. This technique, applied to polymer modified bitumen, makes it possible to determine the distribution of the polymer within the bitumen and to show variations of the polymer content together with the chemical nature (aromatic, aliphatic, etc.) of the bitumen fractions which contribute to the swelling of the polymer (Mouillet *et al.*, 2008a). The main interest of infrared microscopy is to characterize separately different phases in heterogeneous products; therefore it is appropriate for PmB and especially for the change with time in service of two-phase structure material (Planche *et al.*, 2008). Indeed, ageing is already a very complex process in unmodified bitumens that are relatively homogeneous materials at the optical microscopic level, and the degree of complexity increases after polymer modification due to the resulting heterogeneous microstructure. It is therefore important to take this peculiar structure into consideration when trying to identify the process involved during ageing: is PmB ageing a consequence of bitumen ageing, polymer ageing or both at the same time?

12.3.2 Direct and continuous methodological approach for studying PmB ageing

To understand how any changes in composition or processing can affect the evolution of PmB microstructure with time, an ageing simulation method directly observable and analysable by infrared microscopy has been set up to study slow evolution phenomena like oxidation in each of the PmB micro-phases (Lamontagne *et al.*, 2001a). It consists of an ageing cell, purposely designed with a number of requirements: horizontal mode, regulated heating and adaptability to the motorized stage of the microscope. This ageing cell is made up of a metallic body heated by two heating cartridges. Both cartridges are connected to a regulator linked to a temperature probe fitted in the centre of the cell. A heated gas flow is flushed through the cell. Furthermore, the system is equipped with a bypass to select either oxidant gas (air) or neutral (argon) gas, allowing the thermal effect to be dissociated from the oxidative effect during simulated ageing (Lamontagne *et al.*, 2001a).

The experimental conditions for the use of this ageing cell applied to PmB have been optimized according to a validity study (Lamontagne *et al.*, 2001a); they are as follows:

- The PmB simulated oxidation is carried out in the ageing cell placed horizontally, by heating the sample at 130°C for 2 hours in synthetic air (80% N₂, 20% O₂) and at 1 bar pressure. Before this, the cell is heated under neutral gas from 25°C to 130°C at 11°C/min heating rate, permitting the PmB sample to homogeneously reach 130°C. However, the choice

of oxidation temperature had to face a key problem – the compromise between a convenient test time of 2 hours and an ageing mechanism that is highly temperature dependent. Previous research studies have demonstrated that bitumen chemistry oxidation processes in the range 60–130°C are quite similar and representative of ageing occurring at field temperatures (Petersen *et al.*, 1993). So, based on these observations, the heating temperature of the ageing cell was set to 130°C, so that the evolution of the PmB microstructure can be performed relatively quickly in 2 hours.

- The micro-infrared analysis is performed on an infrared microscope fitted with a MCT ('mercury–cadmium telluride') detector cooled with liquid nitrogen. Using a motorized *x*–*y* sample stage allowed the collection of a large number of spectra over a specific area of the sample according to the *x*- and *y*-axes, permitting the mapping of the functional groups formed (Mouillet *et al.*, 2000).
- The standard analytical conditions are $\times 15$ infrared objective, the transmission mode, a background obtained on a clean NaCl window, and samples prepared by letting a hot binder droplet flow on a NaCl window in order to obtain a PmB film thickness of about 20 μm . Moreover, several tests were performed to optimize the technical parameters (Lamontagne *et al.*, 2001a), namely beam size (40 $\mu\text{m} \times 40 \mu\text{m}$), analysis step (20 μm), size of the analysed area (130 $\mu\text{m} \times 100 \mu\text{m}$), number of scans (16) and spectral resolution (8 cm^{-1}).

The use of this tool allows the *in situ* oxidation of PmB to be followed continuously through the visualization and chemical characterization of the different micro-phases without modifying the internal equilibrium between polymeric and bituminous phases. It permits the monitoring of both phases simultaneously and the determination of the kinetics of appearance and disappearance of chemical species. Very useful information can be provided concerning the understanding of the oxidation phenomena that PmB undergoes as a consequence of ageing.

12.3.3 Monitoring of PmB structural changes during ageing kinetics

Coupling of the infrared microscope to the horizontal ageing cell allows for the continuous study of the ageing of PmB. During air oxidation, chemical mapping and video images are recorded every 30 minutes, thereby permitting continuous characterization of the evolution of the polymer network of the sample.

So, it becomes possible to visualize in visible mode the evolution of the different micro-phases, to confirm it by infrared mapping (chemical analysis),

and finally to express in real terms (as a percentage) the copolymer content in each micro-phase. For this purpose, the relative polymer content is based on an index defined as the ratio of the specific copolymer absorption band (not interfering with the bitumen) to the specific bitumen absorption band:

- For SBS modified bitumen: ratio of the out-of-plan bending vibration γCH of *trans*-butadiene at 965 cm^{-1} for SBS copolymer to the in-plan bending vibration δCH_3 at 1376 cm^{-1} for the bitumen
- For EVA modified bitumen: ratios of the stretching vibrations $\nu\text{C—O}$ of vinyl acetate at 1240 cm^{-1} for EVA copolymer to the stretching vibrations $\nu\text{C=C}$ at 1600 cm^{-1} for the bitumen.

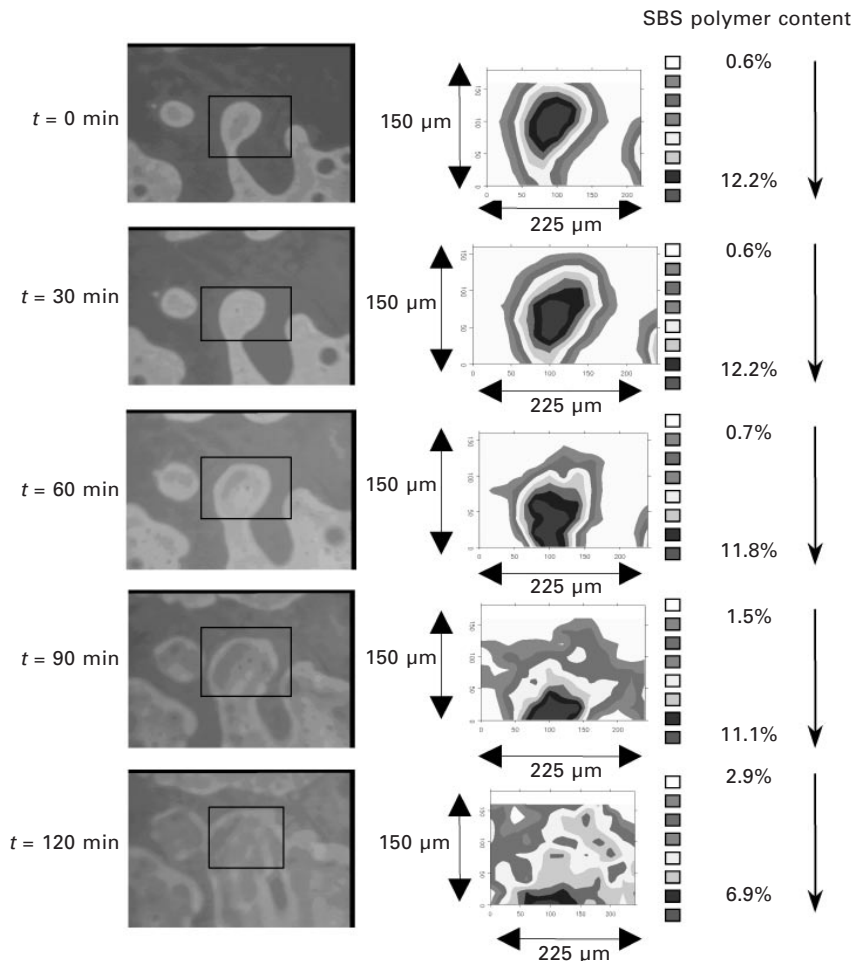
Then, the true percentage of copolymer content in each micro-phase is obtained by comparing this relative polymer content index to a calibration curve obtained by infrared analysis of seven PmBs with known percentage copolymer content from 0.5 to 10 wt% (Lamontagne *et al.*, 2001b; Choquet and Ista, 1992; Masson *et al.*, 2001).

Study of physical blends of styrene–butadiene–styrene (SBS) modified bitumen

The study of ageing of SBS based PmB has been performed on a laboratory-made sample manufactured by adding 6 wt% of unsaturated elastomer (linear styrene–butadiene–styrene, SBS) to a 70/100 penetration-grade bitumen (according to the EN 12591 standard). The physical blend was obtained after 2 hours of moderate shear stirring (about 1000 rpm) at 180°C . The characterization by infrared microscopy of its microstructure at the origin (see Fig. 12.12, $t = 0$ without ageing) reveals a polymer content of 0.6 wt% in the so-called ‘bitumen phase’; this result is in agreement with those published previously (Wilson *et al.*, 2000) in that the polymer is present in very small but significant quantities although it is divided in nodules too small for optical microscopic observation. The polymer seems dissolved in bitumen at this length scale. Although its nominal content in the blend is 6 wt%, the polymer content is 12.2 wt% in the ‘polymer phase’, pointing to local separation of the polymer in the neat PmB.

However, the monitoring of the ageing kinetics using a heating cell under an infrared microscope showed considerable changes in sample micro-morphology with time (see Fig. 12.12, from $t = 30$ to 120 minutes):

- From 0 to 60 minutes’ oxidation, the distribution of both micro-phases remained the same with a quasi-constant SBS content in each domain (about 12 wt% SBS in the polymer-rich area and 0.6 wt% in the surrounding bitumen matrix).
- Between 60 and 120 minutes’ ageing, the micro-morphology of the blend noticeably changed, with the SBS content significantly decreasing in the



12.12 Kinetic evolution of the polymer network of the PmB involving 6 wt% SBS by infrared mapping (130°C in air for 2 hours).

copolymer-rich area (from 11.8 wt% to 6.9 wt%) while increasing in the surrounding bitumen matrix (from 0.6 wt% to 2.9 wt%). The SBS copolymer distribution in the binder appears more homogeneous after ageing.

This homogenization of SBS distribution could be a consequence of polymer chain scission caused by oxidation, as observed in the ageing of pure SBS copolymer (Mouillet *et al.*, 2008a). One can suppose that there is a better compatibility of oxidized SBS molecules with bitumen molecules, leading to a homogenization of SBS. Consequently, from this point of view, the degradation of SBS copolymer could lead to an increase in compatibility

with the base bitumen. There are basically two reasons for this evolution: increase in polarity and/or reduction in the molecular weight of SBS.

Study of chemically reacted SBS modified bitumen (Styrelf®-PmB)

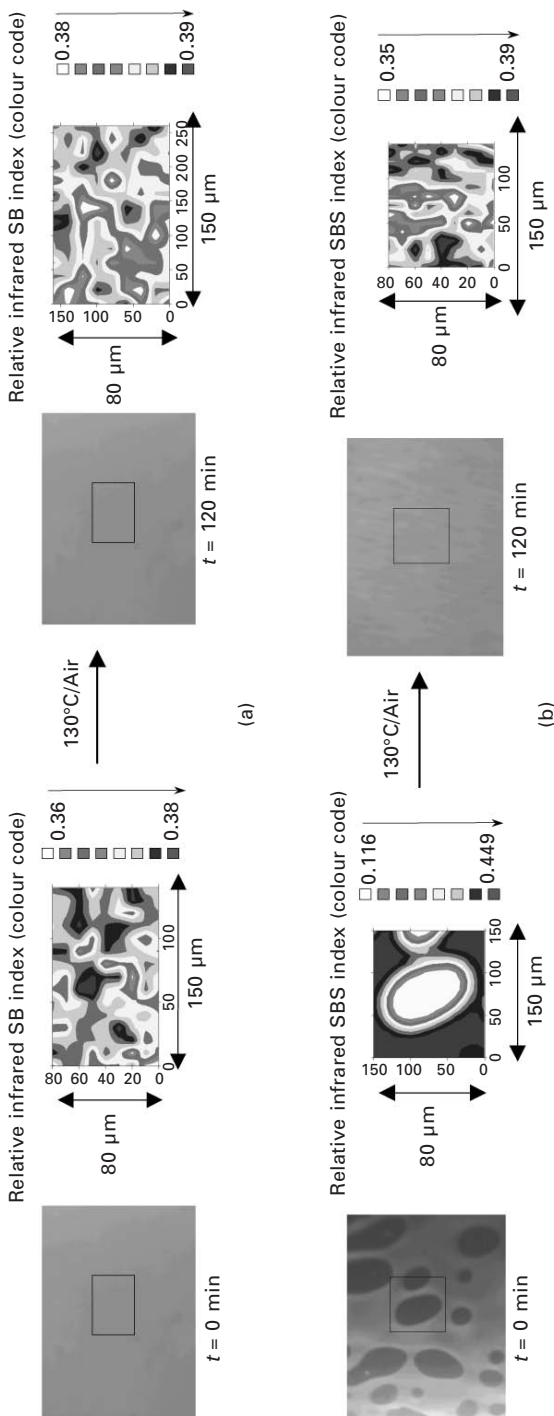
Two chemically reacted PmBs were manufactured on a laboratory scale by adding 6 wt% of two different styrene–butadiene copolymers (copolymer-1 and copolymer-2) to the same 70/100 penetration-grade bitumen (according to the EN 12591 standard). The preparation was carried out according to the industrial proprietary process Styrelf® (patent number FR2376188, 1976) (King *et al.*, 1986) where the PmBs are crosslinked *in situ* by a sulphur derivative under moderate shear stirring for a couple of hours at 180°C.

Copolymer-1 is a linear SB diblock with 25% styrene, whereas copolymer-2 is a radial SBS triblock with around 25% styrene as well. Both polymers have approximately the same molecular weight, around 150 000 Daltons.

At the beginning (see Fig. 12.13(a), $t = 0$), the Styrelf® PmB made with copolymer-1 appears homogeneous when observed on the micro-scale. Globally the polymer content is 6 wt%, that is, identical to the nominal percent. But it is no longer possible to distinguish the polymer phase from the bitumen phase, as clearly shown by the greyscale code mapping where the relative polymer intensity varies only between 0.36 and 0.38. From the resolution of infrared microscopy, the repartition of polymer seems homogeneous.

The Styrelf® PmB manufactured with copolymer-2 on the other hand is less homogeneous, as shown in Fig. 12.13(b), featuring a polymer continuous phase with bitumen nodules inside. It shows that the copolymer structure is another important parameter for compatibility with a given bitumen base (Wilson *et al.*, 2000; Isacsson and Lu, 1999; Kraus, 1982; Lu and Isacsson, 1998; Lu *et al.*, 1999). Although it is a multi-phase system, it is significantly less heterogeneous than the SBS physical blend manufactured with the same compounds: it displays a fourfold relative polymer content gradient (infrared greyscale code) between the phases as opposed to more than 20-fold for the physical blend.

However, it has to be noted that, due to the fineness of the distribution of the copolymer for the chemical blends, the infrared mapping of copolymer repartition is difficult to acquire at the resolution scale. Nevertheless, the kinetic study of Styrelf®-PmB with 6% SB diblock copolymer shows no changes in morphology during ageing (see Fig. 12.13(a)), the binder remaining as homogeneous as that observed without ageing. On the other hand, the PmB becomes more homogeneous for the one manufactured with the radial SBS triblock copolymer (see Fig. 12.13(b)) that was somewhat heterogeneous before ageing, so chemically reacted PmB structure seems to have a stabilizing effect.



12.13 Kinetic evolution of Styrelf®-PmB with SB diblock copolymer (a) and radial SBS triblock copolymer (b) by infrared mapping (130°C in air for 2 hours).

Study of physical blends of ethylene–vinyl acetate (EVA) modified bitumen

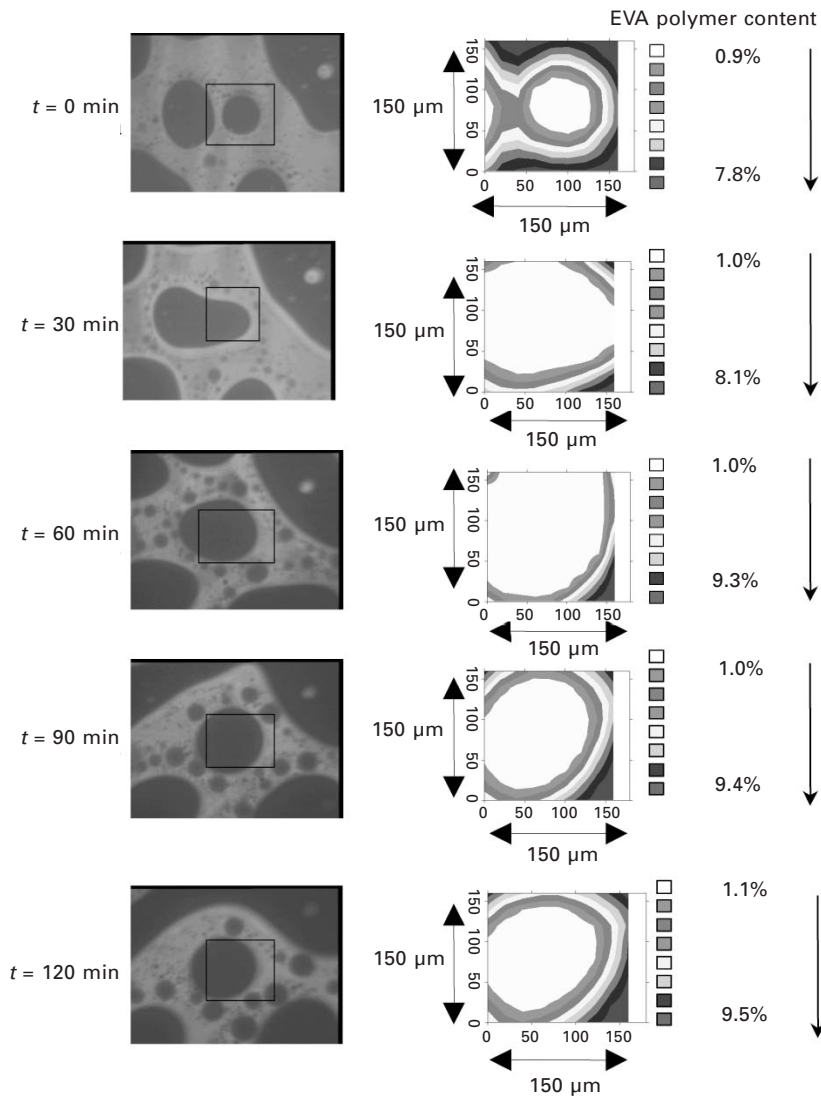
Unlike physical blends of SBS and bitumen, EVA bitumen blends manufactured with the same 70/100 penetration-grade bitumen display an inverse biphasic structure, with bitumen nodules dispersed in the polymeric phase as shown in Fig. 12.14. This structure is highly heterogeneous with polymer content varying more than ninefold between polymer-poor and polymer-rich regions.

The kinetic study of the ageing of this PmB containing 6 wt% EVA also shows changes in morphology during ageing. However, this time, the PmB becomes less homogeneous. The swelling rate of EVA copolymer tends to decrease during controlled oxidation (see Fig. 12.14, from $t = 30$ to 120 minutes).

At the beginning, the blend displays, in visible and infrared modes, a continuous polymeric phase with inclusions of bitumen nodules. During simulated ageing, the EVA copolymer concentrates in the polymer-rich area, the EVA content increasing in the polymer phase from 7.8 wt% to 9.3 wt% after 60 minutes' ageing. The EVA content then no longer increases with ageing up to 120 minutes. The polymeric network seems to partially collapse. This could be due to a weaker compatibility between EVA chains and the oxidized bitumen molecules down to a point where the bitumen fractions swelling the copolymer stop evolving, or get trapped by the polymer network. Moreover, although the morphology changes, the EVA network remains during oxidation in the heating cell with two distinct micro-phases.

12.4 Conclusions

During the service life of a pavement, the bituminous binder is exposed to heat, air and ultraviolet (UV) radiation that lead to the gradual degradation of the physical and mechanical properties of asphalt mixes. This ageing process is of pragmatic importance and consequently is simulated in the laboratory by various accelerated ageing tests, taking into account a thermal oxidation process and the influence of UV radiation. However, there is no available information about the equivalence of these tests with the service years of a binder in a road. At this time, the laboratory simulation techniques of the actions of ageing on modified bitumen are still a substantially open problem because they were developed for unmodified binders and need re-evaluation for polymer-modified bitumen. It seems that the questions of whether an accelerated ageing test performed in the laboratory is truly representative, and of how many years in service it tries to simulate, will certainly never be solved, because binders in pavement age at different rates depending upon climate, air voids, position of the asphalt layer in the pavement layered structure, modified binder oxidation kinetic parameters, initial ageing level when placed in the pavement, and binder hardening susceptibility.



12.14 Kinetic evolution of the polymer network for PmB with 6 wt% EVA by infrared mapping (130°C in air for 2 hours).

Moreover, when a PmB is used to prepare asphalt concrete, what happens after oxidation/ageing is very complex to analyse, due to the number of chemical parameters involved: the nature of the polymer (structure and chemistry), the chemistry of the bitumen, and the type of blending. The majority of physical and chemical techniques used to investigate pure bitumen can be useful in the study of PmB and to follow structural evolution during

thermal or photo-ageing. However, interpretation of results is usually not the same because of differing objectives. For example, the association of two common analytical techniques, namely size exclusion chromatography and Fourier transform infrared spectroscopy applied to PmB, have demonstrated that, on the one hand, inside the bituminous matrix the elastomer architecture does not influence its degradation when exposed to UV radiation and, on the other hand, the bitumen 'protects' the elastomer from UV radiation. In the same way, viscoelastic measurements in the linear domain can be helpful in the evaluation of the role of the polymer during ageing of PmB, namely a reduction of the elasticity attributed to the polymer SBS. It can be noted that this decrease in the ability of the material to relax stress could be the main problem for pavement integrity. However, this effect is also probably dominated by the ageing of the bituminous matrix.

Here one of the most important issues is to describe the process involved: is PmB ageing a consequence of bitumen ageing, polymer ageing or a combination of both at the same time? In order to answer this key question, a new way of characterizing these heterogeneous products has been developed using infrared microscopy without modifying the internal equilibrium between polymeric and bituminous phases. Examination of PmB ageing on the microscopic scale has permitted an understanding of how changes in composition or processing can affect PmB structural evolution with time:

- The general trend for SBS modified bitumen is that the binder becomes more homogeneous upon ageing. This is due both to some polymer degradation (chain scission) and to a better compatibility of the smaller polymer chains with the oxidized bitumen molecules.
- The general trend for EVA modified bitumens is that the binder becomes less homogeneous upon ageing. This is due to a lower compatibility of the polymer chains remaining stable under ageing, with the oxidized bitumen molecules.
- Crosslinked binders appear less sensitive to ageing due to their more homogeneous quasi mono-phase structure (at the length scales investigated) before ageing, which tends to protect them from some kinds of phase change.

These observations permit one to explain how the oxidation and structural modifications of the bitumen after ageing may lead to more or less important modification of the PmBs according to their original composition. Moreover, it seems that during ageing of polymer modified bitumen, oxidation of the bitumen matrix and polymer degradation are important, but above all, the modifications of chemical species exchanges between the two micro-phases during the weathering are primordial. The evolution of structures during ageing depends on the polymer's affinity for the oxidized asphalt molecules, resulting in huge differences in polymer swelling.

In conclusion, the main controlling parameters of PmB ageing are the following:

- The base bitumen, which controls both the PmB structure and its evolution during ageing
- Polymer swelling, which depends on both bitumen and polymer chemistry, and is able to change during ageing
- The manufacturing process, which mainly influences the fineness of the microstructure.

This new tool of characterizing PmB at the microscopic scale provides very useful data to help in the understanding of the oxidation phenomena that occur during both mixing and laying processes in road construction and during further field-service conditions. It can bring new information with regard to durability studies in progress within current national and European standardization frameworks.

12.5 Acknowledgements

The authors wish to thank IFSTTAR and LRPC of Aix-en-Provence laboratory crew members for their helpful contribution.

12.6 References

Airey GD (2003), 'State of the art report on aging test methods for bituminous pavement materials', *International Journal of Pavement Engineering*, 4(3), 165–176.

Airey G (2004), 'Fundamental binder and practical mixture evaluation of polymer modified bituminous materials', *International Journal of Pavement Engineering*, 53, 137–151.

Al-Azri N, Bullin J, Richard R, Ferry A, Glover C, Jung S and Lunsford KM (2006), 'Binder oxidative ageing in Texas pavements: Hardening rates, hardening susceptibilities and the impact of pavement depth', *Transportation Research Board, Annual Meeting 2006*, paper 06-2600.

Anderson D (1999), 'Superpave binder test and specification', *PIARC Seminar SHRP/Superpave*, Luxembourg, pp. 9–10.

Barth EJ (1962), *Asphalt – Science and Technology*, Gordon and Breach, New York and London, pp. 606–609.

Brûlé B and Brion Y (1986), 'Association bitumes-polymères: Relations entre la composition, la structure et les propriétés', *Bulletin de Liaison des Laboratoires des Ponts et Chaussées*, 145, 45–52.

Chailleux E, Ramond G, Such C and de La Roche C (2006), 'A mathematical-based master-curve construction method applied to complex modulus of bituminous materials', *Road Material and Pavement Design*, Vol. 7.

Choquet X and Ista X (1992), 'Determination of SBS, EVA and APP polymers in modified bitumens', *ASTM STP 1108*, 35–49.

Clark DA (1992), 'Fourier transform infrared microscopy: A further dimension in small sample analysis', *Analytica Proceedings*, 29–3, 110.

Cortizo MS, Larsen DO, Bianchetto H and Alessandrini JL (2004), 'Effect of thermal degradation of SBS copolymers during the ageing of modified asphalts', *Polymer Degradation and Stability*, 86, 275–282.

Dong D, Tasaka S, Aikawa S, Kamia S, Inagaki N and Inoue Y (2001), 'Thermal degradation of acrylonitrile–butadiene–styrene terpolymer in bean oil', *Polymer Degradation and Stability*, 75, 319–326.

Duriez M and Arambide J (1962), *Nouveau Traité de Matériaux de Construction, Tome II*, 2ème édition, Dunod, Paris, p. 268.

Durrieu F, Farcas F and Mouillet V (2007), 'Influence of UV radiation on the ageing of a styrene/butadiene/styrene (SBS) modified bitumen: Comparison between laboratory simulations and the on site ageing', *Fuel*, 86(10–11), 1446–1451.

Farcas F (1996), 'Étude d'une méthode de vieillissement des bitumes sur route', PhD, Paris-VI University, France.

Farcas F, Mouillet V, Battaglia V, Besson S, Petiteau C and Le Cunff F (2009), 'Identification et dosage des copolymères SBS et EVA présents dans les liants bitumineux. Analyses par spectrométrie infrarouge à transformée de Fourier', *Testing Method of LPC no. 71*, ISSN 1167–489X, 13 pp.

Goodrich J (1991), 'Asphaltic binder rheology, asphalt concrete rheology and asphalt concrete mix properties', *Association of Asphalt Paving Technologists*, Vol. 60.

Holtzhauer M and Rudolph M (1992), 'Application of colloidal gold for characterization of supports used in size-exclusion chromatography', *Journal of Chromatography A*, 605, 193–198.

Isacsson U and Lu X (1995), 'Testing and appraisal of polymer modified road bitumens – state of the art', *Materials and Structures*, 28, 139–159.

Isacsson U and Lu X (1999), 'Laboratory investigation of polymer modified bitumens', *Proceedings of Association of Asphalt Paving Technologists*, 68, 1–35.

King G, Muncy H and Prudhomme JB (1986), 'Polymer modification: Binder's effect on mix properties', *Journal of Association of Asphalt Paving Technologists*, 28, 519–540.

Korhonen M and Kellomäki A (1996), 'Miscibilities of polymers in bitumen and tall oil pitch under different mixing conditions', *Fuel*, 75(15), 1727–1732.

Kraus G (1982), 'Modification of asphalt by block polymers of butadiene and styrene', *Meeting of the Rubber Division, American Chemical Society*, Philadelphia, PA.

Kubo J, Onzuka H and Akiba M (1994), 'Inhibition of degradation in styrene-based thermoplastic elastomers by hydrogen-donating hydrocarbons', *Polymer Degradation and Stability*, 45(1), 27–37.

Lamontagne J (2002), 'Vieillissement des bitumes modifiés polymères à usage routier par simulations et techniques spectroscopiques', PhD, Aix-Marseille University, France.

Lamontagne J, Durrieu F, Planche JP, Mouillet V and Kister J (2001a), 'Direct and continuous methodological approach to study the ageing of fossil organic material by infrared microspectrometry imaging: Application to polymer modified bitumen', *Analytica Chimica Acta*, 444, 241–250.

Lamontagne J, Dumas Ph, Mouillet V and Kister J (2001b), 'Comparison by FTIR spectroscopy of different ageing techniques: Application to road bitumens', *Fuel*, 80, 483–488.

Lapalu L, Planche JP, Mouillet V, Dumas Ph and Durrieu F (2004), 'Evolution of rheological properties of polymer-modified bitumens during their ageing', *Proceedings of Eurasphalt and Eurobitume Congress*, Vienna, paper 210 (Session 5, 'Ageing, durability and low temperature performance').

Lu X and Isacsson U (1998), 'Chemical and rheological evaluation of ageing properties of SBS polymer modified bitumens', *Fuel*, 77(9–10), 961–972.

Lu X, Isacsson U and Ekblad J (1999), 'Phase separation of SBS polymer modified bitumens', *Journal of Materials in Civil Engineering*, 51–57.

Marechal JC (1982), 'Methods for the study of aging of bitumen-polymer SBS materials', *Durability of Building Materials*, 1, 201–220.

Masson JF, Pelletier L and Collins P (2001), 'Rapid FTIR method for quantification of styrene–butadiene type copolymers in bitumen', *Journal of Applied Polymer Sciences*, 79, 1034–1041.

Migliori F and Corté JF (1998), 'Comparative study of RTFOT and PAV ageing simulation laboratory tests', *Transport Research Boarding*, 1638, 56–63.

Migliori F, Dumas P and Molinengo JC (2000), 'Use of pressure aging vessel (PAV) to study the aging of bituminous mixes with polymer modified bitumens', *2nd Eurasphalt and Eurobitume Congress*, Technical Session 1, paper 0170.

Mill T (1996), 'The role of hydroaromatics in oxidative aging in asphalt', *Preprints of 212th ACS National Meeting*, 41(4), 1245–1249.

Montepara A and Giuliani F (2004), 'Performance testing and specifications for binder and mix: Comparison between ageing simulation tests of road bitumen', *Proceedings of Eurasphalt and Eurobitume Congress*, Vienna, 12–14 May, paper 065.

Montepara A, Santagata E and Tosi G (2000), 'Photochemical degradation of pure bitumen by UV radiation', *1st Eurasphalt and Eurobitume Congress*, paper 5.133.

Mouillet V and Dumas Ph (2008), 'Durability of polymer modified bitumens: comparison of evolution due to conventional standardised ageing tests with the *in situ* ageing of binders in pavements', *Proceedings of Eurasphalt and Eurobitume Congress*, Copenhagen, 21–23 May 2008, paper 406-009 (Session 6, 'Tomorrow's Technical Opportunities and Challenges').

Mouillet V, Kister J, Saury C, Martin D and Planche JP (2000), 'Towards a better understanding of polymer modified bitumens microstructure: Use of FTIR microscopy', *Proceedings of Eurasphalt and Eurobitume Congress*, Session 2, paper 0147.

Mouillet V, Molinengo JC, Durrieu F and Planche JP (2004), 'Effect of ageing on the low temperature cracking properties of bituminous binders: New insights from bending beam rheometer measurements', *Proceedings of 5th RILEM International Conference on Cracking in Pavements*, Limoges (France), RILEM Proceedings PRO37, 'Cracking in Pavements – Mitigation, Risk Assessment and Prevention', ISBN 2-912143-47-0, edited by C. Petit, I.L. Al-Qadi and A. Millien, Session 11, 'Effect of binder properties on HMA cracking – Part A', 351–358.

Mouillet V, Lamontagne J, Durrieu F, Planche JP and Lapalu L (2008a), 'Infrared microscopy investigation of oxidation and phase evolution in bitumen modified with polymers', *Fuel*, 87, 1270–1280.

Mouillet V, Farcas F and Besson S (2008b), 'Ageing by UV radiation of an elastomer modified bitumen', *Fuel*, 87, 2408–2419.

Mouillet V, Farcas F, Battaglia V, Besson S, Petiteau C and Le Cunff F (2010), 'Identification and quantification of bituminous binder's oxygenated species: Analysis by Fourier Transform InfraRed spectroscopy', *Testing Method of LPC no. 69*, ISSN 1167–489X, 9 pp.

Oliver JWH and Tredrea PF (1997), 'The change in properties of polymer modified binders with simulated field exposure', *Proceedings of Association of Asphalt Paving Technologists*, 66, 570–603.

Petersen JC (1998), 'A dual, sequential mechanism for the oxidation of petroleum asphalts', *Petroleum Science and Technology*, 16(9–10), 1023–1059.

Petersen JC (2009), 'A review of the fundamentals of asphalt oxidation: Chemical, physicochemical, physical property and durability relationships', *Transportation Research Circular E-C140*, ISSN 0097-8515, 78 pp.

Petersen JC, Branthaver JF, Robertson RE, Harnsberger PM, Duvall JJ and Ensley EK (1993), 'Effects of physicochemical factors on asphalt oxidation kinetics', *Transport Research Record*, 1391, 1–10.

Pieri N (1994), 'Étude du vieillissement simulé et *in situ* des bitumes routiers par IRTF et fluorescence UV en mode EES', Thèse de doctorat de l'Université d'Aix-Marseille-III, France.

Planche JP, Mouillet V, Dumas Ph and Lapalu L (2008), 'Ageing properties of elastomer modified binders', *Proceedings of Eurasphalt and Eurobitume Congress*, Copenhagen, paper 406-017 (Session 6, 'Tomorrow's technical opportunities and challenges').

Pospišil J, Horák Z, Kruliš Z, Nešpurek S and Kuroda S (1999), 'Degradation and aging of polymer blends – I. Thermomechanical and thermal degradation', *Polymer Degradation and Stability*, 65, 405–414.

Ramond G and Such C (2003), 'Le module complexe des liants bitumineux', *Études et Recherches des Laboratoires des Ponts et Chaussées*, CR32, ISSN 2-7208-2029-6, 84 pp.

Such C, Ballié M, Lombardi B, Migliori F, Ramond G, Samanos J and Simoncelli JP (1997), 'Susceptibilité au vieillissement des bitumes – Expérimentation A08 – Groupe national Bitume', *Études et Recherches des Laboratoires des Ponts et Chaussées*, CR19, 163 pp.

Traxler RN (1963), 'Durability of asphalt cements', *Proceedings of the Association of Asphalt Paving Technology*, 32, 44–58.

Verhasselt A (1999), 'The ageing of hydrocarbon binders and their simulation', *Eurobitume Workshop 99, Performance Related Properties for Bituminous Binders*, Luxembourg, 3–6 May, paper 150.

Wilson A, Fuchs G, Scramoncin C, Martin D and Planche JP (2000), 'Localization of the polymer phase in bitumen/polymer blends by field emission cryo-scanning electron microscopy', *Energy and Fuel*, 14, 575–584.

Wu S, Pang L, Mo L, Qiu J, Zhu G and Xiao Y (2008), 'UV and thermal aging of pure bitumen: Comparison between laboratory simulation and natural exposure aging', *Road Materials and Pavement Design*, EATA 2008, 103–113.

Yau WW, Kirkland JJ and Bly DD (1979), *Modern Size-exclusion Liquid Chromatography: Practice of Gel Permeation and Gel Filtration Chromatography*, Wiley, New York, Chichester, Brisbane, Toronto.

Index

AASHTO criterion, 111, 120
AASHTO MP1, 231, 232
AASHTO R28-06, 253
ageing
chemical characterisation of PMBs, 285–9
high pressure gel permeation chromatography (HP-GPC), 287–8
size exclusion chromatography, 288–9, 290
thin-layer chromatography with flame ionisation detection, 285–7
complex modulus and phase angle at 0.02 Hz
PMB-AS7, 278
PMB-BS7, 278
curves of creep stiffness and creep rate vs loading time
base and SBS 1301 modified bitumens, 285
base and SBS 1301 modified bitumens after TFOT ageing, 286
effect of ageing on temperature dependence of complex modulus and phase angle
EVA1 and EBA modified bitumen A, 279–80
EVA1 and EBA modified bitumen B, 281–2
effect on rheological properties, 275–85
dynamic shear rheology, 277–84
low-temperature creep, 284–5, 286
viscosity, 276–7
future trends in research, 293–4
main causes, 265–9
decreases in ductility with ageing time, 267
effect of intensity of UV radiation on bitumen viscosity, 268
effect of temperature on hardening rate or oxidation rate of base bitumen and PMBs, 266
energy of different chemical bonds found in bitumen, 268
energy of light at different wavelengths, 268
photo-oxidative ageing, 267–9
thermal-oxidative ageing, 265–7
master curves for BA, SEBS2, SEBS4 and SEBS6
loss modulus, 283
storage modulus, 283
methods for improving ageing resistance of PMBs, 292–3
structures of layered silicate/SBS modified bitumen, 293
performance and characterisation of PMBs, 272–92
ageing on SBS modified bitumen physical properties, 274
ageing on viscosity of SBS modified bitumen, 276
FID signal of bitumen before and after ageing, 286
FTIR spectra of SBS modified bitumen, 291
GPC chromatograms of unaged and short-term aged bitumen, 287
master curves of complex modulus for the base and modified bitumens, 284
PAV ageing time effects on softening point of base and SBS modified bitumens, 275
physical properties, 273–5
techniques applied for PMBs ageing evaluation, 273
two-dimensional AFM images of SBS modified bitumen, 292
value of AI for base and modified bitumen, 277
physicochemical techniques for analysing PMB, 366–92
investigation at the microscopic scale, 382–9
usual methods, 367–82
polymer modified bitumen, 264–94
SEC chromatograms
AC-10 + 3% SBR, 290
AC-10 + 3% SBS, 290
PMBs before and after 50 hours of UV exposure, 289
simulative ageing methods, 269–72
natural exposure ageing, 272
pressure ageing vessel, 271
rolling thin film oven test, 270
thin film oven test, 269–70
UV radiation test, 271–2

structural characterisation of PMBs, 289–92
 atomic force microscopy, 291–2
 Fourier transform infrared spectroscopy, 289, 291

ageing index, 276

amplitude ratio, 203

ARES, 46

aromatics, 4–5

Arrhenius equation, 206, 265–6

Arrhenius-like equation, 230

Arrhenius model, 113–14

artificial neural networks

- physical and mechanical properties of polypropylene-modified dense bituminous mixture, 161–81
- % bitumen vs specimen height, 171
- accumulated strain analysis, 180
- bitumen percentage vs air voids, 173
- experimental database, 163, 175
- flow analysis, 172
- Marshall Quotient analysis, 173
- neural network architecture, 164
- optimal architecture, 176
- polypropylene percentage vs voids filled with asphalts, 168
- polypropylene type vs % bitumen, 171
- polypropylene type vs air voids values, 172
- polypropylene type vs pulse count, 179
- polypropylene type vs rest period, 179
- polypropylene type vs unit weight, 178
- polypropylene type vs voids filled with asphalts, 167
- specimen height vs air voids, 169
- specimen height vs voids filled with asphalts, 168
- stability analysis, 170
- statistical parameters, 164, 176
- VMA vs voids filled with asphalt values, 170, 180

asphalt, 299

asphalt concrete, 153

- modification with polypropylene, 136–8
- polypropylene fibres to improve fatigue life, 138–9
- physical properties of polypropylene fibres, 139

asphalt-rubber mixture

- performance of pavement, 90–2
- properties, 87–90
 - changes in asphalt concentrate, 90
 - fatigue life, 89
 - stiffness modulus, 89
 - wheel tracking test, 88

asphaltenes, 3–4

ASTM 1963, 146

ASTM D5, 231

ASTM D36, 231

ASTM D471, 338

ASTM D977, 31

ASTM D2397, 31

ASTM D2872, 253

ASTM D4124, 80

ASTM D7000, 37

ASTM D8, 76

ASTM D1754, 269

ASTM D2872, 269

ASTM D4402, 276

ASTM D6114-97, 352

ASTM D6521, 269

ASTM D1559-76, 139

atomic force microscopy, 10, 65, 291–2

bending beam rheometer, 86, 284–5

binder viscosity, 34

binder–water interfacial tension, 34

bitumen, 1–7, 8–9, 44, 98, 299

- cross-sectional view of asphaltene molecule, 4
- fractional distillation of crude oil, 3
- hypothetical asphaltene molecule, 5
- macrostructure of asphalts, 6
- methods of modification with crumb rubber, 76–8
 - dry process, 78
 - wet process, 76–8
- modification using polyurethanes, 43–68
 - bitumen foaming and future trends, 59–67
 - isocyanate-based reactive polymers, 46–9
 - modification by polymers, 44–5
 - polyurethane/urea-based modified bitumen, 55–9
 - role of colloidal nature, 49–55
- modification using waste polymers, 98–133
 - future trends, 132–3
 - processing of waste polymer modified bitumen, 100–11
 - thermal properties, 111–32
- modification with polypropylene fibre, 136–90
- artificial neural networks for physical and mechanical properties prediction, 161–81
- asphalt concrete modification, 136–8
- creep behaviour analysis, 152–61
- enhancement of physical and mechanical properties, 139–45
- fatigue life analysis, 145–52
- improvement of fatigue life of asphalt concrete, 138–9
- static creep tests, Marshall tests, and fluorescence microscopy analyses, 181–9

rubber modified, 72–93

asphalt-rubber mixture properties, 87–90

economic benefits, 92–3

performance of pavement with asphalt-rubber mixture, 90–2

properties, 84–7

rubber-bitumen interactions, 78–84

shredding of scrap rubber from tyres, 75–6

waste rubber recycling, 73–5

Bitumen Test Data Chart, 245

bituminous binders

- bitumen modification to enhance fuel resistance, 340–62
- polymer modified bitumens, 340–51
- rubber bitumens, 352–6

- wax modified bitumens, 356–62
- fuel resistance, 336–63
 - searching for new solutions, 337–8
 - solutions proposed in the past, 336–7
- solubility, 338–40
 - common and proposed measurement techniques, 338–9
 - simple method to measure fuel solubility, 339–40
- Black diagram, 205, 254, 376
- Boltzmann superposition principle, 200, 201
- branched copolymers, 218
- breaking, 33
- breaking agent, 33–4
- breaking index, 32
- British Standard 3690, 1
- brittleness, 86
- Brookfield viscometer, 276
- BS EN 1426, 244
- BS EN 1427, 244
- BS EN 12593, 245
- BS EN 13398, 245
- BS EN 13587, 245
- BS EN 12607-1, 253
- capillary number, 221
- carbamic acid, 56
- Carreau model, 112–13, 215–16
- CEN EN 12697-43, 338
- chip seals, 35–7
- coalescence, 33
- cold mix asphalt, 25
- Colloidal Indices, 240
- complex compliance, 204–5
- complex modulus, 203–4, 210, 220
- concrete, 138
- confocal laser scanning microscopy, 10
- control, and data acquisition system, 152–3
- crack initiation, 150
- creep, 152
 - analysis of bituminous concrete by wet basis
 - modification, 152–61
 - accumulated strain vs pulse count, 157–8
 - bitumen contents, 155
 - creep stiffness vs pulse count, 159–60
 - M-03 type polypropylene fibre-modified bitumen samples, 155
 - physical properties of coarse aggregates, 154
 - physical properties of fine aggregates, 154
 - physical properties of reference bitumen, 154
 - repeated creep curve, 153
 - type 2 wearing course gradation, 154
 - creep compliance, 202
 - creep stiffness, 157–8, 160–1
 - creep test, 181–4
 - CRM-20, 352
 - crude oil, 2
 - crumb rubber modifier, 352
 - crumb tyre rubber, 338
 - crumb tyre rubber modified bitumen, 99, 206–8
 - cryogenic method, 75–6
 - cutback grades, 2
 - damping function, 217
 - Deborah number, 198
 - dichloromethane, 348–9
 - differential scanning calorimetry, 6, 114–15
 - dry process, 78
 - ductility retention rate, 275
 - dynamic shear rheometer, 239, 247, 248, 277–84
 - EAA6, 341
 - EAA11, 341
 - elasticity, 86
 - elastomers, 218–24
 - electron nuclear double resonance spectroscopy, 7
 - EMA25, 341, 347, 350
 - empirical shift-factor, 206
 - EN 1429, 30
 - EN 13074, 32
 - EN 13588, 32
 - EN 13808, 31
 - EN 14769, 368
 - EN 12607-1, 368
 - EN 13075-1, 32
 - EN ISO 11341, 371
 - Engler, 32
 - environmentally friendly construction technologies, 25
 - ethylene-*bis*-stearamide, 361
 - ethylene vinyl acetate, 239
 - ethylene vinyl acetate copolymers, 341
 - ethylene–acrylic acid copolymers, 341
 - ethylene–methyl acrylate copolymer, 341
 - ethylene–vinyl acetate modified bitumen
 - monitoring PMB structural changes during ageing kinetics, 389
 - European Tyre Recycling Association, 72
 - EVA14, 341, 346
 - EVA28, 341, 346, 350
 - expansion ratio, 61
 - fatigue, 145–6
 - fatigue life analysis, 145–52
 - crack initiation region, 150
 - elastic modulus vs pulse count, 151
 - elastic strain vs pulse count, 148
 - permanent strain vs pulse count, 149
 - fibre-reinforced concrete, 138
 - Fischer–Tropsch waxes, 358, 360
 - flexural creep tests, 199
 - flow tests, 139
 - fluorescence microscope, 185–6
 - fluorescent microscopy imaging, 241
 - Fourier transform infrared spectroscopy, 289, 291, 301–4, 372–6
 - Fraass breaking point, 245
 - Fraass method, 86
 - free radical theory, 268
 - freezing point depression, 6
 - Friedel–Crafts catalysts, 13
 - fuel resistance
 - bituminous binders, 336–63
 - searching for new solutions, 337–8

solutions proposed in the past, 336–7
 enhancement by bitumen modification, 340–62
 polymer modified bitumens, 340–51
 rubber bitumens, 352–6
 wax modified bitumens, 356–62
 functionalised waxes, 358
 Gaestel colloidal index, 51
 gas chromatography–mass spectrometry, 6
 gel contraction, 35
 gel permeation chromatography, 6, 255, 304–8
 bituminous sealant with UV light detection at 210 nm, 254 nm, and 310 nm, 307
 block copolymers of polystyrene and polybutadiene, 304
 GPC responses from two commercial sources of block SB-copolymers, 305
 GPC with UV detection at 210 nm of base bitumen and two sealant batches, 308
 polymer analysis, 304–6
 sulphur analysis, 306–8
 ultraviolet absorbance of important sealant components, 306
 granulation, 85
 hard grades, 2
 high pressure ageing test, 253, 254
 high pressure gel permeation chromatography, 287–8
 high-resolution thermogravimetry, 308–9, 310
 high-shear processing, 104–6
 high-shear-rate-limiting viscosity, 211, 215
 hot mix asphalt, 25, 133
 hydrogen sulphide, 307
 Ietroscan, 6
 indirect tensile fatigue test, 259
 indirect tensile stiffness modulus, 259
 infrared microscopy
 PMB ageing investigation at the microscopic scale, 382–3
 insulation, 62–7
 interaction effect, 80
 International Bitumen Emulsion Federation, 25
 International Union of Pure and Applied Chemistry, 33
 ISO 10512, 7
 Jet Fuel A-1, 340
 Laplace pressure, 221
 large molecular size, 287
 latex, 27
 latex co-emulsification, 27
 latex post-addition, 27
 Leitz Medilux microscope, 241
 Levenberg–Marquardt back-propagation, 162, 174
 life cycle cost analysis, 92–3
 lime stone, 309
 linear constitutive equation, 201
 linear variable displacement transducers, 156
 loss angle, 203
 low-shear processing, 100–3
 low-temperature creep, 284–5
 Marshall Quotient, 144, 152, 162, 170–1, 174
 Marshall stability, 139, 152, 167
 Marshall tests, 151–2, 162, 184–5
 maximum foamability, 61–2
 Maxwell model, 208, 217
 MDI-PPG, 46, 49, 54, 58–9
 mechanical grinding, 76
 medium molecular size, 287
 4,4'-methylenebis(phenyl isocyanate), 46, 67
 'Metravir' viscoanalyser, 378
 Mettler DSC 30 analyser, 250
 microcrystalline waxes, 357
 microsurfacing, 38
 modified rolling thin film oven test, 270
 modulated differential scanning calorimetry, 125–6
 Montan waxes, 357–8, 360
 National Cooperative Highway Research Program project, 231
 natural exposure ageing, 272
 NCHRP 9–10, 231–2
 Newtonian viscosity, 215
 non-Newtonian viscous flow modelling, 211–16
 Carreau's model, 215–16
 Ostwald–De Waele's model, 212–15
 Sisko's model, 215
 Nottingham Asphalt Tester (NAT), 239, 256, 259
 nuclear magnetic resonance spectroscopy, 6
 Ohio State Department of Transportation, 138–9
 organophilic montmorillonite, 293
 Ostwald–De Waele model, 105, 212–15
 oven ageing, 331
 oxidised grades, 2
 Palierne model, 220–1, 224
 paraffin waxes, 357
 particle size, 34, 127–30
 penetration grades, 2
 penetration index, 245
 penetration retention rate, 275
 penetration test, 86
 petroleum waxes, 357
 phase shift, 203
 photo-oxidative ageing, 267–9
 physicochemical techniques
 analysing polymer modified bitumen ageing, 366–92
 Black diagram
 PMB before and after *in situ* ageing, 379
 PMB before and after laboratory ageing procedures, 379
 characterisation methods, 370–84
 C=O index evolution for base bitumen and bitumens modified by linear or radial SBS, 375
 C=O index evolution for bitumen modified with linear and radial SBS, 376

complex modulus of four bituminous binders plotted in Black diagram, 377

follow-up of the degree of oxidation by FTIR spectroscopy, 372–6

FTIR spectra of linear SBS modified binder, 374

isochrones of the norm of complex modulus at 7.8 Hz, 380

isochrones of the phase angle at 7.8 Hz, 380

principle of 'Metravib' viscoanalyser, 378

SBS content of elastomer modified binders aged in laboratory and on site, 382

size exclusion chromatography, 370–2

temperature of iso-angle and iso-modulus for elastomer modified binders, 381

viscoelastic properties evolution, 376–82

kinetic evolution

- polymer network for PMB with 6 wt% EVA by infrared mapping, 390
- polymer network of the PMB, 386
- Styrene-PmB with SB diblock copolymer, 388

laboratory ageing procedures, 367–70

- thermal ageing, 368–9
- UV ray ageing, 369–70

monitoring PMB structural changes during ageing kinetics, 384–9

- chemically reacted SBS modified bitumen, 387–8
- physical blends of EVA modified bitumen, 389
- physical blends of SBS modified bitumen, 385–7

PMB ageing investigation at the microscopic scale, 382–9

- direct and continuous methodological approach, 383–4
- infrared microscopy, 382–3

SEC chromatograms

- bitumen modified by either linear or radial SBS elastomer, 373
- linear and radial SBS elastomer, 372

usual methods, 367–82

plastomers, 218–24

polyblends, 8

polyethylene, 9

polymer modified bitumen, 1–15

- ageing, 264–94
 - future trends in research, 293–4
 - main causes, 265–9
 - performance and characterisation, 272–92
 - simulative ageing methods, 269–72
- bitumen, 1–7
 - cross-sectional view of asphaltene molecule, 4
 - fractional distillation of crude oil, 3
 - hypothetical asphaltene molecule, 5
 - macrostructure of asphalts, 6
- bitumen modification to enhance fuel resistance, 340–51
 - comparative study of different polymeric modifiers, 341–8

content of polar groups in copolymers, 345

fluorescence microscopy of PMBs, 343

penetration and softening point of PMBs, 342

physical and chemical composition of bitumens A and B, 341

PMBs with high polymer content, 350–1

relation between polymer structure and anti-kerosene effect, 348–50

softening point of PMBs with high polymer content, 351

solubility base of bitumen A and PMB, 344

solubility base of bitumen B and PMB, 345

solubility of base bitumen B and PMB with 10% of added polymer, 351

TLC-FID analysis of PMBs from base bitumen A, 348

TLC-FID analysis of residues, 349

factors affecting rheology, 238–61

- advanced rheological characterisation, 248–51

ageing, 251–6

asphalt mixture performance, 256–60

- conventional physical property tests, 243–8

polymer modification, 239–43

physicochemical techniques for ageing analysis, 366–92

ageing investigation at the microscopic scale, 382–9

usual methods, 367–82

rheology, 197–232

case studies, 218–31

characterisation at in-service temperatures, 200–17

future trends, 231–2

stage-wise dispersion of SBS (Shell Cariflex TR1184), 11

types, characterisation and properties, 14–15

polymer modified bitumen emulsions, 14, 25–40

breaking properties, 32–5

effect of route on residual binder morphology, 37

latex-modified emulsion breaking route, 36

routes for emulsion break-up, 32–5

formulation, 28–9

effect of polymer type on particle size distribution, 28

example of emulsion formulas, 29

manufacture, 26–35

categories, 27

properties and specifications, 31–2

recovered binder cohesion for unmodified and modified emulsions, 33

use, 35–8

aggregate loss in the wet abrasion test, 39

average retained aggregate in the sweep test, 38

polypropylene fibre
 bitumen modification, 136–90
 artificial neural networks for physical and mechanical properties prediction, 161–81
 asphalt concrete modification, 136–8
 creep behaviour analysis, 152–61
 fatigue life analysis, 145–52
 improvement of fatigue life of asphalt concrete, 138–9
 enhancement of physical and mechanical properties, 139–45
 effect of polypropylene fibre addition on VMA values, 144
 material properties of polypropylene fibres, 140
 physical properties of bitumen, 141
 physical properties of coarse aggregates, 141
 physical properties of fine aggregates, 141
 polypropylene fibre addition on air voids values, 145
 polypropylene fibre addition on flow values, 146
 polypropylene fibre addition on Marshall Quotient values, 147
 polypropylene fibre addition on stability values, 146
 polypropylene fibre addition on unit weight values, 144
 polypropylene fibre addition on voids with asphalt values, 145
 type 3 wearing course gradation, 141
 types of polypropylene fibres, 143
 static creep tests, Marshall tests, and
 fluorescence microscopy analyses, 181–9
 accumulated strain values for 15 sets of specimens, 183
 accumulated strain vs time graph, 188
 accumulated strain vs time graphs, 183
 average physical and mechanical values, 185
 creep stiffness vs time graph, 184
 economic analysis, 187–9
 polypropylene in base bitumen, 0.5% by weight of aggregate, 186
 polypropylene in base bitumen, 1.5% by weight of aggregate, 186
 polypropylene in base bitumen, 2.5% by weight of aggregate, 186
 polypropylene in base bitumen, 3.5% by weight of aggregate, 186
 polypropylene in base bitumen, 4.5% by weight of aggregate, 187
 polypropylene in base bitumen, 5.5% by weight of aggregate, 187
 polypropylene in base bitumen, 6.5% by weight of aggregate, 187
 poly(propylene glycol), 46, 67
 polyurethane/urea-based modified bitumen, 55–9
 evolution with time of the normalised torque (M/M_0), 58
 frequency dependence of the storage and loss moduli, 55
 FTIR spectra showing C=O (urethane/urea) bands, 57
 temperature dependence of the 'rutting parameter,' 59
 polyurethanes
 bitumen foaming and future trends, 59–67
 AFM micrographs, 66
 evolution of foamed bitumen expansion ratio (ER) with time, 61
 foamed pavement applications, 60–2
 insulation, 62–7
 temperature sweep tests in oscillatory shear, 65
 viscous flow curves, 64
 bitumen modification, 43–68
 modification by polymers, 44–5
 polyurethane/urea-based modified bitumen, 55–9
 isocyanate-based reactive polymers, 46–9
 evolution of M/M_0 (normalised torque) with time, 47
 evolution of zero-shear-limiting viscosity, at 50°C, with curing time at room temperature, 49
 flow curves at 60°C for uncured samples, 48
 role of colloidal nature, 49–55
 AFM images of neat bitumen and 30-day cured MDI-PPG binders, 54
 AFM micrographs of neat bitumens with different microstructure, 53
 AFM of neat bitumen samples, 53
 colloidal index values, 52
 SARAs fractions, 51
 viscous flow curve, 50
 power-law model *see* Ostwald-De Waele model
 pressure ageing, 331
 pressure ageing vessel, 253, 269, 271, 368, 369
 pyrolysis, 73
 radial copolymers, 218
 reclaimed asphalt pavement, 133
 repeated load axial test, 258
 retreading, 73
 rheology, 197
 advanced characterisation, 248–51, 252
 complex modulus master curves at 25°, 252
 DSR rheological parameters, 250–1
 linear viscoelastic response, 248–50
 LVE strain limits as function of complex shear modulus, 249
 modification indices based on complex shear modulus, 250
 phase angle master curves at 25°, 252
 variations in DSC thermal ranges due to EVA modification, 251
 affecting factors, 238–61
 asphalt mixture performance, 256–60
 fatigue cracking resistance, 259
 fatigue functions for unmodified and SBS modified asphalt mixtures, 260

permanent deformation response, 258–9
 RLAT axial strain vs load applications, 258
 case studies, 218–31
 loss tangent for selected bitumen and synthetic binder samples, 227
 plastomers and elastomers, 218–24
 storage and loss moduli for synthetic binders with constant polymer concentration, 229
 storage and loss moduli for synthetic binders with constant resin concentration, 228
 storage and loss moduli for unmodified bitumen and synthetic binder, 226
 synthetic binders, 224–31
 conventional physical property tests, 243–8
 changes in conventional binder properties following EVA and SBS modification, 246
 empirical performance parameters, 245–7
 idealised viscosity–temperature relationship for a PMB, 246
 penetration and softening point, 243–5
 penetration values of EVA and SBS PMBs, 244
 softening point values of EVA and SBS PMBs, 245
 viscosity of PMBs, 247–8
 viscosity–temperature relation for EVA and SBS PMBs, 247
 effect of ageing, 251–6, 257
 Black diagram for unaged, RTFOT and HiPAT aged 7 wt% EVA-Bitumen B, 256
 Black diagram for unaged, RTFOT and HiPAT aged 7 wt% SBS-Bitumen B, 255
 Black diagram for unaged, RTFOT and HiPAT aged Bitumen C, 254
 conventional bitumen ageing, 253–4
 EVA PMBs ageing, 255–6
 morphology of unaged, RTFOT and HiPAT aged 7 wt% EVA-Bitumen B, 257
 SBS PMBs ageing, 254–5
 frequency dependence of the linear storage and loss moduli in oscillatory shear 3 wt% HDPE-modified bitumen, 223 5 wt% SBS-modified bitumen, 222
 future trends, 231–2
 linear viscoelastic behaviour, 200–10
 creep, 201–2
 elastic and viscous moduli curves for CTRMBs, 207
 elastic modulus curves for EVA/LDPE modified bitumens, 209
 linear creep and recovery compliance data vs time, 202
 model, 208–10
 small amplitude oscillatory shear, 202–5
 stress relaxation, 201
 time–temperature superposition principle, 205–8
 non-linear viscoelastic behaviour, 210–17
 log–log scale plot of ‘structured’ fluids flow behaviour, 212
 modelling non-linear viscoelasticity, 216–17
 modelling non-Newtonian viscous flow, 211–16
 viscous flow curves for EVA/LDPE modified bitumen, 213
 viscous flow curves for model crumb tyre rubber-modified bitumen, 214
 polymer modification, 239–43
 fluorescent images of EVA modified Bitumen B, 243
 SARA analysis of three base bitumens, 240
 SBS PMB morphology, 242
 polymer modified bitumens, 197–232
 rheological characterisation at in-service temperatures, 200–17
 road pavement, 90–2
 rolling thin film oven test, 253, 254, 269, 270, 368–9
 rotational viscometer, 247
 rotational viscometry, 199
 rubber-bitumen interactions, 78–84
 generic composition of 70/100 pen. grade bitumen, 81
 percent of rubber swelling in bitumen, 79
 swelling rate of rubber in 70/100 pen grade bitumen, 83
 rubber bitumens, 338
 bitumen modification to enhance fuel resistance, 352–6
 complex modulus of bitumen A and CRM-20, 356
 effect of kerosene on rheological properties, 353–6
 master curves of bitumen A, 354
 master curves of CRM-20, 354
 solubility of base bitumen A and CRM-20, 353
 ‘rutting parameter,’ 58–9, 118, 120
 SARA fractions, 49, 240
 Saybolt–Furol, 32
 SB-copolymers, 299
 scrap rubber shredding, 75–6
 Second Law of Thermodynamics, 197–8
 sinusoidal strain rate, 204
 Sisko’s model, 215
 size exclusion chromatography, 288–9, 370–2
 slurry seals, 38
 small-amplitude oscillatory shear, 199, 202–3
 small molecular size, 287
 sodium montmorillonite, 293
 softening point, 86
 softening point increment, 275
 split tension tests, 139
 stone mastic asphalt, 258
 storage modulus, 205

Strategic Highway Research Program, 118, 199, 231

Stress Absorbent Membrane, 90–1

Stress Absorbent Membrane Interlayer, 90

structured fluids, 211

STV, 32

Stylink, 26

Styrelf, 26

Styrelf-PmB, 387–8

styrene/isoprene/styrene, 371

styrene–butadiene modified bitumen

- bituminous sealants and methods of analysis, 300–9
- common infrared fingerprinting absorbances from bituminous sealants, 303
- Fourier-transform infrared spectroscopy, 301–4
- high-resolution thermogravimetry, 308–9, 310
- mass loss and rate of mass loss upon heating a bituminous sealant, 309
- methods to characterise bituminous sealants, 303
- morphology of bituminous sealants, 302
- typical components in bituminous sealants and their common range, 301
- typical variability in percent mass loss from sealant fractions, 310

copolymer degradation, 317–25

- fragmentation and crosslinking, 318–23
- fragmentation without crosslinking, 323–5
- FTIR spectra of Sealants A and F in their virgin state, 323
- GPC of Sealant A, 322
- GPC of Sealant F, 321
- GPC results at 350 nm for Sealant K, 325

gel permeation chromatography, 304–8

- bituminous sealant with UV light detection at 210 nm, 254 nm, and 310 nm, 307
- block copolymers of polystyrene and polybutadiene, 304
- GPC with UV detection at 210 nm of base bitumen and two sealant batches, 308
- polymer analysis, 304–6
- responses from two commercial sources of block SB-copolymers, 305
- sulphur analysis, 306–8
- ultraviolet absorbance of important sealant components, 306

GPC at 210 nm

- weathering of bituminous Sealant B, 315
- weathering of bituminous Sealant C, 319

GPC at 254 nm

- weathering of bituminous Sealant B, 316
- weathering of bituminous Sealant C, 318

GPC results for Sealant K

- copolymer degradation at 210 nm, 324
- copolymer degradation at 254 nm, 325
- copolymer degradation at 3510 nm, 325

infrared spectra

- Sealant B, 312

Sealant C, 320

Sealant G, 313

natural weathering, 298–331

- future trends, 330–1
- validation cycle for the development of accelerated ageing procedure for bituminous sealants, 331

weathering of bituminous sealants, 309–30

- carbon and sulphur oxidation, 310–14
- change of sealant mass upon weathering as obtained by HRTG, 328

common infrared oxidation frequencies in weathered bituminous sealants, 314

composition and weathering pathways for bituminous sealants as obtained by FTIR, 328

degradation cycle for polymer-modified bituminous sealants, 330

GPC at 350 nm of Sealant B, 317

GPC results for bituminous sealants and the relative effects of weathering, 327

HRTG of light fraction in Sealant C, 319

mass change and loss of aromatics, 316

percent mass loss after weathering of Sealant B, 321

reaction and loss of sulphur compounds, 314–17

synthesis of weathering pathways, 325–30

year-to-year percent mass change in sealant total organic content, 330

styrene–butadiene–styrene block copolymers, 341, 347–8

styrene–butadiene–styrene modified bitumen

- monitoring PMB structural changes during ageing kinetics
- chemically reacted, 387–8
- physical blends, 385–7

styrenic block copolymers, 218

sweep test, 37–8

tensile tests, 151–2

thermal ageing, 368–9

thermal oxidation, 368

thermal-oxidative ageing, 265–7

thermal sensitivity, 86

thermo-rheological simplicity, 251

thermogravimetry, 7, 308

thermoplastic elastomers, 218

thermoplastic polyolefin, 100, 102

thermoplastic rubbers, 218

thin film oven test, 269–70

thin layer chromatography coupled with a flame ionisation detector, 50

thin layer chromatography with flame ionisation detection, 285–7, 342

time–temperature superposition principle, 251

transient shear stress, 217

ultraviolet spectroscopy, 6

uniaxial tension tests, 199

Universal Materials Testing Apparatus for Asphalt and Unbound Specimens tester, 139, 146

US federal specification SS-S-1401-C, 338
 UTM-5P, 152–3, 174, 181
 UV ageing, 331
 UV fluorescence microscopy, 382
 UV radiation test, 271–2
 UV ray ageing, 369–70

vapour pressure osmometry, 6
 viscoelastic properties evolution, 376–82
 viscosity, 86
 voids in mineral aggregate (VMA), 142, 181
 volumetric fraction of dispersed phase, 221

Wagner's model, 216–17

waste polymers
 bitumen modification, 98–133
 future trends, 132–3
 processing of waste polymer modified bitumen, 100–11
 waste thermoplastic polymers, 100–6
 waste thermosetting polymers, 106–11

thermomechanical properties, 111–32
 bitumen modification by waste thermoplastic polymers, 111–22
 bitumen modification by waste thermosetting polymers, 122–30
 combined thermoplastic and thermosetting polymers, 130–2
 linear elastic and viscous moduli in oscillatory shear, at 60°C, 131
 viscous flow curves, at 50°C, 132

waste rubber recycling, 73–5
 energy recovery, 74–5
 material recycling, 73–4

waste thermoplastic polymers, 99, 100–6
 bitumen modification, 111–22
 DSC curves, 115
 frequency dependence of the linear elastic and viscous moduli, 116
 influence of polymer content on Carreau model parameters, 113
 polymer concentration and bitumen type, 111–16
 polymer type, 120–2
 processing, 117–20
 results of penetration and softening temperature tests, 118
 'rutting parameter,' 119
 steady-state viscosity vs shear rate, 112
 temperature dependence of linear elastic modulus in dynamic bending, 119
 temperature dependence of linear elastic modulus in oscillatory shear, 121
 temperature dependence of zero-shear-viscosity, 114
 viscous flow curves at 50°C, 117
 viscous flow curves at 135°C, 120, 122

high-shear processing, 104–6
 evolution of the consistency index with processing time, 105
 fitting parameters, 106
 viscous flow curves, 104

low-shear processing, 100–3

bitumen and waste polymers
 characteristics, 102
 evolution of torque during processing of blends, 101
 fitting parameters, 103
 processing devices, 101

waste thermosetting polymers, 99, 106–11
 bitumen modification, 122–30
 effect of particle size on elastic modulus and loss tangent, 128
 glass transition temperature, 126
 non-reversing heat flow curves, 127
 particle size, 127–30
 rubber concentration, 123–7
 SEM of ground tyre rubber sample, 130
 storage modulus, loss of modulus and loss tangent with temperature, 123
 viscous flow curves of neat bitumen and CTRMB, 50°C, 124
 viscous flow curves of neat bitumen and CTRMB, 125°C, 129
 viscous flow curves of neat bitumen and CTRMB, 135°C, 125

influence of temperature on rheology of crumb tyre rubber modified bitumens, 108–11
 asphalt content, 109
 evolution of storage modulus and loss of modulus, 108
 viscous flow curves at 50°C, 110
 viscous flow curves at 150°C, 110

processing device, 106–8
 evolution of storage modulus and loss of modulus, 107
 solubilised rubber content, 108

wax modified bitumens
 bitumen modification to enhance fuel resistance, 356–62
 DSC analyses of wax and WMBs, 359
 effect of waxes on bitumen solubility, 358–61
 qualitative correlation between fuel resistance and both melting enthalpy and residual crystallinity, 360
 solubility of base bitumen A and WMB with 6% of added wax, 359
 wax concentration, 361–2
 weight loss, softening points and EBS melting temperature as function of EBS content, 361

waxes, 357

weathering, 298

wet process, 76–8
 production diagram of non-stable rubber bitumen binder, 77
 production diagram of stable rubber bitumen binder, 77

Williams–Landel–Ferry's equation, 206

zeolite, 357

zero-shear-rate-limiting viscosity, 211
 zinc dialkyl dithiophosphate, 293
 zinc dibutyl dithiocarbamate, 293